

The Development of Small Molecules that Modulate Molecular
Chaperones Hsp90 and Hsp70

By Leah Kathleen Forsberg

Submitted to the graduate degree program in Medicinal Chemistry and the Graduate Faculty of
the University of Kansas in partial fulfillment of the requirements for the degree of Doctor
of Philosophy.

Co-chairperson: Dr. Brian S. J. Blagg

Co-chairperson: Dr. Apurba Dutta

Dr. Thomas E. Prisinzano

Dr. Rick T. Dobrowsky

Dr. Michael Wolfe

Date Defended: October 18, 2017

The dissertation committee for Leah Kathleen Forsberg certifies that
this is the approved version of the following dissertation:

The Development of Small Molecules that Modulate Molecular
Chaperones Hsp90 and Hsp70

Co-chairperson: Dr. Brian S. J. Blagg

Co-chairperson: Dr. Apurba Dutta

Date Approved: December 7, 2017

Abstract

The heat shock proteins are a highly conserved protein family that are constitutively expressed and function as molecular chaperones. Molecular chaperones 90kDa Heat Shock Protein (Hsp90) and 70kDa Heat Shock Protein (Hsp70) have emerged as promising therapeutic targets for both cancer and neurodegenerative diseases. Hsp90 is responsible for the maturation of more than 300 nascent polypeptides, “clients”. These client proteins are involved in the oncogenic process, as many are associated with all 10 hallmarks of cancer. Hsp70 is involved in protein folding and maintenance of protein homeostasis. Targeting molecular chaperones, Hsp70 and Hsp90, is a viable therapeutic strategy for various neurodegenerative diseases as they prevent protein aggregation via refolding denatured proteins and solubilizing protein aggregates. Therefore, small molecules that interact with Hsp90 are sought, as modulation of Hsp90 can impact the cellular function of Hsp70.

Hsp90 contains a traditional N-terminal ATP-binding site and a C-terminal dimerization domain, which contains an additional binding site. Targeting the Hsp90 C-terminus with inhibitors derived from novobiocin is one approach to modulating molecular chaperones. Structure activity relationship studies on novobiocin have led to the development of either neuroprotective or cytotoxic compounds. Segregation of the pro-survival heat shock response from a cytotoxic response due to client protein degradation is unique to C-terminal inhibitors. Described herein is the design, synthesis and biological evaluation of small molecules that target the C-terminus of Hsp90, for the continued development of potential therapeutics for the treatment of cancer or neurodegenerative diseases.

Acknowledgments

There are many people who contributed to my success in graduate school. These people have made an impact on my life providing support when I needed it, and contributing to my personal and professional growth. I am forever grateful to all of the professors and staff at the University of Kansas who help create the strong Med Chem community that I'm proud to be part of.

I would like to thank my advisor, Dr. Brian S. J. Blagg who has been a great mentor that has helped guide me through graduate school with knowledge, patience, and motivation. Brian has helped me grow as a scientist and as a person. I would also like to thank the members of the Blagg Laboratory who have helped create an environment where scientific creativity can flourish. Specifically, I would like to thank Vincent Crowley and Dr. Jessica Hall for always being there to give suggestions, support, and feedback. Outside of the Blagg Laboratory I would like to thank Dr. Rafferty and Dr. Prisinzano for being supportive and helping me find the right career path.

Thank you to Dr. Molly Lee, Dr. Alex Ford, and Doug Orsi for their friendship outside of the lab, which helped make my time in graduate school more enjoyable. Additionally, I would also like to thank one of my best friends and my forever bench mate, Dr. Anuj Khandelwal. Anuj was always there for me both as a friend and as a scientist. He was a constant inspiration, and will be greatly missed.

Outside of the KU community I would like to thank my family. My parents taught me to never stop trying and to always believe in myself. They are selfless role models, and I am so lucky to be their daughter. I am forever grateful for the love and support I received from them as well as my siblings. Lastly, I would like to thank Chris Strobel for being an incredibly understanding and supportive boyfriend.

Table of Contents

Abstract	iii
Acknowledgements	iii
Table of Contents	iv
List of Figures	vii
List of Schemes	x
List of Tables	xii
List of Abbreviations	xiv

1. Introduction to Hsp90 Structure, Function, and Modulation

Introduction	1
Hsp90 Chaperone Cycle.....	3
Heat Shock Response.....	8
Client-specific Hsp90 Co-chaperones.....	13
Disrupting Hsp90-co-chaperone Interactions.....	14
N-Terminal Hsp90 Inhibitors.....	17
C-Terminal Binding Pocket.....	20
Hsp90 C-Terminal Inhibitors: Novobiocin and Novobiocin Analogs.....	24
EGCG and Silybin.....	26
Post-translational Modification of the Hsp90 Chaperone Cycle.....	27
Future Perspectives.....	32
References	33

2. Development of Noviomimetics that Modulate Molecular Chaperones and Manifest Neuroprotective Effects

Introduction	57
Results and Discussion.....	57
Validation of Hsp90 Modulation.....	69
Conclusion.....	72
Future Directions.....	73
Materials and Methods	75
Luciferase Reporter Assay, Immunoblot Analysis.....	75
c-Jun Assay.....	76
Mitochondrial Bioenergetic (mtBE) Assessment.....	76
Chemistry General.....	77
Synthesis and Compound Characterization.....	78
References	143

3. Modified Biphenyl Hsp90 C-terminal Inhibitors for the Treatment of Cancer

Introduction	152
Design.....	154
Results	155
Chemistry.....	152
Biological Evaluation	161
Conclusion.....	164
Future Directions.....	165

Material and Methods.....	165
Anti-Proliferation MTS Assay.....	165
Western Blot Analysis.....	166
General Chemistry.....	167
Synthesis and Compound Characterization.....	167
References.....	207

4. Development of Phenyl Cyclohexylcarboxamides as a Novel Class of Hsp90 C-terminal Inhibitors

Introduction.....	213
Design.....	215
Chemistry.....	217
Validation of Hsp90 Inhibition via Western Blot Analysis.....	231
Conclusion.....	234
Materials and Methods.....	234
Anti-proliferation MTS Assay.....	234
Western Blot Analysis.....	235
Chemistry General.....	235
Synthesis and Compound Characterization.....	236
References.....	285

5. Probing the Hsp90 C-terminal Binding Pocket with Cytotoxic Noviose Replacements

Introduction.....	291
Results and Discussion.....	293
Validation of Hsp90 Inhibition via Western Blot Analysis.....	306
Chemistry.....	309
Biological Evaluation.....	311
Conclusion.....	320
Materials and Methods.....	321
Anti-proliferation MTS Assay.....	321
Wound Healing Scratch Assay.....	321
Western Blot Analysis.....	322
Chemistry General.....	322
Synthesis and Compound Characterization.....	323
References.....	372

List of Figures

Chapter 1

Introduction to Hsp90 Structure, Function, and Modulation

Figure 1. The Hsp90 Chaperoning Cycle.....	5
Figure 2. Structure of Celastrol and Gedunin.....	14
Figure 3. Structures of Allosteric Modulators of Hsp90.....	16
Figure 4. Structures of Hsp90 N-terminal Inhibitors.....	19
Figure 5. Structures of Hsp90 α/β inhibitors.....	20
Figure 6. Nucleotide binding effects on C-terminal dimerization.....	23
Figure 7. C-terminal Inhibitors of Hsp90.....	25

Chapter 2

Development of Noviomimetics that Modulate Molecular Chaperones and Manifest Neuroprotective Effects

Figure 2.1. Summary of prior and current studies presented.....	59
Figure 2.2. Evaluation of Hsp70 induction via noviomimetics.....	64
Figure 2.3. Immunoblot analysis of Hsp70 induction via novologues.....	67
Figure 2.4. c-Jun assay results.....	70
Figure 2.5. Noviomimetics enhance mitochondrial function.....	71
Figure 2.6 Immunoblot analysis of Hsp70 induction via novologues.....	68

Figure 2.SI1. Hsp70 induction for coumarin containing noviomimetics.....74

Chapter 3

Modified Biphenyl Hsp90 C-terminal Inhibitors for the Treatment of Cancer

Figure 3.1. Rationale for the development of new analogs.....154

Figure 3.2. Molecular modeling of compounds.....155

Figure 3.3. Western Blot analysis in MCF-7 cells.....164

Chapter 4

Development of Phenyl Cyclohexylcarboxamides as a Novel Class of Hsp90C-terminal Inhibitors

Figure 4.1. Hsp90 C-terminal Inhibitors.....215

Figure 4.2. Rationale for proposed molecules.....216

Figure 4.3. Proposed analogs for the exploration of a new core.....217

Figure 4.4. Three-dimensional overlay of **4.3** and proposed analogs.....224

Figure 4.5. Western blot analysis of select compounds233

Chapter 5

Probing the Hsp90 C-terminal Binding Pocket with Cytotoxic Noviose Sugar Replacements

Figure 5.1. Probing the binding pocket with proposed molecules.....293

Figure 5.2. Western blot analysis of select compounds.....	307
Figure 5.3. Overview of proposed analogs.....	308
Figure 5.4. Anti-migratory activities of Hsp90 C-terminal Inhibitors.....	313
Figure 5.5. Anti-Metastatic activity of compounds 5.20-5.27	315
Figure 5.6. Anti-Metastatic Activity of 5.20	316
Figure 5.7. Western blot analysis of 5.20	318
Figure 5.8. Western blot analysis of 5.25	319

List of Schemes

Chapter 2

Development of Noviomimetics that Modulate Molecular Chaperones and Manifest Neuroprotective Effects

Scheme 2.1. Synthesis of phenol 2.9.....	61
Scheme 2.2. Synthesis of intermediates	62

Chapter 3

Modified Biphenyl Hsp90 C-terminal Inhibitors for the Treatment of Cancer

Scheme 3.1. Proposed analogs and synthesis of amine 3.19.....	156
Scheme 3.2 Synthesis of free amines.....	158
Scheme 3.3. Synthesis of final products	160

Chapter 4

Development of Phenyl Cyclohexylcarboxamides as a Novel Class of Hsp90C-terminal Inhibitors

Scheme 4.1. Synthesis of phenylcyclohexyl carboxamides.....	218
Scheme 4.2. Synthesis of phenylpiperidin-4-yl carboxamide.....	219
Scheme 4.3. Synthesis of a cyclohexylphenylamide.....	220
Scheme 4.4. Synthesis of a cyclohexyl derivative.....	221

Scheme 4.5. Synthesis of phenylcyclopentyl carboxamides.....	225
Scheme 4.6. Synthesis of phenylcycloheptyl carboxamides.....	227
Scheme 4.7. Synthesis of phenylcyclopentyl methyl carboxamide.....	228
Scheme 4.8. Synthesis of phenylcyclohexyl methyl carboxamides.....	229

Chapter 5

Probing the Hsp90 C-terminal Binding Pocket with Cytotoxic Noviose Sugar Replacements

Scheme 5.1. Synthesis of phenol 5.36	294
Scheme 5.2. Synthesis of final products.....	297
Scheme 5.3. Synthesis of final products.....	298
Scheme 5.4. Synthesis of final products.....	299
Scheme 5.5. Synthesis of known C-terminal inhibitor cores	305
Scheme 5.6. Synthesis of final products.....	310

List of Tables

Chapter 1

Introduction to Hsp90 Structure, Function, and Modulation

Table 1. Hsp90 Co-Chaperones7

Table 2. Post-translational Modifications to Hsp90.....31

Chapter 3

Modified Biphenyl Hsp90 C-terminal Inhibitors for the Treatment of Cancer

Table 3.1. Anti-proliferative activity of analogs.162

Chapter 4

Development of Phenyl Cyclohexylcarboxamides as a Novel Class of Hsp90C-terminal Inhibitors

Table 4.1. Anti-Proliferative activity of analogs221

Table 4.2. Anti-Proliferative activity of analogs230

Chapter 5

Probing the Hsp90 C-terminal Binding Pocket with Cytotoxic Noviose Sugar Replacements

Table 5.1. Anti-proliferative activity of compounds **5.1-5.4b**.....295

Table 5.2. Anti-proliferative activity of cyclohexylamine derivates.....299

Table 5.3. Core comparison with optimized replacements.....306

Table 5.4. Anti-proliferative activity of compounds 5.20-5.27.....	311
---	------------

List of Abbreviations

17-AAG	17-allylamino-17-demethoxygeldanamycin
17-DMAG	17-dimethylamino-17-demethoxygeldanamycin
ACN	Acetonitrile
ADP	Adenosine Diphosphate
Aha1	Activator of Hsp90 ATPase homologue-1
Akt	Serine/threonine protein kinase
AMP-PNP	Adenylylimidodiphosphate (non-hydrolysable ATP)
ATP	Adenosine triphosphate
BnBr	Benzyl bromide
CDK4	Cyclin-dependent kinase -4
CDK6	Cyclin-dependent kinase -6
CHIP	Carboxy terminus of Hsp70 interacting protein
DCM	Dichloromethane
DIPA	Diisopropylamine
DIPEA	N,N-diisopropylethylamine
DMF	Dimethylformamide
EDCI•HCl	N-(3-Dimethylaminopropyl)-N'-ethylcarbodiimide hydrochloride
EGCG	Epigallocatechin-3-gallate
EGFR	Epidermal growth factor
eHsp90	Extracellular Hsp90
eInt α 2	Extracellular integrin α 2
eMMP2	Extracellular matrix metalloproteinase-2
ER α	Estrogen Receptor α
ERK	Extracellular signal-regulated kinases
EtOAc	Ethyl acetate
GDA	Geldanamycin
Grp94	Glucose regulated protein 94 (endoplasmic reticulum Hsp90 isoform)
Her2	Human epidermal growth factor receptor 2
HCL	Hydrochloric Acid
HOP	Hsp70/Hsp90 organizing protein
HSE	Heat Shock binding element
HSF-1	Heat shock factor 1
Hsp	Heat shock protein
Int α 2	Integrin α 2
LDA	Lithium diisopropylamide
MCF-7	Michigan Cancer Foundation – 7 (breast cancer cell line)
MeOH	Methanol
MMP2	Matrix metalloproteinase-2
MOMCl	Chloromethyl methyl ether
MRC	Maximal respiratory capacity
mtBE	Mitochondrial bioenergetics
NaH	Sodium hydride

NaOH	Sodium hydroxide
OCR	Oxygen consumption rate
on	Overnight
p23	Chaperone associated protein 23 kDa
p53	Tumor protein 53
p-AKT-T308	Phosphorylated Serine/threonine protein kinase —threonine 308
p-ERK1/2	Phosphorylated extracellular signal-regulated kinases 1/2
PTSA	p-Toluenesulfonic acid
Rab10	Ras-related protein 10
rt	Room temperature
SkBr3	Sloan-Kettering breast cancer cell line
TEA	Triethylamine
TFA	Trifluoroacetic acid
THF	Tetrahydrofuran
TMAD	Tetramethylazodicarboxamide
TRAP1	TNF receptor-associated protein
TPR	Tetratricopeptide repeat domain

1. Introduction to Hsp90 Structure, Function, and Modulation

Introduction

Molecular chaperones are an evolutionarily conserved class of proteins that prevent aggregation and assist in the conformational maturation of other cellular proteins (referred to as client proteins). Heat shock proteins (Hsps) are a group of molecular chaperones that are ubiquitously expressed under non-stressed conditions and can be upregulated upon exposure to cellular stress, including elevated temperature. Hsp90 is the most abundant heat shock protein and represents 1-2% of the cellular protein in unstressed cells.¹⁻³ There are four human isoforms of Hsp90: the cytosolic isoforms Hsp90 α and β , Grp94 (localized to the endoplasmic reticulum), and TRAP1 (localized to the mitochondria). Hsp90 facilitates the conformational maturation of Hsp90-dependent proteins via the Hsp90 chaperone cycle, in which the Hsp90 homodimer forms a large, multiprotein complex that relies upon co-chaperones, immunophilins, and partner proteins to fold nascent polypeptides, as well as the rematuration of denatured proteins.⁴⁻⁶ The Hsp90 heteroprotein complex folds these substrates through a series of conformational transitions at the middle and N-terminal domain of Hsp90 that facilitate ATP hydrolysis at the N-terminus.⁷⁻⁸ Inhibition of the Hsp90 protein folding machinery results in client protein ubiquitinylation and subsequent degradation by the proteasome, which can ultimately result in cell death.⁹⁻¹² Many Hsp90-dependent client proteins (e.g., ErbB2, B-Raf, Akt, steroid hormone receptors, mutant p53, HIF-1, survivin, telomerase, etc.) are associated with the ten hallmarks of cancer: self sufficiency in growth signals, insensitivity to anti-growth signals, evading apoptosis, limitless replicative potential, sustained angiogenesis, tissue invasion and metastasis, reprogramming energy metabolism, evading immune response, genome instability and mutation,

and tumor-promoting inflammation.¹³⁻¹⁴ Therefore, oncogenic client protein degradation via Hsp90 inhibition represents a promising approach toward anticancer drug development.¹⁵⁻¹⁷ Additionally chaperones interact with protein degradation pathways to control constitutive protein turnover and to facilitate the elimination of misfolded proteins.¹⁸

Originally, small molecule inhibitors of Hsp90 were designed to perturb the ATPase activity located at the N-terminus and include derivatives of geldanamycin, radicicol, and purine.¹⁹ N-terminal Hsp90 inhibitors are effective at inhibiting Hsp90 function and lead to anti-proliferative activity through client protein degradation; however, Hsp90 N-terminal inhibition also leads to induction of the Heat Shock Response (HSR).²⁰⁻²² The consequence of inducing a pro-survival response concomitantly with inducing client protein degradation is typically, cytostatic activity. However, this induction also leads to dosing and scheduling problems in the clinic, as N-terminal inhibitors induce expression of the target they inhibit. Therefore, Hsp90 inhibitors with novel mechanisms of action are sought to take advantage of the dependence that client protein-driven cancers have upon Hsp90, without concomitant induction of the pro-survival, heat shock response.

Two alternative strategies for inhibiting the function of Hsp90 include disruption of the Hsp90 heteroprotein complex and disruption of the Hsp90 C-terminal dimerization domain. Disruption of the Hsp90 heteroprotein complex has emerged as an effective strategy to prevent client protein maturation without induction of the HSR.²³ More specifically, disruption of interactions between Hsp90 and co-chaperones, such as Cdc37, or direct inhibition of co-chaperones and immunophilins, such as p23, F₁F₀ ATP synthase and FKBP52, prevent the maturation of Hsp90 clients at concentrations that do not induce the HSR.²⁴⁻²⁷

Alternatively, novobiocin was the first Hsp90 C-terminal inhibitor identified, and was found to inhibit Hsp90 in SKBr3 cells at approximately 700 μM concentration.²⁸ As a result, derivatives of the coumarin-containing natural product have been intensely sought and compounds manifesting improved activity identified. These C-terminal inhibitors prevent cancer cell proliferation at concentrations similar to N-terminal inhibitors and induce degradation of Hsp90-dependent client proteins without induction of the HSR.²⁹⁻³⁰ In addition to novobiocin and novobiocin analogs, epigallocatechin-3-gallate (EGCG), silybin and cisplatin have been reported to bind the Hsp90 C-terminus.³¹

Herein, recent progress in Hsp90 structural elucidation and the dynamic aspects of the Hsp90 chaperone cycle will be discussed. Alternative strategies for Hsp90 inhibition that include direct and indirect targets of Hsp90, as well as the current state of traditional small molecule Hsp90 inhibitors will be summarized. Lastly, post-translational modifications to Hsp90 and partner proteins will be described as well as the effect of these modifications on client protein maturation, stability and activity in normal and transformed cells.

Hsp90 Chaperone Cycle

Hsp90 exists primarily as a homodimer. Each monomer contains three domains; an N-terminal domain with an ATP-binding pocket, a C-terminal domain responsible for dimerization, and a middle domain that connects the N- and C-termini through a highly-charged and flexible linker. The Hsp90 protein folding cycle is complex and illustrated in Figure 1. Many conformational switches and changes are needed to obtain the catalytically active state of Hsp90, and various co-chaperones are needed to regulate the protein folding cycle.³² Most of the co-chaperones that interact with Hsp90 at the beginning of the chaperone cycle bind the EEVD

motif located at the C-terminus. Co-chaperone Hsp90-Hsp70 organizing protein (HOP) is responsible for delivering substrates from Hsp70 to Hsp90, and binds Hsp90 to stabilize the open conformation (A brief overview of co-chaperone binding to Hsp90, and its effects are highlighted in Table 1).³³ HOP interacts directly with the EEVD motif through its tetratricopeptide repeat (TPR) domain.

After the binding of HOP, Hsp70 and the bound client protein stabilize the open conformation of Hsp90, and then various immunophilins (specifically, those with prolyl isomerase activity), co-chaperones, and other partner proteins bind to form a heteroprotein complex. When the immunophilins, containing peptidyl-prolyl isomerase activity (e. g. FKBP51, FKBP52, etc.) bind Hsp90, an asymmetric complex is formed.³³ This asymmetric structure is often referred to as the ‘late complex’ and promotes the chaperone cycle through stabilization of the open conformation.³⁴ After formation of the late complex, the activator of Hsp90 ATPase, Aha1, assembles with the heteroprotein complex to dissociate co-chaperones, such as HOP and Hsp70.³⁴ Buchner and coworkers demonstrated that Aha1, the most effective activator of ATPase activity, is needed for HOP release, but not p23, which had been previously reported.³⁴ They found that Aha1 and the co-chaperone Cpr6 bind Hsp90 in a synergistic manner to stabilize the Hsp90 closed conformation.

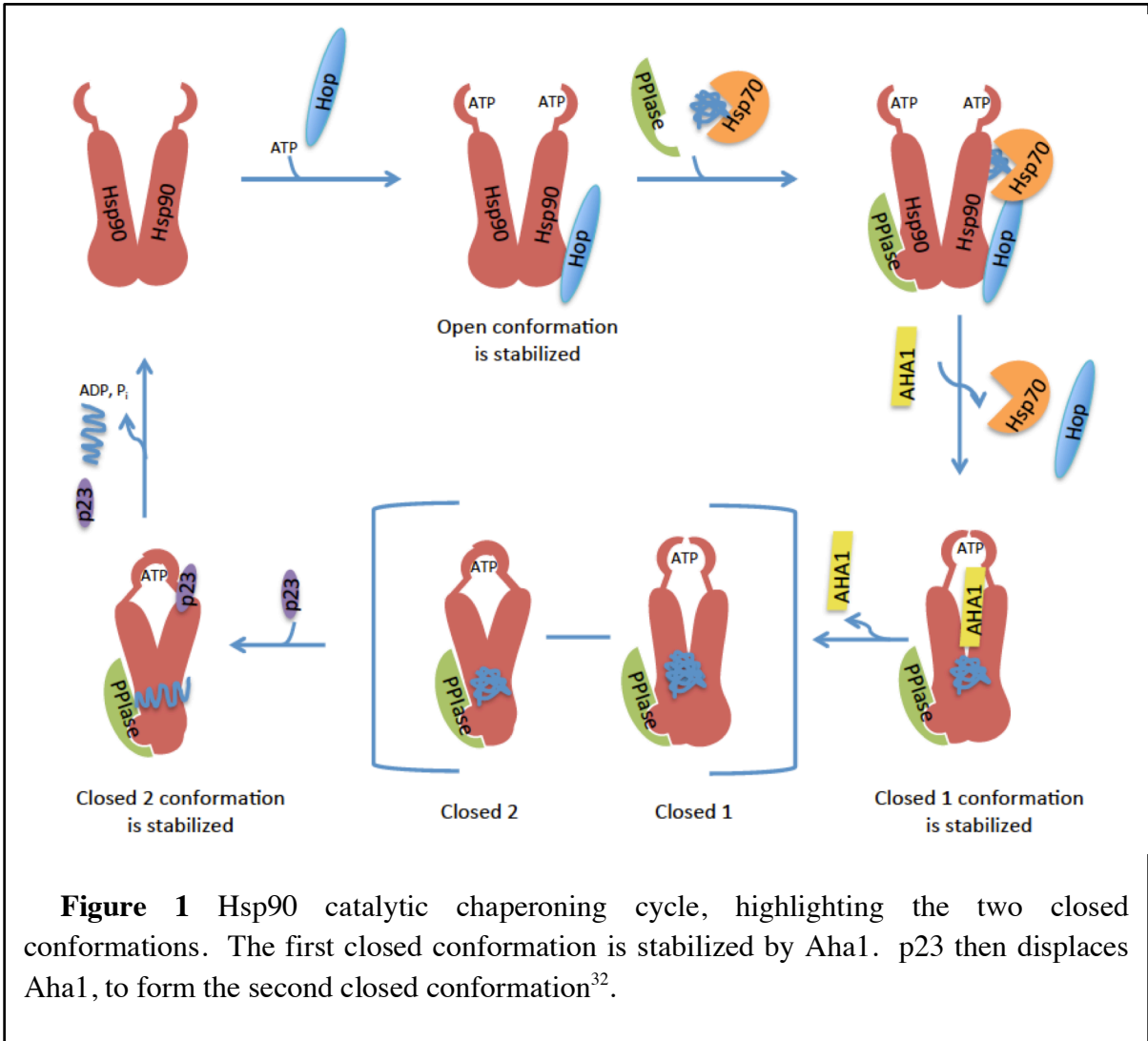


Figure 1 Hsp90 catalytic chaperoning cycle, highlighting the two closed conformations. The first closed conformation is stabilized by Aha1. p23 then displaces Aha1, to form the second closed conformation³².

Hsp90-catalyzed ATP hydrolysis is not only required for folding the bound substrate, but also for release of the properly folded substrate. In order to achieve ATP hydrolysis, Hsp90 must adopt a closed conformation.³² To form the closed state, Aha1 binds in a sequential manner, followed by ATP. Structural reorganization ensues to facilitate closure of the N-terminal ATP lid. Lid closure stabilizes the catalytic loop, which is required for ATP hydrolysis. In addition, the ATP lid establishes contacts between specific residues of the catalytic loop and ATP, in addition to the adjacent Hsp90 monomer, resulting in further stabilization of the Hsp90 complex. This conformational change represents the rate-limiting step in the protein folding cycle, which is not ATP hydrolysis.³²

In addition to establishing that Aha1 and Cpr6 bind Hsp90 in a synergistic manner, it was demonstrated that Aha1 association with Hsp90 accelerates the conformational change required for attainment of the closed state. In fact, the conformation formed upon Aha1 binding is different from the state wherein ATP hydrolysis occurs, as illustrated in Figure 1.³⁴ In the closed state with Aha1, ATP can exchange readily. However, upon p23 displacement of Aha1, a second closed conformation is formed, which is followed by p23 dissociation and ATP hydrolysis.³⁴ The resulting complex disassembles and the folded substrate is released to propagate of the catalytic cycle.

p23 is a well-established regulator of Hsp90 ATPase activity and has been shown to inhibit ATP hydrolysis and client release.³⁵⁻³⁶ McLaughlin et. al demonstrated that p23 interacts with Hsp90 in the presence and absence of ATP; however, affinity for the p23-Hsp90 complex increased when ATP was present. Mass spectral analysis determined that one molecule of p23 bound to each Hsp90 monomer and p23 interacted with truncated fragments that lack a C-terminus. This data indicate that Hsp90 dimerization is not required for p23-Hsp90 association.

Collectively, these data suggest that p23 locks Hsp90 subunits during the ATP-bound state, which exhibits a high affinity for protein substrates.

Another co-chaperone, carboxyl terminus of Hsp70-interacting protein (CHIP), regulates the release of properly folded client proteins, or can target them for degradation.³⁷⁻³⁸ CHIP contains a ubiquitin ligase domain and thus, provides a direct link to protein degradation via the proteasome.³⁹ CHIP interacts with Hsp90 or Hsp70 through its TPR domain, and when bound to Hsp90, CHIP can displace HOP and p23. In the presence of Hsp90 inhibitors, CHIP mediates ubiquitinylation of substrates and ultimately directs them for degradation via the proteasome.⁴⁰

Co-chaperone	Interaction site in co-chaperone	Interaction site in Hsp90	Effect on Hsp90 conformation	Effect on Hsp90 ATPase activity
Hop/Sti1	TPR2A, TPR2B	N, M, C	Stabilizes open state	Inhibition
Cdc37	M, C	N	Stabilizes open state	Inhibition
Sgt1	CS domain	N	Not determined	No effect
Tah1	TPR	C	Not determined	Weak inhibition by Tah1-Pih1 complex
Aha1	N, C	N, M	Stabilizes closed state	Acceleration
Ppt/PP5	TPR1, TPR2, TPR3	C	Not determined	No effect
Cpr6, Cpr7/Cyp40	TPR	C	Not determined	Weak acceleration
FKBP51/FKB P52	TPR	C	Not determined	No effect
p23/Sba1	N	N	Stabilizes closed state	Inhibition

TPR tetratricopeptide repeat, CS = CHORD (cysteine and histidine-rich domain)-containing protein and Sgt1 domain; N = N-terminal domain, M = middle domain, C = C-terminal domain

Other co-chaperones have less defined roles in the inhibition or promotion of Hsp90 ATPase activity; however, proper function of these co-chaperones and direct interaction with Hsp90 appears important for client protein maturation. Small glutamine-rich tetratricopeptide repeat-containing protein α (SGTA) is linked to several cellular processes including cell division, mitosis, cell cycle checkpoint activation, and viral infection. SGTA interacts directly with Hsp70 and may interact with Hsp90 via its TPR domain to facilitate maturation of the growth hormone and androgen receptors.⁴¹ It has also been proposed that SGTA participates in the sequestration of client proteins in an inactive state.

F_1F_0 ATP synthase was proposed to possess co-chaperone function by interacting with Hsp90 in several different cancer cell lines.^{27, 42} Furthermore, inhibition of F_1F_0 ATP synthase directly affected client protein maturation. F_1F_0 ATP synthase is a macromolecular machine that produces the majority of cellular ATP and is localized to the mitochondria and the cell surface in certain cancers.⁴³⁻⁴⁶ F_1F_0 ATP synthase was shown to directly interact with Hsp90, specifically the Hsp90 α isoform.⁴⁷ A selective inhibitor of F_1F_0 ATP synthase, as well as general inhibitors of ATP synthases, have been shown to disrupt interactions between F_1F_0 ATP synthase and Hsp90 α , and ultimately produce client protein Hsp90-dependent degradation.⁴⁷⁻⁴⁸

Heat Shock Response

Traditional discussion of the pro-survival heat shock response (HSR) typically is as follows: “In the presence of degraded client proteins or upon treatment with a N-terminal

inhibitor Hsp90-bound transcription factor Heat Shock Factor-1 (HSF-1) is displaced.⁴⁹⁻⁵⁰ Upon displacement, HSF-1 trimerizes, translocates to the nucleus and binds the Heat Shock Regulatory Elements, which are evolutionarily conserved sequences throughout the genome that lead to increased levels of the heat shock proteins. The HSR is a pro-survival response to cellular stress that cause conditions which induce the denaturation of proteins. Hsp27, Hsp40, Hsp70, and Hsp90, amongst other HSPs, are over-expressed to refold denatured proteins.” While this description is accurate, it is an over-simplification of a complex biological process. HSF-1, the small but mighty player in the heat shock response, has been heavily studied in the last decade and consequently has been found to be involved in many different disease states. HSF-1 is often activated in cancer cells and has been shown to be important in cancer progression.⁵¹ Alternatively, a lack of HSF-1 is connected to neurodegenerative diseases as proteins aggregate.⁵²⁻⁵³ Recently, HSF-1 was implicated in diabetes as HSF-1 expression was altered in islets from diabetic rats and restoring HSF-1 activity prevented glucolipototoxicity-induced endoplasmic reticulum stress and apoptosis.⁵⁴ While it is becoming more apparent how HSF-1 is implicated in many diverse cellular processes, it is still unclear how HSF-1 regulates the heat shock response.

Currently there are two hypotheses in the literature to explain how HSF-1 regulates the heat shock response. The first is the chaperone titration theory and the second is the heat shock-dependent phosphorylation theory. The chaperone titration theory suggests that HSF-1 is bound to chaperones in an inhibitory complex. When cellular stress occurs, HSF-1 dissociates from the inhibitory complex as the chaperones are titrated away by misfolded and unfolded proteins. HSF-1 then forms trimers and localizes to the nucleus to activate transcription. Once proteostasis is restored, chaperones free of client proteins can bind to HSF-1 and deactivate it.⁵⁵ Extensive

studies have determined what chaperone and co-chaperones interact biochemically and pharmacologically with HSF-1. However, due to the observed switching dynamics of HSF-1, direct unequivocal evidence is difficult to obtain.

Bharadwaj and co-workers investigated the Hsp90 chaperone complex and the regulation of HSF-1.⁵⁶ Using electrophoretic mobility shift assay/super shift technique they found that elevated levels of Hsp90, Hsp70, Hip, and Hop decreased the time of HSF-1 deactivation to the non-DNA-binding state. Interestingly, they found that immunophilins had the opposite effect. Thus, they proposed that nascent co-chaperones exert their effect via remodeling existing chaperone complexes and Hip, Hop and Hsp70/90 promote formation of additional chaperone complexes.⁵⁶ Subsequent experiments also evaluated the interaction between various co-chaperones and chaperones and stress-activated HSF-1 to find that Hsp90, p23, and FKBP52 form a heterocomplex with the regulatory domain of HSF-1. Disruption of this complex promotes HSF-1 DNA binding as a heat shock promoter.⁵⁷ Interestingly these co-chaperones are also involved in the chaperone machine that is important for folding the steroid receptors, indicating that HSF-1 oligomerization is regulated by a similar foldosome-type mechanism.

The second theory for HSF-1 regulation is the phosphorylation theory, which simply states that upon site dependent phosphorylation, HSF-1 activates the transcription of chaperone genes.⁵⁸ Unfortunately, recent studies have found that mutation of 15 phosphorylation sites failed to prevent HSF-1 activation during heat shock. Even though phosphorylation of HSF-1 is a hallmark of the heat shock response pathway, no direct evidence of the specific role HSF-1 phosphorylation provides has yet emerged.⁵⁹ Recent studies by Zheng and co workers attempted to link the two theories by studying over 70 phosphorylation sites and examining Hsp70 and HSF-1 involvement. They discovered that HSF-1 is involved with Hsp70 in a titration like

model, as Hsp70 and HSF-1 form a feedback loop controlled by heat shock response and activation. Additionally Zheng and co workers identified that phosphorylation amplifies transcriptional activation of HSF-1, as opposed to phosphorylation triggering the activation of HSF-1.⁶⁰ They hypothesized that introduction of a negative charge via phosphorylation increases the transcription initiated by HSF-1.⁶⁰⁻⁶¹ Based on these findings both theories are correct as HSF-1 uses both phosphorylation and a chaperone switch to regulate the heat shock response.

Control over the pro-survival heat shock response is vital for neuroprotection. Induction of the pro-survival heat shock response occurs in a different manner for N-terminal and C-terminal Hsp90 inhibitors. *Pan* Hsp90 N-terminal inhibition results in induction of the HSR, however C-terminal inhibition can segregate these activities. Treatment with C-terminal inhibitors can result in either client protein degradation or induction of heat shock proteins, but not both.

The pro-survival heat shock response can be beneficial for neuroprotection. Partial folding of proteins leads to a functionally inactive state of the protein, which may lead to toxic insults within the cell, leading to cell death. This partial or inaccurate folding occurs in 30% of nascent proteins, which typically leads to their degradation.⁶²⁻⁶³ It is likely that the toxicity of different neurodegenerative disorders result from an imbalance between normal chaperone activity and misfolded protein species.⁶⁴ HSF-1 protects neuronal cells from death caused by the accumulation of misfolded proteins, which is essential because neurons are post-mitotic and are unable to dilute misfolded or aggregated proteins through cell division.⁶⁵⁻⁶⁶ Consequently HSF-1 has been found to be essential for the survival of rat neurons, and HSF-1 protein expression levels are reduced as cell death is approached.⁶⁷ Verma and co-workers found that overexpression of HSF-1 can protect neurons from death even in non-proteotoxic conditions via

a novel mechanism of action wherein HSF-1 is not a trimer.⁶⁷ While the levels of HSF-1 typically do not change and are tightly regulated, HSF-1 levels in neurons are reduced well before degeneration. This strongly indicates that reduction in HSF-1 expression is a precursor to neurodegeneration. Verma and co workers propose that HSF-1 has an alternate mechanism of action for neuroprotection in which monomer HSF-1 binds non-HSE sequences in conjunction with other transcription factors.⁶⁷⁻⁶⁹

Additional neuroprotection via modulators of HSF-1 have been investigated. Hydroxylamine derivatives like arimoclochol are known to be co-inducers of the HSR and are thought to prolong the binding of HSF-1 to HSE. Additionally, these molecules are thought to cause HSF-1 activation via affecting plasma membrane fluidity.⁷⁰ These compounds are thought to weaken the interactions between lipid chains that can induce disorder effects in membranes, similar to heat shock, ultimately leading to HSF-1 activation.⁷¹⁻⁷²

Current studies have begun to unveil that HSF-1 can segregate its proteostatic activity from its other activities, like metabolic control. For example Qiao and co-workers have reported that HSF-1 is involved with metabolic control via interaction with the *Nampt* promoter, which controls intracellular NAD⁺ levels. Heat shock is known to increase the cellular NAD⁺/NADH ratio. Sirtuin enzymes (SIRT1 and SIRT3) require NAD⁺ as a cofactor for metabolic regulation and are known to play a critical role in the maintenance of mitochondrial function. They found that SIRT1/3 levels are affected in HSF-1 deficient cells. SIRT1 is responsible for the deacetylation of HSF-1, and can prolong HSF-1 DNA binding by deacetylation. HSF-1 removal from chromatin is facilitated by acetylation of K80, which is in direct contact with DNA. This study clearly ties HSF-1 to metabolic control. HSF-1 undoubtedly has many important rolls to play within the cell, and future studies will continue to shed light on what those rolls may entail.

Client-specific Hsp90 Co-chaperones

While Hsp90-co-chaperone interactions continually change throughout the chaperone cycle to either inhibit or promote ATP hydrolysis, co-chaperones also exhibit client specificity during the chaperone cycle and promote the maturation of client protein classes.⁷³ The mechanism by which co-chaperones assist in the delivery of clients to Hsp90 occurs via interactions between specific clients or through interactions with Hsp90 that prime the chaperone machinery for the loading of protein substrates.

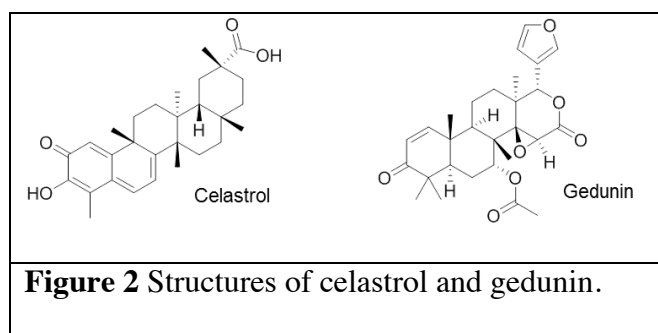
The co-chaperone activity manifested by cell division cycle 37 homolog, or Cdc37, is required for the maturation of all Hsp90-dependent kinases.^{24, 74} This co-chaperone inhibits ATPase activity, but does not affect accessibility to the ATP binding site.⁷⁵⁻⁷⁷ Sgt1 (suppressor of G2 allele of *skp1*) is required for activation of nucleotide-binding leucine-rich repeat receptors (NLRs).⁷⁸ The co-chaperones Tah1 (TRP-containing protein associated with Hsp90) and Pih1 (protein interacting with Hsp90) are associated with chromatin remodeling and temporarily halt the Hsp90 ATPase cycle to prepare Hsp90 for the maturation of small nuclear ribonucleoproteins.⁷⁹

Other co-chaperones that exhibit client protein specificity are the peptidyl-prolyl isomerases (PPIases), and include FK506 binding protein (FKBP) 51, FKBP52, and cyclophilin (Cyp) 40.⁸⁰⁻⁸¹ These remodeling PPIases are commonly utilized in Hsp90-steroid hormone receptor complexes. Interestingly these PPIases are specific hormone receptor clients, for example, FKBP51 in concert with protein phosphatase 5 (Pp5), is responsible for the maturation of the glucocorticoid receptor complexes; however, isolated FKBP51 is found associated with progesterone receptor, whereas Cyp40 associates with the estrogen receptor.

While it remains unknown as to how co-chaperones selectively interact with clients, co-chaperones involved in the maturation of certain clients, or substrate classes, provide an opportunity to selectively prevent the maturation of these client(s) by targeting interactions between Hsp90 and the co-chaperone.

Disrupting Hsp90-co-chaperone Interactions

Disruption of the interactions between Hsp90 and co-chaperones has been a successful strategy for selective and non-selective degradation of client protein substrates. Small molecules can disrupt these interactions and manifest properties unlike N-terminal Hsp90 inhibitors. Celestrol and gedunin (Figure 2) were originally suspected to disrupt interactions between Hsp90 and Cdc37 and induce degradation of kinase client proteins.⁸²⁻⁸⁴ The mechanism by which these compounds affect the Hsp90 chaperone cycle has since been explained. Celestrol is a natural product that exerts potent anti-cancer activity via multiple mechanisms of action. One of these mechanisms is to disrupt Hsp90-Cdc37 interactions. The natural product gedunin was shown to disrupt Hsp90-p23 interactions.



NMR studies by Sreeramulu, et. al. demonstrated that celestrol binds and covalently modifies cysteine residues located at the N-terminus of Cdc37 via Michael adduct formation and

therefore, does not directly bind Hsp90⁸⁵. In addition, Chadli, et. al. report that celastrol inhibits the Hsp90 chaperone cycle by destabilizing p23, which results in the degradation of steroid hormone receptors.⁸⁶ Therefore, celastrol appears to exhibit a multi-faceted mechanism for inhibition of the Hsp90 protein folding cycle. In addition, it was reported that gedunin binds the co-chaperone, p23, and inhibits p23 chaperone activity while blocking interactions between p23 and Hsp90.²⁶ Gedunin inactivated p23 via caspase 7 activation, which led to cleavage of the p23 C-terminus and induction of apoptosis. Interestingly, treatment with gedunin did not increase Hsp27 levels and only slightly elevated Hsp70 levels were observed, suggesting this approach may not induce the HSR.

Hsp90 requires ATP for chaperone activity and inhibition of ATP synthase with pan ATP synthase inhibitors such as oligomycin A, 2-deoxy-D-glucose, antimycin A and efrapeptins prevent Hsp90-dependent client maturation, (Figure 3).^{42, 47-48} ATP synthase inhibitors do not induce the HSR, as oligomycin A and efrapeptins manifest little to no increase in Hsp90, Hsp70 and Hsp27 levels. Furthermore, inhibition of the singular ATP synthase, F₁F₀ ATP synthase, with the selective inhibitor, cruentaren A, retained this activity and resulted in client protein degradation through destabilization of F₁F₀ ATP synthase-Hsp90 α interactions (Figure 3).^{47, 87-88}

Hsp90 and p23 in complex with hTERT, the catalytic subunit of telomerase, is required for the nuclear localization of telomerase, a protein whose unregulated function contributes to unlimited replicative potential. The promiscuous natural product, curcumin, induced cytoplasmic accumulation and degradation of hTERT through disruption of p23-hTERT interactions as one of its many mechanisms of action (Figure 3).⁸⁹ Curcumin decreased association between p23 and hTERT, but did not prevent hTERT from interacting with Hsp90. In contrast, the N-terminal Hsp90 inhibitor, geldanamycin, disrupted both the Hsp90-hTERT and p23-hTERT complexes.

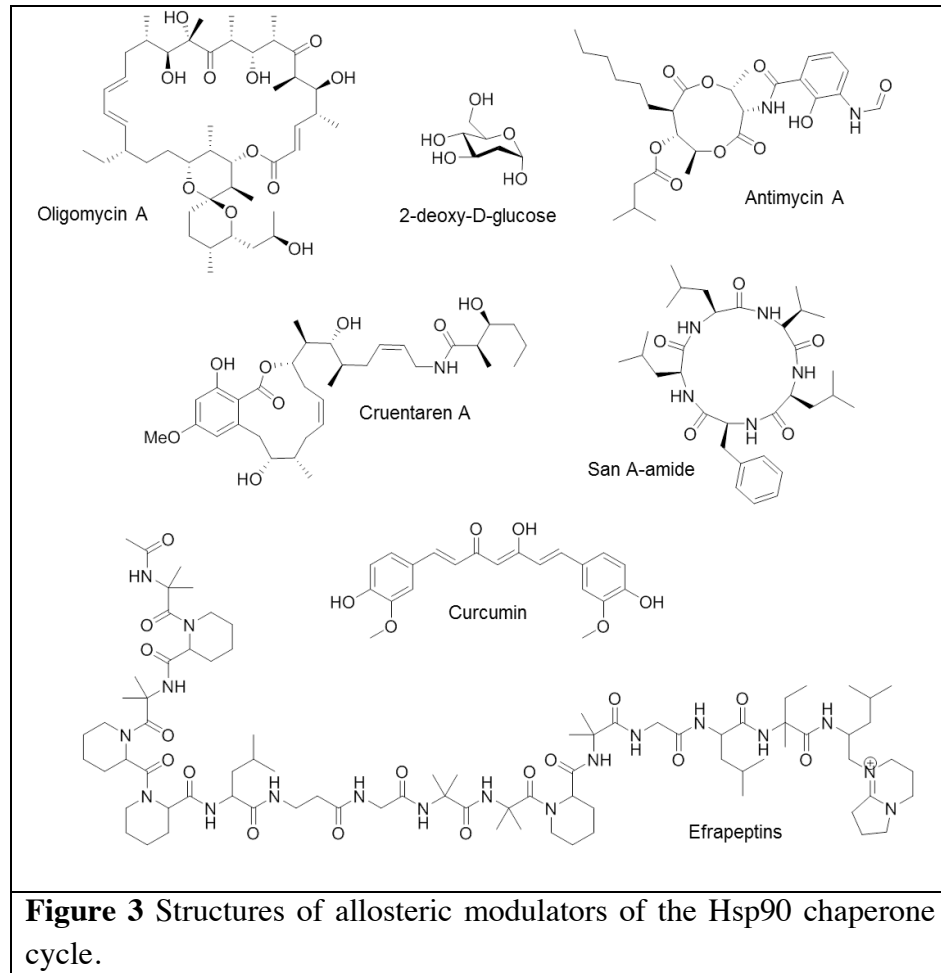


Figure 3 Structures of allosteric modulators of the Hsp90 chaperone cycle.

San A-amide, a derivative of the natural product sansalvamide A, induces apoptosis in various cancer cell lines, including pancreatic, colon, breast and prostate (Figure 3).⁹⁰⁻⁹¹ Vasko et. al. reported that San A-amide-mediated apoptosis in the HCT-116 colon cancer cell line occurred through displacement of inositol hexakisphosphate kinase-2 (IP6K2) and FKBP52 from the Hsp90 C-terminus.⁹² San A-amide binds the N-middle domain of Hsp90 and appears to disrupt the structural equilibrium of this region, which appears to alter the substrate-binding site. In contrast, San A-amide has no effect on the N-terminal client, Her2. This mechanism of action is unique to San A-amide, as the Hsp90 N-terminal inhibitor 17-allylaminogeldanamycin (17-

AAG) does not affect IP6K2 and FKBP52 binding, but does affect Her2 maturation. Furthermore, San A-amide exhibits no effect on Hsp90 ATPase activity, which supports its role as an allosteric modulator and its potential to selectively disrupt Hsp90 C-terminal binding interactions.

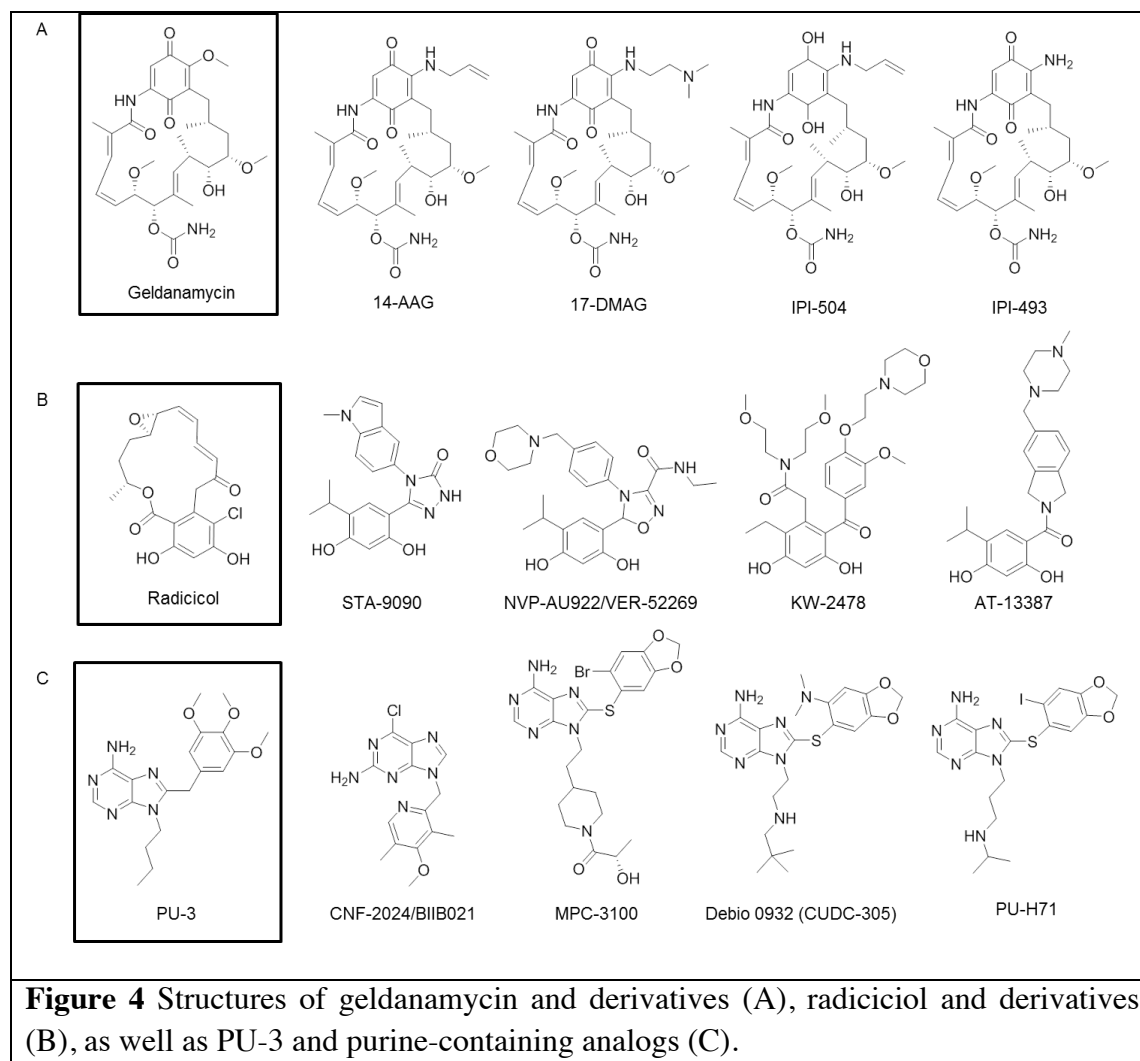
N-Terminal Hsp90 Inhibitors

Hsp90 inhibitors that bind the N-terminus compete with ATP and perturb ATPase activity, thereby disrupting client protein maturation. ATP adopts a unique conformation when bound to Hsp90, due to the presence of a Bergerat fold in the protein structure, which is characteristic of the GHKL (Gyrase, Hsp90, Histidine, Kinase, MutL) subgroup within the ATPase/kinase superfamily.⁹³⁻⁹⁴ Compounds that bind the N-terminal ATP-binding pocket adopt a bent conformation and afford selectivity for Hsp90 over other ATP-binding proteins. All Hsp90 inhibitors under clinical investigation are N-terminal inhibitors and include derivatives of geldanamycin (GDA), radicicol (RDC), and purine (Figure 4). N-terminal inhibitors have been studied in great detail and comprehensive reviews are present throughout the Hsp90 literature.⁹⁵⁻

99

GDA belongs to the benzoquinone class of ansamycins and was originally pursued as an antibiotic until it was shown to reverse v-src oncogenic transformation by destabilization of the Hsp90-src complex.¹⁰⁰ Although GDA is a potent anticancer agent, it did not undergo clinical evaluation due to its poor drug-like properties. However, several derivatives of GDA have entered clinical investigation and include 17-allyl-17-demethoxygeldanamycin (17-AAG), 17-desmethoxy-17-N,N-dimethylaminoethylaminogeldanamycin (17-DMAG), 17-allylamino-17-demethoxygeldanamycin hydroquinone hydrochloride (IPI-504), and 17-desmethoxy-17-

aminogeldanamycin (IPI-493) (Figure 4 A). RDC is a macrocyclic lactone that contains a resorcinol moiety as well as an allylic epoxide and an $\alpha,\beta,\gamma,\delta$ -unsaturated ketone. Although RDC is unstable in serum, the resorcinol moiety of RDC has been utilized to develop several compounds that remain under clinical investigation, such as STA-9090, NVP-AU922/VER-52269, KW-2478, and AT-13387 (Figure 4 B). The crystal structure of ADP bound to Hsp90 provided an opportunity to design inhibitors that take advantage of the unique Bergerat fold. Purine-containing compounds, such as PU-3, CNF 2024/BIIB021, MPC-3100, Debio 0932 (CUDC-305), and PU-H71 have also undergone clinical evaluation (Figure 4 C).



Despite the effectiveness of N-terminal inhibitors as anticancer agents, several concerns have emerged as a consequence of N-terminal inhibition. Induction of the HSR has resulted in dosing and scheduling problems during clinical trials and spurred the development of Hsp90 inhibitors that are devoid of this response, such as C-terminal inhibitors and allosteric modulators of the chaperone cycle. In addition, gastrointestinal distress, hepato- and ocular toxicities have been observed during pre-clinical and clinical trials.¹⁰¹ This may result from off-target effects, metabolic instability and/or on-target effects from pan inhibition of all four Hsp90 isoforms. Recently, it was shown that the hERG channel depends upon the Hsp90 α isoform for its

maturation.¹⁰² Hsp90 inhibitors have been shown to disrupt the proper trafficking and function of hERG.¹⁰³ Therefore, cardiotoxicity has also been observed during the development of Hsp90 inhibitors. All Hsp90 N-terminal inhibitors in the clinic exhibit pan Hsp90 inhibitory activity and target all four isoforms. It appears that other clients (oncogenic or not) may also exhibit a preference for individual Hsp90 isoforms,^{102, 104-105} Therefore, deciphering the role played by each isoform will be important for the development of future Hsp90 inhibitors.

Despite the high sequence similarity and identity possessed among the N-termini of each Hsp90 isoform, inhibitors have recently been developed that manifest selective inhibition. An inhibitor derived from the ansamycin scaffold has been developed that targets Hsp90 α and β , but not Grp94 (Figure 5 A).¹⁰⁶ Likewise, resorcinol- and purine-containing inhibitors have also been reported to selectively inhibit Grp94 based on subtle differences within the N-terminus of Grp94 (Figure 5 B and C).¹⁰⁴⁻¹⁰⁵

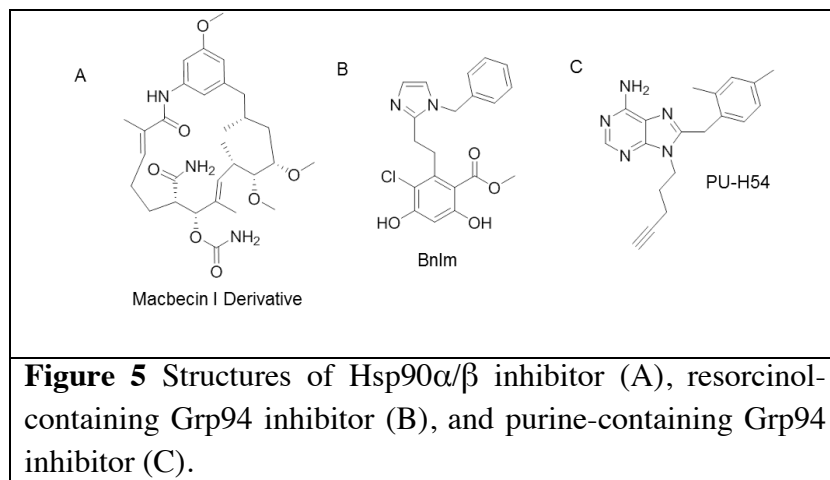


Figure 5 Structures of Hsp90 α/β inhibitor (A), resorcinol-containing Grp94 inhibitor (B), and purine-containing Grp94 inhibitor (C).

C-Terminal Binding Pocket

The C-terminus of Hsp90 contains a second nucleotide-binding site. Matts and coworkers, were the first to note that molybdate inhibited geldanamycin binding to the N-terminus and that molybdate protected the C-terminus from proteolysis.¹⁰⁷ Additional evidence

for a second binding site was presented by Neckers and coworkers, when they determined that novobiocin, a coumarin antibiotic, bound the C-terminus of Hsp90.²⁸ The researchers found that novobiocin bound a carboxy-terminal Hsp90 fragment.²⁸ Later, they were able to demonstrate that the same C-terminal binding site bound ATP and novobiocin, both within amino acids 542-732. More specifically, they found amino acids 657-677 to be essential, as removal of these residues resulted in diminished affinity for novobiocin.¹⁰⁸ In addition, these amino acids revealed that novobiocin bound to a site that is important for Hsp90 dimerization and co-chaperone binding.¹⁰⁸ The ability to interrupt dimerization was therefore, proposed as a useful strategy to prevent client protein maturation.

Matts and coworkers demonstrated that novobiocin binding altered the EEVD motif and consequently impacted Hsp90 interactions with various co-chaperones.¹⁰⁹ Upon further exploration, they showed that novobiocin binding resulted in a conformational change that ultimately led to the dissociation of bound kinases and cochaperones.¹⁰⁹ Csermely and coworkers found the anticancer drug, cisplatin, also bound the C-terminus and strengthened interactions between Hsp90 and Hsp70.¹¹⁰ Their studies suggested that the C-terminal ATP binding site only opens after occupancy of the N-terminal binding site.¹¹⁰ Peyrot and coworkers provided additional evidence for a C-terminal nucleotide binding site using isothermal calorimetry, scanning differential calorimetry, and fluorescence spectroscopy.¹¹¹

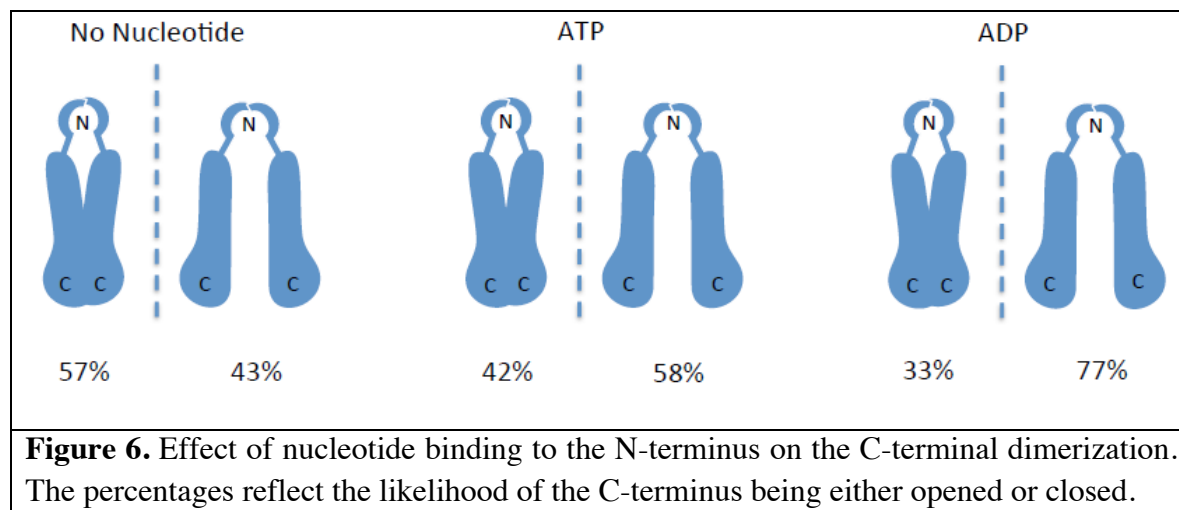
It was proposed that the C-terminus contains a Rossmann fold between amino acids 490 and 630, which could also exhibit NADH reductase activity.¹¹¹ However, Csermely, and coworkers demonstrated that nicotinamide adenine dinucleotides only interacted with the N-terminus and therefore, no such NAD-binding site existed.¹¹² It was found that both purine and pyrimidine nucleotides bound the C-terminus, which is less specific than the N-terminal binding

site that only binds nicotinamide adenine dinucleotides and diadenosine polyphosphate. In fact, GTP and UTP also bind to the C-terminal binding site.¹¹² In addition to exploring the differences in nucleotide specificity of the C-terminal binding site, they determined that a ligand must contain both a charged group as well as a large hydrophobic moiety to effectively bind this region.¹¹²

Agard and coworkers further examined the intra and intermonomer interactions of Hsp90, and demonstrated that dimerization is required for ATP hydrolysis.¹¹³ Removal of the C-terminal dimerization domain resulted in reduced ATPase activity (approximately 6-10 fold). However, it was shown that dimerization could be replaced via a disulfide bond between two monomers, which restored ATPase activity.¹¹³ Additional work by Buchner and coworkers identified a switch point at the C-terminus, in which mutants of alanine 577 caused both higher ATPase activity and increased activation of client proteins.¹¹⁴ Interestingly, these results are consistent with amino acids that are known to stabilize β -sheets. In support of this observation, they showed that mutant A577N produced lower affinity for N-terminal nucleotides, as asparagine is known to destabilize β -sheets.¹¹⁴

Most recently, Matts and Blagg provided additional information about the location of the C-terminal binding site by the use of proteolytic fingerprinting and photoaffinity labeling.¹¹⁵ They showed that Hsp90 C-terminal inhibitors stall the complex into an open confirmation, which results in protection from proteolytic cleavage via trypsin (Arg620 and Lys615), and prevention of N-terminal occupation. Importantly, these results were in agreement with the work of Hugel and coworkers as discussed below.¹¹⁵⁻¹¹⁶ These findings were further supported by Retzlaff and coworkers, who demonstrated that C-terminal inhibitors interact with and stabilize a region about the C-terminal pivot point to prohibit the conformational changes required for

chaperone activity.¹¹⁴⁻¹¹⁵ This work demonstrated that binding to the C-terminus prevents formation of the closed conformation.¹¹⁵



Recent investigation of the Hsp90 dynamic cycle by Hugel and coworkers highlighted conformational activity within the C-terminus that may explain the different biological outcomes observed with C-terminal inhibitors.¹¹⁶ They observed that the Hsp90 C-terminus opens and closes, which is in contrast to prior models. They noted an inverse correlation between the N- and C-terminal domains, in which the Hsp90 dimer was found to open and close several times before dimer dissociation. Interestingly, their data demonstrated that the C-terminus opens and closes regardless of the N-terminal state, which was confirmed by the use of AMP-PNP and caused Hsp90 to remain in the closed state. Their results, as illustrated in Figure 6, showed that when no nucleotide is bound to the N-terminus, the C-terminus exists in an open conformation 43% of the time, and in a closed conformation 57% of the time. However, when ATP is bound to the N-terminus, the C-terminal states reversed. Reversal of the C-terminus state upon ATP binding is caused by destabilization of the C-terminus. Since the N-terminal ATP-binding pocket is far from the C-terminal domain, the protein must communicate through its structure,

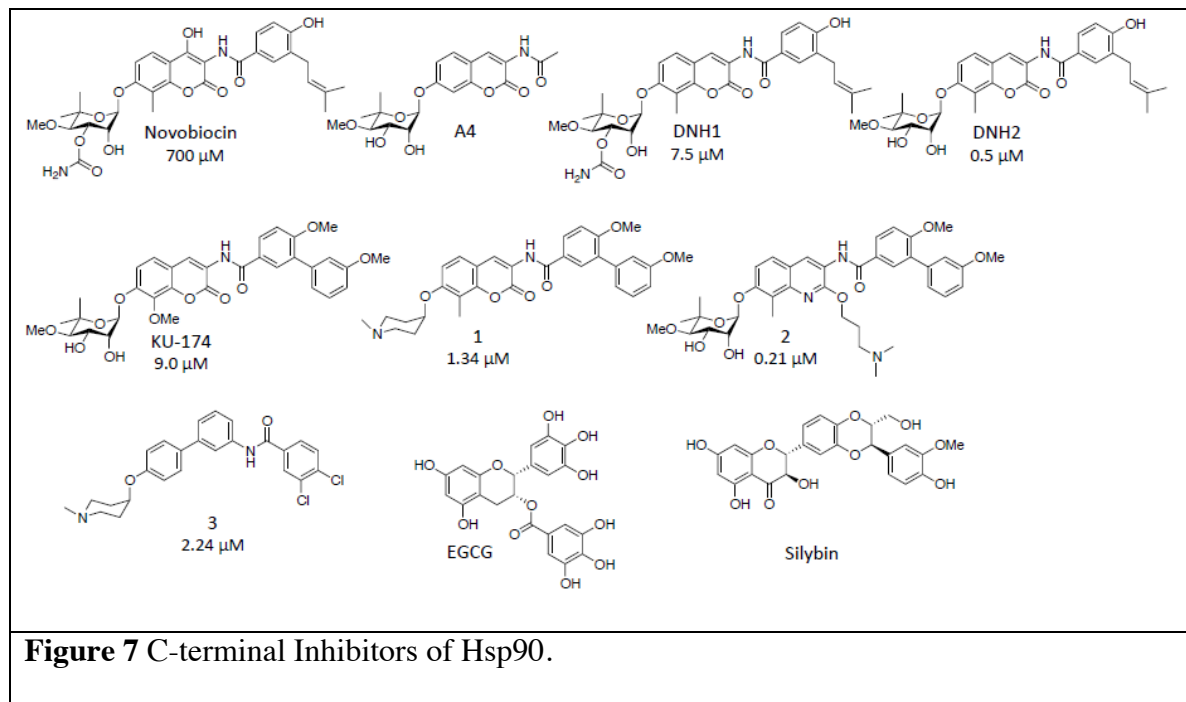
which is important when considering the implication of C-terminal inhibition.¹¹⁶ With Hugel's data and model, one could propose that binding to the C-terminus can occur when the domain is open, which would prevent dimerization, or after dimerization, which would prevent occupation of the N-terminal binding pocket.

Hsp90 C-Terminal Inhibitors: Novobiocin and Novobiocin analogs

Since both Hsp90 and DNA gyrase bind ADP and geldanamycin in a bent conformation, it was proposed that a DNA gyrase inhibitor could also inhibit Hsp90.²⁸ Originally, it was proposed that the coumermycin antibiotics—specifically novobiocin (structure illustrated in Figure 7), chlorobiocin, and coumermycin A1—could bind the N-terminal nucleotide-binding pocket due to structural similarities within the binding site. Indeed, novobiocin was able to compete with radicicol and geldanamycin for Hsp90 binding, but neither geldanamycin nor radicicol could compete with novobiocin.²⁸ Amino-terminal and carboxy-terminal fragments of Hsp90 were prepared for further investigation. As expected, geldanamycin bound the N-terminal fragment, however, novobiocin was found to bind the C-terminal fragment.²⁸

Although novobiocin was found to bind the C-terminus, it manifested low efficacy in cellular models (~700 μM in SkBr₃). To improve upon this low activity, structure-activity relationship studies were pursued. The first novobiocin analog reported was A4 (illustrated in Figure 7), in which the benzamide side chain was replaced with an acetamide and lacked the 4-hydroxyl and the 3'-carbamate.¹¹⁷ A4 induced client protein degradation at approximately 10 μM in the LNCaP prostate cancer cell line (a mutated androgen receptor-dependent prostate cancer cell line).¹¹⁷ However, A4 induced a robust HSR at concentrations approximately 1000-fold lower than that needed for client protein degradation.¹¹⁷ Segregation of the HSR and client

protein degradation had not been previously observed. Recall that, N-terminal inhibitors induce client protein degradation at the same concentration they induce the HSR. Since A4 exhibited heat-shock induction without the degradation of client proteins, it has been evaluated as a neuroprotective agent.¹¹⁷



4-Deshydroxynovobiocin (DHN1) and 3'-descarbamoyl-4-deshydroxynovobiocin (DHN2), as illustrated in Figure 7, were synthesized to examine whether the 4-hydroxy was detrimental to Hsp90 inhibitory activity.¹¹⁸ These studies confirmed that removal of the 4-hydroxy resulted in decreased DNA gyrase activity, but improved Hsp90 inhibitory activity.¹¹⁸ Importantly, these compounds induced client protein degradation at concentrations in which no HSR was observed. Further modifications to the coumarin core were designed to mimic the guanosine nucleus via the addition of hydrogen bond acceptors placed at the 5-, 6-, and 8-positions, since GTP had been shown to bind selectively to the C-terminus.¹¹⁹ The most potent

compound, KU-174 (illustrated in Figure 7), was subjected to a NCI60 screen and showed activity against multiple cancer cell lines.¹²⁰ Other investigational studies on the coumarin core (compound 2) are illustrative of work in this area.^{29, 119, 121-123} Most recently, it was demonstrated that the coumarin core could be replaced with a biphenyl moiety (compound 3 represents such an example). Analogs containing the biphenyl moiety manifest good activity against the SkBr3 and MCF-7 cell lines, and represent a new scaffold for further exploration of the Hsp90 C-terminal binding site.¹²⁴

In addition to the coumarin core, novobiocin contains a noviose sugar and a benzamide side chain. A biaryl ring system that contains a *meta*-methoxy was found to exhibit comparable activity to the benzamide side chain present in KU-174.¹²⁵ Additional studies to replace the benzamide side chain have also been reported.^{125,30, 126-127} Extensive SAR studies have been carried out on the noviose sugar.¹²⁸⁻¹³² It was determined that the 2'- and 3'-hydroxy moieties are essential for activity, whereas, the 6'-gem-dimethyl group and the 5'-methoxy are not.¹²⁸ Additional SAR demonstrated that N-methyl piperidine represents a suitable replacement for the noviose sugar (compound 1 in Figure 7).

EGCG and Silybin

There are two other natural products that have been shown to bind the Hsp90 C-terminus, (-)-Epigallocatechin-3-gallate (EGCG) and silybin (Figure 7). EGCG is the major component of green tea and silybin is the major component of silymarin, which is extracted from the seed of milk thistle.^{133,134} Through the use of proteolytic footprinting, immunoprecipitation, and an ATP-agarose pull-down assay, Gasiewicz and coworkers demonstrated that EGCG binds the same amino acids (538-728) as novobiocin.¹³³ Inhibition of Hsp90 via EGCG binding causes client

protein degradation (telomerase, multiple kinases, and the aryl hydrocarbon receptor), and therefore anti-cancer activity.^{135,136}

Historically, silybin has been used for the treatment of liver and gallbladder disorders.¹³⁷ However, silybin was also shown to manifest cytotoxic activity against various cancer cell lines in addition to enhancing the efficacy of other chemotherapeutic agents. Silybin was identified as an Hsp90 C-terminal inhibitor and Hsp90-dependent client proteins were degraded in a concentration-dependent manner, while Hsp90 levels remained constant.¹³⁸ Overlay of silybin and novobiocin suggest the coumarin and flavonone ring could be interchanged, which led to compounds that exhibited improved Hsp90 inhibitory activity.¹³⁹

Post-translational Modifications of the Hsp90 Chaperone Cycle

The Hsp90 chaperone cycle can be fine-tuned to quickly adapt to changes in the intracellular environment through post-translational modifications (PTMs). Several comprehensive reviews describe these covalent modifications, which include phosphorylation, acetylation, S-nitrosylation, oxidation, ubiquitylation, and SUMOylation. These PTMs can affect ATPase activity, stabilization of Hsp90-client interactions, co-chaperone interactions, and in some cases, target client proteins for maturation or degradation.¹⁴⁰⁻¹⁴² A summary of some Hsp90 PTMs and original references are provided in Table 2. PTMs of the Hsp90 chaperone cycle can enhance or diminish the effects of small molecule Hsp90 inhibitors, such as GDA. Targeting these PTMs can provide an opportunity to enhance the efficacy of Hsp90 inhibitors and gain further insight into the mechanism by which PTMs regulate the Hsp90 protein folding machinery.

Co-chaperones Cdc37, Sgt1, p23, and FKBP52 are susceptible to phosphorylation by casein kinase 2 (CK2).¹⁴³⁻¹⁴⁸ CK2 phosphorylates ser-13 of Cdc37. This modification is required for Cdc37's chaperoning of numerous kinase clients as well as for the binding of Cdc37 to Hsp90. De-phosphorylation of Cdc37 at ser-13 by the phosphatase, PP5/Ppt1, negatively affects the chaperone cycle and prevents maturation of these clients. Phosphorylation of Sgt-1 at ser-361 negatively impacts Sgt-1 dimerization and prevents kinetochore assembly, a process required for chromosome segregation during eukaryotic cell division. CK2-mediated phosphorylation of p23 at ser-113 and -118 was shown to be important for prostaglandin synthase activity and required for formation of the Hsp90-p23-CK2 complex. CK2 also phosphorylated thr-143 of FKBP52. While this modification does not affect FKBP52 from binding FK506, phosphorylated FKBP52 does not bind Hsp90.

Several kinases are capable of phosphorylating Hsp90 and have varying effects on the chaperone cycle. Double-stranded DNA protein kinase (DNA-PK) phosphorylates thr-5 and -7 of the Hsp90 α N-terminal domain and may play a role in DNA damage. Client kinases also phosphorylate Hsp90 and may regulate their own chaperoning via a feedback mechanism. B-Raf was shown to phosphorylate ser-263 of Hsp90 in melanoma and Akt to phosphorylate Hsp90 α and Hsp90 β , Grp78 and Grp94, Hsp70, and protein disulfide isomerase (PDI). c-Src phosphorylates Hsp90 β at tyr-301 in response to vascular endothelial growth factor receptor-2 (VEGFR-2) activation and increases association between Hsp90 β and eNOS. Protein kinase A (PKA) phosphorylates thr-90 of Hsp90 α and reduces association with eNOS, which results in both diminished eNOS activity and nitric oxide production. Phosphorylation of thr-90 of Hsp90 α via PKA was also shown to mediate cellular secretion of Hsp90 α and may play a role in wound healing and/or metastasis. Swe1^{Wee1} kinase phosphorylates tyr-38 of the N-terminus of Hsp90 α

when Hsp90 is in the “open conformation” and positively affects the ability of Hsp90 to chaperone a select group of client kinases (ErbB2, Raf-1, and Cdk4). However, phosphorylation of this residue also negatively affects GDA binding to the Hsp90 N-terminus.

CK2 phosphorylation of ser-231 and -263 in the charged linker of Hsp90 α , as well as the equivalent residues in Hsp90 β (ser-226 and -255) occurs in normal cells, but not leukemic cells. Several leukemogenic kinases, such as Bcr-abl, FLT3/D835Y, and Tel-PDGFR β , suppressed phosphorylation of Hsp90 β at these residues, which resulted in stable interactions between Hsp90 β and apoptotic peptidase activating factor-1 (Apaf-1). Ultimately, this activity led to inhibition of apoptosome function and may contribute to resistance in leukemia. CK2 phosphorylation at these sites also disrupts the Hsp90-aryl hydrocarbon complex and destabilizes the aryl hydrocarbon receptor protein. CK2 was also shown to phosphorylate thr-36 of Hsp90 α . Mutation of this residue to a phospho-mimetic, aspartate, resulted in decreased chaperoning of several clients and reduced interactions between Hsp90 α with Aha1.

Acetylation/deacetylation of Hsp90 has been investigated using HDAC inhibitors.¹⁴⁹⁻
¹⁵¹Acetylation of Hsp90 by p300 resulted in diminished interactions between Hsp90 and clients and ultimately, resulted in client instability and degradation. Mutation of lysine to acetylated lysine was shown to decrease interactions between Hsp90 and several clients/co-chaperones as well as to reduce ATP-binding. De-acetylation of Hsp90 has been shown to occur via several HDACs including HDAC6, HDAC1 and HDAC10, which correlate with the stabilization of Hsp90-client interactions and increased chaperone activity.¹⁵²⁻¹⁵⁵

Other PTMs include S-nitrosylation of Hsp90 α at cys-597 via nitric oxide, oxidation of cys-572 by the oxidized lipid, 4-hydroxy-2-nonenal (4-HNE; is formed during cellular oxidative stress), ubiquitinylation, and more recently, SUMOylation. S-nitrosylation, oxidation, and

ubiquitylation decrease chaperone function by perturbing ATPase activity or destabilizing Hsp90-client interactions, which results in client degradation. Alternatively, SUMOylation of the conserved lysine residue, lys-191, initiated recruitment of the ATPase activating co-chaperone, Aha1. In addition, SUMOylation facilitated binding of several Hsp90 N-terminal inhibitors and sensitized yeast and mammalian Hsp90 to inhibition.

Table 2 Post-translational Modifications of Human Hsp90			
Modification	Catalytic Protein or Moiety	Amino Acid Residue	Effect on Hsp90 Chaperone Activity
Phosphorylation/d e-phosphorylation	DNA-PK	Thr-5 and -7 phosphorylation ¹⁵⁶	Unknown
	B-Raf	Ser-263 phosphorylation of Hsp90 α ¹⁵⁷	Unknown
	Akt	Thr and ser phosphorylation of Hsp90 α , Hsp90 β , and Grp94 ¹⁵⁸	Unknown
	c-Src	Try-301 phosphorylation of Hsp90 β ¹⁵⁹	Increased eNOS activity and NO production.
	PKA	Phosphorylation of ser-452 of Hsp90 β and Thr-90 of Hsp90 α ¹⁶⁰⁻¹⁶¹	Phosphorylation of Hsp90 α decreased eNOS activity and NO production. Also stimulates cellular secretion of Hsp90 α .
	CK2	Phosphorylation of ser-231 and -263 of Hsp90 α and ser-226 and -255 of Hsp90 β in untransformed cells but not leukemic cells ¹⁶²⁻¹⁶³	Phosphorylation of Hsp90 α caused dissociation of Hsp90 and the aryl hydrocarbon receptor.
	Swe1 ^{Wee1} Kinase	Tyr-38 phosphorylation of Hsp90 α ¹⁶⁴	Increased chaperoning activity of select clients. Decreased GDA binding to Hsp90.
S-nitrosylation	NO	Cys-597 nitrosylation ¹⁶⁵⁻¹⁶⁶	Inhibited ATPase activity
Oxidation	4-HNE	Cys-572 oxidation ¹⁶⁷	Decreased chaperone activity
Ubiquitinylation	Ubiquitin pathway	Lys ubiquitinylation ¹⁶⁸⁻¹⁶⁹	Destabilized Hsp90 client interactions and resulted in client degradation.
SUMOylation	SUMOylation	Lys-191 SUMOylation ¹⁴⁰	Initiated recruitment

	pathway		of Aha1 and facilitated binding of N-terminal inhibitors.
--	---------	--	---

Future Perspective

Tumor dependency on pathways regulated by Hsp90 provides clear rationale for the development of Hsp90 inhibitors. Hsp90 inhibition offers a multifaceted treatment strategy, which is in contrast to current cancer therapies that target a single signaling pathway. Despite the potential of Hsp90 as a drug target, no Hsp90 inhibitor has been FDA approved. Alternative methods to target Hsp90 include inhibition of the C-terminus or allosteric modulation of the chaperone machinery.

Recent advances toward elucidation of the Hsp90 structure and intricacies of the chaperone cycle have provided details on the conformational changes required for heteroprotein complex formation during various stages of the chaperone cycle. PTMs of proteins involved in the chaperone cycle have shed light on how quickly Hsp90 adapts to changes in the cellular environment. Alternative methods to modulate Hsp90 may provide an opportunity to select for oncogenic client degradation, while avoiding some of the negative consequences of N-terminal inhibition. In conclusion, the Hsp90 chaperone cycle and inhibitor development have become a diverse and dynamic field of study. As details of the chaperone cycle emerge, more information regarding the regulation of chaperone machinery in normal versus transformed cells will be discovered. Such studies will lead to the development of tailored strategies for modulation of the Hsp90 chaperone machinery for the treatment of cancer as well as other diseases.

References

1. Pratt, W. B., The role of heat shock proteins in regulating the function, folding, and trafficking of the glucocorticoid receptor. *Journal of Biological Chemistry* **1993**, *268* (29), 21455-21458.
2. Csermely, P.; Schnaider, T.; Soti, C.; Prohászka, Z.; Nardai, G., The 90-kDa Molecular Chaperone Family: Structure, Function, and Clinical Applications. A Comprehensive Review. *Pharmacology & Therapeutics* **1998**, *79* (2), 129-168.
3. Taipale, M.; Jarosz, D. F.; Lindquist, S., HSP90 at the hub of protein homeostasis: emerging mechanistic insights. *Nature Reviews Molecular Cell Biology* **2010**, *11* (7), 515-528.
4. Li, J.; Soroka, J.; Buchner, J., The Hsp90 chaperone machinery: Conformational dynamics and regulation by co-chaperones. *Biochimica et Biophysica Acta (BBA) - Molecular Cell Research* **2012**, *1823* (3), 624-635.
5. Li, J.; Buchner, J., Structure, Function and Regulation of the Hsp90 Machinery. *Biomedical Journal* **2013**, *36* (3), 106-117.
6. Prodromou, C.; Pearl, L. H., Structure and functional relationships of Hsp90. *Current Cancer Drug Targets* **2003**, *3* (5), 301-323.
7. Panaretou, B.; Prodromou, C.; Roe, S. M.; O'Brien, R.; Ladbury, J. E.; Piper, P. W.; Pearl, L. H., ATP binding and hydrolysis are essential to the function of the Hsp90 molecular chaperone in vivo. *The EMBO Journal* **1998**, *17* (16), 4829-4836.
8. Prodromou, C.; Roe, S. M.; O'Brien, R.; Ladbury, J. E.; Piper, P. W.; Pearl, L. H., Identification and Structural Characterization of the ATP/ADP-Binding Site in the Hsp90 Molecular Chaperone. *Cell* **1997** *90* (1), 65-75.

9. Bagatell, R.; Khan, O.; Paine-Murrieta, G.; Taylor, C. W.; Akinaga, S.; Whitesell, L., Destabilization of Steroid Receptors by Heat Shock Protein 90-binding Drugs: A Ligand-independent Approach to Hormonal Therapy of Breast Cancer. *Clinical Cancer Research* **2001**, *7* (7), 2076-2084.
10. Chaudhury, S.; Welch, T. R.; Blagg, B. S. J., Hsp90 as a Target for Drug Development. *ChemMedChem* **2006**, *1* (12), 1331-1340.
11. Mimnaugh, E. G.; Chavany, C.; Neckers, L., Polyubiquitination and Proteasomal Degradation of the p185c-erbB-2 Receptor Protein-tyrosine Kinase Induced by Geldanamycin. *Journal of Biological Chemistry* **1996**, *271* (37), 22796-22801.
12. Schneider, C.; Sepp-Lorenzino, L.; Nimmesgern, E.; Ouerfelli, O.; Danishefsky, S.; Rosen, N.; Hartl, F. U., Pharmacologic shifting of a balance between protein refolding and degradation mediated by Hsp90. *Proceedings of the National Academy of Sciences* **1996**, *93* (25), 14536-14541.
13. Hanahan, D.; Weinberg, R. A., The Hallmarks of Cancer. *Cell* **2000**, *100*, 57-70.
14. Hanahan, D.; Weinberg, R. A., Hallmarks of cancer: the next generation. *Cell* **2011**, *144* (5), 646-74.
15. Neckers, L.; Workman, P., Hsp90 Molecular Chaperone Inhibitors: Are We There Yet? *Clinical Cancer Research : an official journal of the American Association for Cancer Research* **2012**, *18* (1), 64-76.
16. da Silva, V. C. H.; Ramos, C. H. I., The network interaction of the human cytosolic 90kDa heat shock protein Hsp90: A target for cancer therapeutics. *Journal of Proteomics* **2012**, *75* (10), 2790-2802.

17. Holzbeierlein, J.; Windsperger, A.; Vielhauer, G., Hsp90: A Drug Target? *Current Oncology Reports* **2010**, *12* (2), 95-101.
18. Ebrahimi-Fakhari, D.; Saidi, L.-J.; Wahlster, L., Molecular chaperones and protein folding as therapeutic targets in Parkinson's disease and other synucleinopathies. *Acta Neuropathological Communications* **2013**, *1* (1), 79.
19. Kamal, A.; Thao, L.; Sensintaffar, J.; Zhang, L.; Boehm, M. F.; Fritz, L. C.; Burrows, F. J., A high-affinity conformation of Hsp90 confers tumour selectivity on Hsp90 inhibitors. *Letters to Nature* **2003**, *425*, 407-410.
20. Kim, H. R.; Kang, H. S.; Kim, H. D., Geldanamycin Induces Heat Shock Protein Expression Through Activation of HSF1 in K562 Erythroleukemic Cells. *IUBMB Life* **1999**, *48* (4), 429-433.
21. Winkelhofer, K. F.; Reintjes, A.; Hoener, M. C.; Voellmy, R.; Tatzelt, J., Geldanamycin Restores a Defective Heat Shock Response in Vivo. *Journal of Biological Chemistry* **2001**, *276* (48), 45160-45167.
22. Whitesell, L.; Bagatell, R.; Falsey, R., The Stress Response: Implications for the Clinical Development of Hsp90 Inhibitors. *Current Cancer Drug Targets* **2003**, *3* (5), 349-358.
23. Brandt, G. E. L.; Blagg, B. S. J., Alternate Strategies of Hsp90 Modulation for the Treatment of Cancer and Other Diseases. *Current Topics in Medicinal Chemistry* **2009**, *9* (15), 1447-1461.
24. Pearl, L. H., Hsp90 and Cdc37 – a chaperone cancer conspiracy. *Current Opinion in Genetics & Development* **2005**, *15* (1), 55-61.
25. Röhl, A.; Rohrber, J.; Buchner, J., The Chaperone Hsp90: Changing Partners for Demanding Clients. *Trends in Biochemical Sciences* **2013**, *38* (5), 253-62.

26. Patwardhan, C. A.; Fauq, A.; Peterson, L. B.; Miller, C.; Blagg, B. S. J.; Chadli, A., Gedunin Inactivates the Co-chaperone p23 Protein Causing Cancer Cell Death by Apoptosis. *Journal of Biological Chemistry* **2013**, *288* (10), 7313-7325.
27. Papathanassiou, A. E.; MacDonald, N. J.; Bencsura, A.; Vu, H. A., F1F0-ATP synthase functions as a co-chaperone of Hsp90–substrate protein complexes. *Biochemical and Biophysical Research Communications* **2006**, *345* (1), 419-429.
28. Marcu, M. G.; Schulte, T. W.; Neckers, L., Novobiocin and Related Coumarins and Depletion of Heat Shock Protein 90-Dependent Signaling Proteins. *Journal of the National Cancer Institute* **2000**, *92* (3), 242-248.
29. Kusuma, B. R.; Khandelwal, A.; Gu, W.; Brown, D.; Liu, W.; Vielhauer, G.; Holzbeierlein, J.; Blagg, B. S. J., Synthesis and Biological Evaluation of Coumarin Replacements of Novobiocin as Hsp90 Inhibitors. *Bioorganic & Medicinal Chemistry* **2014**, *22* (4), 1441-1449.
30. Zhao, H.; Blagg, B. S. J., Novobiocin analogues with second-generation noviose surrogates. *Bioorganic & Medicinal Chemistry Letters* **2013**, *23* (2), 552-557.
31. Zhao, H.; Blagg, B. S. J., Inhibitors of the Hsp90 C-terminus. In *Inhibitors of Molecular Chaperones as Therapeutic Agents*, Machajewski, T.; Gao, Z., Eds. Royal Society of Chemistry: 2013; Vol. 37, pp 259-301.
32. Prodromou, C., The 'Active Life' of Hsp90 Complexes. *Biochimica et Biophysica Acta* **2012**, *1823* (3), 614-23.
33. Rohl, A.; Rohrberg, J.; Buchner, J., The chaperone Hsp90: changing partners for demanding clients. *Trends in Biochemical Sciences* **2013**, *38* (5), 253-62.

34. Li, J.; Richter, K.; Reinstein, J.; Buchner, J., Integration of the Accelerator Aha1 in the Hsp90 Co-Chaperone Cycle. *Nature Structural Molecular Biology* **2013**, *20* (3), 326-31.
35. Martinez-Yamout, M. A.; Venkitakrishnan, R. P.; Preece, N. E.; Kroon, G.; Wright, P. E.; Dyson, H. J., Localization of Sites of Interaction between p23 and Hsp90 in Solution. *Journal of Biological Chemistry* **2006**, *281* (20), 14457-14464.
36. McLaughlin, S. H.; Sobott, F.; Yao, Z.-p.; Zhang, W.; Nielsen, P. R.; Grossmann, J. G.; Laue, E. D.; Robinson, C. V.; Jackson, S. E., The Co-chaperone p23 Arrests the Hsp90 ATPase Cycle to Trap Client Proteins. *Journal of Molecular Biology* **2006**, *356* (3), 746-758.
37. Connell, P.; Ballinger, C. A.; Jiang, J.; Wu, Y.; Thompson, L. J.; Hohfeld, J.; Patterson, C., The co-chaperone CHIP regulates protein triage decisions mediated by heat-shock proteins. *Nature Cell Biology* **2001**, *3* (1), 93-96.
38. Kundrat, L.; Regan, L., Balance between Folding and Degradation for Hsp90-Dependent Client Proteins: A Key Role for CHIP. *Biochemistry* **2010**, *49* (35), 7428-7438.
39. Murata, S.; Minami, Y.; Minami, M.; Chiba, T.; Tanaka, K., CHIP is a chaperone - dependent E3 ligase that ubiquitylates unfolded protein. *EMBO Reports* **2001**, *2* (12), 1133-1138.
40. Xu, W.; Marcu, M.; Yuan, X.; Mimnaugh, E.; Patterson, C.; Neckers, L., Chaperone-dependent E3 ubiquitin ligase CHIP mediates a degradative pathway for c-ErbB2/Neu. *Proceedings of the National Academy of Sciences* **2002**, *99* (20), 12847-12852.
41. Philp, L.; Butler, M.; Hickey, T.; Butler, L.; Tilley, W.; Day, T., SGTA: A New Player in the Molecular Co-Chaperone Game. *Hormones and Cancer* **2013**, *4* (6), 343-357.
42. Papathanassiou, A.; MacDonald, N.; Emlet, D.; Vu, H., Antitumor activity of efrapeptins, alone or in combination with 2-deoxyglucose, in breast cancer in vitro and in vivo. *Cell Stress and Chaperones* **2011**, *16* (2), 181-193.

43. Dakubo, G., The Warburg Phenomenon and Other Metabolic Alterations of Cancer Cells. In *Mitochondrial Genetics and Cancer*, Springer Berlin Heidelberg: 2010; pp 39-66.
44. Capuano, F.; Guerrieri, F.; Papa, S., Oxidative phosphorylation enzymes in normal and neoplastic cell growth. *Journal of Bioenergetics and Biomembranes* **1997**, *29* (4), 379-84.
45. Guppy, M.; Leedman, P.; Zu, X.; Russell, V., Contribution by different fuels and metabolic pathways to the total ATP turnover of proliferating MCF-7 breast cancer cells. *Biochemical Journal* **2002**, *364* (1), 309-315.
46. Wallace, D. C., Mitochondria and cancer. *Nature Reviews Cancer* **2012**, *12* (10), 685-698.
47. Hall, J. A.; Kusuma, B. R.; Brandt, G. E. L.; Blagg, B. S. J., Cruentaren A Binds F1F0 ATP Synthase To Modulate the Hsp90 Protein Folding Machinery. *ACS Chemical Biology* **2014**.
48. Peng, X.; Guo, X.; Borkan, S. C.; Bharti, A.; Kuramochi, Y.; Calderwood, S.; Sawyer, D. B., Heat Shock Protein 90 Stabilization of ErbB2 Expression Is Disrupted by ATP Depletion in Myocytes. *Journal of Biological Chemistry* **2005**, *280* (13), 13148-13152.
49. Ali, A.; Bharadwaj, S.; O'Carroll, R.; Ovsenek, N., HSP90 Interacts with and Regulates the Activity of Heat Shock Factor 1 in Xenopus Oocytes. *Molecular and Cellular Biology* **1998**, *18* (9), 4949-4960.
50. Zou, J.; Guo, Y.; Guettouche, T.; Smith, D. F.; Voellmy, R., Repression of Heat Shock Transcription Factor HSF1 Activation by HSP90 (HSP90 Complex) that Forms a Stress-Sensitive Complex with HSF1. *Cell* **1998**, *94* (4), 471-480.
51. Dai, C.; Whitesell, L.; Rogers, A. B.; Lindquist, S., Heat Shock Factor 1 Is a Powerful Multifaceted Modifier of Carcinogenesis. *Cell* **2007** *130* (6), 1005-1018.

52. Labbadia, J.; Morimoto, R. I., The Biology of Proteostasis in Aging and Disease. *Annual Review of Biochemistry* **2015**, *84* (1), 435-464.
53. Neef, D. W.; Jaeger, A. M.; Thiele, D. J., Heat shock transcription factor 1 as a therapeutic target in neurodegenerative diseases. *Nature Reviews Drug Discovery* **2011**, *10* (12), 930-944.
54. Purwana, I.; Liu, J. J.; Portha, B.; Buteau, J., HSF1 acetylation decreases its transcriptional activity and enhances glucolipotoxicity-induced apoptosis in rat and human beta cells. *Diabetologia* **2017**, *60* (8), 1432-1441.
55. Voellmy, R.; Boellmann, F., Chaperone Regulation of the Heat Shock Protein Response. In *Molecular Aspects of the Stress Response: Chaperones, Membranes and Networks*, Csermely, P.; Vigh, L., Eds. Springer New York: New York, NY, 2007; pp 89-99.
56. Bharadwaj, S.; Ali, A.; Ovsenek, N., Multiple Components of the Hsp90 Chaperone Complex Function in Regulation of Heat Shock Factor 1 in Vivo. *Molecular and Cellular Biology* **1999**, *19* (12), 8033-8041.
57. Guo, Y.; Guettouche, T.; Fenna, M.; Boellmann, F.; Pratt, W. B.; Toft, D. O.; Smith, D. F.; Voellmy, R., Evidence for a mechanism of repression of heat shock factor 1 transcriptional activity by a multichaperone complex. *The Journal of Biological Chemistry* **2001**, *276*, 45791-45799.
58. Anckar, J.; Sistonen, L., Regulation of HSF1 Function in the Heat Stress Response: Implications in Aging and Disease. *Annual Review of Biochemistry* **2011**, *80* (1), 1089-1115.
59. Budzyński, M. A.; Puustinen, M. C.; Joutsen, J.; Sistonen, L., Uncoupling Stress-Inducible Phosphorylation of Heat Shock Factor 1 from Its Activation. *Molecular and Cellular Biology* **2015**, *35* (14), 2530-2540.

60. Zheng, X.; Krakowiak, J.; Patel, N.; Beyzavi, A.; Ezike, J.; Khalil, A. S.; Pincus, D., Dynamic control of Hsf1 during heat shock by a chaperone switch and phosphorylation. *Elife* **2016**, *5*.
61. Sigler, P. B., Acid blobs and negative noodles. *Nature* **1988**, *333* (6170), 210-212.
62. Schubert, U.; Antón, L. C.; Gibbs, J.; Norbury, C. C.; Yewdell, J. W.; Bennink, J. R., Rapid degradation of a large fraction of newly synthesized proteins by proteasomes. *Nature* **2000**, *404* (6779), 770-774.
63. Ellis, R. J.; Pinheiro, T. J. T., Medicine: Danger — misfolding proteins. *Nature* **2002**, *416* (6880), 483-484.
64. Barral, J. M.; Broadley, S. A.; Schaffar, G.; Hartl, F. U., Roles of molecular chaperones in protein misfolding diseases. *Seminars in Cell & Developmental Biology* **2004**, *15* (1), 17-29.
65. Muchowski, P. J.; Wacker, J. L., Modulation of neurodegeneration by molecular chaperones. *Nature Reviews Neuroscience* **2005**, *6* (1), 11-22.
66. Turturici, G.; Sconzo, G.; Geraci, F., Hsp70 and its molecular role in nervous system diseases. *Biochemistry Research International* **2011**, *2011*, 618127.
67. Satoh, T.; Rezaie, T.; Seki, M.; Sunico, C. R.; Tabuchi, T.; Kitagawa, T.; Yanagitai, M.; Senzaki, M.; Kosegawa, C.; Taira, H.; McKercher, S. R.; Hoffman, J. K.; Roth, G. P.; Lipton, S. A., Dual neuroprotective pathways of a pro-electrophilic compound via HSF-1-activated heat-shock proteins and Nrf2-activated phase 2 antioxidant response enzymes. *Journal of Neurochemistry* **2011**, *119* (3), 569-78.
68. Hahn, J.-S.; Hu, Z.; Thiele, D. J.; Iyer, V. R., Genome-Wide Analysis of the Biology of Stress Responses through Heat Shock Transcription Factor. *Molecular and Cellular Biology* **2004**, *24* (12), 5249-5256.

69. Verma, P.; Pfister, J. A.; Mallick, S.; D'Mello, S. R., HSF1 Protects Neurons through a Novel Trimerization- and HSP-Independent Mechanism. *The Journal of Neuroscience* **2014**, *34* (5), 1599-1612.
70. Török, Z.; Tsvetkova, N. M.; Balogh, G.; Horváth, I.; Nagy, E.; Péntzes, Z.; Hargitai, J.; Bensaude, O.; Csermely, P.; Crowe, J. H.; Maresca, B.; Vigh, L., Heat shock protein coinducers with no effect on protein denaturation specifically modulate the membrane lipid phase. *Proceedings of the National Academy of Sciences* **2003**, *100* (6), 3131-3136.
71. Török, Z.; Crul, T.; Maresca, B.; Schütz, G. J.; Viana, F.; Dindia, L.; Piotto, S.; Brameshuber, M.; Balogh, G.; Péter, M.; Porta, A.; Trapani, A.; Gombos, I.; Glatz, A.; Gungo, B.; Peksel, B.; Jr, L. V.; Csoboz, B.; Horváth, I.; Vijaya, M. M.; Hooper, P. L.; Harwood, J. L.; Vigh, L., Plasma membranes as heat stress sensors: From lipid-controlled molecular switches to therapeutic applications. *Biochimica et Biophysica Acta (BBA) - Biomembranes* **2014**, *1838* (6), 1594-1618.
72. Bromberg, Z.; Weiss, Y., The Role of the Membrane-Initiated Heat Shock Response in Cancer. *Frontiers in Molecular Biosciences* **2016**, *3*, 12.
73. Kusuma, B. R.; Peterson, L. B.; Zhao, H.; Vielhauer, G.; Holzbeierlein, J.; Blagg, B. S. J., Targeting the Heat Shock Protein 90 Dimer with Dimeric Inhibitors. *The Journal of Medicinal Chemistry* **2011**, *54* (18), 6234-53.
74. Hartson, S. D.; Irwin, A. D.; Shao, J.; Scroggins, B. T.; Volk, L.; Huang, W.; Matts, R. L., p50cdc37 Is a Nonexclusive Hsp90 Cohort Which Participates Intimately in Hsp90-Mediated Folding of Immature Kinase Molecules. *Biochemistry* **2000**, *39* (25), 7631-7644.

75. Shao, J.; Irwin, A.; Hartson, S. D.; Matts, R. L., Functional Dissection of Cdc37: Characterization of Domain Structure and Amino Acid Residues Critical for Protein Kinase Binding. *Biochemistry* **2003**, *42* (43), 12577-12588.
76. Eckl, J. M.; Rutz, D. A.; Haslbeck, V.; Zierer, B. K.; Reinstein, J.; Richter, K., Cdc37 (Cell Division Cycle 37) Restricts Hsp90 (Heat Shock Protein 90) Motility by Interaction with N-terminal and Middle Domain Binding Sites. *Journal of Biological Chemistry* **2013**, *288* (22), 16032-16042.
77. Gaiser, A. M.; Kretzschmar, A.; Richter, K., Cdc37-Hsp90 Complexes Are Responsive to Nucleotide-induced Conformational Changes and Binding of Further Cofactors. *Journal of Biological Chemistry* **2010**, *285* (52), 40921-40932.
78. Zhang, M.; Kadota, Y.; Prodromou, C.; Shirasu, K.; Pearl, L. H., Structural Basis for Assembly of Hsp90-Sgt1-CHORD Protein Complexes: Implications for Chaperoning of NLR Innate Immunity Receptors. *Molecular Cell* **2010**, *39* (2), 269-281.
79. Eckert, K.; Saliou, J.-M.; Monlezun, L.; Vigouroux, A.; Atmane, N.; Caillat, C.; Quevillon-Chéruef, S.; Madiona, K.; Nicaise, M.; Lazereg, S.; Van Dorsselaer, A.; Sanglier-Cianférani, S.; Meyer, P.; Moréra, S., The Pih1-Tah1 Cochaperone Complex Inhibits Hsp90 Molecular Chaperone ATPase Activity. *Journal of Biological Chemistry* **2010**, *285* (41), 31304-31312.
80. Silverstein, A. M.; Galigniana, M. D.; Chen, M.-S.; Owens-Grillo, J. K.; Chinkers, M.; Pratt, W. B., Protein Phosphatase 5 Is a Major Component of Glucocorticoid Receptor·hsp90 Complexes with Properties of an FK506-binding Immunophilin. *Journal of Biological Chemistry* **1997**, *272* (26), 16224-16230.

81. Barent, R. L.; Nair, S. C.; Carr, D. C.; Ruan, Y.; Rimerman, R. A.; Fulton, J.; Zhang, Y.; Smith, D. F., Analysis of FKBP51/FKBP52 Chimeras and Mutants for Hsp90 Binding and Association with Progesterone Receptor Complexes. *Molecular Endocrinology* **1998**, *12* (3), 342-354.
82. Zhang, T.; Hamza, A.; Cao, X.; Wang, B.; Yu, S.; Zhan, C.-G.; Sun, D., A novel Hsp90 inhibitor to disrupt Hsp90/Cdc37 complex against pancreatic cancer cells. *Molecular Cancer Therapeutics* **2008**, *7* (1), 162-170.
83. Brandt, G. E. L.; Schmidt, M. D.; Prisinzano, T. E.; Blagg, B. S. J., Gedunin, a Novel Hsp90 Inhibitor: Semisynthesis of Derivatives and Preliminary Structure–Activity Relationships. *Journal of Medicinal Chemistry* **2008**, *51* (20), 6495-6502.
84. Zhang, T.; Li, Y.; Yu, Y.; Zou, P.; Jiang, Y.; Sun, D., Characterization of Celastrol to Inhibit Hsp90 and Cdc37 Interaction. *Journal of Biological Chemistry* **2009**, *284* (51), 35381-35389.
85. Sreeramulu, S.; Gande, S. L.; Göbel, M.; Schwalbe, H., Molecular Mechanism of Inhibition of the Human Protein Complex Hsp90–Cdc37, a Kinome Chaperone–Cochaperone, by Triterpene Celastrol. *Angewandte Chemie International Edition* **2009**, *48* (32), 5853-5855.
86. Chadli, A.; Felts, S. J.; Wang, Q.; Sullivan, W. P.; Botuyan, M. V.; Fauq, A.; Ramirez-Alvarado, M.; Mer, G., Celastrol Inhibits Hsp90 Chaperoning of Steroid Receptors by Inducing Fibrillization of the Co-chaperone p23. *Journal of Biological Chemistry* **2010**, *285* (6), 4224-4231.
87. Kunze, B.; Sasse, F.; Wiczorek, H.; Huss, M., Cruentaren A, a highly cytotoxic benzolactone from Myxobacteria is a novel selective inhibitor of mitochondrial F1-ATPases. *FEBS letters* **2007**, *581* (18), 3523-3527.

88. Jundt, L.; Steinmetz, H.; Luger, P.; Weber, M.; Kunze, B.; Reichenbach, H.; Höfle, G., Isolation and Structure Elucidation of Cruentarens A and B — Novel Members of the Benzolactone Class of ATPase Inhibitors from the Myxobacterium *Byssovorax cruenta*. *European Journal of Organic Chemistry* **2006**, 2006 (22), 5036-5044.
89. Lee, J. H.; Chung, I. K., Curcumin inhibits nuclear localization of telomerase by dissociating the Hsp90 co-chaperone p23 from hTERT. *Cancer Letters* **2010**, 290 (1), 76-86.
90. Ardi, V. C.; Alexander, L. D.; Johnson, V. A.; McAlpine, S. R., Macrocycles That Inhibit the Binding between Heat Shock Protein 90 and TPR-Containing Proteins. *ACS Chemical Biology* **2011**, 6 (12), 1357-1366.
91. McConnell, J. R.; Alexander, L. A.; McAlpine, S. R., A heat shock protein 90 inhibitor that modulates the immunophilins and regulates hormone receptors without inducing the heat shock response. *Bioorganic & Medicinal Chemistry Letters* **2014**, 24 (2), 661-666.
92. Vasko, R. C.; Rodriguez, R. A.; Cunningham, C. N.; Ardi, V. C.; Agard, D. A.; McAlpine, S. R., Mechanistic Studies of Sansalvamide A-Amide: An Allosteric Modulator of Hsp90. *ACS Medicinal Chemistry Letters* **2010**, 1 (1), 4-8.
93. Grenert, J. P.; Sullivan, W. P.; Fadden, P.; Haystead, T. A. J.; Clark, J.; Mimnaugh, E.; Krutzsch, H.; Ochel, H.-J.; Schulte, T. W.; Sausville, E.; Neckers, L. M.; Toft, D. O., The Amino-terminal Domain of Heat Shock Protein 90 (hsp90) That Binds Geldanamycin Is an ATP/ADP Switch Domain That Regulates hsp90 Conformation. *Journal of Biological Chemistry* **1997**, 272 (38), 23843-23850.
94. Roe, S. M.; Prodromou, C.; O'Brien, R.; Ladbury, J. E.; Piper, P. W.; Pearl, L. H., Structural Basis for Inhibition of the Hsp90 Molecular Chaperone by the Antitumor Antibiotics Radicicol and Geldanamycin. *Journal of Medicinal Chemistry* **1999**, 42 (2), 260-266.

95. Jhaveri, K.; Taldone, T.; Modi, S.; Chiosis, G., Advances in the clinical development of heat shock protein 90 (Hsp90) inhibitors in cancers. *Biochimica et Biophysica Acta (BBA) - Molecular Cell Research* **2012**, *1823* (3), 742-755.
96. Whitesell, L.; Lin, N. U., HSP90 as a platform for the assembly of more effective cancer chemotherapy. *Biochimica et Biophysica Acta (BBA) - Molecular Cell Research* **2012**, *1823* (3), 756-766.
97. Garcia-Carbonero, R.; Carnero, A.; Paz-Ares, L., Inhibition of HSP90 molecular chaperones: moving into the clinic. *The Lancet Oncology* **2013**, *14* (9), e358-e369.
98. Sidera, K.; Patsavoudi, E., HSP90 Inhibitors: Current Development and Potential in Cancer Therapy. *Recent Patents on Anti-Cancer Drug Discovery* **2014**, *9* (1), 1-20.
99. Kitson, R. R. A.; Moody, C. J., Learning from Nature: Advances in Geldanamycin- and Radicicol-Based Inhibitors of Hsp90. *The Journal of Organic Chemistry* **2013**, *78* (11), 5117-5141.
100. Whitesell, L.; Mimnaugh, E. G.; De Costa, B.; Myers, C. E.; Neckers, L. M., Inhibition of heat shock protein HSP90-pp60v-src heteroprotein complex formation by benzoquinone ansamycins: essential role for stress proteins in oncogenic transformation. *Proceedings of the National Academy of Sciences* **1994**, *91* (18), 8324-8328.
101. Biamonte, M. A.; Van de Water, R.; Arndt, J. W.; Scannevin, R. H.; Perret, D.; Lee, W.-C., Heat Shock Protein 90: Inhibitors in Clinical Trials. *Journal of Medicinal Chemistry* **2009**, *53* (1), 3-17.
102. Peterson, L. B.; Eskew, J. D.; Vielhauer, G. A.; Blagg, B. S. J., The hERG Channel Is Dependent upon the Hsp90 α Isoform for Maturation and Trafficking. *Molecular Pharmaceutics* **2012**, *9* (6), 1841-1846.

103. Ficker, E.; Dennis, A. T.; Wang, L.; Brown, A. M., Role of the Cytosolic Chaperones Hsp70 and Hsp90 in Maturation of the Cardiac Potassium Channel hERG. *Circulation Research* **2003**, *92* (12), e87-e100.
104. Duerfeldt, A. S.; Peterson, L. B.; Maynard, J. C.; Ng, C. L.; Eletto, D.; Ostrovsky, O.; Shinogle, H. E.; Moore, D. S.; Argon, Y.; Nicchitta, C. V.; Blagg, B. S. J., Development of a Grp94 inhibitor. *Journal of the American Chemical Society* **2012**, *134* (23), 9796-9804.
105. Patel, P. D.; Yan, P.; Seidler, P. M.; Patel, H. J.; Sun, W.; Yang, C.; Que, N. S.; Taldone, T.; Finotti, P.; Stephani, R. A.; Gewirth, D. T.; Chiosis, G., Paralog-selective Hsp90 inhibitors define tumor-specific regulation of HER2. *Nature Chemical Biology* **2013**, *9* (11), 677-684.
106. Jeso, V.; Cherry, L.; Macklin, T. K.; Pan, S. C.; LoGrasso, P. V.; Micalizio, G. C., Convergent synthesis and discovery of a natural product-inspired paralog-selective Hsp90 inhibitor. *Organic Letters* **2011**, *13* (19), 5108-5111.
107. Hartson, S. D.; Thulasiraman, V.; Huang, W.; Whitesell, L.; Matts, R. L., Molybdate Inhibits Hsp90, Induces Structural Changes in Its C-Terminal Domain and Alters Its Interactions with Substrates. *Biochemistry* **1999**, *1999* (38), 3837-3849.
108. Marcu, M. G.; Chadli, A.; Bouhouche, I.; Catelli, M.; Neckers, L. M., The Heat Shock Protein 90 Antagonist Novobiocin Interacts with a Previously Unrecognized ATP-binding Domain in the Carboxyl Terminus of the Chaperone. *The Journal of Biological Chemistry* **2000**, *275* (47), 37181-6.
109. Yun, B.-G.; Huang, W.; Leach, N.; Hartson, S. D.; Matts, R. L., Novobiocin Induces a Distinct Conformation of Hsp90 and Alters Hsp90-Cochaperone-Client Interactions. *Biochemistry* **2004**, *43*, 8217-8229.

110. Söti, C.; Rácz, A.; Csermely, P., A Nucleotide-dependent molecular switch controls ATP binding at the C-terminal domain of Hsp90. N-terminal nucleotide binding unmasks a C-terminal binding pocket. *The Journal Biological Chemistry* **2002**, *277* (9), 7066-75.
111. Garnier, C.; Lafitte, D.; Tsvetkov, P. O.; Barbier, P.; Leclerc-Devin, J.; Millot, J.-M.; Briand, C.; Makarov, A. A.; Catelli, M. G.; Peyrot, V., Binding of ATP to Heat Shock Protein 90: Evidence for an ATP-Binding Site in the C-terminal Domain. *The Journal of Biological Chemistry* **2002**, *277* (14), 12208-14.
112. Söti, C.; Vermes, Á.; Haystead, T. A. J.; Csermely, P., Comparative Analysis of the ATP-Binding Sites of Hsp90 by Nucleotide Affinity Cleavage: a Distinct Nucleotide Specificity of the C-terminal ATP-binding Site. *European Journal of Biochemistry* **2003**, *270* (11), 2421-2428.
113. Cunningham, C. N.; Krukenberg, K. A.; Agard, D. A., Intra- and Intermonomer Interactions are Required to Synergistically Facilitate ATP Hydrolysis in Hsp90. *The Journal of Biological Chemistry* **2008**, *283* (30), 21170-8.
114. Retzlaff, M.; Stahl, M.; Eber, H. C.; Lagleder, S.; Beck, J.; Kessler, H.; Buchner, J., Hsp90 is Regulated by a Switch Point in the C-Terminal Domain. *EMBO Reports* **2009**, *10* (10), 1147-53.
115. Matts, R. L.; Dixit, A.; Peterson, L. B.; Sun, L.; Voruganti, S.; Kalyanaraman, P.; Hartson, S. D.; Verkhivker, G. M.; Blagg, B. S., Elucidation of the Hsp90 C-Terminal Inhibitor Binding Site. *ACS Chemical Biology* **2011**, *6* (8), 800-7.
116. Ratzke, C.; Mickler, M.; Hellenkamp, B.; Buchner, J.; Hugel, T., Dynamics of Heat Shock Protein 90 C-terminal dimerization is an important part of its conformational cycle. *Proceedings of the National Academy of Sciences* **2010**, *107* (37), 16101-16106.

117. Yu, X. M.; Shen, G.; Neckers, L.; Blake, H.; Holzbeierlein, J.; Cronk, B.; Blagg, B. S. J., Hsp90 Inhibitor Identified From a Library of Novobiocin Analogues. *Journal of the American Chemical Society* **2005**, *127*, 12778-12779.
118. Burlison, J. A.; Neckers, L.; Smith, A. B.; Maxwell, A.; Blagg, B. S. J., Novobiocin-Redesigning a DNA Gyrase Inhibitor for Selective Inhibitor of Hsp90. *Journal of the American Chemical Society* **2006**, *128* (15529-15536).
119. Donnelly, A. C.; Mays, J. R.; Burlinson, J. A.; Nelson, J. T.; Vielhauer, G.; Holzbeierlein, J.; Blagg, B. S. J., The Design, Synthesis and Evaluation of Coumarin Ring Derivatives of the Novobiocin Scaffold that Exhibit Antiproliferative Activity. *Journal of Organic Chemistry* **2008**, *73*, 8901-8920.
120. Eskew, J. D.; Sadikot, T.; Morales, P.; Duren, A.; Dunwiddie, I.; Swink, M.; Zhang, X.; Hembruff, S.; Donnelly, A.; Rajewski, R. A.; Blagg, B. S.; Manjarrez, J. R.; Matts, R. L.; Holzbeierlein, J. M.; Vielhauer, G. A., Development and Characterization of a Novel C-Terminal Inhibitor of Hsp90 in Androgen Dependent and Independent Prostate Cancer Cells. *BMC cancer* **2011**, *11*, 468.
121. Bras, G. L.; Radanyi, C.; Peyrat, J.-F.; Brion, J.-D.; Alami, M.; Marsaud, V.; Stella, B.; Renoir, J.-M., New Novobiocin Analogues as Antiproliferative Agents in Breast Cancer Cells and Potential Inhibitors of Heat Shock Protein 90. *Journal of Medicinal Chemistry* **2007**, *50*, 6189-6200.
122. Radanyi, C.; Bras, G. L.; Messaoudi, S.; Bouclier, C.; Peyrat, J.-F.; Brion, J.-D.; Marsaud, V.; Renoir, J.-M.; Alami, M., Synthesis and Biological Activity of Simplified Denoviose-Coumarins Related to Novobiocin as Potent Inhibitors of Heat-Shock Protein 90 (hsp90). *Bioorganic & Medicinal Chemistry Letters* **2008**, *18* (7), 2495-8.

123. Radanyi, C.; Bras, G. L.; Marsaud, V.; Peyrat, J.-F.; Messaoudi, S.; Catelli, M.-G.; Brion, J.-D.; Alami, M.; Renoir, J.-M., Antiproliferative and Apoptotic Activities of Tosylcyclonovobiocic Acids as Potent Heat Shock Protein 90 Inhibitors in Human Cancer Cells. *Cancer Letters* **2009**, *274* (1), 88-94.
124. Zhao, H.; Moroni, E.; Colombo, G.; Blagg, B. S. J., Identification of a New Scaffold for Hsp90 C-Terminal Inhibition. *ACS Medicinal Chemistry Letters* **2014**, *5* (1), 84-88.
125. Burlison, J. A.; Avila, C.; Vielhauer, G.; Lubbers, D. J.; Holzbeierlein, J.; Blagg, B. S. J., Development of Novobiocin Analogues that Manifest Anti-Proliferative Activity Against Several Cancer Cell Lines. *Journal of Organic Chemistry* **2008**, *73*, 2130-2137.
126. Peterson, L. B.; Blagg, B. S., Click Chemistry to Probe Hsp90: Synthesis and Evaluation of a Series of Triazole-Containing Novobiocin Analogues. *Bioorganic & Medicinal Chemistry Letters* **2010**, *20* (13), 3957-60.
127. Gunaherath, G. M. K. B.; Marron, M. T.; Wijeratne, E. M. K.; Whitesell, L.; Gunatilaka, A. A. L., Synthesis and Biological Evaluation of Novobiocin Analogues as Potential Heat Shock Protein 90 Inhibitors. *Bioorganic & Medicinal Chemistry* **2013**, *21* (17), 5118-29.
128. Zhao, H.; Donnelly, A. C.; Kusuma, B. R.; Brandt, G. E.; Brown, D.; Rajewski, R. A.; Vielhauer, G.; Holzbeierlein, J.; Cohen, M. S.; Blagg, B. S., Engineering an antibiotic to fight cancer: optimization of the novobiocin scaffold to produce anti-proliferative agents. *Journal of Medicinal Chemistry* **2011**, *54* (11), 3839-53.
129. Shelton, S. N.; Shawgo, M. E.; Matthews, S. B.; Lu, Y.; Donnelly, A. C.; Szabla, K.; Tanol, M.; Vielhauer, G. A.; Rajewski, R. A.; Matts, R. L.; Blagg, B. S.; Robertson, J. D., KU135, a novel novobiocin-derived C-terminal inhibitor of the 90-kDa heat shock protein, exerts

- potent antiproliferative effects in human leukemic cells. *Molecular Pharmacology* **2009**, *76* (6), 1314-22.
130. Kusuma, B. R.; Duerfeldt, A. S.; Blagg, B. S. J., Synthesis and Biological Evaluation of Arylated Novobiocin Analogs as Hsp90 Inhibitors. *Bioorganic & Medicinal Chemistry Letters* **2011**, *21* (23), 7170-7174.
131. Donnelly, A. C.; Zhao, H.; Kusuma, B. R.; Blagg, B. S. J., Cytotoxic Sugar Analogues of an Optimized Novobiocin Scaffold. *Medicinal Chemistry Communication* **2010**, *1* (2), 165-170.
132. Shelton, S. N.; Shawgo, M. E.; Matthews, S. B.; Lu, Y.; Donnelly, A. C.; Szabla, K.; Tanol, M.; Vielhauer, G. A.; Rajewski, R. A.; Matts, R. L.; Blagg, B. S. J.; Robertson, J. D., KU135, a Novel Novobiocin-Derived C-Terminal Inhibitor of the 90-kDa Heat Shock Protein, Exerts Potent Antiproliferative Effects in Human Leukemic Cells. *Molecular Pharmacology* **2009**, *76* (6), 1314-22.
133. Yin, Z.; Henry, E. C.; Gasiewicz, T. A., (-)-Epigallocatechin-3-gallate Is a Novel Hsp90 Inhibitor. *Biochemistry* **2009**, *48*, 336-345.
134. Abenavoli, L.; Capasso, R.; Milic, N.; Capasso, F., Milk Thistle in Liver Diseases: Past, Present, Future. *Phytotherapy Research : PTR* **2010**, *24* (10), 1423-32.
135. Palermo, C. M.; Westlake, C. A.; Gasiewicz, T. A., Epigallocatechin Gallate Inhibits Aryl Hydrocarbon Receptor Gene Transcription through an Indirect Mechanism Involving Binding to a 90 kDa Heat Shock Protein. *Biochemistry* **2005**, *44*, 5041-5052.
136. Khandelwal, A.; Hall, J. A.; Blagg, B. S., Synthesis and Structure-Activity Relationships of EGCG Analogues, a Recently Identified Hsp90 Inhibitor. *The Journal of Organic Chemistry* **2013**, *78* (16), 7859-84.

137. Lu, P.; Mamiya, T.; Lu, L. L.; Mouri, A.; Niwa, M.; Hiramatsu, M.; Zou, L. B.; Nagai, T.; Ikejima, T.; Nabeshima, T., Silibinin Attenuates Amyloid Beta(25-35) Peptide-Induced Memory Impairments: Implication of Inducible Nitric-Oxide Synthase and Tumor Necrosis Factor-Alpha in Mice. *The Journal of Pharmacology and Experimental Therapeutics* **2009**, *331* (1), 319-26.
138. Zhao, H.; Brandt, G. E.; Galam, L.; Matts, R. L.; Blagg, B. S. J., Identification and Initial SAR of Silybin: an Hsp90 Inhibitor. *Bioorganic & Medicinal Chemistry Letters* **2011**, *21* (9), 2659-64.
139. Zhao, H.; Yan, B.; Peterson, L. B.; Blagg, B. S. J., 3-Arylcoumarin Derivatives Manifest Anti-proliferative Activity through Hsp90 Inhibition. *ACS Medicinal Chemistry Letters* **2012**, *3* (4), 327-331.
140. Mollapour, M.; Bourboulia, D.; Beebe, K.; Woodford, Mark R.; Polier, S.; Hoang, A.; Chelluri, R.; Li, Y.; Guo, A.; Lee, M.-J.; Fotooh-Abadi, E.; Khan, S.; Prince, T.; Miyajima, N.; Yoshida, S.; Tsutsumi, S.; Xu, W.; Panaretou, B.; Stetler-Stevenson, William G.; Bratslavsky, G.; Trepel, Jane B.; Prodromou, C.; Neckers, L., Asymmetric Hsp90 N Domain SUMOylation Recruits Aha1 and ATP-Competitive Inhibitors. *Molecular Cell* **2014**, *53* (2), 317-329.
141. Mollapour, M.; Neckers, L., Post-translational modifications of Hsp90 and their contributions to chaperone regulation. *Biochimica et Biophysica Acta (BBA) - Molecular Cell Research* **2012**, *1823* (3), 648-655.
142. Walton-Diaz, A.; Khan, S.; Bourboulia, D.; Trepel, J. B.; Neckers, L.; Mollapour, M., Contributions of co-chaperones and post-translational modifications towards Hsp90 drug sensitivity. *Future Medicinal Chemistry* **2013**, *5* (9), 1059-1071.

143. Miyata, Y., Protein Kinase CK2 in Health and Disease. *Cellular and Molecular Life Sciences* **2009**, *66* (11-12), 1840-1849.
144. Shao, J.; Prince, T.; Hartson, S. D.; Matts, R. L., Phosphorylation of Serine 13 Is Required for the Proper Function of the Hsp90 Co-chaperone, Cdc37. *Journal of Biological Chemistry* **2003**, *278* (40), 38117-38120.
145. Bandhakavi, S.; McCann, R. O.; Hanna, D. E.; Glover, C. V. C., A Positive Feedback Loop between Protein Kinase CKII and Cdc37 Promotes the Activity of Multiple Protein Kinases. *Journal of Biological Chemistry* **2003**, *278* (5), 2829-2836.
146. Bansal, P. K.; Mishra, A.; High, A. A.; Abdulle, R.; Kitagawa, K., Sgt1 Dimerization Is Negatively Regulated by Protein Kinase CK2-mediated Phosphorylation at Ser361. *Journal of Biological Chemistry* **2009**, *284* (28), 18692-18698.
147. Kobayashi, T.; Nakatani, Y.; Tanioka, T.; Tsujimoto, M.; Nakajo, S.; Nakaya, K.; Murakami, M.; Kudo, I., Regulation of cytosolic prostaglandin E synthase by phosphorylation. *Biochemistry Journal* **2004**, *381* (1), 59-69.
148. Miyata, Y.; Chambraud, B.; Radanyi, C.; Leclerc, J.; Lebeau, M.-C.; Renoir, J.-M.; Shirai, R.; Catelli, M.-G.; Yahara, I.; Baulieu, E.-E., Phosphorylation of the immunosuppressant FK506-binding protein FKBP52 by casein kinase II: Regulation of HSP90-binding activity of FKBP52. *Proceedings of the National Academy of Sciences* **1997**, *94* (26), 14500-14505.
149. Yu, X.; Guo, Z. S.; Marcu, M. G.; Neckers, L.; Nguyen, D. M.; Chen, G. A.; Schrupp, D. S., Modulation of p53, ErbB1, ErbB2, and Raf-1 Expression in Lung Cancer Cells by Depsipeptide FR901228. *Journal of the National Cancer Institute* **2002**, *94* (7), 504-513.
150. Nimmanapalli, R.; Fuino, L.; Bali, P.; Gasparetto, M.; Glozak, M.; Tao, J.; Moscinski, L.; Smith, C.; Wu, J.; Jove, R.; Atadja, P.; Bhalla, K., Histone Deacetylase Inhibitor LAQ824 Both

Lowers Expression and Promotes Proteasomal Degradation of Bcr-Abl and Induces Apoptosis of Imatinib Mesylate-sensitive or -refractory Chronic Myelogenous Leukemia-Blast Crisis Cells.

Cancer Research **2003**, *63* (16), 5126-5135.

151. Nimmanapalli, R.; Fuino, L.; Stobaugh, C.; Richon, V.; Bhalla, K., Cotreatment with the histone deacetylase inhibitor suberoylanilide hydroxamic acid (SAHA) enhances imatinib-induced apoptosis of Bcr-Abl-positive human acute leukemia cells. *Blood* **2003**, *101* (8), 3236-3239.

152. Bali, P.; Pranpat, M.; Bradner, J.; Balasis, M.; Fiskus, W.; Guo, F.; Rocha, K.; Kumaraswamy, S.; Boyapalle, S.; Atadja, P.; Seto, E.; Bhalla, K., Inhibition of Histone Deacetylase 6 Acetylates and Disrupts the Chaperone Function of Heat Shock Protein 90: A Novel Basis For Antileukemia Activity of Histone Deacetylase Inhibitors. *Journal of Biological Chemistry* **2005**, *280* (29), 26729-26734.

153. Kovacs, J. J.; Murphy, P. J. M.; Gaillard, S.; Zhao, X.; Wu, J.-T.; Nicchitta, C. V.; Yoshida, M.; Toft, D. O.; Pratt, W. B.; Yao, T.-P., HDAC6 Regulates Hsp90 Acetylation and Chaperone-Dependent Activation of Glucocorticoid Receptor. *Molecular Cell* **2005**, *18* (5), 601-607.

154. Kekatpure, V. D.; Dannenberg, A. J.; Subbaramaiah, K., HDAC6 Modulates Hsp90 Chaperone Activity and Regulates Activation of Aryl Hydrocarbon Receptor Signaling. *Journal of Biological Chemistry* **2009**, *284* (12), 7436-7445.

155. Murphy, P. J. M.; Morishima, Y.; Kovacs, J. J.; Yao, T.-P.; Pratt, W. B., Regulation of the Dynamics of hsp90 Action on the Glucocorticoid Receptor by Acetylation/Deacetylation of the Chaperone. *Journal of Biological Chemistry* **2005**, *280* (40), 33792-33799.

156. Lees-Miller, S. P.; Anderson, C. W., The human double-stranded DNA-activated protein kinase phosphorylates the 90-kDa heat-shock protein, hsp90 alpha at two NH₂-terminal threonine residues. *Journal of Biological Chemistry* **1989**, *264* (29), 17275-17280.
157. Old, W. M.; Shabb, J. B.; Houel, S.; Wang, H.; Coutts, K. L.; Yen, C.-y.; Litman, E. S.; Croy, C. H.; Meyer-Arendt, K.; Miranda, J. G.; Brown, R. A.; Witze, E. S.; Schweppe, R. E.; Resing, K. A.; Ahn, N. G., Functional Proteomics Identifies Targets of Phosphorylation by B-Raf Signaling in Melanoma. *Molecular Cell* **2009**, *34* (1), 115-131.
158. Barati, M. T.; Rane, M. J.; Klein, J. B.; McLeish, K. R., A Proteomic Screen Identified Stress-Induced Chaperone Proteins as Targets of Akt Phosphorylation in Mesangial Cells. *Journal of Proteome Research* **2006**, *5* (7), 1636-1646.
159. Duval, M.; Le Bœuf, F.; Huot, J.; Gratton, J.-P., Src-mediated Phosphorylation of Hsp90 in Response to Vascular Endothelial Growth Factor (VEGF) Is Required for VEGF Receptor-2 Signaling to Endothelial NO Synthase. *Molecular Biology of the Cell* **2007**, *18* (11), 4659-4668.
160. Lei, H.; Venkatakrishnan, A.; Yu, S.; Kazlauskas, A., Protein Kinase A-dependent Translocation of Hsp90 α Impairs Endothelial Nitric-oxide Synthase Activity in High Glucose and Diabetes. *Journal of Biological Chemistry* **2007**, *282* (13), 9364-9371.
161. Wang, X.; Song, X.; Zhuo, W.; Fu, Y.; Shi, H.; Liang, Y.; Tong, M.; Chang, G.; Luo, Y., The regulatory mechanism of Hsp90alpha secretion and its function in tumor malignancy. *Proceedings of the National Academy of Sciences of the United States of America* **2009**, *106* (50), 21288-93.
162. Lees-Miller, S. P.; Anderson, C. W., Two human 90-kDa heat shock proteins are phosphorylated in vivo at conserved serines that are phosphorylated in vitro by casein kinase II. *Journal of Biological Chemistry* **1989**, *264* (5), 2431-2437.

163. Kurokawa, M.; Zhao, C.; Reya, T.; Kornbluth, S., Inhibition of Apoptosome Formation by Suppression of Hsp90 β Phosphorylation in Tyrosine Kinase-Induced Leukemias. *Molecular and Cellular Biology* **2008**, *28* (17), 5494-5506.
164. Mollapour, M.; Tsutsumi, S.; Donnelly, A. C.; Beebe, K.; Tokita, M. J.; Lee, M.-J.; Lee, S.; Morra, G.; Bourboulia, D.; Scroggins, B. T.; Colombo, G.; Blagg, B. S.; Panaretou, B.; Stetler-Stevenson, W. G.; Trepel, J. B.; Piper, P. W.; Prodromou, C.; Pearl, L. H.; Neckers, L., Swe1/Wee1-Dependent Tyrosine Phosphorylation of Hsp90 Regulates Distinct Facets of Chaperone Function. *Molecular Cell* **2010**, *37* (3), 333-343.
165. Martínez-Ruiz, A.; Villanueva, L.; de Orduña, C. G.; López-Ferrer, D.; Higuera, M. Á.; Tarín, C.; Rodríguez-Crespo, I.; Vázquez, J.; Lamas, S., S-nitrosylation of Hsp90 promotes the inhibition of its ATPase and endothelial nitric oxide synthase regulatory activities. *Proceedings of the National Academy of Sciences of the United States of America* **2005**, *102* (24), 8525-8530.
166. Retzlaff, M.; Stahl, M.; Eberl, H. C.; Lagleder, S.; Beck, J.; Kessler, H.; Buchner, J., Hsp90 is regulated by a switch point in the C-terminal domain. *EMBO reports* **2009**, *10* (10), 1147-1153.
167. Carbone, D. L.; Doorn, J. A.; Kiebler, Z.; Ickes, B. R.; Petersen, D. R., Modification of Heat Shock Protein 90 by 4-Hydroxynonenal in a Rat Model of Chronic Alcoholic Liver Disease. *Journal of Pharmacology and Experimental Therapeutics* **2005**, *315* (1), 8-15.
168. Blank, M.; Mandel, M.; Keisari, Y.; Meruelo, D.; Lavie, G., Enhanced Ubiquitinylation of Heat Shock Protein 90 as a Potential Mechanism for Mitotic Cell Death in Cancer Cells Induced with Hypericin. *Cancer Research* **2003**, *63* (23), 8241-8247.

169. Murtagh, J.; Lu, H.; Schwartz, E. L., Taxotere-Induced Inhibition of Human Endothelial Cell Migration Is a Result of Heat Shock Protein 90 Degradation. *Cancer Research* **2006**, *66* (16), 8192-8199.

2. Development of Noviomimetics that Modulate Molecular Chaperones and Manifest Neuroprotective Effects

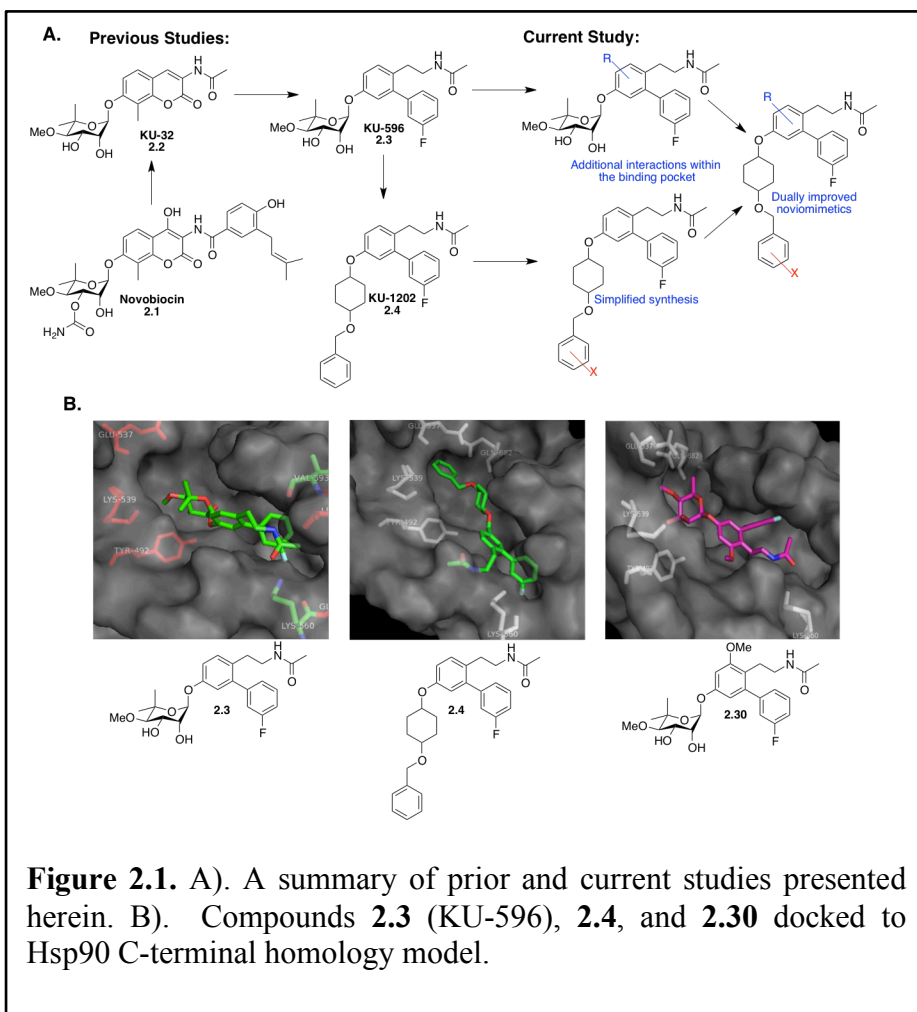
Introduction

Molecular chaperones represent promising therapeutic targets for both cancer and neurodegenerative diseases.¹⁻⁴ The 90kDa Heat Shock Protein 90 (Hsp90) is a molecular chaperone that is responsible for the folding and maturation of more than 300 client protein substrates.⁵ Hsp90 modulates client protein substrates associated with all 10 hallmarks of cancer, supporting that inhibition of this chaperone may be useful for the treatment of cancer.⁶⁻⁸ However, Hsp90 is also a target for neurodegenerative diseases since molecular chaperones can refold denatured proteins and resolubilize protein aggregates.^{3, 9-14} The N-terminus of Hsp90 contains an ATP-binding site, and ATP hydrolysis provides the requisite energy needed to fold client protein substrates.¹⁵⁻¹⁶ Currently, there are six N-terminal inhibitors undergoing clinical evaluation for the potential treatment of cancer.¹⁷⁻¹⁸ Unfortunately, inhibition of the N-terminus and subsequent client protein degradation also leads to induction of the heat shock response (HSR), which results in the overexpression of the heat shock proteins, Hsp27, Hsp40, Hsp70 and Hsp90.¹⁹⁻²¹ In contrast to N-terminal inhibitors, C-terminal inhibitors can segregate client protein degradation from induction of the pro-survival heat shock response.²²

The DNA gyrase inhibitor, novobiocin (**2.1**), was the first Hsp90 C-terminal inhibitor discovered.²³ Through extensive structure-activity relationships, the natural product was modified to exhibit anti-proliferative activity.²⁴⁻²⁶ Continued development of the potential cancer therapeutics led to the identification of cytotoxic replacements of the noviose sugar,²⁷⁻²⁹ which improved inhibitor synthesis, as well as the identification of new cores that target Hsp90, which

could be used in lieu of the coumarin core.³⁰⁻³³ These cytotoxic compounds provide an excellent platform for the treatment of cancer, as these analogs cause degradation of Hsp90-client proteins and leads to the disruption of multiple oncogenic pathways.²

Concurrently, structure-activity relationship studies identified KU-32 (**2.2**), which was shown to manifest neuroprotective activity in cellular models of Alzheimer's disease.³⁴⁻³⁵ Inhibition of Hsp90 by **2.2** results in induction of Hsp70, which decreases the levels of abnormal proteins, prevents aggregation of proteins, and ultimately alleviates the phenotype of many neurodegenerative disorders.³⁶ Subsequent studies demonstrated that **2.2** reversed clinical symptoms of Diabetic Peripheral Neuropathy (DPN) in vivo and protected against neuronal glucotoxicity.³⁷⁻³⁹ A homology model of the Hsp90 C-terminus was utilized to design a second generation of analogues, termed novologues (novobiocin analogues), which exchanged the coumarin core of **2.2** with a biphenyl ring system, and ultimately produced **2.3** (Figure 2.1A: Previous studies).⁴⁰⁻⁴¹ Although **2.3** exhibits promising activity and is undergoing pre-clinical evaluation, modeling studies with **2.3** identified unexplored regions within the C-terminal binding site ultimately led to the identification of noviomimetics (a non-noviosylated compound) **2.4**.⁴² Preliminary studies with **2.4** confirmed that these noviomimetics maintained the desired biological activity of **2.3**, but are more synthetically desirable due to removal of the complex noviose sugar.⁴²⁻⁴⁶ As a result, a new library of novologues and noviomimetics was designed in which modifications were incorporated to gain additional interactions with the binding pocket (Figure 2.1A: Current Study). Several compounds obtained from this third generation library exhibit improved activity as compared to **2.3** and **2.4**.

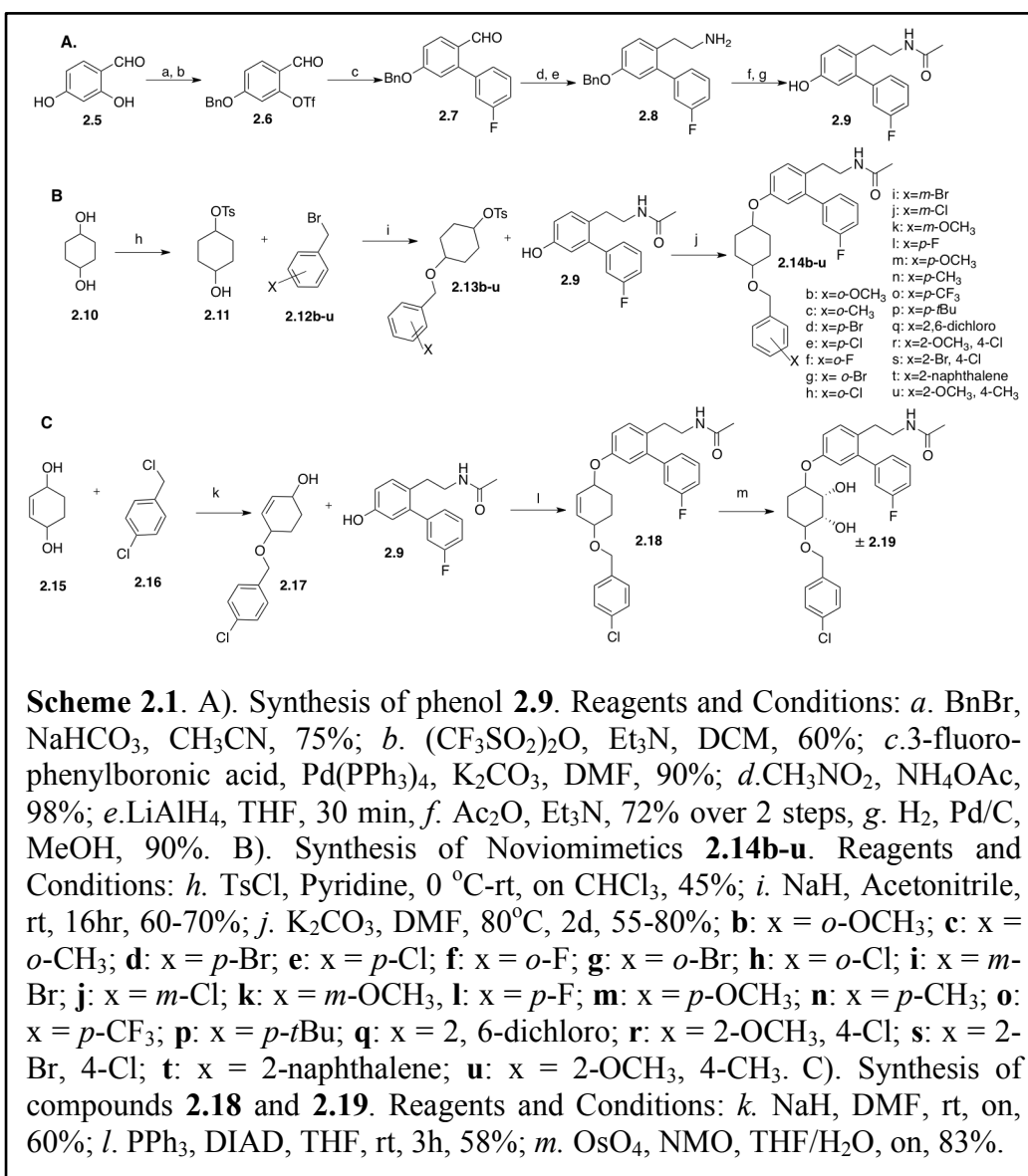


Results and Discussion

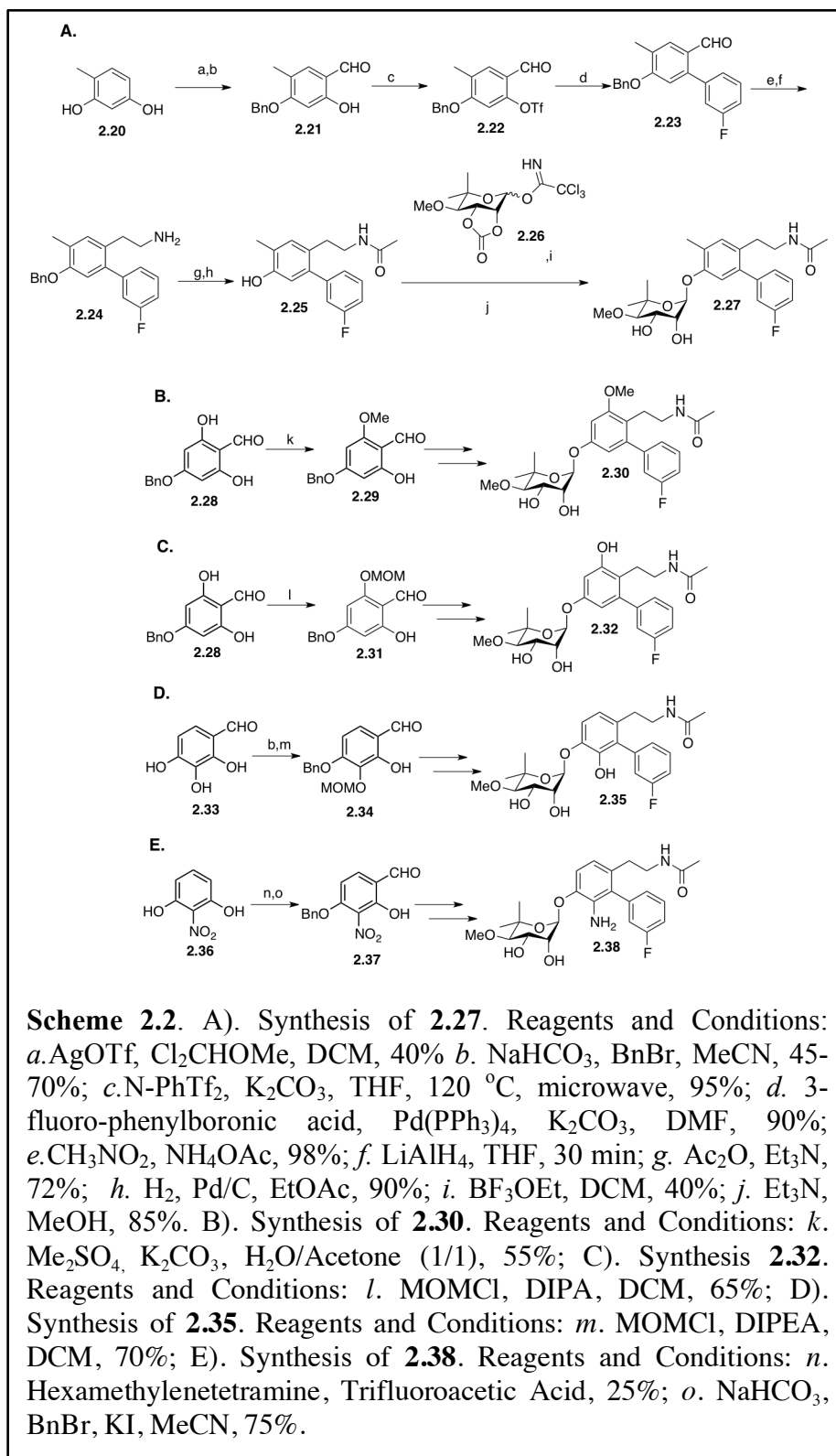
A homology model of the Hsp90 C-terminus was utilized for the design of new novologues, and demonstrated the potential for a binding pocket adjacent to the noviose sugar of **2.3** as illustrated in Figure 2.1B. During prior studies wherein replacements of the noviose sugar were explored, **2.4** was identified as a simplified novologue that exhibited similar biological activity to **2.3**.⁴² As shown in Figure 2.1B, the noviose surrogate could project into this previously unexplored binding pocket and therefore modifications to the benzyl ring on **2.4** were explored to identify improved modulators. Modifications at the *ortho*- position were

investigated to determine whether hydrogen bonding interactions could be established with GLU537, GLN682, or nearby amino acids (Figure 2.1B). Substituents at the *meta*- and *para*-positions were explored to identify potential hydrophobic interactions at this location. In addition, modification to the central ring of **2.3** was sought to determine whether hydrogen bond donors or acceptors would enhance interaction with the binding pocket (Figure 2.1B). Substituents chosen for these studies included both electronic and steric functionalities to establish preliminary structure-activity relationships.

Synthesis of phenol **2.9**⁴¹ (Scheme 2.1A) commenced by benzyl protection of 2,4-dihydroxybenzaldehyde, **2.5**. The resulting benzyl ether was converted to trifluoromethanesulfonate **2.6**, in the presence of N-Phenyl bis-trifluoromethane sulfonimide and potassium carbonate using microwave conditions.⁴⁷ A subsequent Suzuki coupling reaction with commercially available 3-fluorophenyl boronic acid was employed to generate the biaryl ring system found in **2.7**, which was then subjected to a Henry reaction, followed by simultaneous reduction of both the nitro and olefin functionalities with lithium aluminum hydride to yield amine **2.8**. Acylation of **2.8** was followed by cleavage of the benzyl ether under hydrogenolysis conditions to afford the phenol, **2.9**.



Compounds **2.14b-u** were obtained via an S_N2 substitution reaction between phenol **2.9** and the toluenesulfonates of the corresponding sugar surrogates (Scheme 2.1B).⁴⁸ Compound **2.18** was obtained by a Mitsunobu reaction between phenol **2.9** and the corresponding sugar mimic. Novologue **2.18** was then subjected to an osmium tetroxide catalyzed dihydroxylation to obtain the corresponding diol, **2.19** (Scheme 2.1C).

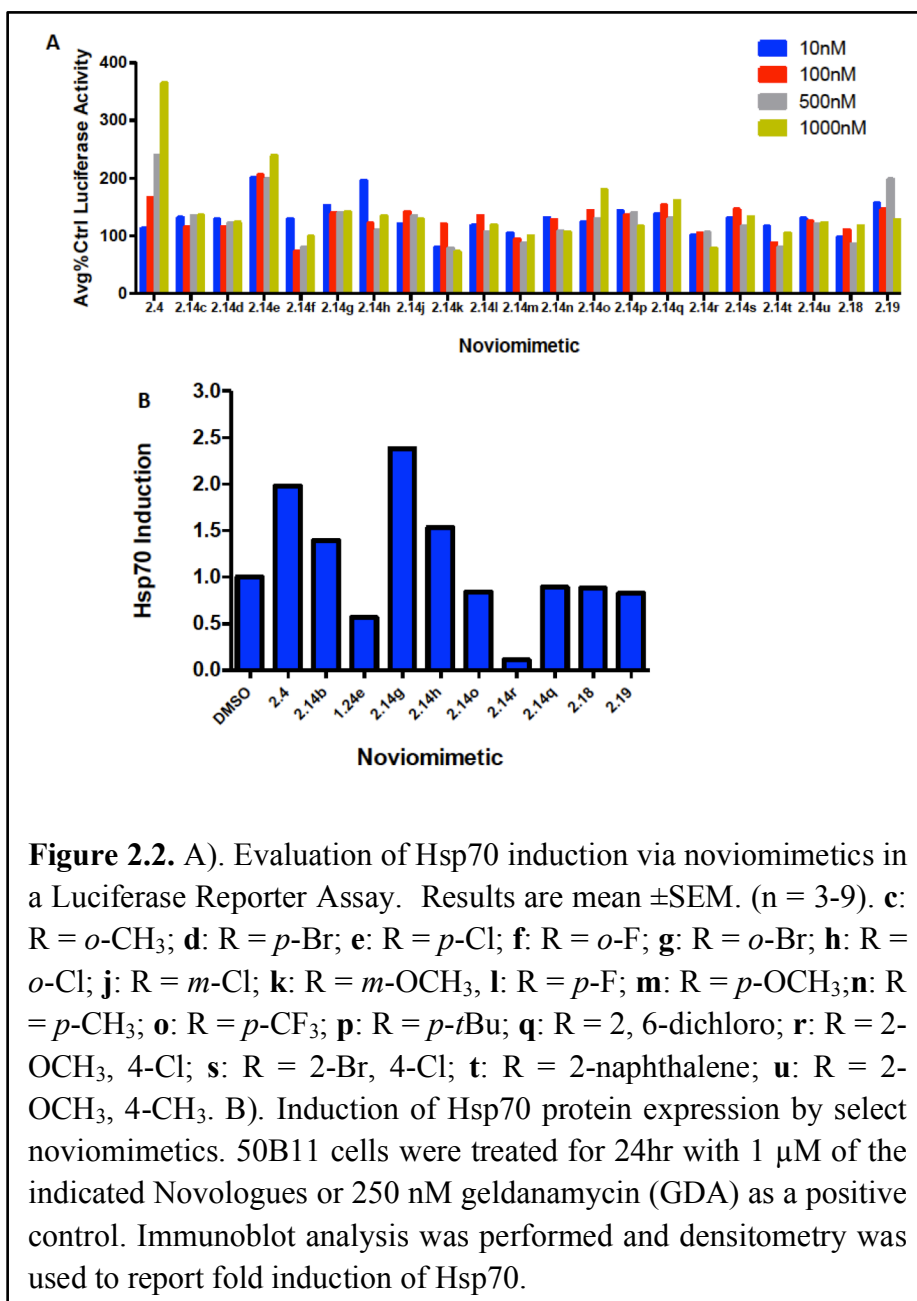


Synthesis of each derivative that contained a modified core began via different starting materials. Synthesis of compound **2.27** commenced by reduction of commercially available 2,4-dihydroxybenzaldehyde with sodium cyanoborohydride in the presence of HCl (Scheme 2.2A).⁴⁹ The resulting methylbenzene (**2.20**) was formylated to obtain 2,4-dihydroxy-5-methylbenzaldehyde, which was then benzyl protected to produce **2.21**.⁵⁰ Compound **2.21** was then subjected to the same conditions utilized to produce phenol **2.9**, and ultimately yielded phenol **2.25** (Scheme 2.2A). The noviose sugar was synthesized using a previously reported procedure.⁴³⁻⁴⁶ The protected sugar was activated (**2.26**)⁵¹⁻⁵² and then coupled with **2.25** using Schmidt conditions.⁵³ Solvolysis of the carbonate with triethylamine and methanol provided the final product, **2.27**. Synthesis of **2.30** and **2.32** began by formylation of phloroglucinol, followed by benzyl protection of 2,4,6-trihydroxybenzaldehyde using potassium carbonate and benzyl bromide to yield **2.28**. To achieve the final product **2.30**, **2.28** was subjected to dimethyl sulfate in water and acetone to yield the methyl ether, **2.29** (Scheme 2.2B).⁵⁴ This key intermediate was then subjected to the conditions previously described in Scheme 2.2B, to obtain **2.30**.

Compound **2.32** was obtained by the treatment of **2.28** with chloromethyl methyl ether to produce the mono-protected phenol **2.31** (Scheme 2.2C),⁵⁵⁻⁵⁶ which was then subjected to the conditions previously described to give **2.32**. Synthesis of compound **2.35** began by selective benzylation of 2,3,4-trihydroxybenzaldehyde, which was then subjected to methoxy methyl ether formation to produce intermediate **2.34**. Similarly, compound **2.34** was subjected to conditions previously described to achieve the free phenol, which was then coupled with the trichloroacetamide of noviose carbonate and upon solvolysis, gave **2.35**. Synthesis of compound **2.38** was initiated by subjecting 2-nitrobenzene 1,3-diol to a Duff reaction.⁵⁷ The resulting

product was then benzyl protected to yield compound **2.37**, which was modified according to the conditions highlighted in Scheme 2.2E to obtain the final product, **2.38**.

We have previously shown that the cytoprotective activity manifested by KU-32 and KU-



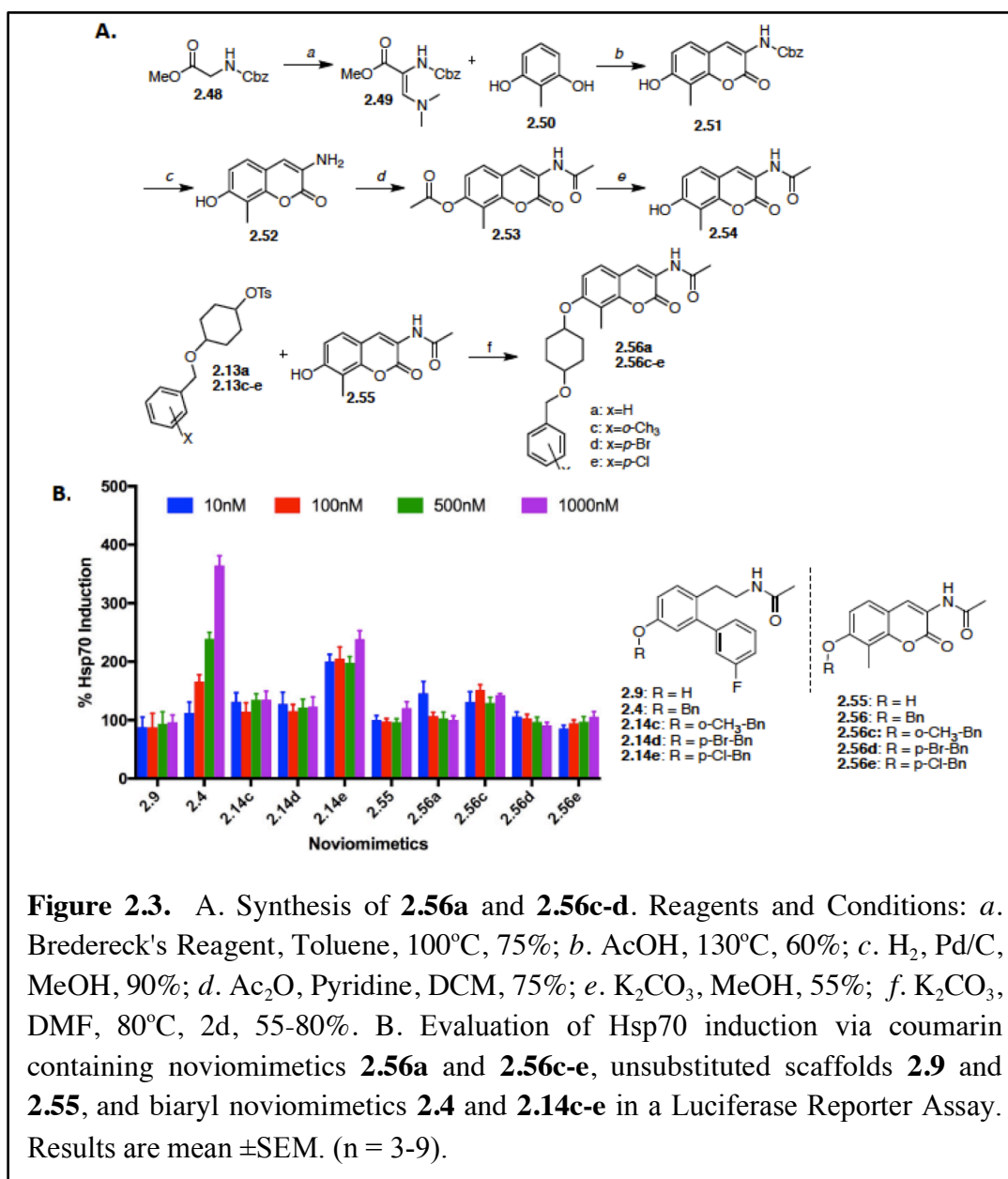
596 requires Hsp70 induction. Therefore, upon construction of the library of noviomimetics, we evaluated Hsp70 induction via a luciferase reporter assay (Figure 2.2A).

As shown in Figure 2.2A, **2.14e** induced the most robust Hsp70 levels for the new noviomimetics. Generally, the noviomimetics with substitutions at the *para*- and *ortho*-positions manifest increased Hsp70 levels in the luciferase reporter assay, Figure 2.2A. Whereas, in the luciferase reporter assay noviomimetics with substitutions at the *meta*-position (**2.14i-k**) appear less favorable as Hsp70 induction was less robust when compared to the similarly substituted *ortho*- and *para*-noviomimetics. The *para*-substituted noviomimetics showed greater induction of Hsp70 than the corresponding *ortho*-noviomimetics (**2.14c**, **2.14f-h**). Generally, electron-withdrawing groups at the *para*- position produced the most Hsp70 induction, followed by electron donating groups at the *ortho*- position. Similarly, *para*-substituted noviomimetic **2.19** contains a cyclohexyl *cis*-diol and also activated the luciferase promoter. The *cis*-diol of **2.19** mimics the noviose sugar more than the unsubstituted cyclohexane ring, which may explain its enhanced activity, Figure 2.2A.

Immunoblot analyses were then performed to further examine the effect of select noviomimetics on Hsp70 protein expression. Compounds **2.4**, **2.14b**, **2.14g**, and **2.14h** resulted in Hsp70 induction, Figure 2.2B. *Meta*-substituted noviomimetics resulted in decreased Hsp70 levels as compared to the similarly substituted *ortho*- and *para*-noviomimetics, **2.14q** and **2.14o**. Dually modified, **2.14r**, demonstrated the least amount of Hsp70 induction, suggesting that the binding pocket does not tolerate modifications at both the *ortho*- and *para*-positions. Surprisingly, **2.19** was less effective in the immunoblot assay, despite promising luciferase activity. Taking the biological activity in both assays into account, noviomimetic side chains on (**2.4** and **2.14 b-e**) were selected for further investigation.

Comparison studies between the noviomimetic side chains and the original KU-32 coumarin scaffold were carried out to further elucidate neuroprotective effects. Additionally,

comparison studies were conducted to determine the core that provides the greatest Hsp70 induction. The coumarin containing noviomimetics (**2.56a** and **2.56c-2.56e**) were synthesized (Figure 2.3A) with selected noviomimetic side chains. Using the luciferase reporter assay, the phenol for each scaffold and noviomimetics **2.56a** and **2.56c-2.56e**, were evaluated (Figure 2.3B). Scaffolds **2.9** and **2.55** did not contain any sugar moiety/surrogate and were found to be inactive. Noviomimetics containing the KU-32 coumarin scaffold exhibited similar or decreased activity compared to their biaryl counterparts (Figure 2.3).



The similar or decreased induction of Hsp70 by **2.56a** and **2.56c-2.56e** could result from the rigid coumarin core. The biphenyl core offers enhanced flexibility that is not available with the coumarin core, which may allow for improved interactions within the binding pocket. Increasing flexibility may also be important due to the increase in length of the noviomimetic side chain as compared to noviose sugar. Substitutions on the central ring were evaluated using immunoblot analysis to observe Hsp70 levels and to support improved interactions with the

binding pocket. The novologues were analyzed at varying concentrations (30, 100, 300, 1000, and 3000nM) as shown in Figure 2.4A.

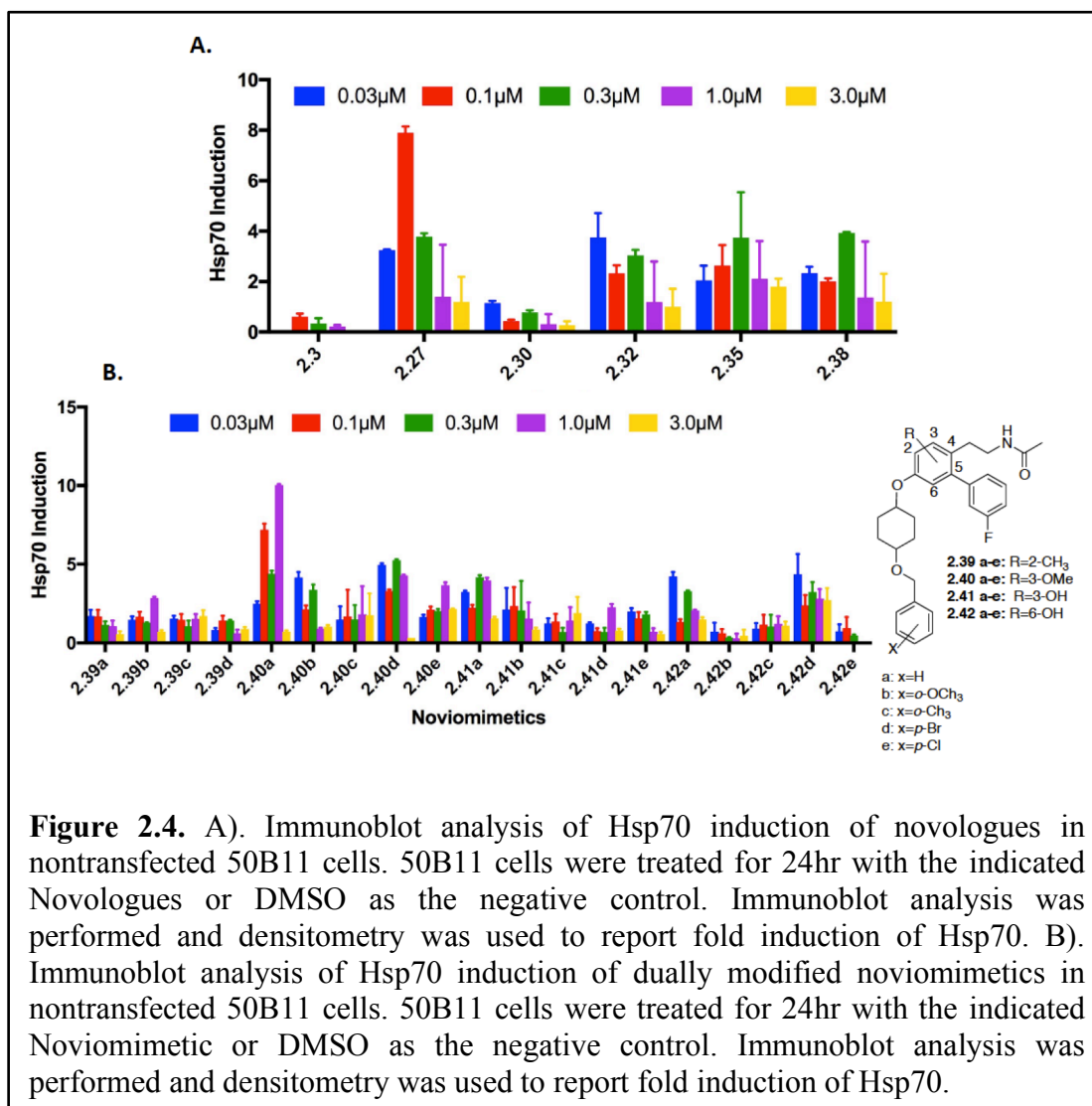


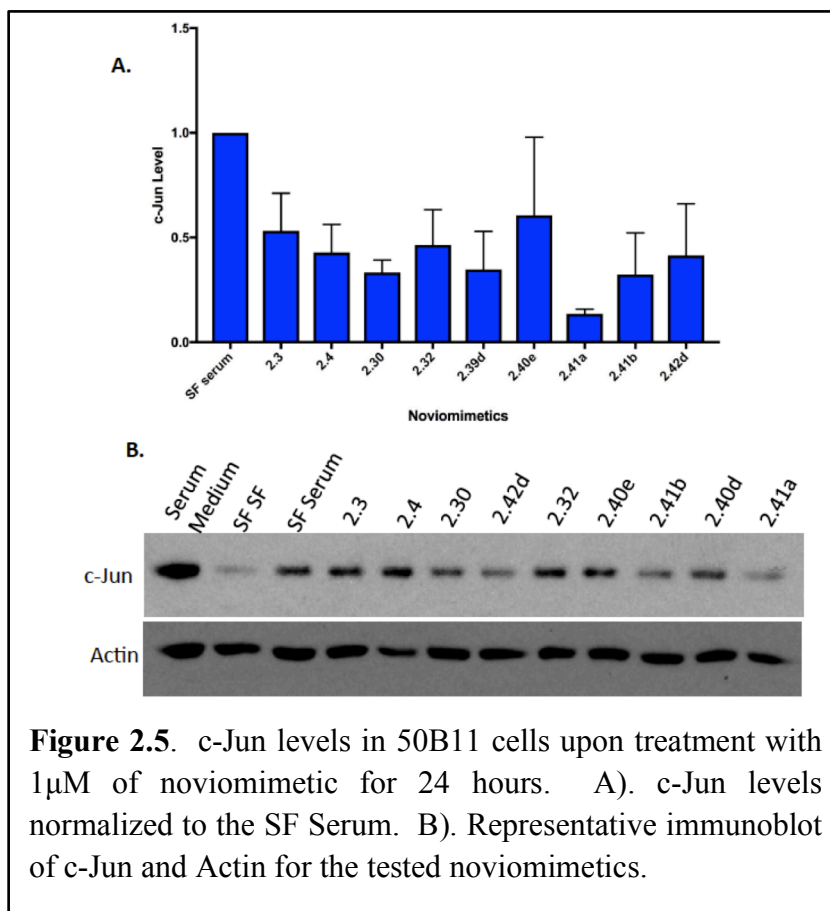
Figure 2.4. A). Immunoblot analysis of Hsp70 induction of novologues in nontransfected 50B11 cells. 50B11 cells were treated for 24hr with the indicated Novologues or DMSO as the negative control. Immunoblot analysis was performed and densitometry was used to report fold induction of Hsp70. B). Immunoblot analysis of Hsp70 induction of dually modified noviomimetics in nontransfected 50B11 cells. 50B11 cells were treated for 24hr with the indicated Noviomimetic or DMSO as the negative control. Immunoblot analysis was performed and densitometry was used to report fold induction of Hsp70.

Novologues containing substituted central rings produced improved Hsp70 induction as compared to **2.3** (Figure 2.4A). Novologues **2.27** and **2.35** resulted in the largest induction of Hsp70. It is possible that the methyl substituent present in **2.27** overlays in three-dimensional space with **2.2**, and reinstates interactions that are lost upon moving from the coumarin to the biphenyl ring system. Furthermore, the data supports the importance of having a hydrophobic substitution on the central core, as **2.27** resulted in the greatest induction of Hsp70. In

continuation, the novologues containing central core substituents were coupled with selected noviomimetics (**2.13a-e**). These noviomimetics were synthesized as described in Scheme 2.2 and then analyzed via immunoblot analysis to evaluate Hsp70 induction.

As shown in Figure 2.4B, noviomimetics **2.40a**, **2.40d**, **2.41a**, and **2.42d** resulted in the greatest Hsp70 induction. Noviomimetics with a methoxy group at the 3-position (**2.40a-e**) generally resulted in increased Hsp70 levels when compared to noviomimetics with other central ring modifications and the same noviomimetic side chain. Interestingly, none of the methyl containing noviomimetics (**2.39a-d**) resulted in improved Hsp70 induction, which was unexpected since **2.27** resulted in the greatest induction of all of the central ring modifications. It is likely that switching from the noviose sugar to a noviomimetic alters binding, and ultimately leads to a decrease in Hsp70 levels. Noviomimetics containing a phenol on the central ring were similarly active when located at the 3- or 6- positions (**2.41a-e** and **2.42a-e**), and only the noviomimetic side chain seemed to impact induction of Hsp70. Noviomimetic side chains **a** and **d** appear to produce the most robust induction of Hsp70, regardless of the central ring modification.

Validation of Hsp90 Inhibition via the c-Jun Assay and Mitochondrial Bioenergetic (mtBE) Assessment



Further assessment of the neuroprotective activity of select noviomimetics was carried out after establishment that the desired cytoprotective response, induction of Hsp70, occurred upon treatment with Hsp90 inhibitors. Noviomimetics **2.30**, **2.32**, **2.40d**, **2.40e**, **2.41a**, **2.41b**, and **2.42d** were selected for further biological evaluation in an assay that evaluates c-jun levels.

Hsp70 regulates c-jun levels by increasing its degradation via the proteasome (Figure 2.5).⁵⁸ Therefore, induction of Hsp70 via noviomimetics results in the degradation of c-jun. The assay was carried out by treating 50B11 cells with serum free media for 24 hours, resulting in cell cycle arrest and a decrease in the expression of c-jun. The cells were then treated with vehicle or 1µM of the indicated noviomimetic, and c-jun was induced by placing the cells in medium containing 10% FBS for 2 hours. The protein was harvested and c-Jun levels were evaluated.

All of the selected noviomimetics decreased c-Jun levels when compared to the untreated control, SF Serum (Figure 2.5). Importantly, most noviomimetics exhibited improved activity when compared to **2.3**, and a few had improved activity as compared to **2.4**. The general trend of the data illustrates that noviomimetics with a free phenol at the 3-position were more effective than noviomimetics with a methoxy at the 3-position. Excitingly, noviomimetic **2.41a** resulted in the greatest reduction in c-Jun levels. Reduction of c-Jun levels by all noviomimetics suggests that the mechanism of action occurs via induction of Hsp70.

Prior work indicated that the neuroprotective efficacy manifested by KU-32 to improve the symptoms of diabetic peripheral neuropathy was associated with an increase in mitochondrial respiration. To determine whether the increase in Hsp70 expression correlated with mitochondrial respiration, 50B11 cells were treated with various noviomimetics for 24 hours

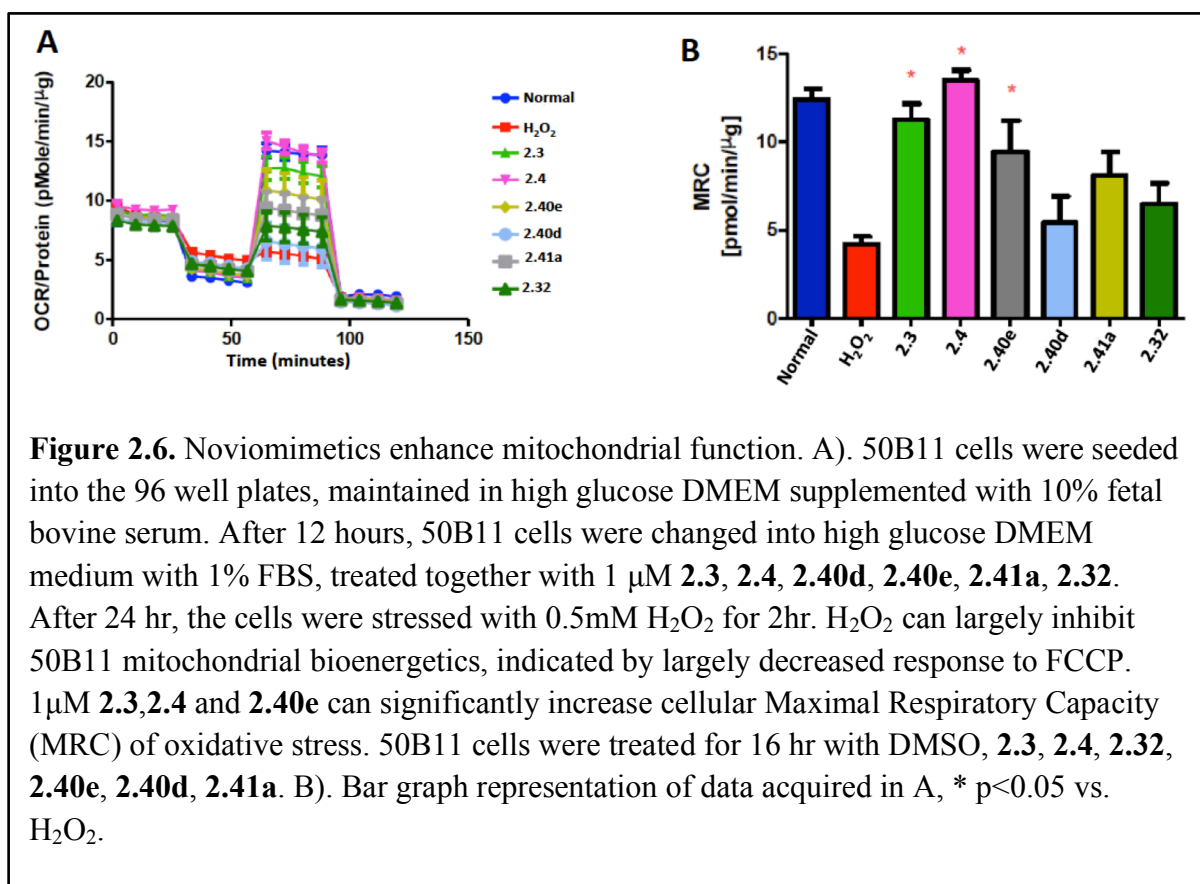


(Figure 2.6). Mitochondrial respiration was then measured in intact cells using an XF96 extracellular flux analyzer, which provides concurrent measures of mitochondrial oxygen consumption rates (OCR) and extracellular acidification rates (ECAR) as an indication of glycolytic activity. A variety of noviomimetics were selected to examine this correlation between Hsp70 expression and mitochondrial respiration effects on mitochondrial respiration.

Hydrogen peroxide can induce cellular apoptosis through mitochondrial dysfunction. 0.5mM hydrogen peroxide can cause mitochondrial bioenergetics (mtBE) loss, indicated by largely decreased response to FCCP. **2.3** and **2.4** effectively improved mtBE, however the dually modified noviomimetics resulted in decreased maximal respiratory capacity (Figure 2.6). Surprisingly, noviomimetic **2.40e** was the most effective at increasing the MRC, even though it was not as efficacious in the c-jun assay as the other noviomimetics. The different results obtained from these two assays are due to each assay relying upon a different cellular mechanism for the analyzed biological result.

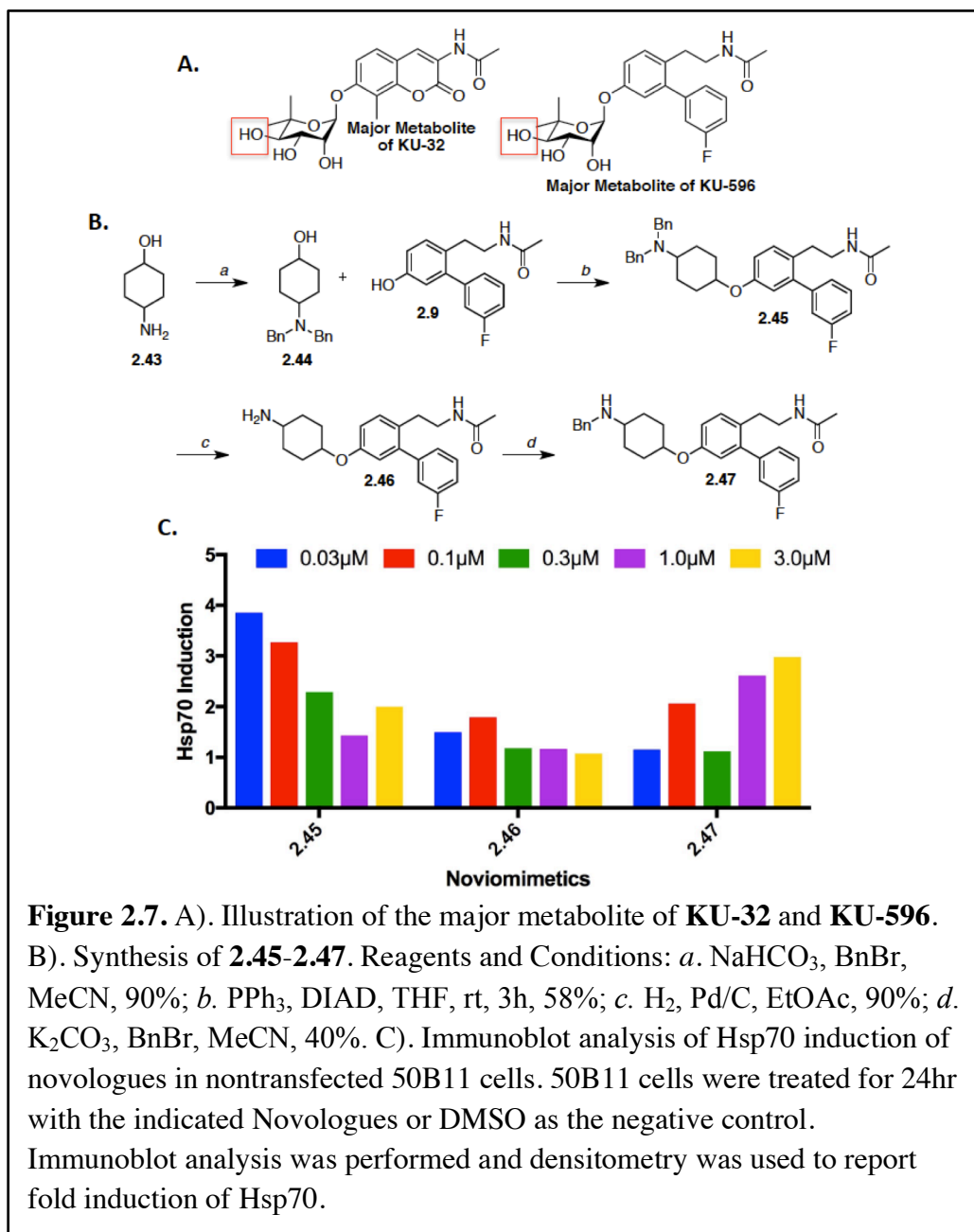
Conclusion

In conclusion, a library of novologues was designed with the goal of replacing the synthetically complex noviose sugar with simplified sugar surrogates. The data support that noviomimetics can successfully retain the ability to increase Hsp70 expression and mitochondrial function, two mechanistic features that are associated with the neuroprotective efficacy of both biaryl-based novologues such as **2.4** and novobiocin-based compounds such as **2.3**. Noviomimetic **2.41a** exhibited promising effects in the c-Jun assay, while **2.40e** was effective at increasing the MRC. Thus, noviomimetics may serve as a new series of simplified,

neuroprotective compounds that may prove useful for the treatment of various neurodegenerative diseases.

Future Directions

We have observed that the major metabolite for both KU-32 and KU-596 lacks the 4'-methyl ether on the noviose sugar and exhibits inconsistent neuroprotective activity (Figure 2.7A). Initial efforts to overcome this short half-life led to the development of noviomimetics like **2.4**, and those investigated in this chapter. Additional efforts can proceed to explore other functional groups that can be used as noviomimetics and exhibit decreased metabolism.



Preliminary exploration led to the synthesis of noviomimetics **2.45-2.47** (Figure 2.7B), which contain a cyclohexylamine group in lieu of the cyclohexane ring. The cyclohexylamine ring was selected because a di-benzylated amine would quickly illustrate how much bulk could be tolerated in the binding pocket while maintaining biological activity. Additionally a di-benzylated amine would be metabolized more slowly than its mono-substituted counterpart,

which is desirable. Immunoblot analysis was used to evaluate Hsp70 induction in 50B11 cells for **2.45-2.47** (Figure 2.7C). Following the trend identified with initial noviomimetics⁴², mono-benzylated **2.47** is more efficacious than non-benzylated **2.46**. Excitingly, **2.45** resulted in the greatest amount of Hsp70 induction. This result highlights that bulk is tolerated within the binding pocket, creating further opportunities to explore different di-substituted amines. These initial results provide an excellent starting point for further exploration of new noviomimetics that contain different di-substituted cyclohexylamine groups and other functional groups that would result in decreased metabolism.

Materials and Methods

Luciferase Reporter Assay, Immunoblot Analysis and Client Protein Degradation

The luciferase reporter assay was performed using a 1.5 kb region upstream of the start codon of the human HSPA1A gene to drive luciferase expression as previously described. 50B11 cells⁵⁹ were grown in 10 cm dishes in maintenance medium and the cells were transfected using lipofectamine. Twenty-four hours after transfection, the cells were re-seeded into 24 well plates at a density of 2×10^5 cells per well. After a 6 hour period to permit attachment, the cells were treated with the indicated compounds for 16 hour. Luciferase activity was assessed and normalized to the total protein concentration of each well.

50B11 cells were treated with the indicated compounds for 24 hours and were scraped into lysis buffer containing 50 mM Tris-HCl, pH 7.4, 150 mM NaCl, 1 mM EDTA, 1% NP-40, 0.5 mM sodium orthovanadate, 40 mM NaF, 10 mM β -glycerophosphate, and Complete Protease Inhibitors (Roche Diagnostics). After 15 minutes on ice, the lysates were sonicated then centrifuged at 10,000 x g for 10 min at 4°C. The protein concentration of the supernatant was

estimated using a Bio-Rad protein assay and bovine serum albumin as the standard. Following SDS-PAGE, the proteins were transferred to nitrocellulose and the membrane incubated with 5% non-fat dry milk in phosphate buffered saline containing 0.1% Tween 20 (PBST) for 1-2hr at room temperature. The blots were probed with primary antibodies recognizing Hsp70 or b-actin at 4°C overnight. The membranes were washed with PBST and subsequently incubated with HRP-conjugated secondary antibodies and immunoreactive proteins were visualized using chemiluminescence detection (GE Healthcare Life Sciences, Little Chalfont, Buckinghamshire, UK). The films were digitally scanned and densitometrically analyzed using ImageJ (NIH) software. Client protein degradation in MCF-7 cells was performed as previously described.⁶⁰

C-jun assay

Immortalized sensory neurons⁶¹ were rendered quiescent to decrease c-jun levels by placing them in serum free medium for 24 hours. During this interval, the cells were treated with vehicle (DMSO or Captisol) or 1 μ M of the indicated compound. C-jun was then upregulated by placing the cells in medium containing 10% serum for 2 hour and cell lysates were collected for western blot analysis. All the data were normalized to c-jun levels in the presence of serum plus vehicle.

Mitochondrial Bioenergetic (mtBE) Assessment

Oxygen consumption rate (OCR) was assessed in the 50B11 transformed sensory neuron cell line, using an XF96 Extracellular Flux Analyzer (Seahorse Biosciences, North Billerica, MA). 50B11 cells were seeded into the 96 well plates at 40,000 cells per well and maintained in high glucose DMEM supplemented with 10% fetal bovine serum (Atlas Biologics, fort Collins

CO), 5 $\mu\text{g/ml}$ blasticidin and antibiotics at 37 °C. The maintenance media was changed to serum free unbuffered DMEM supplemented with 1mM pyruvate and 5.5 mM D-glucose and the cells incubated at 37 °C in room air for one hour before starting the assay. After introducing the plate into the XF96 analyzer, the basal oxygen consumption rate (OCR) was measured prior to the addition of 1 $\mu\text{g/ml}$ oligomycin to inhibit the ATP synthase to measure the portion of the basal OCR that was coupled to ATP synthesis; residual OCR after oligomycin treatment is from uncoupled respiration (proton leak). Next, 1 μM of the protonophore FCCP was injected to dissipate the proton gradient across the inner mitochondrial membrane to measure maximal respiratory capacity (MRC). The final injection of 1 μM rotenone + 1 μM antimycin A was used to assess non-mitochondrial respiration. The XF96 analyzer also measures the rate of extracellular acidification as a marker of glycolytic activity coincident with the assessment of mitochondrial OCR.

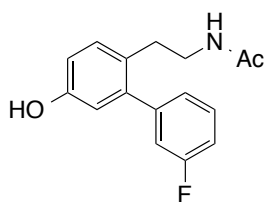
After the respiratory measures, the cells were harvested and the protein content of each well determined using a Bradford protein assay. OCR values were normalized to the total protein content of each well and ATP-linked respiration, proton leak, maximal respiratory capacity, spare respiratory capacity and respiratory control ratio were determined as described.^{60,62}

Chemistry General.

¹H NMR were recorded at 500 MHz (Avance AVIII 500 MHz spectrometer with a dual carbon/proton cryoprobe) or 400 (Bruker AVIIIHD 400 MHz NMR with a broadband X-channel detect gradient probe) and ¹³C NMR were recorded at 125 MHz (Bruker AVIII spectrometer equipped with a cryogenically cooled carbon observe probe). Chemical shifts are reported in δ (ppm) relative to the internal standard (CDCl₃, 7.26 ppm, or as stated). HRMS spectra were

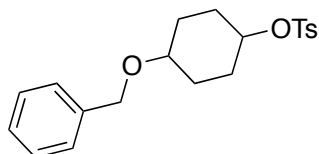
recorded with a LCT Premier with ESI ionization. ^1H and ^{13}C NMR was used to verify that all tested compounds were >95% pure. TLC analysis was performed on glass backed silica gel plates and visualized by UV light. All solvents were reagent grade and used without further purification.

Synthesis and Compound Characterization



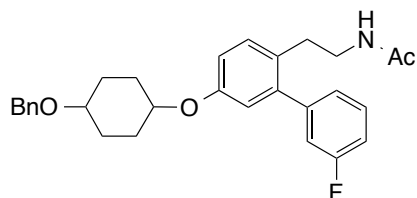
N-(2-(3'-Fluoro-5-hydroxy-[1,1'-biphenyl]-2-yl)ethyl)acetamide (2.9).

Compound **2.9** was synthesized following a previously reported procedure.⁴¹



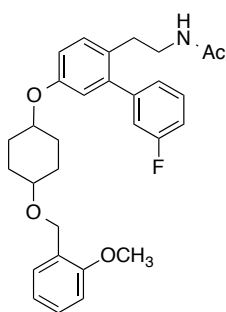
4-(Benzyloxy)cyclohexyl 4-methylbenzenesulfonate.

This compound and the similar side chains were synthesized following a previously reported procedure.^{42, 48}



N-(2-(5-((4-(Benzyloxy)cyclohexyl)oxy)-3'-fluoro-[1,1'-biphenyl]-2-yl)ethyl)acetamide (2.4).

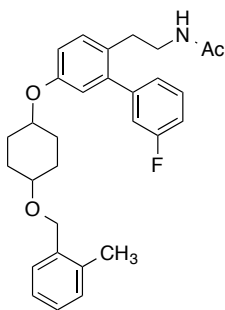
Potassium carbonate (30 mg, 0.19 mmol) was added to a solution of **2.9** (45 mg, 0.16 mmol) in DMF (1 mL) and stirred at rt for 30 min, before 4-(benzyloxy)cyclohexyl 4-methylbenzenesulfonate (75 mg, 0.19 mmol) were added. The solution was heated to 80 °C for 16h. Distilled water (3x 5 mL) was added to the mixture and the organic layer extracted with ethyl acetate. After removal of the solvent on a Rotovap, the crude mixture was purified by column chromatography (Silica gel, 40% EtOAc in hexane) to give **2.4** (8 mg) as a white solid in 75% yield: ¹H NMR (500 MHz, CDCl₃) δ 7.67-7.58 (m, 1H), 7.50-7.46 (m, 1H), 7.41-7.38 (m, 1H), 7.30-7.27 (m, 3H), 7.12 (d, J = 5 Hz, 1H), 7.01-6.92 (m, 3H), 6.82-6.79 (dt, J₁ = 10 Hz, J₂ = 5 Hz, 1H), 6.70-6.67 (dd, J₁ = 10 Hz, J₂ = 5 Hz, 1H), 5.24 (s, 1H), 4.48 (s, 2H), 4.25 (m, 1H), 3.44 (m, 1H), 3.33–3.15 (q, J = 6.7 Hz, 2H), 2.78–2.66 (t, J = 7.2 Hz, 2H), 2.07-1.80 (m, 4H), 1.79 (s, 3H), 1.69-1.61 (m, 2H), 1.50-1.46 (m, 2H). ¹³C NMR (100 MHz, CDCl₃) δ 169.8, 163.4, 156.1, 142.0, 139.0, 132.0, 130.8, 129.8, 128.5, 128.4, 128.3, 128.1, 128.0, 127.4, 124.8, 117.5, 116.0, 115.5, 114.2, 114.1, 74.3, 72.8, 70.1, 40.5, 31.8, 30.9, 28.4, 28.3, 27.4, 23.3. HRMS (ESI+), m/z [M+Na⁺] calculated for C₂₉H₃₂FNO₃Na 484.2264; found 484.2249.



N-(2-(3'-Fluoro-5-(((2-methoxybenzyl)oxy)cyclohexyl)oxy)-[1,1'-biphenyl]-2-yl)ethyl)acetamide (2.14b).

The compound was synthesized following the procedure used for the synthesis of **2.4** to obtain the product as a white solid: ¹H-NMR (400 MHz, Chloroform-d) δ 7.33 (tt, J = 14.7, 7.3

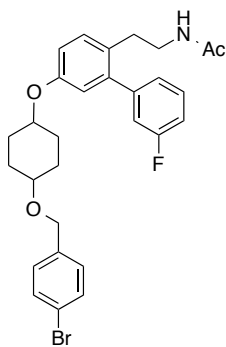
Hz, 2H), 7.23 – 7.06 (m, 2H), 7.04 – 6.85 (m, 4H), 6.79 (dd, $J = 8.0, 5.7$ Hz, 2H), 6.69 (dd, $J = 5.3, 2.2$ Hz, 1H), 5.23 (t, $J = 5.5$ Hz, 1H), 4.51 (s, 2H), 4.31 – 4.17 (m, 1H), 3.75 (s, 3H), 3.45 (td, $J = 7.9, 7.2, 3.5$ Hz, 1H), 3.19 (d, $J = 6.7$ Hz, 2H), 2.65 (t, $J = 7.1$ Hz, 2H), 2.04 (t, $J = 4.1$ Hz, 2H), 1.90 (ddd, $J = 28.1, 12.7, 6.2$ Hz, 2H), 1.79 (s, 3H), 1.67 – 1.58 (m, 2H), 1.55 – 1.41 (m, 2H). ^{13}C NMR (126 MHz, CDCl_3) δ 168.92, 162.45, 160.49, 155.11, 142.58, 141.00, 129.76, 128.84, 127.41, 127.19, 127.02, 126.89, 126.36, 123.81, 119.42, 116.53, 114.46, 112.99, 109.04, 74.57, 73.58, 63.86, 54.26, 39.52, 30.81, 27.44, 26.43, 22.19. HRMS (ESI+), m/z $[\text{M}+\text{Na}^+]$ calculated for $\text{C}_{30}\text{H}_{34}\text{FNO}_4\text{Na}$ 514.2370; found 514.2352.



N-(2-(3'-Fluoro-5-((4-((2-methylbenzyl)oxy)cyclohexyl)oxy)-[1,1'-biphenyl]-2-yl)ethyl)acetamide (2.14c).

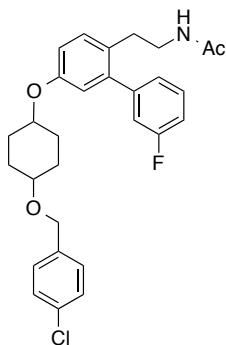
The compound was synthesized following the procedure used for the synthesis of **2.4** to obtain the product as a white solid: ^1H -NMR (500 MHz, Chloroform- d) δ 7.36 (dddd, $J = 14.7, 10.8, 6.6, 2.0$ Hz, 2H), 7.21 – 7.13 (m, 4H), 7.09 – 7.03 (m, 2H), 7.00 (dq, $J = 9.5, 1.1$ Hz, 1H), 6.88 (ddd, $J = 8.5, 4.1, 2.7$ Hz, 1H), 6.76 (dd, $J = 5.8, 2.7$ Hz, 1H), 5.32 – 5.26 (m, 1H), 4.53 (s, 2H), 4.36 (dt, $J = 6.6, 3.4$ Hz, 1H), 4.30 (dq, $J = 8.5, 5.0, 4.1$ Hz, 1H, minor diast.), 3.52 (tt, $J = 6.0, 3.4$ Hz, 1H), 3.27 (td, $J = 7.2, 5.9$ Hz, 2H), 2.72 (t, $J = 7.2$ Hz, 2H), 2.34 (d, $J = 2.4$ Hz, 3H), 2.11 (qt, $J = 6.5, 3.9$ Hz, 2H), 1.97 (m, 3H), 1.92 (tdd, $J = 7.5, 4.2, 2.0$ Hz, 2H), 1.77 – 1.67 (m, 2H), 1.64 – 1.48 (m, 2H). ^{13}C NMR (126 MHz, CDCl_3) δ 169.75, 161.40, 155.80, 143.48,

141.87, 136.64, 136.37, 130.03, 129.67, 128.25, 127.89, 127.49, 125.71, 125.68, 124.73, 117.40, 115.52, 114.08, 113.88, 74.39, 68.66, 68.27, 40.39, 31.74, 30.49, 28.30, 27.40, 27.27, 23.18, 18.76. HRMS (ESI+), m/z [M+Na⁺] calculated for C₃₀H₃₄FNO₃Na 498.2420; found 498.2405.



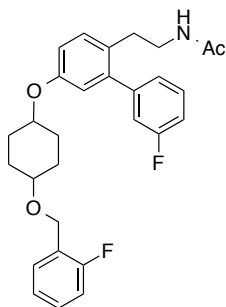
N-(2-(5-((4-(4-Bromobenzyl)oxy)cyclohexyl)oxy)-3'-fluoro-[1,1'-biphenyl]-2-yl)ethyl)acetamide (2.14d).

The compound was synthesized following the procedure used for the synthesis of **2.4** to obtain the product as a white solid: ¹H-NMR (500 MHz, CDCl₃) δ 7.49-7.46 (m, 2H), 7.41-7.36 (m, 1H), 7.26-7.19 (m, 3H) 7.09–6.99 (m, 3H), 6.09-6.87 (m, 1H), 6.77 (dd, J₁ = 10 Hz, J₂ = 5 Hz, 1H), 5.30 (br, s, 1H), 4.50 (s, 2H), 4.38-4.36 (m, 1H), 4.35-4.30 (m, 1H, minor diast.), 3.52-3.48 (m, 1H), 3.28 (q, J = 3 Hz, 2H), 2.73 (t, J = 3 Hz, 2H), 2.13-1.88 (m, 4H), 1.87 (s, 3H). 1.73-1.67 (m, 2H), 1.59-1.51 (m, 2H), ¹³C NMR (125 MHz, CDCl₃) δ 170.09, 161.80, 156.34, 143.87, 142.32, 138.30, 131.73, 131.09, 130.14, 129.35, 128.46, 125.14, 121.53, 117.82, 116.30, 115.90, 114.48, 74.64, 73.05, 69.71, 40.78, 32.15, 28.58, 27.73, 23.57. HRMS (ESI+), m/z [M+Na⁺] calculated for C₂₉H₃₁BrFNO₃Na 562.1369; found 562.1344.



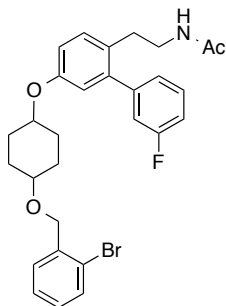
N-(2-(5-((4-(4-Chlorobenzyl)oxy)cyclohexyl)oxy)-3'-fluoro-[1,1'-biphenyl]-2-yl)ethyl)acetamide (2.14e).

The compound was synthesized following the procedure used for the synthesis of **2.4** to obtain the product as a white solid: $^1\text{H-NMR}$ (500 MHz, CDCl_3) δ 7.37-7.32 (m, 1H), 7.29-7.22 (m, 4H), 7.16 (d, $J = 5$ Hz, 1H), 7.05–6.95 (m, 3H), 6.86-6.83 (m, 1H), 6.73-6.71 (m, 1H), 5.33 (br, s, 1H), 4.49 (s, 2H), 4.35-4.26 (m, 1H), 3.49-3.44 (m, 1H), 3.24 (q, $J = 5$ Hz, 2H), 2.71 (t, $J = 5$ Hz, 2H), 2.09-1.81 (m, 4H), 1.84 (s, 3H), 1.71-1.63 (m, 2H), 1.57-1.46 (m, 2H). $^{13}\text{C NMR}$ (125 MHz, CDCl_3) δ 170.15, 161.79, 156.33, 143.91, 142.32, 137.79, 133.42, 131.07, 130.15, 129.01, 128.85, 128.78, 128.45, 125.14, 117.82, 116.46, 115.89, 114.47, 75.84, 74.65, 73.05, 69.68, 40.80, 32.14, 27.73, 23.53. HRMS (ESI+), m/z $[\text{M}+\text{Na}^+]$ calculated for $\text{C}_{29}\text{H}_{31}\text{ClFNO}_3\text{Na}$ 518.1874; found 518.1866.



N-(2-(3'-Fluoro-5-((4-((2-fluorobenzyl)oxy)cyclohexyl)oxy)-[1,1'-biphenyl]-2-yl)ethyl)acetamide (2.14f).

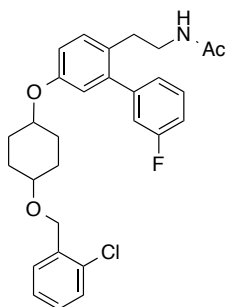
The compound was synthesized following the procedure used for the synthesis of **2.4** to obtain the product as a white solid: ^1H NMR (400 MHz, CDCl_3) δ 7.50-7.36 (m, 2H), 7.28-7.24 (m, 1H), 7.21-7.13 (m, 2H), 7.09-7.00 (m, 4H), 6.91-6.76 (m, 2H), 5.32 (br, s, 1H), 4.62 (s, 2H), 4.38-4.36 (m, 1H), 4.32-4.31 (m, 1H, minor diast.), 3.56-3.52 (m, 1H), 3.27 (q, $J = 5$ Hz, 2H), 2.75-2.71 (t, $J = 7.2$ Hz, 2H), 2.14-1.89 (m, 4H), 1.87 (s, 3H), 1.76-1.53 (m, 4H). ^{13}C NMR (100 MHz, CDCl_3) δ 170.1, 163.7, 159.8, 156.2, 142.3, 131.0, 130.6, 130.0, 129.4, 129.2, 126.4, 126.2, 125.1, 124.3, 117.8, 116.4, 115.7, 114.4, 114.2, 74.6, 73.1, 63.9, 40.7, 32.1, 28.5, 27.6, 23.5. HRMS (ESI+), m/z $[\text{M}+\text{Na}^+]$ calculated for $\text{C}_{29}\text{H}_{31}\text{F}_2\text{NO}_3\text{Na}$ 502.2170; found 502.2158.



N-(2-(5-((4-((2-Bromobenzyl)oxy)cyclohexyl)oxy)-3'-fluoro-[1,1'-biphenyl]-2-yl)ethyl)acetamide (2.14g).

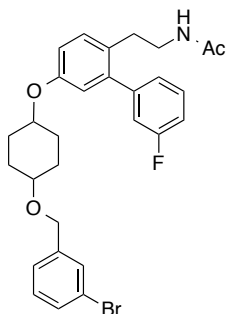
The compound was synthesized following the procedure used for the synthesis of **2.4** to obtain the product as a white solid: ^1H -NMR (500 MHz, CDCl_3) δ 7.57-7.47 (m, 2H), 7.42-7.30 (m, 2H), 7.21-7.12 (m, 2H), 7.10-7.00 (m, 3H), 6.91-6.88 (m, 1H), 6.78-6.76 (m, 1H), 5.33 (br, s, 1H), 4.60 (s, 2H), 4.39-4.33 (m, 1H), 3.60-3.56 (m, 1H), 3.29 (q, $J = 5$ Hz, 2H), 2.74 (t, $J = 5$ Hz, 2H), 2.15-1.92 (m, 4H), 1.88 (s, 3H), 1.78-1.56 (m, 4H). ^{13}C NMR (125 MHz, CDCl_3) δ 169.93, 161.07, 155.98, 142.45, 136.02, 132.79, 131.30, 130.26, 130.19, 129.08, 128.89, 128.77,

128.35, 128.06, 127.06, 125.67, 117.43, 116.38, 115.62, 114.88, 72.06, 71.26, 68.56, 40.81, 32.45, 27.79, 23.38. HRMS (ESI+), m/z [M+Na⁺] calculated for C₂₉H₃₁BrFNO₃Na 562.1369, found 562.1358.



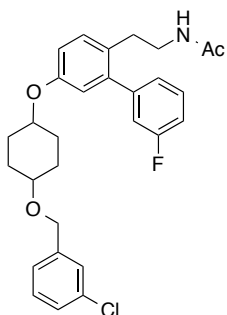
N-(2-(5-((4-((2-Chlorobenzyl)oxy)cyclohexyl)oxy)-3'-fluoro-[1,1'-biphenyl]-2-yl)ethyl)acetamide (2.14h).

The compound was synthesized following the procedure used for the synthesis of **2.4** to obtain the product as a white solid: ¹H-NMR (500 MHz, CDCl₃) δ 7.57-7.51 (m, 1H), 7.14-7.34 (m, 2H), 7.30-7.26 (m, 1H), 7.24-7.19 (m, 2H), 7.09-7.00 (m, 3H), 6.91-6.88 (m, 1H), 6.78-6.676 (m, 1H), 5.31 (br, s, 1H), 4.64 (s, 2H), 4.39-4.32 (m, 1H), 3.59-3.56 (m, 1H), 3.27 (q, J = 5 Hz, 2H), 2.74 (t, J = 5 Hz, 2H), 2.16-1.92 (m, 4H), 1.88 (s, 3H), 1.78-1.55 (m, 4H). ¹³C NMR (125 MHz, CDCl₃) δ 170.13, 163.77, 156.38, 142.35, 137.02, 132.99, 131.10, 130.16, 130.09, 129.48, 129.39, 129.07, 128.67, 128.33, 127.06, 125.15, 117.83, 116.48, 115.92, 114.48, 74.66, 73.23, 67.25, 40.79, 32.15, 27.77, 23.58. HRMS (ESI+), m/z [M+Na⁺] calculated for C₂₉H₃₁ClFNO₃Na 518.1874; found 518.1862.



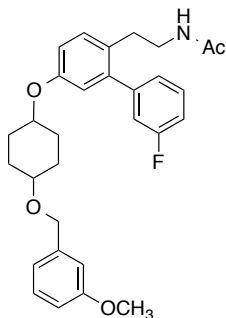
N-(2-(5-((4-(3-Bromobenzyl)oxy)cyclohexyl)oxy)-3'-fluoro-[1,1'-biphenyl]-2-yl)ethyl)acetamide (2.14i).

The compound was synthesized following the procedure used for the synthesis of **2.4** to obtain the product as a white solid: $^1\text{H-NMR}$ (500 MHz, CDCl_3) δ 7.53-7.51 (m, 1H), 7.43-7.36 (m, 2H), 7.30-7.26 (m, 1H), 7.23-7.19 (m, 2H), 7.10-7.05 (m, 2H), 7.03-6.99 (m, 1H), 6.91-6.86 (m, 1H), 6.79-6.76 (m, 1H), 5.30 (br, s, 1H), 4.52 (s, 2H), 4.39-4.29 (m, 1H), 3.53-3.49 (m, 1H), 3.29 (q, $J = 5$ Hz, 2H), 2.74 (t, $J = 5$ Hz, 2H), 2.15-1.87 (m, 4H), 1.87 (s, 3H), 1.67-1.44 (m, 4H). $^{13}\text{C NMR}$ (125 MHz, CDCl_3) δ 170.12, 163.77, 156.16, 143.92, 141.70, 131.10, 130.77, 130.72, 130.62, 130.22, 130.10, 128.45, 127.81, 126.14, 125.15, 117.84, 116.48, 115.91, 115.36, 71.54, 69.63, 69.24, 40.79, 32.15, 28.46, 27.74, 27.59, 23.58. HRMS (ESI+), m/z $[\text{M}+\text{Na}^+]$ calculated for $\text{C}_{29}\text{H}_{31}\text{BrFNO}_3$ 562.1369; found 562.1364.



N-(2-(5-((4-((3-Chlorobenzyl)oxy)cyclohexyl)oxy)-3'-fluoro-[1,1'-biphenyl]-2-yl)ethyl)acetamide (2.14j).

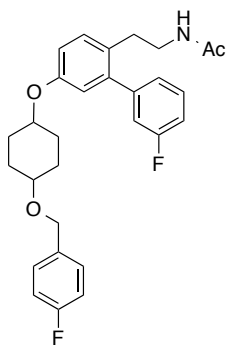
The compound was synthesized following the procedure used for the synthesis of **2.4** to obtain the product as a white solid: $^1\text{H-NMR}$ (500 MHz, CDCl_3) δ 7.41-7.36 (m, 2H), 7.29-7.19 (m, 4H), 7.07-7.00 (m, 3H), 6.91-6.87 (m, 1H), 6.78-6.76 (m, 1H), 5.31 (br, s, 1H), 4.53 (s, 2H), 4.39-4.36 (m, 1H), 3.53-3.49 (m, 1H), 3.28 (q, $J = 5$ Hz, 2H), 2.73 (t, $J = 5$ Hz, 2H), 2.14-2.1.87 (m, 4H), 1.87 (s, 3H), 1.75-1.52 (m, 4H). $^{13}\text{C NMR}$ (125 MHz, CDCl_3) δ 170.10, 161.80, 156.34, 143.92, 142.34, 134.56, 131.09, 130.16, 129.91, 128.46, 128.36, 127.78, 127.69, 125.64, 125.14, 117.83, 116.47, 115.90, 114.47, 75.98, 74.62, 69.68, 40.78, 32.15, 28.55, 27.73, 23.57. HRMS (ESI+), m/z $[\text{M}+\text{Na}^+]$ calculated for $\text{C}_{29}\text{H}_{31}\text{ClFNO}_3\text{Na}$ 518.1874; found 518.1863.



N-(2-(3'-Fluoro-5-((4-((3-methoxybenzyl)oxy)cyclohexyl)oxy)-[1,1'-biphenyl]-2-yl)ethyl)acetamide (2.14k).

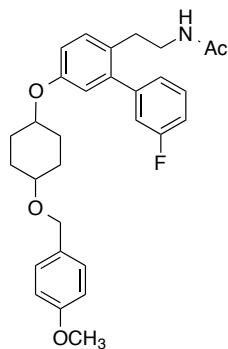
The compound was synthesized following the procedure used for the synthesis of **2.4** to obtain the product as a white solid: $^1\text{H-NMR}$ (500 MHz, CDCl_3) δ 7.41-7.36 (m, 1H), 7.28-7.25 (m, 1H), 7.10 (d, $J = 5$ Hz, 1H), 7.09-7.00 (m, 3H), 6.95-6.87 (m, 3H), 6.84-6.81 (m, 1H), 6.78-6.75 (m, 1H), 5.35 (br, s, 1H), 4.54 (s, 2H), 4.37-4.30 (m, 1H), 3.82 (s, 3H), 3.53-3.49 (m, 1H), 3.28 (q, $J = 5$ Hz, 2H), 2.73 (t, $J = 5$ Hz, 2H), 2.14-1.88 (m, 4H), 1.88 (s, 3H), 1.78-1.51 (m, 4H). $^{13}\text{C NMR}$ (125 MHz, CDCl_3) δ 170.18, 163.76, 159.98, 156.38, 143.93, 142.33, 140.96, 131.08,

130.16, 129.67, 128.40, 125.14, 119.97, 117.83, 116.47, 115.78, 114.47, 114.30, 113.17, 75.66, 74.77, 70.29, 55.49, 40.80, 32.13, 28.58, 27.71, 27.62, 23.54. HRMS (ESI+), m/z [M+Na⁺] calculated for C₃₀H₃₄FNO₄Na 514.2370; found 514.2350.



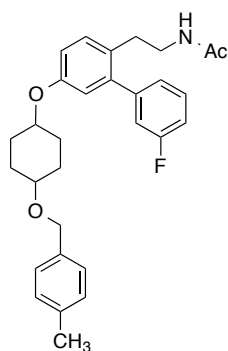
N-(2-(3'-Fluoro-5-((4-((4-fluorobenzyl)oxy)cyclohexyl)oxy)-[1,1'-biphenyl]-2-yl)ethyl)acetamide (2.14l).

The compound was synthesized following the procedure used for the synthesis of **2.4** to obtain the product as a white solid: ¹H-NMR (500 MHz, CDCl₃) δ 7.41-7.30 (m, 3H), 7.20 (d, J = 5 Hz, 1H), 7.10–6.99 (m, 5H), 6.90-6.87 (m, 1H), 6.78-6.75 (m, 1H), 5.33 (br, s, 1H), 4.51 (s, 2H), 4.39-4.29 (m, 1H), 3.53-3.49 (m, 1H), 3.28 (q, J = 5 Hz, 2H), 2.73 (t, J = 5 Hz, 2H), 2.14-1.87 (m, 4H), 1.88 (s, 3H), 1.74-1.48 (m, 4H). ¹³C NMR (125 MHz, CDCl₃) δ 170.14, 163.76, 161.79, 156.16, 143.92, 142.30, 131.09, 130.14, 129.47, 128.34, 125.14, 125.12, 117.79, 116.47, 115.91, 115.53, 115.36, 114.47, 74.80, 73.06, 69.37, 40.79, 32.14, 27.74, 27.71, 27.60, 23.56. HRMS (ESI+), m/z [M+Na⁺] calculated for C₂₉H₃₁F₂NO₃Na 502.2170; found 502.2152.



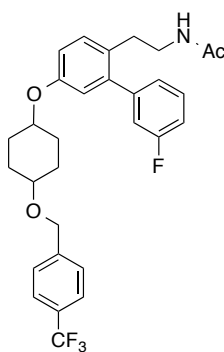
N-(2-(3'-Fluoro-5-(((4-methoxybenzyl)oxy)cyclohexyl)oxy)-[1,1'-biphenyl]-2-yl)ethylacetamide (2.14m).

The compound was synthesized following the procedure used for the synthesis of **2.4** to obtain the product as a white solid: $^1\text{H-NMR}$ (500 MHz, CDCl_3) δ 7.61-7.51 (m, 2H), 7.49-7.46 (m, 2H), 7.41-7.35 (m, 1H), 7.20 (d, $J = 5$ Hz, 1H), 7.09–6.99 (m, 3H), 6.91-6.87 (m, 1H), 6.77-6.75 (m, 1H), 5.38 (br, s, 1H), 4.61 (s, 2H), 4.37-4.31 (m, 1H), 3.83 (s, 3H), 3.55-3.51 (m, 1H), 3.28 (q, $J = 5$ Hz, 2H), 2.73 (t, $J = 5$ Hz, 2H), 2.15-1.86 (m, 4H), 1.87 (s, 3H), 1.75-1.53 (m, 4H). $^{13}\text{C NMR}$ (125 MHz, CDCl_3) δ 170.21, 161.80, 159.34, 156.40, 143.88, 142.33, 131.08, 130.16, 129.34, 128.37, 125.14, 117.84, 116.48, 116.31, 115.78, 114.31, 114.07, 75.39, 74.85, 70.11, 55.57, 40.83, 32.13, 28.75, 23.52. HRMS (ESI+), m/z $[\text{M}+\text{Na}^+]$ calculated for $\text{C}_{30}\text{H}_{34}\text{FNO}_4\text{Na}$ 514.2370 found 514.2347.



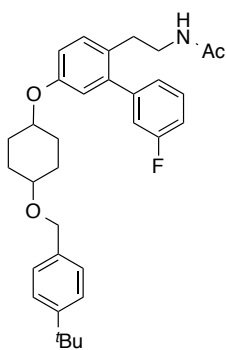
N-(2-(3'-Fluoro-5-((4-((4-methylbenzyl)oxy)cyclohexyl)oxy)-[1,1'-biphenyl]-2-yl)ethyl)acetamide (2.14n).

The compound was synthesized following the procedure used for the synthesis of **2.4** to obtain the product as a white solid: $^1\text{H-NMR}$ (500 MHz, Chloroform- d) δ 7.41 – 7.34 (m, 1H), 7.26 – 7.21 (m, 3H), 7.20 – 7.11 (m, 2H), 7.10 – 7.04 (m, 2H), 7.00 (ddd, $J = 9.6, 2.6, 1.6$ Hz, 1H), 6.87 (ddd, $J = 8.6, 6.0, 2.7$ Hz, 1H), 6.75 (dd, $J = 7.6, 2.7$ Hz, 1H), 5.33 – 5.28 (m, 1H), 4.51 (s, 2H), 4.35 (dt, $J = 6.7, 3.4$ Hz, 1H), 4.29 (tt, $J = 8.2, 3.4$ Hz, 1H, minor diast.), 3.53 – 3.45 (m, 1H), 3.27 (tdd, $J = 7.3, 5.9, 1.4$ Hz, 2H), 2.72 (t, $J = 7.2$ Hz, 2H), 2.34 (s, 3H), 2.15 – 2.02 (m, 2H), 2.00 (dtd, $J = 12.6, 6.7, 2.4$ Hz, 2H), 1.87 (s, 3H), 1.68 (tq, $J = 8.7, 3.9$ Hz, 2H), 1.54 (dddd, $J = 20.1, 15.8, 10.5, 2.8$ Hz, 2H). $^{13}\text{C NMR}$ (126 MHz, CDCl_3) δ 170.08, 161.65, 156.24, 143.73, 142.12, 137.29, 137.20, 136.05, 130.01, 129.93, 129.19, 128.23, 128.10, 127.72, 125.00, 124.98, 117.68, 116.33, 115.78, 114.30, 74.68, 70.14, 69.72, 40.65, 31.98, 28.57, 28.48, 27.59, 27.48, 23.42, 21.31. HRMS (ESI+), m/z $[\text{M}+\text{Na}^+]$ calculated for $\text{C}_{29}\text{H}_{32}\text{FNO}_3\text{Na}$ 498.2420; found 498.2410.



N-(2-(3'-Fluoro-5-((4-((4-(trifluoromethyl)benzyl)oxy)cyclohexyl)oxy)-[1,1'-biphenyl]-2-yl)ethyl)acetamide (2.14o).

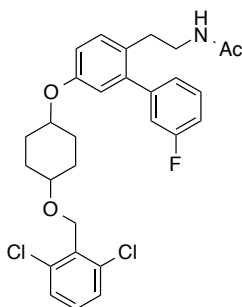
The compound was synthesized following the procedure used for the synthesis of **2.4** to obtain the product as a white solid: $^1\text{H-NMR}$ (500 MHz, CDCl_3) δ 7.61 (d, $J = 5$ Hz, 2H), 7.48 (t, $J = 5$ Hz, 2H), 7.42-7.37 (m, 1H), 7.20 (d, $J = 5$ Hz, 1H), 7.09 (d, $J = 5$ Hz, 1H), 7.09–7.00 (m, 2H), 6.92-6.86 (m, 1H), 6.80-6.75 (m, 1H), 5.38 (br, s, 1H), 4.61 (s, 2H), 4.40-4.30 (m, 1H), 3.55-3.50 (m, 1H), 3.29 (q, $J = 3$ Hz, 2H), 2.74 (t, $J = 3$ Hz, 2H), 2.15-1.87 (m, 4H), 1.88 (s, 3H), 1.77-1.52 (m, 4H). $^{13}\text{C NMR}$ (125 MHz, CDCl_3) δ 170.21, 163.77, 161.81, 156.34, 156.16, 143.91, 143.44, 142.35, 131.11, 130.17, 128.45, 128.36, 127.62, 125.63, 125.14, 117.82, 116.47, 115.90, 114.50, 76.11, 74.56, 69.68, 69.30, 40.84, 32.15, 28.52, 28.41, 27.73, 27.61, 23.53. HRMS (ESI+), m/z [$\text{M}+\text{Na}^+$] calculated for $\text{C}_{30}\text{H}_{31}\text{F}_4\text{NO}_3\text{Na}$ 552.2138; found 552.2111.



N-(2-(5-((4-((*tert*-Butyl)benzyl)oxy)cyclohexyl)oxy)-3'-fluoro-[1,1'-biphenyl]-2-yl)ethyl)acetamide (2.14p**).**

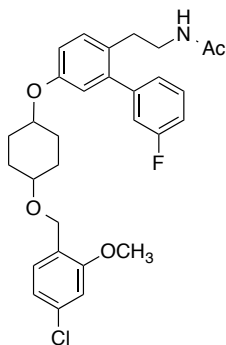
The compound was synthesized following the procedure used for the synthesis of **2.4** to obtain the product as a white solid: $^1\text{H-NMR}$ (500 MHz, CDCl_3) δ 7.40-7.36 (m, 3H), 7.31-7.27 (m, 2H), 7.20 (d, $J = 5$ Hz, 1H), 7.09-6.99 (m, 3H), 6.91-6.87 (m, 1H), 6.78-6.76 (m, 1H), 5.30 (br, s, 1H), 4.53 (s, 2H), 4.36 (dt, $J = 6.7, 3.4$ Hz, 1H), 4.29 (dt, $J = 8.4, 4.5$ Hz, 1H, minor diast.), 3.54-3.51 (m, 1H), 3.29 (q, $J = 5$ Hz, 2H), 2.74 (t, $J = 5$ Hz, 2H), 2.14-1.88 (m 4H), 1.88 (s, 3H), 1.75-1.51 (m, 4H), 1.32 (s, 9H). $^{13}\text{C NMR}$ (126 MHz, CDCl_3) δ 169.98, 163.62, 161.66,

156.25, 150.58, 143.74, 142.13, 135.97, 130.94, 129.95, 128.25, 127.49, 125.46, 124.98, 117.70, 116.34, 115.63, 114.34, 74.70, 70.10, 69.67, 40.64, 34.66, 32.00, 31.51, 28.56, 27.60, 27.49, 23.45. HRMS (ESI+), m/z [M+Na⁺] calculated for C₂₉H₃₂FNO₃Na 540.2890; found 540.2890.



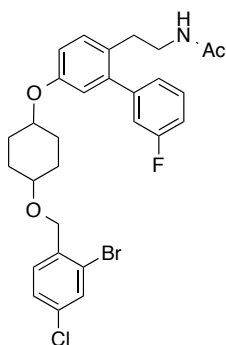
N-(2-(5-((4-((2,6-Dichlorobenzyl)oxy)cyclohexyl)oxy)-3'-fluoro-[1,1'-biphenyl]-2-yl)ethyl)acetamide (2.14q).

The compound was synthesized following the procedure used for the synthesis of **2.4** to obtain the product as a white solid: ¹H-NMR (500 MHz, CDCl₃) δ 7.41-7.36 (m, 1H), 7.33-7.31 (m, 1H), 7.20-7.16 (m, 2H) 7.09–6.99 (m, 3H), 6.90-6.87 (m, 1H), 6.78-6.76 (m, 1H), 5.29 (br, s, 1H), 4.77 (s, 2H), 4.38-4.35 (m, 1H), 4.33-4.28 (m, 1H, minor diast.), 3.61-3.56 (m, 1H), 3.27 (q, J = 3 Hz, 2H), 2.73 (t, J = 3 Hz, 2H), 2.16-1.89 (m, 4H), 1.87 (s, 3H). 1.78-1.67 (m, 2H), 1.63-1.51 (m, 2H), ¹³C NMR (125 MHz, CDCl₃) δ 170.08, 163.76, 161.80, 156.39, 143.89, 137.09, 134.08, 131.08, 130.13, 128.70, 125.15, 117.82, 117.79, 116.47, 115.76, 114.46, 114.30, 74.71, 65.36, 40.77, 32.15, 28.59, 27.79, 23.58. HRMS (ESI+), m/z [M+Na⁺] calculated for C₂₉H₃₀Cl₂FNO₃Na 552.1484; found 552.1494.



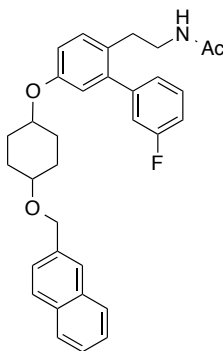
N-(2-(5-((4-(4-Chloro-2-methoxybenzyl)oxy)cyclohexyl)oxy)-3'-fluoro-[1,1'-biphenyl]-2-yl)ethyl)acetamide (2.14r).

The compound was synthesized following the procedure used for the synthesis of **2.4** to obtain the product as a white solid: $^1\text{H-NMR}$ (500 MHz, CDCl_3) δ 7.41-7.31 (m, 2H), 7.21-7.19 (m, 1H), 7.10-7.05 (m, 2H), 7.03-7.00 (m, 1H), 6.97-6.94 (m, 1H), 6.90-6.87 (m, 1H), 6.85-6.84 (m, 1H), 6.78-6.76 (m, 1H), 5.27 (br, s, 1H), 4.53 (s, 2H), 4.38-4.29 (m, 1H), 3.82 (s, 3H), 3.53-3.49 (m, 1H), 3.29 (q, $J = 5$ Hz, 2H), 2.73 (t, $J = 5$ Hz, 2H), 2.15-1.87 (m, 4H), 1.88 (s, 3H), 1.75-1.49 (m, 4H). $^{13}\text{C NMR}$ (125 MHz, CDCl_3) δ 169.27, 161.88, 156.87, 155.57, 144.82, 142.63, 131.10, 131.07, 129.49, 120.72, 117.83, 116.49, 116.32, 115.92, 115.78, 111.13, 64.74, 55.83, 40.79, 32.16, 27.77, 23.59. HRMS (ESI+), m/z $[\text{M}+\text{Na}^+]$ calculated for $\text{C}_{30}\text{H}_{33}\text{ClFNO}_4\text{Na}$ 548.1980; found 548.1957.



N-(2-(5-((4-((2-Bromo-4-chlorobenzyl)oxy)cyclohexyl)oxy)-3'-fluoro-[1,1'-biphenyl]-2-yl)ethyl)acetamide (2.14s).

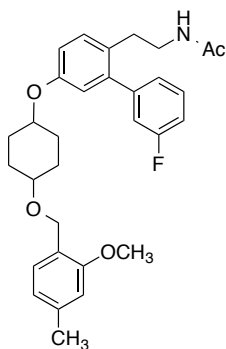
The compound was synthesized following the procedure used for the synthesis of **2.4** to obtain the product as a white solid: $^1\text{H-NMR}$ (500 MHz, CDCl_3) δ 7.56-7.54 (m, 1H), 7.50-7.44 (m, 1H), 7.41-7.36 (m, 1H), 7.32-7.30 (m, 1H), 7.21-7.19 (m, 1H), 7.09-7.00 (m, 3H), 6.91-6.87 (m, 1H), 6.78-6.76 (m, 1H), 5.30 (br, s, 1H), 4.55 (s, 2H), 4.38-4.32 (m, 1H), 3.59-3.55 (m, 1H), 3.29 (q, $J = 5$ Hz, 2H), 2.74 (t, $J = 5$ Hz, 2H), 2.15-1.88 (m, 4H), 1.88 (s, 3H), 1.77-1.55 (m, 4H). $^{13}\text{C NMR}$ (125 MHz, CDCl_3) δ 170.09, 163.76, 156.33, 143.91, 142.35, 137.27, 133.86, 132.26, 132.16, 131.10, 130.16, 129.93, 128.47, 127.90, 125.14, 122.87, 117.81, 116.47, 115.89, 114.48, 76.44, 69.34, 40.78, 32.16, 28.49, 28.38, 27.75, 27.69, 23.58. HRMS (ESI+), m/z $[\text{M}+\text{Na}^+]$ calculated for $\text{C}_{29}\text{H}_{30}\text{BrClFNO}_3\text{Na}$ 596.0979; found 596.0958.



N-(2-(3'-Fluoro-5-((4-(naphthalen-2-ylmethoxy)cyclohexyl)oxy)-[1,1'-biphenyl]-2-yl)ethyl)acetamide (2.14t).

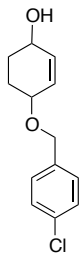
The compound was synthesized following the procedure used for the synthesis of **2.4** to obtain the product as a white solid: $^1\text{H-NMR}$ (500 MHz, CDCl_3) δ 7.86-7.80 (m, 4H), 7.51-7.46 (m, 3H), 7.41-7.37 (m, 1H), 7.21 (d, $J = 5$ Hz, 1H), 7.09-7.00 (m, 3H), 6.91-6.87 (m, 1H), 6.79-6.76 (m, 1H), 5.31 (br, s, 1H), 4.73 (s, 2H), 4.39-4.31 (m, 1H), 3.58-3.55 (m, 1H), 3.29 (q, $J = 5$

Hz, 2H), 2.74 (t, J = 5 Hz, 2H), 2.17-1.89 (m, 4H), 1.88 (s, 3H), 1.77-1.55 (m, 4H). ¹³C NMR (125 MHz, CDCl₃) δ 170.12, 163.76, 156.37, 142.33, 136.77, 133.57, 133.17, 131.08, 130.15, 128.41, 128.10, 127.96, 126.34, 126.00, 125.14, 117.83, 116.47, 115.78, 114.30, 74.78, 70.58, 70.17, 40.78, 32.14, 28.73, 27.78, 27.66, 23.57. HRMS (ESI+), m/z [M+Na⁺] calculated for C₃₃H₃₄FNO₃Na 534.2420; found 534.2397.



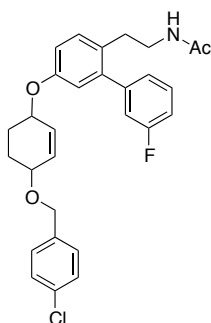
N-(2-(3'-Fluoro-5-(((4-((2-methoxy-4-methylbenzyl)oxy)cyclohexyl)oxy)-[1,1'-biphenyl]-2-yl)ethyl)acetamide (2.14u).

The compound was synthesized following the procedure used for the synthesis of **2.4** to obtain the product as a white solid: ¹H-NMR (500 MHz, CDCl₃) δ 7.41-7.36 (m, 1H), 7.31-7.26 (m, 1H), 7.20-7.18 (m, 1H), 7.10-7.05 (m, 2H), 7.03-7.00 (m, 1H), 6.90-6.87 (m, 1H), 6.79-6.76 (m, 2H), 6.69-6.68 (m, 1H), 5.28 (br, s, 1H), 4.55 (s, 2H), 4.37-4.28 (m, 1H), 3.83 (s, 3H), 3.54-3.48 (m, 1H), 3.28 (q, J = 5 Hz, 2H), 2.73 (t, J = 5 Hz, 2H), 2.35 (s, 3H), 2.14-1.89 (m, 4H), 1.88 (s, 3H), 1.75-1.48 (m, 4H). ¹³C NMR (125 MHz, CDCl₃) δ 170.10, 163.77, 157.19, 156.43, 143.91, 142.33, 138.79, 131.07, 130.15, 128.94, 128.36, 125.15, 124.57, 121.28, 117.84, 116.48, 116.31, 115.94, 115.77, 114.46, 114.43, 111.47, 74.96, 65.07, 55.57, 40.77, 32.14, 28.80, 27.78, 23.59, 21.88. HRMS (ESI+), m/z [M+Na⁺] calculated for C₃₁H₃₆FNO₄Na 528.2526; found 528.2516.



4-((4-Chlorobenzyl)oxy)cyclohex-2-enol (2.17).

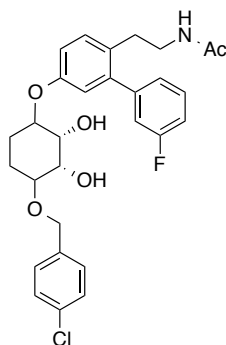
This compound was synthesized following a previously reported procedure.⁶³



N-(2-(5-((4-Chlorobenzyl)oxy)cyclohex-2-en-1-yl)oxy)-3'-fluoro-[1,1'-biphenyl]-2-ylethyl)acetamide (2.18).

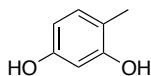
Phenol **2.9** (0.12 g, 0.298 mmol), triphenylphosphine (0.156 g, 0.597 mmol) and alcohol **2.17** (0.128g, 0.597mmol) were dissolved in anhydrous THF (2mL) at rt. After 5 minutes DIAD (0.12 mL, 0.597mmol) was added dropwise to the mixture. After 3 h, the reaction was concentrated, and purified via column chromatography (SiO₂, 1:4, EtOAc: hexane) to afford **2.18** as a solid (58% yield): ¹H NMR (500 MHz, Chloroform-d) δ 7.40 – 7.35 (m, 1H), 7.33 – 7.26 (m, 4H), 7.20 (d, *J* = 8.5 Hz, 1H), 7.09 – 7.05 (m, 2H), 7.00 (ddd, *J* = 9.6, 2.6, 1.6 Hz, 1H), 6.89 (dd, *J* = 8.5, 2.8 Hz, 1H), 6.77 (d, *J* = 2.8 Hz, 1H), 6.00 (td, *J* = 2.3, 1.1 Hz, 2H), 5.25 (s, 1H), 4.87 – 4.82 (m, 1H), 4.10 – 4.04 (m, 1H), 3.27 (td, *J* = 7.2, 5.9 Hz, 2H), 2.73 (t, *J* = 7.2 Hz, 2H), 2.28 – 2.22 (m, 1H), 2.22 – 2.14 (m, 1H), 1.87 (s, 3H), 1.80 – 1.65 (m, 2H). ¹³C NMR (126 MHz, CDCl₃) δ 169.95, 161.68, 156.08, 143.57, 142.30, 137.17, 133.50, 131.88, 131.06, 130.06, 129.67, 129.07,

128.71, 124.98, 117.47, 116.32, 115.51, 114.41, 72.80, 71.63, 69.74, 40.64, 32.04, 26.79, 26.67, 23.46.



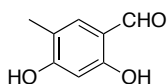
N-(2-(5-(((2R,3S)-4-((4-Chlorobenzyl)oxy)-2,3-dihydroxycyclohexyl)oxy)-3'-fluoro-[1,1'-biphenyl]-2-yl)ethyl)acetamide (2.19).

OsO₄ (0.001g, 0.002mmol) was added at rt to a solution of **2.18** (0.01g, 0.02mmol) and NMO (0.006g, 0.05mmol) in THF/H₂O (1:1, 0.6 mL). The resulting solution was stirred at rt on. After 12 h the THF was evaporated and the residue was extracted with EtOAc (3 x 5mL). The organic layers were collected, dried, concentrated and purified by column chromatography (SiO₂, 1:10, MeOH: DCM) to obtain product **2.19** as a white solid (83% yield): ¹H-NMR (500 MHz, CDCl₃) δ 7.41-7.27 (m, 5H), 7.20 (d, J = 5 Hz, 1H), 7.10–7.06 (m, 2H), 7.01-6.99 (m, 1H), 6.92-6.90 (m, 1H), 6.79 (d, J = 3, 1H), 5.29 (br, s, 1H), 4.62 (dd, J₁ = 3Hz, J₂ = 7.5Hz, 2H), 4.53-4.50 (m, 1H), 4.17-4.15 (m, 1H), 4.06-4.04 (m, 1H), 3.72-3.69 (m, 1H), 3.28 (q, J = 3 Hz, 2H), 2.74 (t, J = 3 Hz, 2H), 2.64 (d, J = 3 Hz, 2H), 1.94-1.72 (m, 4H), 1.88 (s, 3H). ¹³C NMR (125 MHz, CDCl₃) δ 170.13, 161.81, 156.01, 143.65, 142.49, 137.12, 133.77, 130.22, 129.17, 128.92, 125.11, 117.72, 116.45, 115.75, 114.59, 75.83, 72.12, 71.46, 70.52, 40.76, 23.59, 23.45. HRMS (ESI+), m/z [M+Na⁺] calculated for C₂₉H₃₁ClFNO₅Na 550.1773; found 550.1746.



4-Methylbenzene-1,3-diol (2.20).

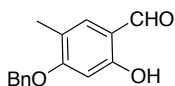
A solution of 2,4-dihydroxybenzaldehyde (0.69 g, 5.0 mmol) and NaBH_3CN (1.0 g, 15 mmol) in THF (30 mL) was stirred at rt. Methyl orange was added as an indicator until the reaction was a light orange color. 1.0 N HCl (15 mL) was added drop wise until the solution turned deep red. After 3 h the reaction was quenched with water (40 mL), extracted with Et_2O (3 x 40 mL), dried (Na_2SO_4), filtered and concentrated to afford **2.20** a light pink solid (0.69g, 5.56 mmol): ^1H NMR (500 MHz, Chloroform-d) δ 6.95 (d, $J = 8.7$ Hz, 1H), 6.33 (dd, $J = 4.3, 2.0$ Hz, 2H), 4.67 (s, 1H), 4.62 – 4.56 (m, 1H), 2.17 (s, 3H). ^{13}C NMR (126 MHz, CDCl_3) δ 154.90, 154.69, 131.53, 115.85, 107.67, 102.72, 15.01.



2,4-Dihydroxy-5-methylbenzaldehyde.

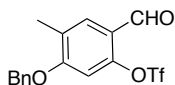
Silver triflate (8.66g, 33.85mmol) was added to a dry round bottom flask, which was then cooled to -78°C . 4-methylbenzene 1,3-diol (1.40g, 11.28mmol) was dissolved in anhydrous DCM (84mL) was added to the round bottom flask drop wise. Dichloromethyl methyl ether (3.063mL, 33.85mmol) in DCM (17.1mL) was then added to the mixture. The reaction was left to stir for 3 h. Saturated NaHCO_3 (45mL) was added to quench the reaction and after stirring for 30 minutes the mixture was filtered through a pad of Celite. The organic layer from the filtrate was removed the aqueous layer was washed with EtOAc (3X60mL). The organic layers were combined, dried, and concentrated. Column chromatography (SiO_2 , 5:1, Hex: EtOAc) was used to obtain the purified product, a white solid in 40% yield: ^1H NMR (500 MHz, Chloroform-d) δ

11.03 (s, 1H), 10.09 (s, 1H), 7.24 (m, 1H), 7.19 (d, J = 1.1 Hz, 1H), 6.37 (s, 1H), 2.12 (d, J = 1.1 Hz, 3H). ¹³C NMR (126 MHz, CDCl₃) δ 194.72, 163.42, 161.56, 134.86, 129.05, 117.53, 99.95, 15.90.



4-(Benzyloxy)-2-hydroxy-5-methylbenzaldehyde (2.21).

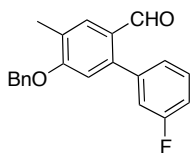
A solution of diol 2,4-dihydroxy-5-methylbenzaldehyde (0.025 g, 0.16 mmol), NaHCO₃ (0.018 g, 0.21 mmol), and BnBr (0.02 mL, 0.18 mmol) in anhydrous acetonitrile (1.6mL) were stirred and heated at reflux for 16 h. The reaction was then quenched by the addition of water (3 mL), extracted with EtOAc (3 x 2mL), dried (Na₂SO₄), filtered and concentrated. The residue was purified by column chromatography (SiO₂, 6:1, Hex: EtOAc) to afford solid phenol **4** (0.015 g, 0.06 mmol): ¹H NMR (500 MHz, Chloroform-d) δ 11.33 (s, 1H), 9.59 (s, 1H), 7.35 – 7.29 (m, 4H), 7.28 – 7.23 (m, 1H), 7.16 (d, J = 1.1 Hz, 1H), 6.37 (s, 1H), 5.02 (s, 2H), 2.12 (d, J = 1.1 Hz, 3H). ¹³C NMR (126 MHz, CDCl₃) δ 194.72, 163.42, 134.86, 129.05, 128.58, 127.53, 99.95, 70.60, 15.90.



5-(Benzyloxy)-2-formyl-4-methylphenyl trifluoromethanesulfonate (2.22).

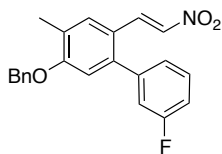
A solution of 4-(benzyloxy)-2-hydroxy-5-methylbenzaldehyde (0.29 g, 1.1mmol), N-bisphenyltriflate (0.59 g, 1.7 mmol), K₂CO₃ (0.61 g, 4.4 mmol) in anhydrous THF (15.7 mL) was stirred in a septum-capped tube. The reaction was heated to 120 °C for 20 minutes in a microwave synthesizer. Upon completion the reaction was cooled to rt and quenched with water

(10 mL), extracted with EtOAc (3 x 5 mL), dried (Na₂SO₄), filtered and concentrated. The residue was used without further purification, a yellow oil (0.16 g, 0.41 mmol): ¹H NMR (500 MHz, Chloroform-d) δ 10.30 (s, 1H), 7.59 (s, 1H), 7.33 (t, J = 2.2 Hz, 5H), 6.42 (s, 1H), 5.05 (s, 2H), 2.13 (s, 3H). ¹³C NMR (126 MHz, CDCl₃) δ 188.38, 163.02, 161.56, 136.15, 129.98, 128.75, 128.29, 127.25, 127.06, 120.23, 118.46, 96.98, 70.15, 15.48.



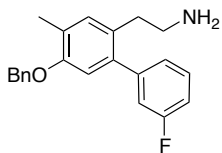
5-(Benzyloxy)-3'-fluoro-4-methyl-[1,1'-biphenyl]-2-carbaldehyde (2.23).

2.22 (0.672g, 2.1 mmol) was dissolved in anhydrous DMF (20mL). 3-fluorophenyl boronic acid (0.32g, 2.31mmol), K₂CO₃ (0.53g, 3.78 mmol), Pd(dppf)Cl₂ (0.154g, 0.21mmol) were added to the mixture. The reaction was degassed and then heated to reflux on. Upon completion of the reaction, it was cooled to rt. The reaction was extracted with saturated LiCl and EtOAc (3 x 50mL). The organic layers were combined, dried, concentrated, and purified via column chromatography (SiO₂, 6:1, Hex: EtOAc) to afford the purified product as a yellow oil: ¹H NMR (400 MHz, Chloroform-d) δ 9.83 (s, 1H), 7.89 (s, 1H), 7.51 – 7.31 (m, 5H), 7.12 (ddd, J = 16.5, 8.6, 2.0 Hz, 3H), 6.86 (s, 1H), 5.19 (s, 2H), 2.36 (d, J = 0.8 Hz, 3H). ¹³C NMR (126 MHz, CDCl₃) δ 190.82, 163.49, 161.01, 136.13, 130.12, 129.87, 129.80, 128.70, 128.22, 127.70, 127.21, 126.71, 125.98, 125.95, 116.98, 114.93, 112.37, 70.19, 16.14. HRMS (ESI+) m/z: [M + H⁺] calculated for C₂₁H₁₇FO₂ 321.0215; found 321.0222.



(E)-5-(Benzyloxy)-3'-fluoro-4-methyl-2-(2-nitrovinyl)-1,1'-biphenyl.

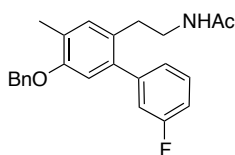
2.23 (0.11g, 0.327mmol) was dissolved in Nitromethane (0.7mL). NH_4OAc (0.05g, 0.654mmol) was added, and then the mixture was heated at reflux for 4 h. After 4 h the reaction was cooled to rt. The product was extracted with EtOAc (3X10mL). The organic layers were combined, dried, concentrated. The residue was purified by column chromatography (SiO_2 , 4:1, Hex: EtOAc) to afford the purified product as a yellow solid in 90% yield: ^1H NMR (500 MHz, Chloroform-d) δ 7.89 (s, 1H), 7.86 (s, 1H), 7.44 – 7.41 (m, 2H), 7.40 – 7.26 (m, 6H), 7.08 (tdd, $J = 8.5, 2.6, 1.0$ Hz, 1H), 6.98 – 6.95 (m, 1H), 6.93 (ddd, $J = 9.5, 2.6, 1.6$ Hz, 1H), 5.08 (s, 2H), 2.28 (s, 3H). ^{13}C NMR (126 MHz, CDCl_3) δ 163.62, 159.68, 137.60, 136.17, 135.74, 130.19, 130.12, 129.69, 128.70, 128.23, 128.01, 127.22, 125.61, 125.59, 120.14, 116.70, 115.07, 113.09, 70.15, 16.26.



2-(5-(Benzyloxy)-3'-fluoro-4-methyl-[1,1'-biphenyl]-2-yl)ethanamine (2.24).

A suspension of Lithium Aluminum Hydride (0.11g, 2.75mmol) in anhydrous THF (5.5mL) was cooled to 0°C . (E)-5-(Benzyloxy)-3'-fluoro-4-methyl-2-(2-nitrovinyl)-1,1'-biphenyl (0.5g, 1.377mmol) was dissolved in anhydrous THF (1.96mL) and added drop wise to the reaction. The reaction slowly warmed to rt and stirred for 12 h. Upon completion, 3N NaOH (1mL), water (1mL), and EtOAc (3mL) were added sequentially to quench the reaction. After stirring

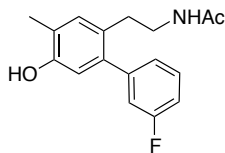
for one h the mixture was filtered through a pad of Celite. The solid was washed with warm EtOAc (100mL). The filtrate was collected, dried, and concentrated. The oil was purified using column chromatography (SiO₂, 2:1, DCM: MeOH) and used directly in the next step: ¹H NMR (500 MHz, Chloroform-d) δ 7.40 – 7.27 (m, 6H), 7.01-6.95 (m, 3H), 6.58 (d, 1H), 5.02 (s, 2H), 3.01 – 2.89 (m, 2H), 2.87 – 2.74 (m, 2H), 2.05 (s, 3H). ¹³C NMR (126 MHz, CDCl₃) δ 163.42, 161.72, 157.77, 143.49, 143.11, 136.84, 129.91, 129.48, 128.06, 127.67, 127.09, 124.79, 116.37, 114.31, 70.28, 40.64, 29.62, 26.89, 16.76. HRMS (ESI+) m/z: [M + H⁺] calculated for C₂₂H₂₂FNO 336.1764; found 336.1765.



N-(2-(5-(Benzyloxy)-3'-fluoro-4-methyl-[1,1'-biphenyl]-2-yl)ethyl)acetamide.

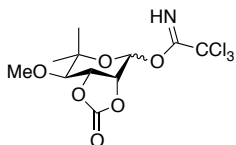
Amine **2.24** (0.10g, 0.29mmol) was dissolved in anhydrous DCM (3mL) and cooled to 0°C. Triethylamine (0.03mL, 0.27mmol) was added dropwise. After 15 minutes acetic anhydride (0.02mL, 0.27mmol) was added and the reaction warmed to rt. The reaction was stirred for 12 h and was then quenched by the addition of water. The mixture was extracted with DCM (2 x 10mL) and the organic layers were combined, dried, and concentrated. The mixture was purified via column chromatography (SiO₂, 2:1, DCM: MeOH) to obtain the product as a white solid in 72% yield: ¹H NMR (500 MHz, Chloroform-d) δ 7.39 – 7.22 (m, 6H), 7.06 – 6.85 (m, 4H), 6.67 (s, 1H), 4.97 (s, 2H), 3.31 – 3.17 (m, 2H), 2.65 (t, J = 7.2 Hz, 2H), 2.24 (s, 3H), 1.97 (s, 3H), 1.55 (s, 1H). ¹³C NMR (126 MHz, CDCl₃) δ 169.87, 161.56, 139.23, 137.17, 132.11, 129.87, 129.80, 128.53, 127.85, 127.83, 127.20, 127.19, 126.97, 125.01, 116.16, 114.06, 113.02, 69.98,

40.68, 31.81, 24.15, 16.12. HRMS (ESI+) m/z : $[M + H^+]$ calculated for $C_{24}H_{24}FNO_2$ 378.3264; found 378.3249.



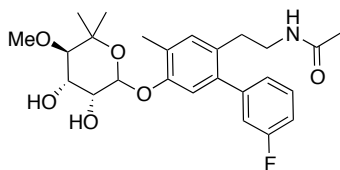
N-(2-(3'-Fluoro-5-hydroxy-4-methyl-[1,1'-biphenyl]-2-yl)ethyl)acetamide (2.25).

Palladium on carbon (10% w/w, 20 mg) was added to a solution of **N-(2-(5-(benzyloxy)-3'-fluoro-4-methyl-[1,1'-biphenyl]-2-yl)ethyl)acetamide** (223 mg, 1.0 mmol) in EtOAc (3 ml) and the suspension was stirred at rt under a hydrogen atmosphere. After 12 h, the reaction mixture was filtrated through Celite and the filtrate was concentrated to get **2.25** as an off-white amorphous solid (~100%): 1H NMR (500 MHz, Chloroform- d) δ 7.33 – 7.24 (m, 1H), 6.98 (d, $J = 1.0$ Hz, 3H), 6.87 (s, 1H), 6.57 (s, 1H), 5.20 (s, 1H), 3.20 (td, $J = 7.3, 5.9$ Hz, 2H), 2.63 (t, $J = 7.3$ Hz, 2H), 2.22 (s, 3H), 1.80 (s, 3H), 1.51 (s, 1H). ^{13}C NMR (126 MHz, $CDCl_3$) δ 169.93, 163.49, 152.19, 132.38, 129.85, 129.79, 128.84, 127.99, 126.34, 124.93, 116.06, 114.10, 113.93, 40.70, 31.75, 23.30, 15.50. HRMS (ESI+), m/z $[M+Na^+]$ calculated for $C_{17}H_{18}FNO_2Na$ 310.1219; found 310.1213.



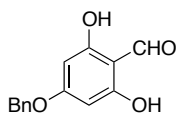
(3aR,7R,7aR)-7-Methoxy-6,6-dimethyl-2-oxotetrahydro-3aH-[1,3]dioxolo[4,5-c]pyran-4-yl 2,2,2-trichloroacetimidate (2.26).

This compound was synthesized following a previously reported procedure.^{41,51}



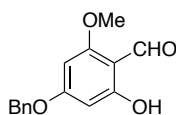
N-(2-(5-(((3R,4S,5R)-3,4-Dihydroxy-5-methoxy-6,6-dimethyltetrahydro-2H-pyran-2-yl)oxy)-3'-fluoro-4-methyl-[1,1'-biphenyl]-2-yl)ethyl)acetamide (2.27).

2.26⁵¹⁻⁵² (0.023g, 0.150mmol) in anhydrous DCM (0.5mL) was added to a mixture of **2.25** (0.035g, 0.066mmol) in anhydrous DCM (0.5mL) at rt. Boron trifluoride diethyl etherate (0.07mL) was then added drop wise. The reaction was monitored via TLC. Upon completion of the reaction (~1 h), triethylamine (0.1mL) was added. The mixture was concentrated and purified via column chromatography (SiO₂, 3:1, Hexane: EtOAc- 20:1, DCM:MeOH). The product was obtained as a white solid in 30% yield and used directly in the next step. The product (0.019g, 0.03mmol) was dissolved in MeOH (12mL) and triethylamine (4mL) was added. The mixture was stirred on. After 12 h the reaction was concentrated and purified via column chromatography (SiO₂, 20:1, DCM: MeOH). The product was obtained in 70% yield to produce a white solid: ¹H NMR (500 MHz, Methylene Chloride-d₂) δ 7.38 (td, *J* = 7.9, 6.0 Hz, 1H), 7.10 – 6.97 (m, 4H), 5.52 – 5.49 (m, 1H), 5.48 (d, *J* = 2.4 Hz, 1H), 4.20 (dd, *J* = 9.1, 3.4 Hz, 1H), 4.13 (dd, *J* = 3.4, 2.4 Hz, 1H), 3.56 (s, 3H), 3.29 (d, *J* = 9.1 Hz, 1H), 3.22 (tdd, *J* = 7.5, 5.8, 2.0 Hz, 2H), 2.69 (td, *J* = 7.1, 4.8 Hz, 2H), 2.20 – 2.17 (s, 3H), 1.81 (s, 3H), 1.30 (s, 3H), 1.17 (s, 3H). ¹³C NMR (126 MHz, CD₂Cl₂) δ 170.53, 164.23, 162.27, 154.05, 144.64, 144.58, 140.03, 132.70, 130.57, 130.50, 129.48, 127.29, 125.97, 125.95, 117.05, 116.88, 115.60, 114.53, 114.36, 98.49, 85.07, 78.84, 72.14, 69.45, 62.36, 41.37, 32.62, 30.45, 29.54, 23.67, 23.26, 16.61. HRMS (ESI+), *m/z* [M+Na⁺] calculated for C₂₅H₃₂FNO₆Na 500.2061; found 500.2054.



4-(Benzyloxy)-2,6-dihydroxybenzaldehyde (**2.28**).

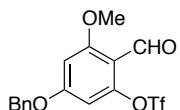
A solution of 2,4,6-trihydroxybenzaldehyde (0.025 g, 0.16 mmol), K_2CO_3 (0.022 g, 0.16 mmol), and BnBr (0.02 mL, 0.16 mmol) in anhydrous DMF (1.6 mL) was stirred at 0 °C for 6 h and then rt for 12 h. The reaction was quenched by the addition of water, extracted with EtOAc (3 x 5 mL), washed with saturated aqueous NaCl solution and a saturated aqueous LiCl solution, dried (Na_2SO_4), filtered and concentrated. The residue was purified by column chromatography (SiO_2 , 4:1. Hex: EtOAc) to afford solid **2.28** (0.014 g, 0.06 mmol): 1H NMR (500 MHz, Chloroform-d) δ 12.36 (s, 1H), 10.09 (s, 1H), 7.38 – 7.26 (m, 5H), 5.93 – 5.87 (m, 2H), 5.03 (s, 2H). ^{13}C NMR (126 MHz, $CDCl_3$) δ 191.95, 166.08, 164.56, 163.41, 135.55, 128.78, 128.46, 127.39, 106.26, 96.04, 91.76, 70.63.



4-(Benzyloxy)-2-hydroxy-6-methoxybenzaldehyde (**2.29**).

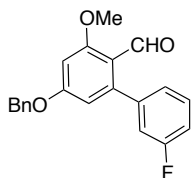
A solution of **2.28** (0.20g, 0.82 mmol) and K_2CO_3 (0.06 g, 0.41 mmol) in water (0.4 mL) and acetone (0.4 mL) was stirred for 30 minutes. A solution of Me_2SO_4 (0.08 mL, 0.82 mmol) in acetone (0.3 mL) was then added drop wise. After 2 h the acetone was evaporated using a Rotovap, water was added (10mL), extracted with EtOAc (3 x 5 mL), dried (Na_2SO_4), filtered and concentrated. The residue was purified by column chromatography (SiO_2 , 4:1, Hex: EtOAc) to afford phenol **2.29** as a colorless solid (0.08 g, 0.31 mmol): 1H NMR (400 MHz, Chloroform-d) δ 12.52 (s, 1H), 10.17 (s, 1H), 7.48 – 7.32 (m, 6H), 6.03 (d, $J = 2.1$ Hz, 1H), 5.99 (d, $J = 2.2$

Hz, 1H), 5.09 (s, 2H), 3.82 (s, 3H). ^{13}C NMR (126 MHz, CDCl_3) δ 191.87, 166.30, 164.41, 163.48, 135.77, 128.91, 128.81, 127.52, 111.66, 98.54, 91.46, 70.65, 56.62.



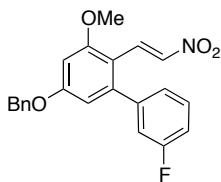
5-(Benzyloxy)-2-formyl-3-methoxyphenyl trifluoromethanesulfonate.

The compound was synthesized following the procedure used for the synthesis of **2.22**: ^1H NMR (400 MHz, Chloroform- d) δ 10.39 (s, 1H), 7.48 – 7.33 (m, 6H), 6.58 (d, $J = 2.1$ Hz, 1H), 6.41 (d, $J = 2.1$ Hz, 1H), 5.19 (s, 2H), 3.88 (s, 3H).



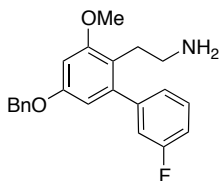
5-(Benzyloxy)-3'-fluoro-3-methoxy-[1,1'-biphenyl]-2-carbaldehyde.

The compound was synthesized following the procedure used for the synthesis of **2.23**: ^1H NMR (400 MHz, Chloroform- d) δ 10.01 (s, 1H), 7.46 – 7.32 (m, 6H), 7.13 – 6.97 (m, 3H), 6.60 (d, $J = 2.3$ Hz, 1H), 6.50 (d, $J = 2.3$ Hz, 1H), 5.14 (s, 2H), 3.92 (s, 3H). ^{13}C NMR (126 MHz, CDCl_3) δ 189.28, 164.17, 162.57, 147.03, 136.22, 129.69, 128.87, 128.25, 127.75, 127.22, 125.10, 116.31, 114.56, 108.92, 99.32, 70.80, 55.76. HRMS (ESI+) m/z : $[\text{M} + \text{H}^+]$ calculated for $\text{C}_{21}\text{H}_{17}\text{FO}_3$ 413.0283; found 413.0273.



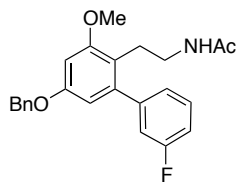
(E)-5-(Benzyloxy)-3'-fluoro-3-methoxy-2-(2-nitrovinyl)-1,1'-biphenyl.

The compound was synthesized following the procedure used for the synthesis of **(E)-5-(benzyloxy)-3'-fluoro-4-methyl-2-(2-nitrovinyl)-1,1'-biphenyl**: ^1H NMR (500 MHz, Chloroform-d) δ 7.89 – 7.75 (m, 2H), 7.41 – 7.24 (m, 7H), 7.11 – 7.04 (m, 1H), 7.02 – 6.92 (m, 3H), 6.84 (d, $J = 9.0$ Hz, 1H), 6.53 (d, $J = 2.4$ Hz, 1H), 5.17 (s, 2H), 3.78 (s, 3H). ^{13}C NMR (126 MHz, CDCl_3) δ 162.58, 160.76, 157.41, 138.14, 137.98, 135.31, 133.50, 130.14, 128.99, 128.61, 128.16, 127.56, 125.50, 116.67, 115.38, 110.99, 108.07, 99.38, 71.19, 55.69.



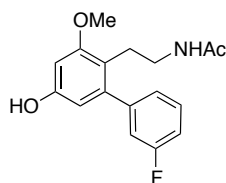
2-(5-(Benzyloxy)-3'-fluoro-3-methoxy-[1,1'-biphenyl]-2-yl)ethanamine.

The compound was synthesized following the procedure used for the synthesis of **2.24**: ^1H NMR (500 MHz, Chloroform-d) δ 7.44 – 7.39 (m, 3H), 7.37 – 7.29 (m, 3H), 7.01 (dd, $J = 7.8, 1.8$ Hz, 2H), 6.98 – 6.93 (m, 1H), 6.52 (d, $J = 2.5$ Hz, 1H), 6.34 (d, $J = 2.5$ Hz, 1H), 5.12 (s, 2H), 3.75 (s, 3H), 2.91 – 2.85 (m, 2H), 2.83 – 2.79 (m, 2H). ^{13}C NMR (126 MHz, CDCl_3) δ 163.48, 161.52, 158.75, 157.70, 143.39, 143.17, 136.64, 129.95, 129.88, 128.76, 127.97, 127.24, 124.70, 116.57, 114.30, 106.54, 99.46, 70.28, 55.37, 40.60, 29.72, 27.09. HRMS (ESI+) m/z : $[\text{M} + \text{H}^+]$ calculated for $\text{C}_{22}\text{H}_{22}\text{FNO}_2$ 352.1713; found 352.1693.



N-(2-(5-(Benzyloxy)-3'-fluoro-3-methoxy-[1,1'-biphenyl]-2-yl)ethyl)acetamide.

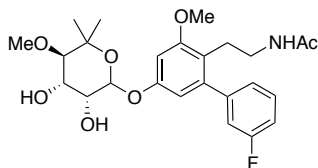
The compound was synthesized following the procedure used for the synthesis of **N-(2-(5-(benzyloxy)-3'-fluoro-4-methyl-[1,1'-biphenyl]-2-yl)ethyl)acetamide**: ^1H NMR (500 MHz, Chloroform- d) δ 7.44 – 7.26 (m, 6H), 7.02 – 6.96 (m, 2H), 6.92 (ddd, $J = 9.5, 2.5, 1.6$ Hz, 1H), 6.53 (d, $J = 2.5$ Hz, 1H), 6.32 (d, $J = 2.5$ Hz, 1H), 5.62 (s, 1H), 5.23 (s, 1H), 5.04 (s, 2H), 3.72 (s, 3H), 3.24 – 3.18 (m, 2H), 2.68 (t, $J = 6.5$ Hz, 2H), 1.62 (s, 3H). ^{13}C NMR (126 MHz, CDCl_3) δ 169.96, 163.44, 161.48, 158.61, 143.29, 136.46, 129.84, 129.77, 128.83, 128.33, 127.50, 124.87, 116.05, 114.29, 106.61, 99.31, 70.55, 55.45, 40.68, 25.87, 22.98. HRMS (ESI+), m/z $[\text{M}+\text{Na}^+]$ calculated for $\text{C}_{24}\text{H}_{24}\text{FNO}_3\text{Na}$ 393.3302; found 393.3311.



N-(2-(3'-Fluoro-5-hydroxy-3-methoxy-[1,1'-biphenyl]-2-yl)ethyl)acetamide.

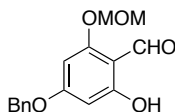
The compound was synthesized following the procedure used for the synthesis of **2.25**: ^1H NMR (500 MHz, Chloroform- d) δ 8.69 (s, 1H), 7.27 (ddd, $J = 8.3, 7.5, 6.0$ Hz, 1H), 6.96 (dddd, $J = 12.6, 6.6, 2.6, 1.1$ Hz, 2H), 6.88 (ddd, $J = 9.7, 2.6, 1.6$ Hz, 1H), 6.48 (d, $J = 2.6$ Hz, 1H), 6.23 (d, $J = 2.6$ Hz, 1H), 6.17 (s, 1H), 3.69 (s, 3H), 3.14 (ddd, $J = 9.0, 7.6, 5.8$ Hz, 2H), 2.63 – 2.56 (m, 2H), 1.91 (s, 3H). ^{13}C NMR (126 MHz, CDCl_3) δ 171.11, 162.29, 160.33, 156.08, 143.12,

141.54, 128.53, 123.67, 114.99, 113.68, 112.99, 106.07, 100.65, 54.26, 39.95, 21.86. HRMS (ESI+), m/z [M+Na⁺] calculated for C₁₇H₁₉FNO₃Na 302.1192; found 302.1183.



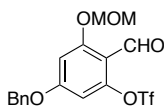
N-(2-(5-(((3R,4S,5R)-3,4-Dihydroxy-5-methoxy-6,6-dimethyltetrahydro-2H-pyran-2-yl)oxy)-3'-fluoro-3-methoxy-[1,1'-biphenyl]-2-yl)ethyl)acetamide (2.30).

The compound was synthesized following the procedure used for the synthesis of **2.27** with phenol **N-(2-(3'-fluoro-5-hydroxy-3-methoxy-[1,1'-biphenyl]-2-yl)ethyl)acetamide** to obtain the product as a white solid: ¹H NMR (400 MHz, Chloroform-d) δ 7.36 (ddd, J = 8.3, 7.6, 5.9 Hz, 1H), 7.09 – 6.99 (m, 1H), 6.95 (ddd, J = 9.6, 2.6, 1.5 Hz, 1H), 6.87 (d, J = 2.6 Hz, 1H), 6.37 (d, J = 2.5 Hz, 1H), 5.64 (s, 1H), 5.46 (d, J = 6.7 Hz, 1H), 5.30 (s, 1H), 4.38 (t, J = 4.2 Hz, 1H), 4.14 (dd, J = 6.7, 3.7 Hz, 1H), 3.78 (s, 3H), 3.50 (s, 3H), 3.19 (d, J = 4.6 Hz, 1H), 2.85 – 2.80 (m, 2H), 2.48 (dd, J = 11.7, 7.0 Hz, 2H), 2.17 (s, 3H), 1.93 (s, 3H), 1.88 – 1.69 (s, 3H). ¹³C NMR (126 MHz, CD₂Cl₂) δ 160.01, 154.63, 144.29, 129.07, 124.22, 115.35, 113.40, 111.65, 105.36, 88.50, 84.79, 75.27, 70.20, 69.23, 60.33, 54.98, 39.26, 25.66, 25.32, 21.78. HRMS (ESI+), m/z [M+Na⁺] calculated for C₂₅H₃₂FNO₇Na 500.2061; found 500.2054.



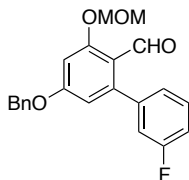
4-(Benzyloxy)-2-hydroxy-6-(methoxymethoxy)benzaldehyde (2.31).

A solution of **2.28** (0.45 g, 1.85 mmol) and DIPA (0.71 mL, 0.74 mmol) in anhydrous DCM (18 mL) was stirred at 0 °C. Chloromethyl methyl ether (0.84 mL, 11.1 mmol) was added drop wise after 10 minutes. After 16 h the reaction was quenched by the addition of water (5 mL), extracted with DCM (3 x 10 mL), dried (Na₂SO₄), filtered and concentrated. The residue was purified by column chromatography (SiO₂, 8:1, Hex:EtOAc) to afford the product as a white solid (0.40 g, 1.38 mmol): ¹H NMR (500 MHz, Chloroform-d) δ 12.36 (s, 1H), 10.20 (s, 1H), 7.44 – 7.40 (m, 5H), 6.97 – 6.94 (m, 2H), 5.18 (s, 2H), 5.10 (s, 2H), 3.48 (s, 3H). ¹³C NMR (126 MHz, CDCl₃) δ 192.17, 149.99, 136.21, 128.84, 128.75, 127.48, 126.34, 95.98, 94.12, 92.39, 70.57, 56.52.



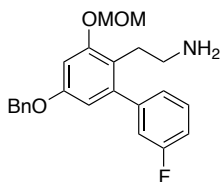
5-(Benzyloxy)-2-formyl-3-(methoxymethoxy)phenyl trifluoromethanesulfonate.

The compound was synthesized following the procedure used for the synthesis of **2.22**: ¹H NMR (500 MHz, Chloroform-d) δ 10.39 (d, J = 1.5 Hz, 1H), 7.43 (dt, J = 4.7, 1.1 Hz, 5H), 6.76 (s, 1H), 6.57 (d, J = 1.7 Hz, 1H), 5.21 (d, J = 1.7 Hz, 2H), 5.18 (t, J = 1.6 Hz, 3H), 3.49 (d, J = 1.6 Hz, 3H). ¹³C NMR (126 MHz, CDCl₃) δ 185.73, 163.19, 162.85, 149.39, 134.78, 128.76, 127.45, 112.66, 103.39, 100.54, 94.53, 71.32, 56.52, 29.60.



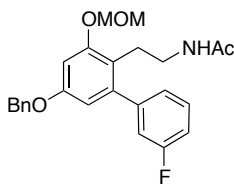
5-(Benzyloxy)-3'-fluoro-3-(methoxymethoxy)-[1,1'-biphenyl]-2-carbaldehyde.

The compound was synthesized following the procedure used for the synthesis of **2.23**: ^1H NMR (500 MHz, Chloroform-d) δ 10.18 (s, 1H), 7.52 – 7.49 (m, 2H), 7.43 – 7.39 (m, 2H), 7.38 – 7.32 (m, 2H), 7.10 – 7.04 (m, 2H), 7.02 (ddd, $J = 9.5, 2.6, 1.8$ Hz, 1H), 6.74 (d, $J = 2.2$ Hz, 1H), 6.56 (d, $J = 2.3$ Hz, 1H), 5.22 (d, 4H), 3.49 (s, 3H). ^{13}C NMR (126 MHz, CDCl_3) δ 189.76, 163.70, 162.55, 161.95, 147.20, 142.27, 136.33, 129.90, 129.08, 128.52, 127.56, 125.35, 118.46, 116.59, 114.90, 111.27, 101.03, 94.62, 71.11, 56.83. HRMS (ESI+) m/z : $[\text{M} + \text{H}^+]$ calculated for $\text{C}_{22}\text{H}_{19}\text{FO}_4$ 367.1404; found 367.1409.



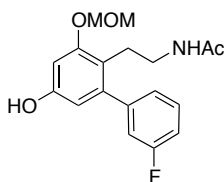
2-(5-(Benzyloxy)-3'-fluoro-3-(methoxymethoxy)-[1,1'-biphenyl]-2-yl)ethanamine.

The compound was synthesized following the procedure used for the synthesis of **2.24**: ^1H NMR (500 MHz, Chloroform-d) δ 7.46 – 7.41 (m, 2H), 7.41 – 7.36 (m, 2H), 7.33 (td, $J = 7.8, 7.3, 1.7$ Hz, 2H), 7.03 (dd, $J = 7.8, 1.5$ Hz, 2H), 6.97 (ddd, $J = 9.6, 2.6, 1.6$ Hz, 1H), 6.69 (d, $J = 2.4$ Hz, 1H), 6.52 (d, $J = 2.4$ Hz, 1H), 5.14 (s, 2H), 5.09 (s, 2H), 3.47 (s, 3H), 2.80 – 2.75 (m, 2H), 2.73 (dd, $J = 6.4, 2.0$ Hz, 2H). ^{13}C NMR (126 MHz, CDCl_3) δ 163.78, 161.82, 158.17, 156.53, 144.04, 143.50, 137.15, 130.11, 130.04, 129.08, 128.40, 127.73, 125.19, 119.38, 114.51, 114.34, 109.88, 101.10, 95.01, 70.66, 56.48, 42.01, 30.10. HRMS (ESI+) m/z : $[\text{M} + \text{H}^+]$ calculated for $\text{C}_{23}\text{H}_{24}\text{FNO}_3$ 382.1662; found 382.1657.



N-(2-(5-(Benzyloxy)-3'-fluoro-3-(methoxymethoxy)-[1,1'-biphenyl]-2-yl)ethyl)acetamide.

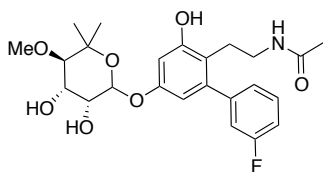
The compound was synthesized following the procedure used for the synthesis of **N-(2-(5-(benzyloxy)-3'-fluoro-4-methyl-[1,1'-biphenyl]-2-yl)ethyl)acetamide**: ^1H NMR (500 MHz, Chloroform- d) δ 7.49 – 7.45 (m, 2H), 7.45 – 7.40 (m, 2H), 7.39 – 7.33 (m, 2H), 7.06 (dd, $J = 7.8$, 1.6 Hz, 2H), 7.00 – 6.96 (m, 1H), 6.73 (d, $J = 2.4$ Hz, 1H), 6.55 (d, $J = 2.4$ Hz, 1H), 5.70 – 5.65 (m, 1H), 5.16 (s, 2H), 5.11 (s, 2H), 3.49 (s, 3H), 3.33 – 3.24 (m, 2H), 2.76 (t, $J = 6.6$ Hz, 2H), 1.68 (s, 3H). ^{13}C NMR (126 MHz, CDCl_3) δ 168.97, 162.38, 160.42, 156.62, 155.25, 142.30, 135.38, 128.77, 127.77, 127.28, 126.52, 123.86, 118.36, 115.04, 113.08, 108.75, 99.64, 93.58, 69.52, 55.11, 39.53, 24.89, 21.99. HRMS (ESI+) m/z : $[\text{M} + \text{H}^+]$ calculated for $\text{C}_{25}\text{H}_{26}\text{FNO}_4$ 423.1891; found 423.1895.



N-(2-(3'-Fluoro-5-hydroxy-3-(methoxymethoxy)-[1,1'-biphenyl]-2-yl)ethyl)acetamide.

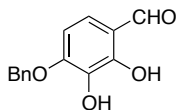
The compound was synthesized following the procedure used for the synthesis of **2.25**: ^1H NMR (500 MHz, Chloroform- d) δ 7.09 – 6.93 (m, 2H), 6.84 (d, $J = 2.5$ Hz, 1H), 6.77 (d, $J = 2.1$ Hz, 1H), 6.74 (d, $J = 2.4$ Hz, 1H), 6.56 (dd, $J = 7.5$, 2.2 Hz, 1H), 6.52 (d, $J = 2.5$ Hz, 1H), 5.71 – 5.67 (m, 1H), 5.17 (d, $J = 4.1$ Hz, 2H), 3.49 (d, $J = 3.2$ Hz, 3H), 3.29 (q, $J = 6.5$ Hz, 2H), 2.75 (dt, $J = 9.9$, 6.8 Hz, 2H), 1.38 (s, 3H). ^{13}C NMR (126 MHz, CDCl_3) δ 169.02, 161.94, 160.41,

142.29, 135.38, 128.36, 123.85, 118.34, 115.20, 113.07, 108.75, 99.63, 93.57, 55.59, 39.52, 28.67, 21.96. HRMS (ESI+), m/z [M+Na⁺] calculated for C₁₈H₂₀FNO₄Na 356.1274; found 356.1241.



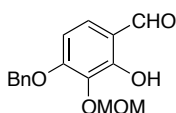
N-(2-(5-(((3R,4S,5R)-3,4-Dihydroxy-5-methoxy-6,6-dimethyltetrahydro-2H-pyran-2-yl)oxy)-3'-fluoro-3-hydroxy-[1,1'-biphenyl]-2-yl)ethyl)acetamide (2.32).

The compound was synthesized following the procedure used for the synthesis of **2.27** using phenol N-(2-(3'-fluoro-5-hydroxy-3-(methoxymethoxy)-[1,1'-biphenyl]-2-yl)ethyl)acetamide. Addition of a slight excess of boron trifluoride diethyl etherate (~0.02mL) resulted in coupling of the activated sugar **2.26** and subsequent removal of the methoxymethyl protecting group⁶⁴ to produce the product as a white solid: ¹H NMR (500 MHz, Methylene Chloride-d₂) δ 7.40 – 7.31 (m, 1H), 7.05 (dddd, J = 9.0, 7.9, 3.7, 2.6, 1.2 Hz, 2H), 6.96 (ddd, J = 9.7, 2.6, 1.6 Hz, 1H), 6.38 (d, J = 2.5 Hz, 1H), 6.30 (d, J = 2.4 Hz, 1H), 5.46 (d, J = 2.5 Hz, 1H), 4.11 (dd, J = 9.0, 3.5 Hz, 1H), 4.04 (dd, J = 3.5, 2.4 Hz, 1H), 3.54 (s, 3H), 3.35 (p, J = 1.7 Hz, 1H), 3.28 (d, J = 9.0 Hz, 1H), 2.67 – 2.61 (m, 2H), 1.88 (s, 3H), 1.35 (s, 3H), 1.33 (s, 3H), ¹³C NMR (126 MHz, CD₂Cl₂) δ 170.94, 162.62, 155.96, 154.95, 143.21, 142.14, 128.92, 124.14, 115.61, 115.08, 112.93, 108.46, 102.21, 97.09, 77.38, 70.39, 67.66, 60.76, 39.64, 27.69, 22.89, 21.99, 21.77, HRMS (ESI+), m/z [M+Na⁺] calculated for C₂₄H₃₀FNO₇Na 486.1904; found 486.1884.



4-(Benzyloxy)-2,3-dihydroxybenzaldehyde.

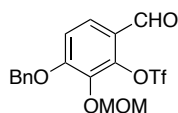
A solution of 2,3,4-trihydroxybenzaldehyde (5g, 32.5mmol) and NaHCO_3 (5.45g, 64.9 mmol) in anhydrous acetonitrile (320mL) was heated at reflux. BnBr (6.9mL, 58.4 mmol) was added over 10 minutes. After 16 h the reaction was cooled to rt, quenched by the addition of water (50ml), extracted with EtOAc (3 x 50mL), washed with saturated aqueous NaCl solution, dried (Na_2SO_4), filtered and concentrated. The residue was purified by column chromatography (SiO_2 , 10:1, DCM: MeOH) to afford the product as a light brown solid (1.5 g, 6.2 mmol): ^1H NMR (500 MHz, DMSO- d_6) δ 10.38 (s, 1H), 9.97 (s, 1H), 8.93 (s, 1H), 7.51 – 7.47 (m, 2H), 7.41 – 7.37 (m, 2H), 7.33 (d, $J = 7.3$ Hz, 1H), 7.18 (d, $J = 8.8$ Hz, 1H), 6.76 (d, $J = 8.8$ Hz, 1H), 5.25 (s, 2H). ^{13}C NMR (126 MHz, DMSO) δ 192.45, 152.91, 150.23, 136.60, 133.88, 128.36, 127.87, 127.59, 122.14, 116.97, 105.46, 69.82. HRMS (ESI+) m/z : $[\text{M} - \text{H}^+]$ calculated for $\text{C}_{33}\text{H}_{43}\text{N}_2\text{O}_4$ 243.0657; found 243.0667.



4-(Benzyloxy)-2-hydroxy-3-(methoxymethoxy)benzaldehyde (2.34).

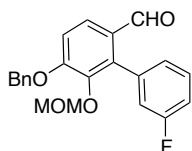
A solution of 4-(benzyloxy)-2,3-dihydroxybenzaldehyde (0.45 g, 1.85 mmol) and DIPEA (0.71mL, 0.74 mmol) in anhydrous DCM (18mL) was stirred at 0 °C. MOMCl (0.84 mL, 11.1 mmol) was added drop wise after 10 minutes. After 16 h the reaction was quenched by the addition of water (5mL), extracted with DCM (3 x 10mL), dried (Na_2SO_4), filtered and concentrated. The residue was purified by column chromatography (SiO_2 , 8:1, Hex:EtOAc) to

afford **23** as a light yellow solid (0.40 g, 1.38 mmol): ^1H NMR (400 MHz, Chloroform- d) δ 11.29 (s, 1H), 9.77 (s, 1H), 7.52 – 7.48 (m, 1H), 7.42 – 7.28 (m, 5H), 6.79 (d, J = 8.8 Hz, 1H), 5.22 (s, 2H), 5.13 (s, 2H), 3.45 (s, 3H).



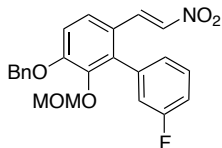
3-(Benzyloxy)-6-formyl-2-(methoxymethoxy)phenyl trifluoromethanesulfonate.

The compound was synthesized following the procedure used for the synthesis of **2.22**: ^1H NMR (500 MHz, Chloroform- d) δ 10.00 (s, 1H), 7.62 (d, J = 8.7 Hz, 1H), 7.37 – 7.24 (m, 5H), 7.02 (dd, J = 8.9, 0.5 Hz, 1H), 5.18 (s, 2H), 5.13 (s, 2H), 3.48 (s, 3H). ^{13}C NMR (126 MHz, CDCl_3) δ 194.93, 157.81, 144.06, 138.45, 134.80, 130.51, 128.89, 128.73, 128.36, 127.63, 126.46, 112.58, 105.34, 98.76, 71.64, 58.06.



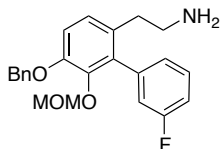
5-(Benzyloxy)-3'-fluoro-6-(methoxymethoxy)-[1,1'-biphenyl]-2-carbaldehyde.

The compound was synthesized following the procedure used for the synthesis of **2.23**: ^1H NMR (500 MHz, Chloroform- d) δ 9.55 (s, 1H), 7.76 (d, J = 8.7 Hz, 1H), 7.39 – 7.27 (m, 6H), 7.26 – 7.19 (m, 2H), 7.08 – 7.04 (m, 2H), 5.15 (s, 2H), 4.83 (s, 2H), 2.82 (s, 3H). ^{13}C NMR (126 MHz, CDCl_3) δ 190.84, 163.26, 156.34, 135.63, 133.76, 129.67, 129.41, 128.79, 128.45, 128.14, 127.47, 127.03, 125.16, 123.64, 118.16, 114.86, 112.97, 98.61, 70.93, 56.76. HRMS (ESI+) m/z : $[\text{M} + \text{H}^+]$ calculated for $\text{C}_{22}\text{H}_{19}\text{FO}_4$ 367.1404; found 367.1401.



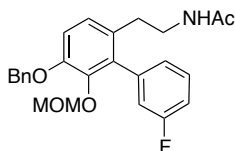
(E)-3-(Benzyloxy)-3'-fluoro-2-(methoxymethoxy)-6-(2-nitrovinyl)-1,1'-biphenyl.

The compound was synthesized following the procedure used for the synthesis of **(E)-5-(benzyloxy)-3'-fluoro-4-methyl-2-(2-nitrovinyl)-1,1'-biphenyl**: ^1H NMR (400 MHz, Chloroform-d) δ 7.84 (d, $J = 8.7$ Hz, 1H), 7.73 (d, $J = 13.6$ Hz, 1H), 7.48 – 7.33 (m, 5H), 7.19 – 7.11 (m, 1H), 7.11 – 7.03 (m, 2H), 5.22 (s, 2H), 4.91 (s, 2H), 2.90 (s, 3H).



2-(5-(Benzyloxy)-3'-fluoro-6-(methoxymethoxy)-[1,1'-biphenyl]-2-yl)ethanamine.

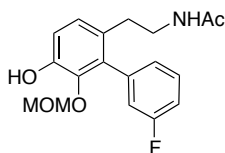
The compound was synthesized following the procedure used for the synthesis of **2.24**: ^1H NMR (400 MHz, Chloroform-d) δ 7.43 – 7.29 (m, 6H), 7.06 – 6.96 (m, 4H), 6.93 (d, $J = 8.4$ Hz, 1H), 5.07 (s, 4H), 4.86 (s, 2H), 2.85 (s, 3H), 2.79 – 2.63 (m, 4H). HRMS (ESI+) m/z : $[\text{M} + \text{H}^+]$ calculated for $\text{C}_{23}\text{H}_{24}\text{FNO}_3$ 382.1662; found 382.1676.



N-(2-(5-(Benzyloxy)-3'-fluoro-6-(methoxymethoxy)-[1,1'-biphenyl]-2-yl)ethyl)acetamide.

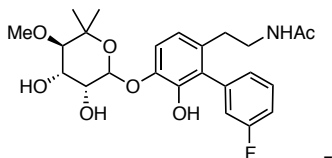
The compound was synthesized following the procedure used for the synthesis of **N-(2-(5-(benzyloxy)-3'-fluoro-4-methyl-[1,1'-biphenyl]-2-yl)ethyl)acetamide**: ^1H NMR (500 MHz, Chloroform-d) δ 7.38 – 7.24 (m, 6H), 7.00 – 6.88 (m, 6H), 5.24 (t, $J = 5.8$ Hz, 1H), 5.04 (s, 2H),

4.81 (s, 2H), 3.15 (tdd, J = 7.0, 5.7, 3.7 Hz, 2H), 2.80 (s, 3H), 2.51 (t, J = 7.2 Hz, 2H), 1.80 (s, 3H). ¹³C NMR (126 MHz, CDCl₃) δ 168.85, 160.45, 149.09, 142.85, 138.19, 135.68, 129.01, 128.51, 128.44, 127.56, 127.00, 126.34, 125.14, 124.16, 116.31, 112.93, 112.50, 97.60, 69.76, 55.54, 39.21, 31.36, 22.25. HRMS (ESI+) m/z: [M + H⁺] calculated for C₂₅H₂₆FNO₄ 423.1891; found 423.1886.



N-(2-(3'-Fluoro-5-hydroxy-6-(methoxymethoxy)-[1,1'-biphenyl]-2-yl)ethyl)acetamide.

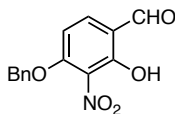
The compound was synthesized following the procedure used for the synthesis of **2.25**: ¹H NMR (500 MHz, Chloroform-d) δ 7.33 (td, J = 8.0, 6.0 Hz, 1H), 7.03 – 6.79 (m, 5H), 5.27 (s, 1H), 4.60 (s, 2H), 3.35 (s, 3H), 3.18 – 3.10 (m, 2H), 2.48 (t, J = 7.2 Hz, 2H), 1.81 (s, 3H). ¹³C NMR (126 MHz, CDCl₃) δ 168.93, 160.56, 146.67, 142.23, 137.91, 133.79, 128.86, 127.78, 125.36, 124.57, 115.90, 115.44, 113.22, 98.69, 56.15, 39.30, 31.28, 22.23. HRMS (ESI+), m/z [M+Na⁺] calculated for C₁₈H₂₀FNO₄Na 356.1274; found 356.1258.



N-(2-(5-(((3R,4S,5R)-3,4-Dihydroxy-5-methoxy-6,6-dimethyltetrahydro-2H-pyran-2-yl)oxy)-3'-fluoro-3-hydroxy-[1,1'-biphenyl]-2-yl)ethyl)acetamide (2.34**).**

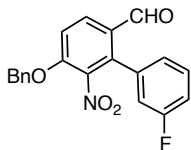
The compound was synthesized following the procedure used for the synthesis of **2.27** using phenol N-(2-(3'-fluoro-5-hydroxy-6-(methoxymethoxy)-[1,1'-biphenyl]-2-yl)ethyl)acetamide.

Addition of a slight excess of boron trifluoride diethyl etherate (~0.02mL) resulted in coupling of the activated sugar **2.26** and subsequent removal of the methoxymethyl protecting group to produce the product as a white solid: ¹H NMR (500 MHz, Methylene Chloride-d₂) δ 7.04 (d, *J* = 8.4 Hz, 1H), 7.00 – 6.80 (m, 3H), 6.65 (dd, *J* = 8.5, 3.6 Hz, 1H), 6.50 (s, 1H), 5.46 – 5.34 (m, 1H), 4.14 (dd, *J* = 6.5, 3.5 Hz, 1H), 3.95 (t, *J* = 4.1 Hz, 1H), 3.42 (s, 3H), 3.14 (dd, *J* = 6.9, 5.2 Hz, 1H), 3.09 (q, *J* = 6.8 Hz, 2H), 2.45 (t, *J* = 7.3 Hz, 2H), 1.74 (s, 3H), 1.34 (s, 3H), 1.17 (s, 3H). ¹³C NMR (126 MHz, CD₂Cl₂) δ 170.51, 162.04, 144.87, 143.76, 139.28, 132.66, 130.23, 128.52, 126.40, 120.84, 117.37, 114.31, 100.15, 83.82, 78.74, 70.35, 69.47, 61.05, 40.66, 32.79, 24.54, 23.33. HRMS (ESI+), *m/z* [M+Na⁺] calculated for C₂₄H₃₀FNO₇Na 486.1904; found 486.1902.



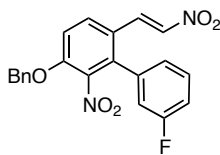
4-(Benzyloxy)-2-hydroxy-3-nitrobenzaldehyde (**2.37**).

2,4-Dihydroxy-3-nitrobenzaldehyde (0.22g, 1.2mmol)⁵⁷ was dissolved in anhydrous acetonitrile (6mL). KI catalyst (0.004g, 0.024mmol) was added and BnBr was added dropwise (0.18mL, 1.56 mmol). The reaction was stirred on at reflux. The reaction was then cool to rt and quenched with water. The mixture was washed with HCl and brine and extracted with EtOAc (3 x 20mL). The organic layers were combined, dried, and concentrated to obtain **2.37** as a yellow solid in 75% yield: ¹H NMR (500 MHz, Chloroform-d) δ 11.75 (s, 1H), 9.80 (s, 1H), 7.60 (d, *J* = 8.8 Hz, 1H), 7.42 – 7.35 (m, 5H), 6.70 (d, *J* = 8.8 Hz, 1H), 5.29 (s, 2H). ¹³C NMR (126 MHz, CDCl₃) δ 194.27, 156.58, 155.00, 136.36, 134.34, 128.90, 128.71, 127.00, 115.77, 104.97, 71.53.



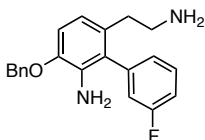
5-(Benzyloxy)-3'-fluoro-6-nitro-[1,1'-biphenyl]-2-carbaldehyde.

The compound was synthesized following the procedure used for the synthesis of **2.23**: ^1H NMR (500 MHz, Chloroform- d) δ 12.72 (s, 1H), 7.63 (d, $J = 9.1$ Hz, 1H), 7.54 – 7.46 (m, 1H), 7.41 – 7.29 (m, 8H), 6.57 (d, $J = 9.1$ Hz, 1H), 5.27 (s, 2H). ^{13}C NMR (126 MHz, CDCl_3) δ 205.99, 197.26, 162.38, 160.40, 155.63, 154.99, 137.79, 135.02, 133.47, 129.43, 127.86, 127.63, 125.95, 123.67, 118.32, 115.03, 112.80, 102.91, 70.36.



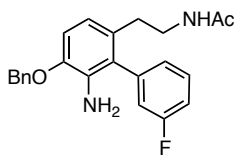
(E)-3-(Benzyloxy)-3'-fluoro-2-nitro-6-(2-nitrovinyl)-1,1'-biphenyl.

The compound was synthesized following the procedure used for the synthesis of **(E)-5-(benzyloxy)-3'-fluoro-4-methyl-2-(2-nitrovinyl)-1,1'-biphenyl**: ^1H NMR (500 MHz, Chloroform- d) δ 7.69 (d, $J = 9.0$ Hz, 1H), 7.61 (d, $J = 13.7$ Hz, 1H), 7.42 – 7.34 (m, 7H), 7.31 (d, $J = 13.6$ Hz, 1H), 7.17 (d, $J = 8.9$ Hz, 1H), 7.03 (ddd, $J = 7.6, 1.6, 1.0$ Hz, 1H), 6.98 (ddd, $J = 8.9, 2.6, 1.6$ Hz, 1H), 5.30 (s, 2H). ^{13}C NMR (126 MHz, CDCl_3) δ 163.50, 161.52, 151.73, 137.67, 135.15, 134.51, 130.84, 129.90, 128.95, 128.74, 127.10, 125.26, 122.28, 116.93, 116.60, 114.06, 71.46.



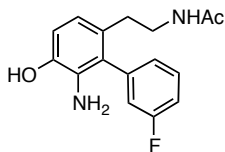
6-(2-Aminoethyl)-3-(benzyloxy)-3'-fluoro-[1,1'-biphenyl]-2-amine.

Lithium Aluminum Hydride (0.22 g, 5.51 mmol) was dissolved in dry THF (10 mL) and cooled to 0°C. **(E)-3-(benzyloxy)-3'-fluoro-2-nitro-6-(2-nitrovinyl)-1,1'-biphenyl** (0.5g, 1.377mmol) was dissolved in anhydrous THF (2.0 mL) and added drop wise to the reaction. The reaction slowly warmed to rt and stirred for 12 h. Upon completion, 3N NaOH (1mL), water (1mL), and EtOAc (3mL) were added sequentially to quench the reaction. After stirring for one h the mixture was filtered through a pad of Celite. The solid was washed with warm EtOAc (100mL). The filtrate was collected, dried, and concentrated and used directly in the next step: HRMS (ESI+), m/z [M+H⁺] calculated for C₂₁H₂₂FN₂O 337.1716; found 337.1729.



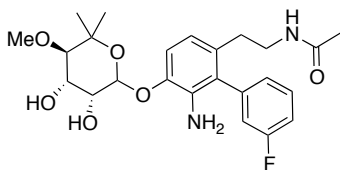
N-(2-(6-Amino-5-(benzyloxy)-3'-fluoro-[1,1'-biphenyl]-2-yl)ethyl)acetamide.

The compound was synthesized following the procedure used for the synthesis of **N-(2-(5-(benzyloxy)-3'-fluoro-4-methyl-[1,1'-biphenyl]-2-yl)ethyl)acetamide**: ¹H NMR (500 MHz, Chloroform-d) δ 7.49 – 7.31 (m, 6H), 7.14 – 6.95 (m, 3H), 6.85 (d, J = 8.3 Hz, 1H), 6.63 (d, J = 8.3 Hz, 1H), 5.20 (s, 1H), 5.11 (s, 2H), 3.24 – 3.19 (m, 2H), 2.54 – 2.45 (m, 2H), 1.88 (s, 3H). ¹³C NMR (126 MHz, CDCl₃) δ 168.73, 161.24, 146.86, 138.69, 134.41, 133.37, 130.60, 129.31, 128.32, 127.71, 127.05, 126.58, 126.08, 124.73, 117.08, 115.90, 113.76, 112.68, 110.02, 70.07, 39.08, 31.53, 22.32. HRMS (ESI+), m/z [M+H⁺] calculated for C₂₃H₂₃FN₂O₂ 378.1781; found 378.1785.



N-(2-(6-Amino-3'-fluoro-5-hydroxy-[1,1'-biphenyl]-2-yl)ethyl)acetamide.

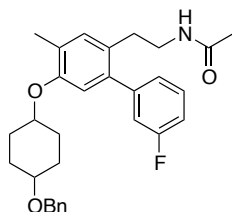
The compound was synthesized following the procedure used for the synthesis of **2.25**: ^1H NMR (500 MHz, Chloroform- d) δ 7.51 (ddd, $J = 8.4, 7.5, 5.9$ Hz, 1H), 7.18 (tdd, $J = 8.4, 2.6, 1.0$ Hz, 1H), 7.11 (d, $J = 8.4$ Hz, 1H), 7.06 (d, $J = 8.4$ Hz, 1H), 7.00 (ddd, $J = 7.5, 1.6, 1.0$ Hz, 1H), 6.96 – 6.92 (m, 2H), 6.74 (s, 1H), 5.33 (d, $J = 6.6$ Hz, 1H), 3.22 (qd, $J = 7.4, 6.0$ Hz, 2H), 2.54 – 2.46 (m, 2H), 2.25 (d, $J = 0.7$ Hz, 2H), 1.89 (s, 3H). ^{13}C NMR (126 MHz, CDCl_3) δ 170.05, 162.27, 138.63, 136.41, 133.89, 131.41, 128.97, 126.46, 125.49, 123.92, 120.32, 116.96, 115.90, 40.31, 32.20, 23.64. HRMS (ESI+), m/z $[\text{M}+\text{H}^+]$ calculated for $\text{C}_{16}\text{H}_{17}\text{FN}_2\text{O}_2$ 288.1381; found 288.1385.



N-(2-(6-Amino-5-(((3R,4S,5R)-3,4-dihydroxy-5-methoxy-6,6-dimethyltetrahydro-2H-pyran-2-yl)oxy)-3'-fluoro-[1,1'-biphenyl]-2-yl)ethyl)acetamide (2.38**).**

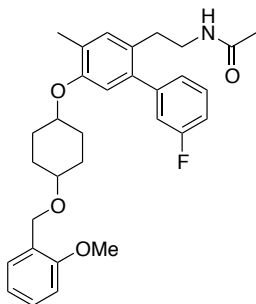
The compound was synthesized following the procedure used for the synthesis of **2.27** to obtain the product as a white solid: ^1H NMR (500 MHz, Chloroform- d) δ 7.45 (tdd, $J = 7.7, 5.8, 1.7$ Hz, 1H), 7.14 – 7.05 (m, 1H), 7.04 – 6.91 (m, 2H), 6.63 (d, $J = 8.3$ Hz, 1H), 5.47 (t, $J = 2.5$ Hz, 1H), 5.35 – 5.27 (m, 1H), 4.22 (dd, $J = 8.4, 3.2$ Hz, 1H), 4.17 (t, $J = 3.2$ Hz, 1H), 3.58 (s, 3H), 3.33 (d, $J = 8.4$ Hz, 1H), 3.22 (dd, $J = 8.3, 4.8$ Hz, 2H), 2.48 (t, $J = 7.1$ Hz, 2H), 1.89 (s, 3H), 1.26 (d, $J = 10.5$ Hz, 6H). ^{13}C NMR (126 MHz, CDCl_3) δ 169.74, 143.09, 139.42, 134.30,

130.85, 130.38, 125.68, 118.50, 117.00, 114.76, 114.06, 98.62, 78.16, 70.91, 68.65, 61.50, 39.98, 32.50, 29.59, 28.40, 23.23. HRMS (ESI+), m/z $[M+Na^+]$ calculated for $C_{24}H_{31}FN_2O_6Na$ 485.2064, found 485.2070.



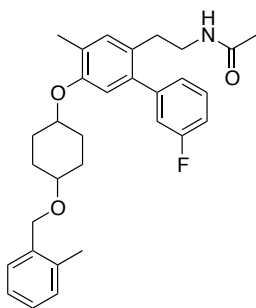
N-(2-(5-((4-(Benzyloxy)cyclohexyl)oxy)-3'-fluoro-4-methyl-[1,1'-biphenyl]-2-yl)ethyl)acetamide (2.39a).

The compound was synthesized following the procedure used for the synthesis of **2.4** using phenol **2.25** to obtain the product as a white solid: 1H -NMR (500 MHz, Chloroform- d) δ 7.39 – 7.32 (m, 5H), 7.08 – 7.02 (m, 2H), 6.99 (ddd, $J = 9.5, 2.6, 1.5$ Hz, 1H), 6.91 – 6.80 (m, 2H), 6.67 (dd, $J = 15.7, 7.1$ Hz, 1H), 5.29 – 5.23 (m, 1H), 4.56 (dd, $J = 11.6, 1.6$ Hz, 2H), 4.36 (dd, $J = 6.0, 3.0$ Hz, 1H), 3.53 – 3.44 (m, 1H), 3.30 – 3.24 (m, 2H), 2.70 (dt, $J = 9.7, 7.1$ Hz, 2H), 2.23 (s, 3H), 2.10 – 1.99 (m, 2H), 1.87 (s, 3H), 1.79 – 1.71 (m, 2H), 1.68 – 1.54 (m, 4H). ^{13}C NMR (126 MHz, $CDCl_3$) δ 168.82, 162.45, 155.80, 153.00, 142.86, 142.08, 138.02, 134.06, 131.17, 130.83, 130.24, 127.43, 124.01, 119.42, 115.31, 113.01, 109.02, 63.52, 54.26, 39.61, 31.31, 30.74, 22.27, 19.04, 15.08. HRMS (ESI+), m/z $[M+Na^+]$ calculated for $C_{30}H_{34}FNO_3Na$ 498.2420; found 498.2414.



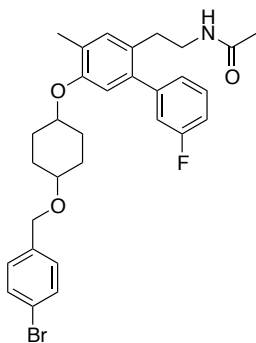
N-(2-(3'-Fluoro-5-((4-((2-methoxybenzyl)oxy)cyclohexyl)oxy)-4-methyl-[1,1'-biphenyl]-2-yl)ethyl)acetamide (2.39b).

The compound was synthesized following the procedure used for the synthesis of **2.39a** to obtain the product as a white solid: $^1\text{H-NMR}$ (500 MHz, Chloroform- d) δ 7.40 – 7.32 (m, 3H), 7.13 – 7.03 (m, 5H), 6.86 (ddd, $J = 8.0, 2.7, 1.1$ Hz, 1H), 6.70 – 6.63 (m, 1H), 5.29 (d, $J = 5.6$ Hz, 1H), 4.59 (d, $J = 10.5$ Hz, 2H), 4.39 – 4.34 (m, 1H), 4.34 – 4.24 (m, 1H, minor diastereomer), 3.83 (d, $J = 2.5$ Hz, 3H), 3.57 – 3.46 (m, 1H), 3.31 – 3.23 (m, 2H), 2.70 (t, $J = 7.3$ Hz, 2H), 2.31 (s, 3H), 2.11 – 1.99 (m, 2H), 1.88 (d, $J = 16.7$ Hz, 3H), 1.81 – 1.70 (m, 2H), 1.71 – 1.53 (m, 4H). $^{13}\text{C NMR}$ (126 MHz, CDCl_3) δ 168.79, 162.45, 160.49, 152.94, 142.88, 137.95, 134.38, 134.06, 131.19, 130.83, 130.24, 128.78, 127.33, 126.75, 126.48, 126.40, 124.01, 123.98, 115.30, 115.14, 112.99, 68.78, 39.60, 30.74, 26.77, 26.38, 22.28, 19.05, 15.14. HRMS (ESI+), m/z $[\text{M}+\text{Na}^+]$ calculated for $\text{C}_{31}\text{H}_{36}\text{FNO}_4\text{Na}$ 528.2526; found 528.2534.



N-(2-(3'-Fluoro-4-methyl-5-((4-((2-methylbenzyl)oxy)cyclohexyl)oxy)-[1,1'-biphenyl]-2-yl)ethyl)acetamide (2.39c).

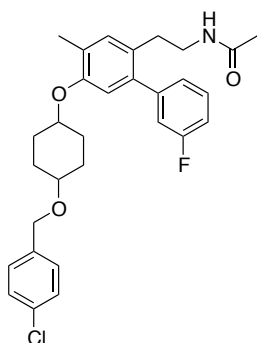
The compound was synthesized following the procedure used for the synthesis of **2.39a** to obtain the product as a white solid: $^1\text{H-NMR}$ (500 MHz, Chloroform- d) δ 7.29 (dddd, $J = 13.5, 8.2, 6.5, 2.7$ Hz, 2H), 7.14 – 7.07 (m, 3H), 6.99 (td, $J = 4.2, 3.4, 1.6$ Hz, 3H), 6.92 (ddd, $J = 9.7, 2.6, 1.6$ Hz, 1H), 6.59 (d, $J = 6.4$ Hz, 1H), 5.23 (t, $J = 5.7$ Hz, 1H), 4.46 (d, $J = 11.1$ Hz, 2H), 4.30 (dt, $J = 6.0, 2.9$ Hz, 1H), 4.22 (dt, $J = 8.2, 4.8$ Hz, 1H), 3.44 (dtt, $J = 23.4, 7.9, 3.6$ Hz, 1H), 3.20 (td, $J = 7.2, 5.9$ Hz, 2H), 2.62 (t, $J = 7.2$ Hz, 2H), 2.27 (d, $J = 9.0$ Hz, 3H), 2.17 (dd, $J = 11.8, 0.7$ Hz, 3H), 2.06 – 1.92 (m, 2H), 1.79 (s, 3H), 1.74 – 1.66 (m, 2H), 1.64 – 1.54 (m, 4H). $^{13}\text{C NMR}$ (126 MHz, CDCl_3) δ 169.86, 163.50, 161.54, 153.99, 144.00, 139.09, 136.73, 132.24, 130.22, 128.46, 127.69, 125.82, 125.03, 116.35, 114.06, 75.20, 74.49, 72.36, 68.45, 40.66, 31.79, 27.86, 27.43, 23.32, 18.90, 16.18. HRMS (ESI+), m/z $[\text{M}+\text{Na}^+]$ calculated for $\text{C}_{31}\text{H}_{36}\text{FNO}_4\text{Na}$ 528.2526; found 528.2504.



N-(2-(5-((4-(4-Bromobenzyl)oxy)cyclohexyl)oxy)-3'-fluoro-4-methyl-[1,1'-biphenyl]-2-yl)ethyl)acetamide (2.39d).

The compound was synthesized following the procedure used for the synthesis of **2.39a** to obtain the product as a white solid: $^1\text{H-NMR}$ (500 MHz, Chloroform- d) δ 7.49 – 7.44 (m, 2H),

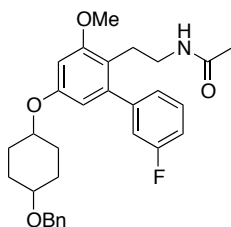
7.41 – 7.30 (m, 2H), 7.23 (dd, $J = 12.4, 8.4$ Hz, 2H), 7.09 – 7.03 (m, 3H), 6.67 (d, $J = 9.5$ Hz, 1H), 5.31 – 5.23 (m, 1H), 4.51 (s, 2H), 4.36 (dt, $J = 6.0, 3.0$ Hz, 1H), 3.47 (dq, $J = 8.0, 4.3, 3.8$ Hz, 1H), 3.27 (td, $J = 7.2, 5.8$ Hz, 2H), 2.71 (dd, $J = 9.6, 7.2$ Hz, 2H), 2.26 (s, 3H), 2.02 (td, $J = 11.9, 5.7$ Hz, 2H), 1.87 (s, 3H), 1.73 (ddd, $J = 13.9, 7.0, 3.8$ Hz, 2H), 1.67 – 1.54 (m, 4H). ^{13}C NMR (126 MHz, CDCl_3) δ 169.95, 161.68, 154.09, 144.04, 139.23, 138.18, 132.39, 131.60, 129.97, 129.28, 127.91, 127.73, 127.53, 125.18, 121.38, 116.48, 114.63, 114.18, 113.98, 72.42, 69.52, 56.14, 40.79, 36.05, 31.94, 29.86, 29.48, 28.20, 27.54, 23.46, 16.32. HRMS (ESI+), m/z $[\text{M}+\text{Na}^+]$ calculated for $\text{C}_{30}\text{H}_{33}\text{BrFNO}_3\text{Na}$ 576.1526; found 576.1499.



N-(2-(5-((4-((4-Chlorobenzyl)oxy)cyclohexyl)oxy)-3'-fluoro-4-methyl-[1,1'-biphenyl]-2-yl)ethyl)acetamide (2.39e).

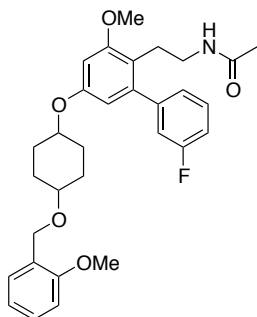
The compound was synthesized following the procedure used for the synthesis of **2.39a** to obtain the product as a white solid: ^1H -NMR (500 MHz, Chloroform- d) δ 7.41 – 7.35 (m, 1H), 7.34 – 7.29 (m, 3H), 7.10 – 7.03 (m, 3H), 6.66 (d, $J = 6.3$ Hz, 1H), 5.33 – 5.28 (m, 1H), 4.52 (s, 1H), 4.37 (dt, $J = 6.0, 3.0$ Hz, 1H), 3.49 – 3.44 (m, 1H), 3.31 – 3.24 (m, 2H), 2.70 (t, $J = 7.2$ Hz, 2H), 2.26 (d, $J = 0.7$ Hz, 3H), 2.12 – 1.99 (m, 2H), 1.87 (s, 3H), 1.77 – 1.70 (m, 4H), 1.68 – 1.58 (m, 2H). ^{13}C NMR (126 MHz, CDCl_3) δ 170.00, 161.66, 154.08, 144.09, 139.23, 137.64, 135.55, 133.25, 132.38, 131.41, 129.96, 128.94, 128.87, 128.64, 127.89, 127.51, 125.15, 116.47, 116.30,

114.63, 114.17, 113.97, 75.30, 72.40, 69.22, 40.80, 32.49, 31.92, 28.20, 27.93, 27.53, 23.43, 20.22, 16.31. HRMS (ESI+), m/z [M+Na⁺] calculated for C₃₀H₃₃ClFNO₃Na 532.2031; found 532.2019.



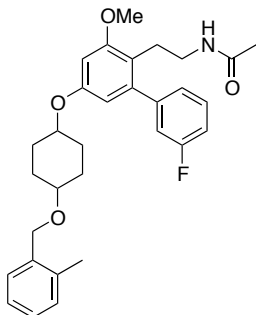
N-(2-(5-((4-(Benzyloxy)cyclohexyl)oxy)-3'-fluoro-3-methoxy-[1,1'-biphenyl]-2-yl)ethyl)acetamide (2.40a).

The compound was synthesized following the procedure used for the synthesis of **2.4** using phenol **N-(2-(3'-fluoro-5-hydroxy-3-methoxy-[1,1'-biphenyl]-2-yl)ethyl)acetamide** to obtain the product as a white solid: ¹H-NMR (500 MHz, Chloroform-d) δ 7.41 – 7.32 (m, 5H), 7.30 – 7.27 (m, 1H), 7.08 – 7.04 (m, 1H), 6.99 (ddt, J = 8.1, 3.1, 1.5 Hz, 1H), 6.50 (t, J = 2.9 Hz, 1H), 6.34 (t, J = 2.8 Hz, 1H), 5.87 (s, 1H), 5.74 (s, 1H), 4.56 (d, J = 1.8 Hz, 2H), 4.42 (dq, J = 6.5, 3.3 Hz, 1H), 3.79 (d, J = 1.9 Hz, 3H), 3.55 (dt, J = 6.7, 3.5 Hz, 1H), 3.28 (qd, J = 6.0, 5.4, 3.1 Hz, 2H), 2.75 – 2.64 (m, 2H), 2.21 – 2.15 (m, 2H), 2.11 – 2.01 (m, 2H), 1.94 – 1.88 (m, 2H), 1.85 (d, J = 4.9 Hz, 3H), 1.78 (tq, J = 12.6, 4.6, 4.1 Hz, 2H). ¹³C NMR (126 MHz, CDCl₃) δ 169.94, 163.43, 161.46, 156.41, 143.82, 138.85, 129.79, 128.40, 127.52, 124.85, 118.92, 116.19, 116.02, 114.23, 114.06, 106.09, 100.02, 73.99, 73.57, 69.90, 55.43, 40.78, 28.33, 27.69, 27.58, 25.81, 23.23. HRMS (ESI+), m/z [M+Na⁺] calculated for C₃₀H₃₅FNO₄H 492.2550; found 492.2543.



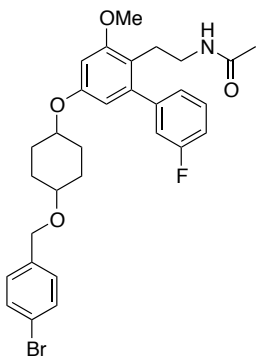
N-(2-(3'-Fluoro-3-methoxy-5-((4-((2-methoxybenzyl)oxy)cyclohexyl)oxy)-[1,1'-biphenyl]-2-yl)ethyl)acetamide (2.40b).

The compound was synthesized following the procedure used for the synthesis of **2.40a** to obtain the product as a white solid: $^1\text{H-NMR}$ (500 MHz, Chloroform- d) δ 7.45 – 7.41 (m, 1H), 7.37 (td, $J = 8.0, 5.9$ Hz, 1H), 7.24 – 7.23 (m, 1H), 7.08 – 7.03 (m, 1H), 7.00 – 6.93 (m, 2H), 6.87 (ddd, $J = 8.2, 3.5, 1.0$ Hz, 1H), 6.50 (d, $J = 2.5$ Hz, 1H), 6.34 (t, $J = 2.4$ Hz, 1H), 5.84 (t, $J = 4.9$ Hz, 1H), 5.69 (q, $J = 5.2, 4.5$ Hz, 1H), 4.59 (d, $J = 3.3$ Hz, 2H), 4.41 (tt, $J = 8.9, 4.5$ Hz, 1H), 3.81 (d, $J = 21.3$ Hz, 6H), 3.57 (td, $J = 5.9, 4.8, 2.6$ Hz, 1H), 3.27 (td, $J = 6.6, 4.8$ Hz, 2H), 2.70 (dt, $J = 15.2, 6.7$ Hz, 2H), 2.19 (ddd, $J = 14.7, 6.0, 3.3$ Hz, 1H), 2.13 – 2.00 (m, 1H), 1.94 (dt, $J = 11.9, 7.7$ Hz, 1H), 1.84 (s, 3H), 1.77 (ddt, $J = 18.3, 9.1, 2.6$ Hz, 2H), 1.66 – 1.56 (m, 2H). ^{13}C NMR (126 MHz, CDCl_3) δ 169.96, 163.56, 161.60, 158.58, 156.59, 143.97, 143.56, 129.90, 128.61, 127.44, 125.00, 120.61, 119.15, 116.33, 114.18, 110.23, 106.20, 100.16, 73.91, 64.76, 55.56, 55.44, 40.93, 29.85, 28.52, 27.91, 27.74, 25.93, 23.43. HRMS (ESI+), m/z $[\text{M}+\text{Na}^+]$ calculated for $\text{C}_{31}\text{H}_{36}\text{FNO}_5\text{Na}$ 544.2475, found 544.2455.



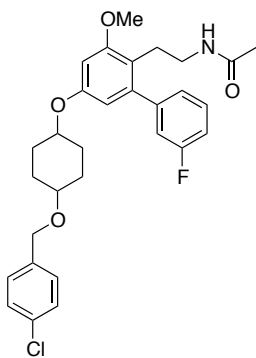
N-(2-(3'-Fluoro-3-methoxy-5-((4-((2-methylbenzyl)oxy)cyclohexyl)oxy)-[1,1'-biphenyl]-2-yl)ethyl)acetamide (2.40c).

The compound was synthesized following the procedure used for the synthesis of **2.40a** to obtain the product as a white solid: $^1\text{H-NMR}$ (500 MHz, Chloroform- d) δ 6.43 (d, $J = 2.7$ Hz, 1H), 6.26 (t, $J = 2.3$ Hz, 1H), 5.77 (t, $J = 4.9$ Hz, 1H), 5.64 (d, $J = 5.1$ Hz, 1H), 4.46 (s, 2H), 4.38 – 4.29 (m, 1H), 3.71 (d, $J = 1.6$ Hz, 3H), 3.48 (dt, $J = 7.5, 3.7$ Hz, 1H), 3.23 – 3.16 (m, 2H), 2.63 (q, $J = 6.4$ Hz, 2H), 2.28 (d, $J = 1.6$ Hz, 3H), 2.15 – 2.10 (m, 1H), 2.05 – 1.96 (m, 1H), 1.90 – 1.81 (m, 1H), 1.77 (d, $J = 10.1$ Hz, 3H), 1.74 – 1.64 (m, 2H), 1.63 – 1.48 (m, 1H). $^{13}\text{C NMR}$ (126 MHz, CDCl_3) δ 168.82, 162.37, 160.41, 157.40, 155.36, 142.36, 135.53, 129.19, 128.73, 127.38, 126.70, 124.78, 123.81, 117.89, 115.14, 113.16, 105.01, 98.95, 74.30, 73.25, 72.43, 67.46, 54.38, 39.65, 27.24, 26.63, 26.58, 24.81, 22.22, 17.84, 16.68, 11.25. HRMS (ESI+), m/z $[\text{M}+\text{Na}^+]$ calculated for $\text{C}_{31}\text{H}_{36}\text{FNO}_4\text{Na}$ 528.2526, found 528.2532.



N-(2-(5-((4-(4-Bromobenzyl)oxy)cyclohexyl)oxy)-3'-fluoro-3-methoxy-[1,1'-biphenyl]-2-yl)ethyl)acetamide (2.40d).

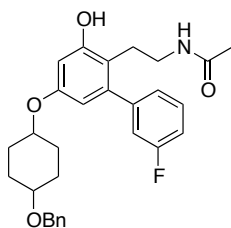
The compound was synthesized following the procedure used for the synthesis of **2.40a** to obtain the product as a white solid: $^1\text{H-NMR}$ (500 MHz, Chloroform- d) δ 7.50 – 7.45 (m, 2H), 7.37 (td, $J = 7.9, 6.0$ Hz, 1H), 7.23 (dd, $J = 8.5, 2.0$ Hz, 1H), 7.06 (tdd, $J = 7.4, 2.8, 1.9$ Hz, 2H), 7.01 – 6.96 (m, 1H), 6.49 (t, $J = 2.9$ Hz, 1H), 6.33 (t, $J = 2.7$ Hz, 1H), 5.74 (s, 1H), 5.62 (s, 1H), 4.50 (s, 2H), 4.41 (dtd, $J = 14.2, 7.7, 7.2, 3.4$ Hz, 1H), 3.79 (d, $J = 1.8$ Hz, 3H), 3.53 (dt, $J = 7.2, 3.7$ Hz, 1H), 3.30 – 3.23 (m, 2H), 2.70 (dt, $J = 18.8, 6.7$ Hz, 2H), 2.21 – 2.14 (m, 2H), 2.05 (ddd, $J = 14.8, 7.5, 3.4$ Hz, 2H), 1.90 – 1.85 (m, 2H), 1.84 (s, 3H), 1.82 – 1.73 (m, 2H), 1.67 – 1.60 (m, 1H). $^{13}\text{C NMR}$ (126 MHz, CDCl_3) δ 168.70, 162.39, 160.42, 155.36, 142.73, 142.37, 136.85, 130.44, 128.68, 128.10, 123.80, 120.26, 117.87, 115.16, 114.99, 113.19, 113.02, 105.01, 98.96, 68.12, 54.39, 39.60, 28.67, 26.60, 26.53, 24.83, 22.27. HRMS (ESI+), m/z $[\text{M}+\text{Na}^+]$ calculated for $\text{C}_{30}\text{H}_{33}\text{BrFNO}_4\text{Na}$ 592.1475; found 592.1473.



N-(2-(5-((4-(4-Chlorobenzyl)oxy)cyclohexyl)oxy)-3'-fluoro-3-methoxy-[1,1'-biphenyl]-2-yl)ethyl)acetamide (2.40e).

The compound was synthesized following the procedure used for the synthesis of **2.40a** to obtain the product as a white solid: $^1\text{H-NMR}$ (500 MHz, Chloroform- d) δ 7.33 – 7.28 (m, 1H),

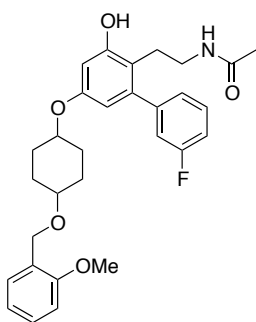
7.27 – 7.22 (m, 3H), 7.01 – 6.96 (m, 2H), 6.94 – 6.89 (m, 1H), 6.43 (t, J = 2.8 Hz, 1H), 6.27 (t, J = 2.8 Hz, 1H), 5.74 (s, 1H), 5.63 (s, 1H), 4.45 (s, 2H), 4.34 (ddq, J = 14.7, 7.6, 3.7, 3.3 Hz, 1H), 3.72 (d, J = 1.7 Hz, 3H), 3.46 (dt, J = 7.2, 3.7 Hz, 1H), 3.23 – 3.17 (m, 2H), 2.63 (dt, J = 18.6, 6.7 Hz, 2H), 2.10 (ddd, J = 10.4, 8.0, 3.9 Hz, 1H), 2.03 – 1.93 (m, 1H), 1.86 – 1.80 (m, 1H), 1.78 (s, 3H), 1.70 (dddt, J = 15.7, 12.3, 8.4, 3.5 Hz, 2H), 1.61 – 1.47 (m, 1H). ¹³C NMR (126 MHz, CDCl₃) δ 170.01, 163.56, 161.60, 156.53, 143.95, 143.54, 137.50, 133.33, 129.94, 128.95, 128.92, 128.67, 124.98, 119.00, 116.32, 116.15, 114.37, 114.20, 106.20, 100.15, 73.54, 69.28, 55.56, 40.82, 28.39, 27.78, 25.99, 23.39. HRMS (ESI+), m/z [M+Na⁺] calculated for C₃₀H₃₄ClFNO₄Na 548.1980; found 548.1996.



N-(2-(5-((4-(Benzyloxy)cyclohexyl)oxy)-3'-fluoro-3-hydroxy-[1,1'-biphenyl]-2-yl)ethyl)acetamide (2.41a).

The compound was synthesized following the procedure used for the synthesis of **2.4** using phenol **N-(2-(3'-fluoro-5-hydroxy-3-(methoxymethoxy)-[1,1'-biphenyl]-2-yl)ethyl)acetamide** to obtain the coupled product in 75% yield (0.1mmol), which was then dissolved in MeOH (5mL) and PTSA (0.017g, 0.1mmol) was added. After 12 hr the reaction was quenched via addition of sat. NH₄Cl (1mL), and then extracted with EtOAc (3 x 7mL). The organic layers were combined, dried, and concentrated. The product was purified by column chromatography (Silica gel, 50% MeOH in DCM) to give **2.41a** as a white solid in 55% yield: ¹H-NMR (500 MHz, Chloroform-d) δ 7.38 – 7.31 (m, 4H), 7.31 – 7.27 (m, 1H), 7.07 – 6.96 (m, 2H), 6.91 (dtd,

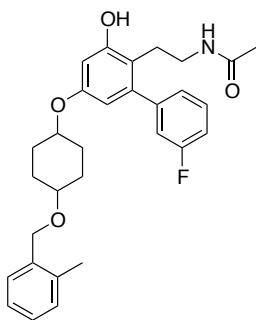
J = 8.5, 2.7, 1.3 Hz, 1H), 6.46 (d, J = 2.4 Hz, 1H), 6.26 (dd, J = 3.8, 2.4 Hz, 1H), 5.88 (d, J = 5.6 Hz, 1H), 5.83 – 5.79 (m, 1H), 5.74 – 5.69 (m, 1H), 4.56 (d, J = 1.8 Hz, 2H), 4.38 (dtd, J = 19.4, 8.0, 7.3, 3.3 Hz, 1H), 3.55 (dt, J = 7.4, 3.7 Hz, 1H), 3.29 – 3.20 (m, 2H), 2.67 (dt, J = 17.5, 6.7 Hz, 2H), 2.17 (dd, J = 11.9, 4.3 Hz, 1H), 2.12 – 1.98 (m, 1H), 1.96 – 1.86 (m, 2H), 1.84 (s, 3H), 1.76 (qt, J = 9.7, 3.7 Hz, 2H), 1.61 (d, J = 16.1 Hz, 2H). ¹³C NMR (126 MHz, CDCl₃) δ 170.56, 163.78, 156.93, 155.23, 143.88, 139.21, 130.10, 130.04, 128.81, 127.92, 125.17, 118.66, 116.48, 114.56, 114.39, 109.47, 100.60, 74.40, 70.63, 70.29, 41.30, 28.76, 28.07, 27.98, 26.05, 23.66. HRMS (ESI+), m/z [M+Na⁺] calculated for C₂₉H₃₂FNO₄Na 500.221; found 500.2192.



N-(2-(3'-Fluoro-3-hydroxy-5-((4-((2-methoxybenzyl)oxy)cyclohexyl)oxy)-[1,1'-biphenyl]-2-yl)ethyl)acetamide (2.41b).

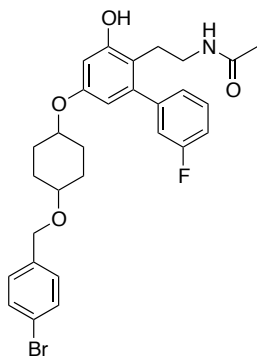
The compound was synthesized following the procedure used for the synthesis of **2.41a** to obtain the product as a white solid: ¹H-NMR (500 MHz, Chloroform-d) δ 7.44 – 7.40 (m, 1H), 7.37 – 7.30 (m, 1H), 7.06 – 6.90 (m, 4H), 6.87 (ddd, J = 8.2, 3.9, 1.0 Hz, 1H), 6.47 (d, J = 2.4 Hz, 1H), 6.28 – 6.23 (m, 1H), 5.90 (s, 1H), 5.73 (s, 1H), 4.59 (s, 2H), 4.38 (ddq, J = 15.2, 7.8, 3.4 Hz, 1H), 3.83 (d, J = 4.7 Hz, 3H), 3.56 (dd, J = 7.1, 3.5 Hz, 1H), 3.33 – 3.18 (m, 2H), 2.69 (t, J = 6.7 Hz, 2H), 2.17 (d, J = 5.6 Hz, 1H), 2.12 – 1.99 (m, 2H), 1.97 – 1.88 (m, 1H), 1.84 (d, J = 6.3 Hz, 3H), 1.82 – 1.71 (m, 2H), 1.65 – 1.51 (m, 2H). ¹³C NMR (126 MHz, CDCl₃) δ 170.26, 163.53, 157.01, 156.75, 154.86, 143.55, 129.86, 128.69, 128.64, 128.55, 127.41, 124.93, 120.61,

118.58, 116.24, 116.07, 114.32, 114.15, 110.24, 109.16, 100.32, 74.31, 73.89, 64.78, 55.44, 41.05, 28.56, 27.90, 27.75, 25.80, 23.40, 22.50. HRMS (ESI+), m/z [M+Na⁺] calculated for C₃₀H₃₄FNO₅Na 530.2319; found 530.2319.



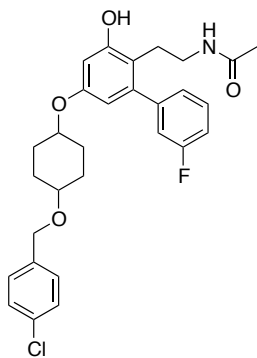
N-(2-(3'-Fluoro-3-hydroxy-5-((4-((2-methylbenzyl)oxy)cyclohexyl)oxy)-[1,1'-biphenyl]-2-yl)ethyl)acetamide (2.41c).

The compound was synthesized following the procedure used for the synthesis of **2.41a** to obtain the product as a white solid: ¹H-NMR (500 MHz, Chloroform-d) δ 7.33 (ddd, J = 10.0, 7.3, 2.2 Hz, 2H), 7.18 (dqt, J = 6.3, 4.0, 1.7 Hz, 3H), 7.06 – 6.95 (m, 2H), 6.91 (ddd, J = 9.5, 2.6, 1.5 Hz, 1H), 6.47 (d, J = 2.4 Hz, 1H), 6.25 (d, J = 2.4 Hz, 1H), 5.91 (s, 1H), 4.54 (s, 2H), 4.40 (dt, J = 7.1, 3.6 Hz, 1H), 3.55 (dq, J = 7.2, 3.8, 3.3 Hz, 1H), 3.24 (q, J = 6.2 Hz, 2H), 2.68 (t, J = 6.6 Hz, 2H), 2.35 (d, J = 2.0 Hz, 3H), 2.09 – 2.00 (m, 1H), 1.95 – 1.86 (m, 1H), 1.84 (s, 2H), 1.81 – 1.73 (m, 4H), 1.63 (q, J = 10.6 Hz, 2H). ¹³C NMR (126 MHz, CDCl₃) δ 170.34, 163.77, 156.92, 155.24, 143.87, 136.98, 130.64, 130.12, 128.16, 126.23, 125.20, 118.61, 116.48, 114.39, 109.47, 100.62, 74.70, 73.88, 68.91, 41.30, 28.03, 26.04, 23.64, 22.75, 19.28. HRMS (ESI+), m/z [M+H⁺] calculated for C₃₀H₃₄FNO₄ 492.2501; found 492.2510.



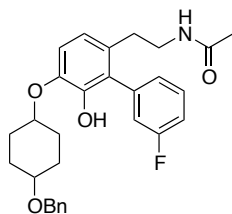
N-(2-(5-((4-((4-Bromobenzyl)oxy)cyclohexyl)oxy)-3'-fluoro-3-hydroxy-[1,1'-biphenyl]-2-yl)ethyl)acetamide (2.41d).

The compound was synthesized following the procedure used for the synthesis of **2.41a** to obtain the product as a white solid: $^1\text{H-NMR}$ (500 MHz, Chloroform- d) δ 7.49 – 7.43 (m, 2H), 7.36 – 7.28 (m, 1H), 7.25 – 7.21 (m, 1H), 7.02 (dddd, $J = 11.1, 8.5, 2.6, 0.9$ Hz, 1H), 6.96 (ddt, $J = 7.6, 5.2, 1.2$ Hz, 1H), 6.89 (dddd, $J = 9.5, 6.3, 2.6, 1.6$ Hz, 1H), 6.46 (d, $J = 2.4$ Hz, 1H), 6.25 (d, $J = 2.4$ Hz, 1H), 6.23 (d, $J = 14.1$ Hz, 1H), 5.86 (t, $J = 5.0$ Hz, 1H), 5.73 (t, $J = 5.1$ Hz, 1H), 4.50 (s, 2H), 4.42 – 4.30 (m, 1H), 3.52 (dt, $J = 7.5, 3.8$ Hz, 1H), 3.24 (td, $J = 6.7, 4.9$ Hz, 2H), 2.66 (dt, $J = 16.8, 6.7$ Hz, 2H), 2.19 – 2.11 (m, 1H), 2.09 – 1.97 (m, 2H), 1.84 (d, $J = 4.4$ Hz, 4H), 1.75 (ddt, $J = 15.0, 11.8, 7.4$ Hz, 2H), 1.65 – 1.51 (m, 2H). $^{13}\text{C NMR}$ (126 MHz, CDCl_3) δ 170.40, 163.52, 156.62, 155.16, 143.57, 137.99, 131.62, 129.84, 129.78, 129.30, 129.27, 124.90, 121.46, 118.16, 116.21, 116.04, 114.28, 114.12, 109.27, 100.40, 74.44, 73.51, 69.31, 41.05, 28.43, 27.77, 25.78, 23.39. HRMS (ESI+), m/z $[\text{M}+\text{Na}^+]$ calculated for $\text{C}_{29}\text{H}_{31}\text{BrFNO}_4\text{Na}$ 578.1318; found 578.1342.



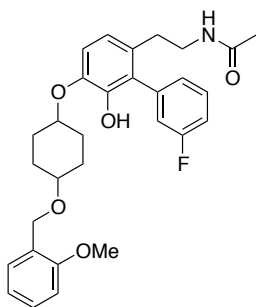
N-(2-(5-((4-((4-Chlorobenzyl)oxy)cyclohexyl)oxy)-3'-fluoro-3-hydroxy-[1,1'-biphenyl]-2-yl)ethyl)acetamide (2.41e).

The compound was synthesized following the procedure used for the synthesis of **2.41a** to obtain the product as a white solid: $^1\text{H-NMR}$ (500 MHz, Chloroform- d) δ 7.35 – 7.27 (m, 4H), 7.02 (dddd, $J = 11.1, 8.5, 2.7, 1.0$ Hz, 1H), 6.99 – 6.94 (m, 1H), 6.90 (dddd, $J = 9.6, 5.8, 2.6, 1.5$ Hz, 1H), 6.46 (d, $J = 2.4$ Hz, 1H), 6.26 (dd, $J = 3.8, 2.4$ Hz, 1H), 6.03 (d, $J = 13.1$ Hz, 1H), 5.85 (t, $J = 5.0$ Hz, 1H), 5.71 (t, $J = 5.2$ Hz, 1H), 4.51 (s, 2H), 4.42 – 4.31 (m, 1H), 3.52 (tt, $J = 6.9, 3.1$ Hz, 1H), 3.24 (td, $J = 6.7, 5.0$ Hz, 2H), 2.71 – 2.63 (m, 2H), 2.18 – 2.12 (m, 1H), 2.03 (tdd, $J = 12.8, 10.5, 7.9$ Hz, 2H), 1.91 – 1.85 (m, 1H), 1.84 (s, 3H), 1.81 – 1.69 (m, 2H), 1.61 (s, 2H). $^{13}\text{C NMR}$ (126 MHz, CDCl_3) δ 169.16, 162.34, 155.46, 153.90, 142.41, 136.29, 132.17, 128.67, 127.78, 127.49, 123.72, 117.07, 115.04, 114.87, 113.12, 112.95, 108.06, 99.19, 73.25, 72.34, 68.11, 39.83, 26.60, 24.62, 22.22. HRMS (ESI+), m/z $[\text{M}+\text{Na}^+]$ calculated for $\text{C}_{29}\text{H}_{31}\text{ClFNO}_4\text{Na}$ 534.1823; found 534.1820.



N-(2-(5-((4-(Benzyloxy)cyclohexyl)oxy)-3'-fluoro-6-hydroxy-[1,1'-biphenyl]-2-yl)ethyl)acetamide (2.42a).

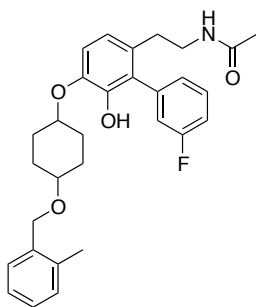
The compound was synthesized following the procedure used for the synthesis of **2.42a** using phenol **N-(2-(3'-fluoro-5-hydroxy-6-(methoxymethoxy)-[1,1'-biphenyl]-2-yl)ethyl)acetamide** to obtain the product as a white solid: ¹H-NMR (500 MHz, Chloroform-d) δ 7.44 – 7.39 (m, 1H), 7.36 – 7.33 (m, 4H), 7.30 – 7.26 (m, 1H), 7.10 – 7.03 (m, 2H), 6.99 (ddd, J = 9.5, 2.6, 1.5 Hz, 1H), 6.86 (d, J = 8.4 Hz, 1H), 6.76 (d, J = 8.4 Hz, 1H), 5.74 (s, 1H), 5.25 (s, 1H), 4.55 (s, 2H), 4.39 (dq, J = 7.2, 3.6 Hz, 1H), 3.56 (tt, J = 6.7, 3.3 Hz, 1H), 3.24 (q, J = 6.8 Hz, 2H), 2.59 (t, J = 7.2 Hz, 2H), 2.03 (dtd, J = 12.3, 8.4, 3.7 Hz, 2H), 1.88 (s, 5H), 1.80 (ddt, J = 12.0, 7.7, 3.6 Hz, 2H), 1.71 (tt, J = 12.6, 3.5 Hz, 2H). ¹³C NMR (126 MHz, CDCl₃) δ 169.93, 163.82, 161.86, 144.19, 143.06, 139.01, 138.70, 130.09, 130.00, 128.53, 127.58, 125.89, 120.40, 117.12, 114.41, 112.75, 73.72, 69.97, 40.44, 32.44, 27.78, 27.63, 23.48. HRMS (ESI+), m/z [M+Na⁺] calculated for C₂₉H₃₂FNO₄Na 500.2213; found 500.2210.



N-(2-(3'-Fluoro-6-hydroxy-5-((4-((2-methoxybenzyl)oxy)cyclohexyl)oxy)-[1,1'-biphenyl]-2-yl)ethyl)acetamide (2.42b).

The compound was synthesized following the procedure used for the synthesis of **2.42a** to obtain the product as a white solid: ¹H-NMR (500 MHz, Chloroform-d) δ 7.45 – 7.38 (m, 2H), 7.11 – 7.02 (m, 2H), 7.02 – 6.93 (m, 2H), 6.88 – 6.82 (m, 2H), 6.76 (d, J = 8.3 Hz, 1H), 5.75 (s,

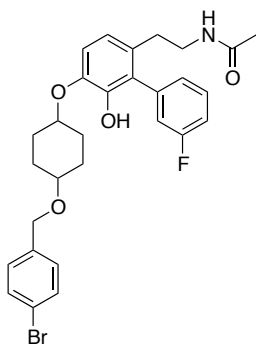
1H), 5.26 (d, J = 6.4 Hz, 1H), 4.58 (s, 2H), 4.39 (tt, J = 7.3, 3.5 Hz, 1H), 3.82 (s, 3H), 3.58 (dt, J = 6.6, 3.3 Hz, 1H), 3.24 (q, J = 6.8 Hz, 2H), 2.59 (t, J = 7.2 Hz, 2H), 2.08 – 1.98 (m, 2H), 1.98 – 1.89 (m, 2H), 1.88 (s, 3H), 1.80 (ddt, J = 11.6, 7.3, 3.4 Hz, 2H), 1.72 (dtd, J = 12.9, 5.2, 4.4, 2.2 Hz, 2H). ¹³C NMR (126 MHz, CDCl₃) δ 168.78, 162.63, 160.68, 155.75, 143.03, 141.93, 137.55, 137.48, 128.85, 128.81, 127.35, 127.28, 126.29, 124.71, 119.45, 119.20, 116.11, 115.94, 113.38, 111.57, 109.01, 72.76, 63.55, 54.26, 39.26, 31.25, 26.69, 26.48, 22.30. HRMS (ESI+), m/z [M+H⁺] calculated for C₃₀H₃₄FNO₅ 508.2425; found 508.2429.



N-(2-(3'-Fluoro-6-hydroxy-5-((4-((2-methylbenzyl)oxy)cyclohexyl)oxy)-[1,1'-biphenyl]-2-yl)ethyl)acetamide (2.42c).

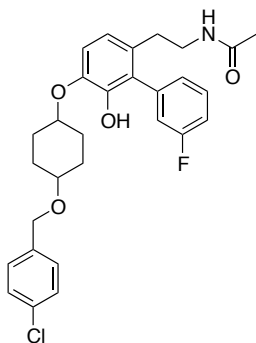
The compound was synthesized following the procedure used for the synthesis of **2.42a** to obtain the product as a white solid: ¹H-NMR (500 MHz, Chloroform-d) δ 7.38 – 7.32 (m, 1H), 7.31 – 7.25 (m, 2H), 7.15 – 7.06 (m, 5H), 7.04 – 6.97 (m, 2H), 6.96 – 6.90 (m, 1H), 6.79 (dd, J = 8.4, 4.8 Hz, 1H), 6.70 (dd, J = 8.4, 3.6 Hz, 1H), 5.67 (s, 1H), 5.62 (s, 1H), 5.19 (d, J = 6.4 Hz, 1H), 5.05 (s, 1H), 4.49 – 4.41 (m, 2H), 4.31 (ddt, J = 19.9, 8.4, 4.2 Hz, 1H), 3.69 (dt, J = 7.8, 3.9 Hz, 1H), 3.49 (dt, J = 6.8, 3.4 Hz, 1H, minor diast.), 3.44 (tt, J = 6.3, 3.1 Hz, 1H), 3.17 (q, J = 6.8 Hz, 2H), 2.52 (t, J = 7.2 Hz, 2H), 2.28 (d, J = 3.6 Hz, 3H), 2.16 – 2.08 (m, 1H), 2.02 (dd, J = 12.0, 4.9 Hz, 1H), 1.98 – 1.91 (m, 1H), 1.88 – 1.83 (m, 2H), 1.81 (s, 3H), 1.74 (dd, J = 8.7, 4.0 Hz, 2H), 1.69 – 1.56 (m, 2H). ¹³C NMR (126 MHz, CDCl₃) δ 169.97, 163.82, 161.86, 144.18,

143.05, 138.65, 136.67, 130.27, 130.06, 128.40, 127.70, 125.94, 120.40, 117.28, 114.41, 112.74, 7574.05, 69.00, 68.44, 40.44, 32.45, 30.76, 29.85, 28.66, 27.80, 23.48, 19.02. HRMS (ESI+), m/z $[M+H^+]$ calculated for $C_{30}H_{34}FNO_4$ 492.2501; found 492.2505.



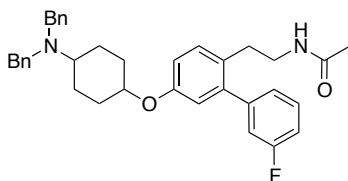
N-(2-(5-((4-(4-Bromobenzyl)oxy)cyclohexyl)oxy)-3'-fluoro-6-hydroxy-[1,1'-biphenyl]-2-yl)ethyl)acetamide (2.42d).

The compound was synthesized following the procedure used for the synthesis of **2.42a** to obtain the product as a white solid: 1H -NMR (500 MHz, Chloroform- d) δ 7.45 (s, 1H), 7.42 (ddd, $J = 8.4, 7.6, 6.0$ Hz, 1H), 7.24 – 7.20 (m, 2H), 7.11 – 7.04 (m, 3H), 6.99 (ddd, $J = 9.6, 2.7, 1.4$ Hz, 1H), 6.86 (dd, $J = 8.4, 4.3$ Hz, 1H), 6.77 (dd, $J = 8.4, 3.2$ Hz, 1H), 5.73 (s, 1H), 5.25 (d, $J = 6.8$ Hz, 1H), 4.49 (s, 2H), 4.39 (dq, $J = 6.9, 3.5$ Hz, 1H), 3.53 (dq, $J = 6.7, 3.3$ Hz, 1H), 3.49 (dq, $J = 5.9, 3.2$ Hz, 2H), 2.59 (td, $J = 7.2, 1.6$ Hz, 2H), 2.20 – 2.14 (m, 1H), 2.02 (dtd, $J = 20.5, 8.0, 7.4, 4.6$ Hz, 3H), 1.88 (s, 3H), 1.79 (ddt, $J = 12.0, 7.7, 3.5$ Hz, 2H), 1.75 – 1.66 (m, 2H). ^{13}C NMR (126 MHz, $CDCl_3$) δ 169.96, 163.82, 161.86, 144.18, 143.01, 138.67, 138.03, 131.61, 130.14, 129.20, 127.49, 125.88, 121.41, 120.42, 117.28, 117.11, 114.59, 114.43, 112.78, 74.00, 69.26, 40.45, 32.44, 29.85, 27.74, 27.60, 23.47. HRMS (ESI+), m/z $[M+Na^+]$ calculated for $C_{29}H_{31}BrFNO_4Na$ 578.1318; found 578.1342.



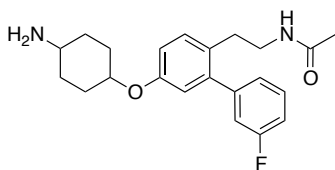
N-(2-(5-((4-(4-Chlorobenzyl)oxy)cyclohexyl)oxy)-3'-fluoro-6-hydroxy-[1,1'-biphenyl]-2-yl)ethyl)acetamide (2.42e).

The compound was synthesized following the procedure used for the synthesis of **2.42a** to obtain the product as a white solid: $^1\text{H-NMR}$ (500 MHz, Chloroform- d) δ 7.45 – 7.39 (m, 1H), 7.33 – 7.27 (m, 4H), 7.10 – 7.03 (m, 2H), 6.99 (ddd, $J = 9.6, 2.7, 1.4$ Hz, 1H), 6.86 (dd, $J = 8.4, 4.3$ Hz, 1H), 6.77 (dd, $J = 8.4, 3.2$ Hz, 1H), 5.73 (s, 1H), 5.26 (s, 1H), 4.50 (s, 2H), 4.42 – 4.34 (m, 1H), 3.54 (dt, $J = 6.8, 3.4$ Hz, 1H), 3.28 – 3.19 (m, 2H), 2.59 (td, $J = 7.2, 1.6$ Hz, 2H), 2.19 – 2.14 (m, 2H), 2.09 – 1.96 (m, 2H), 1.88 (s, 3H), 1.79 (ddt, $J = 12.0, 7.7, 3.6$ Hz, 2H), 1.75 – 1.66 (m, 2H). $^{13}\text{C NMR}$ (126 MHz, CDCl_3) δ 169.81, 163.68, 161.72, 144.04, 142.87, 138.53, 137.37, 133.16, 130.00, 128.73, 128.52, 127.35, 125.74, 120.28, 117.14, 116.97, 114.45, 114.29, 112.64, 73.85, 69.10, 40.31, 32.30, 28.45, 27.60, 27.47, 23.34. HRMS (ESI+), m/z $[\text{M}+\text{H}^+]$ calculated for $\text{C}_{29}\text{H}_{31}\text{ClFNO}_4$ 511.1987; found 511.1980.



N-(2-(5-((4-(Dibenzylamino)cyclohexyl)oxy)-3'-fluoro-[1,1'-biphenyl]-2-yl)ethyl)acetamide (2.46).

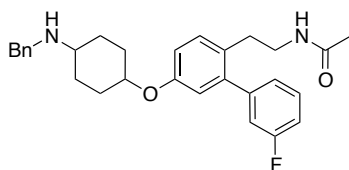
A solution of **2.9** (0.025g, 0.06mmol) and 4-(dibenzylamino)cyclohexanol (0.014mL, 0.12mmol) in anhydrous benzene (0.6 mL) was cooled to 0°C. Tributylphosphine (0.03mL, 0.12mmol) and TMAD (0.021g, 0.12mmol) were added to the mixture. The reaction mixture was stirred at reflux for 12 h. After 12 h the reaction was cooled to rt and purified via column chromatography (SiO₂, 1:20 MeOH:DCM) to afford **2.46** as white amorphous solid (30%): ¹H NMR (500 MHz, Chloroform-d) δ 7.40 – 7.36 (m, 4H), 7.30 – 7.26 (m, 5H), 7.23 – 7.16 (m, 3H), 7.10 – 7.04 (m, 2H), 7.00 (ddd, *J* = 9.7, 2.6, 1.6 Hz, 1H), 6.87 (dd, *J* = 8.5, 2.7 Hz, 1H), 6.76 (d, *J* = 2.7 Hz, 1H), 5.25 (s, 1H), 4.46 (t, *J* = 2.9 Hz, 1H), 3.67 (s, 4H), 3.27 (td, *J* = 7.2, 5.9 Hz, 2H), 2.72 (t, *J* = 7.2 Hz, 2H), 2.58 (ddd, *J* = 11.8, 8.3, 3.5 Hz, 1H), 2.11 (dt, *J* = 14.9, 3.0 Hz, 2H), 1.90 – 1.78 (m, 2H), 1.70 (dd, *J* = 12.9, 3.4 Hz, 2H), 1.56 (s, 3H), 1.45 – 1.33 (m, 2H). ¹³C NMR (126 MHz, CDCl₃) δ 169.95, 163.62, 156.02, 142.17, 141.17, 131.47, 130.92, 129.93, 129.42, 128.54, 128.24, 128.07, 126.70, 125.00, 117.84, 116.18, 115.66, 114.14, 71.26, 56.92, 53.98, 40.64, 32.00, 29.46, 23.47, 22.49. HRMS (ESI+), *m/z* [M+H⁺] calculated for C₃₆H₃₉FN₂O₂ 551.3089; found 551.3077.



***N*-(2-(5-((4-Aminocyclohexyl)oxy)-3'-fluoro-[1,1'-biphenyl]-2-yl)ethyl)acetamide (**2.47**).**

Pd/C (10%wt., 0.05 g) was added to a sealed tube containing a mixture of **2.46** (0.10 g, 0.182mmol) and cyclohexene (3mL). The tube was sealed and heated at 120°C on. After 12 h the mixture was cooled to rt and the mixture was filtered through a pad of Celite. The filtrate was collected, concentrated and purified by column chromatography (Silica gel, 30% EtOAc in Hexane) to give **2.47** as a white solid in 55% yield: ¹H NMR (500 MHz, Chloroform-d) δ 7.33

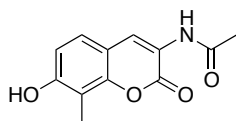
(td, $J = 8.1, 6.0$ Hz, 1H), 7.15 (d, $J = 8.5$ Hz, 1H), 7.04 (dt, $J = 7.7, 1.2$ Hz, 2H), 6.96 (ddd, $J = 9.5, 2.6, 1.5$ Hz, 1H), 6.84 (dd, $J = 8.5, 2.6$ Hz, 1H), 6.73 (d, $J = 2.7$ Hz, 1H), 5.70 (q, $J = 10.8, 8.3$ Hz, 1H), 4.46 – 4.40 (m, 1H), 3.79 – 3.61 (br m, 1H), 3.26 – 3.19 (m, 2H), 2.86 – 2.78 (m, 1H), 2.69 (t, $J = 7.2$ Hz, 2H), 2.06 – 1.99 (m, 2H), 1.83 (s, 3H), 1.74 – 1.67 (m, 2H), 1.67 – 1.48 (m, 4H). ^{13}C NMR (126 MHz, CDCl_3) δ 169.77, 163.22, 155.51, 141.77, 130.57, 129.56, 127.93, 124.66, 117.28, 115.94, 115.37, 113.90, 70.55, 49.15, 40.32, 31.65, 29.33, 28.01, 22.99. HRMS (ESI+), m/z $[\text{M}+\text{H}^+]$ calculated for $\text{C}_{22}\text{H}_{27}\text{FN}_2\text{O}_2$ 371.2135; found 371.2145.



***N*-(2-(5-((4-(benzylamino)cyclohexyl)oxy)-3'-fluoro-[1,1'-biphenyl]-2-yl)ethyl)acetamide (2.48).**

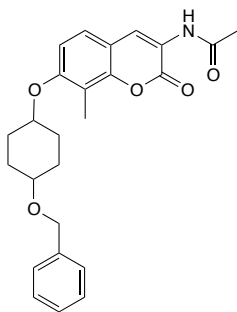
Benzyl Bromide (0.006mL, 0.05mmol) was added to a solution of K_2CO_3 (0.011g, 0.08mmol) and **2.47** (0.04g, 0.1mmol) in MeCN (1mL). The mixture was heated at reflux and monitored by TLC. After 12 h the reaction mixture was determined to be complete and cooled to rt. The reaction was quenched with water (3mL) and extracted with EtOAc (3x 5mL). The organic layers were combined, dried, concentrated, and purified by column chromatography (Silica gel, 30% EtOAc in Hexane) to give **2.48** as a white solid in 40% yield: ^1H NMR (500 MHz, Chloroform- d) δ 7.39 – 7.35 (m, 3H), 7.35 – 7.30 (m, 3H), 7.18 (d, $J = 8.5$ Hz, 1H), 7.06 (dd, $J = 7.9, 1.3$ Hz, 2H), 6.99 (ddd, $J = 9.7, 2.6, 1.6$ Hz, 1H), 6.88 (dd, $J = 8.5, 2.7$ Hz, 1H), 6.76 (d, $J = 2.7$ Hz, 1H), 5.32 (t, $J = 5.9$ Hz, 1H), 4.46 (dt, $J = 4.6, 1.9$ Hz, 1H), 3.86 (s, 2H), 3.26 (td, $J = 7.2, 5.8$ Hz, 2H), 2.72 (t, $J = 7.2$ Hz, 2H), 2.66 (dt, $J = 9.6, 4.0$ Hz, 1H), 2.09 – 2.02 (m, 2H), 1.86 (s, 3H), 1.79 – 1.66 (m, 4H), 1.61 – 1.50 (m, 2H). ^{13}C NMR (126 MHz, CDCl_3) δ 169.98,

163.60, 155.95, 142.13, 130.92, 129.99, 128.64, 128.56, 128.12, 127.33, 125.00, 117.63, 116.32, 115.81, 114.29, 71.64, 54.74, 50.62, 40.64, 31.99, 28.25, 23.43. HRMS (ESI+), m/z [M+H⁺] calculated for C₂₉H₃₃N₂O₂ 461.2523; found 461.2544.



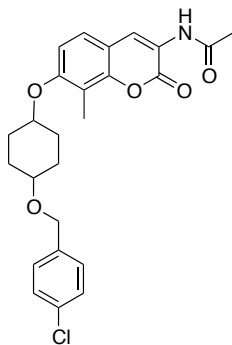
N-(7-Hydroxy-8-methyl-2-oxo-2H-chromen-3-yl)acetamide (2.55).

This compound was synthesized following a previously reported procedure.^{13,41,48,65}



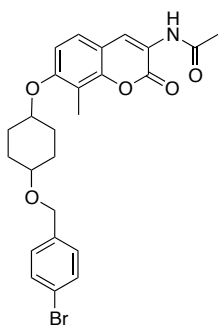
N-(7-((4-(Benzyloxy)cyclohexyl)oxy)-2-oxo-2H-chromen-3-yl)acetamide (2.56a).

The compound was synthesized following the procedure used for the synthesis of **2.4** to obtain the product as a white solid: ¹H-NMR (500 MHz, CDCl₃) δ 8.62 (s, 1H), 8.00 (s, 1H), 7.38–7.35 (m, 2H), 7.30–7.27 (m, 2H), 7.23–7.17 (m, 2H), 6.89–6.86 (m, 1H), 4.56 (s, 2H), 4.51–4.48 (m, 1H), 3.54–3.51 (m, 1H), 2.37 (s, 3H), 2.33 (s, 3H), 2.24 (s, 3H), 2.12–2.03 (m, 2H), 1.95–1.87 (m, 2H), 1.82–1.63 (m, 4H). ¹³C NMR (125 MHz, CDCl₃) δ 169.46, 159.57, 157.39, 149.73, 136.91, 130.50, 128.71, 128.00, 126.10, 125.66, 124.81, 121.41, 115.50, 113.27, 110.62, 75.37, 73.68, 28.02, 27.67, 25.00, 19.16, 8.59. HRMS (ESI+), m/z [M+Na⁺] calculated for C₂₄H₂₅NO₅Na 430.1630; found 430.1623.



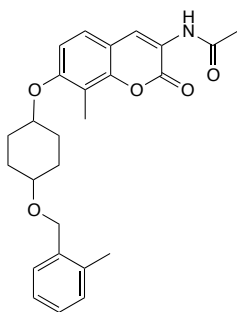
***N*-(7-((4-((4-Chlorobenzyl)oxy)cyclohexyl)oxy)-8-methyl-2-oxo-2*H*-chromen-3-yl)acetamide (2.56e).**

The compound was synthesized following the procedure used for the synthesis of **2.4**, using phenol **2.55**, to obtain the product as a white solid: $^1\text{H-NMR}$ (500 MHz, CDCl_3) δ 8.62 (s, 1H), 7.99 (s, 1H), 7.58–7.52 (m, 2H), 7.36–7.28 (m, 2H), 7.18–7.13 (m, 1H), 6.90–6.87 (m, 1H), 4.62 (s, 2H), 4.52–4.46 (m, 1H), 3.61–3.56 (m, 1H), 2.35 (s, 3H), 2.24 (s, 3H), 2.18–2.05 (m, 2H), 1.97–1.91 (m, 2H), 1.85–1.62 (m, 4H). $^{13}\text{C NMR}$ (125 MHz, CDCl_3) δ 169.45, 159.58, 157.40, 149.74, 138.48, 132.76, 129.27, 129.05, 127.70, 125.68, 124.81, 122.82, 121.43, 115.50, 113.31, 110.65, 75.63, 69.67, 28.01, 27.74, 25.02, 8.63. HRMS (ESI+), m/z $[\text{M}+\text{H}^+]$ calculated for $\text{C}_{25}\text{H}_{26}\text{ClNO}_5$ 455.1502; found 455.1496.



***N*-(7-((4-((4-Bromobenzyl)oxy)cyclohexyl)oxy)-8-methyl-2-oxo-2*H*-chromen-3-yl)acetamide (2.56d).**

The compound was synthesized following the procedure used for the synthesis of **2.4**, using phenol **2.55**, to obtain the product as a white solid: $^1\text{H-NMR}$ (500 MHz, CDCl_3) δ 8.62 (s, 1H), 7.99 (s, 1H), 7.58–7.52 (m, 2H), 7.36–7.28 (m, 2H), 7.18–7.13 (m, 1H), 6.90–6.87 (m, 1H), 4.62 (s, 2H), 4.52–4.46 (m, 1H), 3.61–3.56 (m, 1H), 2.35 (s, 3H), 2.24 (s, 3H), 2.18–2.05 (m, 2H), 1.97–1.91 (m, 2H), 1.85–1.62 (m, 4H). $^{13}\text{C NMR}$ (125 MHz, CDCl_3) δ 169.45, 159.58, 157.40, 149.74, 138.48, 132.76, 129.27, 129.05, 127.70, 125.68, 124.81, 122.82, 121.43, 115.50, 113.31, 110.65, 75.63, 69.67, 28.01, 27.74, 25.02, 8.63. HRMS (ESI+), m/z $[\text{M}+\text{Na}^+]$ calculated for $\text{C}_{25}\text{H}_{26}\text{BrNO}_5\text{Na}$ 522.0892; found 552.0880.



***N*-(8-Methyl-7-((4-((2-methylbenzyl)oxy)cyclohexyl)oxy)-2-oxo-2*H*-chromen-3-yl)acetamide (**2.56c**).**

The compound was synthesized following the procedure used for the synthesis of **2.4**, using phenol **2.55**, to obtain the product as a white solid: $^1\text{H-NMR}$ (500 MHz, CDCl_3) δ 8.62 (s, 1H), 8.00 (s, 1H), 7.38–7.35 (m, 2H), 7.30–7.27 (m, 2H), 7.23–7.17 (m, 1H), 6.89–6.86 (m, 1H), 4.56 (s, 2H), 4.51–4.48 (m, 1H), 3.54–3.51 (m, 1H), 2.37 (s, 3H), 2.33 (s, 3H), 2.24 (s, 3H), 2.12–2.03 (m, 2H), 1.95–1.87 (m, 2H), 1.82–1.63 (m, 4H). $^{13}\text{C NMR}$ (125 MHz, CDCl_3) δ 169.46, 159.57, 157.39, 149.73, 136.91, 130.50, 128.71, 128.00, 126.10, 125.66, 124.81, 121.41, 115.50, 113.27, 110.62, 75.37, 73.68, 28.02, 27.67, 25.00, 19.16, 8.59. HRMS (ESI+), m/z $[\text{M}+\text{Na}^+]$ calculated for $\text{C}_{26}\text{H}_{29}\text{NO}_6\text{Na}$ 458.1901; found 458.1927.

References

1. Khandelwal, A.; Crowley, V. M.; Blagg, B. S. J., Natural Product Inspired N-Terminal Hsp90 Inhibitors: From Bench to Bedside. *Medicinal Research Reviews* **2016**, *36* (1), 92-118.
2. Hall, J. A.; Forsberg, L. K.; Blagg, B. S. J., Alternative Approaches to Hsp90 Modulation for the Treatment of Cancer. *Future Medicinal Chemistry* **2014**, *6* (14), 1587-1605.
3. Zhao, H.; Michaelis, M. L.; Blagg, B. S. J., Hsp90 Modulation for the Treatment of Alzheimer's Disease. *Advances in Pharmacology*, Elias, K. M.; Mary, L. M., Eds. Academic Press: **2012**; Vol. Volume 64, pp 1-25.
4. Zhao, H.; Mary, L. M.; Blagg, B. S. J., Hsp90 Modulation for the Treatment of Alzheimer's Disease. *Advances in Pharmacology* **2012**, *64*.
5. Karagoz, G. E.; Rudiger, S. G. D., Hsp90 interaction with clients. *Trends in Biochemical Sciences* **2015**, *40* (2), 117-25.
6. Miyata, Y.; Nakamoto, H.; Neckers, L., The Therapeutic Target Hsp90 and Cancer Hallmarks. *Current Pharmaceutical Design* **2013**, *19* (3), 347-365.
7. Hanahan, D.; Weinberg, R. A., The Hallmarks of Cancer. *Cell* **2000**, *100*, 57-70.
8. Hanahan, D.; Weinberg, R. A., Hallmarks of cancer: the next generation. *Cell* **2011**, *144* (5), 646-74.
9. Pratt, W. B.; Morishima, Y.; Gestwicki, J. E.; Lieberman, A. P.; Osawa, Y., A model in which heat shock protein 90 targets protein-folding clefts: Rationale for a new approach to neuroprotective treatment of protein folding diseases. *Experimental Biology and Medicine (Maywood)* **2014**, *239* (11), 1405-13.

10. Ebrahimi-Fakhari, D.; Saidi, L.-J.; Wahlster, L., Molecular chaperones and protein folding as therapeutic targets in Parkinson's disease and other synucleinopathies. *Acta Neuropathologica Communications* **2013**, *1* (1), 79.
11. Hoozemans, J. J.; Haastert, E. S. v.; Nijholt, D. A.; Rozemuller, A. J.; Scheper, W., Activation of the unfolded protein response is an early event in Alzheimer's and Parkinson's disease. *Neurodegenerative Disease* **2012**, *10*.
12. Blair, L. J.; Sabbagh, J. J.; Dickey, C. A., Targeting Hsp90 and its co-chaperones to treat Alzheimer's disease. *Expert Opinion Therapeutic Targets* **2014**, *18* (10).
13. Ghosh, S.; Liu, Y.; Garg, G.; Anyika, M.; McPherson, N. T.; Ma, J.; Dobrowsky, R. T.; Blagg, B. S. J., Diverging Novobiocin Anti-Cancer Activity from Neuroprotective Activity through Modification of the Amide Tail. *ACS Medicinal Chemistry Letters* **2016**, *7* (8), 813-8.
14. Saibil, H., Chaperone Machines for Protein Folding, Unfolding and Disaggregation. *Nature Reviews Cancer* **2013**, *14* (10), 630-42.
15. Schopf, F. H.; Biebl, M. M.; Buchner, J., The HSP90 chaperone machinery. *Nature Reviews Molecular Cell Biology* **2017**, *18* (6), 345-360.
16. Röhl, A.; Rohrber, J.; Buchner, J., The Chaperone Hsp90: Changing Partners for Demanding Clients. *Trends in Biochemical Sciences* **2013**, *38* (5), 253-62.
17. Neckers, L.; Trepel, J. B., Stressing the development of small molecules targeting HSP90. *Clinical Cancer Research : an official journal of the American Association for Cancer Research* **2014**, *20* (2), 275-7.
18. Neckers, L.; Workman, P., Hsp90 Molecular Chaperone Inhibitors: Are We There Yet? *Clinical Cancer Research : an official journal of the American Association for Cancer Research* **2012**, *18* (1), 64-76.

19. Bharadwaj, S.; Ali, A.; Ovsenek, N., Multiple Components of the Hsp90 Chaperone Complex Function in Regulation of Heat Shock Factor 1 in Vivo. *Molecular and Cellular Biology* **1999**, *19* (12), 8033-8041.
20. Morimoto, R. I., Regulation of the heat shock transcriptional response: cross talk between a family of heat shock factors, molecular chaperones, and negative regulators. *Genes Development* **1998**, *12*.
21. Whitesell, L.; Bagatell, R.; Falsey, R., The Stress Response; Implications for the Clinical Development of Hsp90 Inhibitors. *Current Cancer Drug Targets* **2003**, *3* (5), 349-358.
22. Isaacs, J.; Whitesell, L., Hsp90 in Cancer: Beyond the Usual Suspects. *Advances in Cancer Research* **2016**, *129*.
23. Marcu, M. G.; Schulte, T. W.; Neckers, L., Novobiocin and Related Coumarins and Depletion of Heat Shock Protein 90-Dependent Signaling Proteins. *Journal of the National Cancer Institute* **2000**, *92* (3), 242-248.
24. Burlison, J. A.; Avila, C.; Vielhauer, G.; Lubbers, D. J.; Holzbeierlein, J.; Blagg, B. S. J., Development of Novobiocin Analogues that Manifest Anti-Proliferative Activity Against Several Cancer Cell Lines. *Journal of Organic Chemistry* **2008**, *73*, 2130-2137.
25. Donnelly, A. C.; Mays, J. R.; Burlinson, J. A.; Nelson, J. T.; Vielhauer, G.; Holzbeierlein, J.; Blagg, B. S. J., The Design, Synthesis and Evaluation of Coumarin Ring Derivatives of the Novobiocin Scaffold that Exhibit Antiproliferative Activity. *Journal of Organic Chemistry* **2008**, *73*, 8901-8920.
26. Zhao, H.; Donnelly, A. C.; Kusuma, B. R.; Brandt, G. E. L.; Brown, D.; Rajewski, R. A.; Vielhauer, G.; Holzbeierlein, J.; Cohen, M. S.; Blagg, B. S. J., Engineering an Antibiotic to Fight

Cancer: Optimization of the Novobiocin Scaffold to Produce Anti-Proliferative Agents. *Journal of Medicinal Chemistry* **2011**, *54* (11), 3839-53.

27. Donnelly, A. C.; Zhao, H.; Kusuma, B. R.; Blagg, B. S. J., Cytotoxic Sugar Analogues of an Optimized Novobiocin Scaffold. *Medicinal Chemistry Communication* **2010**, *1* (2), 165-170.

28. Zhao, H.; Kusuma, B. R.; Blagg, B. S. J., Synthesis and Evaluation of Noviose Replacements on Novobiocin that Manifest Anti-proliferative Activity. *ACS Medicinal Chemistry Letters* **2010**, *1* (7), 311-315.

29. Zhao, H.; Blagg, B. S. J., Novobiocin Analogues with Second-Generation Noviose Surrogates. *Bioorganic & Medicinal Chemistry Letters* **2013**, *23* (2), 552-7.

30. Kusuma, B. R.; Khandelwal, A.; Gu, W.; Brown, D.; Liu, W.; Vielhauer, G.; Holzbeierlein, J.; Blagg, B. S. J., Synthesis and Biological Evaluation of Coumarin Replacements of Novobiocin as Hsp90 Inhibitors. *Bioorganic & Medicinal Chemistry* **2014**, *22* (4), 1441-1449.

31. Zhao, H.; Moroni, E.; Colombo, G.; Blagg, B. S. J., Identification of a New Scaffold for Hsp90 C-Terminal Inhibition. *ACS Medicinal Chemistry Letters* **2014**, *5* (1), 84-88.

32. Byrd, K. M.; Subramanian, C.; Sanchez, J.; Motiwala, H. F.; Liu, W.; Cohen, M. S.; Holzbeierlein, J.; Blagg, B. S. J., Synthesis and Biological Evaluation of Novobiocin Core Analogues as Hsp90 Inhibitors. *Chemistry- A European Journal* **2016**, *22* (20), 6921-31.

33. Forsberg, L. K.; Garg, G.; Zhao, H.; Blagg, B. S. J., Development of Phenyl Cyclohexylcarboxamides as a Novel Class of Hsp90 C-terminal Inhibitors. *Chemistry – A European Journal*, **2017**, in press.

34. Ansar, S.; Burlison, J. A.; Hadden, M. K.; Yu, X. M.; Desino, K. E.; Bean, J.; Neckers, L.; Audus, K. L.; Michaelis, M. L.; Blagg, B. S. J., A non-toxic Hsp90 inhibitor protects neurons from Abeta-induced toxicity. *Bioorganic & Medicinal Chemistry Letters* **2007**, *17* (7), 1984-90.
35. Lu, Y.; Ansar, S.; Michaelis, M. L.; Blagg, B. S. J., Neuroprotective activity and evaluation of Hsp90 inhibitors in an immortalized neuronal cell line. *Bioorganic & Medicinal Chemistry* **2009**, *17* (4), 1709-15.
36. Pratt, W. B.; Gestwicki, J. E.; Osawa, Y.; Lieberman, A. P., Targeting Hsp90/Hsp70-based protein quality control for treatment of adult onset neurodegenerative diseases. *Annual Review Pharmacology Toxicology* **2015**, *55*, 353-71.
37. Urban, M. J.; Li, C.; Yu, C.; Lu, Y.; Krise, J. M.; McIntosh, M. P.; Rajewski, R. A.; Blagg, B. S. J.; Dobrowsky, R. T., Inhibiting heat-shock protein 90 reverses sensory hypoalgesia in diabetic mice. *ASN Neuro* **2010**, *2* (4), e00040.
38. Dobrowsky, R. T., Targeting the Diabetic Chaperome to Improve Peripheral Neuropathy. *Current Diabetes Reports* **2016**, *16* (8), 71.
39. Ma, J.; Pan, P.; Anyika, M.; Blagg, B. S. J.; Dobrowsky, R. T., Modulating Molecular Chaperones Improves Mitochondrial Bioenergetics and Decreases the Inflammatory Transcriptome in Diabetic Sensory Neurons. *ACS Chemical Neuroscience* **2015**, *6* (9), 1637-48.
40. Matts, R. L.; Dixit, A.; Peterson, L. B.; Sun, L.; Voruganti, S.; Kalyanaraman, P.; Hartson, S. D.; Verkhivker, G. M.; Blagg, B. S. J., Elucidation of the Hsp90 C-Terminal Inhibitor Binding Site. *ACS Chemical Biology* **2011**, *6* (8), 800-7.
41. Kusuma, B. R.; Zhang, L.; Sundstrom, T.; Peterson, L. B.; Dobrowsky, R. T.; Blagg, B. S. J., Synthesis and evaluation of novologues as C-terminal Hsp90 inhibitors with cytoprotective

activity against sensory neuron glucotoxicity. *Journal of Medicinal Chemistry* **2012**, *55* (12), 5797-812.

42. Anyika, M.; McMullen, M.; Forsberg, L. K.; Dobrowsky, R. T.; Blagg, B. S. J., Development of Noviomimetics as C-Terminal Hsp90 Inhibitors. *ACS Medicinal Chemistry Letters* **2016**, *7* (1), 67-71.

43. Matsushima, Y.; Kino, J., Novel Concise Synthesis of (\pm)-Noviose and l-(+)-Noviose by Palladium-Catalyzed Epoxide Opening. *Synthesis* **2011**, *2011* (08), 1290-1294.

44. Reddy, D. S.; Srinivas, G.; Rajesh, B. M.; Kannan, M.; Rajale, T. V.; Iqbal, J., Enantiospecific synthesis of (-)-d-noviose from (-)-pantolactone. *Tetrahedron Letters* **2006**, *47* (36), 6373-6375.

45. Rajesh, B. M.; Shinde, M. V.; Kannan, M.; Srinivas, G.; Iqbal, J.; Reddy, D. S., Enantiodivergent routes to (+) and (-)-novioses from (-)-pantolactone. *RSC Advances* **2013**, *3* (43), 20291.

46. Schmidt, B.; Hauke, S., Metathesis-Based De Novo Synthesis of Noviose. *European Journal of Organic Chemistry* **2014**, *2014* (9), 1951-1960.

47. Bengtson, A.; Hallberg, A.; Larhed, M., Fast Synthesis of Aryl Triflates with Controlled Microwave Heating. *Organic Letters* **2002**, *4* (7), 1231-1233.

48. Blagg, B. S. J.; Dobrowsky, R. T.; Anyika, M., Biphenyl amides with modified ether groups as hsp90 inhibitors and hsp70 inducers. US9422320 B2, **2016**.

49. Xie, L.; Takeuchi, Y.; Cosentino, L. M.; Lee, K.-H., Anti-AIDS Agents. 37. Synthesis and Structure-Activity Relationships of (3'R,4'R)-(+)-cis-Khellactone Derivatives as Novel Potent Anti-HIV Agents. *Journal of Medicinal Chemistry* **1999**, *42*, 2662-2672.

50. Ohsawa, K.; Yoshida, M.; Doi, T., A direct and mild formylation method for substituted benzenes utilizing dichloromethyl methyl ether-silver trifluoromethanesulfonate. *Journal of Organic Chemistry* **2013**, *78* (7), 3438-44.
51. Yu, X. M.; Shen, G.; Blagg, B. S. J., Synthesis of (-)-Noviose from 2,3-O-Isopropylidene-D-erythronolactol. *Journal of Organic Chemistry* **2004**, *69*, 7375-7378.
52. Burlison, J. A.; Neckers, L.; Smith, A. B.; Maxwell, A.; Blagg, B. S. J., Novobiocin: Redesigning a DNA Gyrase Inhibitor for Selective Inhibitor of Hsp90. *Journal of the American Chemical Society* **2006**, *128*, 15529-15536.
53. Andrieux, C. P.; Farriol, M.; Gallardo, I.; Marquet, J., Thermodynamics and kinetics of homolytic cleavage of carbon-oxygen bonds in radical anions obtained by electrochemical reduction of alkyl aryl ethers. *Journal of the Chemical Society, Perkin Transactions* **2002**, (5), 985-990.
54. Li, C. C.; Xie, Z. X.; Zhang, Y. D.; Chen, J. H.; Yang, Z., Total Synthesis of Wedelolactone. *Journal of Organic Chemistry* **2003**, *68*, 8500-8504.
55. Kogen, H.; Toda, N.; Tago, K.; Marumoto, S.; Takami, K.; Ori, M.; Yamada, N.; Koyama, K.; Naruto, S.; Abe, K.; Yamazaki, R.; Hara, T.; Aoyagi, A.; Abe, Y.; Kaneko, T., Design and Synthesis of Dual Inhibitors of Acetylcholinesterase and Serotonin Transporter Targeting Potential Agents for Alzheimer's Disease. *Organic Letters* **2002**, *4* (20), 3359-3362.
56. Narihiro Toda; Keiko Tago; Shinji Marumoto; Kazuko Takami; Mayuko Ori; Naho Yamada; Kazuo Koyama; Shunji Naruto; Kazumi Abe; Reina Yamazaki; Takao Hara; Atsushi Aoyagi; Yasuyuki Abe; Tsugio Kaneko; Hiroshi Kogen, A Conformational Restriction Approach to the Development of Dual Inhibitors of Acetylcholinesterase and Serotonin Transporter as

Potential Agents for Alzheimer's Disease. *Bioorganic & Medicinal Chemistry* **2003**, *11* (20), 4389-4415.

57. Garg, G.; Zhao, H.; Blagg, B. S. J., Design, synthesis, and biological evaluation of ring-constrained novobiocin analogues as hsp90 C-terminal inhibitors. *ACS Medicinal Chemistry Letters* **2015**, *6* (2), 204-9.

58. Li, C.; Ma, J.; Zhao, H.; Blagg, B. S. J.; Dobrowsky, R. T., Induction of heat shock protein 70 (Hsp70) prevents neuregulin-induced demyelination by enhancing the proteasomal clearance of c-Jun. *ASN Neuro* **2012**, *4* (7), e00102.

59. Lehmann, H. C.; Chen, W.; Mi, R.; Wang, S.; Liu, Y.; Rao, M.; Höke, A., Human Schwann Cells Retain Essential Phenotype Characteristics After Immortalization. *Stem Cells and Development* **2011**, *21* (3), 423-431.

60. Roy Chowdhury, S. K.; Smith, D. R.; Saleh, A.; Schapansky, J.; Marquez, A.; Gomes, S.; Akude, E.; Morrow, D.; Calcutt, N. A.; Fernyhough, P., Impaired adenosine monophosphate-activated protein kinase signalling in dorsal root ganglia neurons is linked to mitochondrial dysfunction and peripheral neuropathy in diabetes. *Brain* **2012**, *135* (6), 1751-1766.

61. Chen, W.; Mi, R.; Haughey, N.; Oz, M.; Höke, A., Immortalization and characterization of a nociceptive dorsal root ganglion sensory neuronal line. *Journal of the Peripheral Nervous System* **2007**, *12* (2), 121-130.

62. Brand, Martin D.; Nicholls, David G., Assessing mitochondrial dysfunction in cells. *Biochemical Journal* **2011**, *435*, 297-312.

63. Blagg, B., S.J., Dobrowsky, Rick, T., Anyika, Mercy, Biphenyl Amides With Modified Ether Groups as Hsp90 Inhibitors and Hsp70. CA2952029 A1, **2015**.

64. Kieczkowski, G. R.; Schlessinger, R. H., Total synthesis of (+-)-vernolepin. *Journal of the American Chemical Society* **1978**, *100* (6), 1938-1940.
65. Yu, X. M.; Shen, G.; Neckers, L.; Blake, H.; Holzbeierlein, J.; Cronk, B.; Blagg, B. S. J., Hsp90 Inhibitors Identified From a Library of Novobiocin Analogues. *Journal of the American Chemical Society* **2005**, *127*, 12778-12779.

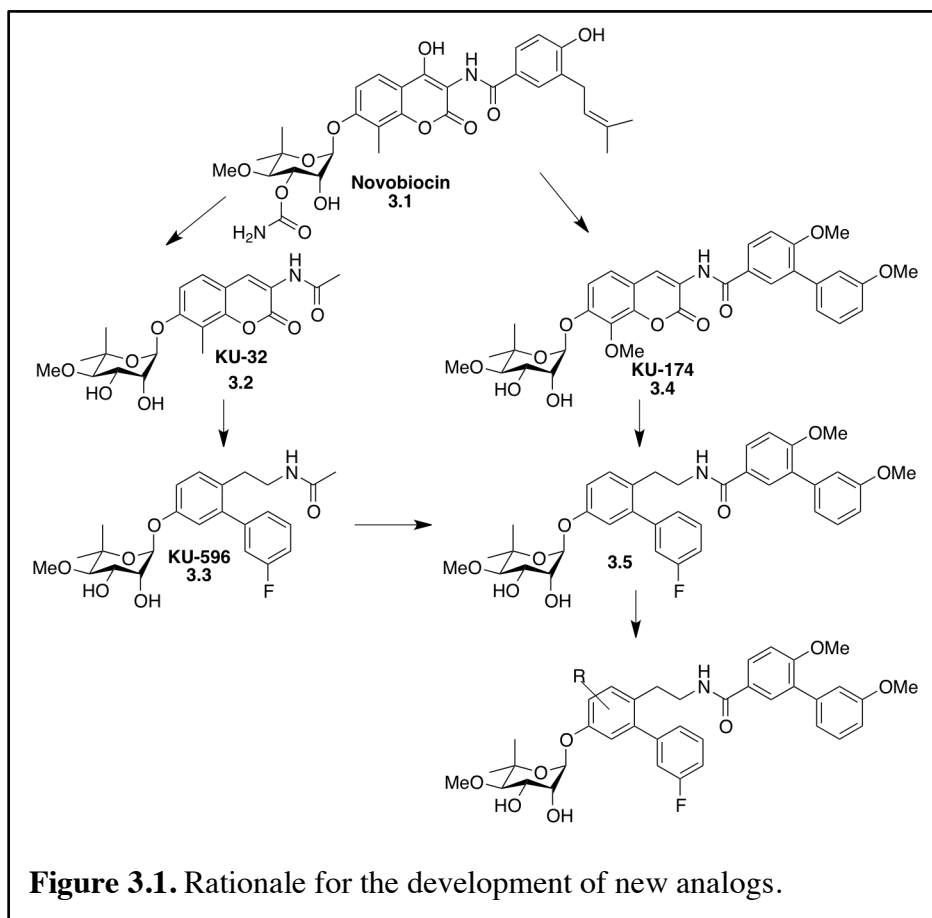
3. Modified Biphenyl Hsp90 C-terminal Inhibitors for the Treatment of Cancer

Introduction

Heat Shock Protein 90 (Hsp90) is a molecular chaperone that is responsible for the maturation of more than 300 nascent polypeptides.¹⁻⁵ Hsp90-dependent client proteins are associated with all 10 hallmarks of cancer, making it an excellent therapeutic target for the treatment of cancer.⁶⁻⁸ As a result, 17 Hsp90 inhibitors have been investigated in clinical trials for the treatment of cancer.⁹⁻¹³ Hsp90 exists as a homodimer and contains a C-terminus, a middle domain, and an N-terminal ATP-binding site.³ In stressed cells, Hsp90 exists as a heteroprotein complex bound to various co-chaperones and partner proteins, and Hsp90 inhibitors exhibit 200-fold higher affinity for the heteroprotein complex versus the homodimer that resides in non-stressed cells.¹⁴⁻²⁰ Inhibition of Hsp90 by traditional inhibitors that bind the N-terminal ATP-binding site results in induction of the heat shock response (HSR) and the overexpression of Hsp27, Hsp40, Hsp70, and Hsp90.²¹⁻²³ Since N-terminal inhibitors induce this HSR, challenges associated with dosing and scheduling have arisen in the clinic.^{9,13,24-25} As a result, new inhibitors that do not induce the heat shock response are actively sought.²⁶⁻²⁷

The natural product, novobiocin, was the first Hsp90 C-terminal inhibitor identified,²⁸⁻²⁹ and preliminary SAR studies resulted in the identification of KU-32, a C-terminal inhibitor that contains an acetamide in lieu of the benzamide side chain present in novobiocin.^{23, 30} Interestingly, KU-32 induces the HSR, but at significantly lower concentrations than that needed to induce the degradation of client proteins.³¹⁻³² Since KU-32 was able to induce the pro-survival HSR, it was investigated for the treatment of neurodegenerative diseases. Studies in mice demonstrated that KU-32 was able to protect against neuronal glucotoxicity and reverse the

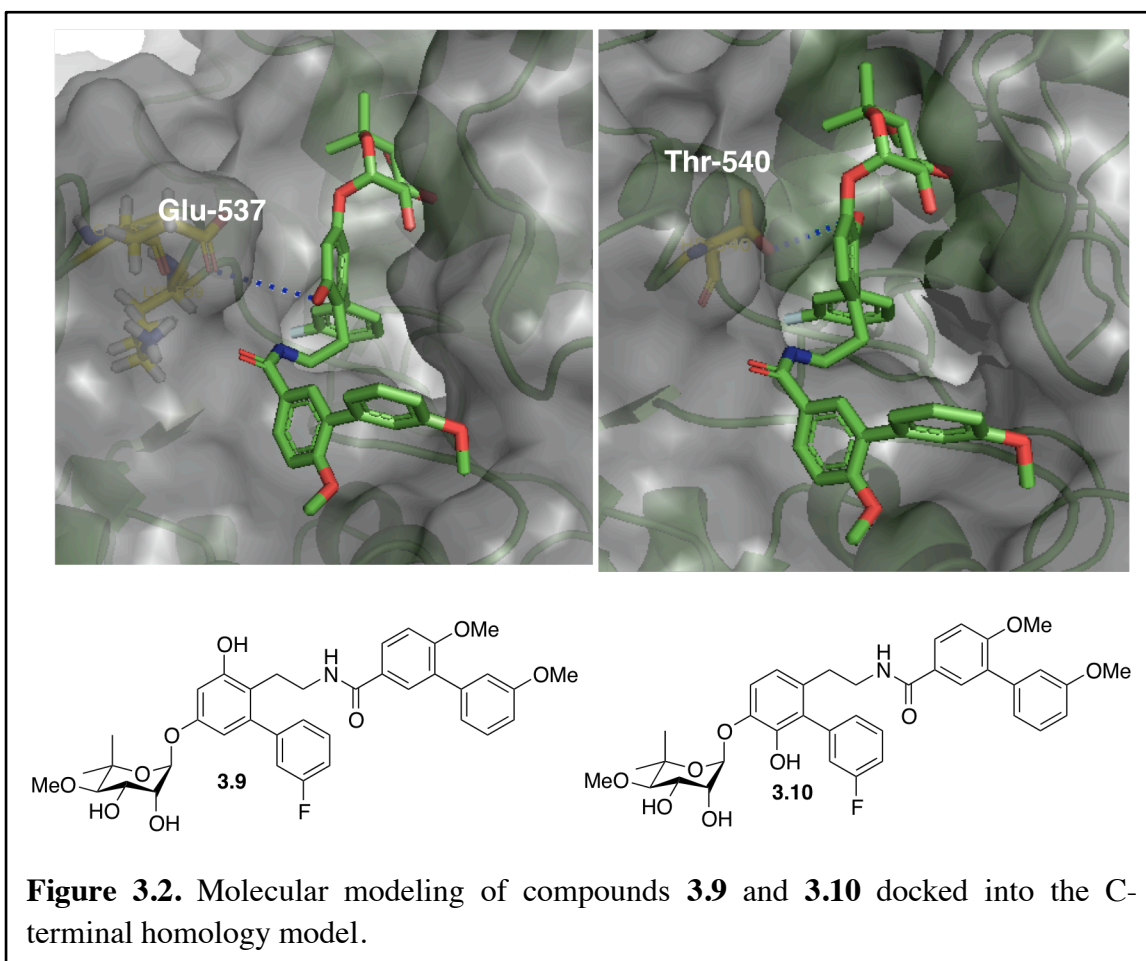
clinical endpoints of diabetic peripheral neuropathy.³³ A second generation of noviosylated analogs contained a biphenyl scaffold in lieu of the coumarin ring, and allowed the preparation of additional analogs. KU-596, the lead compound resulting from this latter generation, was found to exhibit comparable biological activity to KU-32.³⁴⁻³⁵ Since the biphenyl scaffold resulted in improved neuroprotection, compounds containing this new core were investigated for the treatment of cancer. An initial study found that the biphenyl scaffold in KU-596 could be modified to append a biaryl side chain in lieu of the acetamide and replace the noviose sugar with N-methyl piperidine, produced compounds which manifested anti-cancer activity, did not induce the pro-survival HSR, and were similarly active to known cytotoxic C-terminal inhibitor **KU-174**.³⁵ Figure 3.1 illustrates this parallel approach taken during the discovery of Hsp90 C-terminal inhibitors for either the treatment of cancer or neurodegeneration. Furthermore, modifications on the central biaryl ring have not been investigated, therefore analogs were prepared to determine whether such modifications could improve the anti-cancer activity of this class of compounds when compared to parent compound **3.5**, Figure 3.1.



Design

Molecular modeling studies were performed with a homology model of the C-terminal binding site to identify potential interactions with the biaryl core. Two hydrogen-bonding interactions appeared attainable by inclusion of a phenol onto the central biphenyl ring as suggested in Figure 3.2. Molecular modeling studies suggested that compounds containing substituents pointing toward amino acids Glu537 and Thr540 could also form hydrogen-bonding interactions, and consequently may be more efficacious. In silico studies suggested that the attachment of a methyl group onto the biphenyl core could produce hydrophobic interactions within the binding site and increase affinity. These interactions might be similar to previously studied Hsp90 C-terminal inhibitors that contain a coumarin core. Additionally, incorporation of

a methyl group may reinstate interactions lost upon transitioning from the coumarin core to the biaryl ring system.³⁶⁻³⁸ Consequently, analogs were sought to include such modifications.

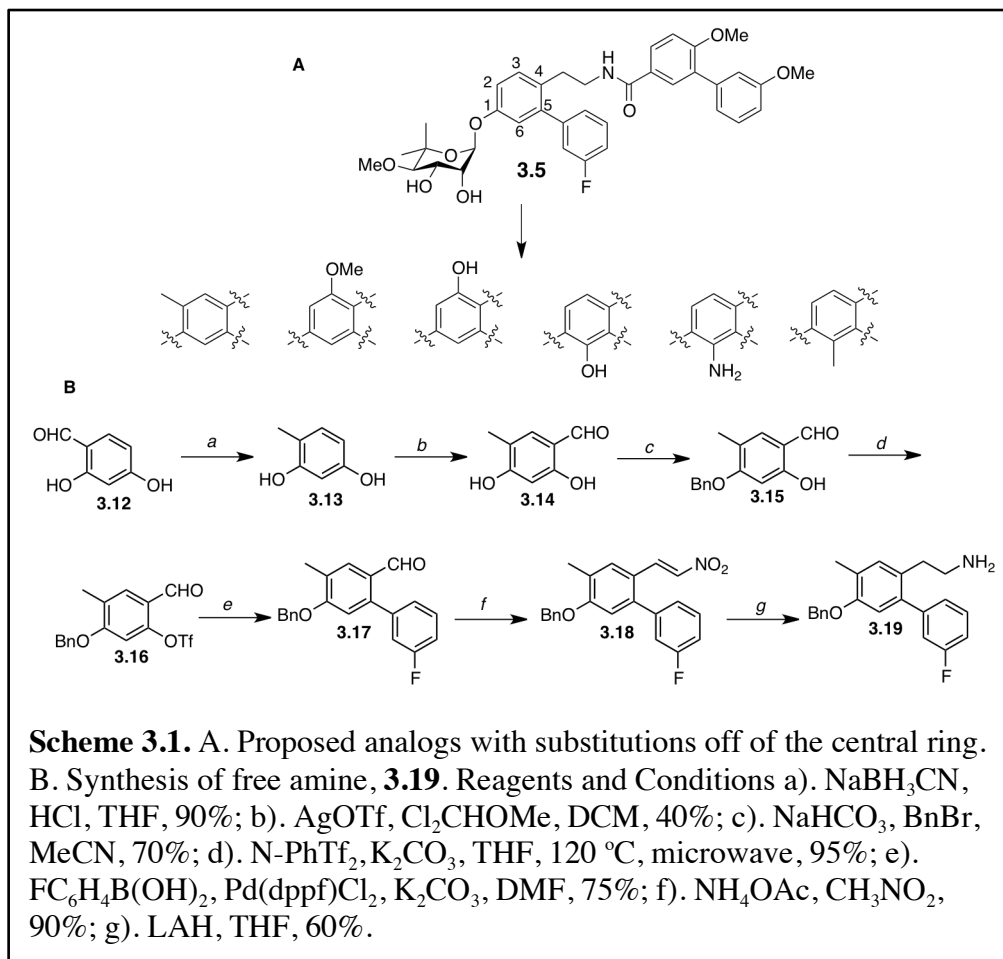


Results

Chemistry

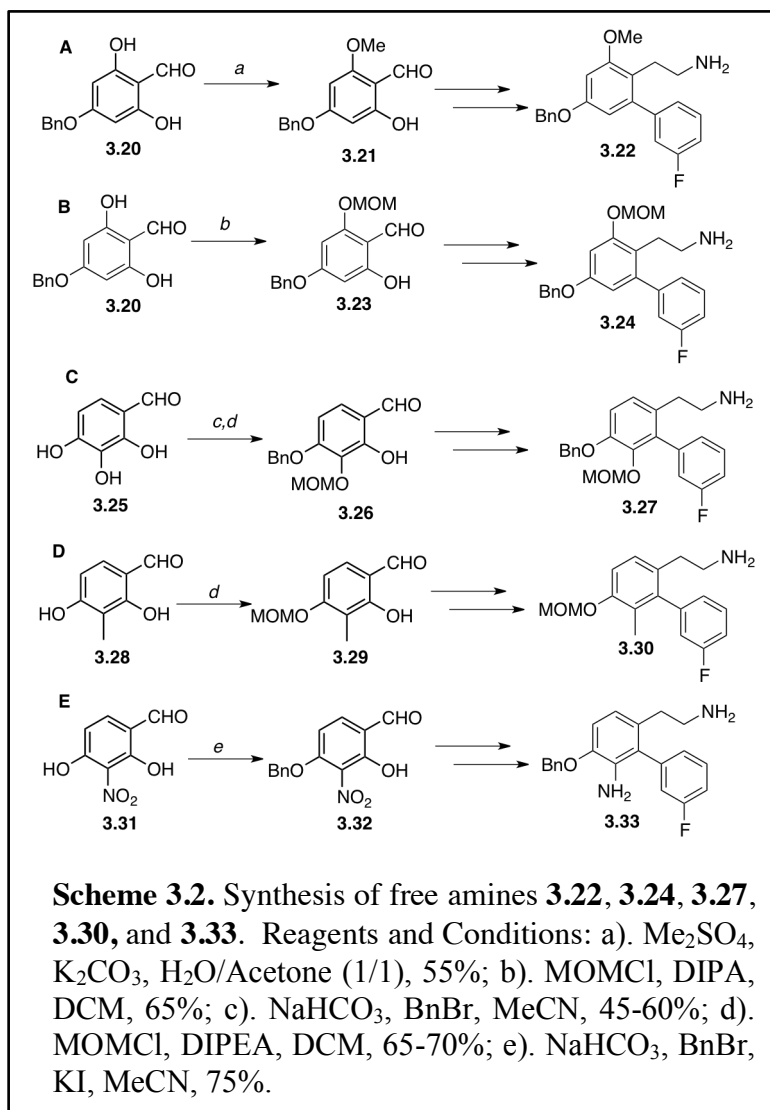
Derivatives of the central ring were selected for initial investigation, as illustrated in Scheme 3.1A. Synthesis of each derivative began via a different core. Synthesis of the derivative containing a methyl substituent (**3.19**) began by reduction of 2,4-dihydroxybenzaldehyde, **3.12**, with sodium cyanoborohydride in acidic THF to yield **3.13** (Scheme 3.1B).³⁹ Silver triflate and dichloro-methyl methyl ether were then used to formylate **3.13**, which produced aldehyde **3.14**.⁴⁰ The resultant methylbenzaldehyde, **3.14**, was then benzylated to give **3.15**, which was then

transformed into the trifluoromethanesulfonate derivative under microwave conditions.⁴¹ Subsequent Suzuki coupling with 3-fluorophenyl boronic acid generated the biaryl core of **3.17**. Henry olefination conditions were used to homologate the aldehyde into the α,β -unsaturated nitro compound **3.18**, which was subsequently reduced to provide amine **3.19**.



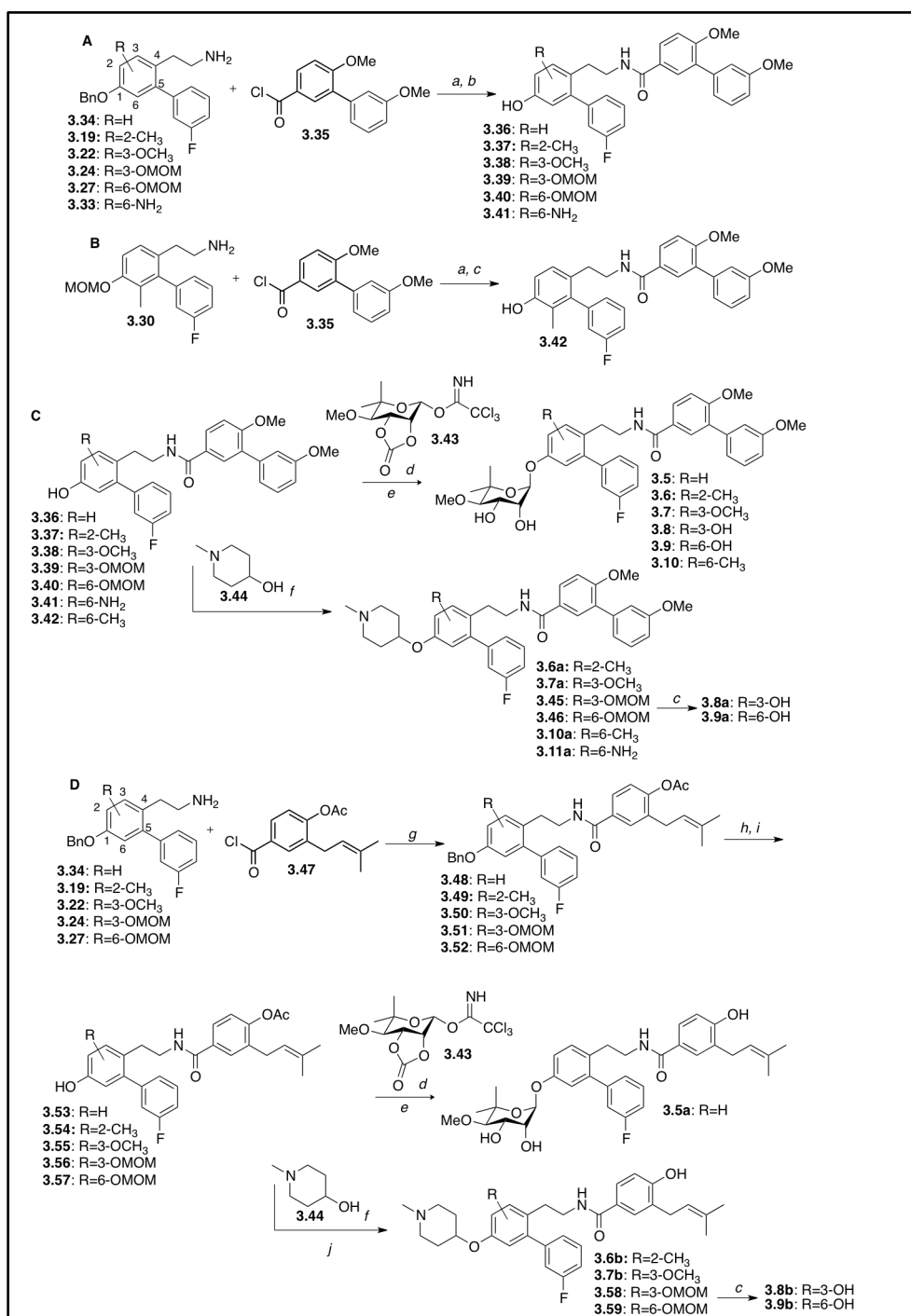
The remaining analogs required alternative routes for their preparation, however installment of the triflate and subsequent steps to yield the free amine were identical to the conditions described for **3.19**, as outlined in Scheme 3.1B. Synthesis of the methoxy and phenol derivatives began by formylation of phloroglucinol, followed by selective benzyl ether formation to give **3.20** (Scheme 3.2A and B). Aldehyde **3.20** was then treated with dimethyl sulfate in water and acetone to yield **3.21** (Scheme 3.2A).⁴² Intermediate **3.21** was subjected to conditions

previously outlined in Scheme 1B to produce amine **3.22**. In order to obtain the phenol, derivative **3.20** was treated with chloromethyl methyl ether to produce **3.23** (Scheme 3.2B),⁴³⁻⁴⁴ which was then subjected to conditions described in Scheme 3.1B to attain amine **3.24**. Synthesis of amine **3.27** began by selective benzylation of 2,3,4-trihydroxybenzaldehyde, which was subsequently reacted with chloromethyl methyl ether and diisopropylamine to yield aldehyde **3.26** (Scheme 3.2C). Compound **3.26** was then subjected to the conditions described in scheme 1B to afford amine **3.27**. Amine **3.30**, was attained via treatment with chloromethyl methyl ether to yield ether **3.29** (Scheme 3.2D), which was subjected to previously described methods to produce amine **3.30**. Analogue **3.33** was synthesized by subjecting 2-nitrobenzene-1,3-diphenol to Duff reaction conditions to yield **3.31** (Scheme 3.2E). Aldehyde **3.31** then underwent selective benzylation to produce the key intermediate, **3.32**, which was subsequently modified to give free amine **3.33**.



Two different amide side chains were investigated with these analogs, the original prenylated side chain present in novobiocin and the optimized biaryl side chain found in **3.4**. Additionally, compounds were made to contain either the noviose sugar or the noviose surrogate, *N*-methyl piperidine.⁴⁵ Installation of the biaryl side chain began by an acid chloride coupling of previously synthesized **3.35** with the free amine of each central ring derivative (Scheme 3.3A and 3.3B). Once the coupled product was obtained, hydrogenolysis was employed to produce the free phenols, **3.36-3.41** (Scheme 3.3A). Phenol **3.42** was obtained via removal of the methoxymethyl protecting group in the presence of *p*-Toluenesulfonic acid (Scheme 3.3B). The

free phenols **3.36-3.40** and **3.42** were then coupled with the activated noviose sugar (**3.43**), using Schmidt conditions.⁴⁶ The carbonate was then removed under solvolysis conditions to procure the corresponding noviose products, **3.5-3.10** (Scheme 3.3C). Simultaneously, free phenols **3.37-3.42** were subjected to Mitsunobu conditions with 1-methylpiperidin-4-ol (**3.44**) to yield the amine-containing products, **3.6a-3.11a** (Scheme 3.3C).

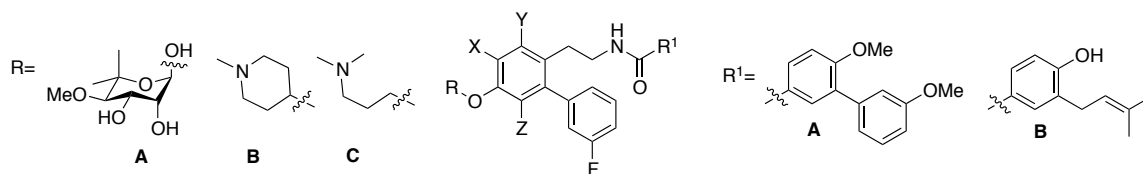


Scheme 3.3. A. Synthesis of phenols **3.36-3.41**. B. Synthesis of phenol **3.42**. C. Synthesis of final products **3.5-3.10** and **3.6a-3.11a**. D. Synthesis of final products **3.5a** and **3.6b-3.9b**. Reagents and Conditions: a). DMAP, Pyridine, DCM, 50-60%; b). H₂ (g), Pd/C, EtOAc, 70-80%; c). PTSA, MeOH, 65-70%; d). BF₃ OEt, DCM, 35-40%; e). Et₃N, MeOH, 85-90%; f). PBu₃, TMAD, Benzene, 30-35%; g). DMAP, Et₃N, DCM, 35-40%; h). Pd(OAc)₂, Et₃Si, Et₃N, DCM, 80-90%; i). TBAF, THF, 0 °C, 15 min, 55-60%; j). K₂CO₃, MeOH, 60-70%.

Analogs that contained the prenylated side chain were synthesized by an acid chloride coupling reaction between **3.47** and the free amine of each analogue (Scheme 3.3D). Coupled products **3.48-3.52** were subjected to Pd(OAc)Cl₂, Et₃SiH, Et₃N, to give the silyl protected phenols. Upon cleavage of the silyl ether with TBAF at 0°C, **3.53-3.57** were obtained in good yields (Scheme 3.3D). The resulting phenols, **3.53-3.57**, were then subjected to a Mitsunobu reaction with **3.44**, to give the amino products, **3.6b-3.9b**, respectively. Additionally phenol **3.53** was coupled with activated noviose sugar **3.43**, followed directly by solvolysis conditions yielded final product **3.5a**.

Biological Evaluation

Upon preparation of these new analogs, an MTS anti-proliferation assay was conducted against two breast cancer cell lines, MCF-7 (estrogen receptor positive cells) and SkBr3 (estrogen receptor negative HER2 overexpressing), and two prostate cancer cell lines, LNCap-LN3 (androgen receptor sensitive prostate cancer cells) and PC3-MM2 (androgen receptor insensitive prostate cancer cells). These cell lines were selected due to their dependency upon Hsp90 client proteins. All new analogs exhibited anti-proliferative activity against the 4 cancer cell lines as detailed in Table 3.1. Compounds containing an N-methyl piperidine exhibited greater inhibitory activity than those containing noviose. Additionally, compounds with a prenylated amide side chain were found to be more efficacious than compounds that contain the biaryl amide side chain.

Table 3.1. Anti-proliferative values of new analogs

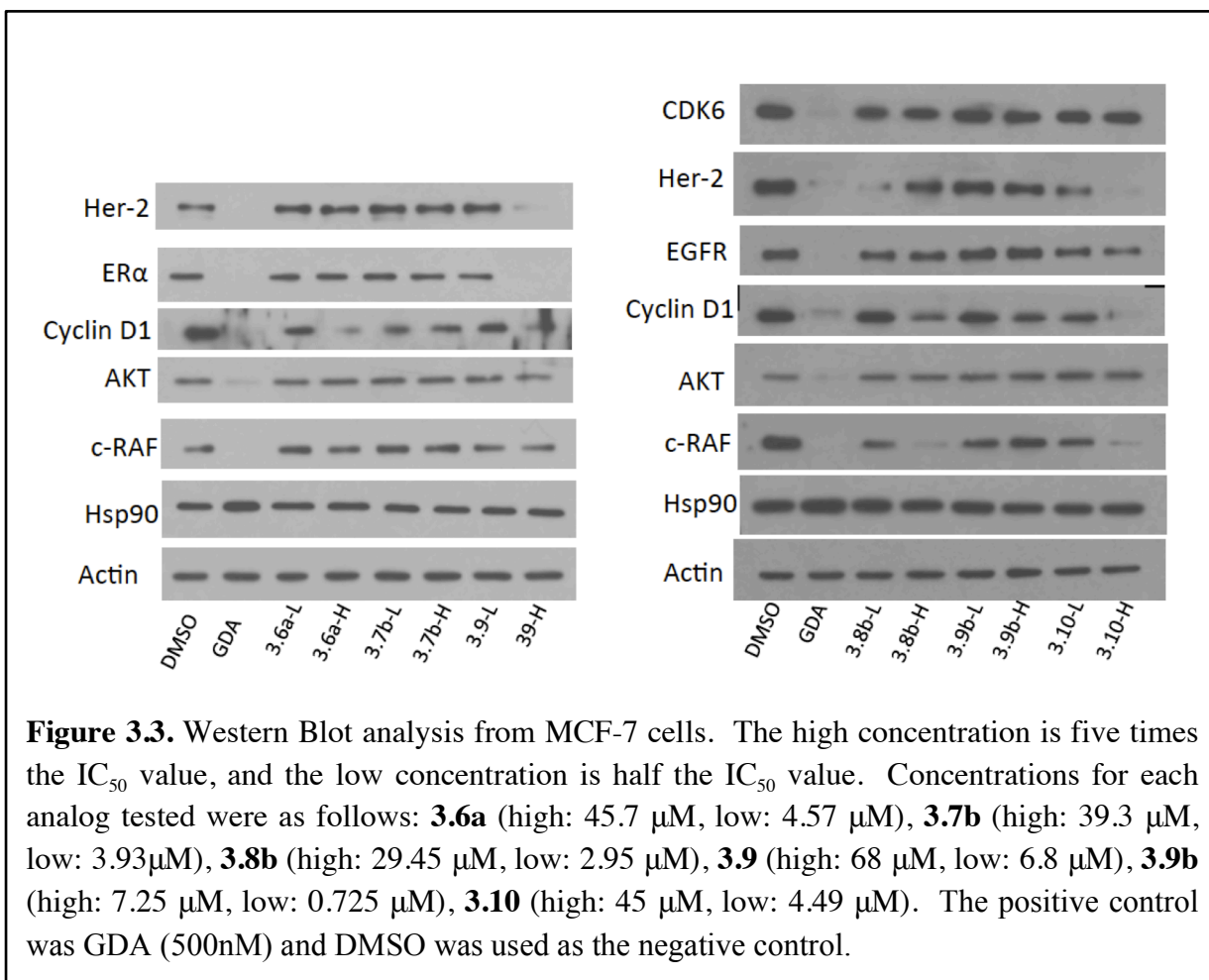
Compound	X	Y	Z	R	R ¹	MCF7 (μM) ^a	SkBr3 (μM) ^a	LNCap- LN3 (μM) ^a	PC3- MM2 (μM) ^a
3.3	H	H	H	A	-	>500	>500	>500	>500
3.5	H	H	H	A	A	>50	>50	>50	>50
3.5a	H	H	H	A	B	15.4±1.75	23.7±0.04	22.5	5.49
3.6	CH ₃	H	H	A	A	>50	43.9 ±4.4	>100	>100
3.6a	CH ₃	H	H	A	B	9.14 ± 2.72	7.81 ±1.1	20.8	13.9
3.6b	CH ₃	H	H	B	B	35.6 ± 3.03	15.2 ±1.67	>100	>100
3.7	H	OCH ₃	H	A	A	44.7 ±4.15	49.4±2.03	8.09	10.6
3.7a	H	OCH ₃	H	A	B	8.71 ±1.20	5.72±0.89	>100	32.1
3.7b	H	OCH ₃	H	B	B	7.86 ±0.20	8.16±0.29	>100	1.84
3.8	H	OH	H	A	A	23.8±0.47	23.5±0.44	>50	>50
3.8a	H	OH	H	A	B	12.2 ±0.89	15.7 ±1.5	44.8	>50
3.8b	H	OH	H	B	B	5.89 ±0.67	7.59 ±0.58	22.8	1.32
3.9	H	H	OH	A	A	13.6 ±2.01	16.7 ±0.93	>100	9.37
3.9a	H	H	OH	A	B	11.3 ± 1.62	9.29±1.07	22.4	8.61
3.9b	H	H	OH	B	B	1.45 ±0.87	3.25 ±1.2	23.1	42.3
3.10	H	H	CH ₃	A	A	8.99±0.28	43.5±1.03	25.1	>50
3.10a	H	H	CH ₃	B	A	17.8±1.48	21.3±2.82	>50	>50
3.10b	H	H	CH ₃	C	A	7.97±0.46	9.34±0.68	44.8	1.32
3.11a	H	H	NH ₂	A	B	11.3±1.3	15.3±2.3	22.4	18.9

^aValues represent mean ± standard deviation for at least two separate experiments performed in triplicate.

Interestingly, the synthesized analogs followed the same trend in activity independent of the sugar surrogate or amide side chain. The methyl derivatives were more active than the parent compound; the methoxy derivatives were more active than the methyl derivatives, and the phenol derivatives more active than both the methoxy and the methyl derivatives. Analogues that contained the sugar surrogate, N-methyl piperidine, were more active than the analogues containing the noviose sugar. Additionally, analogues that contained the prenylated side chain were more

active than analogs containing the biaryl side chain. Analogue **3.6** was similarly active to the parent compound, **3.5**. However analogs **3.6a** and **3.6b**, which contained N-methyl piperidine in lieu of noviose, were more active than **3.6**. In addition, analogs containing moieties that could participate in hydrogen bonding interactions manifested improved inhibitory activity as compared to **3.5**. More specifically, it appears that a hydrogen bond donor is more beneficial as analogs **3.8**, **3.8a**, and **3.8b** exhibited similar or improved activity as compared to analogs **3.7**, **3.7a**, and **3.7b**.

After determination of IC_{50} values, compounds **3.6a**, **3.7b**, **3.8b**, **3.9**, **3.9b**, and **3.10** were further evaluated by western blot analysis of MCF7 cell lysates. Compound **3.10** exhibited significant Hsp90-dependent client protein degradation at concentrations that mirrored its anti-proliferative activity, clearly linking Hsp90 inhibition to cell viability, as illustrated in Figure 3.3. In fact, Hsp90 dependent clients Her-2, Cyclin D1, and c-Raf were degraded upon treatment with **3.10** for 24 hours. **3.6a**, **3.8b**, and **3.9** also demonstrated client protein degradation, but to a lesser extent. Compounds **7b** and **9b** did not demonstrate client protein degradation. Importantly, no increase in Hsp90 levels was observed with these C-terminal inhibitors, which is an important attribute manifested by C-terminal inhibitors that exhibit anti-cancer activity.



Conclusion

In summary, a series of Hsp90 C-terminal inhibitors with modifications to the central ring of the biphenyl scaffold were designed, synthesized, and biologically evaluated. Modifications to the central ring produced compounds that exhibited increased biological activity. Structure-activity relationship studies revealed that modifications, which include a hydrogen bond donor, resulted in the most potent anti-proliferative activity. Finally, western blot analysis confirmed that compounds **3.8b**, **3.9** and **3.10** manifest their anti-proliferative activity via Hsp90 inhibition,

as client protein degradation was observed at concentrations that mirrored anti-proliferative activity.

Future Directions

Recently we began testing select Hsp90 C-terminal inhibitors in a TR-FRET Assay kit that evaluates possible isoform selectivity by measuring %activity against both Hsp90 α and Hsp90 β . Compounds **3.5** and **3.10** were evaluated for activity against both isoforms using this assay. Compound **3.5** did not exhibit selectivity for either isoform as it had 72.2% activity for Hsp90 α and 100% activity for Hsp90 β at 100 μ M. Interestingly compound **3.10** was found to be selective for Hsp90 α as it exhibited 45% activity at 100 μ M and 100% activity for Hsp90 β . The cellular activity of these compounds supports this assay data because the IC₅₀ value of **3.10** is single digit micromolar and only Hsp90 β knockout is known to be lethal, so targeting the *alpha* isoform could result in a compound that is not very cytotoxic.⁴⁷ This initial assay result provides an excellent starting point for the exploration of potential isoform selective inhibitors with these compounds and similar analogs, as Hsp90 α selectivity occurred from the addition of a methyl group. Identification of different structural motifs that result in isoform selectivity would be extremely beneficial for the development of future C-terminal inhibitors. Identifying isoform selective inhibitors would lead to new and interesting studies that would investigate the biological effects of targeting one isoform over the other with a C-terminal inhibitor.

Materials and Methods

Anti-proliferation assays.

Cells were maintained in a 1:1 mixture of Advanced DMEM/F12 (Gibco) supplemented with non-essential amino acids, L-glutamine (2 mM), streptomycin (500 µg/mL), penicillin (100 units/mL), and 10% FBS. Cells were grown to confluence in a humidified atmosphere (37° C, 5% CO₂), seeded (2000/well, 100 µL) in 96-well plates, and allowed to attach overnight. Compound or GDA at varying concentrations in DMSO (1% DMSO final concentration) was added, and cells were returned to the incubator for 72 h. At 72 h, the number of viable cells was determined using an MTT/PMS cell proliferation kit (Promega) per the manufacturer's instructions. Cells incubated in 1% DMSO were used at 100% proliferation, and values were adjusted accordingly. IC₅₀ values were calculated from separate experiments performed in triplicate using GraphPad Prism.

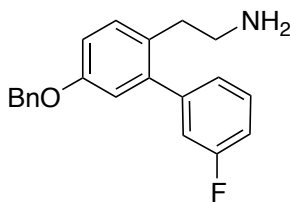
Western blot Analyses.

MCF-7 cells were cultured as described above and treated with various concentrations of drug, GDA in DMSO (1% DMSO final concentration), or vehicle (DMSO) for 24 h. Cells were harvested in cold PBS and lysed in RIPA lysis buffer containing 1 mM PMSF, 2 mM sodium orthovanadate, and protease inhibitors on ice for 1 h. Lysates were clarified at 14000g for 10 min at 4° C. Protein concentrations were determined using the Pierce BCA protein assay kit per the manufacturer's instructions. Equal amounts of protein (20 µg) were electrophoresed under reducing conditions, transferred to a nitrocellulose membrane, and immunoblotted with the corresponding specific antibodies. Membranes were incubated with an appropriate horseradish peroxidase-labeled secondary antibody, developed with a chemiluminescent substrate, and visualized.

Chemistry General.

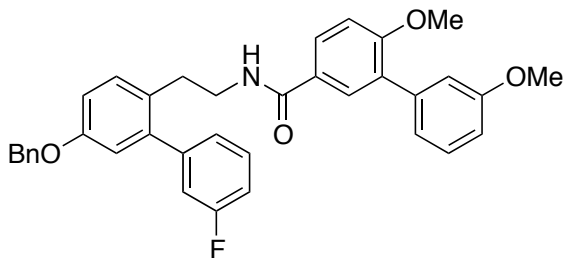
^1H NMR were recorded at 500 MHz (Avance AVIII 500 MHz spectrometer with a dual carbon/proton cryoprobe) or 400 (Bruker AVIIIHD 400 MHz NMR with a broadband X-channel detect gradient probe) and ^{13}C NMR were recorded at 125 MHz (Bruker AVIII spectrometer equipped with a cryogenically cooled carbon observe probe). Chemical shifts are reported in δ (ppm) relative to the internal standard (CDCl_3 , 7.26 ppm, or as stated). HRMS spectra were recorded with a LCT Premier with ESI ionization. ^1H and ^{13}C NMR was used to verify that all tested compounds were >95% pure. TLC analysis was performed on glass backed silica gel plates and visualized by UV light. All solvents were reagent grade and used without further purification.

Synthesis and Compound Characterization



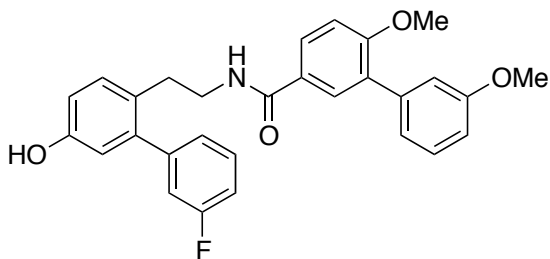
2-(5-(Benzyloxy)-3'-fluoro-[1,1'-biphenyl]-2-yl)ethanamine (3.34).

This compound was synthesized following a previously reported procedure.³⁴



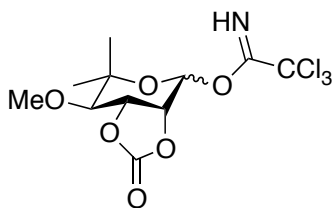
***N*-(2-(5-(Benzyloxy)-3'-fluoro-[1,1'-biphenyl]-2-yl)ethyl)-3',6-dimethoxy-[1,1'-biphenyl]-3-carboxamide.**

Thionyl chloride (0.13 ml, 0.75 mmol) was added to a solution of biaryl acid (97 mg, 0.38 mmol) in anhydrous tetrahydrofuran (2 ml) and the solution was refluxed for 3h. The solution was then concentrated under vacuum to get acid chloride **3.35** (105 mg) as brown semi-solid that was used directly in the next step. Triethylamine (0.13 ml, 0.75 mmol) was added to an ice-cooled solution of acid chloride in anhydrous DCM (1 ml), followed by a dropwise addition of amine **2-(5-(benzyloxy)-3'-fluoro-[1,1'-biphenyl]-2-yl)ethanamine** (50 mg, 0.25 mmol). The solution was then allowed to stir at rt for 12h. The reaction mixture was concentrated and the residue was purified by column chromatography (SiO₂, 1:25, Acetone: DCM) to afford the product as a white amorphous solid (65%): ¹H NMR (500 MHz, Chloroform-d) δ 8.00 – 7.86 (m, 6H), 7.23 (td, *J* = 7.9, 1.9 Hz, 3H), 7.06 – 6.98 (m, 5H), 6.94 – 6.87 (m, 3H), 6.80 (ddt, *J* = 8.3, 2.6, 1.1 Hz, 2H), 5.19 (s, 1H), 4.23 (s, 2H), 3.76 (s, 3H), 3.73 (s, 3H), 3.56 (t, *J* = 6.3 Hz, 2H), 2.90 – 2.69 (m, 2H). ¹³C NMR (126 MHz, CDCl₃) δ 169.38, 160.42, 160.09, 156.59, 138.85, 138.76, 132.74, 132.17, 131.31, 130.78, 130.29, 128.99, 128.52, 127.42, 122.78, 122.77, 122.26, 121.93, 115.28, 112.78, 112.70, 110.56, 70.59, 55.72, 55.20, 44.56, 26.44. HRMS (ESI+) *m/z*: [M + H⁺] calculated for C₃₆H₃₂FNO₄ 562.3145; found 562.3135.



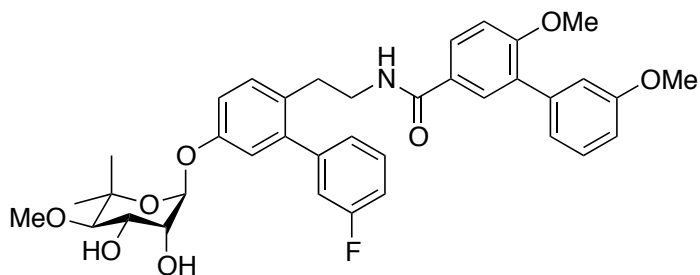
***N*-(2-(3'-Fluoro-5-hydroxy-[1,1'-biphenyl]-2-yl)ethyl)-3',6-dimethoxy-[1,1'-biphenyl]-3-carboxamide (3.36).**

***N*-(2-(5-(Benzyloxy)-3'-fluoro-[1,1'-biphenyl]-2-yl)ethyl)-3',6-dimethoxy-[1,1'-biphenyl]-3-carboxamide** (0.05g) at rt was dissolved in EtOAc (20mL). Pd/C (10% w/w, 20 mg) was added, the mixture was degassed and flushed with argon, then degassed and flushed with hydrogen using a balloon. After 12 h the reaction was filtered through a pad of Celite, washed with EtOAc. The filtrate was concentrated and purified via column chromatography (20-50%EtOAc/Hex). Compound was isolated as an oil in 70% yield: ¹H NMR (500 MHz, Chloroform-d) δ 7.92 – 7.80 (m, 2H), 7.23 (td, *J* = 6.6, 3.9 Hz, 4H), 7.09 – 7.02 (m, 3H), 6.90 – 6.79 (m, 3H), 6.64 (d, 2H), 5.09 (s, 1H), 3.76 (s, 3H), 3.73 (s, 3H), 3.61 (t, *J* = 5.7 Hz, 2H), 2.90 – 2.69 (m, 2H). ¹³C NMR (126 MHz, CDCl₃) δ 169.65, 160.87, 160.11, 159.36, 156.75, 138.43, 132.14, 130.66, 130.43, 128.91, 128.82, 127.43, 122.73, 122.55, 122.26, 121.03, 115.67, 112.14, 112.07, 110.98, 55.66, 55.31, 44.31, 26.48. HRMS (ESI+) *m/z*: [M - H⁺] calculated for C₂₉H₂₆FNO₄ 470.1768; found 470.1771.



(3aR,7R,7aR)-7-Methoxy-6,6-dimethyl-2-oxotetrahydro-3aH-[1,3]dioxolo[4,5-c]pyran-4-yl 2,2,2-trichloroacetimidate (3.43).

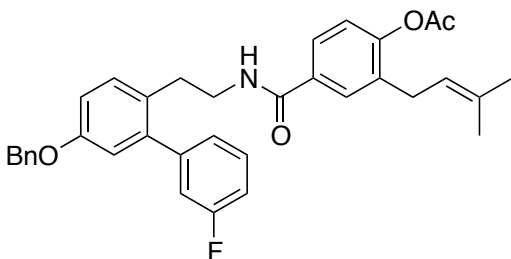
This compound was synthesized following a previously reported procedure.^{34, 48}



***N*-(2-(5-(((2*R*,3*R*,4*S*,5*R*)-3,4-Dihydroxy-5-methoxy-6,6-dimethyltetrahydro-2*H*-pyran-2-yl)oxy)-3'-fluoro-[1,1'-biphenyl]-2-yl)ethyl)-3',6-dimethoxy-[1,1'-biphenyl]-3-carboxamide (3.5).**

Activated noviose sugar **3.47**^{36, 48} in anhydrous dichloromethane (0.5mL) was added to a mixture of **3.36** (0.042g, 0.066mmol) in anhydrous dichloromethane (0.5mL) at rt. Boron trifluoride diethyl etherate (0.07mL) was then added drop wise. The reaction was monitored via TLC. Upon completion of the reaction (~1 hour), triethylamine (0.1mL) was added. The mixture was concentrated and purified via column chromatography (SiO₂, 3:1, Hexane: EtOAc-20:1, DCM:MeOH). The product was obtained as a white solid in 30% yield and used directly in the next step. The product (0.023g, 0.03mmol) was dissolved in MeOH (12mL) and triethylamine (4mL) was added. The mixture was stirred over night. After 12 hours the reaction was concentrated and purified via column chromatography (SiO₂, 20:1, DCM: MeOH) to afford **3.5** as white amorphous solid (70%): ¹H NMR (500 MHz, Chloroform-*d*) δ 7.67 (dd, *J* = 8.6, 2.4 Hz, 1H), 7.57 (d, *J* = 2.4 Hz, 1H), 7.35 – 7.29 (m, 2H), 7.24 (d, *J* = 8.5 Hz, 1H), 7.09 – 6.96 (m, 6H), 6.95 (s, 1H), 6.91 – 6.85 (m, 2H), 5.96 (t, *J* = 5.6 Hz, 1H), 5.53 (d, *J* = 2.3 Hz, 1H), 4.19 (dd, *J* = 9.1, 3.4 Hz, 1H), 4.14 (dd, *J* = 3.4, 2.3 Hz, 1H), 3.84 (d, *J* = 1.9 Hz, 6H), 3.58 (s, 3H), 3.50 – 3.43 (m, 2H), 3.32 (d, *J* = 9.1 Hz, 1H), 2.85 (t, *J* = 7.2 Hz, 2H), 1.34 (s, 3H), 1.19 (s, 3H). ¹³C NMR (126 MHz, CDCl₃) δ 166.99, 161.62, 159.37, 159.05, 155.28, 143.47, 139.06, 131.06, 130.49, 130.03, 129.49, 129.21, 128.11, 126.89, 125.03, 122.09, 117.91, 116.35, 115.56, 115.41,

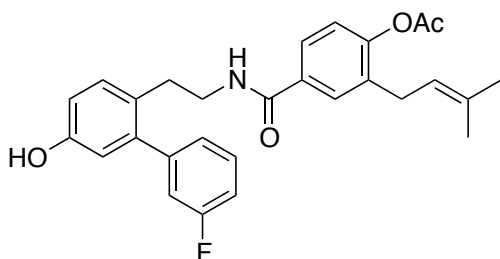
114.18, 112.95, 110.91, 94.46, 78.33, 71.39, 68.66, 61.98, 55.89, 55.45, 41.07, 32.12, 29.83, 29.16. HRMS (ESI+) m/z: [M + H⁺] calculated for C₃₇H₄₀FNO₈ 641.2721; found 641.2730.



4-((2-(5-(Benzyloxy)-3'-fluoro-[1,1'-biphenyl]-2-yl)ethyl)carbamoyl)-2-(3-methylbut-2-en-1-yl)phenyl acetate (3.48).

Oxalyl chloride (0.10 ml, 0.75 mmol) was added to a solution of prenylated acid (97 mg, 0.38 mmol) in anhydrous tetrahydrofuran (2 ml) and the solution was refluxed for 9h. The solution was then concentrated under vacuum to get acid chloride **3.47** (105 mg) as brown semi-solid that was used directly in the next step. Pyridine (0.10 ml, 0.75 mmol) was added to an ice-cooled solution of acid chloride in anhydrous DCM (1 ml), followed by a dropwise addition of amine **2-(5-(benzyloxy)-3'-fluoro-[1,1'-biphenyl]-2-yl)ethanamine** (50 mg, 0.25 mmol). The solution was then allowed to stir at rt for 12h. The reaction mixture was concentrated and the residue was purified by column chromatography (SiO₂, 1:25, Acetone: DCM) to afford the product as a white amorphous solid (40%): ¹H NMR (500 MHz, Chloroform-d) δ 7.58 (d, *J* = 2.2 Hz, 1H), 7.44 (dt, *J* = 8.4, 2.2 Hz, 3H), 7.41 – 7.37 (m, 3H), 7.36 – 7.32 (m, 2H), 7.09 – 7.06 (m, 1H), 7.05 – 7.00 (m, 3H), 6.97 (dd, *J* = 8.5, 2.8 Hz, 1H), 6.87 (d, *J* = 2.7 Hz, 1H), 6.05 (t, *J* = 5.8 Hz, 1H), 5.19 (dddd, *J* = 7.2, 5.8, 2.9, 1.4 Hz, 1H), 5.06 (s, 2H), 3.46 (td, *J* = 7.1, 5.8 Hz, 2H), 3.25 (d, *J* = 7.3 Hz, 2H), 2.86 (t, *J* = 7.1 Hz, 2H), 2.32 (s, 3H), 1.73 (d, *J* = 1.3 Hz, 3H), 1.70 (d, *J* = 1.3 Hz, 3H). ¹³C NMR (126 MHz, CDCl₃) δ 169.16, 166.94, 161.60, 157.28, 151.29, 136.87, 134.15, 133.79,

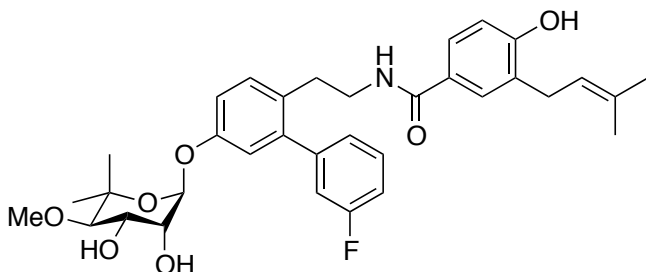
132.54, 131.05, 129.95, 129.27, 128.68, 128.48, 128.12, 127.63, 125.46, 124.97, 122.46, 121.03, 116.55, 116.27, 114.58, 114.32, 70.16, 40.99, 31.97, 28.95, 25.84, 20.96, 17.99. HRMS (ESI+) m/z: [M + H⁺] calculated for C₃₅H₃₄FNO₄ 552.4525; found 552.4520.



4-((2-(3'-Fluoro-5-hydroxy-[1,1'-biphenyl]-2-yl)ethyl)carbamoyl)-2-(3-methylbut-2-en-1-yl)phenyl acetate (3.53).

A catalytic amount of Pd(OAc)₂ was added to a solution of Triethylamine (0.15mL, 1.1mmol) and triethylsilane (0.19 mL, 1.2mmol) in anhydrous dichloromethane (3mL). The reaction was stirred at rt for 15 min and then **4-((2-(5-(benzyloxy)-3'-fluoro-[1,1'-biphenyl]-2-yl)ethyl)carbamoyl)-2-(3-methylbut-2-en-1-yl)phenyl acetate** (0.551 g, 1.0mmol) in anhydrous dichloromethane (2mL) was added dropwise. After 12 h the reaction was quenched with sat. NH₄OAc and worked up with EtOAc (3 x 20mL). The organic layers were dried, concentrated, and purified via column chromatography (SiO₂, 1:4, EtOAc: Hex). The silyl-protected product was obtained as a clear oil in 80% yield. The silyl ether (0.8mmol) was dissolved in anhydrous tetrahydrofuran (2mL) and cooled to 0°C. TBAF, 1.0M in THF (0.1mL, 0.35mmol) was added dropwise and the reaction was stirred at 0°C for 15 minutes. After 15 minutes the reaction progress was monitored by TLC, as soon as the reaction was complete it was quenched via the addition of sat. NH₄Cl. The reaction was worked-up with EtOAc (3 x 5 mL), the organic layers were combined, dried, concentrated and purified via column

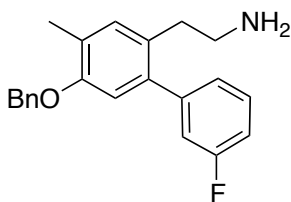
chromatography (SiO₂, 1:2, EtOAc: Hex). **4-((2-(3'-Fluoro-5-hydroxy-[1,1'-biphenyl]-2-yl)ethyl)carbamoyl)-2-(3-methylbut-2-en-1-yl)phenyl acetate** was obtained in 60% yield as a white solid: ¹H NMR (500 MHz, Chloroform-d) δ 7.44 (d, *J* = 2.3 Hz, 1H), 7.36 – 7.30 (m, 2H), 7.06 – 7.02 (m, 3H), 7.02 – 6.96 (m, 2H), 6.94 (d, *J* = 2.5 Hz, 1H), 6.75 (d, *J* = 8.4 Hz, 1H), 6.08 (t, *J* = 5.8 Hz, 1H), 5.27 (dddd, *J* = 7.2, 5.7, 2.8, 1.4 Hz, 1H), 3.50 – 3.44 (m, 2H), 3.33 (d, *J* = 7.2 Hz, 2H), 2.88 (t, *J* = 7.1 Hz, 2H), 2.29 (s, 3H), 1.73 (dd, *J* = 3.8, 1.4 Hz, 6H). ¹³C NMR (126 MHz, CDCl₃) δ 169.61, 167.64, 163.34, 161.38, 157.67, 148.74, 142.43, 141.96, 134.49, 133.82, 130.75, 129.86, 128.80, 127.35, 126.20, 125.76, 124.75, 122.95, 121.25, 121.00, 115.90, 115.24, 114.16, 40.68, 32.11, 29.12, 25.68, 21.00, 17.77. HRMS (ESI+) *m/z*: [M + Na⁺] calculated for C₂₈H₂₈FNO₄Na 484.1900; found 484.1883.



***N*-(2-(3'-Fluoro-5-((1-methylpiperidin-4-yl)oxy)-[1,1'-biphenyl]-2-yl)ethyl)-4-hydroxy-3-(3-methylbut-2-en-1-yl)benzamide (3.5a).**

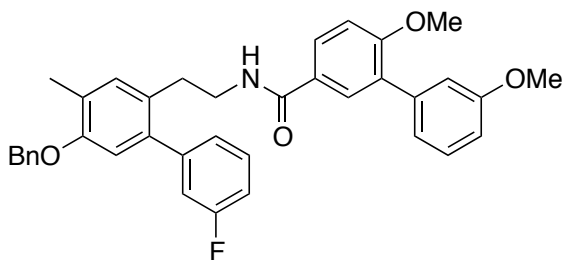
Compound **3.5a** was synthesized following the procedure used for the synthesis of **3.5** to obtain the product as a white solid: ¹H NMR (500 MHz, Chloroform-d) δ 7.42 (d, *J* = 2.4 Hz, 1H), 7.38 (dd, *J* = 8.5, 2.3 Hz, 1H), 7.34 – 7.28 (m, 1H), 7.13 (d, *J* = 8.4 Hz, 1H), 7.07 (d, *J* = 8.6 Hz, 1H), 7.03 – 7.00 (m, 2H), 6.93 (ddd, *J* = 9.6, 2.6, 1.6 Hz, 1H), 6.81 (dd, *J* = 8.3, 2.7 Hz, 1H), 6.71 (d, *J* = 2.7 Hz, 1H), 6.01 (t, *J* = 5.7 Hz, 1H), 5.45 (d, *J* = 2.3 Hz, 1H), 5.13 (tdd, *J* = 5.6, 2.8, 1.4 Hz, 1H), 4.18 (dd, *J* = 9.0, 3.4 Hz, 1H), 4.13 (dd, *J* = 3.4, 2.3 Hz, 1H), 3.58 (s, 3H), 3.45 –

3.40 (m, 2H), 3.34 (d, $J = 9.1$ Hz, 1H), 3.26 – 3.13 (m, 2H), 2.80 (t, $J = 7.2$ Hz, 2H), 1.68 (d, $J = 1.3$ Hz, 6H), 1.65 (d, $J = 1.2$ Hz, 6H). ^{13}C NMR (126 MHz, CDCl_3) δ 167.96, 163.57, 161.61, 157.31, 133.09, 131.09, 130.53, 129.96, 128.67, 127.54, 127.25, 126.18, 124.98, 122.09, 117.26, 116.27, 116.10, 115.36, 114.23, 114.06, 113.30, 97.76, 78.59, 71.27, 68.74, 62.00, 41.20, 31.96, 29.09, 25.85, 22.54, 17.99. HRMS (ESI+) m/z : $[\text{M} + \text{H}^+]$ calculated for $\text{C}_{34}\text{H}_{40}\text{FNO}_7$ 594.0828; found 594.0837.



2-(5-(Benzyloxy)-3'-fluoro-4-methyl-[1,1'-biphenyl]-2-yl)ethanamine (3.19).

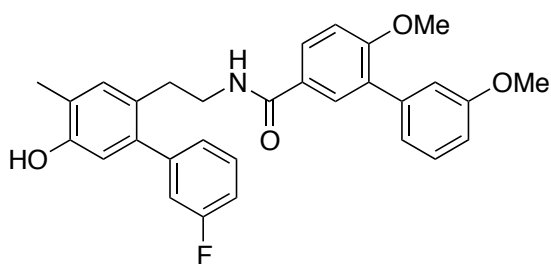
This compound was synthesized following the procedure reported in Chapter 2.



***N*-(2-(5-(Benzyloxy)-3'-fluoro-4-methyl-[1,1'-biphenyl]-2-yl)ethyl)-3',6-dimethoxy-[1,1'-biphenyl]-3-carboxamide.**

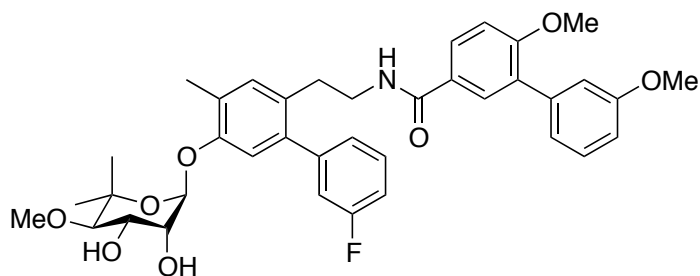
The compound was synthesized following the procedure used for the synthesis of *N*-(2-(5-(benzyloxy)-3'-fluoro-[1,1'-biphenyl]-2-yl)ethyl)-3',6-dimethoxy-[1,1'-biphenyl]-3-carboxamide to obtain the product as a white solid: ^1H NMR (500 MHz, Chloroform- d) δ 7.62 (dd, $J = 8.5, 2.4$ Hz, 1H), 7.49 (d, $J = 2.4$ Hz, 1H), 7.36 (dd, $J = 8.2, 1.5$ Hz, 2H), 7.34 – 7.29 (m,

2H), 7.29 – 7.23 (m, 3H), 7.10 – 7.06 (m, 1H), 7.01 – 6.96 (m, 3H), 6.96 – 6.88 (m, 3H), 6.83 (ddd, $J = 8.3, 2.7, 1.0$ Hz, 1H), 6.67 (s, 1H), 5.85 (d, $J = 5.7$ Hz, 1H), 4.97 (s, 2H), 3.77 (d, $J = 8.5$ Hz, 6H), 3.44 – 3.38 (m, 2H), 2.77 (t, $J = 7.1$ Hz, 2H), 2.22 (d, $J = 0.7$ Hz, 3H). ^{13}C NMR (126 MHz, CDCl_3) δ 166.80, 161.54, 159.27, 158.90, 155.28, 139.26, 138.98, 137.19, 132.30, 130.38, 129.88, 129.81, 129.31, 129.08, 128.51, 128.03, 127.91, 127.84, 127.20, 126.99, 126.90, 125.04, 121.95, 116.19, 115.28, 113.88, 113.10, 112.83, 110.79, 69.98, 55.78, 55.31, 41.11, 31.88, 16.07. HRMS (ESI+) m/z : $[\text{M} + \text{H}^+]$ calculated for $\text{C}_{37}\text{H}_{34}\text{FNO}_4$ 576.3325; found 576.3329.



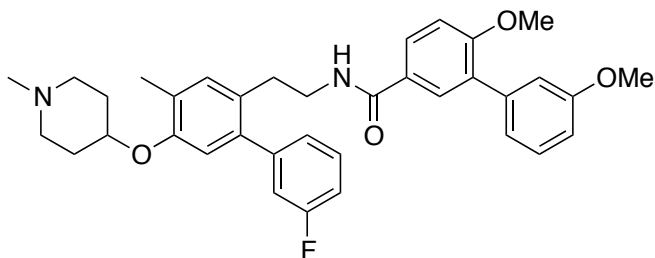
***N*-(2-(3'-Fluoro-5-hydroxy-4-methyl-[1,1'-biphenyl]-2-yl)ethyl)-3',6-dimethoxy-[1,1'-biphenyl]-3-carboxamide (3.37).**

Compound **3.37** was synthesized following the procedure used for the synthesis of **3.36** to obtain the product as a white solid: ^1H NMR (500 MHz, Chloroform- d) δ 7.67 (dd, $J = 8.6, 2.4$ Hz, 1H), 7.52 (d, $J = 2.3$ Hz, 1H), 7.33 (t, $J = 7.9$ Hz, 1H), 7.10 – 7.05 (m, 2H), 7.04 – 6.88 (m, 6H), 6.65 (s, 1H), 5.94 (t, $J = 5.2$ Hz, 1H), 3.84 (d, $J = 1.1$ Hz, 6H), 3.48 – 3.38 (m, 2H), 2.81 (t, $J = 7.2$ Hz, 2H), 2.23 (s, 3H). ^{13}C NMR (126 MHz, CDCl_3) δ 167.18, 161.61, 159.35, 159.09, 152.70, 139.70, 139.07, 132.64, 130.47, 129.94, 129.87, 129.42, 129.21, 128.25, 127.76, 125.07, 125.05, 122.16, 116.34, 115.49, 114.10, 113.94, 112.89, 110.96, 55.90, 55.48, 41.28, 31.85, 15.67. HRMS (ESI+) m/z : $[\text{M} + \text{H}^+]$ calculated for $\text{C}_{30}\text{H}_{28}\text{FNO}_4$ 486.4220; found 486.4211.



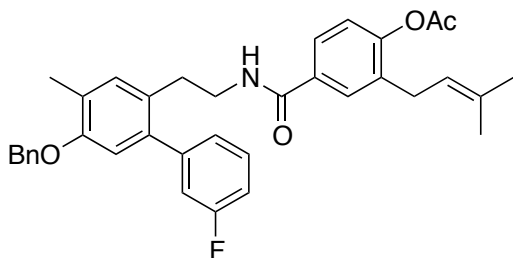
***N*-2-(5-(((2*R*,3*R*,4*S*,5*R*)-3,4-Dihydroxy-5-methoxy-6,6-dimethyltetrahydro-2*H*-pyran-2-yl)oxy)-3'-fluoro-4-methyl-[1,1'-biphenyl]-2-yl)ethyl)-3',6-dimethoxy-[1,1'-biphenyl]-3-carboxamide (**3.6**).**

Compound **3.6** was synthesized following the procedure used for the synthesis of **3.5** to obtain the product as a white solid: ^1H NMR (500 MHz, Chloroform-*d*) δ 7.61 (ddd, $J = 8.6, 4.9, 2.4$ Hz, 2H), 7.49 (d, $J = 2.4$ Hz, 1H), 7.44 (d, $J = 2.4$ Hz, 1H), 7.30 – 7.20 (m, 4H), 7.05 – 7.03 (m, 2H), 7.03 – 6.89 (m, 1H), 6.84 (dtd, $J = 8.2, 2.5, 1.0$ Hz, 2H), 6.58 (s, 1H), 5.82 (dd, $J = 12.2, 5.9$ Hz, 1H), 4.17 (dd, $J = 9.2, 3.3$ Hz, 1H), 4.12 (dd, $J = 3.3, 2.3$ Hz, 1H), 3.78 (d, 6H), 3.77 (s, 3H), 3.69 (dt, $J = 6.8, 3.4$ Hz, 1H), 3.43 – 3.35 (m, 2H), 2.76 (t, $J = 7.2$ Hz, 2H), 2.18 (s, 3H), 1.34 (s, 3H), 1.18 (s, 3H). ^{13}C NMR (126 MHz, CDCl_3) δ 166.99, 161.65, 159.40, 159.06, 153.42, 139.12, 132.72, 132.35, 130.53, 129.94, 129.39, 129.22, 128.90, 128.17, 127.02, 126.70, 125.06, 123.98, 122.19, 116.72, 115.44, 114.05, 112.86, 110.97, 97.71, 73.78, 71.50, 68.83, 62.04, 55.92, 55.47, 41.18, 32.04, 22.79, 15.61. HRMS (ESI+) m/z : $[\text{M} + \text{Na}^+]$ calculated for $\text{C}_{38}\text{H}_{42}\text{FNO}_8$ 682.2792; found 682.2806.



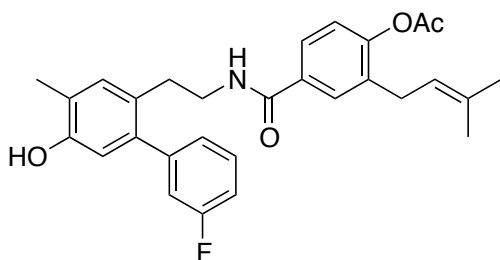
***N*-(2-(3'-Fluoro-4-methyl-5-((1-methylpiperidin-4-yl)oxy)-[1,1'-biphenyl]-2-yl)ethyl)-3',6-dimethoxy-[1,1'-biphenyl]-3-carboxamide (**3.6a**).**

A solution of **3.41** (0.025g, 0.06mmol) and N-Methyl-4-piperidinol (0.014mL, 0.12mmol) in anhydrous benzene (0.6 mL) was cooled to 0°C. Tributylphosphine (0.03mL, 0.12mmol) and TMAD (0.021g, 0.12mmol) were added to the mixture. The reaction mixture was stirred at reflux for 12 h. After 12 h the reaction was cooled to rt and purified via column chromatography (SiO₂, 1:20 MeOH:DCM) to afford **3.6a** as white amorphous solid (30%): ¹H NMR (500 MHz, Chloroform-d) δ 7.70 (dd, *J* = 8.6, 2.3 Hz, 1H), 7.40 (s, 1H), 7.35 (d, *J* = 2.3 Hz, 1H), 7.30 (s, 1H), 7.28 (d, *J* = 2.3 Hz, 1H), 7.24 – 7.22 (m, 1H), 7.11 (d, *J* = 4.3 Hz, 1H), 7.00 – 6.93 (m, 2H), 6.92 (d, *J* = 8.7 Hz, 1H), 6.81 (dd, *J* = 8.8, 3.1 Hz, 1H), 6.74 (d, *J* = 3.0 Hz, 1H), 6.54 (s, 1H), 5.81 (d, *J* = 19.5 Hz, 1H), 4.60 (s, 1H), 3.77 (s, 3H), 3.74 (s, 3H), 3.70 (d, *J* = 4.1 Hz, 2H), 3.45 – 3.39 (m, 4H), 3.28 (m, 2H), 3.06 (s, 3H), 2.74 (d, *J* = 7.6 Hz, 2H), 2.57 (d, *J* = 27.2 Hz, 2H), 2.21 (s, 3H). ¹³C NMR (126 MHz, CDCl₃) δ 166.99, 161.65, 159.40, 159.06, 153.42, 139.12, 132.72, 132.35, 130.53, 129.94, 129.39, 129.22, 128.90, 128.17, 127.02, 126.70, 125.06, 123.98, 122.19, 116.72, 115.44, 114.05, 112.86, 110.97, 97.71, 73.78, 71.50, 68.83, 62.04, 55.92, 55.47, 41.18, 32.04, 22.79, 15.61. HRMS (ESI+) *m/z*: [M + H⁺] calculated for C₃₆H₃₉FN₂O₄ 583.2972; found 583.2952.



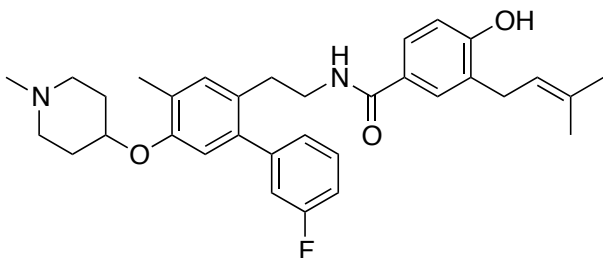
4-((2-(5-(Benzyloxy)-3'-fluoro-4-methyl-[1,1'-biphenyl]-2-yl)ethyl)carbamoyl)-2-(3-methylbut-2-en-1-yl)phenyl acetate (3.49).

Compound **3.49** was synthesized following the procedure used for the synthesis of **3.34** to obtain the product as a white solid: ^1H NMR (500 MHz, Chloroform- d) δ 7.50 (d, $J = 3.0$ Hz, 1H), 7.42 (dt, $J = 7.6, 2.8$ Hz, 3H), 7.36 – 7.30 (m, 3H), 7.22-7.19 (m, 1H), 7.10 (d, $J = 8.0, 5.9, 2.1$ Hz, 1H), 7.03 (d, $J = 11.9$ Hz, 1H), 6.99 – 6.92 (m, 2H), 6.91 – 6.86 (m, 1H), 6.58 (d, $J = 2.0$ Hz, 1H), 5.85 (d, $J = 6.3$ Hz, 1H), 5.28 – 5.21 (m, 1H), 5.14 – 5.07 (m, 2H), 3.38 (dq, $J = 13.4, 7.0$ Hz, 2H), 3.17 (d, $J = 7.3$ Hz, 2H), 2.75 (q, $J = 8.1, 7.2$ Hz, 2H), 2.22 (s, 6H), 2.09 (s, 3H), 1.63 (d, $J = 18.5$ Hz, 6H). ^{13}C NMR (126 MHz, CDCl_3) δ 168.98, 166.86, 161.38, 152.29, 151.10, 139.51, 134.01, 133.61, 132.37, 129.74, 129.04, 127.58, 125.22, 124.82, 123.71, 122.29, 120.80, 116.40, 116.09, 115.92, 113.93, 113.76, 71.09, 41.01, 31.61, 28.76, 25.61, 20.77, 17.77, 15.41. HRMS (ESI+) m/z : $[\text{M} + \text{Na}^+]$ calculated for $\text{C}_{36}\text{H}_{36}\text{FNO}_4$ 588.2526; found 588.2517.



4-((2-(3'-Fluoro-5-hydroxy-4-methyl-[1,1'-biphenyl]-2-yl)ethyl)carbamoyl)-2-(3-methylbut-2-en-1-yl)phenyl acetate (3.54).

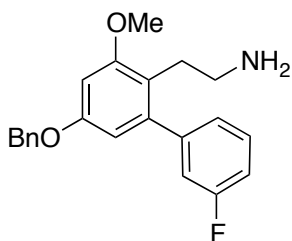
Compound **3.54** was synthesized following the procedure used for the synthesis of **3.53** to obtain the product as a white solid: ^1H NMR (500 MHz, Chloroform- d) δ 7.53 (d, 1H), 7.37 – 7.32 (m, 1H), 7.24-7.21 (m, 1H), 7.18 (d, J = 7.7, 6.1, 2.3 Hz, 1H), 7.08 (d, J = 11.6 Hz, 1H), 6.91 – 6.88 (m, 2H), 6.78 – 6.73 (m, 1H), 6.62 (d, J = 2.4 Hz, 1H), 5.88 (d, J = 6.5 Hz, 1H), 5.10 – 5.05 (m, 1H), 3.40 (dq, J = 13.1, 7.3 Hz, 2H), 3.21 (d, J = 7.6 Hz, 2H), 2.78 (q, J = 8.3, 7.5 Hz, 2H), 2.32 – 2.26 (m, 6H), 1.66 (d, J = 18.1 Hz, 6H). ^{13}C NMR (126 MHz, CDCl_3) δ 168.07, 165.95, 162.43, 151.38, 150.19, 138.59, 133.09, 131.45, 128.82, 128.13, 126.66, 124.30, 123.91, 122.80, 121.37, 119.88, 115.49, 115.01, 113.01, 110.33, 40.09, 30.70, 27.84, 24.70, 19.85, 16.86, 14.50. HRMS (ESI+) m/z : $[\text{M} + \text{H}^+]$ calculated for $\text{C}_{29}\text{H}_{30}\text{FNO}_4$ 476.2237; found 476.2239.



***N*-(2-(3'-Fluoro-4-methyl-5-((1-methylpiperidin-4-yl)oxy)-[1,1'-biphenyl]-2-yl)ethyl)-4-hydroxy-3-(3-methylbut-2-en-1-yl)benzamide (3.6b).**

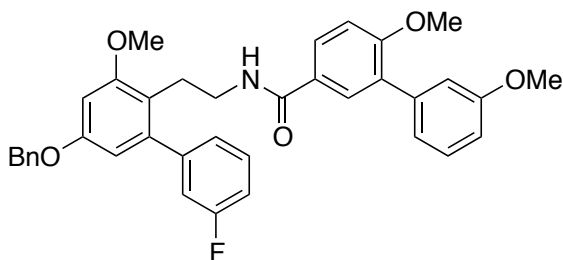
Compound **3.6b** was synthesized following the procedure used for the synthesis of **3.6a**, which was utilized to obtain the acetate-protected product. The acetate group was removed by dissolving the Mitsunobu coupled product (0.02mg) in anhydrous methanol (1mL) and K_2CO_3 (0.02mg). The mixture was stirred at rt. After 8 h the reaction was concentrated and purified via column chromatography (SiO_2 , 1:10, MeOH: DCM) to obtain the product as a white solid (35%): ^1H NMR (500 MHz, Chloroform- d) δ 7.53 – 7.51 (m, 1H), 7.43 (dd, J = 8.5, 2.4 Hz, 1H), 7.34 (td, J = 8.0, 6.0 Hz, 1H), 7.22 (s, 1H), 7.08 – 7.00 (m, 2H), 6.98 (ddd, J = 9.5, 2.6, 1.6 Hz, 1H),

6.88 (s, 1H), 6.78 (d, $J = 8.6$ Hz, 1H), 5.91 (t, $J = 5.7$ Hz, 1H), 5.22 (dddd, $J = 6.9, 5.5, 2.8, 1.4$ Hz, 1H), 4.75 (s, 1H), 3.52 – 3.46 (m, 2H), 3.32 (d, $J = 6.7$ Hz, 2H), 3.07 (s, 2H), 2.88 (t, $J = 7.2$ Hz, 2H), 2.74 (s, 4H), 2.61 (s, 2H), 2.32 (s, 3H), 2.19 (s, 3H), 1.74 (d, $J = 1.4$ Hz, 3H), 1.71 (d, $J = 1.3$ Hz, 3H). ^{13}C NMR (126 MHz, CDCl_3) δ 169.34, 163.50, 161.54, 156.89, 139.65, 133.94, 133.11, 132.61, 129.90, 129.39, 127.41, 126.09, 125.07, 123.40, 122.10, 116.33, 116.16, 114.28, 114.11, 111.28, 78.04, 53.51, 44.03, 40.88, 32.11, 30.98, 28.99, 25.86, 18.08, 15.96. HRMS (ESI+) m/z : $[\text{M} + \text{H}^+]$ calculated for $\text{C}_{33}\text{H}_{39}\text{FN}_2\text{O}_3$ 531.3023; found 531.3033.



2-(5-(Benzyloxy)-3'-fluoro-3-methoxy-[1,1'-biphenyl]-2-yl)ethanamine (3.22).

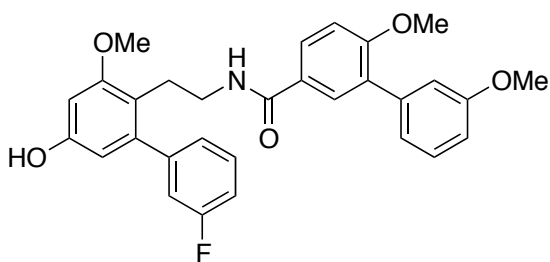
This compound was synthesized following the procedure reported in Chapter 2.



***N*-(2-(5-(Benzyloxy)-3'-fluoro-3-methoxy-[1,1'-biphenyl]-2-yl)ethyl)-3',6-dimethoxy-[1,1'-biphenyl]-3-carboxamide.**

The compound was synthesized following the procedure used for the synthesis of *N*-(2-(5-(benzyloxy)-3'-fluoro-[1,1'-biphenyl]-2-yl)ethyl)-3',6-dimethoxy-[1,1'-biphenyl]-3-

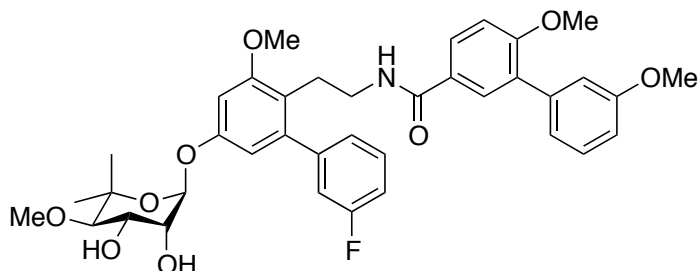
carboxamide to obtain the product as a white solid: ^1H NMR (500 MHz, Chloroform- d) δ 7.57 (dd, $J = 8.5, 2.4$ Hz, 2H), 7.51 (d, $J = 2.3$ Hz, 2H), 7.34 (s, 2H), 7.10 – 6.96 (m, 5H), 6.89 (d, $J = 8.6$ Hz, 3H), 6.57 (d, $J = 2.5$ Hz, 3H), 6.37 (d, $J = 2.4$ Hz, 1H), 6.32 (t, $J = 5.0$ Hz, 1H), 5.05 (s, 2H), 3.85 (s, 3H), 3.84 (s, 3H), 3.77 (s, 3H), 3.51 – 3.44 (m, 2H), 2.89 (t, $J = 6.5$ Hz, 2H). ^{13}C NMR (126 MHz, CDCl_3) δ 167.22, 161.84, 159.68, 159.04, 158.97, 158.16, 139.55, 136.83, 130.57, 130.23, 130.16, 129.74, 129.43, 129.07, 128.49, 128.36, 127.70, 127.53, 118.71, 116.62, 116.45, 115.69, 114.64, 114.47, 113.22, 111.05, 107.32, 99.99, 71.15, 56.13, 55.71 (2Cs), 40.37, 26.00. HRMS (ESI+) m/z : $[\text{M} + \text{Na}^+]$ calculated for $\text{C}_{37}\text{H}_{34}\text{FNO}_5$ 614.2319; found 614.2322.



***N*-(2-(3'-Fluoro-5-hydroxy-3-methoxy-[1,1'-biphenyl]-2-yl)ethyl)-3',6-dimethoxy-[1,1'-biphenyl]-3-carboxamide (3.38).**

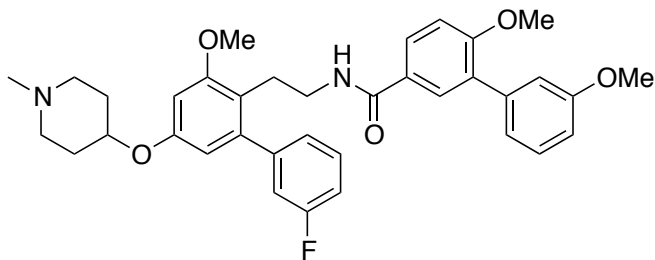
Compound **3.38** was synthesized following the procedure used for the synthesis of **3.36** to obtain the product as a white solid: ^1H NMR (500 MHz, Chloroform- d) δ 7.64 (dd, $J = 6.6, 2.1$ Hz, 2H), 7.56 (d, $J = 3.1$ Hz, 2H), 7.22 (s, 2H), 7.16 – 7.02 (m, 2H), 6.91 (d, $J = 7.9$ Hz, 2H), 6.61 (d, $J = 2.7$ Hz, 2H), 6.39 (d, $J = 3.1$ Hz, 1H), 6.30 (t, $J = 4.8$ Hz, 1H), 3.79 (s, 3H), 3.78 (s, 3H), 3.70 (s, 3H), 3.49 – 3.40 (m, 2H), 2.90 (t, $J = 6.2$ Hz, 2H). ^{13}C NMR (126 MHz, CDCl_3) δ 167.43, 161.64, 159.23, 159.16, 158.96, 158.36, 139.87, 136.33, 130.42, 130.32, 130.06, 129.84, 129.65, 129.37, 128.79, 128.39, 127.60, 127.35, 118.74, 116.66, 116.35, 115.64, 114.74, 114.07,

113.52, 111.35, 107.35, 100.01, 56.33, 55.34 (2Cs), 41.07, 28.05. HRMS (ESI+) m/z : $[M - H^+]$ calculated for $C_{30}H_{28}FNO_5$ 500.1873; found 500.1897.



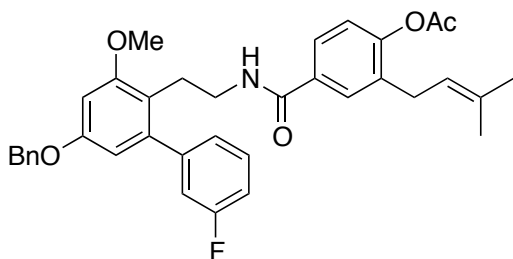
N-**(2-(5-(((2*R*,3*R*,4*S*,5*R*)-3,4-Dihydroxy-5-methoxy-6,6-dimethyltetrahydro-2*H*-pyran-2-yl)oxy)-3'-fluoro-3-methoxy-[1,1'-biphenyl]-2-yl)ethyl)-3',6-dimethoxy-[1,1'-biphenyl]-3-carboxamide (3.7).**

Compound **3.7** was synthesized following the procedure used for the synthesis of **3.5** to obtain the product as a white solid: ^1H NMR (500 MHz, Methylene Chloride- d_2) δ 7.64 (dd, $J = 8.6$, 2.4 Hz, 1H), 7.53 (d, $J = 2.4$ Hz, 1H), 7.33 – 7.27 (m, 1H), 7.27 – 7.21 (m, 1H), 7.02 – 6.97 (m, 3H), 6.97 – 6.91 (m, 2H), 6.81 (ddd, $J = 8.3$, 2.6, 1.0 Hz, 1H), 6.77 (d, $J = 2.6$ Hz, 1H), 6.32 (d, $J = 2.5$ Hz, 1H), 6.24 (dd, $J = 8.3$, 5.0 Hz, 1H), 5.37 (d, $J = 6.6$ Hz, 1H), 5.26 – 5.22 (m, 1H), 4.28 (dd, $J = 4.7$, 3.7 Hz, 1H), 3.99 (dd, $J = 6.6$, 3.6 Hz, 1H), 3.77 (s, 3H), 3.74 (s, 3H), 3.70 (s, 3H), 3.41 (s, 3H), 3.10 (d, $J = 4.7$ Hz, 1H), 2.82 (td, $J = 11.9$, 4.3 Hz, 2H), 2.51 (td, $J = 12.1$, 5.7 Hz, 2H), 1.31 (s, 3H), 1.19 (s, 3H). ^{13}C NMR (126 MHz, CD_2Cl_2) δ 166.33, 160.69, 158.57, 158.37, 156.57, 141.93, 138.30, 129.65, 129.02, 128.61, 128.20, 127.24, 125.67, 124.19, 121.10, 116.25, 115.30, 114.53, 113.18, 113.01, 111.86, 110.06, 107.36, 82.14, 76.69, 69.44, 67.68, 59.02, 54.96, 54.49, 38.97, 24.71, 24.03. HRMS (ESI+) m/z : $[M + \text{Na}^+]$ calculated for $C_{38}H_{42}FNO_9$ 698.2741; found 698.2714.



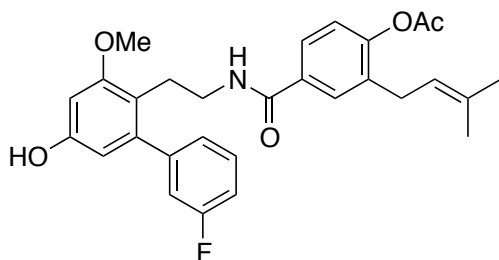
***N*-(2-(3'-Fluoro-3-methoxy-5-((1-methylpiperidin-4-yl)oxy)-[1,1'-biphenyl]-2-yl)ethyl)-3',6-dimethoxy-[1,1'-biphenyl]-3-carboxamide (3.7a).**

Compound **3.7a** was synthesized following the procedure used for the synthesis of **3.6a** to obtain the product as a white solid: ^1H NMR (500 MHz, Methylene Chloride- d_2) δ 7.72 – 7.68 (m, 1H), 7.57 (d, $J = 2.4$ Hz, 1H), 7.40 – 7.31 (m, 2H), 7.10 – 6.98 (m, 5H), 6.97 – 6.86 (m, 2H), 6.50 (d, $J = 2.4$ Hz, 1H), 6.36 (d, $J = 2.4$ Hz, 1H), 6.33 – 6.28 (m, 1H), 4.59 (s, 1H), 3.84 (s, 3H), 3.82 (s, 3H), 3.77 (s, 3H), 3.44 – 3.34 (m, 2H), 2.87 – 2.78 (m, 2H), 2.75 – 2.65 (m, 2H), 2.36 – 2.26 (m, 2H), 2.23 (s, 3H), 2.10 – 1.98 (m, 2H), 1.61 – 1.54 (m, 2H). ^{13}C NMR (126 MHz, CD_2Cl_2) δ 166.45, 163.53, 161.57, 159.47, 159.01, 156.18, 143.96, 139.29, 136.76, 130.35, 129.96, 129.89, 129.29, 129.12, 128.71, 128.09, 127.56, 127.06, 126.29, 125.04, 121.96, 116.18, 116.01, 115.48, 112.64, 110.92, 107.74, 106.87, 77.53, 55.01, 54.22 (2Cs), 53.15(2Cs), 47.10, 40.30, 30.18, 29.78, 22.82. HRMS (ESI+) m/z : $[\text{M} + \text{H}^+]$ calculated for $\text{C}_{36}\text{H}_{39}\text{FN}_2\text{O}_5$ 599.2921; found 599.2914.



4-((2-(5-(Benzyloxy)-3'-fluoro-3-methoxy-[1,1'-biphenyl]-2-yl)ethyl)carbamoyl)-2-(3-methylbut-2-en-1-yl)phenyl acetate (3.50).

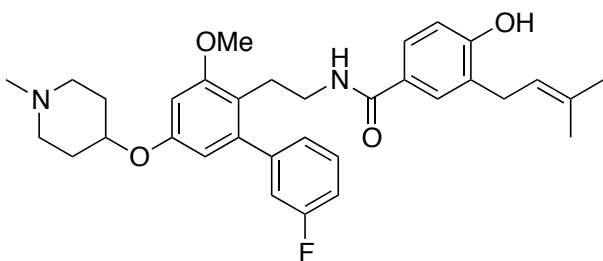
Compound **3.50** was synthesized following the procedure used for the synthesis of **3.48** to obtain the product as a white solid: ^1H NMR (500 MHz, Chloroform- d) δ 7.36 – 7.19 (m, 8H), 7.01 – 6.84 (m, 3H), 6.49 (d, J = 2.5 Hz, 1H), 6.31 – 6.25 (m, 1H), 5.08 – 5.02 (m, 2H), 4.99 (s, 1H), 3.69 – 3.62 (s, 3H), 3.12 (d, J = 7.4 Hz, 2H), 2.80 (d, J = 6.5 Hz, 2H), 2.20 (d, J = 2.5 Hz, 2H), 1.93 (s, 3H), 1.64 – 1.54 (m, 6H). ^{13}C NMR (126 MHz, CDCl_3) δ 167.92, 165.77, 162.33, 160.37, 157.54, 156.70, 142.20, 135.40, 132.33, 128.78, 128.72, 128.25, 127.69, 127.12, 126.29, 126.18, 124.08, 123.87, 121.14, 120.11, 117.11, 115.13, 113.15, 112.99, 105.84, 69.67, 54.30, 39.96, 28.64, 27.87, 24.67, 19.80, 16.83. HRMS (ESI+) m/z : $[\text{M} + \text{Na}^+]$ calculated for $\text{C}_{36}\text{H}_{36}\text{FNO}_5$ 604.2475; found 604.2467.



4-((2-(3'-Fluoro-5-hydroxy-3-methoxy-[1,1'-biphenyl]-2-yl)ethyl)carbamoyl)-2-(3-methylbut-2-en-1-yl)phenyl acetate (3.55).

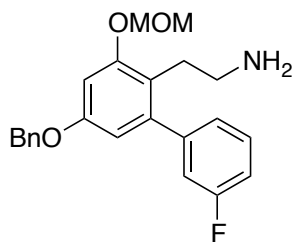
Compound **3.55** was synthesized following the procedure used for the synthesis of **3.53** to obtain the product as a white solid: ^1H NMR (500 MHz, Methylene Chloride- d_2) δ 8.89 (s, 1H), 7.66 (d, J = 2.2 Hz, 1H), 7.58 (dd, J = 8.3, 2.3 Hz, 1H), 7.38 (ddd, J = 8.6, 7.6, 6.0 Hz, 1H), 7.08 (ddd, J = 9.1, 8.2, 2.5 Hz, 2H), 7.03 – 6.96 (m, 1H), 6.81 (t, J = 5.7 Hz, 1H), 6.55 (d, J = 2.7 Hz, 1H), 6.31 (d, J = 2.6 Hz, 1H), 5.24 – 5.16 (m, 1H), 3.76 (s, 3H), 3.37 (ddd, J = 9.8, 7.7, 5.6 Hz,

2H), 3.27 (d, $J = 7.6$ Hz, 2H), 2.76 – 2.69 (m, 2H), 2.30 (s, 3H), 1.72 (dd, $J = 18.9, 1.3$ Hz, 6H). ^{13}C NMR (126 MHz, CD_2Cl_2) δ 169.53, 169.03, 163.90, 161.95, 157.95, 152.35, 135.01, 134.51, 131.71, 130.23, 130.16, 129.53, 126.16, 125.40, 123.21, 121.30, 116.32, 114.43, 114.26, 107.58, 102.12, 55.80, 41.87, 29.25, 26.99, 25.99, 21.22, 18.13. HRMS (ESI+) m/z : $[\text{M} + \text{H}^+]$ calculated for $\text{C}_{29}\text{H}_{30}\text{FNO}_5$ 491.21; found 531.3221.



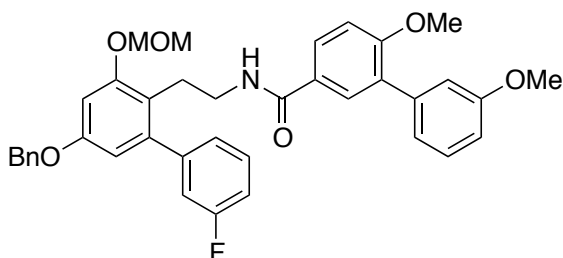
***N*-(2-(3'-Fluoro-3-methoxy-5-((1-methylpiperidin-4-yl)oxy)-[1,1'-biphenyl]-2-yl)ethyl)-4-hydroxy-3-(3-methylbut-2-en-1-yl)benzamide (3.7b).**

Compound **3.7b** was synthesized following the procedure used for the synthesis of **3.6b** to obtain the product as a white solid: ^1H NMR (500 MHz, Chloroform- d) δ 7.41 (ddd, $J = 10.8, 5.4, 2.5$ Hz, 2H), 7.11 (dddd, $J = 9.5, 8.5, 2.6, 1.0$ Hz, 1H), 7.01 (ddd, $J = 9.3, 2.6, 1.5$ Hz, 1H), 6.84 (d, $J = 8.3$ Hz, 1H), 6.46 (d, $J = 2.4$ Hz, 1H), 6.36 (d, $J = 2.4$ Hz, 1H), 6.04 (dt, $J = 29.0, 9.6$ Hz, 2H), 5.28 – 5.21 (m, 1H), 4.83 (q, $J = 6.3$ Hz, 1H), 4.75 (s, 1H), 3.88 (d, $J = 6.6$ Hz, 2H), 3.79 (s, 3H), 3.73 – 3.60 (m, 2H), 3.37 – 3.32 (m, 2H), 3.29 (d, $J = 9.8$ Hz, 2H), 3.01 (dd, $J = 12.6, 5.1$ Hz, 2H), 2.80 – 2.73 (m, 2H), 2.66 (t, $J = 14.9$ Hz, 2H), 2.21 – 2.17 (s, 3H), 1.81 – 1.72 (m, 6H). ^{13}C NMR (126 MHz, CDCl_3) δ 166.85, 158.63, 157.49, 155.59, 143.66, 136.94, 136.16, 135.43, 129.83, 128.73, 127.10, 126.21, 124.54, 120.89, 117.21, 115.94, 115.55, 106.39, 98.91, 66.08, 55.37, 48.88, 43.00, 39.74, 29.56, 27.08, 25.73, 21.73, 17.84. HRMS (ESI+) m/z : $[\text{M} + \text{H}^+]$ calculated for $\text{C}_{33}\text{H}_{39}\text{FN}_2\text{O}_4$ 547.2972; found 547.2962.



2-(5-(Benzyloxy)-3'-fluoro-3-(methoxymethoxy)-[1,1'-biphenyl]-2-yl)ethanamine (3.24).

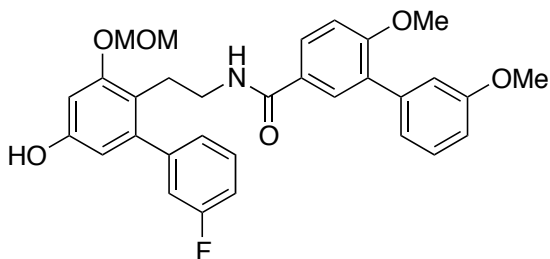
This compound was synthesized following the procedure reported in Chapter 2.



***N*-(2-(5-(Benzyloxy)-3'-fluoro-3-(methoxymethoxy)-[1,1'-biphenyl]-2-yl)ethyl)-3',6-dimethoxy-[1,1'-biphenyl]-3-carboxamide.**

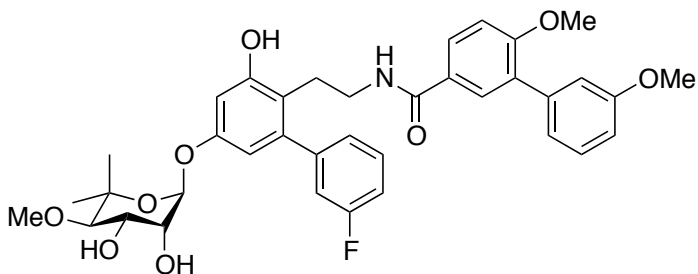
The compound was synthesized following the procedure used for the synthesis of *N*-(2-(5-(benzyloxy)-3'-fluoro-[1,1'-biphenyl]-2-yl)ethyl)-3',6-dimethoxy-[1,1'-biphenyl]-3-carboxamide to obtain the product as a white solid: ^1H NMR (500 MHz, Chloroform- d) δ 7.57 (dd, $J = 8.5, 2.4$ Hz, 1H), 7.51 (d, $J = 2.4$ Hz, 1H), 7.43 – 7.37 (m, 4H), 7.36 – 7.28 (m, 5H), 7.09 – 7.01 (m, 3H), 7.01 – 6.96 (m, 1H), 6.93 – 6.90 (m, 1H), 6.66 (d, $J = 2.4$ Hz, 1H), 6.48 (d, $J = 2.5$ Hz, 1H), 6.31 (t, $J = 5.0$ Hz, 1H), 5.03 (s, 2H), 5.01 (s, 2H), 3.83 (d, $J = 2.4$ Hz, 6H), 3.63 (s, 3H), 3.52 – 3.44 (m, 2H), 2.89 (t, $J = 6.5$ Hz, 2H). ^{13}C NMR (126 MHz, CDCl_3) δ 166.84, 161.45, 159.29, 158.66, 157.82, 139.15, 136.63, 136.40, 130.19, 129.85, 129.78, 129.34, 129.05, 128.67, 128.63, 128.10, 127.97, 127.67, 127.30, 127.13, 124.93, 122.02, 118.60, 116.24, 116.07,

115.30, 114.27, 114.10, 112.82, 110.66, 107.93, 100.29, 95.40, 70.23, 55.74, 55.32, 40.98, 25.65. HRMS (ESI+) m/z: [M + H⁺] calculated for C₃₈H₃₆FNO₆ 622.0725; found 622.0731.



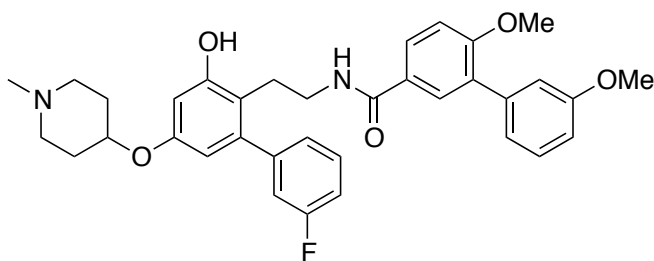
***N*-(2-(3'-Fluoro-5-hydroxy-3-(methoxymethoxy)-[1,1'-biphenyl]-2-yl)ethyl)-3',6-dimethoxy-[1,1'-biphenyl]-3-carboxamide (3.39).**

Compound **3.39** was synthesized following the procedure used for the synthesis of **3.36** to obtain the product as a white solid: ¹H NMR (500 MHz, Chloroform-d) δ 7.58 – 7.47 (m, 2H), 7.19 – 7.06 (m, 2H), 6.92 – 6.87 (m, 3H), 6.85 – 6.75 (m, 2H), 6.78 – 6.66 (m, 3H), 6.46 (d, *J* = 2.4 Hz, 1H), 6.14 (d, *J* = 2.4 Hz, 1H), 5.03 (s, 2H), 3.66 (d, *J* = 1.2 Hz, 6H), 3.63 (s, 3H), 3.32 – 3.27 (m, 2H), 2.66 – 2.58 (m, 2H). ¹³C NMR (126 MHz, CDCl₃) δ 170.44, 167.60, 162.19, 160.23, 158.14, 158.03, 155.26, 154.06, 142.73, 141.97, 137.69, 129.26, 128.54, 128.00, 127.09, 124.64, 123.69, 120.96, 114.26, 113.73, 111.70, 109.85, 108.09, 102.11, 59.50, 54.61, 54.21, 40.37, 24.92. HRMS (ESI+) m/z: [M + H⁺] calculated for C₃₁H₃₀FNO₆ 532.7621, found 532.7617.



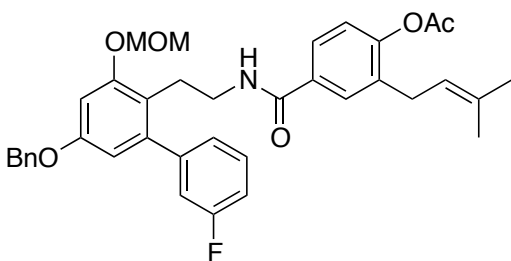
***N*-(2-(5-(((2*R*,3*R*,4*S*,5*R*)-3,4-Dihydroxy-5-methoxy-6,6-dimethyltetrahydro-2*H*-pyran-2-yl)oxy)-3'-fluoro-3-hydroxy-[1,1'-biphenyl]-2-yl)ethyl)-3',6-dimethoxy-[1,1'-biphenyl]-3-carboxamide (3.8).**

Compound **3.8** was synthesized following the procedure used for the synthesis of **3.5** to obtain the product as a white solid: ¹H NMR (500 MHz, Methylene Chloride-d₂) δ 7.80 – 7.74 (m, 1H), 7.70 (dd, *J* = 3.9, 2.3 Hz, 1H), 7.31 (d, *J* = 8.0 Hz, 1H), 7.08 – 7.00 (m, 4H), 6.97 (dtd, *J* = 7.5, 2.6, 1.2 Hz, 1H), 6.89 (ddd, *J* = 8.3, 2.6, 0.9 Hz, 1H), 6.72 (s, 1H), 6.67 (d, *J* = 2.5 Hz, 1H), 6.48 (d, *J* = 2.5 Hz, 1H), 6.42 (d, *J* = 2.5 Hz, 1H), 6.24 (d, *J* = 2.5 Hz, 1H), 5.50 (d, *J* = 2.4 Hz, 1H), 4.16 (dd, *J* = 9.0, 3.4 Hz, 1H), 4.08 (dd, *J* = 3.4, 2.3 Hz, 1H), 3.86 (d, *J* = 0.8 Hz, 6H), 3.82 (s, 3H), 3.55 (d, *J* = 1.0 Hz, 1H), 3.40 – 3.33 (m, 2H), 2.73 (ddd, *J* = 10.6, 7.8, 5.5 Hz, 2H), 1.30 (s, 3H), 1.22 (s, 3H). ¹³C NMR (126 MHz, CD₂Cl₂) δ 169.21, 161.95, 160.05, 159.90, 156.48, 155.50, 143.35, 139.43, 131.08, 130.07, 129.56, 128.61, 125.96, 125.31, 122.40, 122.39, 116.43, 116.26, 115.77, 114.43, 114.27, 113.30, 111.51, 109.48, 98.15, 78.57, 71.80, 69.08, 62.14, 56.31, 55.80, 41.82, 29.22, 23.31. HRMS (ESI+) *m/z*: [M - H⁺] calculated for C₃₇H₄₀FNO₉, 660.2609; found 660.2626.



***N*-(2-(3'-Fluoro-3-hydroxy-5-((1-methylpiperidin-4-yl)oxy)-[1,1'-biphenyl]-2-yl)ethyl)-3',6-dimethoxy-[1,1'-biphenyl]-3-carboxamide (3.8a).**

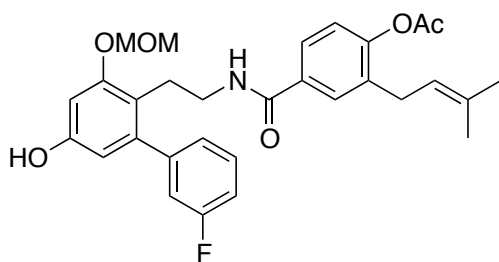
Compound **3.8a** was synthesized following the procedure used for the synthesis of **3.6a**, to obtain the coupled product, which was then dissolved in methanol (3mL). p-TSA (0.1mg, 0.63mmol) was added and the mixture was stirred at rt. After 12 h the reaction mixture was concentrated; the residue was diluted with saturated ammonium chloride and extracted with EtOAc (3x30mL). The organic layers were combined, dried, concentrated, and purified via column chromatography (SiO₂, 1:20, MeOH: DCM) to give **3.8a** as a white solid (60% yield): ¹H NMR (500 MHz, Chloroform-d) δ 7.62 (dd, *J* = 8.6, 2.4 Hz, 1H), 7.46 (d, *J* = 2.4 Hz, 1H), 7.32 – 7.22 (m, 2H), 7.01 (dt, *J* = 7.8, 1.1 Hz, 1H), 6.98 – 6.93 (m, 5H), 6.91 (d, *J* = 8.7 Hz, 1H), 6.88 – 6.83 (m, 1H), 6.45 – 6.42 (m, 1H), 6.27 (d, *J* = 2.2 Hz, 1H), 4.31 (s, 1H), 3.78 (d, *J* = 1.2 Hz, 6H), 3.40 – 3.24 (m, 2H), 2.72 (t, *J* = 7.4 Hz, 2H), 2.61 – 2.45 (m, 2H), 2.28 – 2.10 (m, 2H), 1.86 (s, 3H), 1.61 – 1.49 (m, 2H), 1.39 – 1.28 (m, 2H). ¹³C NMR (126 MHz, CDCl₃) δ 165.99, 162.35, 160.39, 158.20, 155.22, 154.84, 142.56, 137.92, 129.27, 128.78, 128.71, 128.27, 128.15, 127.09, 123.70, 121.02, 114.85, 114.60, 113.18, 111.57, 109.86, 108.93, 78.21, 54.77 (2Cs), 54.39 (2Cs), 48.23, 40.90, 28.68, 28.30, 21.67. HRMS (ESI+) *m/z*: [M + H⁺] calculated for C₃₅H₃₇FN₂O₅ 585.2765; found 585.2793.



4-((2-(5-(Benzyloxy)-3'-fluoro-3-(methoxymethoxy)-[1,1'-biphenyl]-2-yl)ethyl)carbamoyl)-2-(3-methylbut-2-en-1-yl)phenyl acetate (3.51).

Compound **3.51** was synthesized following the procedure used for the synthesis of **3.48** to obtain the product as a white solid: ¹H NMR (500 MHz, Chloroform-d) δ 7.54 (dd, *J* = 5.7, 2.2

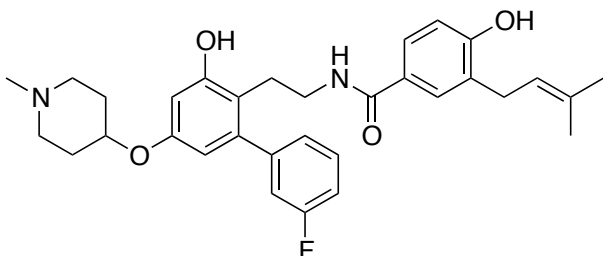
Hz, 1H), 7.46 – 7.29 (m, 8H), 7.11 – 6.92 (m, 4H), 6.68 (d, $J = 2.5$ Hz, 1H), 6.49 (d, $J = 2.5$ Hz, 1H), 6.35 – 6.24 (m, 1H), 5.13 – 5.05 (m, 2H), 5.05 – 4.97 (m, 2H), 4.46 – 4.24 (m, 2H), 3.52 – 3.36 (m, 3H), 2.96 – 2.82 (m, 4H), 2.16 (s, 3H), 1.95 (dq, $J = 5.5, 2.9$ Hz, 3H), 1.74 – 1.69 (m, 3H). ^{13}C NMR (126 MHz, CDCl_3) δ 167.97, 165.81, 162.38, 160.42, 156.80, 154.95, 152.51, 135.58, 135.36, 132.89, 132.41, 131.69, 128.75, 128.31, 127.59, 127.08, 126.33, 124.05, 123.87, 121.15, 120.10, 117.45, 115.18, 115.01, 113.05, 106.87, 99.27, 95.34, 69.75, 59.37, 43.59, 32.35, 28.67, 28.22, 27.91, 24.71, 20.04, 16.87. HRMS (ESI+) m/z : $[\text{M} + \text{H}^+]$ calculated for $\text{C}_{37}\text{H}_{38}\text{FNO}_6$ 612.2761; found 612.2791.



4-((2-(3'-Fluoro-5-hydroxy-3-(methoxymethoxy)-[1,1'-biphenyl]-2-yl)ethyl)carbamoyl)-2-(3-methylbut-2-en-1-yl)phenyl acetate (3.56).

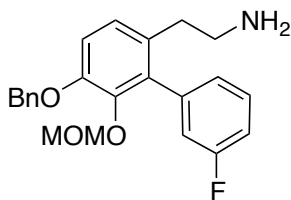
Compound **3.56** was synthesized following the procedure used for the synthesis of **3.53** to obtain the product as a white solid: ^1H NMR (500 MHz, Chloroform- d) δ 8.84 (s, 1H), 7.95 (d, $J = 2.2$ Hz, 1H), 7.66 (d, $J = 2.3$ Hz, 1H), 7.53 (dd, $J = 8.4, 2.3$ Hz, 1H), 7.32 (td, $J = 8.0, 6.0$ Hz, 1H), 7.07 – 6.90 (m, 4H), 6.69 (d, $J = 2.5$ Hz, 1H), 6.44 (d, $J = 2.5$ Hz, 1H), 5.20 – 5.11 (m, 2H), 3.45 (s, 3H), 3.44 – 3.37 (m, 2H), 3.23 (d, $J = 7.3$ Hz, 2H), 2.77 (dt, $J = 8.7, 3.6$ Hz, 2H), 2.31 (s, 3H), 1.71 (d, $J = 1.5$ Hz, 3H), 1.67 (d, $J = 1.4$ Hz, 3H). ^{13}C NMR (126 MHz, CDCl_3) δ 169.19, 168.28, 163.35, 161.39, 156.25, 151.52, 142.80, 134.22, 133.78, 131.49, 129.62, 129.37, 127.82, 125.65, 124.81, 122.51, 120.89, 116.09, 115.92, 114.07, 109.31, 104.00, 94.41, 56.06, 41.45,

28.89, 26.17, 25.75, 20.89, 17.89. HRMS (ESI+) m/z : $[M + H^+]$ calculated for $C_{30}H_{32}FNO_6$ 522.2292; found 522.2271.



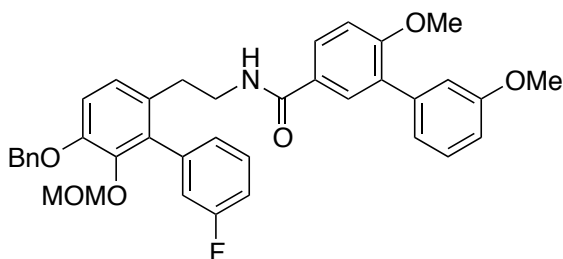
***N*-(2-(3'-Fluoro-3-hydroxy-5-((1-methylpiperidin-4-yl)oxy)-[1,1'-biphenyl]-2-yl)ethyl)-4-hydroxy-3-(3-methylbut-2-en-1-yl)benzamide (3.8b).**

Compound **3.8b** was synthesized following the procedure used for the synthesis of **3.6b**, to obtain the acetate deprotected product, which was then dissolved in methanol (3mL). *p*-TSA (0.1mg, 0.63mmol) was added and the mixture was stirred at rt. After 12 h the reaction mixture was concentrated; the residue was diluted with saturated ammonium chloride and extracted with EtOAc (3x30mL). The organic layers were combined, dried, concentrated, and purified via column chromatography (SiO_2 , 1:20, MeOH: DCM) to give **3.8b** as a white solid (60% yield): 1H NMR (500 MHz, Chloroform- d) δ 7.21 – 7.01 (m, 2H), 6.83 – 6.70 (m, 2H), 6.59 (t, $J = 7.2$ Hz, 2H), 6.48 – 6.33 (m, 2H), 6.15 (dd, $J = 15.4, 7.9$ Hz, 1H), 5.82 (d, $J = 7.2$ Hz, 1H), 5.70 (d, $J = 7.8$ Hz, 1H), 4.71 – 4.59 (m, 1H), 3.33 (dd, $J = 20.5, 8.7$ Hz, 2H), 3.06 – 2.93 (m, 4H), 2.85 – 2.63 (m, 4H), 2.39 (dt, $J = 9.5, 4.0$ Hz, 2H), 2.33 – 2.25 (m, 2H), 2.14 (s, 3H), 1.82 – 1.69 (d, 6H). ^{13}C NMR (126 MHz, $CDCl_3$) δ 168.24, 163.64, 161.69, 143.81, 140.96, 133.24, 129.99, 129.20, 128.68, 126.31, 125.01, 122.19, 116.27, 114.77, 114.08, 109.86, 85.97, 53.21, 53.18, 43.62, 40.10, 32.10, 29.92, 28.58, 27.46, 25.90, 17.91. HRMS (ESI+) m/z : $[M + H^+]$ calculated for $C_{32}H_{37}FN_2O_4$ 533.2816; found 533.2800.



2-(5-(Benzyloxy)-3'-fluoro-6-(methoxymethoxy)-[1,1'-biphenyl]-2-yl)ethanamine (3.27).

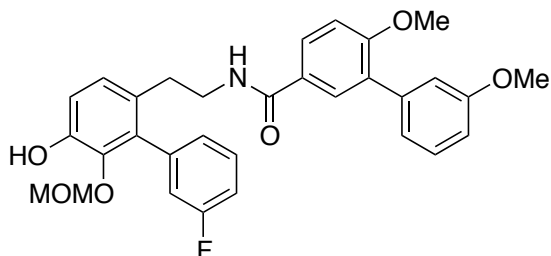
This compound was synthesized following the procedure reported in Chapter 2.



N-(2-(5-(Benzyloxy)-3'-fluoro-6-(methoxymethoxy)-[1,1'-biphenyl]-2-yl)ethyl)-3',6-dimethoxy-[1,1'-biphenyl]-3-carboxamide.

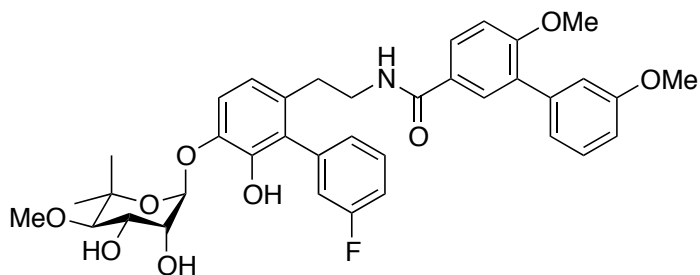
The compound was synthesized following the procedure used for the synthesis of *N*-(2-(5-(benzyloxy)-3'-fluoro-[1,1'-biphenyl]-2-yl)ethyl)-3',6-dimethoxy-[1,1'-biphenyl]-3-carboxamide to obtain the product as a white solid: ^1H NMR (500 MHz, Chloroform- d) δ 8.06 (d, $J = 2.3$ Hz, 1H), 7.69 – 7.60 (m, 3H), 7.37 – 7.21 (m, 7H), 6.98 (s, 1H), 6.93 (dd, $J = 11.5$, 8.6 Hz, 2H), 6.88 – 6.74 (m, 4H), 6.29 (t, $J = 5.5$ Hz, 1H), 5.00 (s, 2H), 4.93 (s, 2H), 3.81 (s, 3H), 3.74 (s, 3H), 3.73 (s, 3H), 3.63 – 3.58 (m, 2H), 2.83 – 2.75 (m, 2H). ^{13}C NMR (126 MHz, CDCl_3) δ 167.43, 161.35, 159.66, 159.61, 151.56, 144.02, 139.43, 139.11, 138.87, 136.98, 133.43, 132.14, 131.20, 130.57, 130.18, 129.53, 129.36, 128.95, 128.43, 127.22, 125.61, 125.19, 122.45, 122.31, 121.30, 115.64, 113.40, 113.26, 112.41, 111.23, 111.01, 98.94, 71.48, 56.26,

56.09, 55.66, 40.58, 30.10. HRMS (ESI+) m/z : $[M + Na^+]$ calculated for $C_{38}H_{36}FNO_6$ 644.2424; found 644.2419.



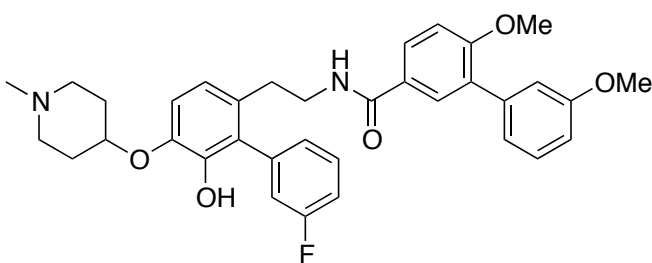
***N*-(2-(3'-Fluoro-5-hydroxy-6-(methoxymethoxy)-[1,1'-biphenyl]-2-yl)ethyl)-3',6-dimethoxy-[1,1'-biphenyl]-3-carboxamide (3.40).**

Compound **3.40** was synthesized following the procedure used for the synthesis of **3.36** to obtain the product as a white solid: 1H NMR (500 MHz, Chloroform- d) δ 7.68 (dd, $J = 8.6, 2.4$ Hz, 1H), 7.60 (d, $J = 2.4$ Hz, 1H), 7.37 – 7.29 (m, 3H), 7.10 – 6.92 (m, 7H), 6.89 (ddd, $J = 8.3, 2.6, 1.0$ Hz, 1H), 6.08 (t, $J = 5.8$ Hz, 1H), 4.66 (s, 2H), 3.83 (d, $J = 4.1$ Hz, 6H), 3.43 – 3.39 (m, 2H), 3.38 (s, 3H), 2.66 (t, $J = 7.1$ Hz, 2H). ^{13}C NMR (126 MHz, $CDCl_3$) δ 165.80, 162.49, 158.20, 157.87, 146.70, 142.22, 137.90, 129.29, 128.85, 128.36, 128.02, 127.86, 126.96, 125.76, 125.47, 124.60, 120.92, 115.91, 115.44, 114.21, 113.33, 111.78, 109.76, 98.62, 56.08, 54.71, 54.25, 39.70, 31.36. HRMS (ESI+) m/z : $[M + H^+]$ calculated for $C_{31}H_{30}FNO_6$ 532.7621, found 532.7611.



***N*-(2-(5-(((2*S*,3*R*,4*S*,5*R*)-3,4-Dihydroxy-5-methoxy-6,6-dimethyltetrahydro-2*H*-pyran-2-yl)oxy)-3'-fluoro-6-hydroxy-[1,1'-biphenyl]-2-yl)ethyl)-3',6-dimethoxy-[1,1'-biphenyl]-3-carboxamide (3.9).**

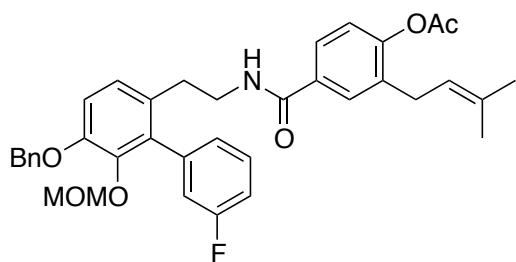
Compound **3.9** was synthesized following the procedure used for the synthesis of **3.5** to obtain the product as a white solid: ¹H NMR (500 MHz, Methylene Chloride-d₂) δ 7.65 (dd, *J* = 8.5, 2.4 Hz, 1H), 7.58 (d, *J* = 2.4 Hz, 1H), 7.42 – 7.34 (m, 1H), 7.31 (t, *J* = 7.9 Hz, 1H), 7.13 (d, *J* = 8.4 Hz, 1H), 7.07 – 6.94 (m, 6H), 6.88 (ddd, *J* = 8.2, 2.6, 1.0 Hz, 1H), 6.79 (d, *J* = 8.4 Hz, 1H), 6.10 (t, *J* = 5.9 Hz, 1H), 5.30 (d, *J* = 4.6 Hz, 1H), 4.19 (dd, *J* = 6.9, 3.5 Hz, 1H), 4.05 – 4.01 (m, 1H), 3.83 (s, 3H), 3.81 (s, 3H), 3.80 – 3.79 (m, 1H), 3.56 – 3.50 (m, 1H), 3.49 (s, 3H), 3.21 (d, *J* = 6.9 Hz, 2H), 2.66 (t, *J* = 7.2 Hz, 2H), 1.39 (s, 3H), 1.23 (s, 3H). ¹³C NMR (126 MHz, CD₂Cl₂) δ 167.13, 162.05, 159.71, 159.37, 156.24, 155.31, 144.92, 143.71, 139.47, 132.75, 130.70, 130.19, 129.74, 129.37, 128.57, 128.25, 127.10, 126.42, 122.26, 121.67, 121.02, 117.55, 115.67, 115.12, 114.51, 114.34, 113.02, 111.19, 100.31, 78.81, 70.52, 69.36, 61.15, 56.09, 55.64, 41.07, 32.93, 24.34. HRMS (ESI+) *m/z*: [M - H⁺] calculated for C₃₇H₄₀FNO₉, 660.2609; found 660.2591.



***N*-(2-(3'-Fluoro-6-hydroxy-5-((1-methylpiperidin-4-yl)oxy)-[1,1'-biphenyl]-2-yl)ethyl)-3',6-dimethoxy-[1,1'-biphenyl]-3-carboxamide (3.9a).**

Compound **3.9a** was synthesized following the procedure used for the synthesis of **3.8a** to obtain the product as a white solid: ¹H NMR (500 MHz, Chloroform-d) δ 7.71 (d, *J* = 8.4 Hz,

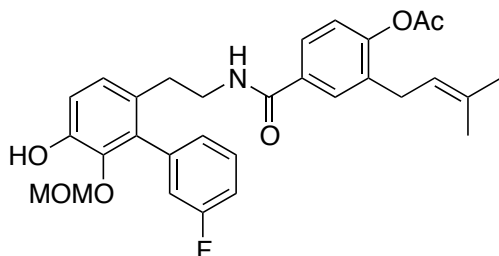
1H), 7.56 (d, $J = 2.1$ Hz, 1H), 7.41 (q, $J = 7.4$ Hz, 1H), 7.34 (t, $J = 7.9$ Hz, 1H), 7.11 – 6.96 (m, 5H), 6.95 – 6.89 (m, 2H), 6.86 (d, $J = 4.9$ Hz, 1H), 5.92 (s, 1H), 5.51 (s, 1H), 4.68 (s, 1H), 3.85 (d, $J = 1.1$ Hz, 6H), 3.43 (d, $J = 6.6$ Hz, 2H), 3.27 (s, 2H), 2.75 (s, 2H), 2.68 (t, $J = 7.0$ Hz, 2H), 2.61 (s, 3H), 2.20 – 2.14 (m, 2H), 1.35 – 1.16 (m, 2H). ^{13}C NMR (126 MHz, CDCl_3) δ 167.14, 162.15, 159.70, 159.38, 144.22, 142.52, 139.33, 138.77, 131.86, 130.98, 130.73, 129.58, 129.52, 128.52, 127.13, 126.21, 122.34, 121.71, 117.65, 117.48, 115.87, 114.60, 113.04, 111.27, 78.30, 56.20, 55.79, 49.83, 44.17, 40.89, 30.10, 27.34 (2Cs). HRMS (ESI+) m/z : $[\text{M} + \text{H}^+]$ calculated for $\text{C}_{35}\text{H}_{37}\text{FN}_2\text{O}_5$, 585.2765; found 585.2738.



4-((2-(5-(Benzyloxy)-3'-fluoro-6-(methoxymethoxy)-[1,1'-biphenyl]-2-yl)ethyl)carbamoyl)-2-(3-methylbut-2-en-1-yl)phenyl acetate (3.52).

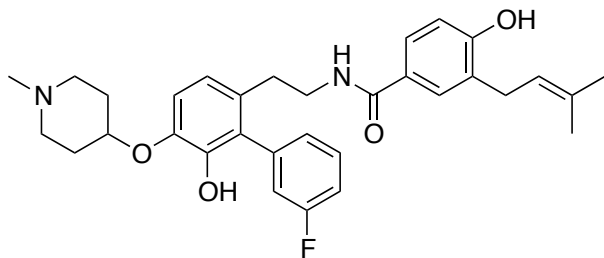
Compound **3.52** was synthesized following the procedure used for the synthesis of **3.48** to obtain the product as a white solid: ^1H NMR (500 MHz, Chloroform- d) δ 7.59 (d, $J = 2.2$ Hz, 1H), 7.46 – 7.41 (m, 4H), 7.38 (td, $J = 8.0, 1.5$ Hz, 4H), 7.35 – 7.32 (m, 1H), 7.11 – 7.01 (m, 4H), 6.98 (d, $J = 8.5$ Hz, 1H), 5.92 – 5.87 (m, 1H), 5.12 (s, 2H), 4.89 (d, $J = 2.4$ Hz, 2H), 3.46 – 3.37 (m, 2H), 3.25 (d, $J = 7.3$ Hz, 2H), 2.87 (s, 3H), 2.70 (t, $J = 7.0$ Hz, 2H), 2.31 (d, $J = 1.5$ Hz, 3H), 1.71 (dd, $J = 19.8, 1.3$ Hz, 6H). ^{13}C NMR (126 MHz, CDCl_3) δ 169.43, 167.17, 163.85, 161.89, 151.60, 150.59, 144.36, 139.56, 137.09, 134.51, 132.89, 130.38, 129.98, 129.91, 129.61, 128.98, 128.42, 127.78, 126.56, 125.73, 125.67, 122.78, 121.34, 117.73, 114.54, 113.94, 99.02,

71.20, 56.96, 41.00, 32.85, 29.27, 26.14, 21.27, 18.30. HRMS (ESI+) m/z : $[M + H^+]$ calculated for $C_{37}H_{38}FNO_6$ 612.2761; found 612.2770.



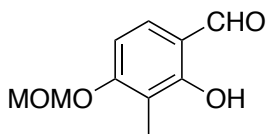
4-((2-(3'-Fluoro-5-hydroxy-6-(methoxymethoxy)-[1,1'-biphenyl]-2-yl)ethyl)carbamoyl)-2-(3-methylbut-2-en-1-yl)phenyl acetate (3.57).

Compound **3.57** was synthesized following the procedure used for the synthesis of **3.53** to obtain the product as a white solid: 1H NMR (500 MHz, Chloroform- d) δ 7.57 (d, $J = 2.2$ Hz, 1H), 7.44 (dd, $J = 8.3, 2.2$ Hz, 1H), 7.37 – 7.32 (m, 2H), 7.08 – 6.91 (m, 5H), 6.13 (t, $J = 5.8$ Hz, 1H), 5.16 (dddd, $J = 7.1, 5.7, 2.8, 1.4$ Hz, 1H), 4.66 (s, 2H), 3.42 – 3.33 (m, 2H), 3.23 (d, $J = 7.4$ Hz, 2H), 3.01 (s, 3H), 2.65 (t, $J = 7.1$ Hz, 2H), 2.30 (d, $J = 6.1$ Hz, 3H), 1.71 (d, $J = 1.6$ Hz, 3H), 1.67 (d, $J = 1.3$ Hz, 3H). ^{13}C NMR (126 MHz, $CDCl_3$) δ 168.92, 166.78, 163.34, 151.05, 147.60, 143.07, 138.68, 134.74, 133.56, 132.18, 129.72, 129.65, 128.98, 128.56, 126.26, 125.49, 125.23, 122.23, 120.71, 116.59, 114.20, 114.03, 99.43, 56.94, 40.56, 32.13, 28.66, 25.54, 20.68, 17.69. HRMS (ESI+) m/z : $[M + Na^+]$ calculated for $C_{30}H_{32}FNO_6$ 544.2111; found 544.2106.



***N*-(2-(3'-Fluoro-6-hydroxy-5-((1-methylpiperidin-4-yl)oxy)-[1,1'-biphenyl]-2-yl)ethyl)-4-hydroxy-3-(3-methylbut-2-en-1-yl)benzamide (3.9b).**

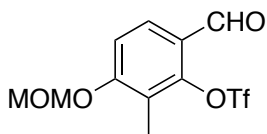
Compound **3.9b** was synthesized following the procedure used for the synthesis of **3.8b** to obtain the product as a white solid: ^1H NMR (500 MHz, Chloroform-*d*) δ 7.53 (d, $J = 2.3$ Hz, 1H), 7.43 (d, $J = 2.3$ Hz, 1H), 7.38 (ddd, $J = 8.2, 5.9, 2.4$ Hz, 2H), 7.31 (dddd, $J = 11.0, 8.2, 5.9, 3.0$ Hz, 2H), 7.07 (d, $J = 8.3$ Hz, 1H), 6.85 (d, $J = 8.5$ Hz, 1H), 6.73 (d, $J = 8.6$ Hz, 1H), 6.47 (s, 1H), 5.11 (tdd, $J = 5.7, 2.9, 1.5$ Hz, 1H), 4.40 (s, 1H), 3.35 (qd, $J = 7.3, 5.9$ Hz, 2H), 3.18 (d, $J = 7.3$ Hz, 2H), 2.63 (t, $J = 7.0$ Hz, 2H), 2.38 (d, $J = 5.4$ Hz, 2H), 2.29 (d, $J = 4.1$ Hz, 2H), 2.25 (d, $J = 5.5$ Hz, 2H), 2.07 – 1.94 (s, 3H), 1.89 – 1.80 (m, 2H), 1.67 – 1.61 (m, 6H). ^{13}C NMR (126 MHz, CDCl_3) δ 167.01, 163.66, 161.73, 143.54, 140.33, 133.74, 129.84, 129.26, 128.53, 126.05, 125.74, 122.34, 116.41, 114.53, 114.11, 109.46, 85.72, 53.44, 53.20, 43.02, 40.11, 33.01, 29.22, 28.82, 27.55, 25.78, 18.01. HRMS (ESI+) m/z : $[\text{M} + \text{H}^+]$ calculated for $\text{C}_{32}\text{H}_{37}\text{FN}_2\text{O}_4$ 533. 2816; found 533.2807.



2-Hydroxy-4-(methoxymethoxy)-3-methylbenzaldehyde (3.29).

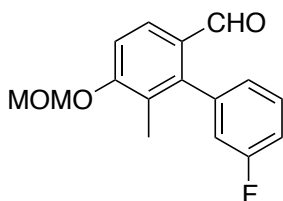
A solution of 2,4-dihydroxy-3-methylbenzaldehyde (0.45 g, 1.85 mmol) and DIPEA (0.71 mL, 0.74 mmol) in anhydrous DCM (18 mL) was stirred at 0 °C. Chloromethyl methyl ether (0.84 mL, 11.1 mmol) was added drop wise after 10 minutes. After 16 h the reaction was quenched by the addition of water (5 mL), extracted with DCM (3 x 10 mL), dried (Na_2SO_4), filtered and concentrated. The residue was purified by column chromatography (SiO_2 , 8:1, Hex:EtOAc) to afford the product as a white solid (75%): ^1H NMR (500 MHz, Chloroform-*d*) δ 11.48 (s, 1H),

9.73 (d, $J = 0.6$ Hz, 1H), 7.39 – 7.29 (m, 1H), 6.75 (d, $J = 8.6$ Hz, 1H), 5.28 (s, 2H), 3.49 (s, 3H), 2.13 (s, 3H). ^{13}C NMR (126 MHz, CDCl_3) δ 195.12, 162.04, 161.45, 132.99, 115.92, 114.49, 105.87, 94.16, 56.51, 7.64.



6-Formyl-3-(methoxymethoxy)-2-methylphenyl trifluoromethanesulfonate.

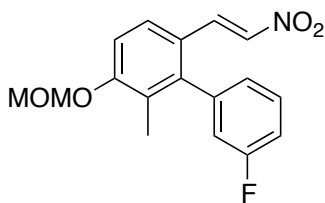
A solution of **3.29** (0.29 g, 1.1 mmol), N-bisphenyltriflate (0.59 g, 1.7 mmol), K_2CO_3 (0.61 g, 4.4 mmol) in anhydrous tetrahydrofuran (15.7 mL) was stirred in a septum-capped tube. The reaction was heated to 120 °C for 20 minutes in a microwave synthesizer. Upon completion the reaction was cooled to rt and quenched with water (10 mL), extracted with EtOAc (3 x 5 mL), dried (Na_2SO_4), filtered and concentrated. The residue was used without further purification, a yellow oil (99%).



3'-Fluoro-5-(methoxymethoxy)-6-methyl-[1,1'-biphenyl]-2-carbaldehyde.

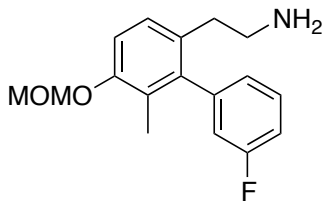
6-Formyl-3-(methoxymethoxy)-2-methylphenyl trifluoromethanesulfonate (5.10 mmol) was dissolved in Dioxane (25 mL). 3-fluorophenyl boronic acid (1.06 g, 7.65 mmol), K_3PO_4 (3.24 g, 15.3 mmol), $\text{Pd}(\text{dba})_3$ (0.117, 0.127 mmol), and S-Phos (0.21 g, 0.51 mmol) were added to the mixture. The reaction was degassed and then heated to reflux on. Upon completion of the reaction, it was cooled to rt. The reaction was extracted with saturated LiCl and EtOAc (3 x 50 mL). The organic layers were combined, dried, concentrated, and purified via column

chromatography (SiO₂, 6:1, Hex: EtOAc) to afford the purified product as a yellow oil (70%): ¹H NMR (500 MHz, Chloroform-d) δ 9.55 (d, *J* = 0.8 Hz, 1H), 7.88 (d, *J* = 8.7 Hz, 1H), 7.47 – 7.35 (m, 1H), 7.21 (d, *J* = 8.7 Hz, 1H), 7.13 (tdd, *J* = 8.5, 2.6, 0.9 Hz, 1H), 7.01 (dt, *J* = 7.5, 1.2 Hz, 1H), 6.97 (ddd, *J* = 9.2, 2.6, 1.5 Hz, 1H), 5.33 (s, 2H), 3.52 (s, 3H), 1.99 (s, 3H). ¹³C NMR (126 MHz, CDCl₃) δ 191.27, 163.51, 161.53, 145.71, 138.97, 129.99, 128.46, 126.99, 123.61, 117.08, 114.92, 114.75, 112.82, 94.18, 56.43, 13.00. HRMS (ESI+) *m/z*: [M + Na⁺] calculated for C₁₆H₁₅FO₃ 297.0903; found 297.0904.



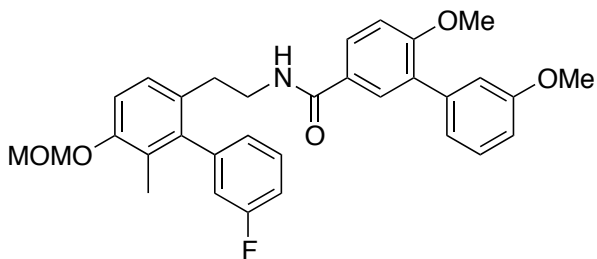
(*E*)-3'-Fluoro-3-(methoxymethoxy)-2-methyl-6-(2-nitrovinyl)-1,1'-biphenyl.

3'-Fluoro-5-(methoxymethoxy)-6-methyl-[1,1'-biphenyl]-2-carbaldehyde (0.11g, 0.327mmol) was dissolved in Nitromethane (0.7mL). NH₄OAc (0.05g, 0.654mmol) was added, and then the mixture was heated at reflux for 4 h. After 4 h the reaction was cooled to rt. The product was extracted with EtOAc (3 x 10mL). The organic layers were combined, dried, concentrated. The residue was purified by column chromatography (SiO₂, 4:1, Hex: EtOAc) to afford the purified product as a yellow solid in 90% yield: ¹H NMR (400 MHz, Chloroform-d) δ 7.58 (d, *J* = 13.6 Hz, 1H), 7.45 (d, *J* = 8.8 Hz, 1H), 7.42 – 7.36 (m, 1H), 7.24 – 7.21 (m, 1H), 7.13 – 7.06 (m, 2H), 6.87 (dt, *J* = 7.5, 1.2 Hz, 1H), 6.81 (ddd, *J* = 9.3, 2.6, 1.5 Hz, 1H), 5.25 (s, 2H), 3.46 (s, 3H), 1.92 (s, 3H).



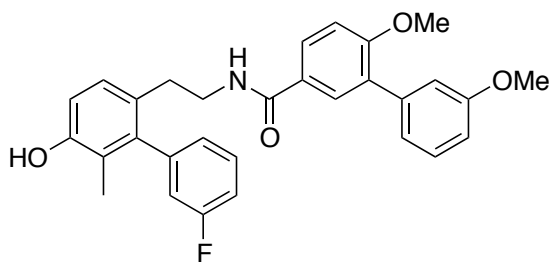
2-(3'-Fluoro-5-(methoxymethoxy)-6-methyl-[1,1'-biphenyl]-2-yl)ethanamine (3.30).

Lithium Aluminum Hydride (0.11g, 2.75mmol) was dissolved in anhydrous tetrahydrofuran (5.5mL) and cooled to 0°C. (*E*)-3'-Fluoro-3-(methoxymethoxy)-2-methyl-6-(2-nitrovinyl)-1,1'-biphenyl (0.5g, 1.377mmol) was dissolved in anhydrous tetrahydrofuran (1.96mL) and added drop wise to the reaction. The reaction slowly warmed to rt and stirred for 12 h. Upon completion, 3N NaOH (1mL), water (1mL), and EtOAc (3mL) were added sequentially to quench the reaction. After stirring for one h the mixture was filtered through a pad of Celite. The solid was washed with warm EtOAc (100mL). The filtrate was collected, dried, and concentrated. The oil was purified using column chromatography (SiO₂, 2:1, DCM: MeOH) and used directly in the next step: ¹H NMR (500 MHz, Chloroform-d) δ 7.38 (td, *J* = 8.0, 6.0 Hz, 1H), 7.06 – 7.02 (m, 3H), 6.91 (dt, *J* = 7.6, 1.2 Hz, 1H), 6.85 (ddd, *J* = 9.5, 2.6, 1.4 Hz, 1H), 5.22 (s, 2H), 3.51 (s, 3H), 2.69 (t, *J* = 7.3 Hz, 2H), 2.46 (t, *J* = 7.3 Hz, 2H), 2.27 (s, 5H), 1.90 (s, 3H). ¹³C NMR (126 MHz, CDCl₃) δ 163.72, 153.78, 137.9, 137.1, 130.25, 129.17, 127.27, 125.15, 123.81, 116.26, 113.80, 113.37, 94.67, 56.06, 42.92, 36.75, 13.73. HRMS (ESI+) *m/z*: [M + H⁺] calculated for C₁₇H₂₀FNO₂ 290.7415; found 290.7422.



***N*-(2-(3'-Fluoro-5-(methoxymethoxy)-6-methyl-[1,1'-biphenyl]-2-yl)ethyl)-3',6-dimethoxy-[1,1'-biphenyl]-3-carboxamide.**

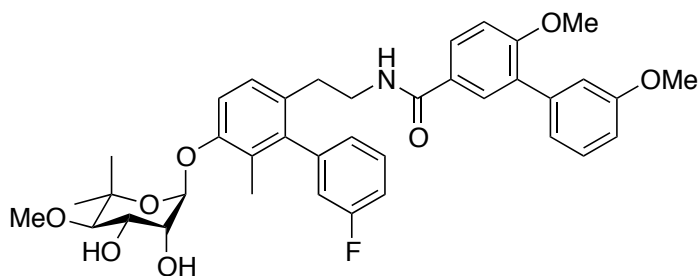
The compound was synthesized following the procedure used for the synthesis of *N*-(2-(5-(benzyloxy)-3'-fluoro-[1,1'-biphenyl]-2-yl)ethyl)-3',6-dimethoxy-[1,1'-biphenyl]-3-carboxamide to obtain the product as a white solid: ¹H NMR (500 MHz, Chloroform-*d*) δ 7.72 (dd, *J* = 8.6, 2.4 Hz, 1H), 7.63 (d, *J* = 2.4 Hz, 1H), 7.40 – 7.29 (m, 2H), 7.13 (d, *J* = 8.4 Hz, 1H), 7.09 – 7.01 (m, 4H), 6.99 – 6.85 (m, 4H), 6.09 (t, *J* = 5.7 Hz, 1H), 5.22 (s, 2H), 3.84 (s, 3H), 3.83 (s, 3H), 3.51 (s, 3H), 3.43 (tdd, *J* = 7.2, 5.7, 2.0 Hz, 2H), 2.62 (t, *J* = 7.2 Hz, 2H), 1.92 (s, 3H). ¹³C NMR (126 MHz, CDCl₃) δ 166.84, 161.85, 159.32, 158.93, 154.00, 141.89, 139.06, 130.37, 130.13, 129.90, 129.47, 129.13, 128.12, 127.48, 127.01, 126.08, 125.21, 122.03, 116.44, 116.28, 115.35, 114.02, 113.44, 112.85, 110.86, 94.68, 56.01, 55.92, 55.89, 40.81, 32.97, 13.84. HRMS (ESI+) *m/z*: [M + Na⁺] calculated for C₃₂H₃₂FNO₅ 552.2161; found 552.2162.



***N*-(2-(3'-Fluoro-5-hydroxy-6-methyl-[1,1'-biphenyl]-2-yl)ethyl)-3',6-dimethoxy-[1,1'-biphenyl]-3-carboxamide (3.42).**

Compound **3.42** was synthesized following the procedure used for the synthesis of **3.36** to obtain the product as a white solid: ¹H NMR (500 MHz, Chloroform-*d*) δ 7.62 (dd, *J* = 8.6, 2.4 Hz, 1H), 7.48 (d, *J* = 2.4 Hz, 1H), 7.15 (s, 1H), 7.02 – 6.97 (m, 1H), 6.96 – 6.88 (m, 3H), 6.86 (d, *J* = 8.5 Hz, 1H), 6.85 – 6.72 (m, 4H), 6.52 – 6.41 (m, 1H), 5.95 (t, *J* = 5.7 Hz, 1H), 3.74 (d, *J* =

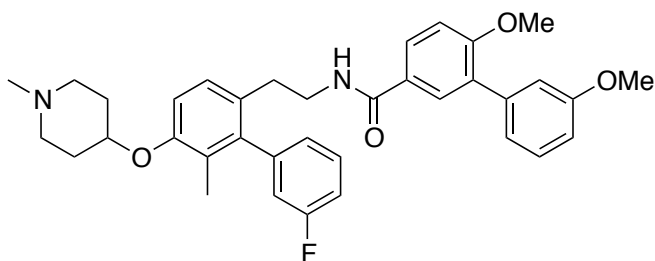
3.0 Hz, 6H), 3.35 – 3.28 (m, 2H), 2.49 (t, $J = 7.1$ Hz, 2H), 1.79 (s, 3H). ^{13}C NMR (126 MHz, CDCl_3) δ 167.55, 162.14, 159.56, 159.39, 153.45, 143.04, 142.14, 139.28, 130.45, 129.74, 129.45, 128.71, 128.58, 128.29, 127.88, 126.99, 125.55, 123.35, 122.48, 116.77, 116.61, 115.86, 115.00, 114.43, 114.26, 113.05, 111.28, 56.14, 55.75, 41.26, 33.20, 13.79. HRMS (ESI+) m/z : $[\text{M} + \text{H}^+]$ calculated for $\text{C}_{30}\text{H}_{28}\text{FNO}_4$ 486.1120; found 486.1109.



***N*-(2-(5-(((2*R*,3*R*,4*S*,5*R*)-3,4-Dihydroxy-5-methoxy-6,6-dimethyltetrahydro-2*H*-pyran-2-yl)oxy)-3'-fluoro-6-methyl-[1,1'-biphenyl]-2-yl)ethyl)-3',6-dimethoxy-[1,1'-biphenyl]-3-carboxamide (3.10).**

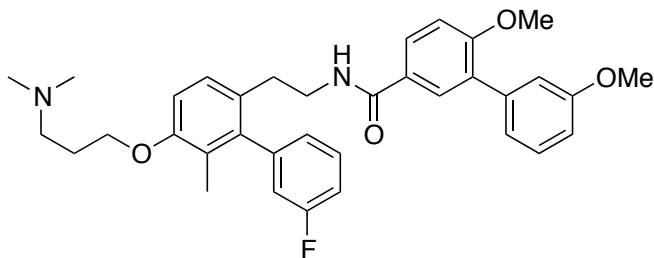
Compound **3.10** was synthesized following the procedure used for the synthesis of **3.5** to obtain the product as a white solid: ^1H NMR (500 MHz, Chloroform- d) δ 7.69 (dd, $J = 8.6, 2.4$ Hz, 1H), 7.59 (t, $J = 2.5$ Hz, 1H), 7.33 (t, $J = 8.0$ Hz, 2H), 7.17 (dd, $J = 8.6, 1.1$ Hz, 1H), 7.12 (s, 1H), 7.08 – 7.00 (m, 3H), 6.97 (d, $J = 8.6$ Hz, 1H), 6.95 – 6.86 (m, 2H), 5.94 (td, $J = 5.7, 2.0$ Hz, 1H), 5.53 (d, $J = 2.2$ Hz, 1H), 4.23 (dd, $J = 9.3, 3.2$ Hz, 1H), 4.19 (t, $J = 2.8$ Hz, 1H), 3.84 (d, $J = 3.0$ Hz, 6H), 3.60 (s, 3H), 3.53 (d, $J = 1.3$ Hz, 1H), 3.49 – 3.38 (m, 2H), 3.39 – 3.31 (m, 1H), 2.81 – 2.77 (m, 1H), 2.64 (d, $J = 25.0$ Hz, 2H), 1.82 (s, 3H), 1.39 (s, 3H), 1.21 (s, 3H). ^{13}C NMR (126 MHz, CDCl_3) δ 166.83, 163.76, 159.25, 158.91, 153.55, 142.44, 141.67, 138.96, 130.38, 130.05, 129.49, 129.38, 129.11, 128.00, 127.49, 126.87, 125.27, 121.97, 116.42, 115.30, 114.15,

112.93, 112.84, 110.81, 97.83, 71.45, 68.75, 61.92, 55.78, 55.34, 40.73, 32.90, 29.25, 22.61, 13.83. HRMS (ESI+) m/z : $[M + Na^+]$ calculated for $C_{38}H_{42}FNO_8Na$ 682.2792; found 682.2806.



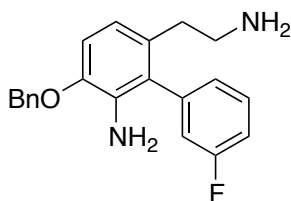
***N*-(2-(3'-Fluoro-6-methyl-5-((1-methylpiperidin-4-yl)oxy)-[1,1'-biphenyl]-2-yl)ethyl)-3',6-dimethoxy-[1,1'-biphenyl]-3-carboxamide (3.10a).**

Compound **3.10a** was synthesized following the procedure used for the synthesis of **3.6a** to obtain the product as a white solid: 1H NMR (500 MHz, DMSO- d_6) δ 7.65 (t, $J = 5.6$ Hz, 1H), 7.12 (dd, $J = 8.6, 2.3$ Hz, 1H), 7.05 (d, $J = 2.4$ Hz, 1H), 6.80 (ddd, $J = 8.1, 7.0, 5.3$ Hz, 1H), 6.65 (t, $J = 7.9$ Hz, 1H), 6.56 – 6.48 (m, 1H), 6.44 (dd, $J = 23.1, 8.7$ Hz, 2H), 6.37 – 6.19 (m, 6H), 3.70 (s, 1H), 3.59 (s, 2H), 3.13 (s, 3H), 3.10 (s, 3H), 2.68 (s, 2H), 2.60 – 2.52 (m, 2H), 2.49 (s, 2H), 2.12 (s, 3H), 1.96 (d, $J = 20.2$ Hz, 4H), 1.92 (s, 3H). ^{13}C NMR (126 MHz, DMSO) δ 167.03, 162.11, 159.72, 159.30, 158.43, 152.71, 142.12, 142.09, 140.96, 138.50, 129.95, 128.84, 128.57, 127.99, 127.57, 126.78, 126.32, 125.03, 124.17, 121.23, 115.61, 114.70, 113.44, 112.06, 111.92, 110.72, 77.62, 55.28, 54.61, 51.54 (2Cs), 48.14, 45.00, 35.35, 32.10 (2Cs), 13.11. HRMS (ESI+) m/z : $[M + H^+]$ calculated for $C_{36}H_{39}FN_2O_4$ 571.2972; found 571.2978.



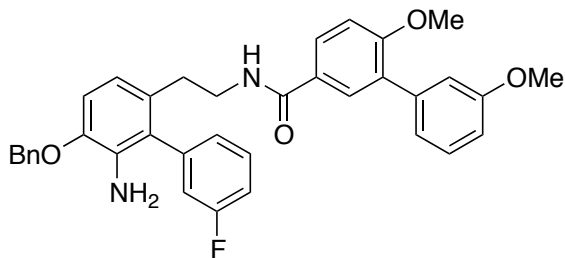
***N*-(2-(5-(3-(Dimethylamino)propoxy)-3'-fluoro-6-methyl-[1,1'-biphenyl]-2-yl)ethyl)-3',6-dimethoxy-[1,1'-biphenyl]-3-carboxamide (3.10b).**

Compound **3.10b** was synthesized following the procedure used for the synthesis of **3.6a** to obtain the product as a white solid: ^1H NMR (500 MHz, DMSO- d_6) δ 8.02 (t, $J = 5.6$ Hz, 1H), 7.50 (dd, $J = 8.6, 2.3$ Hz, 1H), 7.43 (d, $J = 2.4$ Hz, 1H), 7.21 – 7.15 (m, 1H), 7.03 (t, $J = 7.9$ Hz, 1H), 6.90 (td, $J = 8.6, 2.5$ Hz, 1H), 6.82 (dd, $J = 17.9, 8.6$ Hz, 2H), 6.76 – 6.66 (m, 4H), 6.65 – 6.60 (m, 2H), 3.68 (t, $J = 6.2$ Hz, 2H), 3.51 (s, 3H), 3.48 (s, 3H), 2.95 – 2.88 (m, 2H), 2.20 (s, 3H), 2.19 – 2.15 (m, 2H), 2.09 (t, $J = 7.1$ Hz, 2H), 1.85 (s, 6H), 1.58 – 1.53 (m, 2H). ^{13}C NMR (126 MHz, DMSO) δ 165.36, 161.12, 158.92, 158.68, 158.21, 154.86, 141.16, 138.99, 130.43, 129.33, 129.06, 128.78, 128.48, 127.34, 126.82, 125.42, 123.66, 121.72, 116.11, 115.19, 113.76, 112.41, 111.22, 110.70, 65.88, 55.77, 55.09, 48.63, 45.16, 35.80, 32.59, 26.98, 13.43. HRMS (ESI+) m/z : $[\text{M} + \text{H}^+]$ calculated for $\text{C}_{35}\text{H}_{39}\text{FN}_2\text{O}$ 571.2972; found 571.2965.



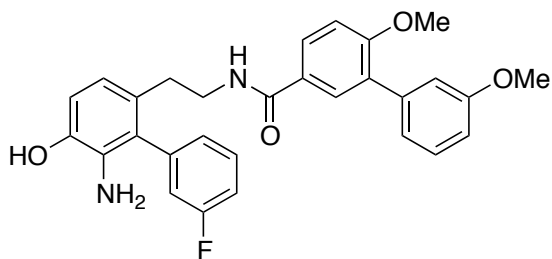
6-(2-Aminoethyl)-3-(benzyloxy)-3'-fluoro-[1,1'-biphenyl]-2-amine (3.33).

This compound was synthesized following the procedure reported in Chapter 2.



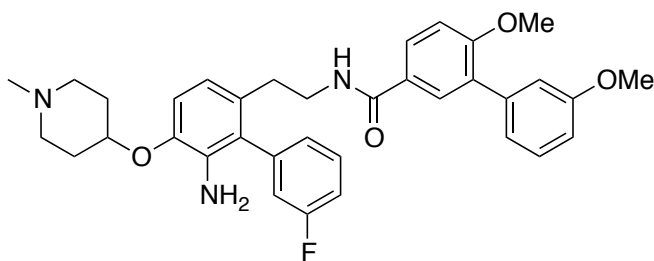
***N*-(2-(6-Amino-5-(benzyloxy)-3'-fluoro-[1,1'-biphenyl]-2-yl)ethyl)-3',6-dimethoxy-[1,1'-biphenyl]-3-carboxamide.**

The compound was synthesized following the procedure used for the synthesis of *N*-(2-(5-(benzyloxy)-3'-fluoro-[1,1'-biphenyl]-2-yl)ethyl)-3',6-dimethoxy-[1,1'-biphenyl]-3-carboxamide to obtain the product as a white solid: ^1H NMR (500 MHz, Chloroform- d) δ 7.70 (t, $J = 5.5$ Hz, 1H), 7.18 (dd, $J = 8.5, 2.2$ Hz, 1H), 7.09 (d, $J = 2.5$ Hz, 1H), 6.85 – 6.79 (m, 5H), 6.60 (t, $J = 8.1$ Hz, 1H), 6.51 (td, $J = 8.5, 2.6$ Hz, 1H), 6.42 (dd, $J = 18.1, 8.5$ Hz, 2H), 6.37 – 6.29 (m, 5H), 6.26 – 6.21 (m, 3H), 5.58 (s, 1H), 5.09 (s, 2H), 3.68 (s, 3H), 3.63 (s, 3H), 3.40 (d, $J = 6.7$ Hz, 2H), 2.58 (t, $J = 6.8$ Hz, 2H). ^{13}C NMR (126 MHz, DMSO) δ 167.04, 161.35, 159.25, 159.00, 144.32, 139.53, 138.07, 131.77, 130.45, 130.02, 129.82, 129.54, 128.62, 127.43, 126.71, 122.34, 121.60, 120.19, 117.67, 117.45, 115.72, 114.65, 113.77, 111.07, 110.43, 70.11, 56.45, 55.71, 42.01, 38.66. HRMS (ESI+) m/z : $[\text{M} + \text{H}^+]$ calculated for $\text{C}_{36}\text{H}_{33}\text{FN}_2\text{O}_4$ 577.2475; found 577.2492.



***N*-(2-(6-Amino-3'-fluoro-5-hydroxy-[1,1'-biphenyl]-2-yl)ethyl)-3',6-dimethoxy-[1,1'-biphenyl]-3-carboxamide (3.41).**

Compound **3.41** was synthesized following the procedure used for the synthesis of **3.36** to obtain the product as a white solid which was verified using HRMS and used immediately due to stability concerns: HRMS (ESI+) m/z : $[M + H^+]$ calculated for $C_{29}H_{27}FN_2O_4$ 485.1877; found 485.1863.



***N*-(2-(6-Amino-3'-fluoro-5-((1-methylpiperidin-4-yl)oxy)-[1,1'-biphenyl]-2-yl)ethyl)-3',6-dimethoxy-[1,1'-biphenyl]-3-carboxamide (3.11a).**

Compound **3.11a** was synthesized following the procedure used for the synthesis of **3.6a** to obtain the product as a white solid: 1H NMR (500 MHz, DMSO- d_6) δ 7.65 (t, $J = 5.6$ Hz, 1H), 7.13 (dd, $J = 8.6, 2.3$ Hz, 1H), 7.06 (d, $J = 2.4$ Hz, 1H), 6.84 – 6.78 (m, 1H), 6.66 (t, $J = 7.9$ Hz, 1H), 6.53 (td, $J = 8.6, 2.5$ Hz, 1H), 6.45 (dd, $J = 17.9, 8.6$ Hz, 2H), 6.39 – 6.29 (m, 5H), 6.28 – 6.22 (m, 2H), 5.58 (s, 1H), 3.75 (s, 1H), 3.65 (s, 3H), 3.62 (s, 3H), 3.46 (d, $J = 6.6$ Hz, 2H), 2.68 (t, $J = 7.0$ Hz, 2H), 2.53 – 2.48 (m, 2H), 2.38-2.30 (m, 2H), 2.19 (s, 3H), 1.92 – 1.86 (m, 2H). ^{13}C NMR (126 MHz, DMSO) δ 167.34, 162.05, 159.65, 159.08, 142.12, 139.03, 138.77, 131.89, 130.90, 130.62, 129.55, 129.32, 128.72, 127.43, 126.44, 122.14, 121.61, 120.09, 117.63, 117.08, 115.55, 114.45, 113.72, 111.67, 110.01, 78.90, 56.00, 55.39, 48.43, 40.79, 30.16, 27.74. HRMS (ESI+) m/z : $[M + H^+]$ calculated for $C_{35}H_{38}FN_3O_4$ 584.2832; found 584.2818.

References:

1. Karagoz, G. E.; Rudiger, S. G. D., Hsp90 interaction with clients. *Trends in Biochemical Sciences* **2015**, *40* (2), 117-25.
2. Frydman, J.; Nimmesgern, E.; Ohtsuka, K.; Hartl, F. U., Folding of nascent polypeptide chains in a high molecular mass assembly with molecular chaperones. *Nature* **1994**, *370*, 111-117.
3. Csermely, P.; Schnaider, T.; Söti, C.; Prohászka, Z.; Nardai, G., The 90-kDa Molecular Chaperone Family: Structure, Function, and Clinical Applications. A Comprehensive Review. *Pharmacology Therapy* **1998**, *79* (2), 129-168.
4. Röhl, A.; Rohrber, J.; Buchner, J., The Chaperone Hsp90: Changing Partners for Demanding Clients. *Trends in Biochemical Sciences* **2013**, *38* (5), 253-62.
5. Taipale, M.; Krykbaeva, I.; Koeva, M.; Kayatekin, C.; Westover, K. D.; Karras, G. I.; Lindquist, S., Quantitative analysis of HSP90-client interactions reveals principles of substrate recognition. *Cell* **2012**, *150* (5), 987-1001.
6. Miyata, Y.; Nakamoto, H.; Neckers, L., The Therapeutic Target Hsp90 and Cancer Hallmarks. *Current Pharmaceutical Design* **2013**, *19* (3), 347-365.
7. Hanahan, D.; Weinberg, R. A., The Hallmarks of Cancer. *Cell* **2000**, *100*, 57-70.
8. Hanahan, D.; Weinberg, R. A., Hallmarks of cancer: the next generation. *Cell* **2011**, *144* (5), 646-74.
9. Jhaveri, K.; Taldone, T.; Modi, S.; Chiosis, G., Advances in the Clinical Development of Heat Shock Protein 90 (Hsp90) Inhibitors in Cancers. *Biochimica et Biophysica Acta* **2012**, *1823* (3), 742-55.

10. Garcia-Carbonero, R.; Carnero, A.; Paz-Ares, L., Inhibition of HSP90 Molecular Chaperones: Moving into the Clinic. *The Lancet Oncology* **2013**, *14* (9), e358-e369.
11. Katerina, S.; Evangelia, P., HSP90 Inhibitors: Current Development and Potential in Cancer Therapy. *Recent Patents on Anti-Cancer Drug Discovery* **2014**, *9* (1), 1-20.
12. Ozgur, A.; Tutar, Y., Heat Shock Protein 90 Inhibition in Cancer Drug Discovery: From Chemistry to Futural Clinical Applications. *Anti-Cancer Agents in Medicinal Chemistry* **2016**, *16*, 280-290.
13. Neckers, L.; Workman, P., Hsp90 Molecular Chaperone Inhibitors: Are We There Yet? *Clinical Cancer Research : an official journal of the American Association for Cancer Research* **2012**, *18* (1), 64-76.
14. Trepel, J.; Mollapour, M.; Giaccone, G.; Neckers, L., Targeting the Dynamic HSP90 Complex in Cancer. *Nature Reviews Cancer* **2010**, *10* (8), 537-549.
15. Holzbeierlein, J. M.; Windsperger, A.; Vielhauer, G., Hsp90: A Drug Target? *Current Oncology Reports* **2010**, *12* (2), 95-101.
16. Li, J.; Soroka, J.; Buchner, J., The Hsp90 Chaperone Machinery: Conformational Dynamics and Regulation by Co-Chaperones. *Biochimica et Biophysica Acta* **2012**, *1823* (3), 624-35.
17. Jego, G.; Hazoumé, A.; Seigneuric, R.; Garrido, C., Targeting Heat Shock Proteins in Cancer. *Cancer Letters* **2013**, *332* (2), 275-285.
18. Blagg, B. S. J.; Kerr, T. D., Hsp90 inhibitors: Small molecules that transform the Hsp90 protein folding machinery into a catalyst for protein degradation. *Medicinal Research Reviews* **2006**, *26* (3), 310-338.

19. Zhang, H.; Burrows, F., Targeting multiple signal transduction pathways through inhibition of Hsp90. *Journal of Molecular Medicine* **2004**, *82* (8), 488-499.
20. Kamal, A.; Thao, L.; Sensintaffar, J.; Zhang, L.; Boehm, M. F.; Fritz, L. C.; Burrows, F. J., A high-affinity conformation of Hsp90 confers tumour selectivity on Hsp90 inhibitors. *Letters to Nature* **2003**, *425*, 407-410.
21. Zou, J.; Guo, Y.; Guettouche, T.; Smith, D. F.; Voellmy, R., Repression of Heat Shock Transcription Factor HSF1 Activation by HSP90 (HSP90 Complex) that Forms a Stress-Sensitive Complex with HSF1. *Cell* **1998**, *94* (4), 471-480.
22. Morimoto, R. I., The heat shock response: systems biology of proteotoxic stress in aging and disease. *Cold Spring Harbor symposia on quantitative biology* **2011**, *76*, 91-9.
23. Ansar, S.; Burlison, J. A.; Hadden, M. K.; Yu, X. M.; Desino, K. E.; Bean, J.; Neckers, L.; Audus, K. L.; Michaelis, M. L.; Blagg, B. S. J., A non-toxic Hsp90 inhibitor protects neurons from Abeta-induced toxicity. *Bioorganic & Medicinal Chemistry Letters* **2007**, *17* (7), 1984-90.
24. Whitesell, L.; Bagatell, R.; Falsey, R., The Stress Response; Implications for the Clinical Development of Hsp90 Inhibitors. *Current Cancer Drug Targets* **2003**, *3* (5), 349-358.
25. Whitesell, L.; Santagata, S.; Lin, N. U., Inhibiting HSP90 to Treat Cancer: A Strategy in Evolution. *Current Molecular Medicine* **2012**, *12* (9), 1108-1124.
26. Hall, J. A.; Forsberg, L. K.; Blagg, B. S. J., Alternative Approaches to Hsp90 Modulation for the Treatment of Cancer. *Future Medicinal Chemistry* **2014**, *6* (14), 1587-1605.
27. Whitesell, L.; Lindquist, S. L., HSP90 and the Chaperoning of Cancer. *Nature Reviews Cancer* **2005**, *5* (10), 761-772.

28. Marcu, M. G.; Schulte, T. W.; Neckers, L., Novobiocin and Related Coumarins and Depletion of Heat Shock Protein 90-Dependent Signaling Proteins. *Journal of the National Cancer Institute* **2000**, *92* (3), 242-248.
29. Marcu, M. G.; Chadli, A.; Bouhouche, I.; Catelli, M.; Neckers, L. M., The Heat Shock Protein 90 Antagonist Novobiocin Interacts with a Previously Unrecognized ATP-binding Domain in the Carboxyl Terminus of the Chaperone. *The Journal of Biological Chemistry* **2000**, *275* (47), 37181-6.
30. Lu, Y.; Ansar, S.; Michaelis, M. L.; Blagg, B. S. J., Neuroprotective activity and evaluation of Hsp90 inhibitors in an immortalized neuronal cell line. *Bioorganic & Medicinal Chemistry* **2009**, *17* (4), 1709-15.
31. Zhang, L.; Zhao, H.; Blagg, B. S.; Dobrowsky, R. T., C-terminal heat shock protein 90 inhibitor decreases hyperglycemia-induced oxidative stress and improves mitochondrial bioenergetics in sensory neurons. *Journal of Proteome Research* **2012**, *11* (4), 2581-93.
32. Li, C.; Ma, J.; Zhao, H.; Blagg, B. S. J.; Dobrowsky, R. T., Induction of heat shock protein 70 (Hsp70) prevents neuregulin-induced demyelination by enhancing the proteasomal clearance of c-Jun. *ASN Neuro* **2012**, *4* (7), e00102.
33. Urban, M. J.; Li, C.; Yu, C.; Lu, Y.; Krise, J. M.; McIntosh, M. P.; Rajewski, R. A.; Blagg, B. S. J.; Dobrowsky, R. T., Inhibiting heat-shock protein 90 reverses sensory hypoalgesia in diabetic mice. *ASN Neuro* **2010**, *2* (4), e00040.
34. Kusuma, B. R.; Zhang, L.; Sundstrom, T.; Peterson, L. B.; Dobrowsky, R. T.; Blagg, B. S. J., Synthesis and evaluation of novologues as C-terminal Hsp90 inhibitors with cytoprotective activity against sensory neuron glucotoxicity. *Journal of Medicinal Chemistry* **2012**, *55* (12), 5797-812.

35. Zhao, H.; Anyika, M.; Girgis, A.; Blagg, B. S., Novologues containing a benzamide side chain manifest anti-proliferative activity against two breast cancer cell lines. *Bioorganic & Medicinal Chemistry Letters* **2014**, *24* (15), 3633-7.
36. Donnelly, A. C.; Mays, J. R.; Burlinson, J. A.; Nelson, J. T.; Vielhauer, G.; Holzbeierlein, J.; Blagg, B. S. J., The Design, Synthesis and Evaluation of Coumarin Ring Derivatives of the Novobiocin Scaffold that Exhibit Antiproliferative Activity. *Journal of Organic Chemistry* **2008**, *73*, 8901-8920.
37. Burlison, J. A.; Neckers, L.; Smith, A. B.; Maxwell, A.; Blagg, B. S. J., Novobiocin: Redesigning a DNA Gyrase Inhibitor for Selective Inhibitor of Hsp90. *Journal of the American Chemical Society* **2006**, *128*, 15529-15536.
38. Burlison, J. A.; Avila, C.; Vielhauer, G.; Lubbers, D. J.; Holzbeierlein, J.; Blagg, B. S. J., Development of Novobiocin Analogues that Manifest Anti-Proliferative Activity Against Several Cancer Cell Lines. *Journal of Organic Chemistry* **2008**, *73*, 2130-2137.
39. Xie, L.; Takeuchi, Y.; Cosentino, L. M.; Lee, K.-H., Anti-AIDS Agents. 37. Synthesis and Structure-Activity Relationships of (3'R,4'R)-(+)-cis-Khellactone Derivatives as Novel Potent Anti-HIV Agents. *Journal of Medicinal Chemistry* **1999**, *42*, 2662-2672.
40. Ohsawa, K.; Yoshida, M.; Doi, T., A direct and mild formylation method for substituted benzenes utilizing dichloromethyl methyl ether-silver trifluoromethanesulfonate. *Journal of Organic Chemistry* **2013**, *78* (7), 3438-44.
41. Bengtson, A.; Hallberg, A.; Larhed, M., Fast Synthesis of Aryl Triflates with Controlled Microwave Heating. *Organic Letters* **2002**, *4* (7), 1231-1233.
42. Li, C. C.; Xie, Z. X.; Zhang, Y. D.; Chen, J. H.; Yang, Z., Total Synthesis of Wedelolactone. *Journal of Organic Chemistry* **2003**, *68*, 8500-8504.

43. Kogen, H.; Toda, N.; Tago, K.; Marumoto, S.; Takami, K.; Ori, M.; Yamada, N.; Koyama, K.; Naruto, S.; Abe, K.; Yamazaki, R.; Hara, T.; Aoyagi, A.; Abe, Y.; Kaneko, T., Design and Synthesis of Dual Inhibitors of Acetylcholinesterase and Serotonin Transporter Targeting Potential Agents for Alzheimer's Disease. *Organic Letters* **2002**, *4* (20), 3359-3362.
44. Narihiro Toda; Keiko Tago; Shinji Marumoto; Kazuko Takami; Mayuko Ori; Naho Yamada; Kazuo Koyama; Shunji Naruto; Kazumi Abe; Reina Yamazaki; Takao Hara; Atsushi Aoyagi; Yasuyuki Abe; Tsugio Kaneko; Hiroshi Kogen, A Conformational Restriction Approach to the Development of Dual Inhibitors of Acetylcholinesterase and Serotonin Transporter as Potential Agents for Alzheimer's Disease. *Bioorganic & Medicinal Chemistry* **2003**, *11* (20), 4389-4415.
45. Donnelly, A. C.; Zhao, H.; Kusuma, B. R.; Blagg, B. S. J., Cytotoxic Sugar Analogues of an Optimized Novobiocin Scaffold. *Medicinal Chemistry Communication* **2010**, *1* (2), 165-170.
46. Andrieux, C. P.; Farriol, M.; Gallardo, I.; Marquet, J., Thermodynamics and kinetics of homolytic cleavage of carbon-oxygen bonds in radical anions obtained by electrochemical reduction of alkyl aryl ethers. *Journal of the Chemical Society, Perkin Transactions* **2002**, (5), 985-990.
47. Zou, M.; Bhatia, A.; Dong, H.; Jayaprakash, P.; Guo, J.; Sahu, D.; Hou, Y.; Tsen, F.; Tong, C.; O'Brien, K.; Situ, A. J.; Schmidt, T.; Chen, M.; Ying, Q.; Ulmer, T. S.; Woodley, D. T.; Li, W., Evolutionarily conserved dual lysine motif determines the non-chaperone function of secreted Hsp90alpha in tumour progression. *Oncogene* **2017**, *36* (15), 2160-2171.
48. Yu, X. M.; Shen, G.; Blagg, B. S. J., Synthesis of (-)-Noviose from 2,3-O-Isopropylidene-D-erythronolactol. *Journal of Organic Chemistry* **2004**, *69*, 7375-7378.

4. Development of Phenyl Cyclohexylcarboxamides as a Novel Class of Hsp90 C-terminal Inhibitors

Introduction

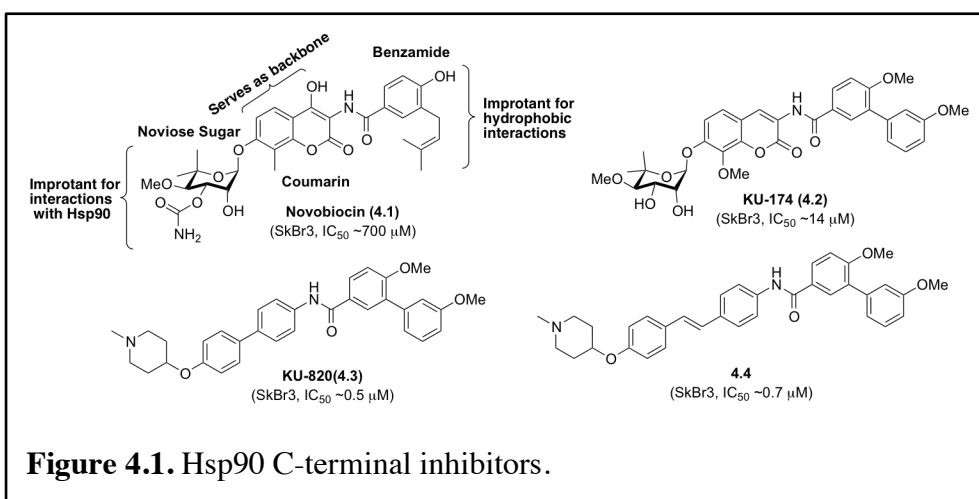
Heat shock protein 90 (Hsp90) is an evolutionarily conserved molecular chaperone that plays a critical role in the maintenance of protein homeostasis as well as an adaptive response to cell stress.¹ Hsp90 is a core component of the protein folding machinery that regulates the folding, stability, function, and proteolytic turnover of more than 300 client proteins, including protein kinases, transcription factors, and signal transducers.² These client proteins control a wide range of cellular functions, such as cell signaling, protein trafficking, chromatin remodeling, cell proliferation and survival.²⁻⁴ However, in cancer, these clients are frequently mutated and/or over-expressed to drive oncogenic processes, such as dysregulated proliferation, metastasis, and angiogenesis. In fact, ~25% of the Hsp90-dependent clients (eg. Her-2, CDK6, Raf1, Akt, survivin, telomerase) represent oncoproteins that are directly associated with all ten hallmarks of cancer.^{3, 5-7} Moreover, Hsp90 is overexpressed in cancer cells to stabilize these oncoproteins against proteotoxic stresses and to fold mutants that enable the growth and/or survival of tumorigenic cells.⁸⁻⁹ Consequently, Hsp90 inhibition provides an opportunity to simultaneously disrupt multiple oncogenic pathways that are required for cancer cell survival. As a result, Hsp90 has emerged as a promising therapeutic target for the development of cancer chemotherapeutics.¹⁰⁻¹¹ 17 Small molecules that target the Hsp90 N-terminus have entered clinical trials for the treatment of cancer, demonstrating proof-of-concept for Hsp90 inhibitors as potential anticancer agents.¹² Although these molecules have shown some promising clinical responses, several concerns have arisen such as concomitant induction of the pro-survival heat shock response (HSR), hepatotoxicity, and cardiotoxicity amongst others, which represent

additional risks that must be overcome during the development of new inhibitors.⁴ Therefore, small molecules that modulate Hsp90 via alternative mechanisms represent a novel approach towards the evolution of Hsp90 inhibitors.^{4,13}

In 2000, Neckers and co-workers discovered that novobiocin, a clinically used antibiotic and DNA gyrase inhibitor, binds the Hsp90 C-terminus, and allosterically inhibits Hsp90 function.¹⁴⁻¹⁵ Importantly, novobiocin and related natural products do not induce the HSR and therefore, can avoid the clinical limitations associated with Hsp90 N-terminal inhibitors. Unfortunately, novobiocin exhibits low cellular activity (SkBr3 IC₅₀ ~ 700 μM) and thus, has limited therapeutic potential. Preliminary studies with novobiocin identified key structural features required for Hsp90 inhibitory activity, which led to analogues with improved inhibitory activity.¹⁶⁻¹⁷ Subsequent studies revealed that the benzamide side chain of novobiocin is important for anti-proliferative activity and modification of this side chain produced several promising compounds, such as KU-174 (Figure 4.1).¹⁸ Additional studies demonstrated that the stereochemically complex sugar moiety could be replaced with ionizable amines, which produced analogues that manifest mid-nanomolar to low micromolar activity against multiple cancer cell lines.¹⁹⁻²² In contrast to these side chains, limited structural investigations have been performed on the coumarin core of novobiocin.

Recent investigation of the novobiocin scaffold demonstrated that an aromatic or heteroaromatic ring system could be used in lieu of the coumarin core without compromising activity, suggesting that the central core may serve as a backbone to orient both the benzamide and sugar/side chains within the binding pocket.²³⁻²⁴ Consequently, it was proposed that the coumarin core could be replaced with other scaffolds to identify compounds upon which more potent inhibitors could be realized. Moreover, the development of a structurally diverse set of

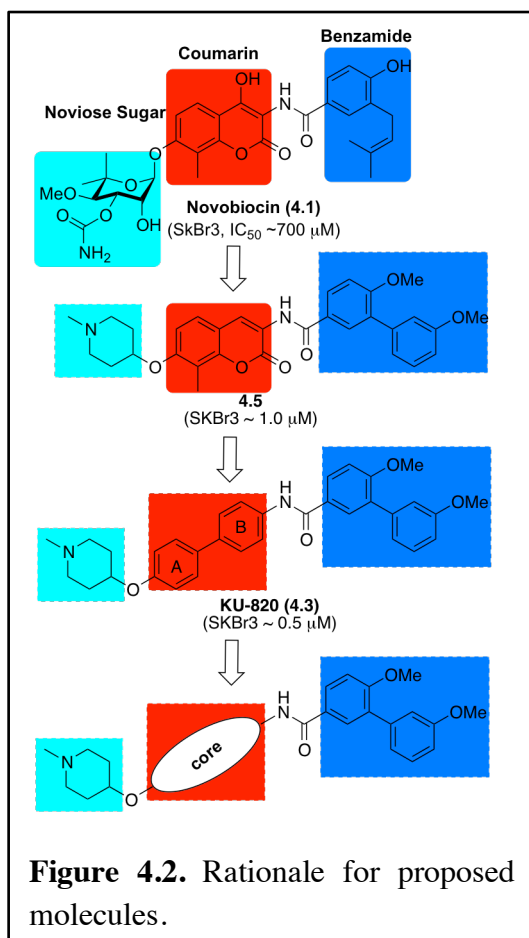
compounds is necessary to better understand the mechanism by which the C-terminal domain regulates the Hsp90 chaperone cycle. Towards this objective, we discovered the coumarin core of novobiocin could be replaced with a biphenyl scaffold, which led to analogues that exhibit potent anti-proliferative activity, like **4.3** (Figure 4.1).²⁵⁻²⁶ More recently, we demonstrated that a stilbene core (**4.4**) could be used in lieu of the coumarin core as well.²⁷ In continuation of these studies, the current work identifies a novel core, which has led to the development of more efficacious Hsp90 inhibitors.



Design

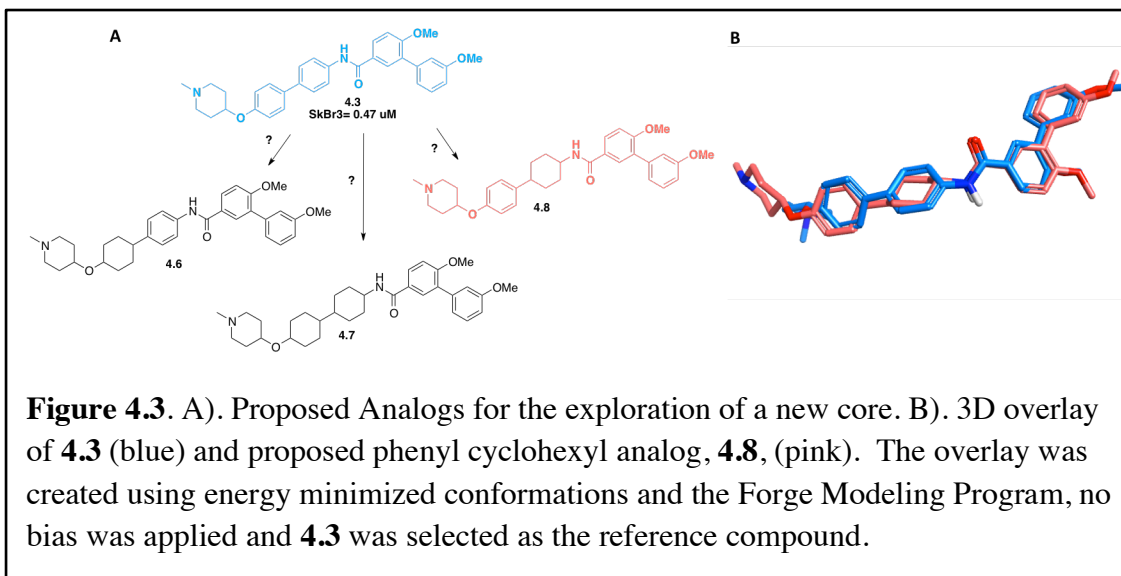
Prior SAR studies on novobiocin revealed the benzamide side chain and sugar are critical for Hsp90 inhibitory activity and that modification to these moieties has produced several promising compounds, such as **4.5** (Figure 4.2), which manifests improved activity against several cancer cell lines.^{18-22, 28} Recently, it was demonstrated that a biphenyl scaffold could be used in lieu of the coumarin core, which also led to potent inhibitors, such as KU-820 (Figure 4.2), presumably due to the favorable conformation adopted by the relatively flexible biphenyl core within the binding pocket.^{25, 29} In addition, it was determined that the planarity and

flexibility of the central core are important for Hsp90 inhibitory activity.²⁷ Therefore, it was hypothesized that the central core could be modified to optimize orientation of the side chains for increased inhibitory activity. Since biphenyl analogues manifest superior activity, this scaffold was chosen as the starting point for the discovery of more efficacious Hsp90 inhibitors.



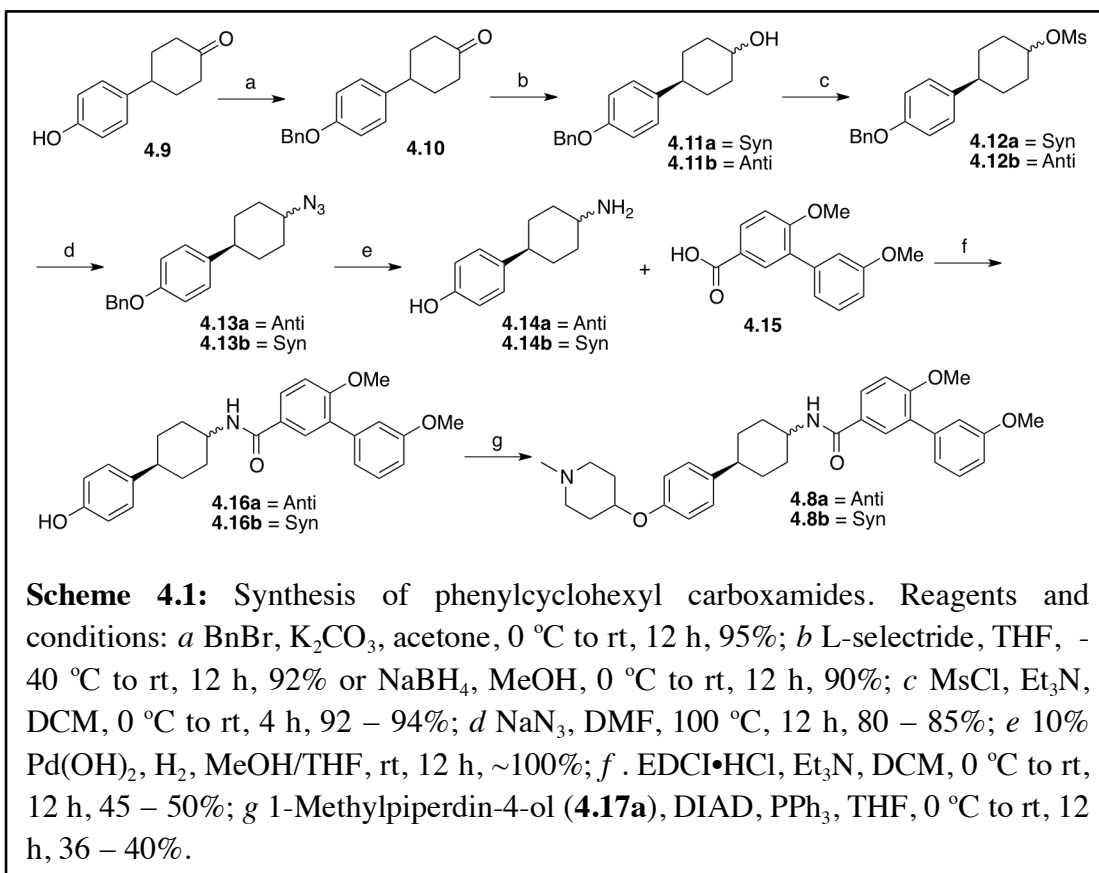
Increasing evidence suggests that molecules with aromatic scaffolds offer limited spatial diversity, while the incorporation of a saturated ring system can improve drug-like properties, such as ligand/receptor interactions as well as solubility.³⁰⁻³¹ As a flexible structure, the saturated ring system has the ability to adopt multiple conformations and to project substituents into optimal orientations within the binding pocket. Therefore, optimization of the core began by replacement of the A- and/or B-ring of the biphenyl core with a saturated ring system (Figure

4.3). The previously optimized biaryl amide side chain and *N*-methylpiperidine present in **4.3** were appended to these new cores for evaluation of preliminary structure-activity relationships. A 3D overlay was used to verify that the general three-dimensional structure would be similar with the proposed analogs when compared to **4.3** (Figure 4.3).

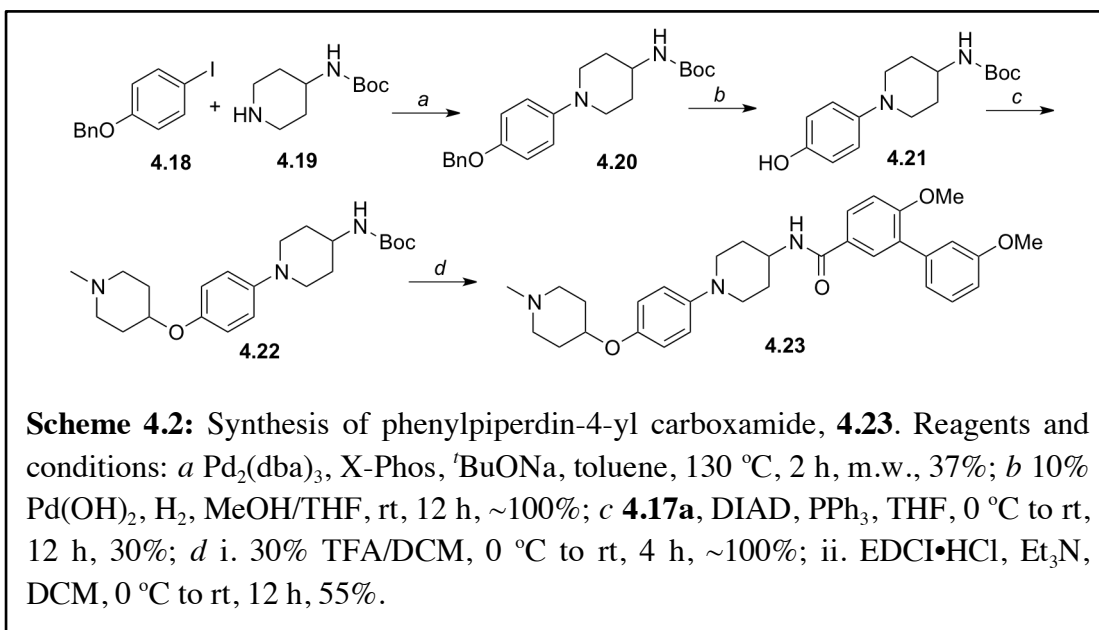


Chemistry

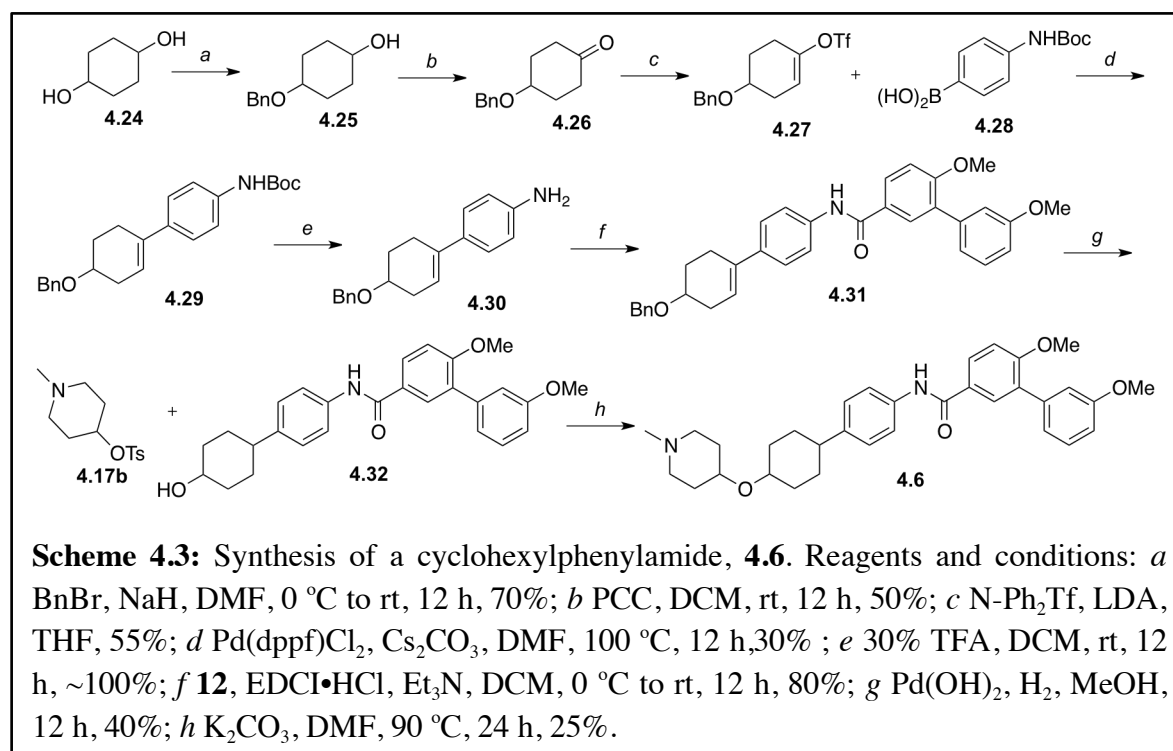
As shown in Scheme 4.1, the preparation of analogues that contain a saturated B-ring (**4.8a** and **4.8b**) commenced via benzyl-protection of phenol **4.9** to afford ketone **4.10**, which was then stereoselectively reduced with either L-selectride or sodium borohydride to give the syn (**4.11a**) or anti (**4.11b**) diastereomers in >90% de, respectively. Inversion of stereochemistry was made possible by mesylation of the alcohols (**4.11a**, **4.11b**), followed by S_N2 substitution with sodium azide to yield **4.13a** and **4.13b**. Reduction of the azides with palladium on carbon under a hydrogen atmosphere gave amines **4.14a** and **4.14b**, which were then coupled with biaryl acid **4.15** using standard coupling conditions to afford the corresponding amides, **4.16a** and **4.16b**. Mitsunobu etherification of the resulting amides with 1-methyl-4-hydroxypiperidine (**4.17a**) gave the desired products, **4.8a** and **4.8b**, in moderate yields.



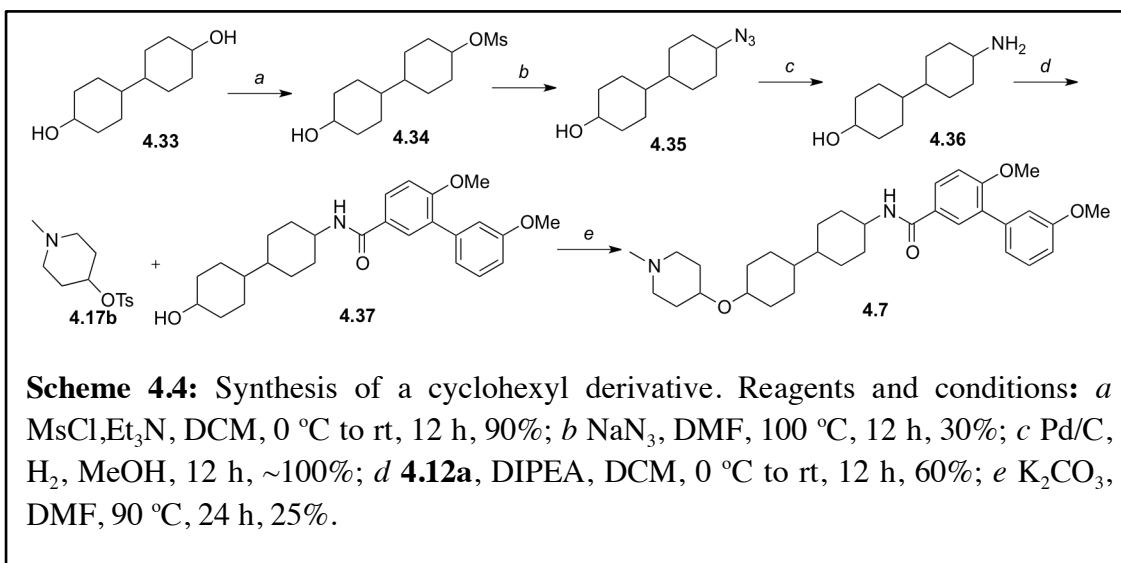
In addition, an analogue that contains a piperidine ring (**4.23**) was designed to determine whether orientation of the cyclohexyl ring is important for activity. Synthesis of **4.23** was achieved via a Buchwald coupling between aryl bromide **4.18** and piperidine **4.19** to produce **4.20**, which then underwent hydrogenolysis with palladium hydroxide under a hydrogen atmosphere to give the free phenol, **4.21** (Scheme 4.2). Mitsunobu etherification of **4.21** with 1-methyl-4-hydroxypiperidine (**4.17a**) yielded the *N*-Boc-protected amine **4.22**, which was then treated with trifluoroacetic acid to remove the Boc- protecting group before the resulting amine was coupled with biaryl acid **4.15** to afford the desired product, **4.23**.



In parallel, an analogue containing a saturated A-ring (**4.6**) was prepared as illustrated in Scheme 4.3. Synthesis of compound **4.6** was initiated by selective mono-benylation of cyclohexane-1,4-diol to give **4.25**,³² which was then oxidized with pyridinium chlorochromate to yield ketone **4.26**.³³ The ketone was then converted to the vinyl triflate (**4.27**), before Suzuki coupling with boronic acid **4.28** to give the cyclohexyl phenyl core, **4.29**. Acid-catalyzed hydrolysis of the Boc-protecting group on **4.30** yielded aniline **4.29**, which underwent an amide coupling reaction with acid chloride **4.15** to afford **4.31**. Hydrogenolysis of **4.31** with palladium on carbon under a hydrogen atmosphere gave the free alcohol, **4.32**, which underwent an S_N2 substitution reaction with **4.17b** to afford **4.6** in moderate yield. Following a similar protocol as standardized for **4.8a** and **4.8b**, compound **4.7** was prepared to contain two cyclohexyl rings as shown in Scheme 4.4.

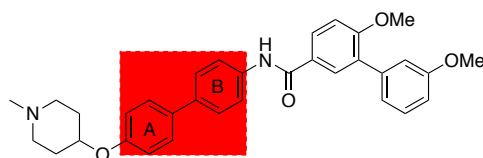


Upon construction, analogues containing saturated A- and/or B-rings were evaluated for their anti-proliferative activity against two cancer cell lines, SkBr3 (estrogen receptor negative, Her-2 overexpressing breast cancer cells) and MCF-7 (estrogen receptor positive breast cancer cells).

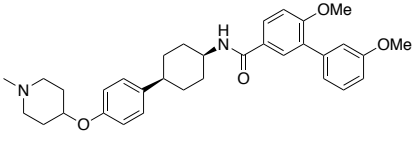
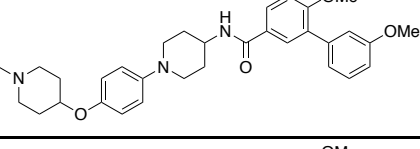
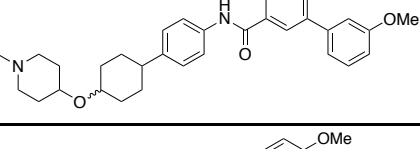
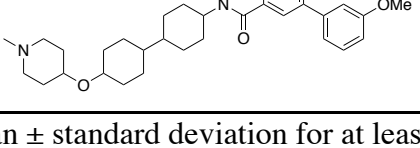


As shown in Table 4.1, compound **4.8a** (*anti*) exhibited 4-fold greater anti-proliferative activity than the lead compound **4.3**, and 10-15 fold better activity than **4.8b** and **4.23**, indicating the *anti*-stereochemistry is important for anti-proliferative activity. Incorporation of a saturated ring into the A-position was detrimental, as compounds **4.6** and **4.7** were both inactive up to 50 μM, suggesting that planarity of the A-ring is important for anti-proliferative activity.

Table 4.1. Anti-proliferative activity of analogues with the modified A- and/or B-rings.



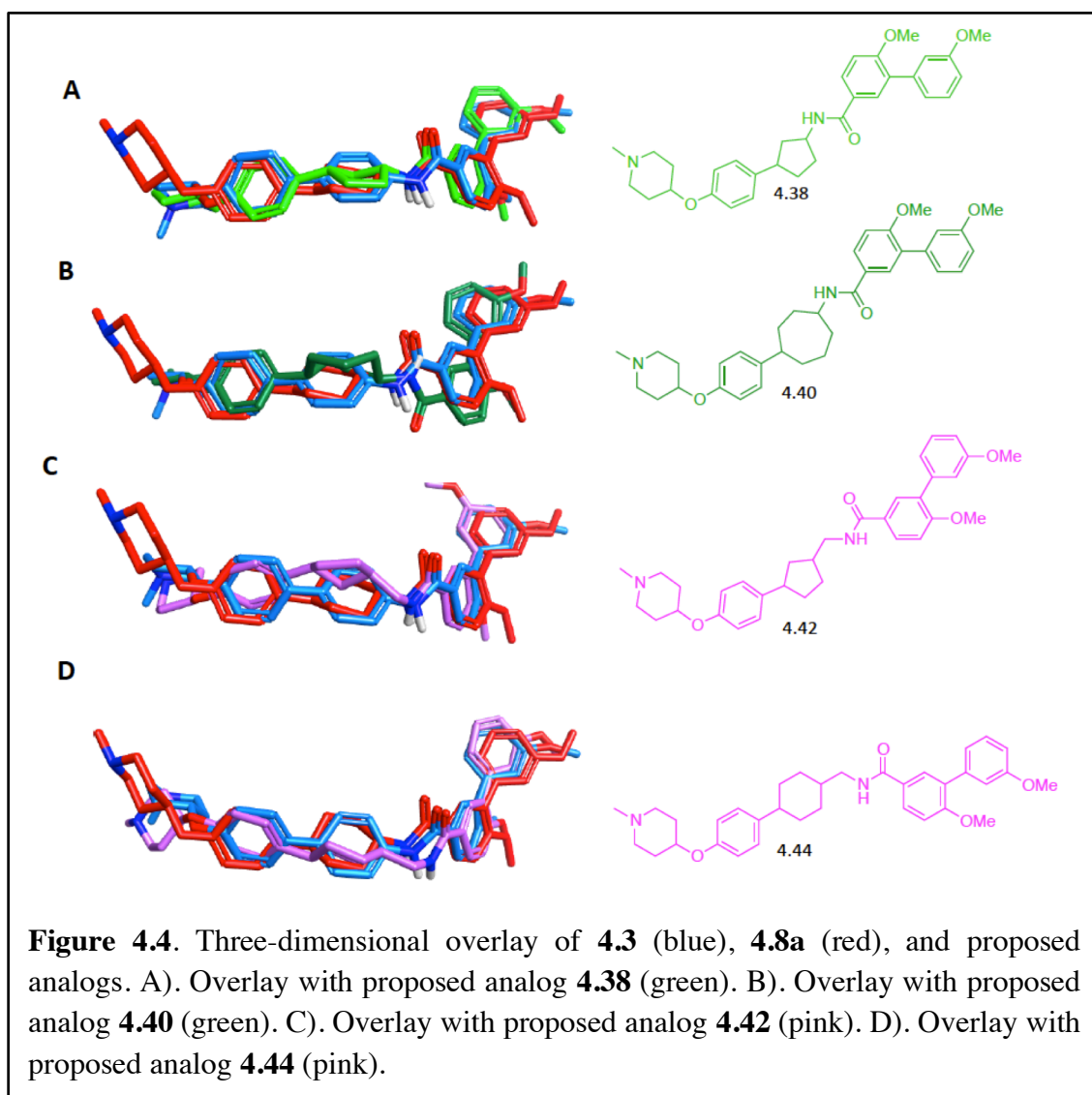
Entry	Compound	SKBr3	MCF-7
		(IC ₅₀ , μM) ^a	(IC ₅₀ , μM) ^a
4.3	-	0.47 ± 0.06	0.71 ± 0.02
4.8a		0.17 ± 0.02	0.22 ± 0.01

4.8b		2.57 ± 0.08	2.43 ± 0.05
4.23		2.87 ± 0.13	3.37 ± 0.14
4.6		>50	>50
4.7		>50	>50

^aValues represent mean \pm standard deviation for at least two separate experiments performed in triplicate.

Preliminary SARs indicate that the phenyl A-ring is necessary for maintaining anti-proliferative activity, while modifications to the B-ring could improve activity. Since no co-crystal structure of Hsp90 bound to C-terminal inhibitors has been solved, there is limited knowledge about the size and nature of this binding pocket. Therefore, a library of analogues containing the phenyl A-ring attached to various appendages in lieu of the cyclohexyl B-ring was pursued to identify an optimal scaffold that could orient both side chains and maximize interactions for increased inhibitory activity. Recent studies have suggested that an optimal distance between 7.7 and 12.1 Å from the amine to the amide is important for Hsp90 inhibitory activity.²⁷ Therefore, analogues containing five-, six- and seven-membered rings with varying distance and orientation of both the amine and amide were pursued. Additionally all compounds were synthesized with either the open or closed chain amine, as the dimethyl-propylamine has been identified as a noviose surrogate.³⁴ A three-dimensional overlay of the proposed analogs

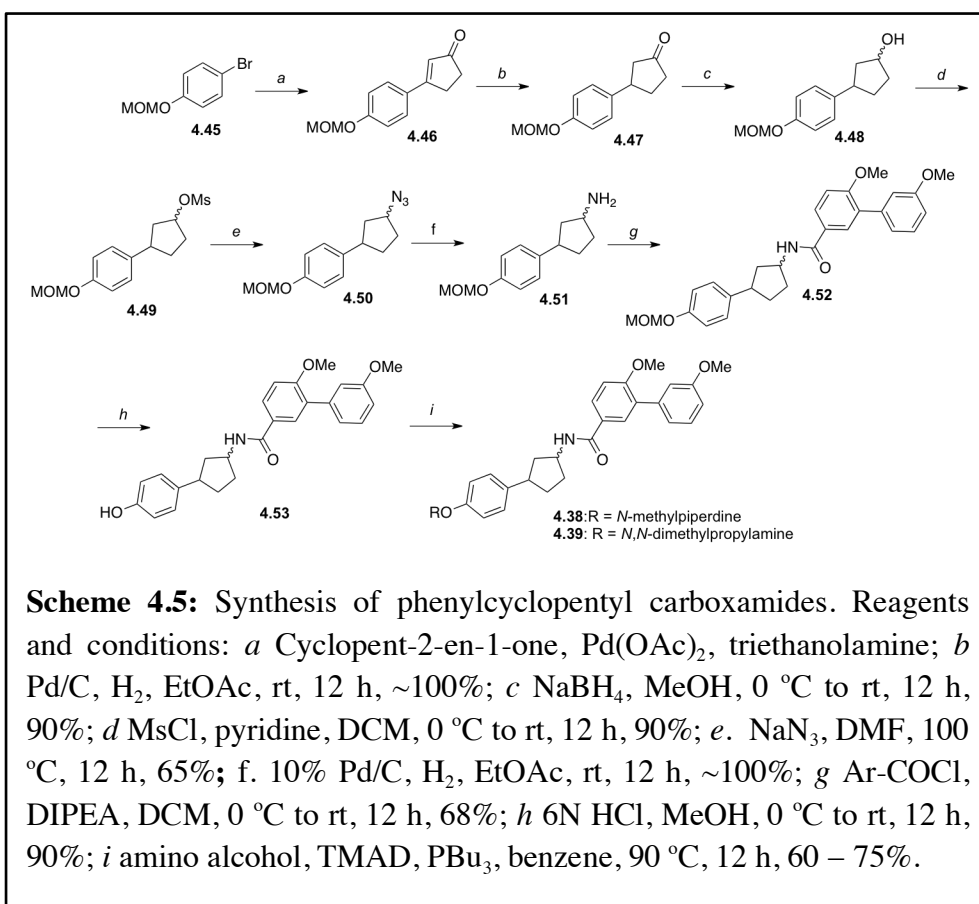
compared to the phenyl cyclohexyl was performed in order to better understand how the geometry would change with the various saturated B rings (Figure 4.4). The 3-D overlay study was carried out using the Forge Modeling Program, no bias was applied and **4.3** was used as the reference compound. Compounds **4.38** and **4.44** overlaid most similarly to **4.3** and **4.8a** and might be expected to bind similarly within the binding pocket and exhibit similar biological activity. Interestingly, the amide moiety in **4.40** doesn't overlay with **4.3** and **4.8a**, and from previous analog development we know that amide positioning is critical for inhibitor activity.³⁵⁻³⁶ This shift in the amide positioning may lead to decreased biological activity when compared to compounds **4.3** and **4.8a**.



Lastly, analog **4.42** does not overly well with **4.3** and **4.8a** and therefore might not be expected to exhibit similar biological activity as the cyclopentane ring is contorted out. Once the modeling studies were complete, analogues containing five-, six- and seven-membered rings with varying distances and orientations of both the amine and amide were synthesized.

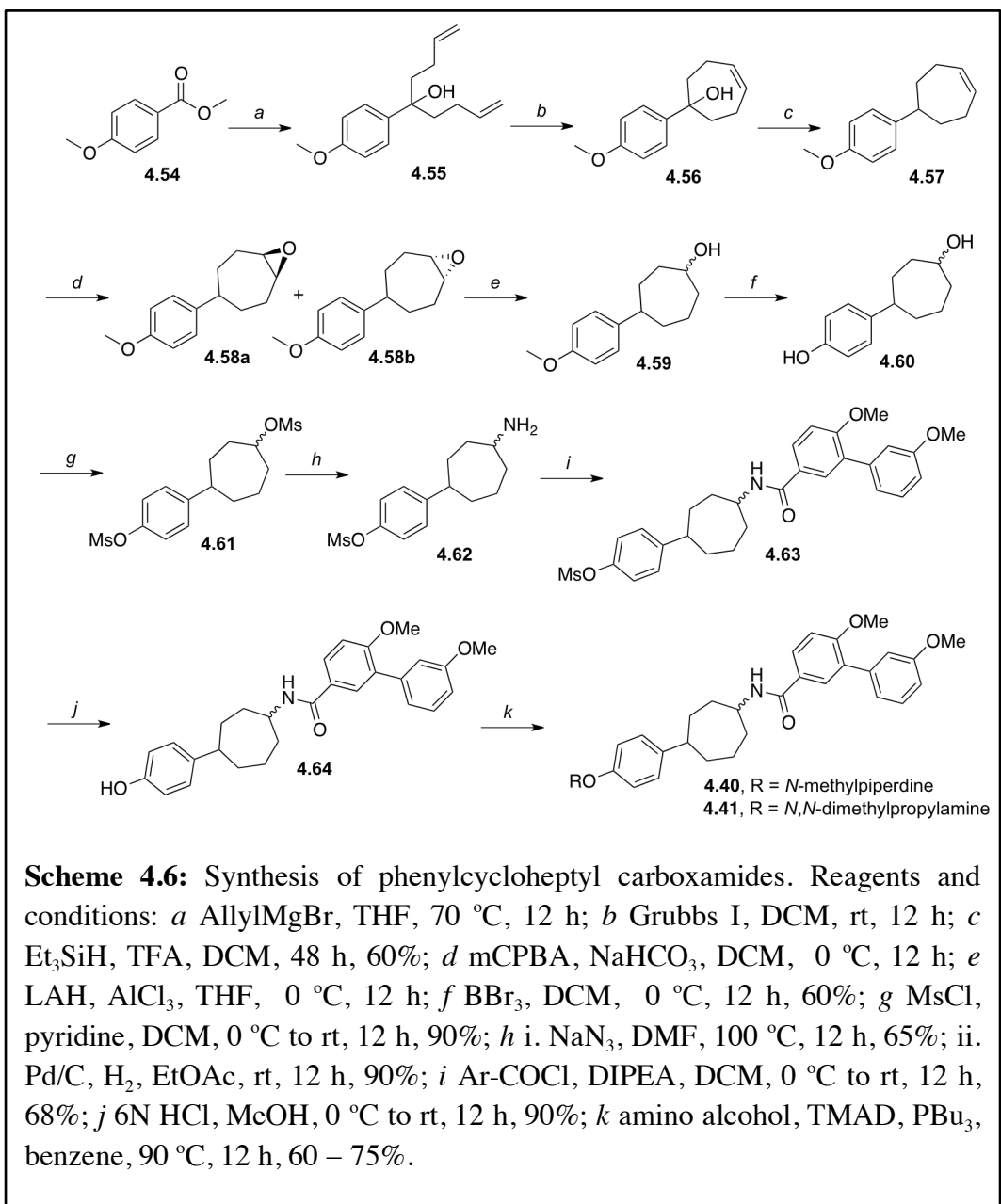
Preparation of analogues (**4.38** and **4.39**) that contain a five-membered saturated ring is illustrated in Scheme 4.5. Synthesis began by a Heck coupling between aryl bromide **4.45** and cyclopent-2-enone to yield **4.46**, which was subsequently reduced via palladium on carbon and hydrogen gas to afford cyclopentanone **4.47**.³⁷ Reduction of **4.47** with sodium borohydride gave

an inseparable mixture of *anti* and *syn* diastereomers, **4.48**, in a 7:3 ratio, respectively. The mixture of **4.48** was converted to the methanesulfonate ester, **4.49**, before nucleophilic substitution with sodium azide to produce **4.50**. Following reduction of the azide, the resulting amine was coupled with biaryl acid **4.15** to form the corresponding amide **4.52**. Removal of the methoxymethyl-protecting group present in **4.52** provided the free phenol, **4.53**. Mixture of diastereomers **4.53** was submitted to the KU Specialized Chemistry Center for separation. Unfortunately even with a chiral HPLC column the *syn* and *anti* were inseparable. Mitsunobu etherification of the resulting phenol, **4.53**, with 1-methyl-4-hydroxypiperidine (**4.17a**) finally furnished the desired product **4.38** and **4.39** in moderate yield.



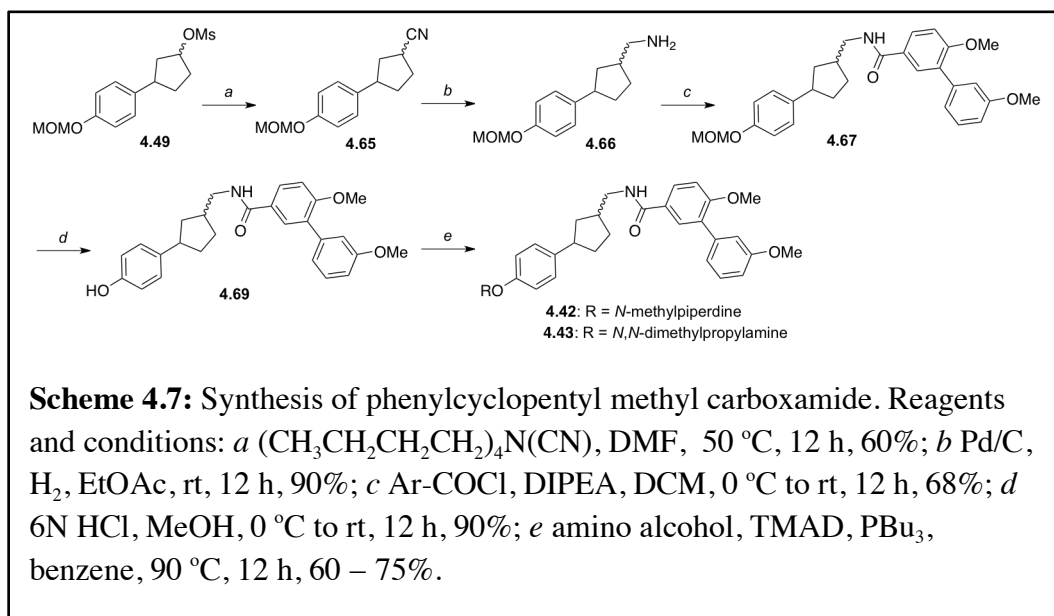
As shown in Scheme 4.6, synthesis of analogues that contain a seven-membered ring began via a Grignard coupling reaction of commercially available ester **4.54** with allyl

magnesium bromide to yield **4.55**.³⁸ Ring-closing metathesis using Grubbs first-generation catalyst, followed by removal of the hydroxyl group using triethylsilane provided the desired phenylcycloheptyl core, **4.57**. Oxidation of alkene **4.57** with meta-chloroperoxybenzoic acid resulted in an inseparable mixture of epoxides **4.58a** and **4.58b**, in a 1:1 ratio. Reduction of these epoxides with lithium aluminum hydride resulted in alcohol **4.59**, which upon acid-catalyzed cleavage of the methyl ether, provided **4.60**. Next, **4.60** was converted to methanesulfonate ester **4.61** before nucleophilic substitution with sodium azide and then subsequently reduced to afford amine **4.62**. Amide coupling of **4.62** with acid chloride **4.15** produced **4.63**, which after base-catalyzed deprotection of the methanesulfonate group gave the free phenol, **4.64**. Again phenol **4.64** was submitted to the KU Specialized Chemistry Center for hopeful separation and again separation of *syn* and *anti* was unattainable. Finally, Mitsunobu etherification of the resulting phenol with 1-methyl-4-hydroxypiperidine (**4.17a** and **4.17b**) furnished **4.40** and **4.41**.

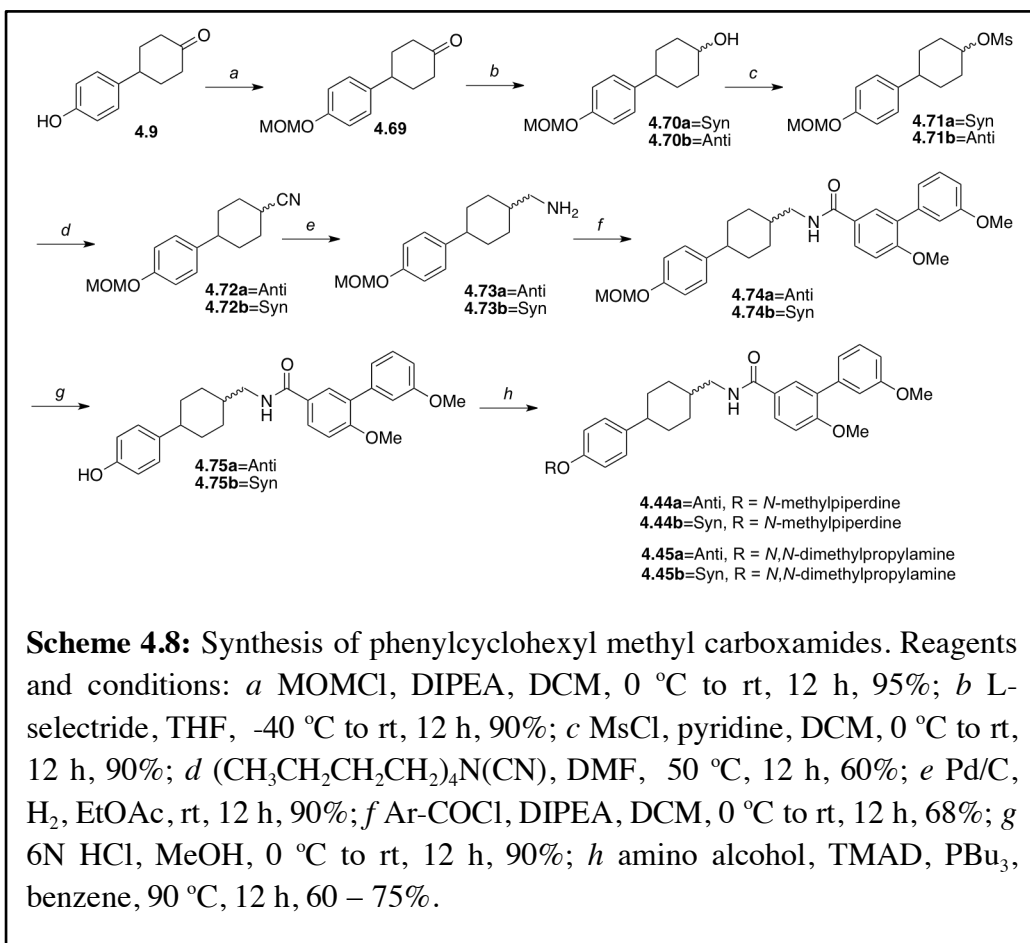


Compounds (**4.42** and **4.44**) that contain a methylene linker were envisioned to impart additional flexibility and explore potential binding interactions as a consequence of the flexible benzamide side chain. As shown in Scheme 4.7, construction of the phenylcyclopentyl methyl derivative (**4.42** and **4.43**) was accomplished by employing the methanesulfonate ester **4.49** as a key intermediate. Briefly, **4.49** was first converted to cyanide **4.65** via a nucleophilic substitution

reaction with tetra-butylammonium cyanide and then reduced with lithium aluminum hydride to afford the free amine, **4.66**.³⁹⁻⁴¹ Amide coupling of the resulting amine with acid chloride **4.15** gave the corresponding amide **4.67**. Acid-catalyzed deprotection of the methoxymethyl-protecting group generated the free phenol, **4.68**, which underwent Mitsunobu etherification to yield an inseparable mixture of *anti* and *syn* diastereomers of **4.42** and **4.43** in a 6:4 ratio respectively.



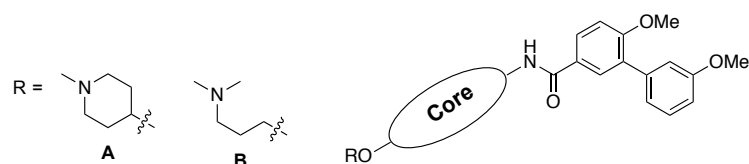
As outlined in Scheme 4.8, the phenylcyclohexyl methyl derivatives (**4.44a/b** and **4.45a/b**) were assembled following the general strategy described earlier.



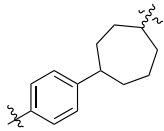
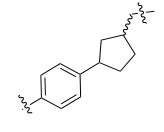
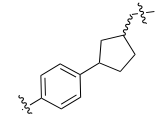
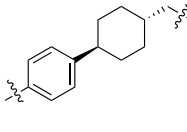
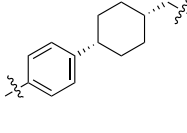
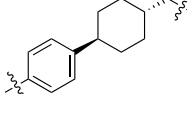
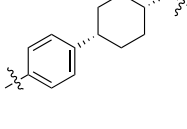
Upon construction of the modified B-ring analogues, the compounds were evaluated for their anti-proliferative activity against both breast cancer cell lines as summarized in Table 4.2. In general, compounds containing other ring systems were less active than the lead compound **4.8a**, suggesting the 1,4-*anti*-cyclohexyl core is optimal. Incorporation of either a five- or seven-membered ring system resulted in less potent analogues as evidenced by **4.38/4.39** and **4.40/4.41**, which were 25-40 fold less active than **4.8a**, highlighting the importance of orientation of the side chains for increased anti-proliferative activity. Inclusion of a methylene linker (**4.42**, **4.43**, **4.44a/b**, and **4.45a/b**, vs. **4.8a**) did not improve activity, suggesting that flexibility is not necessary for maximal activity. Surprisingly, the stereochemistry of analogues **4.44a/b** and

4.45a/b was not important for anti-proliferative activity, as both the *syn* and *anti*-diastereomers manifested similar activities. Additionally, compounds with noviose replacement N,N-dimethylaminopropoyl did not improve activity when compared to those analogs with N-methylpiperidine.

Table 4.2. Anti-proliferative activity of analogues containing various central core.



Entry	Core	Amine	SKBr3 (IC ₅₀ , μM) ^a	MCF-7 (IC ₅₀ , μM) ^a
4.8a		A	0.17 ± 0.02	0.22 ± 0.01
4.46		B	0.25 ± 0.05	0.34 ± 0.02
4.38		A	5.56±0.40	8.88±0.26
4.39		B	6.047±0.04	9.405±0.68
4.40		A	3.51 ± 0.14	4.17 ± 0.01

4.41		B	3.387±0.16	5.908±0.06
4.42		A	4.101±0.06	5.325±0.15
4.43		B	4.336±0.11	6.198±0.04
4.44a		A	2.98 ± 0.43	3.16 ± 0.31
4.45a		A	4.13 ± 0.74	5.0 ± 0.29
4.44b		B	1.023±0.04	0.92±0.22
4.45b		B	4.65±0.51	5.908±0.64

“Values represent mean ± standard deviation for at least two separate experiments performed in triplicate.

Validation of Hsp90 inhibition via Western Blot Analysis.

Western blot analyses were performed on MCF-7 cell lysates treated with six representative compounds (**4.8a**, **4.46**, **4.38**, **4.39**, **4.40** and **4.41**) to confirm these analogues manifest anti-proliferative activity via Hsp90 inhibition. As shown in Figure 4.5A, incubation with compound **4.8a** caused degradation of Hsp90-dependent clients EGFR and ER α , while

treatment with compound **4.46** led to the degradation of Her-2, EGFR, ER α , and Akt, clearly linking cell viability to Hsp90 inhibition. In addition, treatment of MCF-7 cells with **4.38** and **4.39** induced the degradation of the Hsp90-dependent client substrates c-Raf, and Akt (Figure 4.5B). Unfortunately, compounds **4.40** and **4.41** did not result in any client protein degradation (Figure 4.5C). The Hsp90-independent protein, actin remained unchanged, suggesting selective degradation of Hsp90-dependent client proteins. In addition, Hsp90 levels remained constant, which is a hallmark shared by Hsp90 C-terminal inhibitors. The 3-D overlay (Figure 4.4) supports the western blot data as compound **4.38** overlaid well with the parent compound **4.3**, however **4.40** did not overlay well as the position of the amide moiety was different from the parent compound. Clearly the size and geometry of the 7-membered ring affected the interaction of the compound with the C-terminal binding site, and resulted in **4.40** and **4.41** not targeting Hsp90.

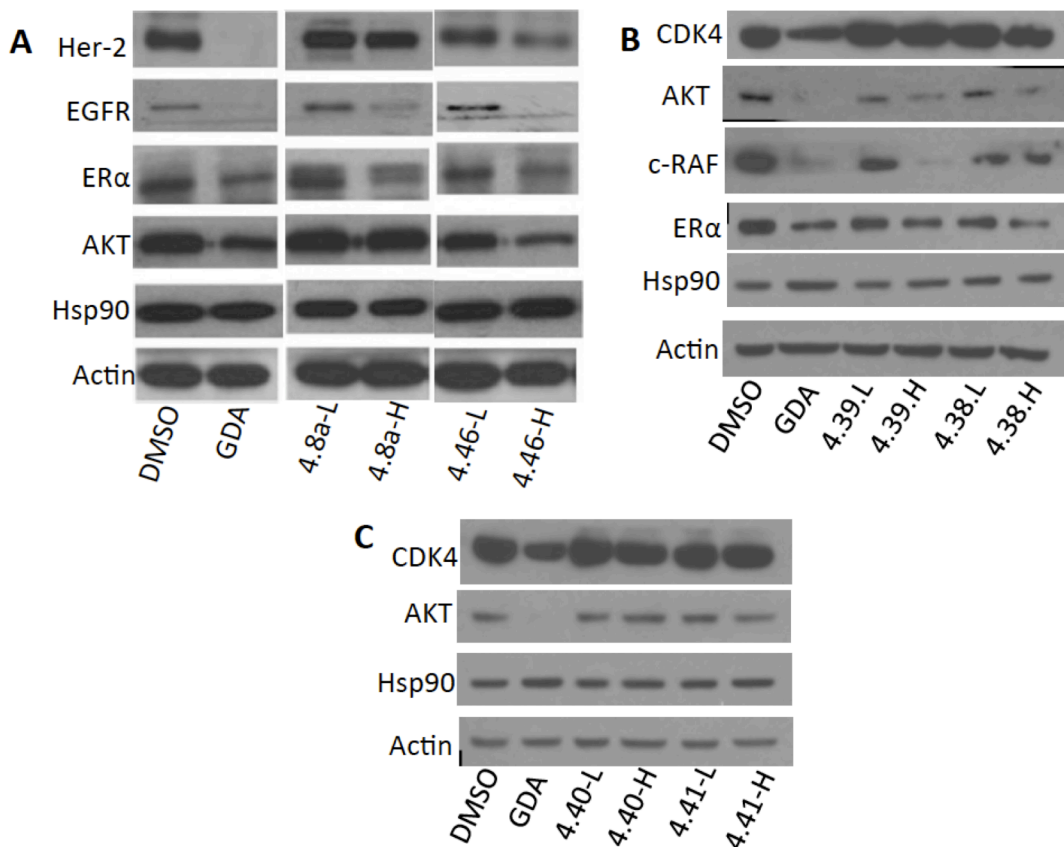


Figure 4.5. Western blot analyses of compounds after incubation with MCF-7 breast cancer cells for 24 h. A). Western blot analyses of Hsp90-dependent client proteins (Her2, EGFR, ER α and Akt) degradation after treatment with **4.8a** and **4.46**. B). Western blot analyses of Hsp90-dependent client proteins (CDK4, Akt, c-Raf, and ER α) degradation after treatment with **4.38** and **4.39**. C). Western blot analyses of Hsp90-dependent client proteins (CDK4 and Akt) degradation after treatment with **4.40** and **4.41**. L represents a concentration 1/2 of the anti-proliferative IC₅₀ value, while H represents a concentration 5-fold of the anti-proliferative IC₅₀ value. Geldanamycin (G, 0.5 μ M) and dimethylsulfoxide (D, 100%) were employed as positive and negative controls, respectively. Protein levels were measured compared to the level of Actin.

Conclusion

In summary, the biphenyl core was explored to identify an optimized scaffold for Hsp90 C-terminal inhibition. These studies led to the development of phenyl cyclohexyl carboxamides that manifest sub-micromolar to mid-nanomolar anti-proliferative activity against breast cancer cell lines. Structural investigations suggest that the central core is important for projection of the amine and amide side chains as evidenced by increased anti-proliferative activity. Furthermore, SAR studies on these side chains indicate the phenyl cyclohexyl derivatives exhibit a different binding mode as compared to other scaffolds. Discovery of the phenyl cyclohexyl core provides a new platform on which the development of more efficacious Hsp90 C-terminal inhibitors can be explored.

Materials and Methods

Anti-proliferation assays.

Cells were maintained in a 1:1 mixture of Advanced DMEM/F12 (Gibco) supplemented with non-essential amino acids, L-glutamine (2 mM), streptomycin (500 µg/mL), penicillin (100 units/mL), and 10% FBS. Cells were grown to confluence in a humidified atmosphere (37° C, 5% CO₂), seeded (2000/well, 100 µL) in 96-well plates, and allowed to attach overnight. Compound or GDA at varying concentrations in DMSO (1% DMSO final concentration) was added, and cells were returned to the incubator for 72 h. At 72 h, the number of viable cells was determined using an MTS/PMS cell proliferation kit (Promega) per the manufacturer's instructions. Cells incubated in 1% DMSO were used at 100% proliferation, and values were adjusted accordingly. IC₅₀ values were calculated from separate experiments performed in triplicate using GraphPad Prism.

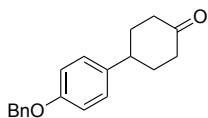
Western Blot Analyses.

MCF-7 cells were cultured as described above and treated with various concentrations of drug, GDA in DMSO (1% DMSO final concentration), or vehicle (DMSO) for 24 h. Cells were harvested in cold PBS and lysed in RIPA lysis buffer containing 1 mM PMSF, 2 mM sodium orthovanadate, and protease inhibitors on ice for 1 h. Lysates were clarified at 14000g for 10 min at 4° C. Protein concentrations were determined using the Pierce BCA protein assay kit per the manufacturer's instructions. Equal amounts of protein (20 µg) were electrophoresed under reducing conditions, transferred to a nitrocellulose membrane, and immunoblotted with the corresponding specific antibodies. Membranes were incubated with an appropriate horseradish peroxidase-labeled secondary antibody, developed with a chemiluminescent substrate, and visualized.

Chemistry General.

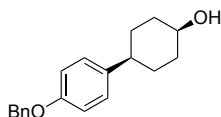
¹H NMR were recorded at 500 MHz (Avance AVIII 500 MHz spectrometer with a dual carbon/proton cryoprobe) or 400 (Bruker AVIIIHD 400 MHz NMR with a broadband X-channel detect gradient probe) and ¹³C NMR were recorded at 125 MHz (Bruker AVIII spectrometer equipped with a cryogenically cooled carbon observe probe). Chemical shifts are reported in δ (ppm) relative to the internal standard (CDCl₃, 7.26 ppm, or as stated). HRMS spectra were recorded with a LCT Premier with ESI ionization. ¹H and ¹³C NMR was used to verify that all tested compounds were >95% pure. TLC analysis was performed on glass backed silica gel plates and visualized by UV light. All solvents were reagent grade and used without further purification.

Synthesis and Compound Characterization



4-(4-(Benzyloxy)phenyl)cyclohexan-1-one (4.10).

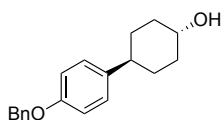
A solution of phenol **4.9** (1.0 g, 5.26 mmol) in anhydrous acetone was cooled to 0 °C and potassium carbonate (1.46 g, 11.5 mmol) was added, followed by a dropwise addition of benzyl bromide (0.94 ml, 7.89 mmol). The reaction mixture was then allowed to stir at rt. After 12 h, the reaction mixture was concentrated and the residue purified by column chromatography (SiO₂, 1:5, EtOAc: hexane) to afford **4.10** as a white amorphous solid (1.4 g, 95%): ¹H NMR (400 MHz, Chloroform-*d*) δ 7.46 – 7.35 (m, 4H), 7.35 – 7.30 (m, 1H), 7.19 – 7.14 (m, 2H), 6.96 – 6.91 (m, 2H), 5.05 (s, 2H), 3.03 – 2.90 (m, 1H), 2.53 – 2.45 (m, 4H), 2.25 – 2.13 (m, 2H), 1.99 – 1.82 (m, 2H). ¹³C NMR (126 MHz, CDCl₃) δ 211.48, 157.58, 137.31, 137.19, 128.74, 128.11, 127.74, 127.61, 115.02, 70.19, 42.08, 41.55, 34.34.



(1s,4s)-4-(4-(Benzyloxy)phenyl)cyclohexan-1-ol (4.11a).

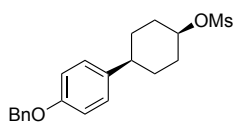
4-(4-(Benzyloxy)phenyl)cyclohexan-1-one **4.10** (1g, 3.57 mmol) was dissolved in anhydrous tetrahydrofuran (10 ml) and the solution was cooled to -40 °C. L-selectride (1.0 M in THF, 4.29 ml) was added dropwise to the solution and the reaction mixture was allowed to stir at rt for 12 h. The reaction mixture was concentrated and the residue was diluted with water. The suspension was acidified with 1N HCl and extracted with ethyl acetate. The organic layers were combined, dried (over Na₂SO₄), concentrated and purified by column chromatography (SiO₂, 1:4, EtOAc :

hexane) to afford **4.11a** as a white amorphous solid (920 mg, 92%): ^1H NMR (400 MHz, Chloroform-*d*) δ 7.49 – 7.37 (m, 4H), 7.37 – 7.32 (m, 1H), 7.22 – 7.17 (m, 2H), 6.98 – 6.92 (m, 2H), 5.06 (s, 2H), 4.14 (m, 1H), 2.52 (tt, $J = 11.4, 2.9$ Hz, 1H), 1.96 – 1.86 (m, 4H), 1.69 (tdd, $J = 12.2, 5.4, 2.3$ Hz, 4H). ^{13}C NMR (101 MHz, CDCl_3) δ 157.08, 139.96, 137.30, 128.63, 127.96, 127.79, 127.57, 114.70, 70.09, 65.70, 43.01, 33.10, 28.04.



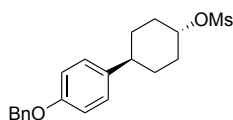
(1*r*,4*r*)-4-(4-(Benzyloxy)phenyl)cyclohexan-1-ol(4.11b).

Sodium borohydride (202.4 mg, 5.35 mmol) was added to an ice-cooled solution of 4-(4-(benzyloxy)phenyl)cyclohexan-1-one **4.10** (1g, 3.57 mmol) in methanol (10 ml) and the reaction mixture was allowed to stir at rt for 12 h. The reaction mixture was concentrated and the residue was diluted with water. The suspension was acidified with 1N HCl and extracted with ethyl acetate. The organic layers were combined, dried (over Na_2SO_4), concentrated and purified by column chromatography (SiO_2 , 1:4, EtOAc: hexane) to afford **4.11b** as a white amorphous solid (900 mg, 90%): ^1H NMR (400 MHz, Chloroform-*d*) δ 7.45 – 7.35 (m, 4H), 7.35 – 7.29 (m, 1H), 7.14 – 7.08 (m, 2H), 6.93 – 6.87 (m, 2H), 5.04 (s, 2H), 3.67 (dd, $J = 9.4, 5.5$ Hz, 1H), 2.45 (td, $J = 11.8, 3.5$ Hz, 1H), 2.08 (d, $J = 11.4$ Hz, 2H), 1.91 (d, $J = 12.7$ Hz, 2H), 1.56 – 1.39 (m, 4H). ^{13}C NMR (126 MHz, CDCl_3) δ 157.26, 139.13, 137.32, 128.71, 128.05, 127.78, 127.63, 114.80, 70.82, 70.17, 42.67, 36.12, 32.79.



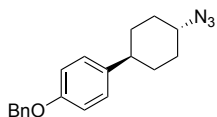
(1*s*,4*s*)-4-(4-(Benzyloxy)phenyl)cyclohexyl methanesulfonate (4.12a).

Triethylamine (0.28 ml, 2 mmol) was added to an ice-cooled solution of alcohol **4.11a** (282.4 mg, 1 mmol) in anhydrous THF (3 ml), followed by a dropwise addition of methanesulfonyl chloride (0.12 ml, 1.5 mmol). The reaction mixture was then allowed to stir at rt for 4 h. The reaction mixture was diluted with water and extracted with ethyl acetate. The organic layers were combined, dried (over Na₂SO₄), concentrated to yield **4.12a** as a white amorphous solid (339 mg, 94%) that was used in the next step without further purification.



(1*r*,4*r*)-4-(4-(Benzyloxy)phenyl)cyclohexyl methanesulfonate (4.12b).

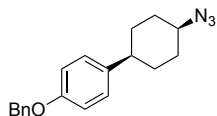
Compound **4.12b** was obtained following the procedure used for the synthesis of **4.12a**, as a white amorphous solid (92%): ¹H NMR (400 MHz, Chloroform-*d*) δ 7.45 – 7.35 (m, 4H), 7.35 – 7.29 (m, 1H), 7.12 – 7.07 (m, 2H), 6.94 – 6.89 (m, 2H), 5.04 (s, 2H), 4.69 (td, *J* = 11.2, 5.5 Hz, 1H), 3.03 (s, 3H), 2.53 – 2.42 (m, 1H), 2.27 (d, *J* = 11.9 Hz, 2H), 1.98 (d, *J* = 13.7 Hz, 2H), 1.72 (qd, *J* = 12.4, 11.8, 3.5 Hz, 2H), 1.55 (qd, *J* = 13.4, 3.1 Hz, 2H). ¹³C NMR (126 MHz, CDCl₃) δ 157.45, 137.98, 137.23, 128.72, 128.09, 127.71, 127.61, 114.93, 81.46, 70.18, 42.01, 39.00, 33.31, 32.47.



1-((1*r*,4*r*)-4-Azidocyclohexyl)-4-(benzyloxy)benzene (4.13a).

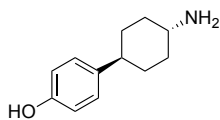
A mixture of methanesulfonate ester **4.12a** (361 mg, 1.0 mmol) and sodium azide (195 mg, 3.0 mmol) in DMF was heated at 100 °C. After 12 h, the reaction mixture was cooled to rt and

concentrated. The residue was diluted with water and extracted with ethyl acetate. The organic layers were combined, concentrated and purified by column chromatography (SiO₂, 1:20, EtOAc : hexane) to afford **4.13a** as a white amorphous solid (246 mg, 80%): ¹H NMR (400 MHz, Chloroform-*d*) δ 7.53 – 7.30 (m, 5H), 7.21 – 7.08 (m, 2H), 6.97 (tt, *J* = 5.7, 3.1 Hz, 2H), 5.07 (s, 2H), 3.36 (qt, *J* = 7.6, 3.4 Hz, 1H), 2.51 (ddd, *J* = 12.1, 7.7, 3.8 Hz, 1H), 2.23 – 2.07 (m, 2H), 2.00 (d, *J* = 8.4 Hz, 2H), 1.93-1.85 (m, 4H). ¹³C NMR (101 MHz, CDCl₃) δ 157.29, 138.59, 137.22, 128.63, 127.99, 127.66, 127.54, 114.79, 70.07, 59.97, 42.35, 32.84, 32.16.



1-((1s,4s)-4-Azidocyclohexyl)-4-(benzyloxy)benzene (4.13b).

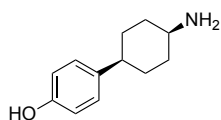
Compound **4.13b** was obtained following the procedure used for the synthesis of **4.13a**, as a white amorphous solid (85%): ¹H NMR (400 MHz, Chloroform-*d*) δ 7.46 – 7.35 (m, 4H), 7.35 – 7.30 (m, 1H), 7.17 – 7.12 (m, 2H), 6.95 – 6.90 (m, 2H), 5.03 (s, 2H), 3.95 (t, *J* = 3.1 Hz, 1H), 2.54 – 2.43 (m, 1H), 2.01 – 1.94 (m, 2H), 1.82 – 1.62 (m, 6H). ¹³C NMR (126 MHz, CDCl₃) δ 157.28, 139.43, 137.32, 128.71, 128.05, 127.81, 127.64, 114.82, 70.18, 57.23, 42.77, 30.18, 28.68.



4-((1r,4r)-4-Aminocyclohexyl)phenol (4.14a)

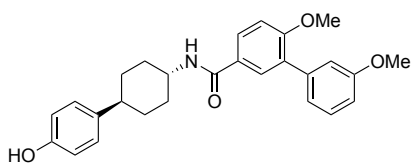
Palladium hydroxide (20% w/w, 20 mg) was added to a solution of **4.13a** (225 mg, 0.73 mmol) in MeOH/THF (3:1, 4 ml) and the resulting mixture was stirred under a hydrogen atmosphere. After 12 h, the reaction mixture was filtrated through Celite and the filtrate was

concentrated to get **4.14a** as a white amorphous solid (140 mg, ~100%): ^1H NMR (400 MHz, Chloroform-*d*) δ 6.98 (t, $J = 8.0$ Hz, 2H), 6.74 – 6.63 (m, 2H), 2.67 (tt, $J = 11.2, 4.0$ Hz, 1H), 2.34 (tt, $J = 12.1, 3.4$ Hz, 1H), 1.97 – 1.58 (m, 4H), 1.48 – 1.10 (m, 4H). ^{13}C NMR (126 MHz, $\text{CDCl}_3 + \text{CD}_3\text{OD}$) δ 154.79, 137.94, 127.60, 115.10, 50.04, 42.60, 34.75, 33.19. HRMS (ESI+) m/z : $[\text{M} + \text{H}^+]$ calculated for $\text{C}_{12}\text{H}_{18}\text{NO}$ 192.1388; found 192.1394.



4-((1*s*,4*s*)-4-Aminocyclohexyl)phenol (4.14b).

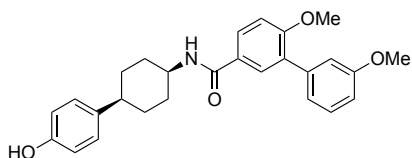
Compound **4.14b** was obtained following the procedure used for the synthesis of **4.14a**, as a white amorphous solid (~100%): ^1H NMR (400 MHz, Chloroform-*d*) δ 7.06 (dd, $J = 27.1, 8.2$ Hz, 2H), 6.73 (dd, $J = 8.7, 2.4$ Hz, 2H), 3.44 – 3.34 (m, 1H), 2.43 (d, $J = 32.2$ Hz, 1H), 2.18 (d, $J = 17.1$ Hz, 5H), 1.90 (d, $J = 11.6$ Hz, 1H), 1.86 – 1.60 (m, 4H). ^{13}C NMR (126 MHz, CDCl_3) δ 154.80, 137.33, 127.97, 115.32, 46.69, 43.77, 29.50, 27.05. HRMS (ESI+) m/z : $[\text{M} + \text{H}^+]$ calculated for $\text{C}_{12}\text{H}_{18}\text{NO}$ 192.1388; found 192.1398.



***N*-((1*r*,4*r*)-4-(4-Hydroxyphenyl)cyclohexyl)-3',6-dimethoxy-[1,1'-biphenyl]-3-carboxamide (4.16a).**

Triethylamine (0.11 ml, 0.79 mmol) was added to a solution of amine **4.14a** (50mg, 0.26 mmol) and acid **4.15** (81 mg, 0.32 mmol) in anhydrous dichloromethane (0.5 ml) and the solution was cooled to 0 $^{\circ}\text{C}$. At this temperature, EDCI•HCl (100 mg, 0.53 mmol) was added to

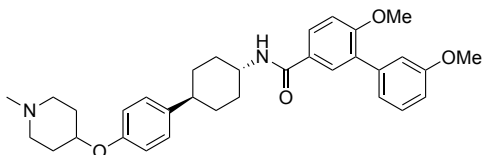
the reaction mixture and the resulting solution was then allowed to stir at rt. After 12 h, the reaction mixture was concentrated; the residue was diluted with water, and extracted with ethyl acetate. The organic layers were combined, concentrated and purified by column chromatography (SiO₂, 1:25, Acetone: DCM) to afford **4.16a** as a white amorphous solid (56 mg, 50%): ¹H NMR (500 MHz, Chloroform-*d*) δ 7.82 (dd, *J* = 8.5, 2.4 Hz, 1H), 7.68 (d, *J* = 2.4 Hz, 1H), 7.35 (t, *J* = 7.9 Hz, 1H), 7.10 (dt, *J* = 7.6, 1.2 Hz, 1H), 7.09 – 7.05 (m, 3H), 7.01 (d, *J* = 8.6 Hz, 1H), 6.92 (ddd, *J* = 8.4, 2.7, 1.0 Hz, 1H), 6.83 – 6.79 (m, 2H), 5.94 (d, *J* = 8.1 Hz, 1H, NH), 5.48 (s, 1H, OH), 4.03 (dtt, *J* = 12.7, 8.8, 4.4 Hz, 1H), 3.86 (s, 3H), 3.85 (s, 3H), 2.45 (tt, *J* = 12.1, 3.5 Hz, 1H), 2.19 (dd, *J* = 13.9, 3.4 Hz, 2H), 1.96 – 1.88 (m, 2H), 1.63 – 1.50 (m, 2H), 1.36 (qd, *J* = 12.7, 3.4 Hz, 2H). ¹³C NMR (126 MHz, CDCl₃) δ 166.52, 159.43, 159.10, 154.24, 139.16, 138.73, 130.57, 129.41, 129.25, 128.36, 127.87, 127.19, 122.14, 115.50, 115.42, 112.94, 111.02, 55.95, 55.48, 48.97, 42.73, 33.75, 33.34. HRMS (ESI+) *m/z*: [M + H⁺] calculated for C₂₇H₂₉NO₄Na 454.1994; found 454.1988.



***N*-((1*s*,4*s*)-4-(4-Hydroxyphenyl)cyclohexyl)-3',6-dimethoxy-[1,1'-biphenyl]-3-carboxamide (**4.16b**).**

Compound **4.16b** was obtained following the procedure used for the synthesis of **4.16a**, as an off-white amorphous solid (45%): ¹H NMR (400 MHz, Chloroform-*d*) δ 8.30 (s, 1H, OH), 7.80 (dd, *J* = 8.5, 2.4 Hz, 1H), 7.74 (d, *J* = 2.5 Hz, 1H), 7.33 (dd, *J* = 4.4, 2.9 Hz, 1H), 7.13 – 7.05 (m, 4H), 7.01 (d, *J* = 8.6 Hz, 1H), 6.90 (ddd, *J* = 8.2, 2.6, 1.0 Hz, 1H), 6.87 – 6.82 (m, 2H), 6.37 (d, *J* = 7.4 Hz, 1H), 4.36 (dt, *J* = 7.3, 3.6 Hz, 1H), 3.85 (s, 3H), 3.83 (s, 3H), 2.63 – 2.54 (m, 1H), 2.05

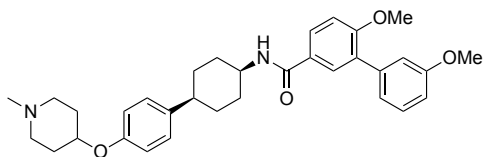
– 1.93 (m, 2H), 1.88 – 1.71 (m, 4H), 1.64 (qd, $J = 14.4, 13.3, 4.8$ Hz, 2H). ^{13}C NMR (126 MHz, CDCl_3) δ 166.49, 159.40, 159.01, 155.42, 139.13, 139.10, 130.60, 129.48, 129.22, 128.07, 127.86, 127.56, 122.10, 116.06, 115.54, 112.94, 110.96, 55.92, 55.43, 45.64, 41.89, 30.28, 29.11. HRMS (ESI+) m/z : $[\text{M} + \text{H}^+]$ calculated for $\text{C}_{27}\text{H}_{29}\text{NO}_4$ 432.2175; found 432.2170.



3',6-Dimethoxy-N-((1*r*,4*r*)-4-(4-((1-methylpiperidin-4-yl)oxy)phenyl)cyclohexyl)-[1,1'-biphenyl]-3-carboxamide (4.8a).

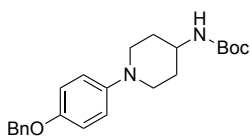
Diisopropylazodicarboxylate (23 μL , 0.12 mmol) was added to an ice-cooled solution of phenol **4.13a** (25 mg, 0.06 mmol), N-methyl-4-hydroxy-piperidine (10.4 mg, 0.09 mmol) and triphenylphosphine (24 mg, 0.09 mmol) in anhydrous THF (0.25 mL) and resulting solution was then allowed to stir at room temperature for 12 hours. The reaction mixture was concentrated under reduced pressure and the residue was purified by column chromatography (SiO_2 , Methanol: CH_2Cl_2 , 1:25) to afford a white amorphous solid (12 mg, 40%): ^1H NMR (500 MHz, Chloroform- d) δ 7.81 (dd, $J = 8.6, 2.3$ Hz, 1H), 7.68 (d, $J = 2.4$ Hz, 1H), 7.35 (t, $J = 7.9$ Hz, 1H), 7.15 – 7.08 (m, 3H), 7.07 (dd, $J = 2.7, 1.6$ Hz, 1H), 7.01 (d, $J = 8.7$ Hz, 1H), 6.91 (ddd, $J = 8.3, 2.6, 0.9$ Hz, 1H), 6.87 – 6.81 (m, 2H), 5.93 (d, $J = 8.1$ Hz, NH), 4.45 – 4.35 (m, 1H), 4.03 (dtt, $J = 16.4, 8.5, 4.3$ Hz, 1H), 3.86 (s, 3H), 3.85 (s, 3H), 2.94 – 2.80 (m, 2H), 2.75 – 2.56 (m, 2H), 2.53 – 2.41 (m, 4H), 2.20 (ddd, $J = 11.2, 7.8, 3.8$ Hz, 4H), 1.95 (ddd, $J = 14.6, 10.6, 5.9$ Hz, 4H), 1.62 (qd, $J = 13.2, 3.3$ Hz, 2H), 1.36 (qd, $J = 12.6, 3.4$ Hz, 2H). ^{13}C NMR (126 MHz, CDCl_3) δ 166.33, 159.42, 159.02, 155.35, 139.54, 139.19, 130.52, 129.39, 129.23, 128.31, 127.93, 127.33, 122.13, 116.06, 115.50, 112.90, 110.98, 77.37, 55.93, 55.47, 51.82, 48.82, 45.43, 42.85, 33.75,

33.33, 29.84. HRMS (ESI+) m/z : $[M + H^+]$ calculated for $C_{33}H_{41}N_2O_4$ 529.3066; found 529.3058.



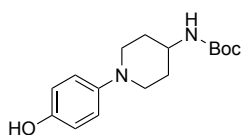
3',6-Dimethoxy-N-((1*s*,4*s*)-4-(4-((1-methylpiperidin-4-yl)oxy)phenyl)cyclohexyl)-[1,1'-biphenyl]-3-carboxamide (4.8b).

Compound **4.8b** was obtained following the procedure utilized for the synthesis of **4.8a**, as a white amorphous solid (36%): 1H NMR (400 MHz, Chloroform-*d*) δ 7.80 (dd, $J = 8.5, 2.4$ Hz, 1H), 7.72 (d, $J = 2.4$ Hz, 1H), 7.36 (t, $J = 7.9$ Hz, 1H), 7.18 – 7.06 (m, 4H), 7.02 (d, $J = 8.6$ Hz, 1H), 6.92 (ddd, $J = 8.3, 2.6, 1.0$ Hz, 1H), 6.87 – 6.81 (m, 2H), 6.27 (d, $J = 7.2$ Hz, NH), 4.43 – 4.31 (m, 2H), 3.87 (s, 3H), 3.85 (s, 3H), 2.81 (d, $J = 9.3$ Hz, 2H), 2.66 – 2.55 (m, 1H), 2.55 – 2.35 (m, 5H), 2.11 (d, $J = 10.1$ Hz, 2H), 2.01 (dd, $J = 13.2, 3.3$ Hz, 2H), 1.96 – 1.73 (m, 4H), 1.72 – 1.58 (m, 2H). ^{13}C NMR (126 MHz, $CDCl_3$) δ 166.60, 159.51, 159.12, 155.53, 139.23, 139.22, 130.71, 129.59, 129.32, 128.18, 127.97, 127.67, 122.21, 116.17, 115.56, 113.05, 111.07, 77.48, 56.03, 55.54, 52.09, 45.75, 45.05, 42.00, 30.39, 29.92, 29.22. HRMS (ESI+) m/z : $[M + H^+]$ calculated for $C_{33}H_{41}N_2O_4$ 529.3066; found 529.3066.



tert-Butyl (1-(4-(benzyloxy)phenyl)piperidin-4-yl)carbamate (4.20).

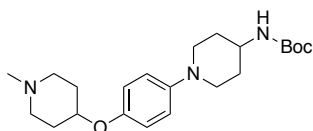
A mixture of iodide **4.18** (200 mg, 0.65 mmol), *tert*-butyl piperidin-4-ylcarbamate (194 mg, 0.97 mmol), sodium *tert*-butoxide (93 mg, 0.97 mmol), 2-dicyclohexylphosphino-2',4',6'-triisopropylbiphenyl (15.4 mg, 0.03 mmol) and tris(dibenzylideneacetone)dipalladium(29.3 mg, 0.03 mmol) was suspended in toluene (2 mL) and the resulting mixture was purged with argon for 20 min before being heated at 130 °C for 1 h under microwave conditions. The reaction mixture was concentrated and the residue was purified by column chromatography (SiO₂, 1:9, EtOAc : hexane) to afford **4.20** as a yellow amorphous solid (90 mg, 37%): ¹H NMR (400 MHz, Chloroform-*d*) δ 7.44 – 7.34 (m, 4H), 7.32 (d, *J* = 7.1 Hz, 1H), 6.89 (s, 4H), 5.01 (s, 2H), 4.51 – 4.42 (m, 1H), 3.58 (s, 1H), 3.44 (d, *J* = 12.3 Hz, 2H), 2.75 (t, *J* = 11.3 Hz, 2H), 2.04 (d, *J* = 12.6 Hz, 2H), 1.55 (qd, *J* = 11.7, 3.8 Hz, 2H), 1.46 (s, 9H). ¹³C NMR (101 MHz, CDCl₃) δ 156.68, 146.20, 135.87, 130.26, 128.67, 127.99, 127.62, 118.89, 115.69, 77.36, 70.65, 50.32, 50.26, 32.83, 28.58. HRMS (ESI+) *m/z*: [M + H⁺] calculated for C₂₃H₃₁N₂O₃ 383.2335; found 383.2334.



***tert*-Butyl (1-(4-hydroxyphenyl)piperidin-4-yl)carbamate (4.21).**

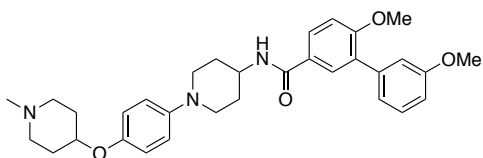
Palladium hydroxide (20% w/w, 20 mg) was added to a solution of **4.20** (85 mg, 0.22 mmol) in MeOH/THF (2:1, 3 ml) and the resulting mixture was stirred under a hydrogen atmosphere for 12 h. The reaction mixture was filtrated through Celite and the filtrate was concentrated to get **4.21** as a white amorphous solid (65 mg, ~100%): ¹H NMR (400 MHz, Chloroform-*d*) δ 6.85 (d, *J* = 8.4 Hz, 2H), 6.75 (d, *J* = 8.4 Hz, 2H), 4.63 – 4.41 (m, 1H), 4.48 (s, 1H), 3.56 (s, 1H), 3.40 (d, *J* = 12.0 Hz, 2H), 2.73 (t, *J* = 11.8 Hz, 2H), 2.04 (d, *J* = 12.5 Hz, 2H), 1.56 (qd, *J* = 11.7, 3.8 Hz,

2H), 1.46 (s, 9H). ^{13}C NMR (101 MHz, CDCl_3) δ 151.47, 119.24, 115.95, 77.36, 50.52, 50.50, 32.83, 28.55. HRMS (ESI+) m/z : $[\text{M} + \text{H}^+]$ calculated for $\text{C}_{16}\text{H}_{25}\text{N}_2\text{O}_3$ 293.1865; found 293.1867.



***tert*-Butyl (1-(4-((1-Methylpiperidin-4-yl)oxy)phenyl)piperidin-4-yl)carbamate (4.22).**

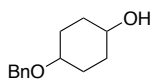
Diisopropylazodicarboxylate (85 μL , 0.43 mmol) was added to an ice-cooled solution of phenol **4.21** (63 mg, 0.21 mmol), N-methyl-4-hydroxy-piperidine (37 mg, 0.32 mmol) and triphenylphosphine (87 mg, 0.43 mmol) in anhydrous THF (0.20 mL) and the resulting solution was then allowed to stir at rt for 12 h. The reaction mixture was concentrated under reduced pressure and the residue was purified by column chromatography (SiO_2 , Methanol: CH_2Cl_2 , 1:25) to afford **4.22** as a brownish amorphous solid (42 mg, 50%): ^1H NMR (400 MHz, Chloroform-*d*) δ 6.89 (d, $J = 8.7$ Hz, 2H), 6.81 (d, $J = 8.7$ Hz, 2H), 4.61 – 4.52 (m, 1H), 4.51 – 4.41 (m, 1H), 3.58 (s, 1H, NH), 3.46 (d, $J = 12.4$ Hz, 2H), 3.39 – 3.16 (m, 4H), 2.76 (d, $J = 4.8$ Hz, 5H), 2.67 – 2.50 (m, 2H), 2.19 (d, $J = 15.2$ Hz, 2H), 2.09 – 1.99 (m, 2H), 1.55 (qd, $J = 11.7$, 3.8 Hz, 2H), 1.45 (s, 9H). ^{13}C NMR (101 MHz, CDCl_3) δ 155.33, 149.87, 147.09, 118.84, 117.17, 77.48, 77.36, 51.63, 50.05, 49.93, 44.00, 32.70, 28.57, 27.02. HRMS (ESI+) m/z : $[\text{M} + \text{H}^+]$ calculated for $\text{C}_{22}\text{H}_{36}\text{N}_3\text{O}_3$ 390.2757; found 390.2760.



3',6-Dimethoxy-N-(1-(4-((1-methylpiperidin-4-yl)oxy)phenyl)piperidin-4-yl)-[1,1'-biphenyl]-3-carboxamide (4.23).

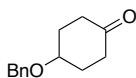
Trifluoroacetic acid (30% v/v in DCM, 0.27 mmol) was added to a solution of **4.22** (40 mg, 0.11 mmol) in dichloromethane (0.5 ml) and the resulting solution was stirred at rt for 4 h. The reaction mixture was then neutralized with 7N-ammoniated methanol and concentrated to get amine, which was used in the next step without further purification.

Triethylamine (0.05 ml, 0.33 mmol) was added to a solution of amine (0.11 mmol) and biaryl acid **4.15** (43 mg, 0.17 mmol) in dry dichloromethane (0.5 ml) and the solution was cooled to 0 °C. At this temperature, EDCI•HCl (33 mg, 0.17 mmol) was added to the reaction mixture and the resulting solution was then allowed to stir at rt for 16 h. The reaction mixture was concentrated and the residue was purified by column chromatography (SiO₂, methanol:DCM, 1:25) to afford **4.23** as a white amorphous solid (29%); ¹H NMR (400 MHz, Chloroform-*d*) δ 7.80 (d, *J* = 8.7 Hz, 1H), 7.67 (d, *J* = 2.2 Hz, 1H), 7.35 (t, *J* = 8.1 Hz, 1H), 7.13 – 7.03 (m, 2H), 7.01 (d, *J* = 8.7 Hz, 1H), 6.91 (d, *J* = 8.7 Hz, 3H), 6.83 (d, *J* = 8.7 Hz, 1H), 5.95 (d, *J* = 7.9 Hz, 1H), 4.49 – 4.41 (m, 1H), 4.18 – 4.05 (m, 1H), 3.86 (s, 3H), 3.85 (s, 3H), 3.56 – 3.48 (m, 2H), 3.12 – 2.91 (m, 4H), 2.86 (t, *J* = 11.7 Hz, 2H), 2.62 (s, 3H), 2.48 – 2.30 (m, 3H), 2.19 – 2.02 (m, 4H), 1.67 (q, *J* = 11.6, 11.1 Hz, 2H). ¹³C NMR (101 MHz, CDCl₃) δ 166.49, 159.48, 159.20, 146.76, 141.72, 139.14, 130.69, 129.44, 129.26, 128.29, 127.09, 122.13, 118.83, 117.30, 115.57, 112.94, 111.06, 77.36, 55.96, 55.49, 53.56, 50.08, 47.10, 44.68, 32.50, 28.29. HRMS (ESI+) *m/z*: [M + Na⁺] calculated for C₃₂H₃₉N₃O₄Na 552.2838; found 552.2838.



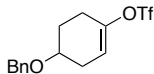
4-(Benzyloxy)cyclohexanol (4.25).

Sodium hydride (0.480g, 20mmol) was added to an ice-cooled solution of cyclohexane-1,4-diol (1.16g, 10mmol) in anhydrous DMF (25mL), followed by a dropwise addition of benzyl bromide (1.43mL, 12.5mmol). The reaction mixture was allowed to stir at rt for 12 h. The reaction mixture was quenched with brine and 1M HCl, and extracted with EtOAc. The organic layers were combined, dried, concentrated and purified via column chromatography (SiO₂, 1:1 EtOAc:Hex) to afford **4.25** as a white amorphous solid (70% yield): ¹H NMR (500 MHz, Chloroform-d) δ 7.27 (d, *J* = 4.4 Hz, 3H), 7.19 (s, 2H), 4.47 (s, 2H), 3.64 (tt, *J* = 9.5, 4.1 Hz, 1H), 3.32 (tt, *J* = 9.7, 4.0 Hz, 1H), 2.04 – 1.96 (m, 2H), 1.92 (dddd, *J* = 10.3, 6.1, 2.8, 1.5 Hz, 2H), 1.51 – 1.42 (m, 3H), 1.41 – 1.18 (m, 4H). ¹³C NMR (126 MHz, CDCl₃) δ 138.94, 128.37 (2Cs), 127.49 (2Cs), 127.45, 86.21, 70.17, 69.70, 32.71 (2Cs), 29.32 (2Cs). HRMS (ESI+) *m/z*: [M + Na⁺] calculated for C₁₃H₁₈O₂Na 229.1205; found 229.1214.



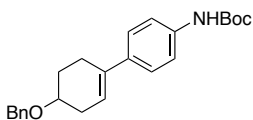
4-(Benzyloxy)cyclohexanone (4.26).

Pyridinium chlorochromate (1.4g, 6.49mmol) and 4A molecular sieves (1.4g) were added to a solution of **4.25** (0.89g, 4.32mmol) in anhydrous DCM (40mL) and the reaction mixture was stirred at rt for 12 h. The reaction was concentrated and the residue was purified via column chromatography (SiO₂, 1:1 EtOH:Hex) to yield **4.26** as a white amorphous solid product (50% yield): ¹H NMR (500 MHz, Chloroform-d) δ 7.32 – 7.29 (m, 4H), 4.54 (s, 2H), 3.76 (tt, *J* = 5.7, 2.9 Hz, 1H), 2.56 (dddd, *J* = 15.2, 10.7, 5.2, 1.2 Hz, 2H), 2.24 – 2.18 (m, 2H), 2.09 (dtdd, *J* = 11.7, 5.9, 4.4, 1.2 Hz, 2H), 1.96 – 1.84 (m, 2H). ¹³C NMR (126 MHz, CDCl₃) δ 211.30, 138.49, 128.47 (2Cs), 127.45, 127.41, 86.21, 72.22, 37.23 (2Cs), 30.55 (2Cs).



4-(Benzyloxy)cyclohex-1-en-1-yl trifluoromethanesulfonate (4.27).

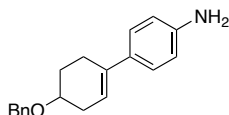
Freshly prepared LDA (1.18 mmol) was taken in a 25 ml 2-neck round flask and cooled to -78°C. A solution of ketone **4.26** (0.20 g, 0.98 mmol) in anhydrous THF (2 ml) was added dropwise to the flask and the reaction mixture was stirred for 15 min at the same temperature. A solution of *N*-bisphenyltriflate (385 mg, 1.08 mmol) in THF (1 mL) was added and the reaction mixture was then allowed to stir at rt for 90 minutes. The reaction was quenched with saturated NH₄Cl, diluted with water, and extracted with EtOAc (3x 15mL). The organic layers were combined, dried, and concentrated to obtain **4.27** as white amorphous solid (185 mg, 55%) that was used in the next step without further purification.



tert-Butyl (4'-(benzyloxy)-2',3',4',5'-tetrahydro-[1,1'-biphenyl]-4-yl)carbamate (4.29).

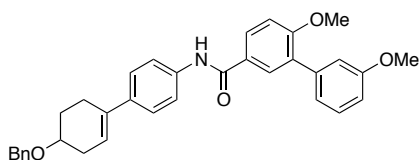
A mixture of triflate **4.27** (160 mg, 0.48 mmol), 4-boc-aminophenyl boronic acid **4.28** (170 mg, 0.71 mmol), cesium carbonate (310 mg, 0.95 mmol) and tetrakis(triphenylphosphine)palladium (10 mg, 0.14 mmol) was suspended in anhydrous DMF (4 mL) was purged with argon for 20 min before heating at 100 °C for 12 h. The reaction mixture was cooled to rt; diluted with saturated LiCl and extracted with EtOAc (3x 15mL). The organic layers were combined, dried, concentrated and the residue purified by column chromatography (SiO₂, 1:3, EtOAc : hexane) to afford **4.29** as a solid (30%): ¹H NMR (400 MHz, Chloroform-d) δ 7.45 – 7.34 (m, 4H), 7.32 – 7.25 (m, 5H), 6.48 (s, 1H), 5.97 (dt, *J* = 5.0, 1.6 Hz, 1H), 4.65 (d, *J* = 4.8 Hz, 2H), 3.76 (ddq, *J* = 9.9, 5.1, 3.0, 2.6 Hz, 1H), 2.66 – 2.53 (m, 2H), 2.52 – 2.39 (m, 1H),

2.35 – 2.24 (m, 1H), 2.13 (dtd, $J = 9.8, 4.7, 2.4$ Hz, 1H), 1.86 (dtd, $J = 12.6, 9.5, 5.5$ Hz, 1H), 1.53 (d, $J = 4.7$ Hz, 9H). ^{13}C NMR (126 MHz, CDCl_3) δ 172.18, 138.80, 136.84, 135.74, 134.31, 129.65 (2C), 128.51, 127.80, 127.67, 127.31, 125.61, 123.50 (2C), 118.66, 80.95, 73.63, 70.13, 32.25, 29.82, 28.71, 28.42, 28.18, 26.07. HRMS (ESI+) m/z : $[\text{M} + \text{Na}^+]$ calculated for $\text{C}_{24}\text{H}_{29}\text{NO}_3\text{Na}$ 402.2045; found 402.2027.



4'-(Benzyloxy)-2',3',4',5'-tetrahydro-[1,1'-biphenyl]-4-amine (4.30).

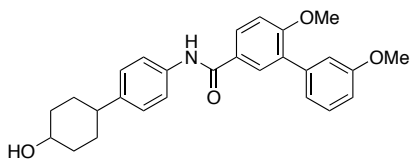
4.29 (0.1g, 0.36 mmol) was dissolved in anhydrous DCM (1 mL) and the solution was cooled to 0°C . Trifluoroacetic Acid (30% wt./vol, 0.5 mL) was added to the solution and the reaction mixture was allowed stir at rt for 3 h. The reaction was concentrated and the crude product (~100%) was used directly in the next step without further purification: HRMS (ESI+) m/z : $[\text{M} + \text{H}^+]$ calculated for $\text{C}_{19}\text{H}_{21}\text{NO}$ 280.1701; found 280.1700.



N-(4'-(Benzyloxy)-2',3',4',5'-tetrahydro-[1,1'-biphenyl]-4-yl)-3',6-dimethoxy-[1,1'-biphenyl]-3-carboxamide (4.31).

Thionyl chloride (0.13 ml, 0.75 mmol) was added to a solution of biaryl acid **4.15** (97 mg, 0.38 mmol) in anhydrous tetrahydrofuran (2 ml) and the solution was refluxed for 3h. The solution was then concentrated under vacuum to get acid chloride **4.15a** (105 mg) as brown semi-solid that was used directly in the next step.

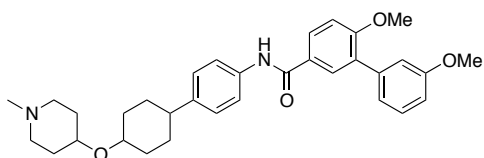
DIPEA (0.13 ml, 0.75 mmol) was added to an ice-cooled solution of acid chloride in anhydrous DCM (1 ml), followed by a dropwise addition of amine **4.30** (50 mg, 0.25 mmol). The solution was then allowed to stir at rt for 12h. The reaction mixture was concentrated and the residue was purified by column chromatography (SiO₂, 1:25, Acetone: DCM) to afford **4.31** as a white amorphous solid (80%): ¹H NMR (400 MHz, Chloroform-d) δ 7.87 (s, 1H), 7.82 (dd, *J* = 8.6, 2.4 Hz, 1H), 7.74 (d, *J* = 2.4 Hz, 2H), 7.51 (d, *J* = 8.7 Hz, 2H), 7.37 – 7.21 (m, 8H), 7.07 – 6.95 (m, 2H), 6.85 – 6.77 (m, 1H), 5.92 (td, *J* = 3.6, 1.9 Hz, 1H), 4.56 – 4.51 (m, 2H), 3.78 (d, *J* = 12.4 Hz, 6H), 3.73 – 3.64 (m, 1H), 2.56 – 2.46 (m, 2H), 2.43 – 2.33 (m, 1H), 2.26 – 2.17 (m, 1H), 2.08 – 1.98 (m, 2H). ¹³C NMR (101 MHz, CDCl₃) δ 169.56, 158.32 (2Cs), 143.69, 139.09, 137.23 (2Cs), 133.03, 130.41, 129.62, 128.74(2Cs), 128.36 (2Cs), 127.93 (2Cs), 127.69 (2Cs), 127.55, 124.68, 121.09 (2Cs), 119.08, 118.75, 115.84 (2Cs), 114.07, 79.86, 68.98, 55.25(2Cs), 27.41, 25.73, 23.11. HRMS (ESI+) *m/z*: [M + H⁺] calculated for C₃₄H₃₃NO₄ 520.2488; found 520.2485.



***N*-(4-(4-Hydroxycyclohexyl)phenyl)-3',6-dimethoxy-[1,1'-biphenyl]-3-carboxamide
(4.32).**

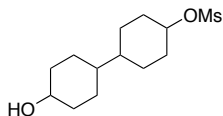
Palladium on carbon (10% w/w, 20 mg) was added to a solution of **4.31** (223 mg, 1.0 mmol) in MeOH (3 ml) and the suspension was stirred at rt under a hydrogen atmosphere. After 12 h, the reaction mixture was filtrated through Celite and the filtrate was concentrated to get **4.32** as an off-white amorphous solid (~100%): ¹H NMR (500 MHz, Chloroform-d) δ 7.85 (d, *J* = 8.0 Hz, 1H), 7.81 – 7.77 (m, 1H), 7.71 (d, *J* = 2.3 Hz, 1H), 7.44 (d, *J* = 8.4 Hz, 2H), 7.25 (ddd, *J* =

7.9, 4.3, 3.4 Hz, 1H), 7.21 – 7.16 (m, 2H), 7.12 (d, $J = 8.5$ Hz, 1H), 7.03 – 6.98 (m, 1H), 6.93 (d, $J = 8.7$ Hz, 1H), 6.83 (ddd, $J = 8.3, 2.6, 1.0$ Hz, 1H), 4.07 – 4.04 (m, 1H), 3.78 (d, $J = 1.1$ Hz, 3H), 3.75 (s, 3H), 2.48 – 2.35 (m, 1H), 2.03 – 1.98 (m, 2H), 1.83 – 1.73 (m, 3H), 1.63 – 1.53 (m, 3H). ^{13}C NMR (126 MHz, CDCl_3) δ 165.38, 159.16 (2Cs), 143.55, 138.68, 135.60, 130.49, 129.45, 129.33, 128.99, 128.27, 127.20, 126.95, 123.33, 121.84, 120.44, 115.16, 112.81, 110.91, 65.65, 55.68, 55.18, 43.04, 32.76 (2Cs), 27.61 (2Cs). HRMS (ESI+) m/z : $[\text{M} + \text{H}^+]$ calculated for $\text{C}_{27}\text{H}_{29}\text{NO}_4$ 432.2175; found 432.2182.



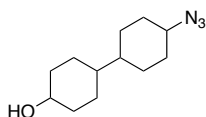
3',6-Dimethoxy-*N*-(4-(4-((1-methylpiperidin-4-yl)oxy)cyclohexyl)phenyl)-[1,1'-biphenyl]-3-carboxamide (4.6).

Compound **4.6** was obtained following the procedure utilized for the synthesis of **4.8a**, as a white amorphous solid (25%): ^1H NMR (500 MHz, Chloroform- d) δ 7.96 (dd, $J = 8.6, 2.4$ Hz, 1H), 7.71 – 7.65 (m, 2H), 7.58 – 7.51 (m, 2H), 7.36 (dd, $J = 8.5, 0.6$ Hz, 4H), 7.24 (d, $J = 8.5$ Hz, 1H), 7.05 (s, 1H), 6.92 – 6.82 (m, 1H), 4.14 (q, $J = 3.3$ Hz, 1H), 3.87 (s, 3H), 3.81 (s, 3H), 3.06 – 2.99 (m, 1H), 2.56 – 2.50 (m, 2H), 1.94 – 1.85 (m, 2H), 1.68 (d, $J = 5.8$ Hz, 3H), 1.56 (d, $J = 14.6$ Hz, 4H), 1.25 (s, 6H). ^{13}C NMR (126 MHz, CDCl_3) δ 158.54, 157.04, 142.56, 136.40, 134.80, 128.99, 128.54, 128.11, 126.37, 124.26, 119.25, 115.67, 113.83, 109.88, 64.61, 54.92, 54.56, 42.24, 31.97, 28.68, 26.73. HRMS (ESI+) m/z : $[\text{M} + \text{H}^+]$ calculated for $\text{C}_{33}\text{H}_{40}\text{N}_2\text{O}_4$ 529.3066; found 529.3092.



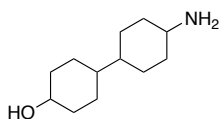
4'-Hydroxy-[1,1'-bi(cyclohexan)]-4-yl methanesulfonate (4.34).

Triethylamine (0.140 mL, 1.009 mmol) was added to a solution of [1,1'-bi(cyclohexane)]-4,4'-diol (0.1g, 0.505mmol) in anhydrous DCM (2.5mL) and the solution was cooled to 0 °C. Methanesulfonyl chloride (0.07mL, 0.909 mmol) was added dropwise and the reaction mixture was then allowed to stir at rt. After 12 h, water was added to quench the reaction and the suspension was extracted using EtOAc (3 x 20mL). The organic layers was combined, dried and concentrated to yield **4.34** as an amorphous solid (90%) that was used directly in the next step: HRMS (ESI+) m/z: [M + H⁺] calculated for C₁₃H₂₄O₄S 283.1555; found 283.1566.



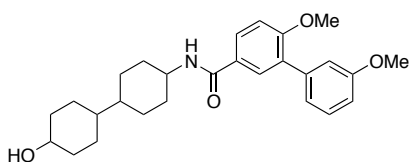
4'-Azido-[1,1'-bi(cyclohexan)]-4-ol (4.35).

Compound **4.35** was obtained as a white amorphous solid (30%) by following the general procedure D: ¹H NMR (500 MHz, Chloroform-d) δ 5.69 – 5.63 (m, 1H), 4.03 – 3.97 (m, 1H), 3.82 (t, *J* = 3.6 Hz, 1H), 2.06 – 1.97 (m, 1H), 1.88 – 1.79 (m, 4H), 1.78 – 1.70 (m, 2H), 1.58 – 1.45 (m, 4H), 1.47 – 0.97 (m, 6H). ¹³C NMR (126 MHz, CDCl₃) δ 71.14, 57.82, 41.59 (2Cs), 35.77 (2Cs), 32.67, 31.89, 29.69, 28.07, 24.55, 23.81. HRMS (ESI+) m/z: [M + Na⁺] calculated for C₁₂H₂₁N₃ONa 246.1582; found 246.1593.



4'-Amino-[1,1'-bi(cyclohexan)]-4-ol (4.36).

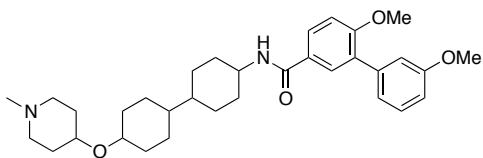
Palladium on carbon (10% w/w, 20 mg) was added to a solution of **4.35** (223 mg, 1.0 mmol) in MeOH (3 ml) and the resulting mixture was stirred at rt under a hydrogen atmosphere. After 12 h, the reaction mixture was filtrated through Celite and the filtrate was concentrated to get **4.36** as a white amorphous solid (~100%): ^1H NMR (500 MHz, Chloroform-d) δ 5.67 – 5.64 (m, 2H), 3.99 (q, $J = 3.6$ Hz, 1H), 3.53 (tt, $J = 10.9, 4.2$ Hz, 1H), 3.09 – 3.00 (m, 1H), 2.07 – 1.94 (m, 2H), 1.85 – 1.69 (m, 2H), 1.65 – 1.38 (m, 10H), 1.30 – 1.15 (m, 4H), 1.15 – 0.94 (m, 2H). ^{13}C NMR (126 MHz, CDCl_3) δ 70.18, 52.54, 42.34 (2Cs), 35.98 (2Cs), 32.82 (2Cs), 28.55 (2Cs), 24.22 (2Cs). HRMS (ESI+) m/z : $[\text{M} + \text{H}^+]$ calculated for $\text{C}_{12}\text{H}_{23}\text{NO}$ 198.1858; found 198.1861.



N-(4'-Hydroxy-[1,1'-bi(cyclohexan)]-4-yl)-3',6-dimethoxy-[1,1'-biphenyl]-3-carboxamide (4.37).

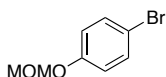
Compound **4.37** was obtained following the procedure used for the synthesis of **4.31**, as an off-white amorphous solid (60%): ^1H NMR (500 MHz, Chloroform-d) δ 7.78 (dd, $J = 8.6, 2.4$ Hz, 1H), 7.67 (d, $J = 2.4$ Hz, 1H), 7.35 (t, $J = 7.9$ Hz, 1H), 7.16 – 7.06 (m, 2H), 7.01 (d, $J = 8.6$ Hz, 1H), 6.92 (ddd, $J = 8.3, 2.6, 1.0$ Hz, 1H), 6.11 (d, $J = 7.5$ Hz, 1H), 4.24 (dt, $J = 8.1, 4.2$ Hz, 1H), 3.85 (d, $J = 5.2$ Hz, 6H), 3.54 (ddd, $J = 11.0, 6.6, 4.3$ Hz, 1H), 2.03 – 1.95 (m, 1H), 1.87 – 1.75 (m, 4H), 1.63 (dt, $J = 12.2, 3.5$ Hz, 3H), 1.60 – 1.47 (m, 1H), 1.34 – 1.11 (m, 6H), 1.08 – 0.94 (m, 2H). ^{13}C NMR (126 MHz, CDCl_3) δ 165.19, 158.24, 157.81, 138.00, 129.39, 128.24, 128.06 (2Cs), 126.96, 120.97, 114.34 (2Cs), 111.73, 70.03, 54.76, 54.29, 41.96 (2Cs), 34.67

(2Cs), 28.77 (2Cs), 27.29 (2Cs), 24.35 (2Cs). HRMS (ESI+) m/z : $[M + Na^+]$ calculated for $C_{27}H_{35}NO_4Na$ 460.2464; found 460.2462.



***N*-(4'-Hydroxy-[1,1'-bi(cyclohexan)]-4-yl)-3',6-dimethoxy-[1,1'-biphenyl]-3-carboxamide (4.7).**

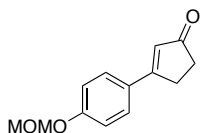
Compound **4.7** was obtained following the procedure utilized for the synthesis of **4.8a**, as a white amorphous solid (25%): 1H NMR (500 MHz, Chloroform- d) δ 7.78 (dd, $J = 8.6, 2.4$ Hz, 1H), 7.67 (d, $J = 2.4$ Hz, 2H), 7.35 (t, $J = 7.9$ Hz, 2H), 7.16 – 7.06 (m, 4H), 7.01 (d, $J = 8.6$ Hz, 1H), 6.92 (ddd, $J = 8.3, 2.6, 1.0$ Hz, 1H), 6.11 (d, $J = 7.5$ Hz, 1H), 4.24 (dt, $J = 8.1, 4.2$ Hz, 1H), 3.85 (d, $J = 5.2$ Hz, 6H), 3.54 (ddd, $J = 11.0, 6.6, 4.3$ Hz, 1H), 2.03 – 1.95 (m, 1H), 1.87 – 1.75 (m, 8H), 1.63 (dt, $J = 12.2, 3.5$ Hz, 3H), 1.60 – 1.47 (m, 2H), 1.34 – 1.11 (m, 12H), 1.08 – 0.94 (m, 4H). ^{13}C NMR (126 MHz, $CDCl_3$) δ 165.19, 158.24, 157.81, 138.00, 129.39, 128.24, 128.06, 126.96, 120.97, 114.34, 111.73, 109.80, 76.24, 70.03, 54.76, 54.29, 34.67, 28.77, 27.29, 24.35. HRMS (ESI+) m/z : $[M + Na^+]$ calculated for $C_{31}H_{37}N_2O_2Na$ 557.3355; found 557.3345.



1-Bromo-4-(methoxymethoxy)benzene (4.45).

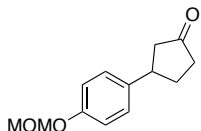
DIPEA (30mL, 173.4mmol) was added to a solution of 4-bromophenol (10g, 57.8mmol) in anhydrous DCM (289mL) and the solution was cooled to 0 °C. Chloromethyl methyl ether (6.5mL, 86.7mmol) was added dropwise and the reaction mixture was allowed or stir at rt for 12

h. The reaction mixture was quenched with water; extracted with DCM (3x 80mL). The organic layers was combined, dried, concentrated, and purified via column chromatography (SiO₂, 1:4, EtOAc: Hex). The product was isolated as oil in 48% yield: ¹H NMR (500 MHz, Chloroform-d) δ 7.38 (d, *J* = 9.0 Hz, 2H), 6.93 (d, *J* = 9.0 Hz, 2H), 5.14 (s, 2H), 3.47 (s, 3H). ¹³C NMR (126 MHz, CDCl₃) δ 156.44, 132.44 (2Cs), 118.19 (2Cs), 114.32, 94.60, 56.18. HRMS (ESI+) *m/z*: [M - H⁺] calculated for C₈H₉BrO₂ 214.9708; found 214.9704.



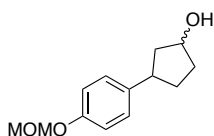
3-(4-(Methoxymethoxy)phenyl)cyclopent-2-enone (4.46).

1-bromo-4-(methoxymethoxy)benzene **4.45** (1.2g, 5.53mmol), 2-Cyclopenten-1-one (0.23mL, 2.76mmol), and Pd(OAc)₂ (0.06g, 0.276mmol) were suspended in anhydrous toluene (10 ml) and the suspension was stirred at rt for 15 minutes. Triethanolamine (11mL) was added and the mixture was heated at 110°C. After 12 h, the reaction mixture was cooled to rt and extracted with ether (3 x 50mL). The organic layers were combined, dried, concentrated and purified via column chromatography (SiO₂, 1:3, EtOAc: Hex). Compound was isolated was a yellow oil, 75%yield: ¹H NMR (500 MHz, Chloroform-d) δ 7.51 (d, *J* = 8.8 Hz, 2H), 7.00 (d, *J* = 8.8 Hz, 2H), 6.38 (t, *J* = 1.7 Hz, 1H), 5.13 (s, 2H), 3.39 (s, 3H), 2.93 – 2.87 (m, 2H), 2.48 – 2.42 (m, 2H). ¹³C NMR (126 MHz, CDCl₃) δ 209.65, 159.85, 153.92, 130.22, 128.74, 127.81, 125.89, 116.49 (2Cs), 94.27, 56.39, 35.41, 28.79. HRMS (ESI+) *m/z*: [M + H⁺] calculated for C₁₃H₁₄O₃ 219.1021; found 219.0992.



\pm 3-(4-(Methoxymethoxy)phenyl)cyclopentanone (4.47).

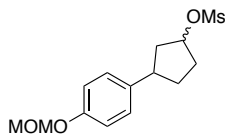
10% Pd/C (0.015g) was added to the solution of **4.46** (0.05g) in EtOAc (2 mL) and the suspension was stirred under a hydrogen atmosphere. After 12 h, the reaction mixture was filtered through a pad of Celite; the residue was washed with EtOAc. The filtrate was concentrated and purified by column chromatography (SiO₂, 1:3, EtOAc: Hex) to yield **4.47** as an oil (60% yield): ¹H NMR (500 MHz, Chloroform-d) δ 7.14 (d, J = 8.7 Hz, 2H), 6.99 (d, J = 8.7 Hz, 2H), 5.12 (s, 2H), 3.43 (s, 3H), 3.36 – 3.26 (m, 1H), 2.63 – 2.53 (m, 1H), 2.43 – 2.32 (m, 2H), 2.29 – 2.18 (m, 2H), 1.94 – 1.85 (m, 1H). ¹³C NMR (126 MHz, CDCl₃) δ 210.05, 155.94, 136.45, 127.70 (2Cs), 116.41 (2Cs), 94.43, 55.90, 45.94, 41.50, 38.86, 31.34.



3-(4-(Methoxymethoxy)phenyl)cyclopentanol (4.48).

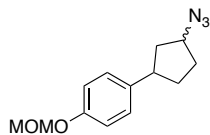
NaBH₄ (0.001 g, 0.227mmol) was added to an ice-cooled solution of **4.47** (0.05g, 0.227mmol) in MeOH (0.5mL) and the reaction mixture was then allowed to stir at rt. After 1 h, the reaction mixture was concentrated; the residue was diluted with water and extracted with ethyl acetate (3 x10 mL). The combined organic layers were dried, concentrated, and purified via column chromatography (SiO₂, 1:3, EtOAc: Hex) to yield a mixture of diastereomers. The product was isolated as a clear oil, 90% yield: ¹H NMR (500 MHz, Chloroform-d) δ 7.12 (d, J = 8.6 Hz, 2H), 6.97 (d, J = 8.7 Hz, 2H), 5.15 (s, 2H), 3.68 (tt, J = 10.5, 4.3 Hz, 1H), 3.48 (s, 3H), 2.45 (tt, J = 12.0, 3.6 Hz, 1H), 2.11 – 2.05 (m, 2H), 1.94 – 1.85 (m, 2H), 1.65 (dt, J = 12.2, 2.2 Hz, 1H), 1.55

– 1.48 (m, 1H). ^{13}C NMR (126 MHz, CDCl_3) δ 155.36, 139.91, 127.55 (2Cs), 116.04 (2Cs), 94.45, 70.54, 55.85, 51.53, 42.47, 35.84, 32.50, 27.80.



3-(4-(Methoxymethoxy)phenyl)cyclopentyl methanesulfonate (4.48).

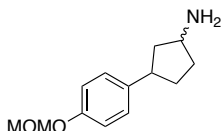
Triethylamine (0.1 mL, 0.68 mmol) was added to a solution of **4.48** (75 mg, 0.34 mmol) in anhydrous THF (0.5 mL) and the solution was cooled to 0°C. Methanesulfonyl chloride (0.039 mL, 0.51 mmol) was added dropwise and the reaction mixture was allowed to stir at rt for 1 h. The mixture was quenched by the addition of water, and extracted with EtOAc (3 x 15mL). The combined organic layers were dried, and concentrated to get **4.49** (90%) was used as such without further purification.



1-(3-Azidocyclopentyl)-4-(methoxymethoxy)benzene (4.49).

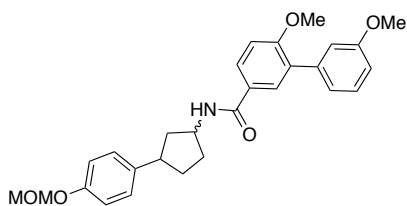
Sodium Azide (0.026g, 0.41 mmol) was added to a solution of **4.49** (60 mg, 0.21 mmol) in anhydrous DMF (0.84 mL) and the reaction mixture was heated at 100 °C. After 12 h, the reaction mixture was cooled to rt and diluted with water. The mixture was worked up with saturated LiCl and EtOAc (3 x 30mL). The combined organic layers were dried and purified via column chromatography, (SiO_2 , 1:4, EtOAc: Hex). The product was isolated in 85% yield: ^1H NMR (500 MHz, Chloroform- d) δ 7.21 – 7.07 (m, 2H), 6.98 (dd, J = 8.8, 2.6 Hz, 2H), 5.16 (d, J = 1.1 Hz, 2H), 4.16 (tdd, J = 6.2, 3.4, 2.3 Hz, 1H), 4.04 (qd, J = 6.8, 4.4 Hz, 1H), 3.48 (d, J = 0.6

Hz, 3H), 3.24 (tt, $J = 10.4, 7.4$ Hz, 1H), 3.03 (tt, $J = 10.3, 7.7$ Hz, 1H), 2.48 – 2.39 (m, 1H), 2.27 – 2.11 (m, 2H), 2.10 – 1.93 (m, 1H), 1.93 – 1.74 (m, 1H), 1.73 – 1.57 (m, 2H). ^{13}C NMR (126 MHz, CDCl_3) δ 155.70, 139.93, 128.31 (2Cs), 116.54 (2Cs), 94.96, 56.33, 52.92, 44.01, 43.22, 34.20, 32.84.



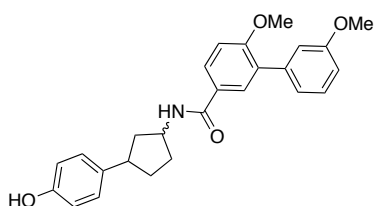
3-(4-(Methoxymethoxy)phenyl)cyclopentanamine (4.51).

Compound **4.51** was obtained as a mixture of diastereomers (71%) by following the procedure for **4.32**. ^1H NMR (500 MHz, Chloroform- d) δ 7.19 – 7.11 (m, 4H), 6.96 (ddd, $J = 8.6, 2.0, 0.9$ Hz, 4H), 5.15 (d, $J = 1.1$ Hz, 4H), 3.47 (d, $J = 1.0$ Hz, 6H), 3.43 – 3.37 (m, 1H), 3.34 – 3.27 (m, 1H), 3.22 (t, $J = 8.4$ Hz, 1H), 2.98 (ddd, $J = 11.3, 5.4, 2.8$ Hz, 1H), 2.41 – 2.33 (m, 2H), 2.21 – 2.10 (m, 2H), 2.04 (td, $J = 5.0, 3.2$ Hz, 1H), 1.99 – 1.84 (m, 2H), 1.82 – 1.54 (m, 4H), 1.52 – 1.38 (m, 1H). ^{13}C NMR (126 MHz, CDCl_3) δ 155.40, 138.85, 127.94 (2Cs), 116.16 (2Cs), 94.53, 55.90, 52.29, 43.04, 42.56, 34.48, 32.63. HRMS (ESI+) m/z : $[\text{M} + \text{H}^+]$ calculated for $\text{C}_{13}\text{H}_{19}\text{NO}_2$ 222.1494; found 222.1507.



3',6-Dimethoxy-N-(3-(4-(methoxymethoxy)phenyl)cyclopentyl)-[1,1'-biphenyl]-3-carboxamide (4.52).

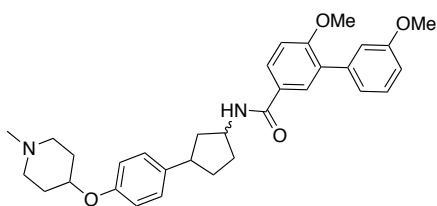
DIPEA (0.35 mL, 2.0 mmol) was added to a solution of 3-(4-(methoxymethoxy)phenyl)cyclopentanamine **4.51** (0.3g, 1.0 mmol), biaryl acid **4.15** (0.31g, 1.2mmol), and HOBt-H₂O (0.382g, 2.0mmol) in anhydrous DCM (10 mL) and the solution was cooled to 0 °C. EDCI•HCl (0.382 g, 2.0 mmol) was added to the reaction mixture and the resulting solution was then allowed to stir at rt. After 12 h, the reaction mixture was concentrated; the residue was diluted with water, and extracted with DCM (3x 40mL). The organic layers were combined, concentrated and purified by column chromatography (SiO₂, 1:4 EtOAc:Hex) to afford **4.52** as a white amorphous solid (80%): ¹H NMR (500 MHz, Chloroform-d) δ 7.89 – 7.76 (m, 2H), 7.31 (td, *J* = 7.9, 2.0 Hz, 1H), 7.15 – 7.05 (m, 4H), 6.99 – 6.92 (m, 3H), 6.91 – 6.87 (m, 1H), 6.82 – 6.74 (m, 1H), 5.13 (d, *J* = 6.2 Hz, 2H), 4.54 (dt, *J* = 7.5, 2.0 Hz, 1H), 3.85 – 3.75 (m, 6H), 3.46 (d, *J* = 4.1 Hz, 3H), 2.26 – 2.18 (m, 1H), 2.18 – 2.13 (m, 1H), 2.09 – 2.02 (m, 3H), 1.75 – 1.55 (m, 2H). ¹³C NMR (126 MHz, CDCl₃) δ 171.15, 159.18, 158.75, 155.40, 139.01, 138.50, 130.18, 129.51, 128.98, 128.25, 127.84, 127.78, 125.06, 121.95, 116.14 (2Cs), 115.28, 112.66, 110.70, 94.45, 55.85, 55.65, 55.18, 51.04, 42.94, 41.65, 33.64, 32.22. HRMS (ESI+) *m/z*: [M + H⁺] calculated for C₂₈H₃₁NO₅ 484.2100; found 484.2124.



***N*-(3-(4-Hydroxyphenyl)cyclopentyl)-3',6-dimethoxy-[1,1'-biphenyl]-3-carboxamide (4.53).**

6N HCl (1mL/1g starting material, 0.2mL) was added to a solution of **4.52** (158 mg, 0.34 mmol) was dissolved in a mixture of MeOH/THF (10mL/1g of starting material, 2mL: 2mL) and

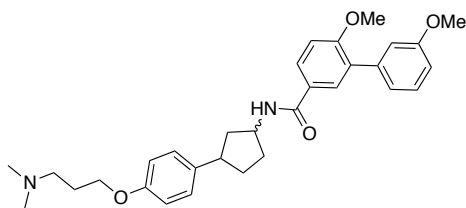
the reaction mixture was stirred at rt for 12 h. The reaction mixture was concentrated under reduced pressure to get **4.53** as a mixture of diastereomers, white solid (60%): ¹H NMR (500 MHz, Chloroform-d) δ 7.83 (dd, *J* = 8.6, 2.4 Hz, 1H), 7.79 (dd, *J* = 8.6, 2.4 Hz, 1H), 7.70 (d, *J* = 2.4 Hz, 1H), 7.65 (d, *J* = 2.3 Hz, 1H), 7.33 (td, *J* = 7.9, 2.6 Hz, 2H), 7.11 – 7.01 (m, 7H), 6.98 (dd, *J* = 8.7, 7.6 Hz, 2H), 6.90 (ddd, *J* = 8.3, 2.5, 0.9 Hz, 1H), 6.81 (dd, *J* = 8.5, 6.1 Hz, 6H), 6.34 (d, *J* = 7.2 Hz, 1H), 6.31 (d, *J* = 7.5 Hz, 1H), 4.66 – 4.58 (m, 1H), 4.53 (q, *J* = 7.7, 7.1 Hz, 1H), 3.84 (s, 6H), 3.83 (s, 6H), 3.17 (p, *J* = 8.8 Hz, 1H), 3.11 – 2.99 (m, 1H), 2.53 (dt, *J* = 13.1, 6.8 Hz, 1H), 2.40 – 2.33 (m, 2H), 2.30 – 2.22 (m, 1H), 2.19 – 1.96 (m, 4H), 1.82 – 1.66 (m, 2H), 1.66 – 1.52 (m, 2H). ¹³C NMR (126 MHz, CDCl₃) δ 167.11, 167.00, 159.29, 159.09, 154.64, 154.55, 138.96 (2Cs), 136.53, 136.29, 130.48, 130.40, 129.34, 129.32, 129.12, 129.09, 128.35, 128.32, 127.88, 127.84, 126.71, 126.66, 122.12, 122.02, 115.41(2Cs), 115.37 (2Cs), 112.86 (2Cs), 112.75 (2Cs), 110.99 (2Cs), 55.81 (2Cs), 55.79 (2Cs), 55.34 (2Cs), 42.04 (2Cs), 41.40 (2Cs), 33.84, 33.60, 32.74, 31.93. HRMS (ESI+) *m/z*: [M + Na⁺] calculated for C₂₆H₂₇NO₄Na 440.1838; found 440.1847.



3',6-Dimethoxy-N-(3-(4-((1-methylpiperidin-4-yl)oxy)phenyl)cyclopentyl)-[1,1'-biphenyl]-3-carboxamide (4.38).

A solution of **4.53** (0.025g, 0.06mmol) and N-Methyl-4-piperidinol (0.014mL, 0.12mmol) in anhydrous benzene (0.6 mL) was cooled to 0°C. Tributylphosphine (0.03mL, 0.12mmol) and TMAD (0.021g, 0.12mmol) were added to the mixture. The reaction mixture was stirred at reflux

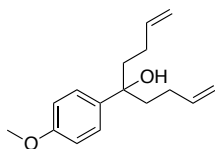
for 12 h. After 12 h the reaction was cooled to rt and purified via column chromatography (SiO₂, 1:20 MeOH:DCM) to afford **4.38** as white amorphous solid (27%): ¹H NMR (500 MHz, Chloroform-d) δ 7.82 (dd, *J* = 8.6, 2.4 Hz, 1H), 7.67 (d, *J* = 2.4 Hz, 1H), 7.35 (td, *J* = 7.9, 2.9 Hz, 1H), 7.15 (dd, *J* = 8.3, 5.9 Hz, 2H), 7.11 (ddd, *J* = 7.6, 1.6, 1.0 Hz, 1H), 7.07 (dd, *J* = 2.6, 1.5 Hz, 1H), 7.01 (dd, *J* = 8.6, 5.4 Hz, 1H), 6.92 (ddd, *J* = 8.3, 2.6, 1.0 Hz, 1H), 6.84 (d, *J* = 8.6 Hz, 2H), 6.08 (d, *J* = 7.1 Hz, 1H), 4.64 (td, *J* = 7.1, 4.5 Hz, 1H), 4.56 (q, *J* = 8.0 Hz, 1H), 4.35 (s, 2H), 3.86 (d, *J* = 1.8 Hz, 3H), 3.85 (d, *J* = 1.8 Hz, 3H), 3.25 – 3.15 (m, 1H), 3.14 – 3.06 (m, 2H), 2.79 (s, 3H), 2.40 (td, *J* = 6.3, 4.9, 2.7 Hz, 4H), 2.26 – 2.16 (m, 1H), 2.15 – 1.99 (m, 2H), 1.91 (s, 2H), 1.80 – 1.51 (m, 1H). ¹³C NMR (126 MHz, CDCl₃) δ 166.89, 159.68, 159.31, 155.84, 139.43, 137.96, 130.80, 129.62, 129.51, 129.51, 128.60, 128.39, 128.30, 127.43, 122.39, 116.42 (2Cs), 115.77, 113.17, 111.26, 56.19 (2Cs), 55.74, 51.49, 43.32, 41.84, 34.34, 33.96, 32.58 (2Cs), 30.10 (2Cs). HRMS (ESI+) *m/z*: [M + H⁺] calculated for C₃₂H₃₈N₂O₄ 515.2910; found 515.2899.



***N*-(3-(4-(3-(Dimethylamino)propoxy)phenyl)cyclopentyl)-3',6-dimethoxy-[1,1'-biphenyl]-3-carboxamide (**4.39**).**

A solution of **4.53** (0.025g, 0.06mmol) and 3-dimethylamino-1-propanol (0.014mL, 0.12mmol) in anhydrous benzene (0.6 mL) was cooled to 0°C. Tributylphosphine (0.03mL, 0.12mmol) and TMAD (0.021g, 0.12mmol) were added to the mixture. The reaction mixture was stirred at reflux for 12 h. After 12 h the reaction was cooled to rt and purified via column

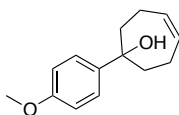
chromatography (SiO₂, 1:20 MeOH:DCM) to afford **4.39** as white amorphous solid (29%): ¹H NMR (500 MHz, Chloroform-d) δ 7.82 (dd, *J* = 8.6, 2.4 Hz, 1H), 7.67 (d, *J* = 2.4 Hz, 1H), 7.35 (t, *J* = 7.9 Hz, 1H), 7.16 – 7.04 (m, 4H), 7.01 (d, *J* = 8.6 Hz, 1H), 6.91 (ddd, *J* = 8.2, 2.6, 1.0 Hz, 1H), 6.83 (d, *J* = 8.7 Hz, 2H), 6.08 (d, *J* = 7.2 Hz, 1H), 4.64 (td, *J* = 7.1, 4.4 Hz, 1H), 4.00 (t, *J* = 6.3 Hz, 2H), 3.86 (d, *J* = 5.9 Hz, 6H), 3.20 (t, *J* = 8.2 Hz, 1H), 2.56 (m, 2H), 2.34 (s, 6H), 2.23 – 2.16 (m, 1H), 2.12 (ddd, *J* = 13.7, 9.7, 8.0 Hz, 1H), 2.08 – 1.97 (m, 4H), 1.78 – 1.51 (m, 2H). ¹³C NMR (126 MHz, CDCl₃) δ 166.63, 159.43, 159.04, 157.34, 139.18, 137.28, 130.54, 129.38, 129.25, 128.34, 128.00, 127.20, 122.14, 115.51 (2Cs), 114.53, 112.93, 111.00, 66.14, 56.49, 55.94, 55.48, 51.26, 45.26 (2Cs), 43.08, 41.60, 34.11, 33.76, 29.85. HRMS (ESI+) *m/z*: [M + H⁺] calculated for C₃₁H₃₈N₂O₄ 503.2910; found 503.2888.



5-(4-Methoxyphenyl)nona-1,8-dien-5-ol (4.55).

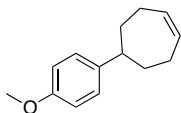
Magnesium turnings (1.46 g, 60.2 mmol) were suspended in anhydrous THF (12 mL) in a 3-neck flask. 4-Bromo-1-butene (1.02 mL of total 3.08 mL, 9.84 mmol) in anhydrous THF (7.5 mL) was added dropwise and the mixture was heated at reflux while the remaining bromide (2.06 mL, 20.29 mmol) was added. The reaction mixture was refluxed until all of the magnesium had reacted, approximately 2h. The mixture was then cooled to rt and methyl 4-methoxybenzoate (1.0 g, 6.02 mmol) in anhydrous THF (12 mL) was added dropwise over 30min. The reaction was stirred overnight at rt. After 12 h the reaction was quenched with saturated NH₄Cl (15mL), and the emulsion was stirred for 2h. The mixture was then extracted with ether (3 x 50 mL), dried, concentrated, and purified via column chromatography (SiO₂, 1:8 EtOAc:Hex). Product

was isolated as a colorless oil, 84% yield: ^1H NMR (500 MHz, Chloroform- d) δ 7.29 – 7.27 (m, 2H), 6.88 (d, J = 8.8 Hz, 2H), 5.84 – 5.73 (m, 2H), 4.97 (d, J = 1.7 Hz, 1H), 4.94 – 4.87 (m, 3H), 3.81 (s, 3H), 2.08 – 1.99 (m, 2H), 1.97 – 1.80 (m, 6H). ^{13}C NMR (126 MHz, CDCl_3) δ 158.23, 139.01 (2Cs), 137.82, 126.52 (2Cs), 114.72 (2Cs), 113.58 (2Cs), 75.62, 55.36, 42.26 (2Cs), 28.20 (2Cs).



1-(4-Methoxyphenyl)cyclohept-4-enol (4.56).

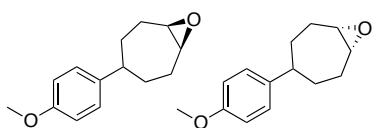
Grubbs 1st generation catalyst (0.2g, 0.04mol%) was added to a solution of **4.55** (1.5 g, 6.09 mmol) and the reaction mixture was heated at 40°C for 12 h. The reaction mixture was concentrated and purified by column chromatography (SiO_2 , 1:10 EtOAc:Hex) to yield **4.56** as a white solid (54%): ^1H NMR (500 MHz, Chloroform- d) δ 7.13 – 7.07 (m, 2H), 6.83 (d, J = 8.7 Hz, 2H), 5.91 – 5.85 (m, 2H), 3.79 (s, 3H), 2.69 (tt, J = 11.2, 3.2 Hz, 1H), 2.34 – 2.24 (m, 1H), 2.22 – 2.13 (m, 2H), 1.86 (dddd, J = 11.8, 5.2, 2.8, 1.2 Hz, 1H), 1.56 (s, 1H), 1.48 (dtd, J = 13.5, 11.4, 2.2 Hz, 2H). ^{13}C NMR (126 MHz, CDCl_3) δ 157.97, 141.89, 132.87 (2Cs), 127.93 (2Cs), 114.07 (2Cs), 79.16, 55.63, 49.82 (2Cs), 28.29 (2Cs).



5-(4-Methoxyphenyl)cyclohept-1-ene (4.57).

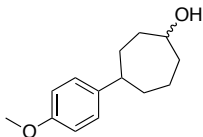
Et_3SiH (0.257 mL, 1.61 mmol) was added to a solution of 1-(4-methoxyphenyl)cyclohept-4-enol **4.56** (0.32g, 1.47mmol) in anhydrous DCM (9mL), followed by addition of trifluoroacetic

acid (1.12 mL, 14.7 mmol) and the solution was stirred at rt for 48h. The reaction mixture was concentrated and purified via column chromatography (SiO₂, 1:20 EtOAc:Hex) to yield **4.57** as a clear oil (50% yield): ¹H NMR (500 MHz, Chloroform-d) δ 7.14 – 7.07 (m, 2H), 6.83 (d, *J* = 8.7 Hz, 2H), 5.91 – 5.86 (m, 2H), 3.79 (s, 3H), 2.69 (tt, *J* = 11.2, 3.2 Hz, 1H), 2.34 – 2.24 (m, 2H), 2.17 (ddt, *J* = 14.4, 11.5, 1.9 Hz, 2H), 1.86 (dddd, *J* = 11.7, 5.1, 3.3, 1.8 Hz, 1H), 1.48 (dtd, *J* = 13.5, 11.4, 2.1 Hz, 2H). ¹³C NMR (126 MHz, CDCl₃) δ 157.72, 141.63, 132.62 (2Cs), 127.68 (2Cs), 113.81(2Cs), 55.38, 49.57, 35.05 (2Cs), 28.04 (2Cs). HRMS (ESI+) *m/z*: [M + Na⁺] calculated for C₁₄H₁₈ONa 225.1255; found 225.1277.



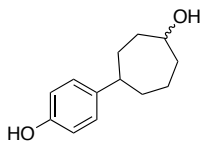
(1R,7S)-4-(4-Methoxyphenyl)-8-oxabicyclo[5.1.0]octane (4.58).

A solution of **4.57** (0.25g, 1.24mmol) in anhydrous DCM (8.5mL) was added dropwise to an ice-cooled solution of *m*-CPBA (0.36g, 2.10mmol) in anhydrous DCM (5mL). NaHCO₃ (0.26g, 3.1mmol) was added and the reaction was stirred at rt for 12 h. The reaction mixture was extracted with DCM (3 x 30mL) and saturated NaHCO₃. The organic layers were collected, dried, concentrated, and purified via column chromatography (SiO₂, 1:5 EtOAc:Hex) to yield a mixture of diastereomers **4.58** (89% yield): ¹H NMR (500 MHz, Chloroform-d) δ 7.13 – 7.03 (m, 4H), 6.87 – 6.77 (m, 4H), 3.79 (s, 3H), 3.78 (s, 3H), 3.20 – 3.15 (m, 1H), 3.13 – 3.06 (m, 1H), 2.55 (tt, *J* = 11.5, 3.3 Hz, 4H), 2.41 – 2.29 (m, 2H), 2.16 – 2.10 (m, 2H), 1.92 – 1.56 (m, 10H), 1.50 – 1.39 (m, 2H). ¹³C NMR (126 MHz, CDCl₃) δ 158.19, 157.98, 141.64, 140.27, 127.94 (2Cs), 127.64 (2Cs), 114.18 (2 Cs), 114.09 (2Cs), 56.49 (4 Cs), 55.64, 55.48, 49.61, 33.01 (2Cs), 32.43 (2Cs), 29.18 (2Cs), 27.88 (2Cs).



4-(4-Methoxyphenyl)cycloheptanol (4.59).

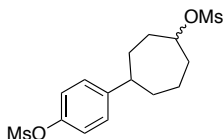
Lithium aluminum hydride (0.12 g, 2.97 mmol) was added to a solution of (1*R*,7*S*)-4-(4-methoxyphenyl)-8-oxabicyclo[5.1.0]octane **4.58** (0.20 g, 0.99 mmol) was dissolved in anhydrous THF (20 mL), followed by addition of AlCl₃ (0.05 mL, 0.99 mmol) and the mixture was stirred at rt. After 12 h, 30 drops of water were added, followed by 6mL of 3M NaOH and 20mL of water. The reaction mixture was stirred for one hour and then filtered through a pad of Celite. The filtrate was concentrated and purified via column chromatography (SiO₂, 1:3 EtOAc:Hex) to yield **4.59** as mixture of diastereomers, white solid (60% yield): ¹H NMR (500 MHz, Chloroform-*d*) δ 7.10 (dd, *J* = 10.0, 7.9 Hz, 4H), 6.83 (dt, *J* = 8.7, 1.5 Hz, 4H), 4.07 – 4.00 (m, 1H), 3.98 – 3.91 (m, 1H), 3.78 (d, *J* = 0.8 Hz, 6H), 2.67 (tdd, *J* = 7.2, 4.8, 1.6 Hz, 1H), 2.60 (ddd, *J* = 8.6, 6.9, 4.3 Hz, 1H), 2.10 (dddt, *J* = 9.8, 7.3, 4.1, 1.5 Hz, 2H), 2.00 – 1.87 (m, 4H), 1.86 – 1.78 (m, 4H), 1.80 – 1.65 (m, 4H), 1.65 – 1.45 (m, 6H). ¹³C NMR (126 MHz, CDCl₃) δ 157.70 (2Cs), 141.61, 141.47, 127.63 (2Cs), 113.84 (2Cs), 72.90, 71.76, 55.39 (2Cs), 46.35, 46.09, 38.33, 37.79, 37.30, 37.10, 36.99, 35.86, 31.84, 29.71, 23.42, 21.47.



4-(4-Hydroxyphenyl)cycloheptanol (4.60).

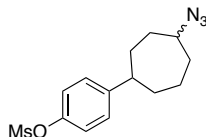
4.59 (0.75g, 3.41 mmol) was dissolved in anhydrous DCM (340mL) and the solution was cooled to -78°C. Boron tribromide (1.16mL, 1.0M in DCM, 6.82mmol) was added dropwise and

the solution was stirred at same temperature for ~30minutes before warming to rt over 2 h. The mixture was quenched with water and extracted with DCM (3 x 70mL). The combined organic layers were dried and concentrated to yield a mixture of diastereomers **4.60** as white solid (46% yield): ¹H NMR (500 MHz, Chloroform-d) δ 7.08 – 7.05 (m, 2H), 7.04 – 7.01 (m, 2H), 6.81 – 6.70 (m, 4H), 4.78 – 4.68 (m, 2H), 4.52 (dtd, *J* = 9.5, 5.3, 4.4 Hz, 1H), 4.38 (ddt, *J* = 10.6, 7.2, 4.8 Hz, 1H), 2.72 (tdd, *J* = 10.5, 5.1, 3.5 Hz, 1H), 2.68 – 2.61 (m, 1H), 2.53 – 2.45 (m, 2H), 2.45 – 2.38 (m, 2H), 2.38 – 2.28 (m, 2H), 2.16 – 2.07 (m, 2H), 2.03 – 1.91 (m, 2H), 1.90 – 1.68 (m, 8H), 1.68 – 1.53 (m, 2H). ¹³C NMR (126 MHz, CDCl₃) δ 153.94, 153.93, 141.45, 141.32, 128.10 (2Cs), 115.56 (2Cs), 70.90, 56.36, 56.00, 46.15, 45.71, 39.79, 39.59, 38.17, 37.95, 36.75, 34.60, 31.65, 25.61, 23.91, 21.49. HRMS (ESI+) *m/z*: [M + H⁺] calculated for C₁₃H₁₈O₂ 207.1385; found 207. 1410.



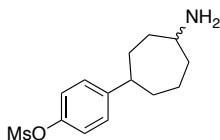
4-(4-((Methylsulfonyl)oxy)cycloheptyl)phenyl methanesulfonate (4.61).

Compound **4.61** was obtained as a brown amorphous solid (90% yield) by following the procedure used for the synthesis of **4.12a**: ¹H NMR (400 MHz, Chloroform-d) δ 7.20 (s, 3H), 7.16 (s, 1H), 7.14 (s, 1H), 7.13 (d, *J* = 0.6 Hz, 3H), 4.47 (dq, *J* = 9.6, 4.9 Hz, 1H), 4.36 – 4.28 (m, 1H), 3.08 (s, 6H), 3.06 (d, *J* = 1.4 Hz, 6H), 2.79 – 2.71 (m, 1H), 2.65 (dq, *J* = 10.0, 5.1, 4.3 Hz, 1H), 2.48 – 2.41 (m, 2H), 2.38 – 2.10 (m, 4H), 2.10 – 1.98 (m, 4H), 1.97 – 1.88 (m, 2H), 1.87 – 1.63 (m, 4H), 1.62 – 1.47 (m, 4H). ¹³C NMR (101 MHz, CDCl₃) δ 149.78, 147.87, 139.12 (2Cs), 128.16 (4Cs), 121.95 (4Cs), 55.52, 55.09, 45.91 (2Cs), 39.73 (2Cs), 37.27, 36.10, 33.89, 33.23, 31.55 (2Cs), 25.05 (2Cs), 23.53 (2Cs).



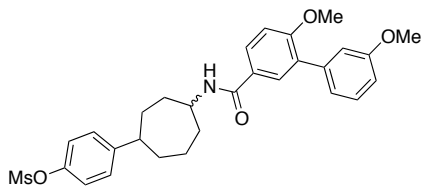
4-(4-Azidocycloheptyl)phenyl methanesulfonate (4.62a).

Compound **4.62a** was obtained as a white amorphous solid (40% yield) by following the procedure used for the synthesis of **4.13a**: ^1H NMR (500 MHz, Chloroform-d) δ 6.99 (dd, $J = 8.7, 6.6$ Hz, 4H), 6.76 – 6.69 (m, 4H), 3.66 (s, 6H), 3.65 – 3.60 (m, 1H), 3.51 (ddt, $J = 10.1, 7.4, 4.7$ Hz, 1H), 2.60 – 2.47 (m, 2H), 2.06 – 1.96 (m, 2H), 1.90 – 1.67 (m, 9H), 1.64 – 1.42 (m, 9H). ^{13}C NMR (126 MHz, CDCl_3) δ 157.70 (2Cs), 140.93, 140.81, 127.46 (4Cs), 113.76 (4Cs), 62.45, 61.72, 55.19 (2Cs), 46.02, 45.70, 37.87, 36.62, 33.87, 33.37, 33.10, 32.38, 32.00, 29.97, 23.66, 22.16.



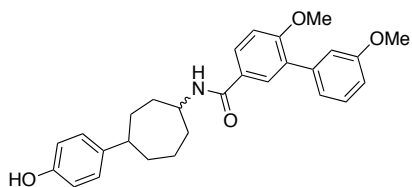
4-(4-Aminocycloheptyl)phenyl methanesulfonate (4.62).

Compound **4.62** was obtained as a white amorphous solid (85% yield) by following the procedure used for the synthesis of **4.32**. The amine was used immediately after synthesis: ^1H NMR (400 MHz, Methanol-d₄) δ 6.84 (q, $J = 8.8$ Hz, 4H), 3.74 (q, $J = 7.1$ Hz, 1H), 3.08 – 2.94 (m, 2H), 2.78 (d, $J = 2.3$ Hz, 3H), 2.33 (ddd, $J = 12.2, 8.0, 3.3$ Hz, 1H), 2.28 – 2.13 (m, 2H), 1.89 – 1.78 (m, 2H), 1.66 – 1.05 (m, 6H). HRMS (ESI+) m/z : $[\text{M} + \text{H}^+]$ calculated for $\text{C}_{14}\text{H}_{21}\text{NO}_3\text{S}$ 284.1320; found 284.1324.



4-(4-(3',6-Dimethoxy-[1,1'-biphenyl]-3-ylcarboxamido)cycloheptyl)phenyl methanesulfonate (4.63).

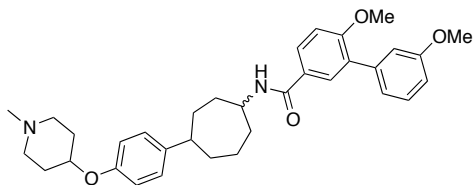
Compound **4.63** was obtained as a white amorphous solid (90% yield) by following the procedure used for the synthesis of **4.16a**: ^1H NMR (500 MHz, Chloroform- d) δ 7.82 (ddd, $J = 8.6, 3.6, 2.3$ Hz, 2H), 7.74 (t, $J = 2.6$ Hz, 2H), 7.35 – 7.28 (m, 2H), 7.20 – 7.12 (m, 8H), 7.12 – 7.04 (m, 4H), 6.97 (d, $J = 8.7$ Hz, 2H), 6.88 (ddt, $J = 8.3, 2.4, 1.1$ Hz, 2H), 6.46 (d, $J = 7.8$ Hz, 1H), 6.40 (d, $J = 7.9$ Hz, 1H), 4.31 – 4.26 (m, 1H), 4.21 (ddt, $J = 8.9, 4.5, 2.5$ Hz, 1H), 3.83 – 3.82 (m, 6H), 3.81 (d, $J = 1.7$ Hz, 6H), 3.08 (s, 3H), 3.07 (s, 3H), 2.72 (ddd, $J = 14.6, 7.2, 3.6$ Hz, 1H), 2.69 – 2.64 (m, 1H), 2.16 (dt, $J = 7.2, 4.0$ Hz, 2H), 2.09 – 1.95 (m, 4H), 1.92 – 1.79 (m, 4H), 1.79 – 1.47 (m, 7H). ^{13}C NMR (126 MHz, CDCl_3) δ 171.19 (2Cs), 159.25 (2Cs), 158.84 (2Cs), 148.38, 148.24, 139.05 (2Cs), 130.26 (2Cs), 129.43 (2Cs), 129.07 (2Cs), 128.25, 128.13 (2Cs), 127.19 (2Cs), 122.00 (2Cs), 121.85 (2Cs), 115.39 (2Cs), 115.37 (2Cs), 112.71 (2Cs), 112.68 (2Cs), 55.77 (2Cs), 55.29 (2Cs), 50.91, 49.98, 46.67, 45.74, 37.91, 37.12, 36.08, 35.44, 34.78, 34.34, 33.13, 32.83, 30.93, 24.95, 22.67, 21.06. HRMS (ESI+) m/z : $[\text{M} + \text{Na}^+]$ calculated for $\text{C}_{29}\text{H}_{33}\text{NO}_6\text{SNa}$ 546. 1926; found 546. 1910.



***N*-(4-(4-Hydroxyphenyl)cycloheptyl)-3',6-dimethoxy-[1,1'-biphenyl]-3-carboxamide**

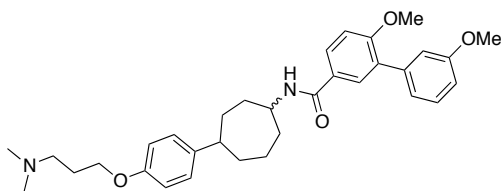
(4.64).

3.2N NaOH (0.05 mL, 1.15 mmol) was added to a solution of **4.63** (0.20 g, 0.38 mmol) in ethanol (3 mL) and the solution was refluxed for 3 h. The reaction mixture was cooled to rt and concentrated under vacuum. The residue was neutralized with 1N HCl and extracted with EtOAc (3 x 10mL). The organic layers were collected, dried and concentrated to get **4.64** as a white solid (60% yield): ¹H NMR (500 MHz, Chloroform-d) δ 7.81 (dd, *J* = 8.6, 2.4 Hz, 1H), 7.67 (d, *J* = 2.3 Hz, 1H), 7.35 (t, *J* = 7.9 Hz, 2H), 7.12 – 6.99 (m, 7H), 6.91 (ddd, *J* = 8.3, 2.6, 0.9 Hz, 1H), 6.77 (dd, *J* = 8.4, 6.1 Hz, 2H), 6.03 (dd, *J* = 13.2, 7.9 Hz, 1H), 4.31 (s, 1H), 4.25 (dt, *J* = 10.9, 4.4 Hz, 1H), 3.86 (d, *J* = 4.8 Hz, 8H), 2.73 – 2.59 (m, 1H), 2.25 – 2.16 (m, 1H), 2.15 – 1.96 (m, 1H), 1.96 – 1.76 (m, 3H), 1.76 – 1.62 (m, 2H), 1.55 (qd, *J* = 11.4, 3.5 Hz, 1H). ¹³C NMR (126 MHz, CDCl₃) δ 165.81 (2Cs), 159.71 (2Cs), 159.31 (2Cs), 154.13 (2Cs), 139.45 (2Cs), 130.85 (2Cs), 129.62 (2Cs), 129.50 (2Cs), 128.58 (2Cs), 128.07 (2Cs), 128.05 (2Cs), 122.42 (2Cs), 122.41 (2Cs), 115.79, 115.77, 115.60, 115.58, 113.22 (2Cs), 113.20 (2Cs), 111.31 (2Cs), 51.42, 50.40, 46.92, 45.79, 38.49, 36.70, 35.35, 35.01, 33.93, 33.38, 31.71, 30.11, 25.32, 23.17. HRMS (ESI+) *m/z*: [M + Na⁺] calculated for C₂₈H₃₁NO₄Na 468.2151; found 468.2147.



3',6-Dimethoxy-*N*-(4-(4-((1-methylpiperidin-4-yl)oxy)phenyl)cycloheptyl)-[1,1'-biphenyl]-3-carboxamide (4.40).

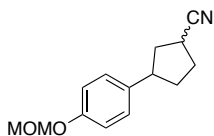
Compound **4.40** was obtained following the procedure utilized for the synthesis of **4.38**, as a white amorphous solid (32%): ^1H NMR (500 MHz Chloroform- d) δ 7.81 (ddd, $J = 8.6, 2.4, 1.3$ Hz, 2H), 7.67 (d, $J = 2.4$ Hz, 2H), 7.34 (t, $J = 7.9$ Hz, 2H), 7.14 – 7.04 (m, 8H), 7.00 (d, $J = 8.6$ Hz, 2H), 6.91 (ddd, $J = 8.3, 2.6, 0.9$ Hz, 2H), 6.81 (dd, $J = 8.7, 2.5$ Hz, 4H), 6.09 (dd, $J = 15.4, 8.0$ Hz, 2H), 4.43 – 4.38 (m, 2H), 4.33 – 4.27 (m, 1H), 4.27 – 4.20 (m, 1H), 3.85 (s, 6H), 3.84 (s, 6H), 2.94 – 2.85 (m, 5H), 2.75 – 2.61 (m, 6H), 2.53 – 2.48 (m, 4H), 2.22 – 2.15 (m, 7H), 2.08 (qd, $J = 11.2, 9.8, 6.2$ Hz, 1H), 2.04 – 1.92 (m, 5H), 1.92 – 1.85 (m, 2H), 1.82 – 1.76 (m, 1H), 1.75 – 1.62 (m, 4H), 1.54 (dddd, $J = 13.7, 10.9, 8.9, 2.5$ Hz, 3H). ^{13}C NMR (126 MHz, CDCl_3) δ 165.96, 159.38, 158.96, 155.00, 141.94, 139.15, 130.46, 129.36, 129.20, 128.26 (2Cs), 127.82, 127.35, 122.10, 116.03 (2Cs), 115.46, 112.87, 110.95, 55.90, 55.44, 51.04, 50.08, 46.60, 45.56, 45.32, 38.22, 36.44, 34.65, 33.48, 33.06, 25.02, 22.84. HRMS (ESI+) m/z : $[\text{M} + \text{H}^+]$ calculated for $\text{C}_{34}\text{H}_{42}\text{N}_2\text{O}_4$ 543.3223; found 543.3201.



***N*-(4-(4-(3-(Dimethylamino)propoxy)phenyl)cycloheptyl)-3',6-dimethoxy-[1,1'-biphenyl]-3-carboxamide (4.41).**

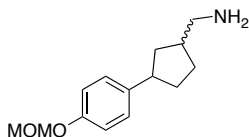
Compound **4.41** was obtained following the procedure utilized for the synthesis of **4.39**, as a yellow amorphous solid (35%): ^1H NMR (500 MHz, Chloroform- d) δ 7.80 (ddd, $J = 8.5, 2.4, 1.2$ Hz, 2H), 7.70 (d, $J = 2.3$ Hz, 2H), 7.32 (t, $J = 7.9$ Hz, 2H), 7.11 – 7.03 (m, 8H), 6.98 (d, $J = 8.6$ Hz, 2H), 6.89 (ddd, $J = 8.3, 2.6, 1.0$ Hz, 2H), 6.79 (dd, $J = 8.7, 2.6$ Hz, 4H), 6.22 (dd, $J = 15.2, 8.0$ Hz, 2H), 4.28 (dt, $J = 10.2, 5.0$ Hz, 1H), 4.26 – 4.18 (m, 1H), 3.98 (td, $J = 6.1, 2.8$ Hz, 4H),

3.83 (d, $J = 4.8$ Hz, 12H), 2.94 (d, $J = 3.7$ Hz, 2H), 2.73 (td, $J = 7.7, 3.6$ Hz, 4H), 2.69 – 2.58 (m, 4H), 2.46 (d, $J = 2.5$ Hz, 12H), 2.22 – 2.13 (m, 1H), 2.12 – 2.04 (m, 6H), 2.01 – 1.96 (m, 1H), 1.93 – 1.73 (m, 4H), 1.73 – 1.61 (m, 4H), 1.57 – 1.47 (m, 4H). ^{13}C NMR (126 MHz, CDCl_3) δ 165.88, 159.27, 158.83, 156.70, 141.51, 139.06, 130.31, 129.35, 129.09, 128.17 (2Cs), 127.55, 127.29, 122.01, 115.34 (2Cs), 114.31, 112.78, 110.83, 65.55, 56.24, 55.79, 55.33, 50.96, 46.48, 45.48, 44.56, 38.18, 36.41, 35.63, 34.91, 34.53, 33.40, 31.24, 26.44, 24.91, 22.75. HRMS (ESI+) m/z : $[\text{M} + \text{H}^+]$ calculated for $\text{C}_{33}\text{H}_{42}\text{N}_2\text{O}_4$ 531.3223; found 531.3204.



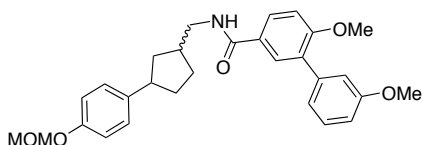
3-(4-(Methoxymethoxy)phenyl)cyclopentanecarbonitrile (4.65).

Tetrabutylammonium cyanide was added to a solution of mesylate **4.49** (0.10g, 0.33 mmol) in anhydrous DMF (0.6 mL) and the solution was heated at 85°C. After 12 h, the reaction was cooled to rt; diluted with water and extracted with EtOAc (3 x 10mL). The organic layers were combined, dried, concentrated, and purified via column chromatography (SiO_2 , 1:4, EtOAc:Hex) to afford **4.65** as an oil (55% yield): ^1H NMR (500 MHz, Chloroform- d) δ 7.16 – 7.09 (m, 2H), 7.00 – 6.95 (m, 2H), 5.14 (d, $J = 1.5$ Hz, 2H), 3.46 (d, $J = 1.0$ Hz, 3H), 3.30 – 3.21 (m, 2H), 3.04 – 2.97 (m, 1H), 2.39 – 2.32 (m, 1H), 2.30 – 2.20 (m, 1H), 2.14 (ddt, $J = 6.9, 5.0, 1.8$ Hz, 1H), 2.08 – 1.87 (m, 1H), 1.70 – 1.59 (m, 1H), 1.42 (q, $J = 7.4$ Hz, 1H). ^{13}C NMR (126 MHz, CDCl_3) δ 154.77, 135.55, 126.81 (2Cs), 122.55, 115.32 (2Cs), 93.44, 57.78, 42.81, 38.26, 37.83, 32.59, 29.48.



(3-(4-(Methoxymethoxy)phenyl)cyclopentyl)methanamine (4.66).

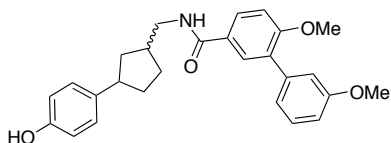
A solution of **4.65** (0.60g, 2.45mmol) in anhydrous THF (4mL) was added to an ice-cooled suspension of Lithium Aluminum Hydride (0.48 g, 12.24 mmol) in anhydrous THF (4 mL) and the reaction mixture was allowed to stir at rt for 3 h. The reaction was quenched by sequential addition of 3M NaOH, water, and EtOAc. The emulsion was stirred for one hour and then filtered through Celite. The filtrate was concentrated and purified via column chromatography (SiO₂, 1:20, MeOH: DCM) to yield **4.66** as a white solid (88% yield): ¹H NMR (500 MHz, Chloroform-d) δ 7.15 – 7.07 (m, 2H), 6.99 – 6.92 (m, 2H), 5.22 – 5.08 (m, 2H), 3.47 (d, *J* = 1.3 Hz, 2H), 3.46 (d, *J* = 0.7 Hz, 3H), 3.12 – 2.96 (m, 1H), 2.89 – 2.76 (m, 1H), 2.12 – 2.01 (m, 1H), 1.82 (ddd, *J* = 8.9, 6.8, 3.5 Hz, 1H), 1.71 – 1.56 (m, 1H), 1.46 – 1.20 (m, 3H). ¹³C NMR (126 MHz, CDCl₃) δ 154.43, 138.05, 127.02, 126.80, 115.13, 115.09, 93.52, 54.89, 44.02, 41.17, 38.59, 34.93, 33.79, 31.75, 29.81.



3',6-Dimethoxy-N-((3-(4-(methoxymethoxy)phenyl)cyclopentyl)methyl)-[1,1'-biphenyl]-3-carboxamide (4.67).

DIPEA (0.11mL, 0.596mmol) was added to a mixture of **4.66** (0.07g, 0.298mmol), biaryl acid **4.15** (0.09g, 0.357mmol), and HOBt (0.114g, 0.596mmol) in anhydrous DCM (3 mL) and the suspension was cooled to 0 °C. EDCI (0.114g, 0.6 mmol) was added and the reaction mixture was stirred at rt for 12 h. The reaction mixture was diluted with water and extracted with DCM

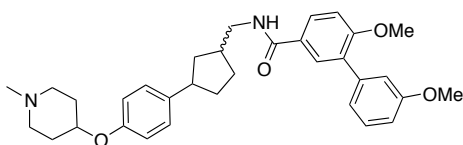
(3 x 15mL). The organic layers were combined, dried, concentrated, and purified by column chromatography (SiO₂, 1:4, EtOAc: Hex) to yield **4.67** as a white foam (80% yield): ¹H NMR (500 MHz, Chloroform-d) δ 7.83 (ddd, *J* = 11.2, 8.5, 2.4 Hz, 1H), 7.76 (t, *J* = 2.4 Hz, 1H), 7.32 (td, *J* = 7.9, 2.2 Hz, 1H), 7.16 – 7.05 (m, 4H), 6.96 (ddd, *J* = 8.6, 3.6, 2.4 Hz, 3H), 6.89 (dtd, *J* = 8.2, 2.4, 0.9 Hz, 1H), 6.59 (d, *J* = 7.3 Hz, 1H), 5.15 (s, 1H), 5.14 (s, 1H), 4.62 (q, *J* = 6.3 Hz, 1H), 4.54 (qd, *J* = 8.7, 7.9, 2.0 Hz, 1H, minor), 3.83 (d, *J* = 1.1 Hz, 3H), 3.82 (d, *J* = 1.7 Hz, 3H), 3.47 (s, 2H), 3.46 (s, 1H minor), 3.11-3.00 (m, 1H), 2.53 (dt, *J* = 12.9, 6.7 Hz, 1H minor), 2.41 – 2.29 (m, 1H), 2.26 – 2.11 (m, 1H), 2.09 – 2.04 (m, 1H), 1.81 – 1.69 (m, 1H), 1.68 – 1.53 (m, 1H). ¹³C NMR (126 MHz, CDCl₃) δ 166.65, 159.27, 158.85, 155.50, 139.08, 138.54, 130.30, 129.50, 128.30, 128.24, 127.86, 127.13, 125.07, 122.03, 116.23 (2 Cs), 115.37, 112.76, 110.80, 94.55, 55.95, 55.76, 55.30, 43.21, 41.34, 33.81, 33.70, 32.68, 32.28, 21.08. HRMS (ESI+) *m/z*: [M + Na⁺] calculated for C₂₉H₃₃NO₅Na 498.2256; found 498.2236.



***N*-((3-(4-Hydroxyphenyl)cyclopentyl)methyl)-3',6-dimethoxy-[1,1'-biphenyl]-3-carboxamide (**4.68**).**

PTSA (360 mg, 1.89 mmol) was added to a solution **4.67** (300 mg, 0.63 mmol) was dissolved in MeOH (3 mL) and the reaction mixture was stirred at rt for 12 h. The reaction mixture was concentrated; the residue was diluted with saturated ammonium chloride and extracted with EtOAc (3x30mL). The organic layers were combined, dried, concentrated, and purified via column chromatography (SiO₂, 1:20, MeOH: DCM) to give **4.68** as a white solid (60% yield): ¹H NMR (500 MHz, Chloroform-d) δ 7.80 (ddd, *J* = 8.6, 5.3, 2.4 Hz, 1H), 7.69 (t, *J* = 2.7 Hz, 1H),

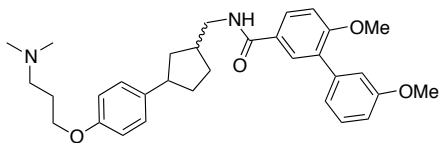
7.33 (t, $J = 7.9$ Hz, 1H), 7.11 – 7.01 (m, 4H), 6.99 (dd, $J = 8.6, 0.9$ Hz, 1H), 6.90 (ddd, $J = 8.2, 2.6, 0.9$ Hz, 1H), 6.80 – 6.75 (m, 2H), 6.26 (q, $J = 6.0$ Hz, 1H), 3.85 (s, 3H), 3.83 (s, 3H), 3.54 – 3.45 (m, 1H), 3.40 (ddd, $J = 13.1, 7.2, 5.6$ Hz, 1H), 3.12 – 3.02 (m, 1H), 2.97 (td, $J = 10.8, 5.4$ Hz, 1H), 2.47 – 2.38 (m, 1H), 2.37 – 2.28 (m, 1H), 2.26 – 2.15 (m, 1H), 2.13 – 1.97 (m, 1H), 1.94 – 1.73 (m, 2H), 1.72 – 1.47 (m, 1H), 1.42 – 1.36 (m, 1H), 1.34 – 1.22 (m, 1H). ^{13}C NMR (126 MHz, CDCl_3) δ 167.41, 159.28, 159.05, 154.23, 138.95, 137.37, 130.52, 129.36, 129.10, 128.18, 127.96, 127.91, 126.83, 122.00, 115.32, 115.22, 115.20, 112.89, 110.95, 55.80, 55.33, 45.39, 43.55, 39.86, 34.76, 33.29, 30.69, 29.47. HRMS (ESI+) m/z : $[\text{M} + \text{H}^+]$ calculated for $\text{C}_{27}\text{H}_{29}\text{NO}_4$ 432.2175; found 432.2176.



***N*-((3-(4-(3-(Dimethylamino)propoxy)phenyl)cyclopentyl)methyl)-3',6-dimethoxy-[1,1'-biphenyl]-3-carboxamide (4.42).**

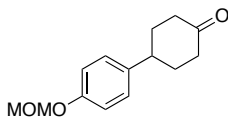
Compound **4.42** was obtained following the procedure utilized for the synthesis of **4.38**, as a white amorphous solid (33%): ^1H NMR (500 MHz, Chloroform- d) δ 7.79 (ddd, $J = 8.5, 3.8, 2.4$ Hz, 1H), 7.69 (d, $J = 2.3$ Hz, 1H), 7.36 – 7.31 (m, 1H), 7.17 – 7.04 (m, 4H), 7.00 (dd, $J = 8.7, 0.9$ Hz, 1H), 6.90 (ddd, $J = 8.3, 2.6, 1.0$ Hz, 1H), 6.79 (dd, $J = 8.8, 1.0$ Hz, 2H), 6.18 – 6.11 (m, 1H), 4.02 (t, $J = 5.9$ Hz, 1H), 3.85 (s, 3H), 3.84 (s, 3H), 3.48 – 3.40 (m, 1H), 3.15 – 3.05 (m, 1H), 2.91 (d, $J = 8.0$ Hz, 2H), 2.61 (s, 3H), 2.48 – 2.36 (m, 1H), 2.24 – 2.15 (m, 4H), 2.15 – 2.01 (m, 2H), 1.94 – 1.76 (m, 2H), 1.72 – 1.49 (m, 2H), 1.47 – 1.23 (m, 4H). ^{13}C NMR (126 MHz, CDCl_3) δ 167.03, 159.28, 158.92, 156.63, 139.00, 130.44, 129.33, 129.11, 127.99, 127.08, 121.99, 115.32, 114.22, 112.82, 110.85, 65.22, 56.16, 55.80, 55.34, 45.26, 44.02, 43.59, 39.72, 39.01, 38.25,

34.77, 33.32, 30.75, 29.52, 25.76. HRMS (ESI+) m/z : $[M + H^+]$ calculated for $C_{33}H_{40}N_2O_4$ 517.3066; found 517.3061.



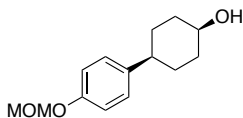
***N*-((3-(4-(3-(Dimethylamino)propoxy)phenyl)cyclopentyl)methyl)-3',6-dimethoxy-[1,1'-biphenyl]-3-carboxamide (4.43)**

Compound **4.43** was obtained following the procedure utilized for the synthesis of **4.39**, as a yellow amorphous solid (27%): 1H NMR (500 MHz, Chloroform- d) δ 7.79 (ddd, $J = 8.5, 3.8, 2.4$ Hz, 1H), 7.69 (d, $J = 2.3$ Hz, 1H), 7.36 – 7.31 (m, 1H), 7.17 – 7.04 (m, 4H), 7.00 (dd, $J = 8.7, 0.9$ Hz, 1H), 6.90 (ddd, $J = 8.3, 2.6, 1.0$ Hz, 1H), 6.79 (dd, $J = 8.8, 1.0$ Hz, 2H), 6.18 – 6.11 (m, 1H), 4.02 (t, $J = 5.9$ Hz, 2H), 3.85 (s, 3H), 3.84 (s, 3H), 3.48 – 3.40 (m, 1H), 3.15 – 3.05 (m, 1H), 2.91 (d, $J = 8.0$ Hz, 2H), 2.61 (s, 6H), 2.48 – 2.36 (m, 1H), 2.24 – 2.15 (m, 2H), 2.15 – 2.01 (m, 1H), 1.94 – 1.76 (m, 1H), 1.72 – 1.49 (m, 1H), 1.47 – 1.23 (m, 2H). ^{13}C NMR (126 MHz, $CDCl_3$) δ 167.03, 159.28, 158.92, 156.63, 139.00, 130.44, 129.33, 129.11, 127.99, 127.08, 121.99, 115.32, 114.22, 112.82, 110.85, 65.22, 56.16, 55.80, 55.34, 45.26, 44.02, 43.59, 39.72, 39.01, 38.25, 34.77, 33.32, 30.75, 29.52, 25.76. HRMS (ESI+) m/z : $[M + H^+]$ calculated for $C_{32}H_{40}N_2O_4$ 517.3066; found 517.3061.



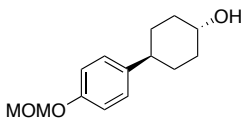
4-(4-(Methoxymethoxy)phenyl)cyclohexanone (4.69).

DIPEA (13.7 mL, 78.95 mmol) was added to a solution of 4-(4-hydroxyphenyl)cyclohexanone (10 g, 52.63 mmol) in anhydrous DCM (500 mL), and the mixture was cooled to 0°C. MOMCl was added dropwise (11.2 mL, 157.89 mmol) and the solution was allowed to stir at rt. After 12 h, the reaction mixture was quenched by water and extracted with DCM. The organic layers were combined, dried, concentrated, and purified via column chromatography (SiO₂, 1:4, EtOAc: Hex) to afford **4.69** as a white solid (65% yield): ¹H NMR (500 MHz, Chloroform-d) δ 7.16 (d, *J* = 8.6 Hz, 2H), 7.00 – 6.96 (m, 2H), 5.15 (d, *J* = 1.9 Hz, 2H), 3.48 (d, *J* = 1.6 Hz, 3H), 2.56 – 2.42 (m, 1H), 2.11 – 2.05 (m, 2H), 1.94 – 1.83 (m, 2H), 1.71 – 1.61 (m, 2H), 1.54 – 1.31 (m, 2H). ¹³C NMR (126 MHz, CDCl₃) δ 211.13, 158.94, 134.55, 129.90 (2Cs), 115.31 (2Cs), 96.25, 56.10, 44.91 (2Cs), 41.20, 35.86 (2Cs).



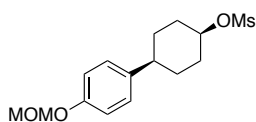
(1*s*,4*s*)-4-(4-(Methoxymethoxy)phenyl)cyclohexanol (4.70a).

Compound **4.70a** was obtained as an oil (70% yield) by following the procedure used for the synthesis of **4.11a**: ¹H NMR (500 MHz, Chloroform-d) δ 7.15 – 7.09 (m, 2H), 6.97 (d, *J* = 8.7 Hz, 2H), 5.15 (s, 2H), 3.73 – 3.62 (m, 1H), 3.48 (s, 3H), 2.45 (tt, *J* = 11.9, 3.4 Hz, 1H), 2.13 – 2.06 (m, 2H), 1.94 – 1.84 (m, 2H), 1.52 – 1.35 (m, 4H). ¹³C NMR (126 MHz, CDCl₃) δ 155.49, 140.04, 127.67 (2Cs), 116.17 (2Cs), 94.57, 70.67, 55.97, 42.60, 35.97 (2Cs), 32.62 (2Cs).



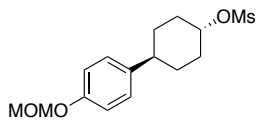
(1*r*,4*r*)-4-(4-(Methoxymethoxy)phenyl)cyclohexanol (4.70b).

Compound **4.70b** was obtained as an oil (85% yield) by following the procedure used for the synthesis of **4.11b**: ^1H NMR (500 MHz, Chloroform- d) δ 7.12 (d, J = 8.6 Hz, 2H), 6.97 (d, J = 8.7 Hz, 2H), 5.15 (s, 2H), 3.68 (tt, J = 10.5, 4.3 Hz, 1H), 3.48 (d, J = 1.6 Hz, 3H), 2.45 (tt, J = 12.0, 3.6 Hz, 1H), 2.13 – 2.05 (m, 2H), 1.94 – 1.87 (m, 2H), 1.56 – 1.47 (m, 2H), 1.47 – 1.35 (m, 2H). ^{13}C NMR (126 MHz, CDCl_3) δ 155.87, 140.42, 128.05 (2Cs), 116.55 (2Cs), 94.95, 71.05, 56.35, 42.98, 36.35 (2Cs), 33.44 (2Cs).



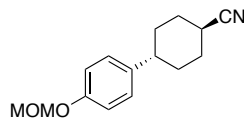
(1*s*,4*s*)-4-(4-(Methoxymethoxy)phenyl)cyclohexyl methanesulfonate (4.71a).

Compound **4.71a** was obtained as an oil (85 % yield) by following the procedure used for the synthesis of **4.12a** and used directly in the next step.



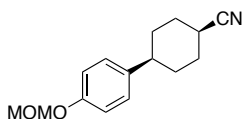
(1*r*,4*r*)-4-(4-(Methoxymethoxy)phenyl)cyclohexyl methanesulfonate (4.71b).

Compound **4.71b** was obtained as a white solid (85 % yield) by following the procedure used for the synthesis of **4.12a** and used directly in the next step.



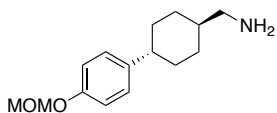
(1*r*,4*r*)-4-(4-(Methoxymethoxy)phenyl)cyclohexanecarbonitrile (4.72a).

Compound **4.72a** was obtained as a light yellow oil (45%) by following the procedure used for the synthesis of **4.65**: ^1H NMR (500 MHz, Chloroform- d) δ 7.15 (d, $J = 8.6$ Hz, 2H), 7.01 – 6.96 (m, 2H), 5.16 (s, 2H), 3.48 (s, 3H), 3.06 – 2.97 (m, 1H), 2.48 (tt, $J = 11.5, 4.0$ Hz, 1H), 2.15 – 2.07 (m, 2H), 1.93 – 1.76 (m, 4H), 1.75 – 1.64 (m, 2H). ^{13}C NMR (126 MHz, CDCl_3) δ 155.69, 139.58, 127.71(2Cs), 122.02, 116.29 (2Cs), 94.55, 55.99, 42.79, 30.13 (2Cs), 28.78, 26.72 (2Cs).



(1s,4s)-4-(4-(Methoxymethoxy)phenyl)cyclohexanecarbonitrile (4.72b).

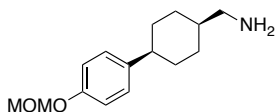
Compound **4.72b** was obtained as a light yellow solid (49%) by following the procedure used for the synthesis of **4.65**: ^1H NMR (500 MHz, Chloroform- d) δ 7.18 – 7.12 (m, 2H), 7.01 – 6.97 (m, 2H), 5.16 (s, 2H), 3.47 (s, 3H), 3.00 (td, $J = 3.9, 1.4$ Hz, 1H), 2.48 (tt, $J = 11.5, 4.0$ Hz, 1H), 2.12 – 2.07 (m, 2H), 1.89 – 1.77 (m, 4H), 1.72 – 1.64 (m, 1H). ^{13}C NMR (126 MHz, CDCl_3) δ 155.72, 138.62, 126.96, 126.79, 122.02, 116.29, 96.53, 54.95, 42.05, 31.04 (2Cs), 28.77, 25.30 (2Cs).



((1r,4r)-4-(4-(Methoxymethoxy)phenyl)cyclohexyl)methanamine (4.73a).

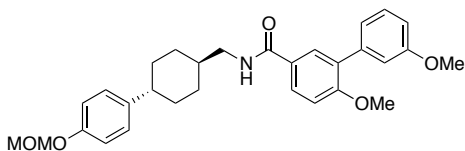
Compound **4.73a** was obtained as a light yellow solid (75%) by following the procedure used for the synthesis of **4.66**: ^1H NMR (500 MHz, Chloroform- d) δ 7.18 (m, 2H), 6.99 (qd, $J = 5.9, 2.9$ Hz, 2H), 5.10 (d, 2H), 3.41 (s, 3H), 3.41 – 3.27 (m, 1H), 3.08 – 3.00 (m, 1H), 2.56 – 2.47 (m, 1H), 2.44 – 2.31 (m, 1H), 2.29 – 2.17 (m, 1H), 2.16 – 1.98 (m, 1H), 1.90 – 1.76 (m, 1H), 1.71 –

1.62 (m, 1H). ¹³C NMR (126 MHz, CDCl₃) δ 156.33, 136.43, 127.59 (2Cs), 115.67 (2Cs), 95.04, 54.37, 45.09, 41.95, 33.55 (2Cs), 24.89 (2Cs).



((1*s*,4*s*)-4-(4-(Methoxymethoxy)phenyl)cyclohexyl)methanamine (4.73b).

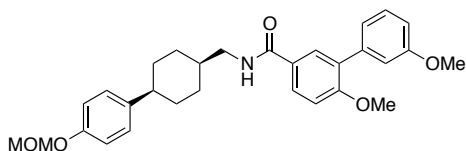
Compound **4.73b** was obtained as a light yellow solid (65%) by following the procedure used for the synthesis of **4.66**: ¹H NMR (500 MHz, Chloroform-*d*) δ 7.20 – 7.13 (m, 2H), 6.99 (qd, *J* = 5.6, 3.1 Hz, 2H), 5.16 (d, *J* = 1.2 Hz, 2H), 3.48 (s, 3H), 3.41 – 3.27 (m, 1H), 3.08 – 3.00 (m, 1H), 2.56 – 2.47 (m, 1H), 2.44 – 2.31 (m, 1H), 2.29 – 2.17 (m, 1H), 2.16 – 1.98 (m, 1H), 1.90 – 1.76 (m, 1H), 1.71 – 1.62 (m, 1H). ¹³C NMR (126 MHz, CDCl₃) δ 155.52, 138.40, 128.16 (2Cs), 116.31 (2Cs), 94.56, 55.97, 46.65, 42.95, 32.43 (2Cs), 25.44 (2Cs).



3',6-Dimethoxy-*N*-(((1*r*,4*r*)-4-(4-(methoxymethoxy)phenyl)cyclohexyl)methyl)-[1,1'-biphenyl]-3-carboxamide (4.74a).

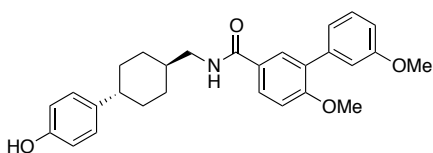
Compound **4.74a** was obtained as a light yellow solid (80%) by following the procedure used for the synthesis of **4.31**: ¹H NMR (500 MHz, Chloroform-*d*) δ 7.82 (ddd, *J* = 8.6, 3.7, 2.4 Hz, 1H), 7.73 (t, *J* = 2.3 Hz, 1H), 7.37 – 7.32 (m, 1H), 7.17 – 7.13 (m, 3H), 7.13 – 7.05 (m, 2H), 7.02 – 6.93 (m, 2H), 6.93 – 6.87 (m, 1H). 6.27 (t, *J* = 5.8 Hz, 1H), 5.15 (d, *J* = 0.8 Hz, 2H), 3.84 (dd, *J* = 6.7, 1.1 Hz, 6H), 3.48 (d, *J* = 3.1 Hz, 3H), 3.34 (t, *J* = 6.5 Hz, 2H), 2.56 (dt, *J* = 9.7, 5.1 Hz, 1H), 2.25 (ddt, *J* = 24.0, 12.0, 3.2 Hz, 1H), 1.95 – 1.83 (m, 2H), 1.75 – 1.61 (m, 6H). ¹³C NMR

(126 MHz, CDCl₃) δ 165.62, 161.02, 159.95, 155.07, 140.89, 139.61, 130.06, 129.19, 129.08, 127.94, 127.73, 127.44, 124.91, 122.14, 116.21 (2Cs) 114.69, 112.63, 111.31, 96.05, 56.45, 55.05, 55.01, 43.56, 42.59, 37.84, 31.23 (2Cs), 28.07 (2Cs). HRMS (ESI+) m/z : [M + H⁺] calculated for C₃₀H₃₅NO₅ 490.2593; found 490.2576.



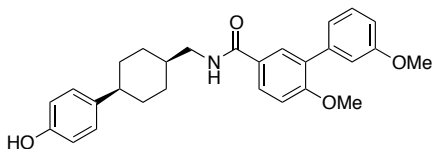
3',6-Dimethoxy-N-(((1*S*,4*S*)-4-(4-(methoxymethoxy)phenyl)cyclohexyl)methyl)-[1,1'-biphenyl]-3-carboxamide (4.74b).

Compound **4.74b** was obtained as a light yellow solid (70%) by following the procedure used for the synthesis of **4.31**: ¹H NMR (400 MHz, Chloroform-*d*) δ 7.84 (d, J = 1.0 Hz, 1H), 7.32 – 7.23 (m, 1H), 7.13 – 7.01 (m, 5H), 6.97 – 6.89 (m, 4H), 6.86 (ddd, J = 8.3, 2.4, 1.2 Hz, 1H), 5.11 (s, 2H), 3.78 (d, J = 4.2 Hz, 6H), 3.50 (dd, J = 7.7, 5.8 Hz, 2H), 3.44 (s, 3H), 2.55 – 2.47 (m, 1H), 1.99 (dd, J = 7.8, 4.1 Hz, 1H), 1.76 – 1.54 (m, 8H). ¹³C NMR (126 MHz, CDCl₃) δ 167.14, 159.34, 158.95, 155.46, 140.54, 139.10, 130.46, 129.45, 128.20, 127.91, 127.81, 127.74, 127.17, 122.07, 116.18 (2Cs), 115.39, 112.87, 110.91, 94.65, 56.02, 55.85, 55.38, 43.11, 41.93, 36.01, 29.13 (2Cs), 28.01 (2Cs). HRMS (ESI+) m/z : [M + Na⁺] calculated for C₃₀H₃₅NO₅Na 512.2413; found 512.2408.



***N*-(((1*r*,4*r*)-4-(4-Hydroxyphenyl)cyclohexyl)methyl)-3',6-dimethoxy-[1,1'-biphenyl]-3-carboxamide (4.75a).**

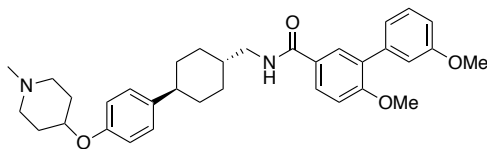
Compound **4.75a** was obtained as a white solid (66%) by following the procedure used for the synthesis of **4.53**: ¹H NMR (400 MHz, Chloroform-*d*) δ 7.86 – 7.80 (m, 1H), 7.70 (dd, *J* = 5.4, 2.4 Hz, 1H), 7.34 (t, *J* = 7.9 Hz, 1H), 7.12 – 7.05 (m, 3H), 7.01 (t, *J* = 7.5 Hz, 1H), 6.91 (dd, *J* = 8.1, 2.6 Hz, 1H), 6.85 – 6.75 (m, 1H), 6.21 (t, *J* = 6.1 Hz, 1H), 3.88 – 3.80 (d, 6H), 3.58 (t, *J* = 6.9 Hz, 2H), 2.56 – 2.44 (m, 1H), 2.15 (dd, 1H), 1.75 – 1.59 (m, 8 H). ¹³C NMR (126 MHz, CDCl₃) δ 166.19, 159.75 (2Cs), 154.09, 139.67, 131.04, 129.83, 129.64, 128.39 (2Cs), 128.17, 127.33, 122.15, 114.71, 114.46, 112.77, 110.99, 55.86, 55.52, 42.53, 42.06, 38.84, 33.89, 29.27, 28.12.



***N*-(((1*s*,4*s*)-4-(4-Hydroxyphenyl)cyclohexyl)methyl)-3',6-dimethoxy-[1,1'-biphenyl]-3-carboxamide (4.75b).**

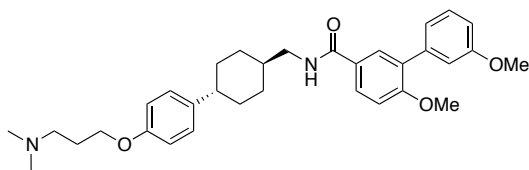
Compound **4.75b** was obtained as a white solid (72%) by following the procedure used for the synthesis of **4.53**: ¹H NMR (500 MHz, Chloroform-*d*) δ 7.74 (dd, *J* = 8.6, 2.4 Hz, 1H), 7.61 (d, *J* = 2.4 Hz, 1H), 7.27 (t, *J* = 7.9 Hz, 1H), 7.05 – 7.02 (m, 3H), 7.00 (dd, *J* = 2.6, 1.5 Hz, 1H), 6.94 (d, *J* = 8.6 Hz, 1H), 6.84 (ddd, *J* = 8.3, 2.6, 0.9 Hz, 1H), 6.71 (d, *J* = 8.5 Hz, 2H), 6.02 (t, *J* = 6.1 Hz, 1H), 3.79 (s, 3H), 3.78 (s, 3H), 3.50 (dd, *J* = 7.7, 5.6 Hz, 2H), 2.47 (dt, *J* = 9.7, 5.9 Hz, 1H), 1.91 (dt, *J* = 7.5, 3.9 Hz, 1H), 1.64 (ddq, *J* = 11.0, 7.3, 3.5 Hz, 7H). ¹³C NMR (126 MHz, CDCl₃) δ 167.45, 159.45 (2Cs), 153.95, 139.15, 130.66, 129.43, 129.24, 128.35, 128.09 (2Cs), 127.07,

122.17, 115.51, 115.26 (2Cs), 112.99, 111.10, 55.95, 55.49, 42.57, 42.06, 39.26, 33.89, 29.27, 28.12. HRMS (ESI+) m/z : $[M + H^+]$ calculated for $C_{28}H_{31}NO_4$ 446.2331; found 446.2328.



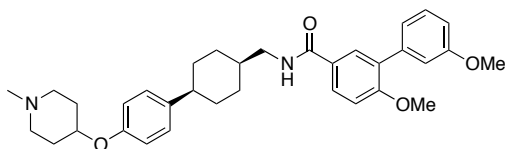
3',6-Dimethoxy-N-(((1*r*,4*r*)-4-(4-((1-methylpiperidin-4-yl)oxy)phenyl)cyclohexyl)methyl)-[1,1'-biphenyl]-3-carboxamide (4.44a).

Compound **4.44a** was obtained following the procedure utilized for the synthesis of **4.38**, as a white amorphous solid (39%): 1H NMR (500 MHz, Chloroform- d) δ 7.81 (dd, $J = 8.6, 2.4$ Hz, 1H), 7.69 (d, $J = 2.4$ Hz, 1H), 7.34 (t, $J = 7.9$ Hz, 1H), 7.17 – 7.13 (m, 2H), 7.10 (dt, $J = 7.6, 1.3$ Hz, 1H), 7.07 (dd, $J = 2.7, 1.6$ Hz, 1H), 7.01 (d, $J = 8.6$ Hz, 1H), 6.91 (ddd, $J = 8.3, 2.6, 0.9$ Hz, 1H), 6.83 (d, $J = 8.6$ Hz, 2H), 6.07 (t, $J = 5.9$ Hz, 1H), 4.88 (s, 1H), 3.86 (s, 3H), 3.84 (s, 3H), 3.54 (dd, $J = 7.3, 5.8$ Hz, 2H), 3.35-3.24 (m, 2H), 3.14 (d, 2H), 2.84 (s, 3H), 2.40 (d, 2H), 2.35 (s, 4H), 3.15-2.05 (m, 2H), 1.99 (m, 1H), 1.80 (m, 4H). ^{13}C NMR (126 MHz, $CDCl_3$) δ 167.03, 159.31, 158.96, 142.66, 140.47, 139.76, 139.01, 130.48, 129.28, 129.09, 128.73, 128.21, 128.09, 127.05, 125.92, 121.98, 115.71, 115.38, 112.78, 110.90, 55.82 (2Cs), 55.35 (2Cs), 44.31, 41.78, 329.03, 27.93, 23.80, 23.67, 23.12, 22.65, 21.32. HRMS (ESI+) m/z : $[M + H^+]$ calculated for $C_{34}H_{42}N_2O_4$ 543.3223; found 543.3221.



***N*-(((1*r*,4*r*)-4-(4-(3-(Dimethylamino)propoxy)phenyl)cyclohexyl)methyl)-3',6-dimethoxy-[1,1'-biphenyl]-3-carboxamide (4.44b)**

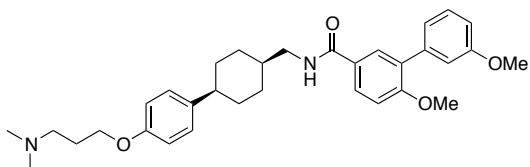
Compound **4.44b** was obtained following the procedure utilized for the synthesis of **4.39**, as a yellow amorphous solid (27%): ¹H NMR (500 MHz, Chloroform-*d*) δ 7.83 (dd, *J* = 8.8, 2.2 Hz, 1H), 7.70 (d, *J* = 2.6 Hz, 1H), 7.36 (t, 1H), 7.18 – 7.14 (m, 2H), 7.11 (dt, *J* = 7.7, 1.5 Hz, 1H), 7.08 (dd, *J* = 2.8, 1.4 Hz, 1H), 7.03 (d, 1H), 6.90 (ddd, *J* = 8.1, 2.6, 0.8 Hz, 1H), 6.82 (d, *J* = 8.8 Hz, 2H), 6.05 (t, *J* = 5.8 Hz, 1H), 4.00 (t, *J* = 6.6 Hz, 2H), 3.86 (s, 3H), 3.84 (s, 3H), 3.55 (dd, *J* = 7.5, 5.6 Hz, 2H), 2.60 (m, 3H), 2.31 (s, 6H), 1.99 (t, *J* = 7.2 Hz, 3H), 1.70 (dd, *J* = 10.3, 4.4 Hz, 8H).). ¹³C NMR (126 MHz, CDCl₃) δ 167.05, 159.35, 158.72, 157.34, 139.44, 139.11, 130.67, 129.75, 129.18, 128.58, 127.45, 127.12, 125.34, 121.79, 115.04, 114.20, 112.55 (2Cs), 110.44, 66.56, 56.64, 55.59, 55.30, 44.07, 41.37, 32.67, 29.60, 28.19. HRMS (ESI+) *m/z*: [M + H⁺] calculated for C₃₃H₄₂N₂O₄ 530.7045; found 530.7040.



3',6-Dimethoxy-*N*-(((1*s*,4*s*)-4-(4-((1-methylpiperidin-4-yl)oxy)phenyl)cyclohexyl)methyl)-[1,1'-biphenyl]-3-carboxamide (4.45a).

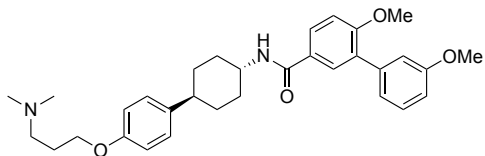
Compound **4.45a** was obtained following the procedure utilized for the synthesis of **4.38**, as a white amorphous solid (31%): ¹H NMR (500 MHz, Chloroform-*d*) δ 7.81 (dd, *J* = 8.6, 2.4 Hz, 1H), 7.78 (d, *J* = 8.2 Hz, 1H), 7.69 (d, *J* = 2.3 Hz, 1H), 7.34 (t, *J* = 7.9 Hz, 1H), 7.17 (dd, *J* = 8.3, 3.0 Hz, 2H), 7.11 – 7.05 (m, 2H), 7.01 (d, *J* = 8.7 Hz, 1H), 6.91 (ddd, *J* = 8.3, 2.6, 1.0 Hz, 1H), 6.81 (d, *J* = 8.7 Hz, 1H), 6.08 (t, *J* = 5.9 Hz, 1H), 4.96 (s, 1H), 4.59 (s, 1H), 3.86 (s, 3H), 3.84 (s, 3H), 3.56 (dd, *J* = 7.8, 5.9 Hz, 2H), 3.38 – 3.26 (m, 1H), 3.16 (d, *J* = 12.6 Hz, 2H), 2.83 (s, 3H),

2.59 – 2.52 (m, 1H), 2.39 (d, $J = 11.9$ Hz, 2H), 2.35 (s, 4H), 2.18 – 2.07 (m, 2H), 1.70 (dtt, $J = 12.8, 8.1, 3.4$ Hz, 5H). ^{13}C NMR (126 MHz, CDCl_3) δ 167.03, 159.31, 158.96, 142.66, 140.47, 139.76, 139.01, 130.48, 129.28, 129.09, 128.73, 128.21, 128.09, 127.05, 125.92, 121.98, 115.71, 115.38, 112.78 (2Cs), 110.90, 55.80 (2Cs), 55.33 (2Cs), 44.34, 42.40, 33.84 (2Cs), 29.03 (2Cs), 27.93 (2Cs). HRMS (ESI+) m/z : $[\text{M} + \text{H}^+]$ calculated for $\text{C}_{34}\text{H}_{42}\text{N}_2\text{O}_4$ 543.3223; found 543.3198.



***N*-(((1*s*,4*s*)-4-(4-(3-(Dimethylamino)propoxy)phenyl)cyclohexyl)methyl)-3',6-dimethoxy-[1,1'-biphenyl]-3-carboxamide (4.45b).**

Compound **4.45b** was obtained following the procedure utilized for the synthesis of **4.39**, as a yellow amorphous solid (30%): ^1H NMR (500 MHz, Chloroform- d) δ 7.81 (dd, $J = 8.6, 2.4$ Hz, 1H), 7.69 (d, $J = 2.4$ Hz, 1H), 7.34 (t, $J = 7.9$ Hz, 1H), 7.17 – 7.13 (m, 2H), 7.10 (dt, $J = 7.6, 1.3$ Hz, 1H), 7.07 (dd, $J = 2.7, 1.6$ Hz, 1H), 7.01 (d, $J = 8.6$ Hz, 1H), 6.91 (ddd, $J = 8.3, 2.6, 0.9$ Hz, 1H), 6.83 (d, $J = 8.6$ Hz, 2H), 6.07 (t, $J = 5.9$ Hz, 1H), 4.00 (t, $J = 6.3$ Hz, 2H), 3.86 (s, 3H), 3.84 (s, 3H), 3.55 (dd, $J = 7.7, 5.8$ Hz, 2H), 2.53 (m, 3H), 2.31 (s, 6H), 2.05 (t, $J = 7.0$ Hz, 3H), 1.65 (m, 8H). ^{13}C NMR (126 MHz, CDCl_3) δ 167.00, 159.30, 158.92, 157.04, 139.13, 139.03, 130.47, 129.30, 129.08, 128.08, 127.77, 127.13, 121.99, 115.34, 114.28, 112.83 (2Cs), 110.88, 66.06, 56.44, 55.79, 55.33, 45.27, 41.87, 33.66, 29.10, 28.02. HRMS (ESI+) m/z : $[\text{M} + \text{H}^+]$ calculated for $\text{C}_{33}\text{H}_{42}\text{N}_2\text{O}_4$ 530.7045; found 530.7061.



***N*-((1*r*,4*r*)-4-(4-(3-(Dimethylamino)propoxy)phenyl)cyclohexyl)-3',6-dimethoxy-[1,1'-biphenyl]-3-carboxamide (**4.46a**).**

Compound **4.46a** was obtained following the procedure utilized for the synthesis of **4.39**, as a yellow amorphous solid (27%): $^1\text{H NMR}$ (400 MHz, Chloroform-*d*) δ 7.82 (dd, $J = 8.6, 2.5$ Hz, 1H), 7.68 (t, $J = 2.4$ Hz, 1H), 7.35 (t, $J = 7.9$ Hz, 1H), 7.12 (dt, $J = 7.8, 3.1$ Hz, 3H), 7.07 (q, $J = 3.6, 2.9$ Hz, 1H), 7.01 (dd, $J = 9.0, 3.7$ Hz, 1H), 6.92 (dd, $J = 8.2, 2.7$ Hz, 1H), 6.84 (dd, $J = 9.5, 2.9$ Hz, 2H), 5.92 (d, $J = 8.0$ Hz, 1H), 4.10 – 3.95 (m, 3H), 3.86 (s, 3H), 3.85 (s, 3H), 2.53 – 2.41 (m, 3H), 2.27 (s, 6H), 2.24 – 2.16 (m, 2H), 1.96 (dq, $J = 10.9, 5.3, 4.0$ Hz, 4H), 1.62 (qd, $J = 13.2, 3.0$ Hz, 2H), 1.38 (td, $J = 12.3, 3.5$ Hz, 2H). $^{13}\text{C NMR}$ (126 MHz, CDCl_3) δ 166.32, 159.42, 159.00, 157.41, 139.19, 138.83, 130.52, 129.40, 129.23, 128.30, 127.70, 127.37, 122.13, 115.48, 114.49, 112.92, 110.97, 66.27, 56.59, 55.93, 55.47, 48.84, 45.55, 42.86, 33.79, 33.35, 27.62. HRMS (ESI+) m/z : $[\text{M} + \text{H}^+]$ calculated for $\text{C}_{32}\text{H}_{41}\text{N}_2\text{O}_4$ 517.3066; found 517.3069.

Reference

1. Taipale, M.; Jarosz, D. F.; Lindquist, S., HSP90 at the hub of protein homeostasis: emerging mechanistic insights. *Nature Reviews Molecular Cell Biology* **2010**, *11* (7), 515-528.
2. Taipale, M.; Krykbaeva, I.; Koeva, M.; Kayatekin, C.; Westover, Kenneth D.; Karras, Georgios I.; Lindquist, S., Quantitative Analysis of Hsp90-Client Interactions Reveals Principles of Substrate Recognition. *Cell* **2012**, *150* (5), 987-1001.

3. Garg, G.; Khandelwal, A.; Blagg, B. S., Anticancer Inhibitors of Hsp90 Function: Beyond the Usual Suspects. *Advances in Cancer Research* **2016**, *129*, 51-88.
4. Whitesell, L.; Lindquist, S. L., HSP90 and the chaperoning of cancer. *Nature Reviews Cancer* **2005**, *5* (10), 761-772.
5. Hanahan, D.; Weinberg, R. A., The Hallmarks of Cancer. *Cell* **2000**, *100* (1), 57-70.
6. Hanahan, D.; Weinberg, Robert A., Hallmarks of Cancer: The Next Generation. *Cell* **2011**, *144* (5), 646-674.
7. Powers, M. V.; Workman, P., Targeting of multiple signalling pathways by heat shock protein 90 molecular chaperone inhibitors. *Endocrine-Related Cancer* **2006**, *13*, S125-S135.
8. Dai, C.; Dai, S.; Cao, J., Proteotoxic stress of cancer: Implication of the heat-shock response in oncogenesis. *Journal of Cellular Physiology* **2012**, *227* (8), 2982-2987.
9. Stephanie, C. B.; Joseph, A. B.; Brian, S. J. B., Hsp90: A Novel Target for the Disruption of Multiple Signaling Cascades. *Current Cancer Drug Targets* **2007**, *7* (4), 369-388.
10. Chaudhury, S.; Welch, T. R.; Blagg, B. S. J., Hsp90 as a Target for Drug Development. *ChemMedChem* **2006**, *1* (12), 1331-1340.
11. Bishop, S. C.; Burlison, J. A.; Blagg, B. S., Hsp90: a novel target for the disruption of multiple signaling cascades. *Current Cancer Drug Targets* **2007**, *7* (4), 369-88.
12. Neckers, L.; Workman, P., Hsp90 Molecular Chaperone Inhibitors: Are We There Yet? *Clinical Cancer Research* **2012**, *18* (1), 64-76.
13. Brandt, G. E.; Blagg, B. S., Alternate strategies of Hsp90 modulation for the treatment of cancer and other diseases. *Current Topics in Medicinal Chemistry* **2009**, *9* (15), 1447-61.

14. Marcu, M. G.; Schulte, T. W.; Neckers, L., Novobiocin and Related Coumarins and Depletion of Heat Shock Protein 90-Dependent Signaling Proteins. *Journal of the National Cancer Institute* **2000**, *92* (3), 242-248.
15. Marcu, M. G.; Chadli, A.; Bouhouche, I.; Catelli, M.; Neckers, L. M., The Heat Shock Protein 90 Antagonist Novobiocin Interacts with a Previously Unrecognized ATP-binding Domain in the Carboxyl Terminus of the Chaperone. *Journal of Biological Chemistry* **2000**, *275* (47), 37181-37186.
16. Yu, X. M.; Shen, G.; Neckers, L.; Blake, H.; Holzbeierlein, J.; Cronk, B.; Blagg, B. S. J., Hsp90 Inhibitors Identified from a Library of Novobiocin Analogues. *Journal of the American Chemical Society* **2005**, *127* (37), 12778-12779.
17. Burlison, J. A.; Neckers, L.; Smith, A. B.; Maxwell, A.; Blagg, B. S. J., Novobiocin: Redesigning a DNA Gyrase Inhibitor for Selective Inhibition of Hsp90. *Journal of the American Chemical Society* **2006**, *128* (48), 15529-15536.
18. Burlison, J. A.; Avila, C.; Vielhauer, G.; Lubbers, D. J.; Holzbeierlein, J.; Blagg, B. S. J., Development of Novobiocin Analogues That Manifest Anti-proliferative Activity against Several Cancer Cell Lines. *The Journal of Organic Chemistry* **2008**, *73* (6), 2130-2137.
19. Zhao, H.; Reddy Kusuma, B.; Blagg, B. S. J., Synthesis and Evaluation of Noviose Replacements on Novobiocin That Manifest Antiproliferative Activity. *ACS Medicinal Chemistry Letters* **2010**, *1* (7), 311-315.
20. Zhao, H.; Donnelly, A. C.; Kusuma, B. R.; Brandt, G. E. L.; Brown, D.; Rajewski, R. A.; Vielhauer, G.; Holzbeierlein, J.; Cohen, M. S.; Blagg, B. S. J., Engineering an Antibiotic to Fight Cancer: Optimization of the Novobiocin Scaffold to Produce Anti-proliferative Agents. *Journal of Medicinal Chemistry* **2011**, *54* (11), 3839-3853.

21. Sadikot, T.; Swink, M.; Eskew, J. D.; Brown, D.; Zhao, H.; Kusuma, B. R.; Rajewski, R. A.; Blagg, B. S. J.; Matts, R. L.; Holzbeierlein, J. M.; Vielhauer, G. A., Development of a High-Throughput Screening Cancer Cell-Based Luciferase Refolding Assay for Identifying Hsp90 Inhibitors *Assay and Drug Development Technologies* **2013**, *11* (8), 478-488.
22. Garg, G.; Zhao, H.; Blagg, B. S. J., Design, Synthesis, and Biological Evaluation of Ring-Constrained Novobiocin Analogues as Hsp90 C-Terminal Inhibitors. *ACS Medicinal Chemistry Letters* **2014**.
23. Donnelly, A. C.; Mays, J. R.; Burlison, J. A.; Nelson, J. T.; Vielhauer, G.; Holzbeierlein, J.; Blagg, B. S. J., The Design, Synthesis, and Evaluation of Coumarin Ring Derivatives of the Novobiocin Scaffold that Exhibit Antiproliferative Activity. *The Journal of Organic Chemistry* **2008**, *73* (22), 8901-8920.
24. Kusuma, B. R.; Khandelwal, A.; Gu, W.; Brown, D.; Liu, W.; Vielhauer, G.; Holzbeierlein, J.; Blagg, B. S. J., Synthesis and biological evaluation of coumarin replacements of novobiocin as Hsp90 inhibitors. *Bioorganic & Medicinal Chemistry* **2014**, *22* (4), 1441-1449.
25. Zhao, H.; Garg, G.; Zhao, J.; Moroni, E.; Girgis, A.; Franco, L. S.; Singh, S.; Colombo, G.; Blagg, B. S. J., Design, synthesis and biological evaluation of biphenylamide derivatives as Hsp90 C-terminal inhibitors. *European Journal of Medicinal Chemistry* **2015**, *89* (0), 442-466.
26. Zhao, H.; Moroni, E.; Colombo, G.; Blagg, B. S. J., Identification of a New Scaffold for Hsp90 C-Terminal Inhibition. *ACS Medicinal Chemistry Letters* **2013**, *5* (1), 84-88.
27. Byrd, K. M.; Subramanian, C.; Sanchez, J.; Motiwala, H. F.; Liu, W.; Cohen, M. S.; Holzbeierlein, J.; Blagg, B. S. J., Synthesis and Biological Evaluation of Novobiocin Core Analogues as Hsp90 Inhibitors. *Chemistry – A European Journal* **2016**, *22* (20), 6921-6931.

28. Zhao, J.; Zhao, H.; Hall, J. A.; Brown, D.; Brandes, E.; Bazzill, J.; Grogan, P. T.; Subramanian, C.; Vielhauer, G.; Cohen, M. S.; Blagg, B. S. J., Triazole containing novobiocin and biphenyl amides as Hsp90 C-terminal inhibitors. *MedChemComm* **2014**, *5* (9), 1317-1323.
29. Garg, G.; Zhao, H.; Blagg, B. S., Design, synthesis and biological evaluation of alkylamino biphenylamides as Hsp90 C-terminal inhibitors. *Bioorganic & Medicinal Chemistry* **2017**, *25* (2), 451-457.
30. Lovering, F.; Bikker, J.; Humblet, C., Escape from Flatland: Increasing Saturation as an Approach to Improving Clinical Success. *Journal of Medicinal Chemistry* **2009**, *52* (21), 6752-6756.
31. Aldeghi, M.; Malhotra, S.; Selwood, D. L.; Chan, A. W. E., Two- and Three-dimensional Rings in Drugs. *Chemical Biology & Drug Design* **2014**, *83* (4), 450-461.
32. Uyanik, M.; Akakura, M.; Ishihara, K., 2-Iodoxybenzenesulfonic Acid as an Extremely Active Catalyst for the Selective Oxidation of Alcohols to Aldehydes, Ketones, Carboxylic Acids, and Enones with Oxone. *Journal of the American Chemical Society* **2009**, *131* (1), 251-262.
33. Allen, J. R.; Bourbeau, M. P.; Chen, N.; Hu, E.; Kunz, R.; Rumfelt, S., Pyrazine compounds as phosphodiesterase 10 inhibitors. WO2010057121 A1, **2010**.
34. Zhao, H.; Blagg, B. S. J., Novobiocin Analogues with Second-Generation Noviose Surrogates. *Bioorganic & Medicinal Chemistry Letters* **2013**, *23* (2), 552-7.
35. Huang, Y.-T.; Blagg, B. S. J., A Library of Noviosylated Coumarin Analogues. *Journal of Organic Chemistry* **2007**, *72* (10), 3609-3613.

36. Burlison, J. A.; Avila, C.; Vielhauer, G.; Lubbers, D. J.; Holzbeierlein, J.; Blagg, B. S. J., Development of Novobiocin Analogues that Manifest Anti-Proliferative Activity Against Several Cancer Cell Lines. *Journal of Organic Chemistry* **2008**, *73*, 2130-2137.
37. Lu, Z.; Chen, Y. H.; Smith, C.; Li, H.; Thompson, C. F.; Sweis, R.; Sinclair, P.; Kallashi, F.; Hunt, J.; Adamson, S. E., Cyclic amine substituted oxazolidinone cetp inhibitor. WO2012058187 A1, **2012**.
38. Donaldson, W. A.; Sem, D. S.; Neumann, T. S., Substituted (4'-hydroxyphenyl)cycloalkane compounds and uses thereof as selective agonists of the estrogen receptor beta isoform. US20160340279 A1, **2016**.
39. Trah, S.; Lamberth, C., Pyridazine derivatives, processes for their preparation and their use as fungicides. WO2011095459 A1, **2011**.
40. Lewis, H. D.; Harrison, T.; Shearman, M. S., Cyclohexyl sulphones for treatment of cancer. WO2006123182 A3, **2006**.
41. Nolte, B.; Schröder, W.; Linz, K.; Englberger, W.; Schick, H.; Graubaum, H.; Roloff, B.; Ozegowski, S.; Bálint, J.; Sonnenschein, H., Substituted 4-aminocyclohexane derivatives. US9580386 B2, **2014**.

5. Probing the Hsp90 C-terminal Binding Pocket with Cytotoxic Noviose Replacements

Introduction

Molecular chaperones maintain cellular protein homeostasis via the proper folding, maturation, and degradation of proteins. The 90-kDa heat shock protein, Hsp90, is a molecular chaperone that is responsible for the maturation and folding of more than 300 client protein substrates.¹⁻² Hsp90-dependent client proteins are associated with a variety of disease states, including neurodegenerative disorders, infectious diseases, and cancer.³⁻⁴ Hsp90 exists as a homodimer with an N-terminal ATP-binding site that hydrolyzes ATP to provide the requisite energy for the protein folding cycle, a middle domain that maintains co-chaperone and substrate interactions, and a C-terminal dimerization domain that contains an EEVD motif that is critical for the interactions with various co-chaperone. There are four Hsp90 isoforms: Hsp90 α and Hsp90 β reside in the cytoplasm, TRAP1 is localized to the mitochondria, and Grp94 is found in the endoplasmic reticulum.⁵⁻⁶

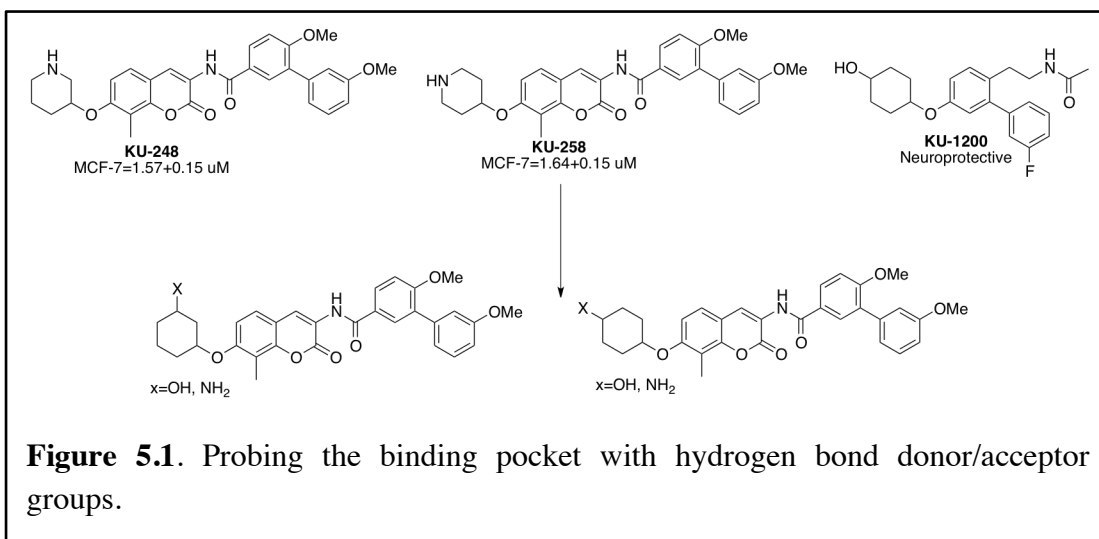
Client proteins of Hsp90 are associated with all 10 Hallmarks of cancer, making it an ideal drug target for the development of cancer therapeutics.⁷⁻¹¹ Due to the cellular stressful nature of tumor cells, Hsp90 exists in a heteroprotein complex that exhibits 200-fold greater affinity for ATP as compared to the Hsp90 complex in non-stressed cells.¹⁰⁻¹² The higher affinity manifested by the heteroprotein complex produces an inherent selectivity for cancer cells versus normal cells. Consequently, inhibitors of the N-terminal ATP-binding site have been pursued clinically for the treatment of cancer, and 17 small molecules have been evaluated in clinical trials.^{9, 13} Unfortunately toxicity, dosing and scheduling issues have been observed for most of these compounds during clinical evaluations and therefore no Hsp90 inhibitor has been FDA

approved. As a consequence of these issues, C-terminal inhibitors or isoform selective inhibitors are sought to overcome these clinical detriments. Hsp90 C-terminal inhibitors are sought because they are able to segregate client protein degradation from induction of the pro-survival heat shock response, which could overcome the dosing issues observed in the clinic. The second approach is the development of isoform selective inhibitors as certain toxicities are associated with specific Hsp90 isoforms.¹⁴⁻¹⁵

The first Hsp90 C-terminal inhibitor identified was the natural product, novobiocin, which is also a clinically used DNA gyrase inhibitor.¹⁶⁻¹⁷ In contrast to N-terminal inhibitors, treatment of cancer cells with novobiocin did not induce of the heat shock response at concentrations that led to client protein degradation. Initial structure activity relationship studies demonstrated that modifications to novobiocin could result in compounds that were either cytotoxic or neuroprotective.¹⁸⁻¹⁹ The Hsp90 C-terminal inhibitor, **KU-32**, replaced the benzamide side chain with an acetamide, which induced the pro-survival HSR without concomitant client protein degradation and upon further evaluation manifested efficacious neuroprotective activity in Alzheimer's disease, animal models of Diabetic Peripheral Neuropathy, and chemo-brain.²⁰

Synthetic complexity of the noviose sugar resulted in discovery efforts focused on simplified groups with similar or improved biological activity.²¹ Initial exploration of simplified functional groups and sugars, yielded a new series of non-noviosylated compounds "Noviomimetics", that maintained desired neuroprotective activity.²² Exploration of cytotoxic replacements for the noviose sugar identified piperidines that include **KU-248** and **KU-258** (Figure 5.1).²³⁻²⁴ Exploration of replacements for the noviose sugar replacement in both neuroprotective and cytotoxic analogs highlighted the importance of having a hydrogen bond

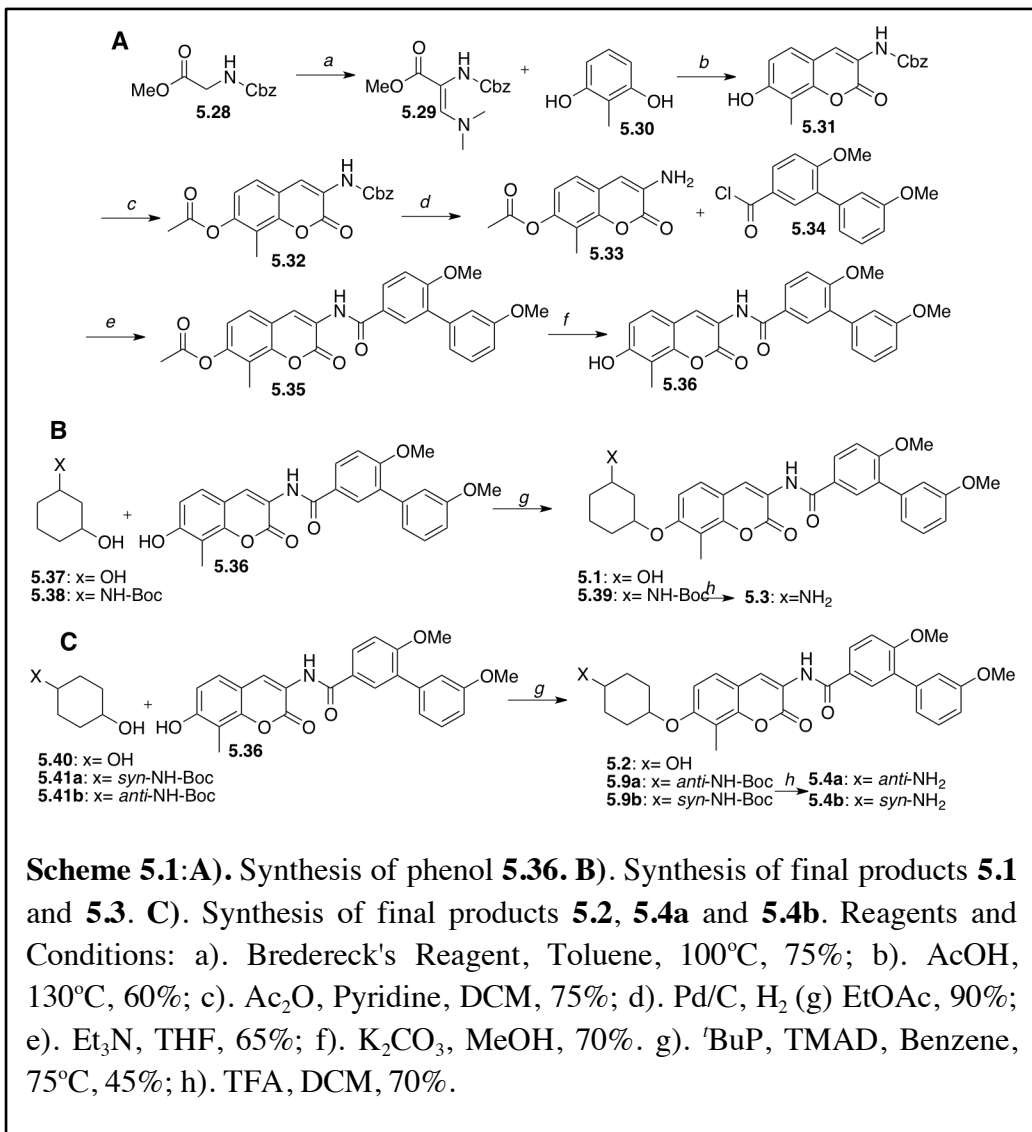
donor/acceptor at specific positions on the noviose sugar and sugar replacements.²⁵⁻²⁶ Improved C-terminal inhibitors are constantly pursued, thus potential anti-cancer therapeutics that maintains those important interactions were designed. These compounds contained simple alkyl rings with either an alcohol or an amine and were coupled to a previously optimized coumarin core that yields anti-cancer activity (Figure 5.1).²³⁻²⁴ The four initial compounds were designed to explore possible electronic interactions when the hydrogen bond donor/acceptor was removed from the ring. Additionally the simplified replacements were selected because similar biological results were obtained when the noviose sugar was replaced with a cyclohexanol ring.²² Synthesis of these compounds commenced.



Results and Discussion

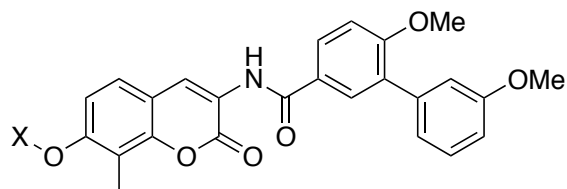
Synthesis of coumarin core **5.36** began by coupling Cbz-protected glycine **5.28** with Bredreck's Reagent in Toluene (Scheme 5.1A). Resulting enamine **5.29** was coupled with 2,4-dihydroxytoluene **5.30** in Acetic Acid for 72 hours to produce the Cbz-protected coumarin core **5.31**. Treatment of **5.31** with acetic acid and pyridine in dichloromethane resulted **5.32**. Hydrogenolysis gave free amine **5.33**, which was subsequently coupled with acid chloride **5.34**

to yield coumarin **5.35**. Removal of the acetate resulted in phenol **5.36** (Scheme 5.1A). Mitsunobu conditions were utilized to obtain coupled products **5.1**, **5.39**, **5.2**, **5.9a**, and **5.9b** (Scheme 5.1B and 5.1C). Subsequent removal of the Boc protecting group produced final products **5.3**, **5.4a**, and **5.4b**.



Upon synthetic completion the anti-proliferative activity was determined by an MTS assay. Analogs were evaluated in two breast cancer cell lines MCF-7 (estrogen receptor positive cells) and SkBr3 (estrogen receptor negative HER2 overexpressing).

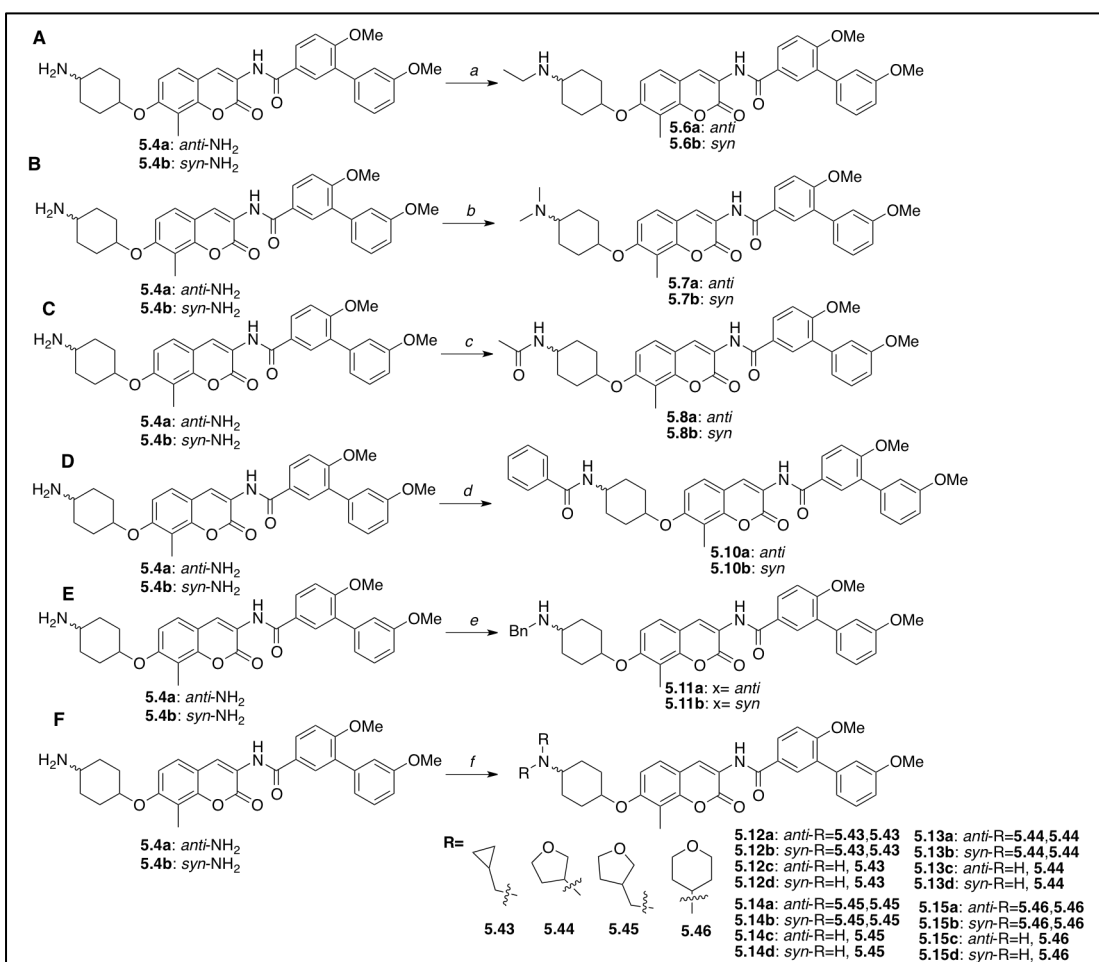
Table 5.1. Anti-proliferative activity of cyclohexylamine and cyclohexanol analogs.



Compound	X	MCF-7 (IC ₅₀ , μM) ^a	SkBr3 (IC ₅₀ , μM) ^a
5.1		4.21±0.59	6.882±0.43
5.2		4.68±0.53	5.368±0.61
5.3		5.76 ±0.12	3.82±0.12
5.4a		1.625±0.22	0.7745±0.36
5.4b		0.9±0.19	0.79±0.30

^aValues represent mean ± standard deviation for at least two separate experiments performed in triplicate.

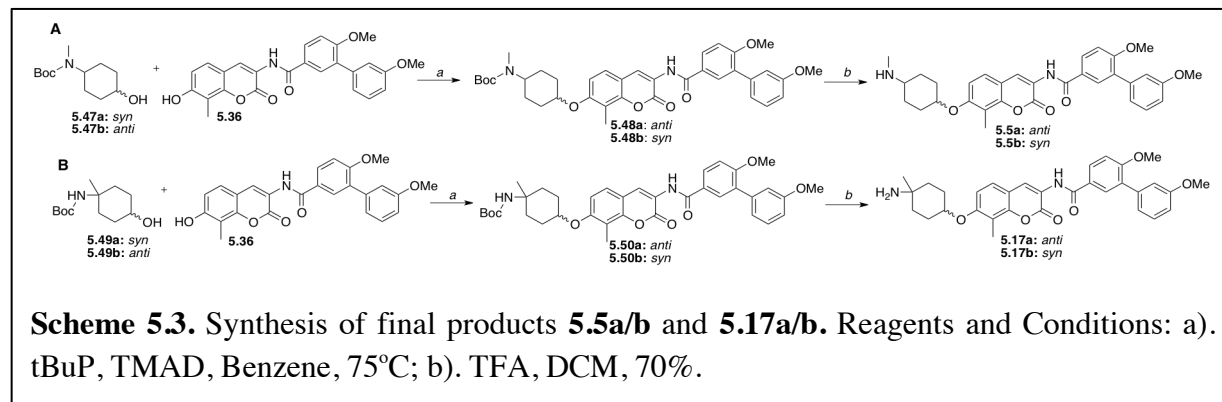
All analogs displayed anti-proliferative activity against the breast cancer cell lines illustrated in Table 5.1. Analogs **5.1**, **5.2**, and **5.3**, diastereomeric mixtures, exhibited similar activity in both cell lines. Interestingly the 4-*syn*-amine (**5.4b**) produced the best anti-proliferative activity of all of the new analogs. This data suggests that extending the hydrogen bond donor/acceptor from the ring is equally beneficial as the biological activity is similar to the parent compounds **KU-248** and **KU-258** (Figure 5.1). Due to these promising initial results, new analogs were designed that extended a variety of functional groups off of both the *syn*- and *anti*-amine at the 4-position. The functional groups selected continued to explore electrostatic interactions and investigate if a bulky substituent could be tolerated within the binding pocket at the 4- position. Noviomimetic exploration highlighted that groups as large as a benzyl could be tolerated at the 4 position of a cyclohexane ring, so both a benzyl and benzamide functional group will be utilized in this study.²² These new analogs were synthesized in the following manner (Scheme 5.2).



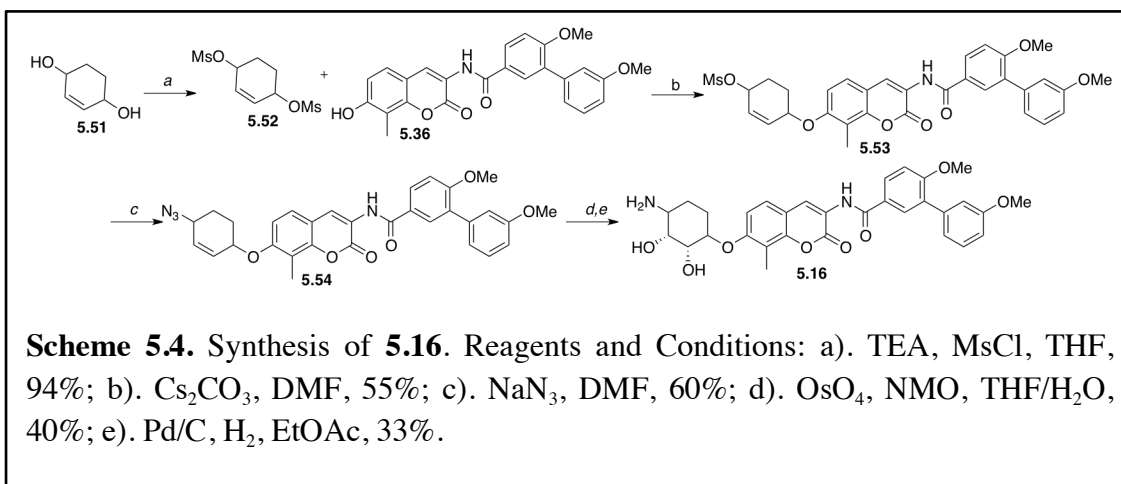
Scheme 5.2. Synthesis of final products **5.6a/b**, **5.7a/b**, **5.8a/b**, **5.9a/b**, **5.10a/b**, **5.11a/b**, **5.12a/b/c/d**, **5.13a/b/c/d**, **5.14a/b/c/d**, and **5.15a/b/c/d**. Reagents and Conditions: a). Pt/C, H₂ (g), MeCN, MeOH, 60%; b). Acetic Acid, Formaldehyde, NaBH₃CN, MeOH, 40%; c). Acetic Anhydride, TEA, DCM, rt, on, 70%; d). Benzoyl Chloride, TEA, THF, rt, on, 70%; e). BnBr, K₂CO₃, MeCN, 40%; f). RBr, DIPEA, MeCN, *m*120°C, 1hr, 30%.

Each mono-substituted product was synthesized in the manner described in Scheme 5.2. Analogs **5.6a** and **5.6b** were obtained via treatment of **5.4a/b** with Pt/C, acetonitrile, and hydrogen gas. These conditions ensured mono addition to the amine. **5.4a** or **5.4b** was subjected to acetic acid, formaldehyde, and sodium cyanoborohydride to obtain di-methylated amine **5.7a** or **5.7b**. Acetate **5.8a** or **5.8b** was obtained by subjecting **5.4a/b** in

dichloromethane. Similarly, the benzamide analogs **5.10a** and **5.10b** were obtained via addition of triethylamine and benzoyl chloride at 0 °C to **5.4a/b**. Benzyl substituted amines **5.11a** and **5.11b** were obtained *via* refluxing **5.4a/b** with benzyl bromide and K₂CO₃ in acetonitrile overnight.

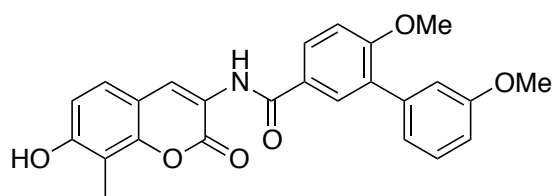


Mono-methyl derivatives **5.5a** and **5.5b** were obtained by selective reduction of *tert*-butyl methyl(4-oxocyclohexyl)carbamate to either the *syn* or *anti* alcohol (**5.47a** and **5.47b**) using NaBH₄ or L-selectride. Mitsunobu conditions were used to couple alcohols **5.47a/b** with phenol **5.36**. Subsequent Boc-deprotection of **5.48a/b** yielded methylamine **5.5a/b**. Methylcyclohexamine analogs **5.17a/b** were obtained *via* coupling **5.49a/b** with phenol **5.36** using Mitsunobu conditions. Removal of the Boc-protecting group provided final products **5.17a/b**.

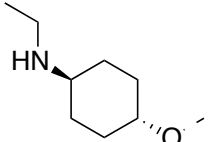
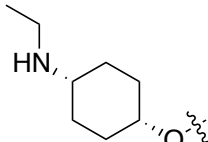
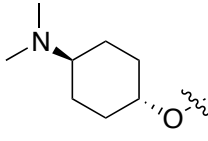
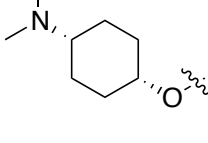
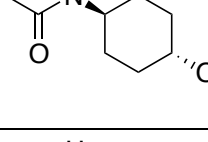
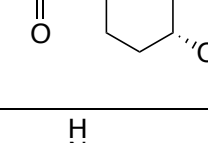
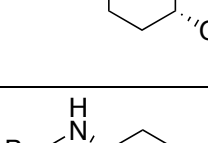
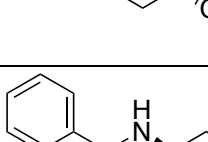
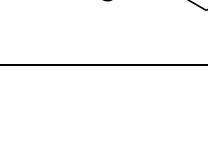


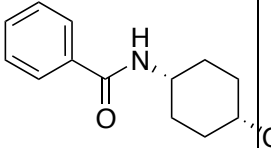
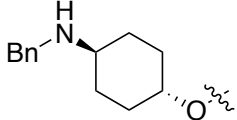
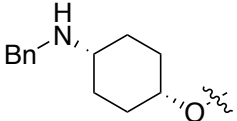
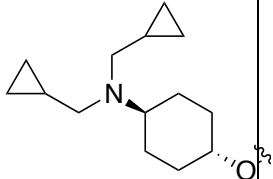
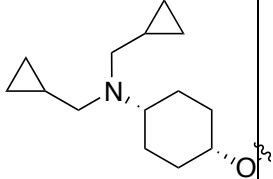
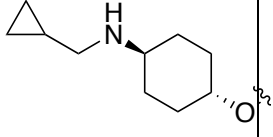
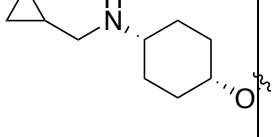
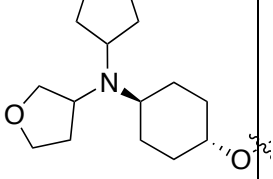
Analog **5.16** was synthesized *via* coupling mesylate **5.52** with phenol **5.36**. The coupled mesylate was subsequently subjected to NaN₃, to obtain azide **5.54**. Osmium tetroxide was added to obtain cis-diol **5.55**. Hydrogenolysis was used to acquire amine **5.16**. Upon completion of synthesis the analogs were evaluated in the MTS anti-proliferation assay in MCF-7 and SkBr3 cells.

Table 5.2. Anti-proliferative activity of cyclohexylamine derivatives

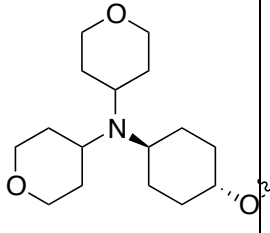
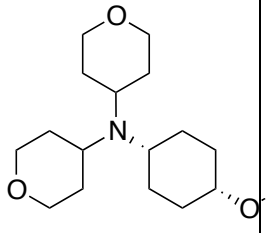
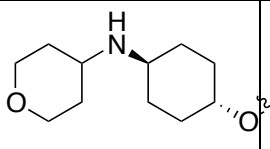
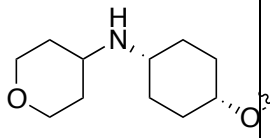
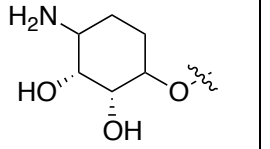
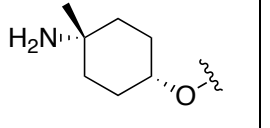
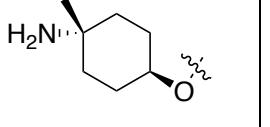


Compound	Side Chain	MCF-7 (IC ₅₀ , μM) ^a	SkBr3 (IC ₅₀ , μM) ^a
5.5a		6.79±0.77	4.16±0.33
5.5b		4.35±1.06	3.38±0.15

5.6a		8.91±0.76	7.45±0.45
5.6b		7.76±0.08	6.21±0.32
5.7a		1.231±0.23	0.962±0.15
5.7b		3.803±0.08	3.485±0.07
5.8a		1.16±0.01	1.74 ±0.71
5.8b		>50	>50
5.9a		>50	>50
5.9b		>50	>50
5.10a		>50	>50

5.10b		>50	>50
5.11a		1.924±0.08	1.568±0.64
5.11b		>50	>50
5.12a		14.45±0.98	14.1±0.64
5.12b		12.34±0.65	12.8±0.31
5.12c		0.97±0.05	1.03±0.14
5.12d		4.98±0.06	3.56±0.21
5.13a		6.31±0.06	5.78±0.18

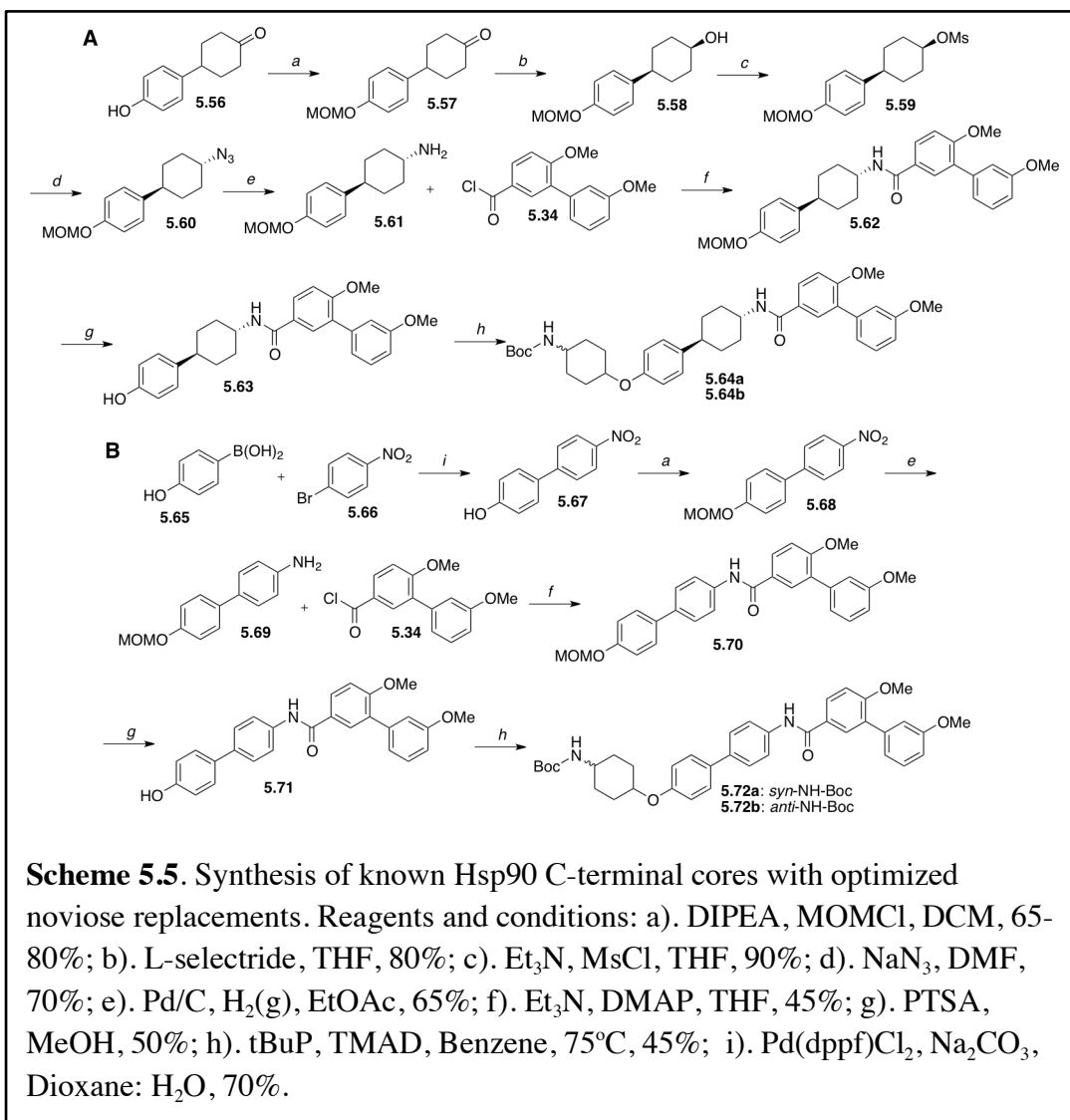
5.13b		2.3±0.22	2.45±0.11
5.13c		0.89±0.05	0.81±0.02
5.13d		1.04±0.09	2.15±0.31
5.14a		2.6±0.28	3.02±0.20
5.14b		1.6±0.41	0.98±0.08
5.14c		1.39±0.17	1.48±0.09
5.14d		1.29±0.29	1.54±0.43

5.15a		5.32±0.65	4.87±0.38
5.15b		7.12±.066	6.56±0.53
5.15c		4.76±0.39	3.87±0.46
5.15d		5.62±0.33	4.77±0.55
5.16		1.21±0.06	1.02±0.19
5.17a		4.02±0.35	2.91±0.9
5.17b		3.00±0.71	2.83±0.10

^aValues represent mean ± standard deviation for at least two separate experiments performed in triplicate.

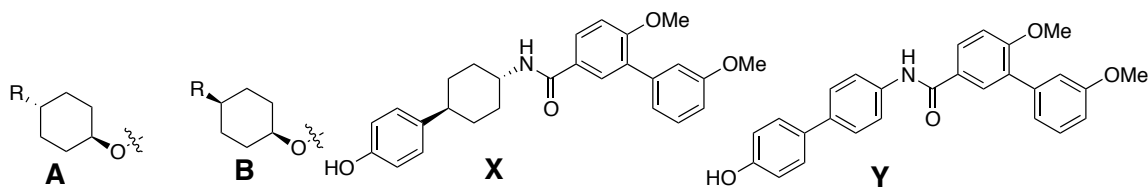
The modified amines did not exhibit improved biological activity when compared to **5.4a/b**. The *anti* analogs exhibited slightly improved activity when compared to the

corresponding *syn* analog. The larger mono-substituted amines had improved activity when compared to the corresponding di-substituted amine (**5.13a** versus **5.13c**). It is possible that the bulk of the di-substituted amines decreased the binding affinity of the compound, resulting in the loss of biological activity. In contrast, the smaller di-methyl analogs **5.7a/b** exhibited improved activity compared to the mono-methyl, **5.5a/b**. Interesting *anti* analogs **5.8a** and **5.11a** exhibited anti-proliferative activity while the corresponding *syn* derivatives were not active even at high concentrations. To determine what causes this dramatic difference in activity, more analogs will need to be synthesized and additional biological studies should be carried on these compounds. Since analogs did not improve anti-proliferative activity as compared to **5.4a/b**, new cores were selected to replace the coumarin core in order to see what effect increasing core flexibility and length would have on the biological activity of these compounds. The phenyl cyclohexyl and biphenyl core were selected as they are both validated cores of Hsp90 C-terminal inhibitors.



The synthesis of analogs with a phenyl cyclohexyl and biphenyl core was carried out as illustrated in Scheme 5.5. Upon completion of synthesis the analogs were evaluated in the MTS assay in MCF-7 and SkBr3 breast cancer cell lines.

Table 5.3. Core comparison with optimized replacements



Compound	Side Chain	R	Core	MCF-7 (IC ₅₀ , μM) ^a	SkBr3 (IC ₅₀ , μM) ^a
5.18a	A		X	4.7±1.21	3.43±0.14
5.18b	B		X	2.33±1.02	1.58±0.32
5.19a	A		Y	3.21±0.35	3.56±0.11
5.19b	B		Y	3.62±0.1	3.52±0.05

^aValues represent mean ± standard deviation for at least two separate experiments performed in triplicate.

The anti-proliferative activity of these compounds is relatively flat. Even with the increased length and flexibility of the phenyl cyclohexyl and biphenyl cores compared to the coumarin, the anti-proliferative activity of all analogs is very similar. Additionally, the stereochemistry of the cyclohexylamine does not appear to have any impact on anti-proliferative activity.

Validation of Hsp90 inhibition via Western Blot Analysis

After determination of the IC₅₀ values, a few compounds were selected for western blot analysis in MCF-7 cells. Analogs **5.4a**, **5.4b**, and **5.7a** were selected to explore the effect of stereochemistry on Hsp90 inhibition.

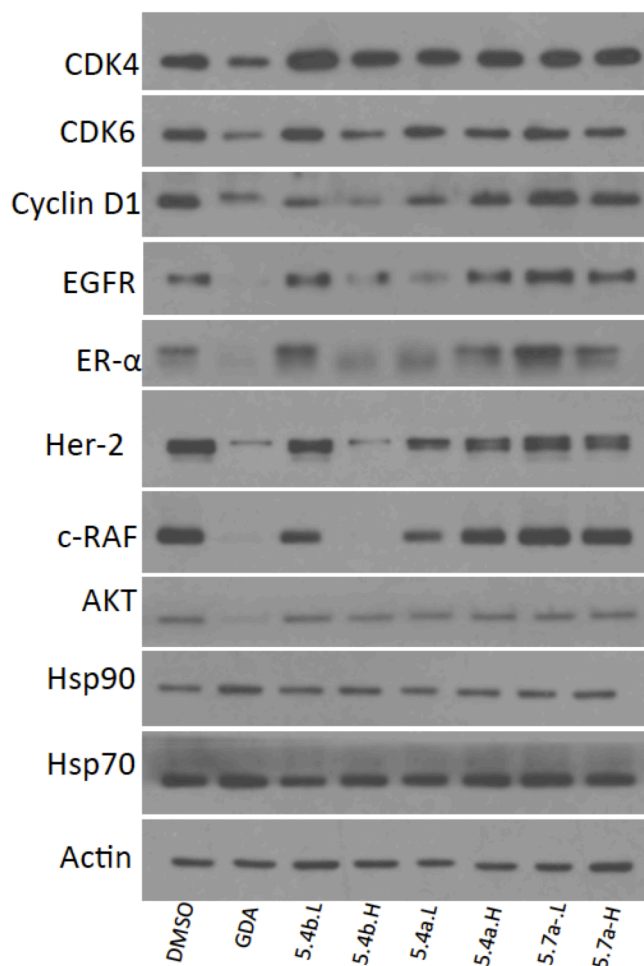
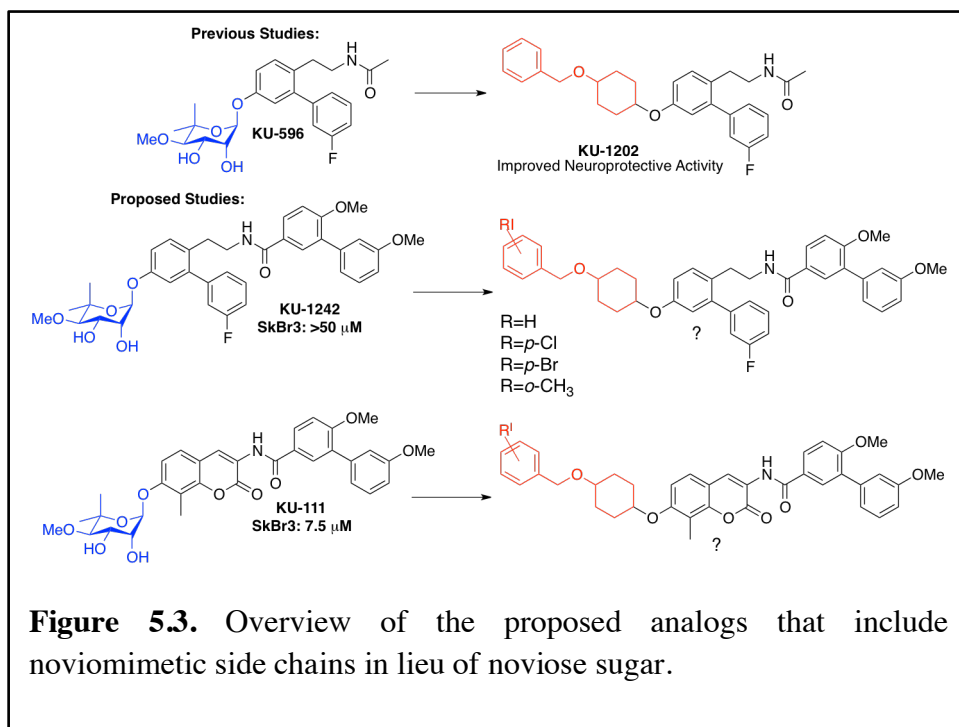


Figure 5.2. Western blot analyses of **5.4a**, **5.4b**, and **5.7a** after incubation with MCF-7 breast cancer cells for 24 h. The high concentration is five times the IC_{50} value, and the low concentration is half the IC_{50} value. Concentrations for each analog tested were as follows: **5.4a** (high: 8.25 μ M, low: 0.83 μ M), **5.4b** (high: 4.50 μ M, low: 0.45 μ M), and **5.7a** (high: 6.15 μ M, low: 3.08 μ M). GDA (500nM) was the positive control and DMSO was used as the negative control.

Compound **5.4b** caused the degradation of many Hsp90 client proteins. **5.7a** resulted in slight degradation of ER- α , however **5.4a** did not result in degradation of any of the client proteins. No compounds resulted in induction of the heat shock proteins, which is a hallmark of

C-terminal inhibitors. Additionally Actin, a Hsp90 independent protein, levels did not change in response to compound treatment. This data strongly suggests that for cyclohexylamine analogs *syn* stereochemistry is important for Hsp90 activity.

The current study was then expanded upon to include noviomimetic side chains that were utilized in neuroprotective compounds (**KU-1202**, Figure 5.3). These noviomimetic side chains were coupled with anti-cancer scaffolds (coumarin and biaryl **KU-1242** and **KU-111**, Figure 5.3) to investigate potential anti-cancer activity (Figure 5.3). Noviomimetic side chains were able to produce similar and often improved neuroprotective activity as compared to the noviose sugar for a variety of scaffolds.²²

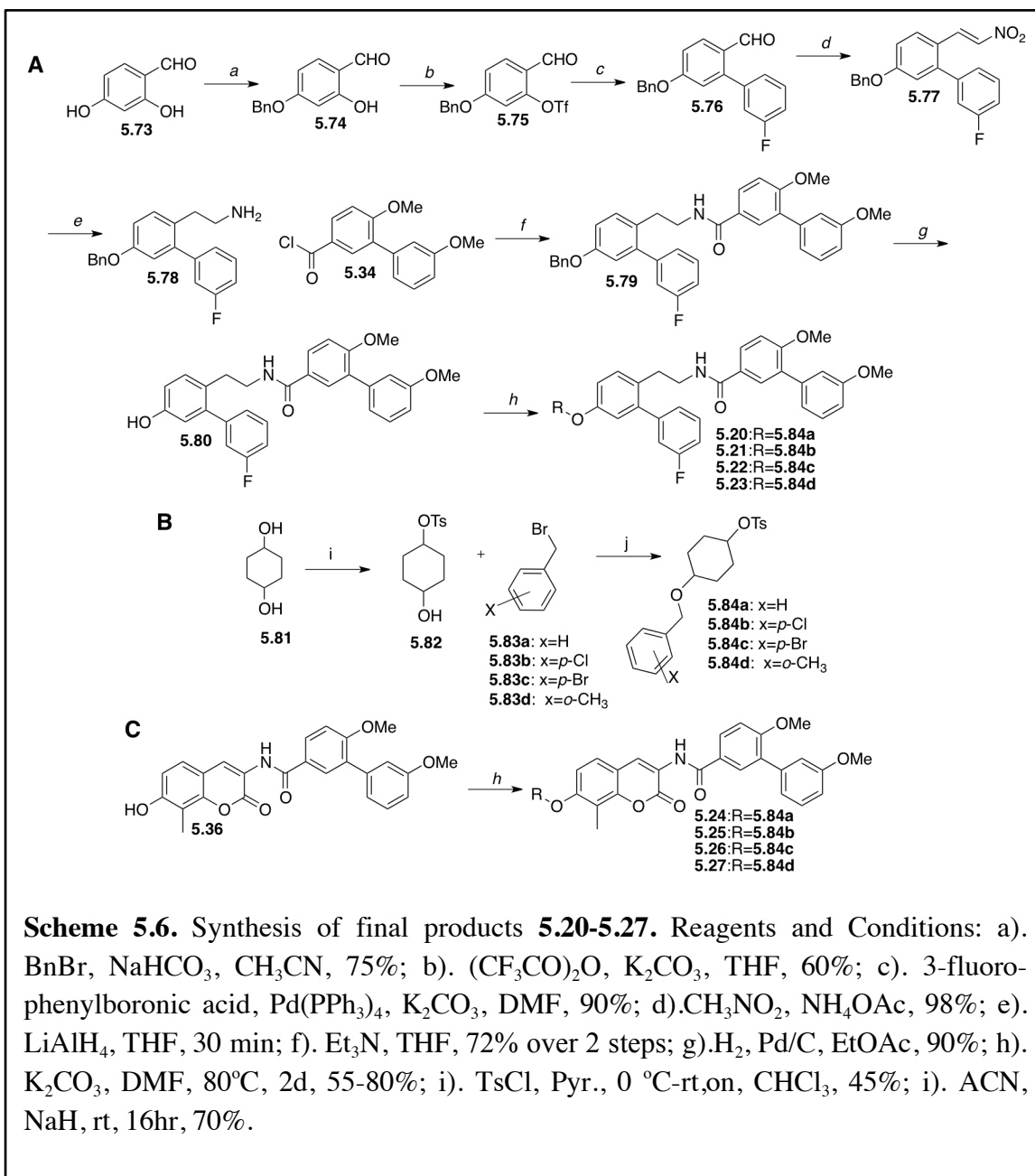


These compounds were selected to verify whether the noviomimetic side chains were non-toxic in cells and to explore how different side chains may impact anti-cancer activity.

Chemistry

Biaryl containing analogs were synthesized beginning with selective benzyl protection of 2, 4-dihydroxybenzaldehyde, **5.73** (Scheme 5.6). Microwave conditions were used to convert benzyl ether **5.74** to the corresponding trifluoromethanesulfonate, which was then coupled with 3-fluorophenyl boronic acid using Suzuki coupling conditions to generate the biaryl ring system found in **5.76**. Henry reaction conditions were utilized to obtain the α - β unsaturated nitro **5.77**. Treatment with lithium aluminum hydride reduced both the nitro and olefin to amine **5.78**. Acid chloride **5.34** was coupled with amine **5.78** in the presence of triethylamine and DMAP, to generate **5.79**. Hydrogenolysis conditions were then utilized to cleave the benzyl ether and obtain phenol **5.80**.

The toluenesulfonates of the noviomimetic side chains were synthesized (Scheme 5.6b) and coupled with phenol **5.80** via S_N2 substitution reaction to obtain compounds **5.20-5.23**. (Scheme 5.6a).

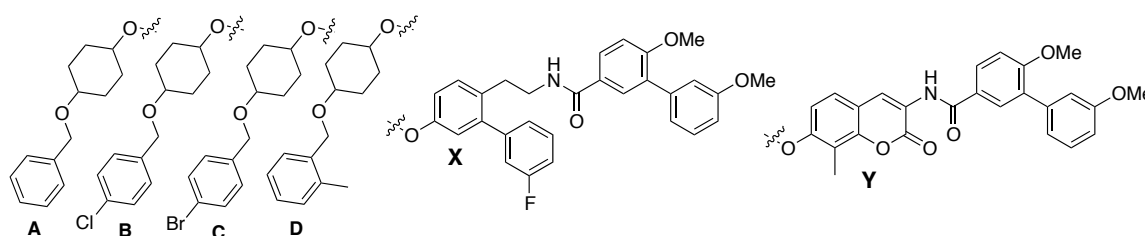


Coumarin core phenol **5.36** was synthesized as described in Scheme 1. S_N2 substitution reaction conditions were then utilized to couple toluenesulfonate noviomimetics to yield compounds **5.24-5.27** (Scheme 5.6c).

Biological Evaluation

Upon completion of the synthesis, the analogs were evaluated in a MTS anti-proliferation assay in MCF-7 (estrogen receptor positive cells), SkBr3 (estrogen receptor negative HER-2 overexpressing), and MDA-MB-231 (triple negative) breast cancer cell lines, and non-cancerous HEK-293 cells (human embryonic kidney).

Table 5.4. Anti-proliferative activity of Compounds 5.20-5.27.

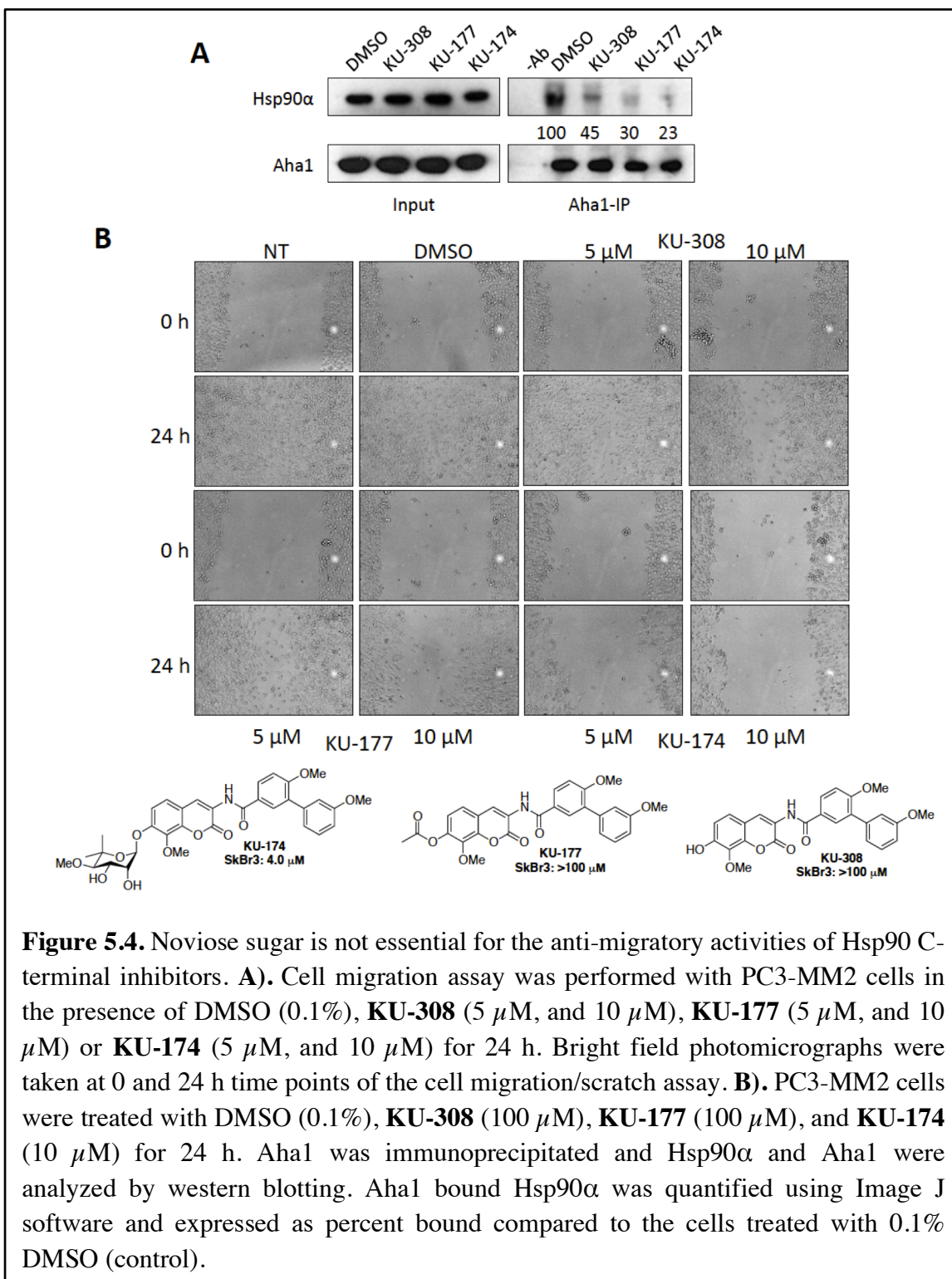


Compound	Side Chain	Core	MCF-7 (IC ₅₀ , μM) ^a	SkBr3 (IC ₅₀ , μM) ^a	MDA-MB-231 (IC ₅₀ , μM) ^a	HEK293 (IC ₅₀ , μM) ^a
5.20	A	X	>50	>50	>50	>10
5.21	B	X	>50	>50	>50	>10
5.22	C	X	>50	>50	>50	>10
5.23	D	X	>50	>50	>50	>10
5.24	A	Y	>50	>50	>50	>10
5.25	B	Y	>50	>50	>50	>10
5.26	C	Y	>50	>50	>50	>10
5.27	D	Y	>50	>50	>50	>10

^aValues represent mean ± standard deviation for at least two separate experiments performed in triplicate.

The analogs did not exhibit cytotoxic activity against any of the breast cancer cell lines nor did they exhibit cytotoxicity in the non-cancerous cell line HEK-293, Table 5.4. The absence of cytotoxicity is significant because these side chains were originally designed to replace the noviose sugar for the treatment of neurodegenerative diseases. Development of compounds that replace the noviose sugar with a surrogate have lead to new studies which investigate the biological importance of the noviose sugar.

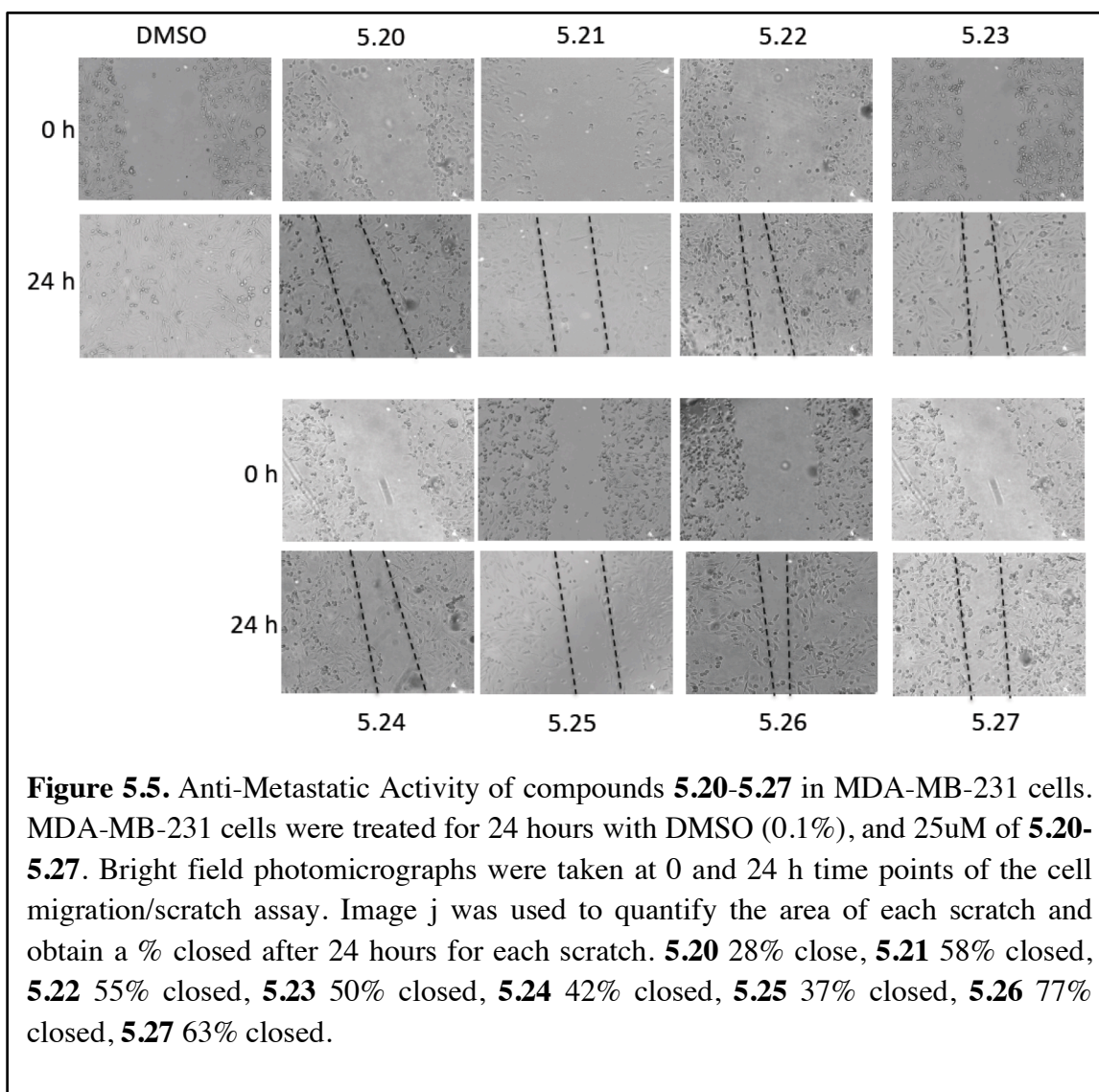
Recently, the Hsp90 C-terminal inhibitor **KU-174**, which contains the biaryl side chain, was able to prevent cancer cell migration.²⁷ Due to these promising results, analogs of **KU-174** were evaluated to determine the importance of the noviose sugar with regards to the desired anti-migratory activity. Two analogs, **KU-177** and **KU-308**, were selected for initial studies due to their lack of cytotoxicity in a variety of immortalized cancer cell lines. These two analogs were void of any cytotoxic moiety in lieu of the noviose sugar. It is possible that the lack of cytotoxicity is because these two analogs are unable to interact with several amino acids within the binding pocket known to form important binding interactions with noviose sugar (Thr540, Gln682, and Asn686). Unpublished co-immunoprecipitation results show that the three analogs disrupted the Hsp90a/AHA1 complex (Figure 5.4a).



Highly metastatic PC3-MM2 prostate cancer cells were utilized to verify anti-migratory activity via a wound healing scratch assay (WHA) of the compounds due to disruption of the

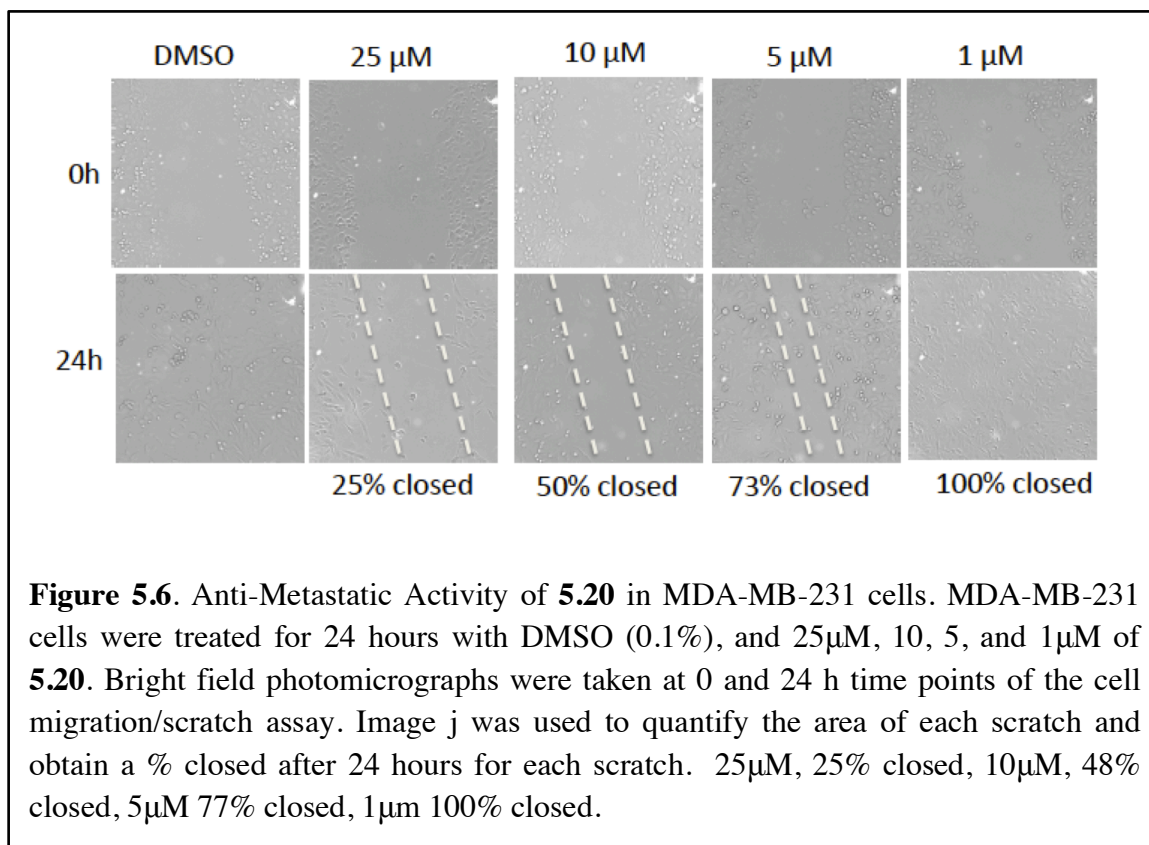
Hsp90 α /Aha1 complex. Both **KU-308** and **KU-177** inhibit cancer cell migration at $\sim 10 \mu\text{M}$ concentration (Figure 5.4b). **KU-177**, which contains the acetyl ester, was more effective than the non-acetylated derivative **KU-308** at inhibition of cell motility. Because **KU-177** and **KU-308** are non-toxic, the therapeutic window is very large since the IC_{50} value exhibited by these compounds is $>100 \mu\text{M}$ and anti-migratory activity were observed at low micro-molar concentrations (Figure 5.4b).

These preliminary results highlight that the noviose sugar is not essential for anti-migratory activity, and verification that there were no unintended cytotoxic effects upon treatment with **5.20-5.27**. A WHSA was carried out with MDA-MB-231 cells to evaluate potential anti-metastatic activity of these compounds (Figure 5.5).



Compounds **5.20**, **5.24**, and **5.25** resulted in promising anti-metastatic activity (Figure 5.5). The increased length of C-terminal inhibitors that contain the biaryl core appear too long to fit within the binding pocket, whereas the coumarin core is shorter in length, and produced two analogs that manifest the most promising activity and are also the shortest.

After a promising initial screen (Figure 5.5), compound **5.20** was selected for further evaluation. A dose response WHSA in MDA-MB-231 breast cancer cells was carried out using 1µM, 5µM, 10µM, and 25µM concentrations (Figure 5.6).



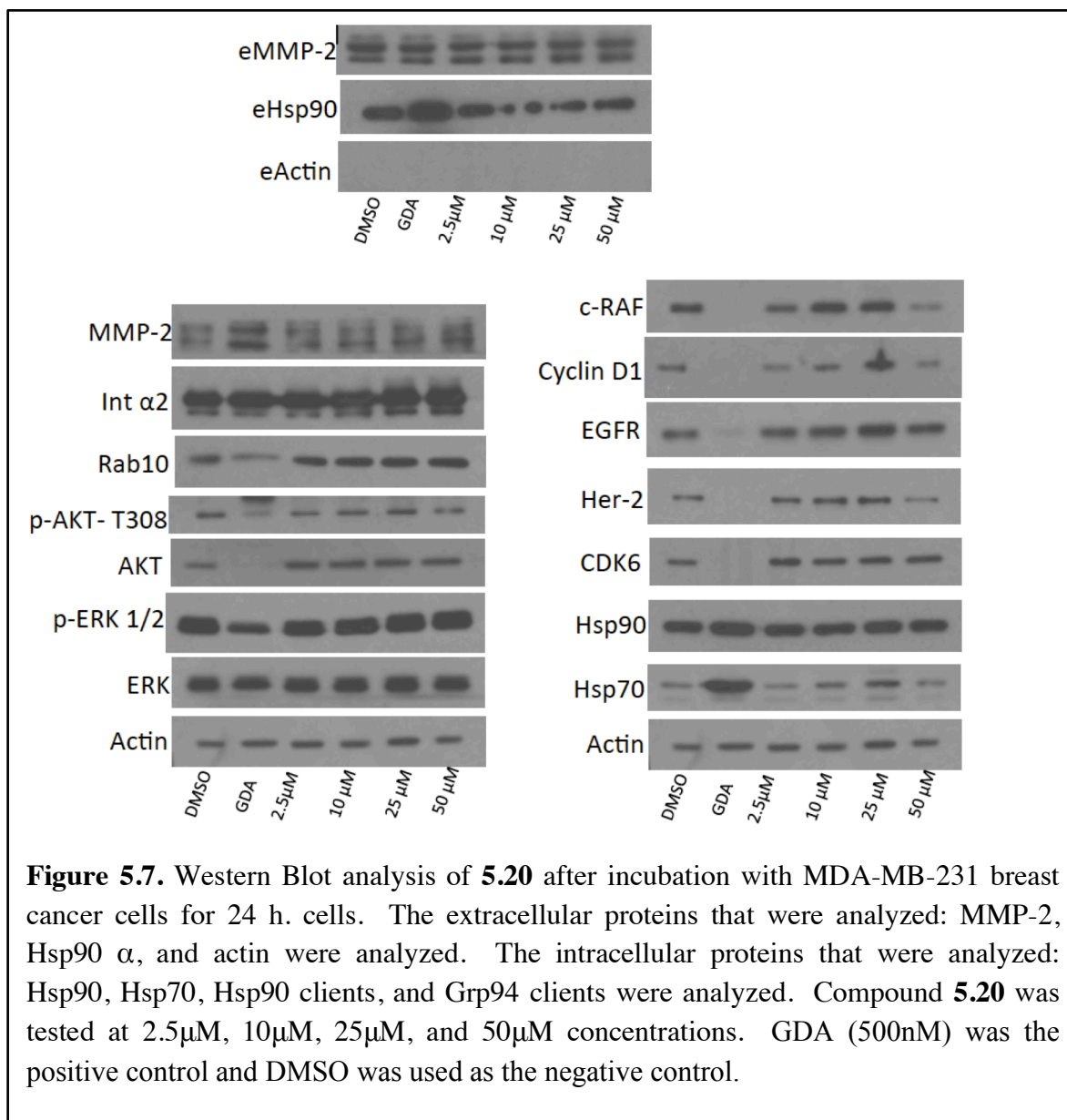
Compound **5.20** exhibits excellent anti-metastatic activity with only 50% of the wound being closed after 24 hours at 10 μ M (Figure 5.6). Because **5.20** does not exhibit any cytotoxicity the therapeutic window is quite large, making it an interesting biological probe with therapeutic potential. Therefore investigation of the mechanism of action for compounds **5.20** and **5.25** began. Compound **5.25** was also selected for further evaluation because it exhibited promising anti-metastatic activity. These compounds were first evaluated for potential Grp94 activity because there is a well-established connection between Grp94 selective inhibitors and prevention of cell migration.

Recent studies have shown that Hsp90 isoform Grp94, is responsible for the maturation of toll-like receptors, immunoglobulins, and integrins.²⁸ Integrins are important for cell adhesion and metastasis; therefore inhibition of Grp94 would prevent metastasis. Also, inhibition of

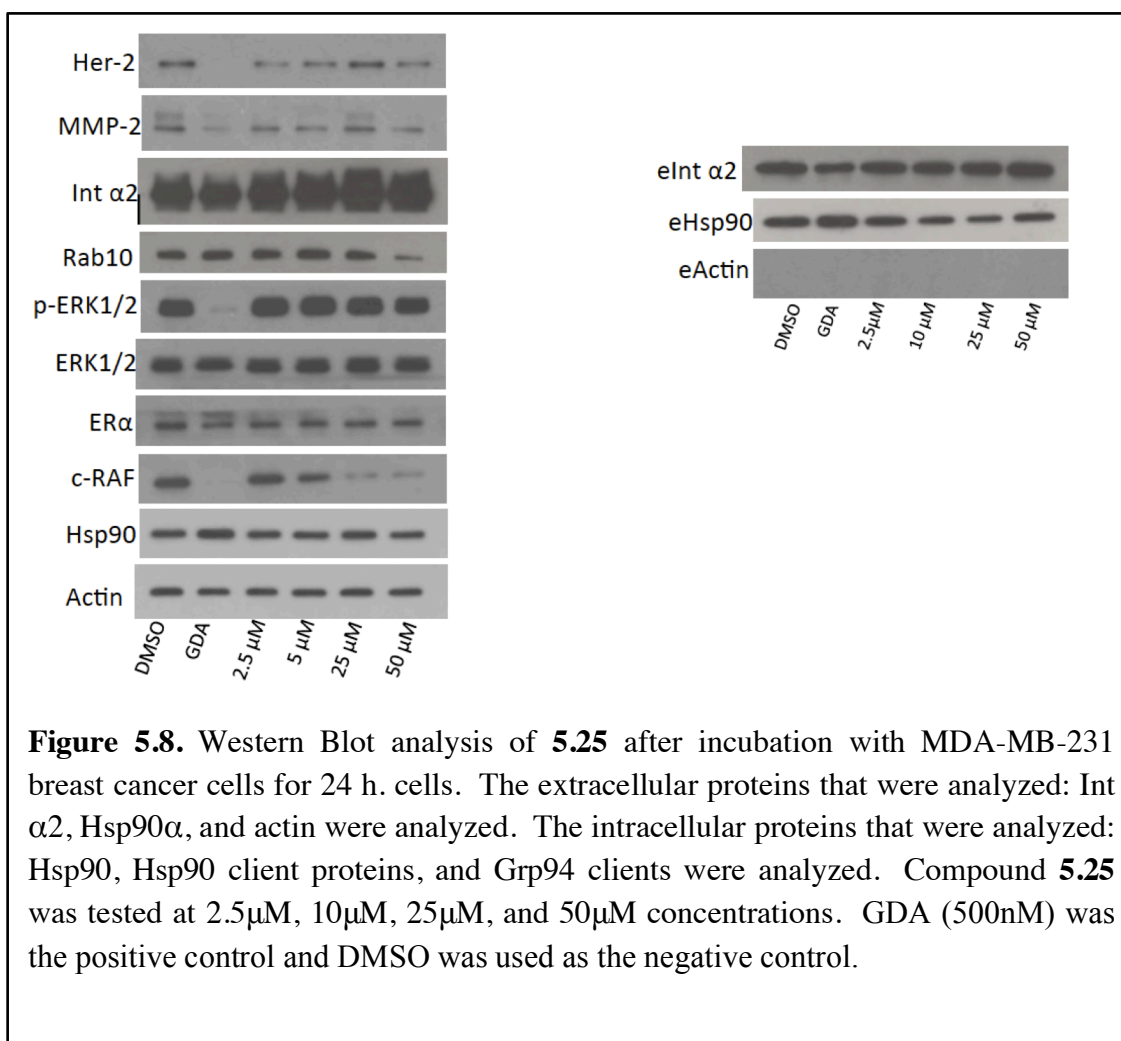
Grp94 prevents the Grp94-mediated toll-like receptor trafficking to the cell surface, which is also important for cancer cell migration.¹⁴ Collectively these studies have shown that Grp94-selective inhibitors are promising anti-metastatic agents.

As a result of these findings and the anti-metastatic properties, the analogs were assessed for Grp94, e Hsp90 (extracellular Hsp90), and general Hsp90 activity. Immunoblot analysis of MDA-MB-231 cells was performed and client proteins involved in cellular metastasis pathways, such as pERK1/2 and pAKT, and client proteins associated with the Hsp90 isoform Grp94 (Int α 2 and Rab10) were visualized. Additionally levels of select extracellular proteins were selected to determine if **5.20** and **5.25** have an effect on extracellular heat shock protein 90.²⁹ MMP-2, metalloproteinase-2, is a protein that plays a pivotal role in wound healing and relies upon Hsp90 for cleavage into its active form. Levels of both pro- and active MMP-2 were analyzed in response to treatment with different concentrations of **5.20** and **5.25**. Unfortunately there was no clear down regulation of the active form of MMP-2, meaning compounds were not acting via extracellular Hsp90 inhibition, which would result in a decrease of MMP-2 active levels.

Immunoblot analysis of **5.20** (Figure 5.7), did not clarify a possible mechanism of action. There was no observed degradation of extracellular proteins, specifically no change in extracellular MMP-2 pro to active levels. Importantly, no extracellular actin was found, thus verifying that cellular contents were not in the extracellular space due to cell lysis from stress. Therefore, we were able to conclude that we only isolated the extracellular proteins. Due to an absence of change in eHsp90 α and MMP-2 levels, compound **5.20** is likely not targeting



extracellular Hsp90. Additionally, there were no changes in intracellular p-AKT and pErk1/2 levels, indicating that the compounds are not preventing metastasis by targeting intracellular pathways. There was no decrease in Grp94-dependent clients Int α 2 and Rab10 indicating that the compounds are not causing anti-metastatic activity through a Grp94-isoform-dependent effect. There is slight client protein degradation of Her2, C-Raf, and Cyclin D1 at the highest concentration tested, however it is unlikely that this client protein degradation is related to the anti-metastatic activity. The degradation of these client proteins confirms that at 50 μ M these



compounds are exhibiting characteristics associated with C-terminal inhibition (lack of heat

shock protein induction at concentrations where there is client protein degradation). Simultaneously immunoblot analysis of **5.25** was carried out in MDA-MB-231 cells (Figure 5.8).

Similar to compound **5.20**, immunoblot analysis of **5.25** did not confirm a possible mechanism of action for these compounds. The difference between these compounds was that **5.25** exhibited significant degradation at the highest concentrations of C-Raf. Again, degradation of C-Raf is likely unrelated to the anti-metastatic activity, but is indicative of Hsp90 C-terminal inhibition. Interestingly there appears to be slight degradation of Rab10 at the highest concentration of **5.25**. It is possible that at very high concentrations of inhibitor some Grp94-dependent clients could be affected. However without observed degradation of Grp94-dependent client Integrin $\alpha 2$, it is difficult to say compound **5.25** targets Grp94.

Conclusion

Two series of compounds were synthesized in attempt to probe the C-terminal binding site. One series of compounds were either coumarin or biaryl containing compounds with noviomimetic side chains that were synthesized and found to exhibit anti-metastatic activity. These compounds were non-toxic and exhibited good anti-migratory activity in a wound healing scratch assay. An initial study to determine the mechanism of action for these compounds was inconclusive. Moving forward, co-IP studies between Hsp90 isoforms and co-chaperones are necessary to continue to probe mechanism of action. Once the mechanism of action can be determined this series of compounds could be expanded to evaluate all noviomimetic side chains explored for KU-596 derivatives. This series of compounds represent a promising new scaffold of non-toxic compounds with a large therapeutic window that exhibit anti-metastatic activity.

The second series of compounds were designed and synthesized to project hydrogen bond donor/acceptor moieties into unexplored regions of the binding pocket. Both *syn* and *anti*

derivatives of the cyclohexylamine compounds were similarly cytotoxic, however western blot analysis highlighted that *syn* stereochemistry is important for Hsp90 inhibition. Cyclohexylamine derivative development should continue and more cyclohexylamines should be coupled with the phenyl cyclohexyl core to further explore anti-cancer activity due to inhibition of the Hsp90 C-terminus.

Materials and Methods

Anti-proliferation assays.

Cells were maintained in a 1:1 mixture of Advanced DMEM/F12 (Gibco) supplemented with non-essential amino acids, L-glutamine (2 mM), streptomycin (500 µg/mL), penicillin (100 units/mL), and 10% FBS. Cells were grown to confluence in a humidified atmosphere (37° C, 5% CO₂), seeded (2000/well, 100 µL) in 96-well plates, and allowed to attach overnight. Compound or GDA at varying concentrations in DMSO (1% DMSO final concentration) was added, and cells were returned to the incubator for 72 h. At 72 h, the number of viable cells was determined using an MTT/PMS cell proliferation kit (Promega) per the manufacturer's instructions. Cells incubated in 1% DMSO were used at 100% proliferation, and values were adjusted accordingly. IC₅₀ values were calculated from separate experiments performed in triplicate using GraphPad Prism.

Wound Healing Scratch Assay.

Trypan blue exclusion was utilized to count MDA-MB-231 cells and seed 12-well plates at 200,000 cells/mL/well, which were then placed in an incubator for 24 h. After 12 h, two scratches per well were made with a 0.1-10 µL pipette tip, then cells were washed with PBS and

then fresh media was added to each well. The compound or DMSO control was then added (0.25% DMSO final concentration) and pictures taken were taken (0h) with a camera-mounted Olympus IX-71 microscope (10X objective). Plates were then returned to the incubator until 24 h, at which point pictures were taken again. Images were processed and % migration determined via ImageJ. All experiments were performed in at least duplicate.

Western blot Analysis.

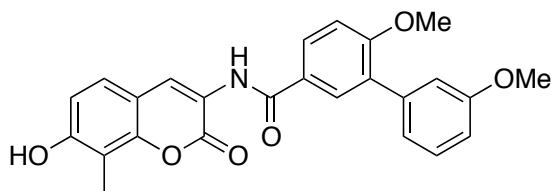
MCF-7 cells were cultured as described above and treated with various concentrations of drug, GDA in DMSO (1% DMSO final concentration), or vehicle (DMSO) for 24 h. Cells were harvested in cold PBS and lysed in RIPA lysis buffer containing 1 mM PMSF, 2 mM sodium orthovanadate, and protease inhibitors on ice for 1 h. Lysates were clarified at 14000g for 10 min at 4° C. Protein concentrations were determined using the Pierce BCA protein assay kit per the manufacturer's instructions. Equal amounts of protein (20 µg) were electrophoresed under reducing conditions, transferred to a nitrocellulose membrane, and immunoblotted with the corresponding specific antibodies. Membranes were incubated with an appropriate horseradish peroxidase-labeled secondary antibody, developed with a chemiluminescent substrate, and visualized.

Chemistry General.

¹H NMR were recorded at 500 MHz (Avance AVIII 500 MHz spectrometer with a dual carbon/proton cryoprobe) or 400 (Bruker AVIIIHD 400 MHz NMR with a broadband X-channel detect gradient probe) and ¹³C NMR were recorded at 125 MHz (Bruker AVIII spectrometer equipped with a cryogenically cooled carbon observe probe). Chemical shifts are reported in δ

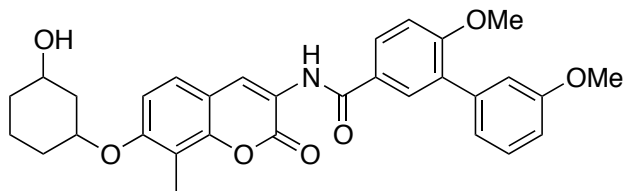
(ppm) relative to the internal standard (CDCl₃, 7.26 ppm, or as stated). HRMS spectra were recorded with a LCT Premier with ESI ionization. ¹H and ¹³C NMR was used to verify that all tested compounds were >95% pure. TLC analysis was performed on glass backed silica gel plates and visualized by UV light. All solvents were reagent grade and used without further purification.

Synthesis and Compound Characterization



***N*-(7-Hydroxy-8-methyl-2-oxo-2*H*-chromen-3-yl)-3',6-dimethoxy-[1,1'-biphenyl]-3-carboxamide (5.36).**

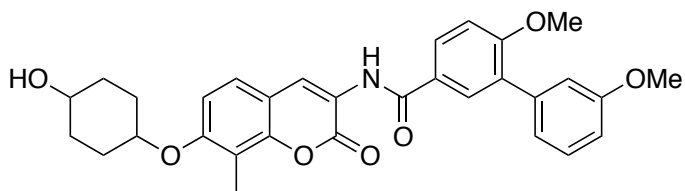
Compound **5.36** was synthesized following a previously reported procedure.²³



***N*-(7-((3-Hydroxycyclohexyl)oxy)-8-methyl-2-oxo-2*H*-chromen-3-yl)-3',6-dimethoxy-[1,1'-biphenyl]-3-carboxamide (5.1).**

Phenol **5.36** (0.12 g, 0.298 mmol), and cyclohexane-1,3-diol (0.128g, 0.597mmol) were dissolved in anhydrous Benzene (2mL). Tri-butylphosphine (0.147mL, 0.597 mmol) was added dropwise and the reaction was stirred at 0°C. After 5 minutes the mixture was covered and Diamide (0.103g, 0.597mmol) was added. The mixture was stirred for 15 minutes and then

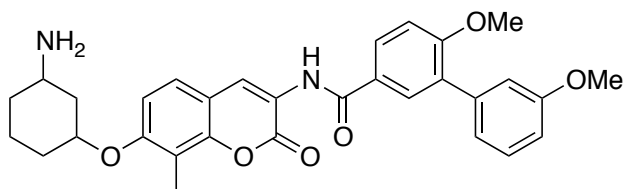
heated to reflux. The reaction was stirred at reflux for 12 h, cooled to rt, concentrated, and purified via column chromatography (SiO₂, 1:4, EtOAc: hexane) to afford **5.1** as a white amorphous solid (35% yield): ¹H NMR (500 MHz, Chloroform-d) δ 8.80 (s, 1H), 8.70 (d, *J* = 2.8 Hz, 1H), 7.93 – 7.88 (m, 3H), 7.35 (dt, *J* = 15.6, 8.3 Hz, 3H), 7.12 (dt, *J* = 7.6, 1.2 Hz, 2H), 7.10 – 7.04 (m, 4H), 6.95 – 6.87 (m, 3H), 4.81 (dt, *J* = 6.0, 3.2 Hz, 1H), 4.39 (tt, *J* = 8.9, 3.8 Hz, 1H), 4.14 (ddd, *J* = 14.5, 9.9, 5.8 Hz, 1H), 3.90 (s, 4H), 3.86 (s, 4H), 3.83 – 3.77 (m, 1H), 2.33 (s, 3H), 2.13 (dt, *J* = 12.6, 4.6 Hz, 1H), 2.04 – 1.98 (m, 1H), 1.94 – 1.86 (m, 2H), 1.70 (ddt, *J* = 21.7, 12.5, 7.0 Hz, 3H), 1.60 – 1.33 (m, 2H). ¹³C NMR (126 MHz, CDCl₃) δ 165.67, 159.92, 159.64, 159.47, 157.23, 149.56, 138.75, 131.19, 130.10, 129.31, 128.29, 125.67, 124.43, 122.15, 121.85, 115.39, 113.30, 111.15, 110.90, 75.58, 73.70, 68.47, 67.04, 40.49, 39.11, 34.41, 30.89, 19.27, 8.58. HRMS (ESI+), *m/z* [M+H⁺] calculated for C₃₁H₃₁NO₇ 530.2179; found 530.2162.



***N*-(7-((4-Hydroxycyclohexyl)oxy)-8-methyl-2-oxo-2*H*-chromen-3-yl)-3',6-dimethoxy-[1,1'-biphenyl]-3-carboxamide (**5.2**).**

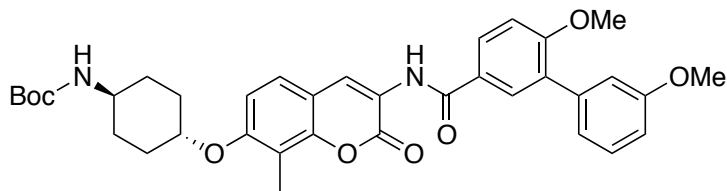
Compound **5.2** was obtained following the procedure for the synthesis of **5.1** as a white amorphous solid (35%): ¹H NMR (500 MHz, Chloroform-d) δ 8.80 (d, *J* = 1.0 Hz, 2H), 8.70 (d, *J* = 2.6 Hz, 2H), 7.95 – 7.87 (m, 5H), 7.39 – 7.31 (m, 4H), 7.12 (dt, *J* = 7.6, 1.2 Hz, 2H), 7.10 – 7.05 (m, 5H), 6.95 – 6.88 (m, 4H), 4.53 (dt, *J* = 5.4, 2.7 Hz, 1H), 4.40 (dt, *J* = 8.6, 4.6 Hz, 1H), 3.90 (s, 6H), 3.86 (s, 7H), 2.36 (d, *J* = 2.7 Hz, 3H), 2.32 (s, 3H), 2.14 (ddd, *J* = 12.5, 5.0, 2.5 Hz, 2H), 2.05 (td, *J* = 8.5, 7.6, 4.3 Hz, 2H), 1.78 (t, *J* = 4.0 Hz, 1H), 1.64 (ddd, *J* = 12.8, 8.6, 3.2 Hz,

2H), 1.49 (dq, $J = 8.6, 2.8, 2.3$ Hz, 2H). ^{13}C NMR (126 MHz, CDCl_3) δ 165.51, 159.76, 159.56, 159.33, 157.30, 138.61, 131.04, 129.95, 129.17, 128.15, 126.13, 125.53, 124.41, 122.01, 115.24, 113.16, 111.01, 110.66, 75.24, 68.59, 31.54, 28.17, 28.15, 8.32, 1.03. HRMS (ESI+), m/z $[\text{M}+\text{Na}^+]$ calculated for $\text{C}_{31}\text{H}_{31}\text{NO}_7$ 552.1998; found 552.2015.



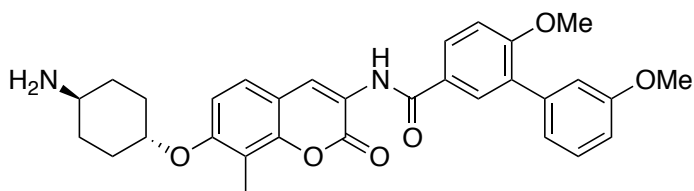
***N*-(7-((3-Aminocyclohexyl)oxy)-8-methyl-2-oxo-2*H*-chromen-3-yl)-3',6-dimethoxy-[1,1'-biphenyl]-3-carboxamide (**5.3**).**

Compound **5.3** was obtained following the procedure for the synthesis of **5.1** as a white amorphous solid (35%). The boc-protected amine was then subjected to the conditions utilized to obtain **5.4a** to obtain compound **5.3** in (70%) yield as a white solid: ^1H NMR (500 MHz, Methanol- d_4) δ 8.73 (s, 1H), 7.87 (dd, $J = 8.6, 2.4$ Hz, 1H), 7.84 (d, $J = 2.4$ Hz, 1H), 7.31 (d, $J = 8.2$ Hz, 2H), 7.10 – 7.01 (m, 4H), 6.89 (ddd, $J = 8.3, 2.6, 0.9$ Hz, 1H), 6.83 (d, $J = 8.7$ Hz, 1H), 4.82 (t, $J = 3.1$ Hz, 1H), 3.85 (s, 3H), 3.81 (s, 3H), 3.50 – 3.43 (m, 1H), 2.37 – 2.32 (m, 2H), 2.28 (s, 3H), 2.07 (d, $J = 12.6$ Hz, 2H), 2.03 – 1.96 (m, 2H), 1.76 – 1.64 (m, 2H). ^{13}C NMR (126 MHz, MeOD) δ 166.59, 160.67, 160.10, 157.13, 150.21, 139.40, 131.83, 130.74, 129.98, 129.01, 126.59, 125.44, 122.82, 122.37, 116.05, 114.37, 113.93, 111.89, 110.92, 72.74, 56.66, 56.11, 49.98, 47.22, 30.49, 28.76, 19.65, 8.95. HRMS (ESI+), m/z $[\text{M}+\text{H}^+]$ calculated for $\text{C}_{31}\text{H}_{32}\text{N}_2\text{O}_6$ 529.2339; found 529.2326.



tert-Butyl ((1*r*,4*r*)-4-((3-(3',6-dimethoxy-[1,1'-biphenyl]-3-yl)carboxamido)-8-methyl-2-oxo-2*H*-chromen-7-yl)oxy)cyclohexyl)carbamate (5.9a).

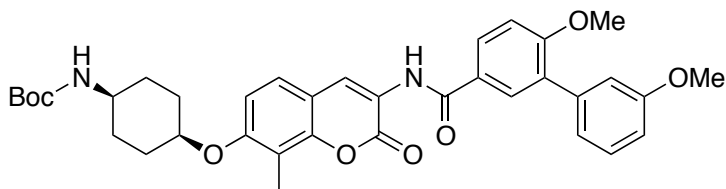
Compound **5.9a** was obtained following the procedure for the synthesis of **5.1** as a white amorphous solid (35%): ^1H NMR (500 MHz, Chloroform-*d*) δ 8.79 (d, $J = 4.0$ Hz, 1H), 8.70 (d, $J = 6.6$ Hz, 1H), 7.94 – 7.87 (m, 2H), 7.39 – 7.29 (m, 1H), 7.14 – 7.03 (m, 3H), 6.93 (dt, $J = 8.3$, 4.5 Hz, 1H), 6.86 (d, $J = 8.7$ Hz, 1H), 4.58 (d, $J = 18.7$ Hz, 1H), 3.88 (d, $J = 20.6$ Hz, 6H), 3.62 – 3.51 (m, 1H), 2.34 (s, 3H), 2.05 (dt, $J = 10.3$, 4.5 Hz, 2H), 1.88 – 1.81 (m, 1H), 1.76 – 1.54 (m, 4H), 1.46 (s, 7H), 1.38 (s, 1H), 1.30 – 1.21 (m, 3H). ^{13}C NMR (126 MHz, CDCl_3) δ 165.96, 160.14, 159.96, 159.68, 157.22, 156.56, 149.99, 149.83, 138.96, 131.38, 130.33, 129.56, 128.54, 126.42, 126.00, 124.90, 122.38, 121.86, 115.61, 113.51, 111.37, 110.56, 79.80, 77.16, 71.95, 48.79, 30.09, 28.94, 28.82, 8.74, 8.37. HRMS (ESI+), m/z $[\text{M}+\text{H}^+]$ calculated for $\text{C}_{36}\text{H}_{40}\text{N}_2\text{O}_8$ 628.2811; found 628.2831.



***N*-(7-(((1*r*,4*r*)-4-Aminocyclohexyl)oxy)-8-methyl-2-oxo-2*H*-chromen-3-yl)-3',6-dimethoxy-[1,1'-biphenyl]-3-carboxamide(5.4a).**

Compound **5.9a** (0.05mg, 0.0795mmol) was dissolved in anhydrous dichloromethane (1mL). Trifluoroacetic acid (0.3mL, 30% vol.) was added to the mixture at 0°C. The mixture was

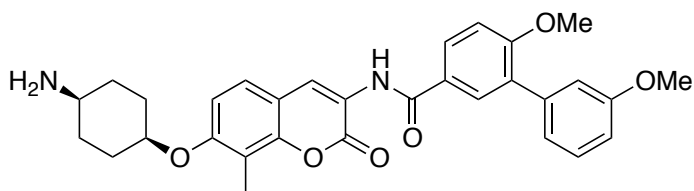
warmed to rt and after 12 h the reaction was concentrated and purified via column chromatography (SiO₂, 1:10, MeOH: DCM) to afford **5.4a** as a white amorphous solid (70% yield): ¹H NMR (500 MHz, Chloroform-d) δ 8.77 (d, *J* = 4.0 Hz, 1H), 8.71 (d, *J* = 6.8 Hz, 1H), 7.90 – 7.82 (m, 2H), 7.38 – 7.30 (m, 1H), 7.10 – 7.02 (m, 3H), 6.90 (dt, *J* = 8.1, 4.6 Hz, 1H), 6.84 (d, *J* = 8.5 Hz, 1H), 4.53 (d, *J* = 18.5 Hz, 1H), 3.88 (d, 6H), 3.60 – 3.54 (m, 1H), 2.24 (s, 3H), 2.09 (m, 2H), 1.88 – 1.81 (m, 2H), 1.76 – 1.54 (m, 4H). ¹³C NMR (126 MHz, CDCl₃) δ 165.99, 160.44, 159.91, 159.58, 157.02, 155.06, 149.00, 148.83, 138.16, 131.28, 130.53, 129.86, 128.52, 126.22, 126.01, 124.40, 122.88, 121.83, 115.63, 113.52, 111.57, 110.50, 79.00, 77.36, 71.05, 48.29, 30.39, 28.12, 8.17. HRMS (ESI+), *m/z* [M+H⁺] calculated for C₃₁H₃₂N₂O₆ 529.2339; found 529.2333.



***tert*-Butyl ((1*s*,4*s*)-4-((3-(3',6-dimethoxy-[1,1'-biphenyl]-3-ylcarboxamido)-8-methyl-2-oxo-2*H*-chromen-7-yl)oxy)cyclohexyl)carbamate (**5.9b**).**

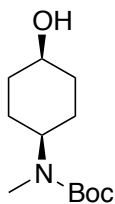
Compound **5.9b** was obtained following the procedure for the synthesis of **5.1** as a white amorphous solid (35%): ¹H NMR (500 MHz, Chloroform-d) 8.78 (s, 1H), 8.69 (s, 1H), 7.92 (m, 1H), 7.87 (m, 2H), 7.37 (m, 1H), 7.29 (m, 2H), 7.12 (dt, *J* = 7.6, 1.2 Hz, 1H), 7.09 (dd, *J* = 2.7, 1.6 Hz, 1H), 7.06 (d, *J* = 8.6 Hz, 1H), 6.92 (ddd, *J* = 8.3, 2.6, 1.0 Hz, 1H), 6.85 (d, *J* = 8.7 Hz, 1H), 4.62 (s, 1H) 4.53 (m, 1H), 3.89 (s, 3H), 3.85 (s, 3H), 3.52 (m, 1H), 2.33 (s, 3H), 1.98 (m, 2H), 1.77 (m, 2H), 1.70 (tt, *J* = 14.2, 2.8 Hz, 2H), 1.54 (m, 2H), 1.45 (s, 9H). ¹³C NMR (126 MHz, CDCl₃) δ 165.59, 159.83, 159.63, 159.39, 156.90, 149.52, 138.68, 132.34, 131.06, 130.03,

129.26, 128.25, 126.14, 125.69, 124.54, 122.09, 121.58, 117.42, 115.31, 113.27, 113.21, 111.07, 110.27, 79.41, 71.68, 48.49, 28.64, 28.52, 27.98. HRMS (ESI+), m/z $[M+H^+]$ calculated for $C_{36}H_{40}N_2O_8$ 628.2811; found 628.2807.



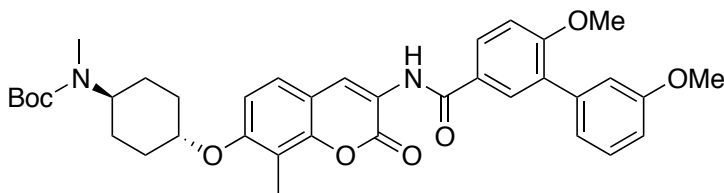
***N*-(7-(((1*s*,4*s*)-4-Aminocyclohexyl)oxy)-8-methyl-2-oxo-2*H*-chromen-3-yl)-3',6-dimethoxy-[1,1'-biphenyl]-3-carboxamide (**5.4b**).**

Compound **5.4b** was obtained following the procedure for the synthesis of **5.4a** as a white amorphous solid (70%): 1H NMR (500 MHz, Methanol- d_4) δ 8.47 (d, $J = 1.3$ Hz, 1H), 7.61 (dt, $J = 8.6, 1.9$ Hz, 1H), 7.57 (d, $J = 2.4$ Hz, 1H), 7.08 – 7.03 (m, 2H), 6.82 (dt, $J = 7.6, 1.2$ Hz, 1H), 6.80 – 6.76 (m, 2H), 6.63 (ddd, $J = 8.2, 2.7, 1.0$ Hz, 1H), 6.57 (d, $J = 8.7$ Hz, 1H), 4.39 (t, $J = 3.1$ Hz, 1H), 3.60 (d, $J = 1.3$ Hz, 3H), 3.55 (d, $J = 1.3$ Hz, 3H), 2.84 (ddt, $J = 11.2, 7.9, 3.9$ Hz, 1H), 2.06 (s, 3H), 1.92 – 1.83 (m, 2H), 1.65 – 1.58 (m, 2H), 1.55 – 1.45 (m, 2H), 1.39 (tt, $J = 13.6, 3.3$ Hz, 2H). ^{13}C NMR (126 MHz, MeOD) δ 165.81, 159.77, 159.54, 159.17, 156.47, 149.36, 138.51, 130.90, 129.84, 129.11, 128.16, 125.70, 124.81, 121.93, 121.33, 115.14, 113.01, 111.00, 109.98, 70.03, 55.78, 55.22, 27.85, 25.39, 7.93. HRMS (ESI+), m/z $[M+H^+]$ calculated for $C_{31}H_{32}N_2O_6$ 529.2339; found 529.2336.



***tert*-Butyl ((1*s*,4*s*)-4-hydroxycyclohexyl)(methyl)carbamate (5.47a).**

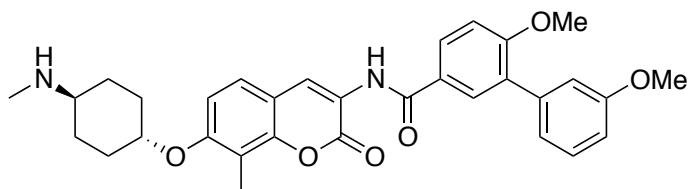
tert-Butyl (4-oxocyclohexyl)carbamate (0.10 g, 0.44 mmol) was dissolved in anhydrous tetrahydrofuran (4 mL) and the solution was cooled to -40 °C. L-selectride (1.0 M in THF, 0.12 ml) was added dropwise to the solution and the reaction mixture was allowed to stir at rt for 12 h. The reaction mixture was concentrated and the residue was diluted with water. The suspension was acidified with 1N HCl and extracted with ethyl acetate. The organic layers were combined, dried (over Na₂SO₄), concentrated and purified by column chromatography (SiO₂, 1:2, EtOAc : hexane) to afford **5.47a** as a white amorphous solid (30%): ¹H NMR (500 MHz, Chloroform-*d*) δ 3.87 (tt, *J* = 10.0, 4.5 Hz, 1H), 2.80 (s, 1H), 2.58 (s, 1H), 2.20 – 2.12 (m, 2H), 2.04 – 1.90 (m, 2H), 1.86 – 1.79 (m, 2H), 1.69 – 1.58 (m, 2H), 1.38 (d, *J* = 2.4 Hz, 9H). ¹³C NMR (126 MHz, CDCl₃) δ 155.33, 79.01, 69.79, 34.29, 28.43, 28.34, 27.84.



***tert*-Butyl ((1*r*,4*r*)-4-((3-(3',6-Dimethoxy-[1,1'-biphenyl]-3-yl)carboxamido)-8-methyl-2-oxo-2*H*-chromen-7-yl)oxy)cyclohexyl)(methyl)carbamate (5.48a).**

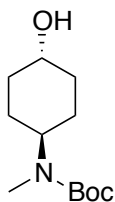
Compound **5.48a** was obtained following the procedure for the synthesis of **5.1** as a white amorphous solid (35%): ¹H NMR (500 MHz, Methanol-*d*₄) δ 8.00 (s, 1H), 7.20 (dd, *J* = 8.9, 2.3 Hz, 1H), 7.10 (d, *J* = 2.5 Hz, 1H), 6.60 – 6.52 (m, 3H), 6.40 – 6.32 (m, 4H), 6.24 – 6.18 (m, 2H), 4.02 (t, *J* = 3.1 Hz, 1H), 3.14 (s, 3H), 3.10 (s, 3H), 2.60 (p, *J* = 1.8 Hz, 1H), 2.30 (tt, *J* = 11.9, 4.3 Hz, 1H), 1.96 (s, 3H), 1.87 (s, 3H), 1.65-1.55 (m, 2H), 1.45 (m, 4H), 1.32 – 1.25 (m, 2H), 1.11 – 1.07 (s, 9H). ¹³C NMR (126 MHz, MeOD) δ 165.66, 159.56, 159.35, 158.42, 156.05, 149.21,

138.07, 130.35, 129.06, 128.71, 127.28, 125.17, 124.37, 121.09, 121.00, 114.89, 112.75, 110.09, 109.14, 69.74, 56.54, 55.49, 54.00, 29.52, 28.02, 27.09, 22.38, 7.58. HRMS (ESI+), m/z $[M+Na^+]$ calculated for $C_{37}H_{42}N_2O_8Na$ 665.2839; found 665.2825.



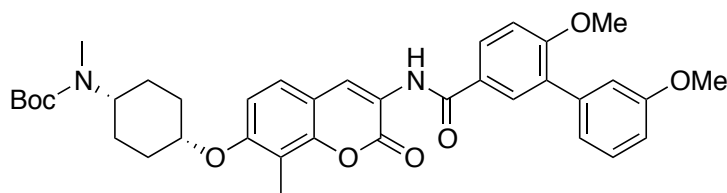
3',6-Dimethoxy-*N*-(8-methyl-7-(((1*r*,4*r*)-4-(methylamino)cyclohexyl)oxy)-2-oxo-2*H*-chromen-3-yl)-[1,1'-biphenyl]-3-carboxamide (5.5a).

Compound **5.5a** was obtained following the procedure for the synthesis of **5.4a** as a white amorphous solid (70%): 1H NMR (500 MHz, Methanol- d_4) δ 8.02 (s, 1H), 7.18 (dd, $J = 8.6, 2.5$ Hz, 1H), 7.14 (d, $J = 2.4$ Hz, 1H), 6.67 – 6.58 (m, 3H), 6.41 – 6.34 (m, 4H), 6.22 – 6.13 (m, 2H), 3.99 (t, $J = 2.9$ Hz, 1H), 3.17 (s, 3H), 3.12 (s, 3H), 2.62 (p, $J = 1.6$ Hz, 1H), 2.34 (tt, $J = 11.7, 4.1$ Hz, 1H), 1.94 (d, $J = 2.6$ Hz, 3H), 1.62 (s, 3H), 1.50 (dt, $J = 16.0, 2.9$ Hz, 2H), 1.26 (dd, $J = 13.0, 3.8$ Hz, 2H), 1.18 – 1.07 (m, 2H), 1.04 – 0.92 (m, 2H). ^{13}C NMR (126 MHz, MeOD) δ 165.63, 159.55, 159.25, 158.92, 156.15, 149.11, 138.27, 130.65, 129.56, 128.81, 127.88, 125.47, 124.67, 121.65, 121.07, 114.89, 112.71, 110.79, 109.74, 69.73, 56.58, 55.46, 54.90, 29.22, 27.49, 22.88, 7.57. HRMS (ESI+), m/z $[M+H^+]$ calculated for $C_{32}H_{34}N_2O_6$ 543.2495; found 543.2462.



***tert*-Butyl ((1*r*,4*r*)-4-hydroxycyclohexyl)(methyl)carbamate (5.47b).**

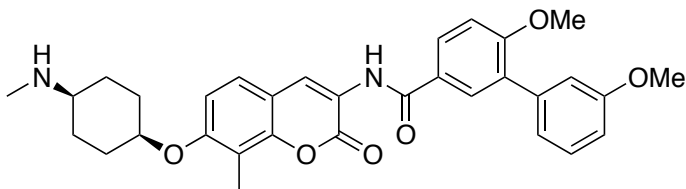
Sodium borohydride (0.02g, 0.53 mmol) was added to an ice-cooled solution of *tert*-butyl (4-oxocyclohexyl)carbamate (0.1g, 0.44 mmol) in methanol (4.5 ml) and the reaction mixture was allowed to stir at rt for 12 h. The reaction mixture was concentrated and the residue was diluted with water. The suspension was acidified with 1N HCl and extracted with ethyl acetate. The organic layers were combined, dried (over Na₂SO₄), concentrated and purified by column chromatography (SiO₂, 1:2, EtOAc: hexane) to afford **5.47b** as a white amorphous solid (60%): ¹H NMR (500 MHz, Chloroform-d) δ 3.50 (tt, *J* = 10.7, 4.3 Hz, 1H), 2.71 (s, 1H), 2.66 (s, 1H), 2.17 – 2.08 (m, 2H), 2.01 – 1.93 (m, 2H), 1.85 – 1.78 (m, 2H), 1.67 – 1.56 (m, 2H), 1.42 (d, *J* = 2.2 Hz, 9H). ¹³C NMR (126 MHz, CDCl₃) δ 155.46, 79.19, 69.77, 34.39, 28.33, 28.31, 27.64.



***tert*-Butyl ((1*s*,4*s*)-4-((3-(3',6-dimethoxy-[1,1'-biphenyl]-3-yl)carboxamido)-8-methyl-2-oxo-2*H*-chromen-7-yl)oxy)cyclohexyl(methyl)carbamate (5.48b).**

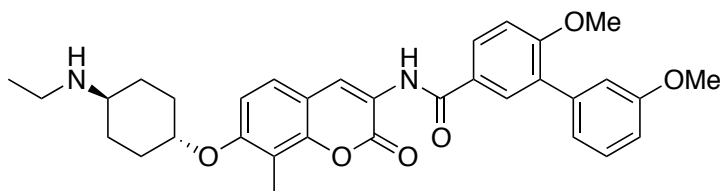
Compound **5.48b** was obtained following the procedure for the synthesis of **5.1** as a white amorphous solid (35%): ¹H NMR (500 MHz, Chloroform-d) δ 9.35 (d, *J* = 9.7 Hz, 2H), 9.02 (s, 1H), 8.67 (d, *J* = 10.2 Hz, 1H), 8.60 (s, 1H), 7.90 – 7.82 (m, 2H), 7.35 (dt, *J* = 21.7, 8.3 Hz, 2H), 7.16 – 7.08 (m, 3H), 6.90 (dd, *J* = 8.1, 2.5 Hz, 1H), 6.82 (dd, *J* = 12.0, 8.5 Hz, 1H), 4.55 (d, *J* = 3.9 Hz, 1H), 3.95 (s, 3H), 3.91 (s, 3H), 2.67 (d, *J* = 5.1 Hz, 1H), 2.32 (m, 2H), 2.29 (s, 3H), 2.20 (d, *J* = 15.5 Hz, 2H), 2.04 – 1.92 (m, 4H), 1.52 (s, 3H), 1.29 (s, 9H). ¹³C NMR (126 MHz, CDCl₃) δ 165.04, 159.66, 159.25, 149.02, 138.99, 130.93, 129.56, 129.25, 128.03, 126.54, 125.61, 125.43, 124.47, 122.23, 121.09, 115.43, 113.13, 110.88, 109.34, 55.65, 55.01, 30.58,

29.62, 29.17, 27.45, 26.03, 23.60, 7.93. HRMS (ESI+), m/z $[M+Na^+]$ calculated for $C_{37}H_{42}N_2O_8Na$ 665.2839; found 665.2860.



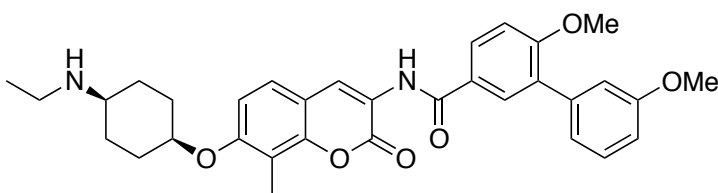
3',6-Dimethoxy-N-(8-methyl-7-(((1*S*,4*S*)-4-(methylamino)cyclohexyl)oxy)-2-oxo-2*H*-chromen-3-yl)-[1,1'-biphenyl]-3-carboxamide (5.5b).

Compound **5.5b** was obtained following the procedure for the synthesis of **5.4a** as a white amorphous solid (70%): 1H NMR (500 MHz, Chloroform- d) δ 9.39 (d, $J = 9.9$ Hz, 2H), 9.22 (s, 1H), 8.77 (d, $J = 10.0$ Hz, 1H), 8.67 (s, 1H), 7.92 – 7.85 (m, 2H), 7.33 (dt, $J = 21.9, 8.1$ Hz, 2H), 7.14 – 7.03 (m, 3H), 6.92 (dd, $J = 7.9, 2.5$ Hz, 1H), 6.83 (dd, $J = 12.0, 8.7$ Hz, 1H), 4.68 (d, $J = 3.7$ Hz, 1H), 4.30 (d, $J = 9.6$ Hz, 1H), 3.89 (d, $J = 6.3$ Hz, 3H), 3.85 (s, 3H), 3.06 – 2.93 (m, 2H), 2.67 (d, $J = 5.1$ Hz, 5H), 2.32 (s, 2H), 2.29 (s, 1H), 2.22 (d, $J = 15.8$ Hz, 3H), 2.04 – 1.92 (m, 5H), 1.70 – 1.52 (m, 3H), 1.29 (d, $J = 33.7$ Hz, 3H). ^{13}C NMR (126 MHz, $CDCl_3$) δ 165.34, 159.65, 159.21, 149.32, 138.49, 130.91, 129.86, 129.05, 128.00, 126.94, 125.91, 125.42, 124.07, 122.21, 121.89, 115.13, 113.03, 110.89, 109.74, 55.75, 55.21, 30.28, 29.60, 29.07, 27.85, 26.00, 23.10, 8.22, 7.93. HRMS (ESI+), m/z $[M+H^+]$ calculated for $C_{32}H_{34}N_2O_6$ 543.2495; found 543.2490.



***N*-(7-(((1*r*,4*r*)-4-(Ethylamino)cyclohexyl)oxy)-8-methyl-2-oxo-2*H*-chromen-3-yl)-3',6-dimethoxy-[1,1'-biphenyl]-3-carboxamide (**5.6a**).**

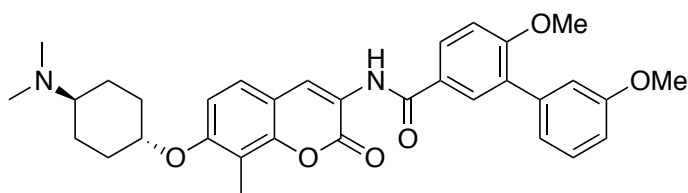
Compound **5.4a** (0.04g, 0.06mmol) was dissolved in methanol (0.6mL). 10% Pt/C (0.002, 0.008mmol) and acetonitrile (0.01mL) were added to the mixture and the suspension was stirred under a hydrogen atmosphere. After 25 h, the reaction mixture was filtered through a pad of Celite; the residue was washed with ethyl acetate. The filtrate was concentrated and purified by column chromatography (SiO₂, 1:10, MeOH: DCM) to yield **5.6a** as a white solid (60% yield): ¹H NMR (500 MHz, Methanol-d₄) δ 8.02 (s, 1H), 7.18 (dd, *J* = 8.6, 2.5 Hz, 1H), 7.14 (d, *J* = 2.4 Hz, 1H), 6.67 – 6.58 (m, 3H), 6.41 – 6.34 (m, 4H), 6.22 – 6.13 (m, 2H), 3.99 (t, *J* = 2.9 Hz, 1H), 3.17 (s, 3H), 3.12 (s, 3H), 2.62 (p, *J* = 1.6 Hz, 2H), 2.34 (tt, *J* = 11.7, 4.1 Hz, 1H), 2.20-2.15 (m, 4H), 1.94 (d, *J* = 2.6 Hz, 3H), 1.88 (t, 4H), 1.62 (s, 3H). ¹³C NMR (126 MHz, MeOD) δ 165.63, 159.55, 159.25, 158.92, 156.15, 149.11, 138.27, 130.65, 129.56, 128.81, 127.88, 125.47, 124.67, 121.65, 121.07, 114.89, 112.71, 110.79, 109.74, 69.73, 56.58, 55.46, 54.90, 29.22, 27.49, 22.88, 7.57. HRMS (ESI+), *m/z* [M+H⁺] calculated for C₃₃H₃₆N₂O₆, 571.2682; found 571.2667.



***N*-(7-(((1*s*,4*s*)-4-(Ethylamino)cyclohexyl)oxy)-8-methyl-2-oxo-2*H*-chromen-3-yl)-3',6-dimethoxy-[1,1'-biphenyl]-3-carboxamide (**5.6b**).**

Compound **5.6b** was obtained following the procedure for the synthesis of **5.6a** as a white amorphous solid (60%): ¹H NMR (500 MHz, Chloroform-d) δ 9.39 (d, *J* = 9.9 Hz, 2H), 9.22 (s, 1H), 8.77 (d, *J* = 10.0 Hz, 1H), 8.67 (s, 1H), 7.92 – 7.85 (m, 2H), 7.33 (dt, *J* = 21.9, 8.1 Hz, 2H),

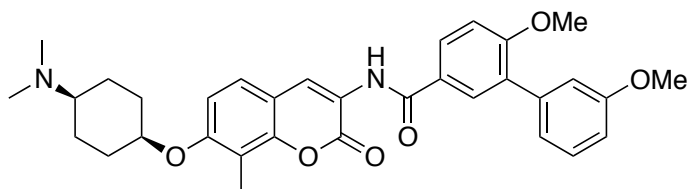
7.14 – 7.03 (m, 3H), 6.92 (dd, $J = 7.9, 2.5$ Hz, 1H), 6.83 (dd, $J = 12.0, 8.7$ Hz, 1H), 4.68 (d, $J = 3.7$ Hz, 1H), 4.30 (d, $J = 9.6$ Hz, 1H), 3.89 (d, $J = 6.3$ Hz, 3H), 3.85 (s, 3H), 3.06 – 2.93 (m, 2H), 2.67 (d, $J = 5.1$ Hz, 2H), 2.22 (d, $J = 15.8$ Hz, 1H), 2.11 (s, 3H), 2.04 – 1.92 (m, 4H), 1.70 – 1.64 (m, 2H), 1.61 (s, 3H). ^{13}C NMR (126 MHz, CDCl_3) δ 165.34, 159.65, 159.21, 149.32, 138.49, 130.91, 129.86, 129.05, 128.00, 126.94, 125.91, 125.42, 124.07, 122.21, 121.89, 115.13, 113.03, 110.89, 109.74, 55.75, 55.21, 30.28, 29.60, 29.07, 27.85, 26.00, 23.10, 8.22, 7.93. HRMS (ESI+), m/z $[\text{M}+\text{H}^+]$ calculated for $\text{C}_{33}\text{H}_{36}\text{N}_2\text{O}_6$ 571.2682; found 571.2688.



***N*-(7-(((1*r*,4*r*)-4-(Dimethylamino)cyclohexyl)oxy)-8-methyl-2-oxo-2*H*-chromen-3-yl)-3',6-dimethoxy-[1,1'-biphenyl]-3-carboxamide (**5.7a**).**

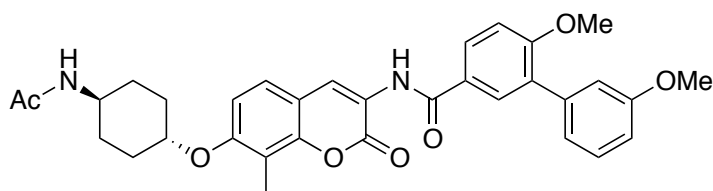
Acetic Acid (0.5mg, 8.5mmol) was added to a solution of **5.4a** (0.20g, 1.7mmol) in methanol (20mL). Formaldehyde (0.10g, 3.4mmol) and NaBH_3CN (0.23g, 3.7mmol) were added and the mixture was stirred at rt. After 12h the reaction was diluted with 40mL of H_2O and then extracted with DCM (3 x 30mL). The organic layers were combined, dried, and concentrated. The crude mixture was purified by column chromatography (SiO_2 , 1:10, MeOH: DCM) to yield **5.7a** as a white solid (40% yield): ^1H NMR (500 MHz, Chloroform- d) δ 8.80 (s, 1H), 8.70 (s, 1H), 7.94 – 7.87 (m, 2H), 7.39 – 7.32 (m, 2H), 7.12 (dt, $J = 7.6, 1.2$ Hz, 1H), 7.10 – 7.08 (m, 2H), 7.06 (s, 1H), 6.93 (ddd, $J = 8.3, 2.6, 0.9$ Hz, 1H), 6.85 (d, $J = 8.8$ Hz, 1H), 4.70 (t, $J = 2.9$ Hz, 1H), 3.90 (s, 3H), 3.86 (s, 3H), 3.18 – 3.03 (m, 1H), 2.69 (s, 6H), 2.35 (s, 3H), 2.31 – 2.21 (m, 2H), 1.99 – 1.79 (m, 4H), 1.76 – 1.62 (m, 2H). ^{13}C NMR (126 MHz, CDCl_3) δ 165.66,

159.92, 159.56, 159.45, 156.33, 149.56, 138.71, 131.15, 130.07, 129.32, 128.31, 126.15, 125.87, 124.31, 122.13, 115.37, 113.26, 111.13, 110.18, 70.33, 63.46, 39.57, 28.61, 21.12, 8.54. HRMS (ESI+), m/z $[M+H^+]$ calculated for $C_{33}H_{36}N_2O_6$ 557.2652; found 557.2641.



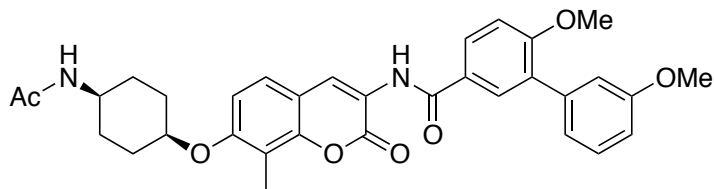
***N*-(7-(((1*s*,4*s*)-4-(Dimethylamino)cyclohexyl)oxy)-8-methyl-2-oxo-2*H*-chromen-3-yl)-3',6-dimethoxy-[1,1'-biphenyl]-3-carboxamide (5.7b).**

Compound **5.7b** was obtained following the procedure for the synthesis of **5.7a** as a white amorphous solid (60%): 1H NMR (500 MHz, Chloroform- d) δ 8.80 (s, 1H), 8.70 (s, 1H), 7.94 – 7.87 (m, 2H), 7.40 – 7.30 (m, 2H), 7.13 (ddd, $J = 7.6, 1.6, 1.0$ Hz, 1H), 7.09 (dd, $J = 2.6, 1.6$ Hz, 1H), 7.07 (d, $J = 8.6$ Hz, 1H), 6.93 (ddd, $J = 8.3, 2.6, 0.9$ Hz, 1H), 6.86 (d, $J = 8.7$ Hz, 1H), 4.65 (t, $J = 3.0$ Hz, 1H), 3.90 (s, 3H), 3.86 (s, 3H), 2.51 (t, $J = 11.4$ Hz, 1H), 2.43 (s, 7H), 2.36 (s, 3H), 2.23 – 2.14 (m, 2H), 1.81 – 1.72 (m, 5H), 1.63 (ddt, $J = 14.0, 11.1, 2.7$ Hz, 2H). ^{13}C NMR (126 MHz, $CDCl_3$) δ 165.64, 159.88, 159.68, 159.45, 156.86, 149.60, 138.73, 131.13, 130.08, 129.32, 128.29, 126.23, 125.71, 124.52, 122.14, 115.35, 113.28, 111.11, 110.29, 71.46, 62.92, 40.99, 28.94, 22.62, 8.50. HRMS (ESI+), m/z $[M+H^+]$ calculated for $C_{33}H_{36}N_2O_6$ 557.2652; found 557.2652.



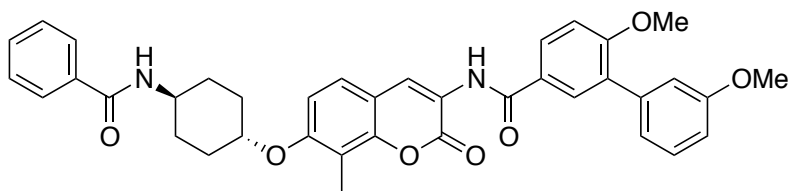
***N*-(7-(((1*r*,4*r*)-4-Acetamidocyclohexyl)oxy)-8-methyl-2-oxo-2*H*-chromen-3-yl)-3',6-dimethoxy-[1,1'-biphenyl]-3-carboxamide (5.8a).**

Compound **5.4a** (0.03g, 0.08mmol) was dissolved in anhydrous dichloromethane (0.8mL). Triethylamine (0.013mL, 0.08mmol) was added and the mixture was cooled to 0°C. After 10 minutes, acetic anhydride (0.008mL, 0.08mmol) was added dropwise. The reaction was quenched after 12 h, via the addition of water. The mixture was worked-up with dichloromethane (3 x 5mL), dried, concentrated, and purified via column chromatography (SiO₂, 1:10, MeOH: DCM) to afford **5.8a** as a white amorphous solid (70% yield): ¹H NMR (500 MHz, Chloroform-*d*) δ 8.79 (d, *J* = 1.3 Hz, 1H), 8.70 (s, 1H), 7.94 – 7.86 (m, 2H), 7.40 – 7.34 (m, 1H), 7.31 (d, *J* = 8.6 Hz, 1H), 7.12 (dd, *J* = 7.6, 1.4 Hz, 1H), 7.10 – 7.05 (m, 2H), 6.96 – 6.90 (m, 1H), 6.87 (d, *J* = 8.6 Hz, 1H), 5.34 (d, *J* = 7.8 Hz, 1H), 4.31 – 4.22 (m, 1H), 3.88 (dd, *J* = 20.0, 1.4 Hz, 6H), 2.31 (d, *J* = 1.4 Hz, 3H), 2.19 – 2.05 (m, 4H), 1.98 (d, *J* = 1.4 Hz, 3H), 1.71 – 1.57 (m, 4H). ¹³C NMR (126 MHz, CDCl₃) δ 169.42, 165.52, 159.77, 159.51, 159.33, 157.25, 138.61, 131.04, 129.96, 129.17, 128.13, 126.10, 125.44, 124.30, 122.00, 121.64, 115.25, 113.15, 111.01, 110.77, 55.89, 55.33, 47.44, 30.42, 30.30, 23.57, 8.37. HRMS (ESI+), *m/z* [M+Na⁺] calculated for C₃₃H₃₄N₂O₇Na 593.2264; found 593.2264.



***N*-(7-(((1*s*,4*s*)-4-Acetamidocyclohexyl)oxy)-8-methyl-2-oxo-2*H*-chromen-3-yl)-3',6-dimethoxy-[1,1'-biphenyl]-3-carboxamide (5.8b).**

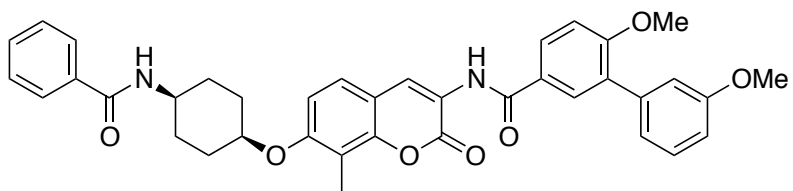
Compound **5.8b** was obtained following the procedure for the synthesis of **5.8a** as a white amorphous solid (70%): ¹H NMR (500 MHz, Chloroform-d) δ 8.81 (s, 1H), 8.70 (s, 1H), 7.92 (dd, *J* = 8.6, 2.4 Hz, 1H), 7.89 (d, *J* = 2.4 Hz, 1H), 7.38 (d, *J* = 7.9 Hz, 1H), 7.36 – 7.32 (m, 1H), 7.13 (ddd, *J* = 7.6, 1.6, 1.0 Hz, 1H), 7.09 (dd, *J* = 2.6, 1.6 Hz, 1H), 7.07 (d, *J* = 8.7 Hz, 1H), 6.93 (ddd, *J* = 8.3, 2.6, 1.0 Hz, 1H), 6.87 (d, *J* = 8.8 Hz, 1H), 5.40 (d, *J* = 8.1 Hz, 1H), 4.63 (t, *J* = 3.3 Hz, 1H), 3.90 (s, 3H), 3.86 (s, 3H), 2.36 (s, 3H), 2.11 – 2.03 (m, 2H), 2.00 (s, 3H), 1.86 – 1.81 (m, 2H), 1.78 – 1.69 (m, 2H), 1.65 – 1.57 (m, 7H). ¹³C NMR (126 MHz, CDCl₃) δ 169.41, 165.64, 159.90, 159.70, 159.45, 156.91, 149.58, 138.74, 131.15, 130.07, 129.33, 128.32, 126.21, 125.80, 124.54, 122.14, 121.70, 115.37, 114.98, 113.39, 113.28, 111.13, 110.28, 71.51, 47.44, 28.74, 27.68, 23.78, 8.56. HRMS (ESI+), *m/z* [M+Na⁺] calculated for C₃₃H₃₄N₂O₇Na 593.2264; found 593.2270.



***N*-(7-(((1*r*,4*r*)-4-Benzamidocyclohexyl)oxy)-8-methyl-2-oxo-2*H*-chromen-3-yl)-3',6-dimethoxy-[1,1'-biphenyl]-3-carboxamide (**5.10a**).**

Compound **5.4a** (0.03g, 0.08mmol) was dissolved in anhydrous tetrahydrofuran (0.8mL). Triethylamine (0.013mL, 0.08mmol) was added and the mixture was cooled to 0°C. After 10 minutes, benzyl chloride (0.013mL, 0.08mmol) was added dropwise. The reaction was quenched after 12 hours, via the addition of water. The mixture was worked-up with ethyl acetate (3 x 5mL), dried, concentrated, and purified via column chromatography (SiO₂, 1:10, MeOH: DCM) to afford **5.10a** as a white amorphous solid (70% yield): ¹H NMR (500 MHz, Chloroform-d) δ 8.78 (s, 1H), 8.70 (s, 1H), 7.90 (d, *J* = 8.7 Hz, 2H), 7.78 – 7.73 (m, 2H), 7.49

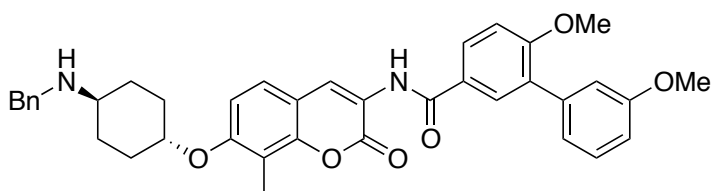
(d, $J = 7.1$ Hz, 1H), 7.42 (t, $J = 7.5$ Hz, 2H), 7.36 (t, $J = 7.9$ Hz, 1H), 7.30 (d, $J = 8.6$ Hz, 1H), 7.12 (d, $J = 7.7$ Hz, 1H), 7.09 (t, $J = 2.0$ Hz, 1H), 7.06 (d, $J = 8.4$ Hz, 1H), 6.93 (dd, $J = 8.2, 2.5$ Hz, 1H), 6.87 (d, $J = 8.7$ Hz, 1H), 6.10 (d, $J = 7.8$ Hz, 1H), 4.30 (tt, $J = 9.8, 3.5$ Hz, 1H), 4.09 (dq, $J = 10.5, 3.6$ Hz, 1H), 3.87 (d, $J = 18.7$ Hz, 6H), 2.32 (s, 3H), 2.21 (td, $J = 11.5, 10.1, 5.1$ Hz, 5H), 1.71 (tdd, $J = 13.1, 9.9, 4.0$ Hz, 2H), 1.49 – 1.38 (m, 2H). ^{13}C NMR (126 MHz, CDCl_3) δ 167.34, 165.86, 160.13, 159.86, 159.69, 157.62, 149.80, 138.97, 135.06, 131.84, 130.32, 129.54, 128.94, 128.49, 127.22, 125.82, 124.66, 122.36, 115.62, 113.50, 111.38, 111.11, 76.44, 56.25, 55.69, 48.25, 30.77, 30.70, 8.74. HRMS (ESI+), m/z $[\text{M}+\text{Na}^+]$ calculated for $\text{C}_{38}\text{H}_{36}\text{N}_2\text{O}_7\text{Na}$ 655.2420; found 655.2437.



***N*-(7-(((1*s*,4*s*)-4-Benzamidocyclohexyl)oxy)-8-methyl-2-oxo-2*H*-chromen-3-yl)-3',6'-dimethoxy-[1,1'-biphenyl]-3-carboxamide (5.10b).**

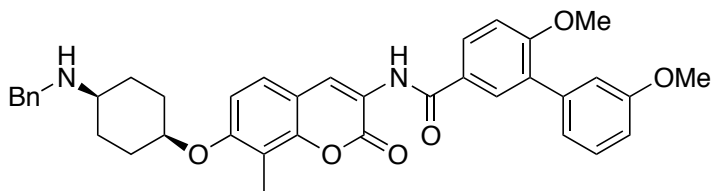
Compound **5.10b** was obtained following the procedure for the synthesis of **5.10a** as a white amorphous solid (70%): ^1H NMR (500 MHz, Chloroform- d) δ 8.80 (s, 1H), 8.70 (s, 1H), 8.10 (dd, $J = 8.3, 1.3$ Hz, 1H), 7.93 – 7.87 (m, 2H), 7.81 – 7.76 (m, 2H), 7.52 – 7.40 (m, 3H), 7.40 – 7.30 (m, 2H), 7.14 – 7.03 (m, 3H), 6.93 (ddd, $J = 8.3, 2.6, 0.9$ Hz, 1H), 6.88 (d, $J = 8.8$ Hz, 1H), 6.16 (d, $J = 8.0$ Hz, 1H), 4.66 (dd, $J = 4.7, 2.5$ Hz, 1H), 4.17 – 4.08 (m, 1H), 3.99 – 3.90 (m, 1H), 3.89 (s, 3H), 3.85 (s, 3H), 2.37 (s, 2H), 2.18 – 2.07 (m, 2H), 1.99 – 1.92 (m, 2H), 1.83 – 1.67 (m, 4H). ^{13}C NMR (126 MHz, CDCl_3) δ 170.23, 167.04, 165.63, 159.86, 159.66, 159.41, 156.93, 149.53, 138.70, 134.82, 133.56, 131.58, 131.09, 130.21, 130.03, 129.29, 128.69, 128.53, 128.28,

127.00, 126.16, 125.77, 124.55, 122.11, 121.63, 115.34, 114.96, 113.23, 111.10, 110.27, 71.57, 70.90, 48.54, 47.94, 28.81, 28.57, 27.71, 26.92, 8.56. HRMS (ESI+), m/z $[M+Na^+]$ calculated for $C_{38}H_{36}N_2O_7Na$ 655.2420; found 655.2391.



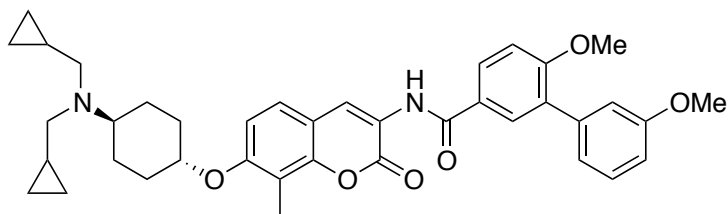
***N*-(7-(((1*r*,4*r*)-4-(Benzylamino)cyclohexyl)oxy)-8-methyl-2-oxo-2*H*-chromen-3-yl)-3',6-dimethoxy-[1,1'-biphenyl]-3-carboxamide (**5.11a**).**

Benzyl Bromide (0.12mL, 1.0mmol), was added to a solution of **5.4a** (1.32g, 2.5mmol), K_2CO_3 (0.15g, 1.1mmol), in MeCN (30mL) and heated at reflux. After 24 h. the reaction was cooled to rt, quenched with water, and worked-up with EtOAc (3 x 50mL). The organic layers were combined, dried, concentrated and purified via column chromatography (SiO_2 , 1:10, MeOH: DCM) to afford **5.10a** as a white amorphous solid (50% yield): 1H NMR (500 MHz, Chloroform- d) δ 8.79 (s, 1H), 8.69 (s, 1H), 7.92 – 7.87 (m, 2H), 7.53 (d, $J = 7.4$ Hz, 2H), 7.41 – 7.30 (m, 6H), 7.12 (ddd, $J = 7.6, 1.6, 1.0$ Hz, 1H), 7.09 (dd, $J = 2.6, 1.6$ Hz, 1H), 7.06 (d, $J = 8.7$ Hz, 1H), 6.93 (ddd, $J = 8.2, 2.6, 1.0$ Hz, 1H), 6.87 (d, $J = 8.7$ Hz, 1H), 4.32 (ddt, $J = 9.5, 6.7, 3.4$ Hz, 1H), 3.96 (s, 2H), 3.89 (s, 3H), 3.85 (s, 3H), 2.82 (dd, $J = 12.3, 8.8$ Hz, 1H), 2.27 (s, 3H), 2.21 (d, $J = 11.3$ Hz, 5H), 1.71 – 1.62 (m, 2H), 1.49 (td, $J = 11.2, 9.9, 2.6$ Hz, 2H). ^{13}C NMR (126 MHz, $CDCl_3$) δ 165.62, 159.87, 159.64, 159.44, 157.10, 149.53, 138.73, 131.12, 130.07, 129.31, 129.11, 128.31, 126.22, 125.69, 124.43, 122.14, 121.81, 115.34, 113.64, 113.28, 111.11, 110.85, 75.48, 54.42, 49.13, 29.76, 27.59, 8.48. HRMS (ESI+), m/z $[M+H^+]$ calculated for $C_{38}H_{38}N_2O_6$ 619.2808; found 619.2791.



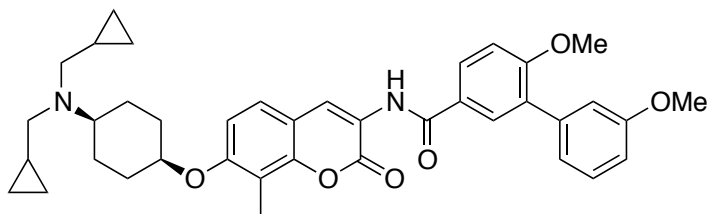
***N*-(7-(((1*s*,4*s*)-4-(benzylamino)cyclohexyl)oxy)-8-methyl-2-oxo-2*H*-chromen-3-yl)-3',6-dimethoxy-[1,1'-biphenyl]-3-carboxamide (11b).**

Compound **5.11b** was obtained following the procedure for the synthesis of **5.11a** as a white amorphous solid (70%): ^1H NMR (500 MHz, Chloroform-*d*) δ 8.79 (d, $J = 2.0$ Hz, 1H), 8.70 (d, $J = 2.9$ Hz, 1H), 7.94 – 7.88 (m, 3H), 7.41 – 7.36 (m, 3H), 7.35 – 7.27 (m, 5H), 7.23 – 7.19 (m, 1H), 7.13 (dt, $J = 7.6, 1.2$ Hz, 2H), 7.10 – 7.04 (m, 3H), 6.93 (dd, $J = 8.3, 2.5$ Hz, 1H), 6.86 (dd, $J = 11.6, 8.7$ Hz, 1H), 4.66 (s, 1H), 4.60 (dd, $J = 7.4, 4.3$ Hz, 1H), 3.90 (s, 4H), 3.86 (d, $J = 5.3$ Hz, 5H), 3.69 (s, 2H), 2.64 (dt, $J = 11.5, 3.7$ Hz, 1H), 2.36 (d, $J = 1.2$ Hz, 3H), 2.18 – 2.02 (m, 2H), 1.79 (ddd, $J = 26.3, 13.3, 6.6$ Hz, 2H), 1.69 – 1.55 (m, 6H). ^{13}C NMR (126 MHz, CDCl_3) δ 165.90, 160.15, 159.73, 149.83, 141.33, 139.02, 131.44, 130.36, 129.57, 128.82, 128.57, 128.49, 127.05, 126.56, 125.89, 124.88, 122.43, 115.64, 113.56, 111.41, 110.62, 72.12, 57.15, 56.29, 55.73, 54.24, 51.40, 29.82, 28.83, 28.43, 22.85, 8.83. HRMS (ESI+), m/z $[\text{M}+\text{H}^+]$ calculated for $\text{C}_{38}\text{H}_{38}\text{N}_2\text{O}_6$ 619.2808; found 619.2811.



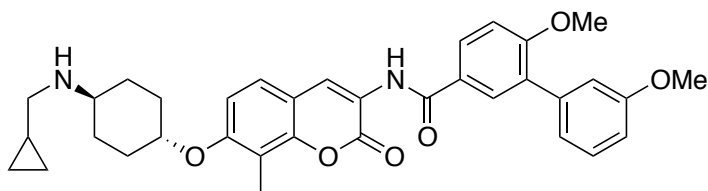
***N*-(7-(((1*r*,4*r*)-4-(bis(cyclopropylmethyl)amino)cyclohexyl)oxy)-8-methyl-2-oxo-2*H*-chromen-3-yl)-3',6-dimethoxy-[1,1'-biphenyl]-3-carboxamide (5.12a).**

Cyclopropylmethyl methanesulfonate (0.18g, 1.2mmol) was added to a solution of DIPEA (0.32 mL, 1.8mmol), **5.4b** (0.528g, 1.0mmol), and anhydrous MeCN (10mL). The mixture was placed in a sealed microwave safe septum-capped tube, and heated to 120 °C in a microwave synthesizer. After 1h the reaction was complete and the vial was cooled to rt and quenched with water. The reaction was worked-up with EtOAc (3 x 20mL). The organic layers were combined, dried, concentrated, and purified via column chromatography (SiO₂, 1:10, MeOH:DCM) to afford **5.12a** as a white amorphous solid (30% yield): ¹H NMR (500 MHz, Methanol-d₄) δ 8.69 (d, *J* = 3.4 Hz, 1H), 7.86 (dd, *J* = 8.8, 2.3 Hz, 1H), 7.82 (d, *J* = 2.4 Hz, 1H), 7.35 (d, *J* = 2.2 Hz, 1H), 7.33 – 7.28 (m, 2H), 7.10 – 7.05 (m, 3H), 6.85 – 6.82 (m, 2H), 4.32 – 4.30 (m, 1H), 3.85 (d, *J* = 25.3 Hz, 6H), 2.80 (m, 1H), 2.25 (s, 3H), 2.20 (m, 4H), 2.07 (d, *J* = 12.9 Hz, 3H), 1.90 – 1.85 (m, 2H), 1.80 (td, *J* = 11.5, 3.1 Hz, 1H), 1.69 (d, *J* = 12.3 Hz, 2H). -0.10 – -0.15 (m, 2H), -0.69 (m, 4H), -0.79 – -0.95 (m, 4H). ¹³C NMR (126 MHz, MeOD) δ 166.39, 160.42, 160.02, 157.76, 150.42, 139.12, 131.81, 130.23, 129.76, 129.21, 126.86, 125.52, 122.27, 122.11, 116.31, 115.96, 114.34, 113.75, 113.04, 111.62, 110.72, 70.44, 56.51, 55.93, 54.34, 30.41, 28.22, 25.54, 13.16, 8.02, 3.91. HRMS (ESI+), *m/z* [M+H⁺] calculated for C₃₉H₄₄N₂O₆ 637.3278; found 637.3266.



***N*-(7-(((1*s*,4*s*)-4-(Bis(cyclopropylmethyl)amino)cyclohexyl)oxy)-8-methyl-2-oxo-2*H*-chromen-3-yl)-3',6-dimethoxy-[1,1'-biphenyl]-3-carboxamide (**5.12b**).**

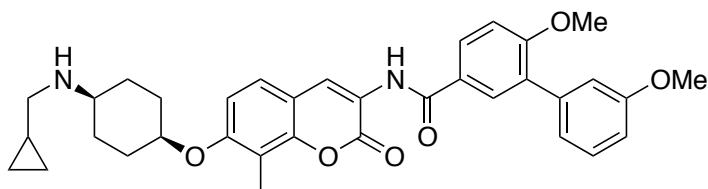
Compound **5.12b** was obtained following the procedure for the synthesis of **5.12a** as a white amorphous solid (30%): ¹H NMR (500 MHz, Methanol-d₄) δ 8.75 (d, *J* = 3.6 Hz, 1H), 7.82 (dd, *J* = 8.7, 2.4 Hz, 1H), 7.79 (d, *J* = 2.6 Hz, 1H), 7.35 (d, *J* = 2.7 Hz, 1H), 7.33 – 7.29 (m, 2H), 7.07 – 7.02 (m, 3H), 6.88 – 6.82 (m, 2H), 4.66 – 4.63 (m, 1H), 3.84 (d, *J* = 24.6 Hz, 6H), 3.13 – 3.09 (m, 1H), 2.32 (s, 3H), 2.27 (m, 4H), 2.18 (d, *J* = 13.4 Hz, 3H), 1.93 – 1.88 (m, 2H), 1.81 (td, *J* = 12.1, 3.3 Hz, 1H), 1.68 (d, *J* = 12.4 Hz, 2H). -0.04 – -0.14 (m, 2H), -0.65 (m, 4H), -0.83 – -1.00 (m, 4H). ¹³C NMR (126 MHz, MeOD) δ 166.20, 160.15, 160.46, 157.42, 150.45, 139.48, 131.38, 130.69, 129.95, 129.00, 126.64, 125.75, 122.74, 122.34, 116.02, 115.36, 114.51, 113.13, 113.00, 111.52, 110.11, 70.49, 56.66, 55.75, 54.81, 30.32, 28.75, 25.91, 13.11, 8.07, 3.55. HRMS (ESI+), *m/z* [M+H⁺] calculated for C₃₉H₄₄N₂O₆ 637.3278; found 637.3292.



***N*-(7-(((1*r*,4*r*)-4-((Cyclopropylmethyl)amino)cyclohexyl)oxy)-8-methyl-2-oxo-2*H*-chromen-3-yl)-3',6-dimethoxy-[1,1'-biphenyl]-3-carboxamide (**5.12c**).**

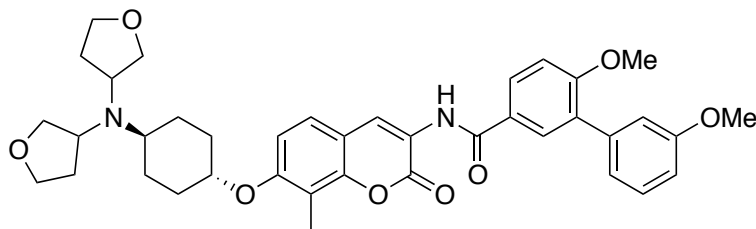
Compound **5.12c** was obtained following the procedure for the synthesis of **5.12a** as a white amorphous solid (30%): ¹H NMR (500 MHz, Methanol-d₄) δ 8.68 (d, *J* = 3.3 Hz, 1H), 7.85 (dd, *J* = 8.7, 2.6 Hz, 1H), 7.80 (d, *J* = 2.6 Hz, 1H), 7.33 (d, *J* = 2.4 Hz, 1H), 7.32 – 7.29 (m, 2H), 7.06 – 7.04 (m, 3H), 6.87 – 6.82 (m, 2H), 4.52 (s, 1H), 4.35 – 4.30 (m, 1H), 3.81 (d, *J* = 24.9 Hz, 6H), 2.83 (m, 1H), 2.29 (s, 3H), 2.24 (t, *J* = 5.5 Hz, 2H), 2.10 (d, *J* = 13.0 Hz, 3H), 1.94 – 1.89 (m, 2H), 1.81 (td, *J* = 11.7, 3.4 Hz, 1H), 1.68 (d, *J* = 12.2 Hz, 2H) -0.08 – -0.16 (m, 1H), -0.66 (dt, *J* = 7.7, 2.7 Hz, 2H), -0.82 – -1.01 (m, 2H). ¹³C NMR (126 MHz, MeOD) δ 166.72, 160.53,

160.11, 157.39, 150.36, 139.43, 131.66, 130.08, 129.42, 129.30, 126.45, 125.77, 122.32, 122.06, 116.31, 115.83, 114.33, 113.11, 113.00, 111.67, 110.22, 70.84, 56.59, 55.97, 54.33, 30.53, 28.05, 25.67, 13.36, 8.32, 3.19. HRMS (ESI+), m/z $[M+H^+]$ calculated for $C_{35}H_{38}N_2O_6$ 583.2808; found 583.2806.



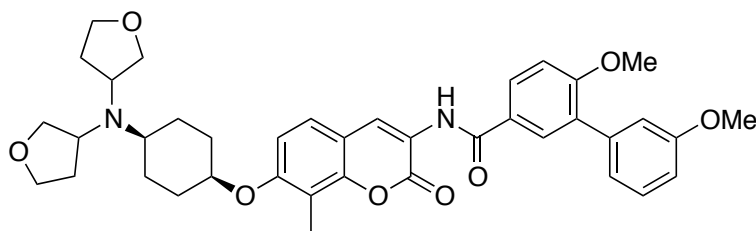
***N*-(7-(((1*s*,4*s*)-4-((Cyclopropylmethyl)amino)cyclohexyl)oxy)-8-methyl-2-oxo-2*H*-chromen-3-yl)-3',6-dimethoxy-[1,1'-biphenyl]-3-carboxamide (5.12d).**

Compound **5.12d** was obtained following the procedure for the synthesis of **5.12a** as a white amorphous solid (30%): 1H NMR (500 MHz, Methanol- d_4) δ 8.70 (d, $J = 3.4$ Hz, 1H), 7.86 (dd, $J = 8.5, 2.5$ Hz, 1H), 7.81 (d, $J = 2.7$ Hz, 1H), 7.36 (d, $J = 2.6$ Hz, 1H), 7.34 – 7.27 (m, 2H), 7.08 – 7.01 (m, 3H), 6.89 – 6.83 (m, 2H), 4.69 – 4.62 (m, 1H), 4.49 (s, 1H), 3.82 (d, $J = 24.7$ Hz, 6H), 3.15 – 3.06 (m, 1H), 2.30 (s, 3H), 2.25 (t, $J = 5.7$ Hz, 2H), 2.14 (d, $J = 13.3$ Hz, 3H), 1.92 – 1.83 (m, 2H), 1.79 (td, $J = 11.9, 3.2$ Hz, 1H), 1.66 (d, $J = 12.3$ Hz, 2H). -0.04 – -0.15 (m, 1H), -0.64 (dt, $J = 7.9, 2.9$ Hz, 2H), -0.85 – -1.03 (m, 2H). ^{13}C NMR (126 MHz, MeOD) δ 166.82, 160.71, 160.06, 157.41, 150.25, 139.42, 131.78, 130.68, 129.92, 129.90, 126.60, 125.95, 122.77, 122.14, 116.00, 115.66, 114.11, 113.83, 113.80, 111.92, 110.91, 70.89, 56.56, 55.99, 54.21, 30.40, 28.65, 25.90, 13.81, 8.67, 3.29. HRMS (ESI+), m/z $[M+H^+]$ calculated for $C_{35}H_{38}N_2O_6$ 583.2808; found 583.2786.



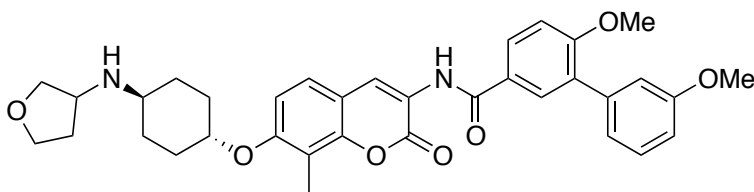
***N*-(7-(((1*r*,4*r*)-4-(Bis(tetrahydrofuran-3-yl)amino)cyclohexyl)oxy)-8-methyl-2-oxo-2*H*-chromen-3-yl)-3',6-dimethoxy-[1,1'-biphenyl]-3-carboxamide (5.13a).**

Compound **5.13a** was obtained following the procedure for the synthesis of **5.12a** as a white amorphous solid (30%): ^1H NMR (500 MHz, Methanol- d_4) δ 8.72 (d, $J = 3.4$ Hz, 1H), 7.81 (dd, $J = 8.9, 2.5$ Hz, 1H), 7.79 (d, $J = 2.6$ Hz, 1H), 7.36 (d, $J = 2.5$ Hz, 1H), 7.31 – 7.29 (m, 2H), 7.09 – 7.02 (m, 3H), 6.90 – 6.86 (m, 2H), 4.39-4.37 (m, 2H), 4.32 – 4.29 (m, 1H), 3.88-3.85 (m, 2H), 3.82 (d, $J = 24.8$ Hz, 6H), 3.70 (m, 2H), 3.66-3.63 (m, 2H), 2.80 (m, 1H), 2.22 (s, 3H), 2.11-2.09 (m, 4H), 1.97 (m, 1H), 1.92 – 1.86 (m, 2H), 1.83-1.80 (m, 4H), 1.69 (m, 2H). ^{13}C NMR (126 MHz, MeOD) δ 162.31, 159.07, 159.02, 157.79, 144.57, 131.71, 129.99, 129.77, 129.19, 128.28, 127.62, 125.65, 123.02, 123.12, 122.02, 120.31, 117.82, 115.57, 115.35, 114.28, 75.32, 71.07, 66.69, 58.49, 57.71, 53.69, 52.39, 51.31, 35.24, 31.02, 27.67, 27.39 7.55. HRMS (ESI+), m/z [$M+H^+$] calculated for $\text{C}_{39}\text{H}_{44}\text{N}_2\text{O}_8$ 669.3187; found 669.3200.



***N*-(7-(((1*s*,4*s*)-4-(Bis(tetrahydrofuran-3-yl)amino)cyclohexyl)oxy)-8-methyl-2-oxo-2*H*-chromen-3-yl)-3',6-dimethoxy-[1,1'-biphenyl]-3-carboxamide (5.13b).**

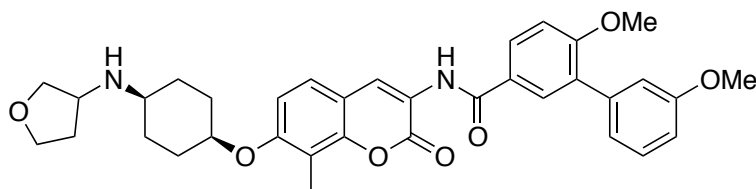
Compound **5.13b** was obtained following the procedure for the synthesis of **5.12a** as a white amorphous solid (30%): ^1H NMR (500 MHz, Methanol- d_4) δ 8.82 (d, $J = 3.5$ Hz, 1H), 7.80 (dd, $J = 8.6, 2.3$ Hz, 1H), 7.75 (d, $J = 2.6$ Hz, 1H), 7.50 (d, $J = 2.3$ Hz, 1H), 7.34 – 7.28 (m, 2H), 7.05 – 7.01 (m, 3H), 6.87 – 6.82 (m, 2H), 4.68 – 4.63 (m, 1H), 4.42-4.38 (m, 2H), 3.90-3.87 (m, 2H), 3.79 (d, $J = 24.8$ Hz, 6H), 3.75 (m, 2H), 3.65-3.60 (m, 2H), 3.11 – 3.06 (m, 1H), 2.28 (s, 3H), 2.10 (d, 4H), 1.99-1.93 (m, 2H), 1.89 – 1.80 (m, 5H), 1.72 (m, 1H), 1.66 (m, 1H). ^{13}C NMR (126 MHz, MeOD) δ 162.45, 159.35, 159.02, 157.17, 144.02, 131.86, 129.95, 129.45, 129.23, 128.37, 127.14, 125.01, 123.28, 123.02, 122.09, 120.55, 117.85, 115.51, 115.21, 114.67, 75.34, 71.31, 66.49, 58.62, 57.51, 53.66, 52.12, 51.14, 35.54, 31.13, 27.56, 27.23 7.55. HRMS (ESI+), m/z [M+H $^+$] calculated for $\text{C}_{39}\text{H}_{44}\text{N}_2\text{O}_8$ 669.3187; found 669.3165.



3',6-Dimethoxy-N-(8-methyl-2-oxo-7-(((1*r*,4*r*)-4-((tetrahydrofuran-3-yl)amino)cyclohexyl)oxy)-2*H*-chromen-3-yl)-[1,1'-biphenyl]-3-carboxamide (5.13c**).**

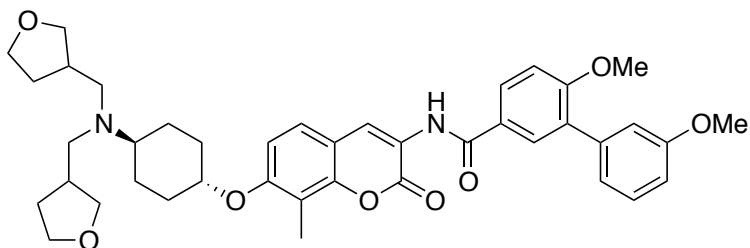
Compound **5.13c** was obtained following the procedure for the synthesis of **5.12a** as a white amorphous solid (30%): ^1H NMR (500 MHz, Methanol- d_4) δ 8.72 (d, $J = 3.5$ Hz, 1H), 7.89 (dd, $J = 8.8, 2.5$ Hz, 1H), 7.80 (d, $J = 2.6$ Hz, 1H), 7.33 (d, $J = 2.6$ Hz, 1H), 7.30 – 7.27 (m, 2H), 7.06 – 7.01 (m, 3H), 6.86 – 6.80 (m, 2H), 4.55 (s, 1H), 4.38 (t, $J = 5.9$ Hz, 1H), 4.32 – 4.29 (m, 1H), 3.88 (q, $J = 7.5$ Hz, 1H), 3.80 (d, $J = 24.7$ Hz, 6H), 3.74 (dt, $J = 8.3, 4.2$ Hz, 1H), 3.67 (dq, $J = 12.9, 4.5, 3.8$ Hz, 1H), 2.82 (m, 1H), 2.23 (s, 3H), 2.11 (d, $J = 13.2$ Hz, 3H), 1.99 (ddd, $J = 14.2, 9.4, 6.0$ Hz, 1H), 1.94 – 1.88 (m, 2H), 1.83-1.80 (m, 2H), 1.67 (m, 2H). ^{13}C NMR (126 MHz,

MeOD) δ 162.01, 159.37, 159.32, 157.72, 144.53, 131.41, 129.97, 129.47, 129.39, 128.48, 127.32, 125.61, 123.82, 123.02, 122.00, 120.41, 117.85, 115.50, 115.15, 114.22, 75.22, 71.27, 66.62, 58.19, 57.71, 53.29, 52.39, 51.11, 35.02, 31.72, 27.97, 27.69 7.31. HRMS (ESI+), m/z $[M+H^+]$ calculated for $C_{35}H_{38}N_2O_7$ 599.2709; found 599.2720.



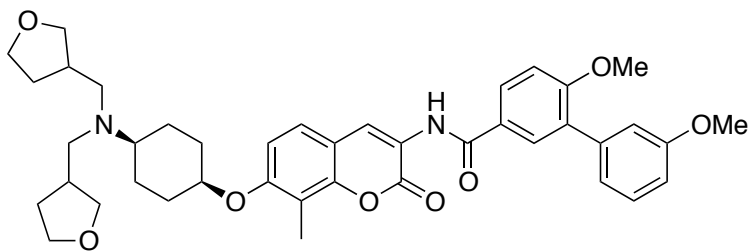
3',6-Dimethoxy-N-(8-methyl-2-oxo-7-(((1*S*,4*S*)-4-((tetrahydrofuran-3-yl)amino)cyclohexyl)oxy)-2*H*-chromen-3-yl)-[1,1'-biphenyl]-3-carboxamide (5.13d).

Compound **5.13d** was obtained following the procedure for the synthesis of **5.12a** as a white amorphous solid (30%): 1H NMR (500 MHz, Methanol- d_4) δ 8.80 (d, $J = 3.4$ Hz, 1H), 7.85 (dd, $J = 8.8, 2.6$ Hz, 1H), 7.79 (d, $J = 2.9$ Hz, 1H), 7.49 (d, $J = 2.4$ Hz, 1H), 7.34 – 7.28 (m, 2H), 7.03 – 7.00 (m, 3H), 6.85 – 6.82 (m, 2H), 4.70 – 4.65 (m, 1H), 4.50 (s, 1H), 4.40 (t, $J = 5.9$ Hz, 1H), 3.88 (q, $J = 7.6$ Hz, 1H), 3.81 (d, $J = 24.5$ Hz, 6H), 3.76 (dt, $J = 8.4, 4.3$ Hz, 1H), 3.62 (dq, $J = 12.7, 4.5, 3.7$ Hz, 1H), 3.12 – 3.07 (m, 1H), 2.32 (s, 3H), 2.14 (d, 4H), 1.99 (ddd, $J = 14.2, 9.4, 6.0$ Hz, 1H), 1.92 – 1.80 (m, 3H), 1.75 (td, $J = 11.7, 3.1$ Hz, 1H), 1.68 (d, $J = 12.4$ Hz, 1H). ^{13}C NMR (126 MHz, MeOD) δ 162.11, 159.33, 159.02, 157.76, 144.52, 131.44, 129.90, 129.67, 129.23, 128.67, 127.02, 125.61, 123.22, 123.02, 122.00, 120.11, 117.05, 115.59, 115.45, 114.67, 75.09, 71.32, 66.45, 58.65, 57.71, 53.48, 52.23, 51.16, 35.12, 31.45, 27.22, 27.13 7.33. HRMS (ESI+), m/z $[M+H^+]$ calculated for $C_{35}H_{38}N_2O_7$ 599.2709; found 599.2720.



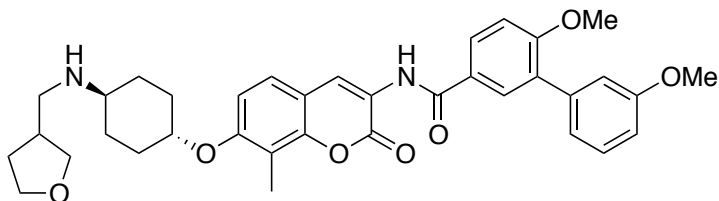
***N*-(7-(((1*r*,4*r*)-4-(Bis((tetrahydrofuran-3-yl)methyl)amino)cyclohexyl)oxy)-8-methyl-2-oxo-2*H*-chromen-3-yl)-3',6-dimethoxy-[1,1'-biphenyl]-3-carboxamide (5.14a).**

Compound **5.14a** was obtained following the procedure for the synthesis of **5.12a** as a white amorphous solid (30%): ^1H NMR (500 MHz, Methanol- d_4) δ 7.91 (d, $J = 2.4$ Hz, 1H), 7.11 – 7.06 (m, 1H), 7.02 (d, $J = 2.4$ Hz, 1H), 6.60 (d, $J = 3.0$ Hz, 1H), 6.55 – 6.46 (m, 2H), 6.35 (ddt, $J = 8.1, 6.7, 2.2$ Hz, 3H), 6.29 – 6.21 (m, 2H), 6.00 (ddd, $J = 7.0, 5.1, 3.2$ Hz, 1H), 3.56 – 3.42 (m, 1H), 3.17 (d, $J = 1.6$ Hz, 3H), 3.11 (d, $J = 3.0$ Hz, 3H), 2.99 – 2.88 (m, 2H), 2.79 (m, 2H), 2.75 – 2.68 (m, 2H), 2.63 – 2.58 (m, 2H), 2.50 (s, 3H), 2.48 (dt, $J = 3.3, 1.5$ Hz, 1H), 2.30 (m, 2H), 1.88 – 1.76 (m, 1H), 1.62-1.57 (m, 4H), 1.42 – 1.30 (m, 2H), 1.25 (m, 2H), 1.09 – 1.02 (m, 1H). ^{13}C NMR (126 MHz, MeOD) δ 165.06, 159.63, 158.41, 149.33, 144.21, 138.74, 130.39, 129.36, 128.23, 128.07, 125.56, 123.06, 121.59, 114.61, 112.31, 110.98, 70.08, 67.90, 63.52, 55.06, 54.00, 53.17, 49.37, 40.99, 33.76, 28.48, 7.04. HRMS (ESI+), m/z $[\text{M}+\text{H}^+]$ calculated for $\text{C}_{41}\text{H}_{48}\text{N}_2\text{O}_8$ 697.3464; found 697.3487.



***N*-(7-(((1*s*,4*s*)-4-(Bis((tetrahydrofuran-3-yl)methyl)amino)cyclohexyl)oxy)-8-methyl-2-oxo-2*H*-chromen-3-yl)-3',6-dimethoxy-[1,1'-biphenyl]-3-carboxamide (5.14b).**

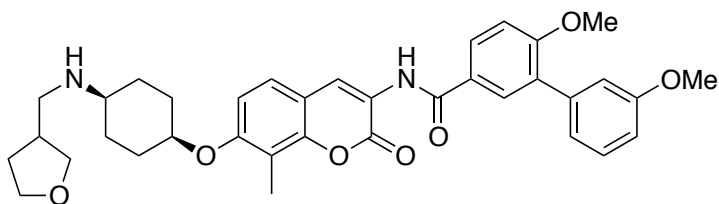
Compound **5.14b** was obtained following the procedure for the synthesis of **5.12a** as a white amorphous solid (30%): ¹H NMR (500 MHz, Methanol-d₄) δ 7.93 (d, *J* = 2.7 Hz, 1H), 7.20 – 7.15 (m, 1H), 7.10 (d, *J* = 2.5 Hz, 1H), 6.66 (d, *J* = 3.0 Hz, 1H), 6.55 – 6.40 (m, 2H), 6.30 (ddt, *J* = 7.7, 6.3, 2.4 Hz, 3H), 6.21 – 6.17 (m, 2H), 6.09 (ddd, *J* = 6.4, 5.1, 3.8 Hz, 1H), 3.55 – 3.40 (m, 1H), 3.10 (s, 3H), 3.06 (s, 3H), 2.95 – 2.89 (m, 2H), 2.77 (m, 2H), 2.73 – 2.68 (m, 2H), 2.60 – 2.53 (m, 2H), 2.45 (s, 3H), 2.30 (dt, *J* = 3.3, 1.8 Hz, 1H), 2.22 (m, 2H), 1.88 – 1.65 (m, 1H), 1.58 (m, 4H), 1.39 – 1.28 (m, 2H), 1.22 (m, 2H), 1.13 – 1.06 (m, 1H). ¹³C NMR (126 MHz, MeOD) δ 165.53, 159.41, 158.89, 149.05, 144.40, 138.22, 130.44, 129.78, 128.69, 128.19, 125.56, 123.93, 121.88, 114.23, 112.15, 110.63, 70.78, 67.22, 63.42, 55.06, 54.10, 53.57, 49.27, 40.99, 33.82, 28.58, 7.66. HRMS (ESI+), *m/z* [M+H⁺] calculated for C₄₁H₄₈N₂O₈ 697.3464; found 697.3436.



3',6-Dimethoxy-*N*-(8-methyl-2-oxo-7-(((1*r*,4*r*)-4-(((tetrahydrofuran-3-yl)methyl)amino)cyclohexyl)oxy)-2*H*-chromen-3-yl)-[1,1'-biphenyl]-3-carboxamide (5.14c).

Compound **5.14c** was obtained following the procedure for the synthesis of **5.12c** as a white amorphous solid (30%): ¹H NMR (500 MHz, Methanol-d₄) δ 7.95 (d, *J* = 2.9 Hz, 1H), 7.19 – 7.15 (m, 1H), 7.05 (d, *J* = 2.3 Hz, 1H), 6.57 (d, *J* = 2.7 Hz, 1H), 6.55 – 6.49 (m, 2H), 6.34 (ddt, *J* = 7.7, 6.5, 2.4 Hz, 3H), 6.29 – 6.22 (m, 2H), 6.03 (ddd, *J* = 6.5, 5.5, 3.6 Hz, 1H), 3.62 (s, 1H), 3.54 – 3.38 (m, 1H), 3.15 (d, *J* = 1.8 Hz, 3H), 3.11 (d, *J* = 3.2 Hz, 3H), 2.98 – 2.86 (m, 1H), 2.77 (td, *J* = 5.8, 2.9 Hz, 1H), 2.76 – 2.69 (m, 1H), 2.64 – 2.55 (m, 1H), 2.52 (s, 3H), 2.49 (dt, *J* = 3.5,

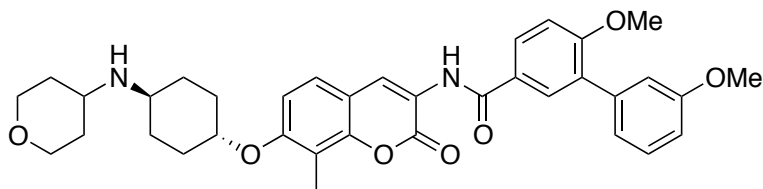
1.3 Hz, 1H), 2.40 (dd, $J = 8.9, 4.5$ Hz, 1H), 1.70 – 1.56 (m, 1H), 1.40 (dd, $J = 5.6, 3.4$ Hz, 4H), 1.30 – 1.24 (m, 2H), 1.18 (dddd, $J = 17.5, 14.8, 10.3, 4.5$ Hz, 2H), 0.99 – 0.84 (m, 1H). ^{13}C NMR (126 MHz, MeOD) δ 165.47, 159.47, 158.37, 149.04, 144.19, 138.32, 130.51, 129.49, 128.41, 128.09, 125.73, 123.58, 121.19, 114.11, 112.61, 110.78, 70.48, 67.09, 63.34, 55.35, 54.82, 53.07, 49.15, 41.00, 33.72, 28.08, 7.66. HRMS (ESI+), m/z $[\text{M}+\text{H}^+]$ calculated for $\text{C}_{36}\text{H}_{40}\text{N}_2\text{O}_7$ 613.2807; found 613.2801.



3',6-Dimethoxy-*N*-(8-methyl-2-oxo-7-(((1*s*,4*s*)-4-(((tetrahydrofuran-3-yl)methyl)amino)cyclohexyl)oxy)-2*H*-chromen-3-yl)-[1,1'-biphenyl]-3-carboxamide (5.14d).

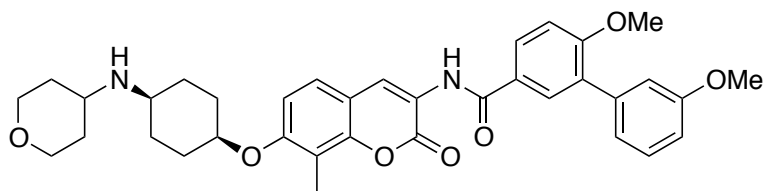
Compound **5.14d** was obtained following the procedure for the synthesis of **5.12c** as a white amorphous solid (30%): ^1H NMR (500 MHz, Methanol- d_4) δ 7.90 (d, $J = 2.7$ Hz, 1H), 7.09 – 7.05 (m, 1H), 7.04 (d, $J = 2.5$ Hz, 1H), 6.56 (d, $J = 2.9$ Hz, 1H), 6.55 – 6.46 (m, 2H), 6.34 (ddt, $J = 7.9, 6.7, 2.4$ Hz, 3H), 6.30 – 6.22 (m, 2H), 6.09 (ddd, $J = 6.8, 5.3, 3.8$ Hz, 1H), 3.52 – 3.36 (m, 1H), 3.05 (d, $J = 1.8$ Hz, 3H), 3.01 (d, $J = 3.2$ Hz, 3H), 2.93 – 2.86 (m, 1H), 2.76 (td, $J = 5.6, 2.7$ Hz, 1H), 2.73 – 2.68 (m, 1H), 2.67 – 2.58 (m, 1H), 2.54 (d, $J = 3.3$ Hz, 3H), 2.50 (dt, $J = 3.4, 1.6$ Hz, 1H), 2.41 (dd, $J = 8.8, 4.7$ Hz, 1H), 1.66 – 1.53 (m, 1H), 1.44 (dd, $J = 5.8, 3.3$ Hz, 4H), 1.32 – 1.24 (m, 2H), 1.15 (dddd, $J = 17.3, 15.0, 10.3, 4.3$ Hz, 2H), 0.86 – 0.67 (m, 1H). ^{13}C NMR (126 MHz, MeOD) δ 165.57, 159.47, 158.87, 149.07, 144.49, 138.25, 130.54, 129.49, 128.71, 128.09, 125.23, 123.56, 121.59, 114.81, 112.61, 110.72, 70.18, 67.39, 63.50, 55.36, 54.80, 53.27,

49.17, 40.94, 33.70, 28.18, 7.64. HRMS (ESI+), m/z $[M+H^+]$ calculated for $C_{36}H_{40}N_2O_7$ 613.2807; found 613.2792.



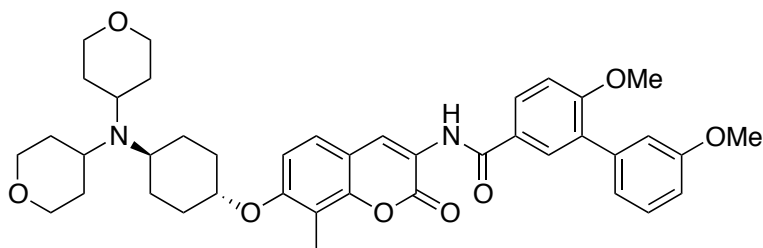
3',6-Dimethoxy-*N*-(8-methyl-2-oxo-7-(((1*r*,4*r*)-4-((tetrahydro-2*H*-pyran-4-yl)amino)cyclohexyl)oxy)-2*H*-chromen-3-yl)-[1,1'-biphenyl]-3-carboxamide (5.15c).

Compound **5.15c** was obtained following the procedure for the synthesis of **5.12a** as a white amorphous solid (30%): 1H NMR (500 MHz, Methanol- d_4) δ 8.59 (s, 1H), 7.75 (dd, $J = 8.6, 2.5$ Hz, 1H), 7.70 (d, $J = 2.4$ Hz, 1H), 7.26 (d, $J = 2.3$ Hz, 1H), 7.22 – 7.15 (m, 2H), 6.97 – 6.90 (m, 3H), 6.78 – 6.70 (m, 2H), 4.62, (s, 1H), 4.55 (t, $J = 3.1$ Hz, 1H), 3.77 (dt, $J = 11.8, 4.2$ Hz, 2H), 3.73 (s, 3H), 3.68 (s, 3H), 3.61 (tt, $J = 9.1, 4.2$ Hz, 1H), 3.27 (ddd, $J = 12.1, 10.3, 2.6$ Hz, 2H), 3.05 – 2.92 (m, 1H), 2.19 (s, 3H), 2.09 – 1.98 (m, 2H), 1.69 (m, 4H), 1.60 – 1.47 (m, 2H), 1.37 (dtd, $J = 13.6, 9.7, 4.2$ Hz, 2H), 1.31 (dd, $J = 7.1, 2.3$ Hz, 4H). ^{13}C NMR (126 MHz, MeOD) δ 165.64, 159.50, 158.86, 156.21, 149.07, 138.22, 130.59, 129.50, 128.73, 127.84, 125.43, 124.76, 121.59, 114.83, 112.63, 110.75, 109.73, 79.98, 69.68, 59.67, 55.38, 54.81, 53.05, 34.62, 34.47, 27.46, 24.69, 7.49. HRMS (ESI+), m/z $[M+H^+]$ calculated for $C_{36}H_{40}N_2O_7$ 613.2867; found 613.2854.



3',6-Dimethoxy-N-(8-methyl-2-oxo-7-(((1*s*,4*s*)-4-((tetrahydro-2*H*-pyran-4-yl)amino)cyclohexyl)oxy)-2*H*-chromen-3-yl)-[1,1'-biphenyl]-3-carboxamide (5.15d).

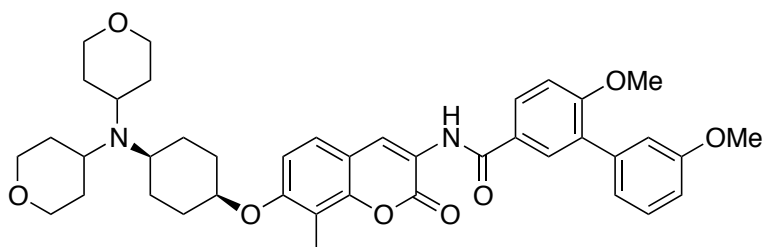
Compound **5.15d** was obtained following the procedure for the synthesis of **5.12a** as a white amorphous solid (30%): ¹H NMR (500 MHz, Methanol-*d*₄) δ 8.68 (d, *J* = 2.8 Hz, 1H), 7.83 (dt, *J* = 8.5, 3.2 Hz, 1H), 7.79 (t, *J* = 3.1 Hz, 1H), 7.30 (m, 2H), 7.04 – 6.97 (m, 4H), 6.81 (ddd, *J* = 16.9, 8.8, 4.7 Hz, 2H), 4.65 (s, 1H), 4.62 – 4.56 (m, 1H), 3.85 – 3.70 (m, 2H), 3.55 (ddd, *J* = 10.5, 6.6, 3.3 Hz, 2H), 3.25 (dt, *J* = 3.1, 1.6 Hz, 6H), 3.02 (qd, *J* = 7.5, 2.9 Hz, 1H), 2.66 (d, *J* = 2.6 Hz, 1H), 2.27 (d, *J* = 3.0 Hz, 3H), 2.14 – 2.04 (m, 2H), 1.83 (d, *J* = 13.0 Hz, 2H), 1.72 (d, *J* = 12.3 Hz, 2H), 1.62 (dd, *J* = 14.0, 3.1 Hz, 2H), 1.33 (dt, *J* = 6.7, 2.2 Hz, 2H), 1.29 (dd, *J* = 6.7, 2.9 Hz, 2H). ¹³C NMR (126 MHz, MeOD) δ 165.64, 159.50, 158.86, 156.21, 149.07, 138.22, 130.59, 129.50, 128.73, 127.84, 125.43, 124.76, 121.59, 114.83, 112.63, 110.75, 109.73, 80.02, 69.68, 59.67, 55.38, 54.81, 53.05, 34.62, 34.47, 27.46, 24.69, 7.49. HRMS (ESI+), *m/z* [M+H⁺] calculated for C₃₆H₄₀N₂O₇ 613.2867; found 613.2854.



N-(7-(((1*r*,4*r*)-4-(Bis(tetrahydro-2*H*-pyran-4-yl)amino)cyclohexyl)oxy)-8-methyl-2-oxo-2*H*-chromen-3-yl)-3',6-dimethoxy-[1,1'-biphenyl]-3-carboxamide (5.15a).

Compound **5.15a** was obtained following the procedure for the synthesis of **5.12a** as a white amorphous solid (30%): ¹H NMR (500 MHz, Methanol-*d*₄) δ 8.50 (s, 1H), 7.78 (dd, *J* = 8.4, 2.2 Hz, 1H), 7.71 (d, *J* = 2.4 Hz, 1H), 7.30 (d, *J* = 2.4 Hz, 1H), 7.23 – 7.17 (m, 2H), 6.90 – 6.84 (m,

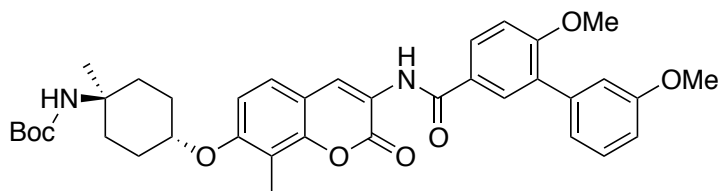
3H), 6.76 – 6.70 (m, 2H), 4.50 (t, $J = 3.2$ Hz, 1H), 3.78 (dt, $J = 11.9, 4.0$ Hz, 4H), 3.70 (s, 3H), 3.67 (s, 3H), 3.60 (tt, $J = 9.1, 4.2$ Hz, 2H), 3.30 (ddd, $J = 12.0, 10.1, 2.5$ Hz, 4H), 3.05 – 2.92 (m, 1H), 2.10 (s, 3H), 2.02 – 1.96 (m, 2H), 1.65 (m, 4H), 1.58 – 1.49 (m, 2H), 1.39 (dtd, $J = 13.5, 9.9, 4.2$ Hz, 4H) 1.31 (dd, $J = 7.1, 2.3$ Hz, 4H). ^{13}C NMR (126 MHz, MeOD) δ 165.94, 159.55, 158.06, 155.71, 149.00, 138.42, 130.51, 129.00, 128.33, 127.14, 125.44, 124.56, 121.50, 114.89, 112.03, 110.55, 109.43, 79.90, 69.68, 59.63, 55.18, 54.21, 53.15, 34.64, 34.40, 27.56, 24.60, 7.89. HRMS (ESI+), m/z $[\text{M}+\text{H}^+]$ calculated for $\text{C}_{41}\text{H}_{48}\text{N}_2\text{O}_8$ 697.3403; found 697.3421.



***N*-(7-(((1*s*,4*s*)-4-(Bis(tetrahydro-2*H*-pyran-4-yl)amino)cyclohexyl)oxy)-8-methyl-2-oxo-2*H*-chromen-3-yl)-3',6-dimethoxy-[1,1'-biphenyl]-3-carboxamide (5.15b).**

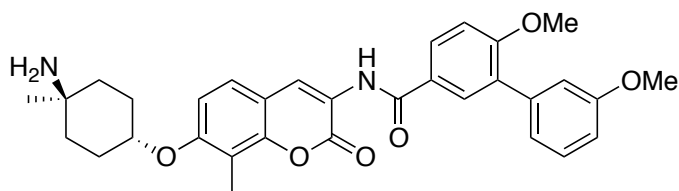
Compound **5.15b** was obtained following the procedure for the synthesis of **5.12a** as a white amorphous solid (30%): ^1H NMR (500 MHz, Methanol- d_4) δ 8.66 (d, $J = 2.8$ Hz, 1H), 7.82 (dt, $J = 8.6, 3.0$ Hz, 1H), 7.77 (t, $J = 2.8$ Hz, 1H), 7.28 (m, 2H), 7.01 – 6.92 (m, 4H), 6.80 (ddd, $J = 16.7, 8.9, 4.5$ Hz, 2H), 4.60 – 4.51 (m, 1H), 3.83 – 3.72 (m, 4H), 3.50 (ddd, $J = 10.7, 6.6, 3.1$ Hz, 4H), 3.27 (d, 6H), 3.02 (qd, $J = 7.5, 2.9$ Hz, 2H), 2.62 (d, $J = 2.8$ Hz, 1H), 2.20 (s, 3H), 2.13 – 2.08 (m, 2H), 1.80 (d, $J = 12.8$ Hz, 2H), 1.75 (d, $J = 12.5$ Hz, 2H), 1.60 (dd, $J = 14.2, 3.0$ Hz, 2H), 1.35 (dt, $J = 6.5, 2.4$ Hz, 4H), 1.30 (dd, $J = 6.9, 2.6$ Hz, 4H). ^{13}C NMR (126 MHz, MeOD) δ 165.04, 159.51, 158.82, 156.22, 149.27, 138.52, 130.50, 129.51, 128.70, 127.14, 125.42, 124.26, 121.50, 114.84, 112.63, 110.25, 109.53, 80.12, 69.08, 59.47, 55.08, 54.82, 53.05, 34.22,

34.44, 27.66, 24.09, 7.59. HRMS (ESI+), m/z $[M+H]^+$ calculated for $C_{41}H_{48}N_2O_8$ 697.3403; found 697.3390.



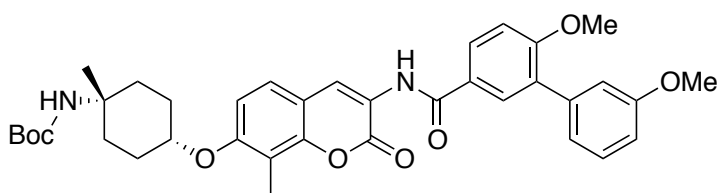
tert-Butyl ((1*r*,4*r*)-4-((3-(3',6-dimethoxy-[1,1'-biphenyl]-3-yl)carboxamido)-8-methyl-2-oxo-2*H*-chromen-7-yl)oxy)-1-methylcyclohexyl)carbamate (5.50a).

Compound **5.50a** was obtained following the procedure for the synthesis of **5.1** as a white amorphous solid (35%): 1H NMR (500 MHz, Chloroform- d) δ 8.80 (s, 1H), 8.70 (s, 1H), 7.94 – 7.87 (m, 2H), 7.39 – 7.30 (m, 2H), 7.13 – 7.10 (m, 1H), 7.10 – 7.05 (m, 2H), 6.93 (ddd, $J = 8.3, 2.6, 0.9$ Hz, 1H), 6.87 (d, $J = 8.7$ Hz, 1H), 4.40 (s, 1H), 4.32 (dt, $J = 9.2, 4.9$ Hz, 1H), 3.90 (s, 3H), 3.86 (s, 3H), 2.34 (s, 3H), 2.19 – 2.12 (m, 2H), 1.93 (dq, $J = 12.9, 4.5$ Hz, 2H), 1.81 – 1.69 (m, 2H), 1.57 (s, 3H), 1.46 (s, 9H), 1.37 (s, 3H). ^{13}C NMR (126 MHz, $CDCl_3$) δ 165.40, 159.65, 159.45, 159.23, 157.20, 149.35, 138.51, 130.94, 129.85, 129.06, 128.04, 126.04, 125.39, 124.28, 121.92, 121.47, 115.14, 113.22, 113.06, 110.91, 110.58, 55.79, 55.23, 51.07, 28.38, 27.26, 8.32. HRMS (ESI+), m/z $[M+Na]^+$ calculated for $C_{37}H_{42}N_2O_8Na$ 665.2839; found 665.2854.



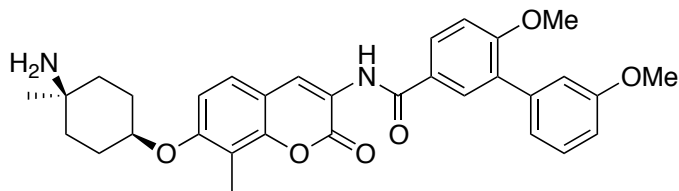
N-(7-(((1*r*,4*r*)-4-Amino-4-methylcyclohexyl)oxy)-8-methyl-2-oxo-2*H*-chromen-3-yl)-3',6-dimethoxy-[1,1'-biphenyl]-3-carboxamide (5.17a).

Compound **5.17a** was obtained following the procedure for the synthesis of **5.4a** as a white amorphous solid (70%): ^1H NMR (500 MHz, Chloroform- d) δ 9.65 (s, 1H), 8.50 (s, 1H), 8.32 (s, 1H), 8.01 (dd, $J = 8.7, 2.4$ Hz, 1H), 7.94 (d, $J = 2.4$ Hz, 1H), 7.59 (d, $J = 8.6$ Hz, 1H), 7.38 (t, $J = 7.9$ Hz, 1H), 7.27 (d, $J = 8.8$ Hz, 1H), 7.14 – 7.08 (m, 3H), 6.97 (ddd, $J = 8.3, 2.6, 0.9$ Hz, 1H), 5.76 (s, 1H), 4.71 (s, 1H), 3.89 (s, 3H), 3.82 (s, 3H), 2.21 (s, 3H), 1.88 (td, $J = 15.0, 13.3, 9.1$ Hz, 6H), 1.62 (dd, $J = 10.2, 5.9$ Hz, 2H), 1.33 (s, 3H). ^{13}C NMR (126 MHz, CDCl_3) δ 165.61, 159.42, 157.05, 150.23, 139.15, 129.86, 126.24, 122.19, 121.67, 95.24, 56.38, 55.57, 53.15, 25.93, 8.69. HRMS (ESI+), m/z $[\text{M}+\text{H}^+]$ calculated for $\text{C}_{32}\text{H}_{34}\text{N}_2\text{O}_6$ 543.2495; found 543.2470.



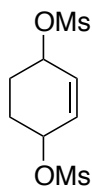
tert-Butyl ((1s,4s)-4-((3-(3',6-dimethoxy-[1,1'-biphenyl]-3-yl)carboxamido)-8-methyl-2-oxo-2H-chromen-7-yl)oxy)-1-methylcyclohexyl)carbamate (5.50b**).**

Compound **5.50b** was obtained following the procedure for the synthesis of **5.1** as a white amorphous solid (35%): ^1H NMR (500 MHz, Chloroform- d) δ 8.79 (s, 1H), 8.69 (s, 1H), 7.94 – 7.88 (m, 2H), 7.38 – 7.30 (m, 2H), 7.12 (dt, $J = 7.6, 1.1$ Hz, 1H), 7.10 – 7.05 (m, 2H), 4.56 (t, $J = 4.2$ Hz, 1H), 4.38 (s, 1H), 3.88 (d, $J = 19.7$ Hz, 5H), 2.34 (s, 3H), 1.95 (d, $J = 12.3$ Hz, 2H), 1.84 (dt, $J = 9.2, 4.1$ Hz, 4H), 1.78 – 1.72 (m, 2H), 1.60 (s, 3H), 1.45 (s, 9H), 1.37 (s, 3H). ^{13}C NMR (126 MHz, CDCl_3) δ 165.65, 159.90, 159.71, 159.48, 157.18, 149.61, 138.76, 131.18, 130.10, 129.31, 128.28, 126.29, 125.72, 124.58, 122.17, 121.67, 115.38, 113.36, 111.16, 110.49, 72.88, 56.03, 55.47, 51.82, 32.06, 28.63, 26.37, 8.45. HRMS (ESI+), m/z $[\text{M}+\text{Na}^+]$ calculated for $\text{C}_{37}\text{H}_{42}\text{N}_2\text{O}_8\text{Na}$ 665.2839; found 665.2830.



***N*-7-(((1*s*,4*s*)-4-((Cyclopropylmethyl)amino)cyclohexyl)oxy)-8-methyl-2-oxo-2*H*-chromen-3-yl)-3',6-dimethoxy-[1,1'-biphenyl]-3-carboxamide (**5.17b**).**

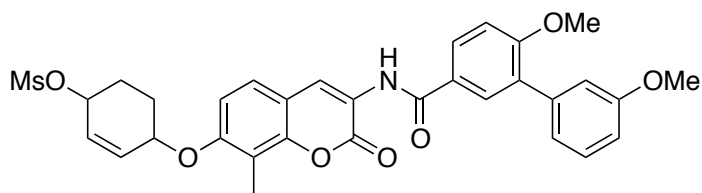
Compound **5.17b** was obtained following the procedure for the synthesis of **5.4a** as a white amorphous solid (70%): ^1H NMR (500 MHz, Methanol- d_4) δ 8.59 (s, 1H), 7.74 (dd, $J = 8.6, 2.4$ Hz, 1H), 7.70 (d, $J = 2.4$ Hz, 1H), 7.20 – 7.16 (m, 3H), 6.96 – 6.90 (m, 3H), 6.76 (ddd, $J = 8.4, 2.7, 1.0$ Hz, 2H), 4.33 (dt, $J = 7.3, 3.7$ Hz, 1H), 3.73 (s, 3H), 3.68 (s, 3H), 3.20 (s, 1H), 2.14 (s, 3H), 1.92 – 1.84 (m, 2H), 1.78 – 1.69 (m, 2H), 1.69 – 1.54 (m, 4H), 1.26 (s, 3H). ^{13}C NMR (126 MHz, MeOD) δ 165.65, 159.59, 158.98, 156.56, 149.14, 138.32, 130.72, 129.62, 128.87, 127.94, 125.52, 124.71, 121.73, 121.14, 114.95, 113.19, 112.81, 110.84, 110.31, 73.03, 55.54, 54.98, 31.98, 28.53, 25.93, 7.87. HRMS (ESI+), m/z $[\text{M}+\text{H}^+]$ calculated for $\text{C}_{32}\text{H}_{34}\text{N}_2\text{O}_6$ 543.2495; found 543.2510.



Cyclohex-2-ene-1,4-diyl dimethanesulfonate (5.52**).**

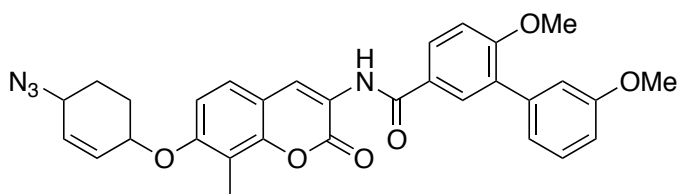
Triethylamine (0.07 mL, 0.526 mmol) was added to an ice-cooled solution of alcohol **5.51**³¹ (0.03 g, 0.26 mmol) in anhydrous tetrahydrofuran (2.5 ml), followed by a dropwise addition of methanesulfonyl chloride (0.03 ml, 0.39 mmol). The reaction mixture was then allowed to stir at rt for 4 h. The reaction mixture was diluted with water and extracted with ethyl acetate. The

organic layers were combined, dried (over Na₂SO₄), concentrated to yield **5.52** as a white amorphous solid (94%) that was used in the next step without further purification.



4-((3-(3',6-Dimethoxy-[1,1'-biphenyl]-3-yl)carboxamido)-8-methyl-2-oxo-2H-chromen-7-yl)oxy)cyclohex-2-en-1-yl methanesulfonate (5.53**).**

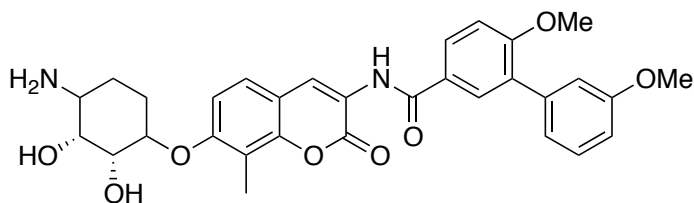
Compound **5.52** (0.67g, 2.5mmol) was added to a solution of Cs₂CO₃ (0.65, 2.0mmol), **5.36** (0.431g, 1.0mmol) in anhydrous DMF (10mL). The mixture was heated 70°C for 12 h. The reaction was then cooled to rt and worked up with sat. LiCl (3 x 20mL) and EtOAc (30mL). The organic layer was dried and concentrated to yield mesylate **5.53**, which was used immediately and without further purification.



N-(7-((4-Azidocyclohex-2-en-1-yl)oxy)-8-methyl-2-oxo-2H-chromen-3-yl)-3',6-dimethoxy-[1,1'-biphenyl]-3-carboxamide (5.54**).**

A mixture of methanesulfonate ester **5.53** (mg, 1.0 mmol) and sodium azide (mg, 3.0 mmol) in anhydrous dimethylformamide was heated at 100 °C. After 12 h, the reaction mixture was cooled to rt and concentrated. The residue was diluted with water and extracted with ethyl acetate. The organic layers were combined, concentrated and purified by column

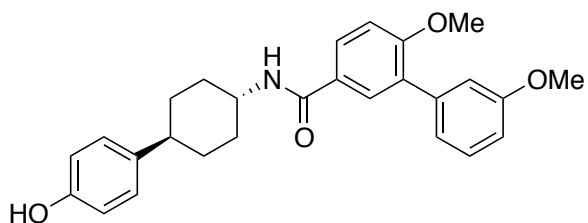
chromatography (SiO₂, 1:20, EtOAc : hexane) to afford **5.54** as a white amorphous solid (60%):
¹H NMR (500 MHz, Methanol-d₄) δ 8.60 (s, 1H), 7.76 (dd, *J* = 8.1, 2.4 Hz, 1H), 7.60 (d, *J* = 2.3 Hz, 1H), 7.20 – 7.12 (m, 3H), 6.90 – 6.85 (m, 3H), 6.70 (ddd, *J* = 8.2, 2.3, 1.2 Hz, 2H), 5.62 (d, 2H), 4.27-4.20 (m, 1H), 3.86 (s, 3H), 3.82 (s, 3H), 2.25 (m, 1H), 2.21 (m, 1H), 2.11 (s, 3H), 1.96-1.72 (m, 4H). ¹³C NMR (126 MHz, MeOD) δ 165.55, 159.39, 158.08, 155.00, 150.32, 138.79, 130.92, 129.22, 128.45, 127.17, 125.99, 125.05, 124.11, 121.83, 121.14, 114.98, 113.59, 112.77, 110.04, 79.02, 55.02, 54.33, 23.44, 23.02, 8.10.



***N*-(7-(((2*R*,3*R*)-4-Amino-2,3-dihydroxycyclohexyl)oxy)-8-methyl-2-oxo-2*H*-chromen-3-yl)-3',6-dimethoxy-[1,1'-biphenyl]-3-carboxamide (**5.16**).**

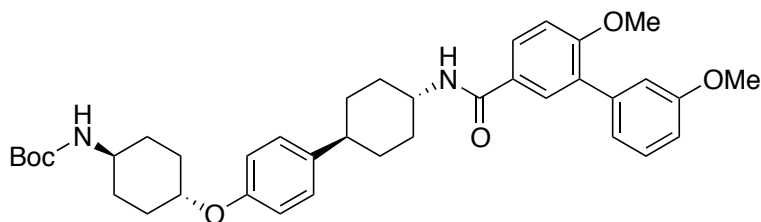
OsO₄ (0.001g, 0.002mmol) was added at rt to a solution of **5.54** (0.01g, 0.02mmol) and NMO (0.006g, 0.05mmol) in THF/H₂O (1:1, 0.6 mL). The resulting solution was stirred at rt on. After 12 h the THF was evaporated and the residue was extracted with EtOAc (3 x 5mL). The organic layers were collected, dried, concentrated and purified by column chromatography (SiO₂, 1:10, MeOH: DCM) to give a white solid, which was then dissolved in EtOAc (4 mL). Pd/C (10% w/w, 20 mg) was added, the mixture was degassed and flushed with argon, then degassed and flushed with hydrogen using a balloon. After 12 h the reaction was filtered through a pad of Celite, washed with EtOAc. The filtrate was concentrated and purified via column chromatography (SiO₂, 1:10, MeOH: DCM) to give **5.16** as a white solid (33% yield): ¹H NMR (500 MHz, Methanol-d₄) δ 8.51 (s, 1H), 7.72 (dd, *J* = 8.2, 2.1 Hz, 1H), 7.68 (d, *J* = 2.2 Hz, 1H),

7.18 – 7.10 (m, 3H), 6.93 – 6.88 (m, 3H), 6.71 (ddd, $J = 8.2, 2.4, 1.3$ Hz, 2H), 4.07-4.05 (m, 1H), 3.96-3.94 (m, 1H), 3.83 (s, 3H), 3.80 (s, 3H), 3.72-3.69 (m, 1H), 2.74 (t, $J = 3$ Hz, 1H), 2.16 (s, 3H), 1.94-1.72 (m, 4H). ^{13}C NMR (126 MHz, MeOD) δ 165.87, 159.09, 158.78, 156.16, 149.34, 138.72, 130.32, 129.62, 128.17, 127.77, 125.55, 124.31, 121.23, 121.04, 114.98, 113.49, 112.31, 110.34, 73.03, 72.42, 71.06, 55.52, 54.18, 23.89, 23.40, 7.80. HRMS (ESI+), m/z $[\text{M}+\text{H}^+]$ calculated for $\text{C}_{31}\text{H}_{32}\text{N}_2\text{O}_8$ 561.2254; found 561.2231.



***N*-((1*R*,4*R*)-4-(4-Hydroxyphenyl)cyclohexyl)-3',6-dimethoxy-[1,1'-biphenyl]-3-carboxamide (5.63).**

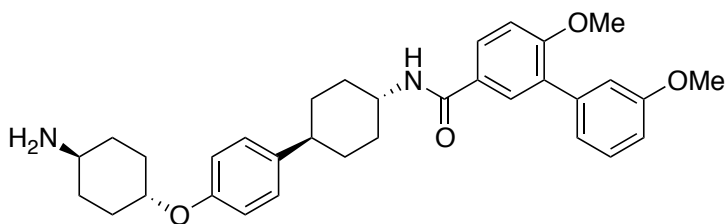
Compound **5.63** was synthesized following the procedure reported in Chapter 4.



***tert*-Butyl ((1*R*,4*R*)-4-(4-((1*R*,4*R*)-4-(3',6-dimethoxy-[1,1'-biphenyl]-3-ylcarboxamido)cyclohexyl)phenoxy)cyclohexyl)carbamate (5.64a).**

Compound **5.64a** was obtained following the procedure for the synthesis of **5.1** as a white amorphous solid (35%): ^1H NMR (500 MHz, Chloroform- d) δ 7.73 (ddd, $J = 10.5, 8.3, 2.4$ Hz, 1H), 7.63 (dd, $J = 10.5, 2.1$ Hz, 1H), 7.30 (t, $J = 8.1$ Hz, 1H), 7.11 (q, $J = 9.2, 8.1$ Hz, 3H), 7.05

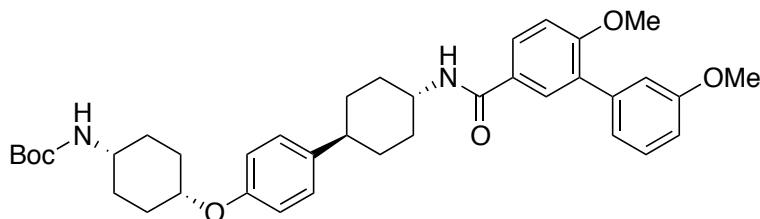
(t, $J = 2.4$ Hz, 1H), 6.89 – 6.84 (m, 1H), 6.80 (dd, $J = 8.1, 2.3$ Hz, 1H), 6.76 (dt, $J = 9.5, 2.6$ Hz, 2H), 4.53 (s, 1H), 4.42 (t, $J = 3.3$ Hz, 1H), 4.33– 4.24 (m, 1H), 3.96 (m, 1H), 3.85 (d, 6H), 3.11 (dt, $J = 10.2, 4.8$ Hz, 1H), 2.32 (tt, $J = 11.8, 3.6$ Hz, 1H), 2.12 (ddt, $J = 19.1, 12.5, 3.7$ Hz, 4H), 1.92 (ddd, $J = 27.5, 14.0, 3.1$ Hz, 2H), 1.86 – 1.73 (m, 6H), 1.58 (dtd, $J = 18.2, 10.5, 8.3, 4.3$ Hz, 4H), 1.45 (s, 9H). ^{13}C NMR (126 MHz, CDCl_3) δ 167.44, 159.67, 159.19, 155.00, 140.93, 139.33, 131.01, 130.06, 129.79, 128.40, 128.03, 122.12, 116.41, 116.08, 113.66, 113.07, 111.32, 70.52, 56.16, 55.00, 43.45, 34.19, 33.88, 30.34, 29.15, 28.55, 25.70. HRMS (ESI+), m/z $[\text{M}+\text{H}^+]$ calculated for $\text{C}_{38}\text{H}_{48}\text{N}_2\text{O}_6$ 629.3535; found 629.3032.



***N*-((1*R*,4*r*)-4-(4-(((1*r*,4*R*)-4-Aminocyclohexyl)oxy)phenyl)cyclohexyl)-3',6-dimethoxy-[1,1'-biphenyl]-3-carboxamide. (5.18a).**

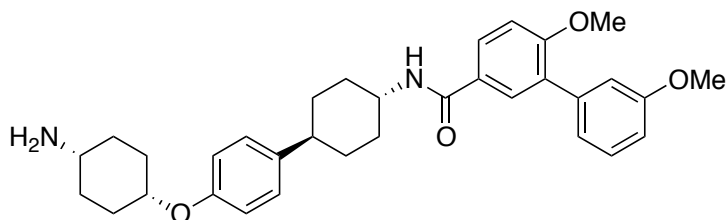
Compound **5.18a** was obtained following the procedure for the synthesis of **5.4a** as a white amorphous solid (70%): ^1H NMR (500 MHz, Chloroform- d) δ 7.75 (ddd, $J = 10.7, 8.5, 2.4$ Hz, 1H), 7.64 (dd, $J = 10.5, 2.3$ Hz, 1H), 7.30 (t, $J = 7.9$ Hz, 1H), 7.08 (q, $J = 9.1, 8.3$ Hz, 3H), 7.03 (t, $J = 2.2$ Hz, 1H), 6.99 – 6.94 (m, 1H), 6.87 (dd, $J = 8.3, 2.5$ Hz, 1H), 6.78 (dt, $J = 9.8, 2.6$ Hz, 2H), 4.46 (t, $J = 3.1$ Hz, 1H), 4.30 – 4.23 (m, 1H), 3.96 (ddd, $J = 11.9, 7.7, 4.3$ Hz, 1H), 3.81 (dt, $J = 7.1, 3.4$ Hz, 6H), 3.09 (dt, $J = 10.0, 5.0$ Hz, 1H), 2.42 (tt, $J = 12.0, 3.4$ Hz, 1H), 2.12 (ddt, $J = 19.2, 12.6, 3.3$ Hz, 4H), 1.93 (ddd, $J = 27.7, 14.2, 3.2$ Hz, 2H), 1.84 – 1.72 (m, 6H), 1.56 (dtd, $J = 18.1, 10.8, 8.1, 4.3$ Hz, 4H). ^{13}C NMR (126 MHz, CDCl_3) δ 167.49, 159.97, 159.69, 155.90, 140.03, 139.73, 131.11, 130.01, 129.79, 128.90, 128.45, 122.72, 116.71, 116.08, 113.56, 113.47,

111.62, 70.22, 56.46, 55.99, 43.40, 34.09, 33.86, 30.74, 29.65, 28.45, 25.78. HRMS (ESI+), m/z [M+H⁺] calculated for C₃₃H₄₀N₂O₄ 529.3076; found 529.3082.



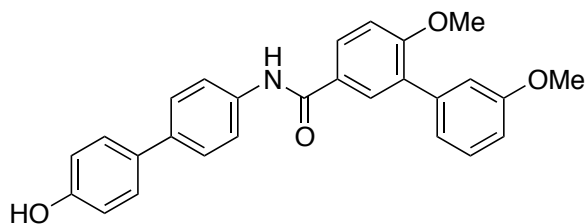
tert-Butyl ((1*S*,4*s*)-4-(4-((1*r*,4*R*)-4-(3',6-dimethoxy-[1,1'-biphenyl]-3-ylcarboxamido)cyclohexyl)phenoxy)cyclohexyl)carbamate (**5.64b**).

Compound **5.64b** was obtained following the procedure for the synthesis of **5.1** as a white amorphous solid (35%): ¹H NMR (500 MHz, Methylene Chloride-d₂) δ 7.80 (ddd, *J* = 8.4, 6.1, 2.3 Hz, 1H), 7.65 (t, *J* = 3.0 Hz, 1H), 7.30 (t, *J* = 8.1 Hz, 1H), 7.10 – 7.00 (m, 2H), 6.95 (td, *J* = 9.2, 6.4 Hz, 2H), 6.87 (dd, *J* = 8.3, 2.2 Hz, 1H), 6.80 – 6.72 (m, 2H), 4.48 (s, 1H) 4.22 (t, *J* = 3.9 Hz, 1H), 4.07 (dd, *J* = 9.5, 4.6 Hz, 1H), 3.91 (ddt, *J* = 10.8, 7.4, 4.1 Hz, 1H), 3.85 (s, 3H), 3.81 (s, 3H), 3.10 – 3.01 (m, 1H), 2.55 – 2.40 (m, 1H), 2.22 – 2.09 (m, 4H), 2.03 – 1.96 (m, 1H), 1.90 – 1.86 (m, 1H), 1.80 – 1.73 (m, 1H), 1.71 – 1.35 (m, 8H), 1.31 (s, 9H). ¹³C NMR (126 MHz, CD₂Cl₂) δ 159.83, 159.00, 155.18, 139.89, 139.46, 130.57, 129.50, 129.06, 127.45, 122.10, 116.28, 115.59, 112.08, 111.01, 74.45, 55.65, 55.22, 42.07, 33.45, 29.67, 29.37, 29.02, 28.29. HRMS (ESI+), m/z [M+H⁺] calculated for C₃₈H₄₈N₂O₆ 629.3535; found 629.3010.



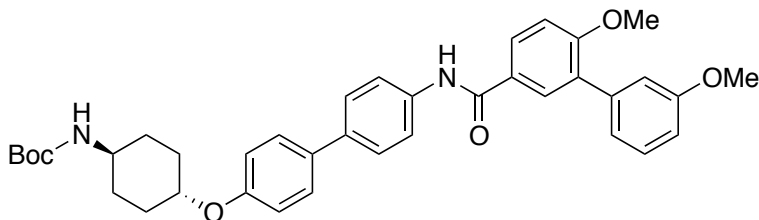
***N*-((1*R*,4*r*)-4-(4-(((1*s*,4*S*)-4-Aminocyclohexyl)oxy)phenyl)cyclohexyl)-3',6-dimethoxy-[1,1'-biphenyl]-3-carboxamide (5.18b).**

Compound **5.18b** was obtained following the procedure for the synthesis of **5.4a** as a white amorphous solid (70%): ¹H NMR (500 MHz, Methylene Chloride-d₂) δ 7.78 (ddd, *J* = 8.7, 6.2, 2.5 Hz, 1H), 7.69 (t, *J* = 2.9 Hz, 1H), 7.32 (t, *J* = 7.9 Hz, 1H), 7.15 – 7.10 (m, 2H), 7.05 (td, *J* = 9.0, 6.2 Hz, 2H), 6.89 (dd, *J* = 8.3, 2.6 Hz, 1H), 6.84 – 6.78 (m, 2H), 4.26 (t, *J* = 3.8 Hz, 1H), 4.17 (dd, *J* = 9.7, 4.6 Hz, 1H), 3.94 (ddt, *J* = 11.4, 7.5, 4.3 Hz, 1H), 3.85 (d, *J* = 2.6 Hz, 3H), 3.82 (d, *J* = 2.3 Hz, 3H), 3.13 – 3.07 (m, 1H), 2.52 – 2.42 (m, 1H), 2.23 – 2.05 (m, 5H), 2.01 – 1.96 (m, 1H), 1.94 – 1.88 (m, 1H), 1.83 – 1.73 (m, 1H), 1.71 – 1.35 (m, 8H). ¹³C NMR (126 MHz, CD₂Cl₂) δ 159.53, 159.50, 155.78, 139.81, 139.36, 130.51, 129.56, 129.16, 127.85, 122.11, 116.21, 115.51, 112.88, 111.05, 74.40, 55.85, 55.40, 42.87, 33.41, 29.65, 29.60, 29.12, 28.49. HRMS (ESI+), *m/z* [M+H⁺] calculated for C₃₃H₄₀N₂O₄ 529.3076; found 529.3056.



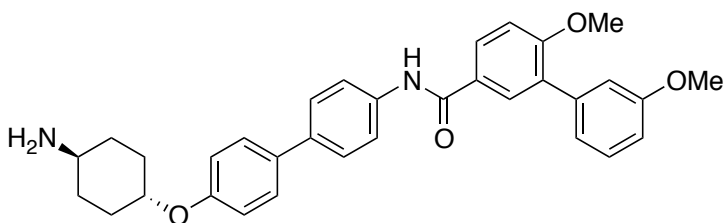
***N*-(4'-Hydroxy-[1,1'-biphenyl]-4-yl)-3',6-dimethoxy-[1,1'-biphenyl]-3-carboxamide (5.71)**

Compound **5.71** was synthesized following a reported procedure.³⁰



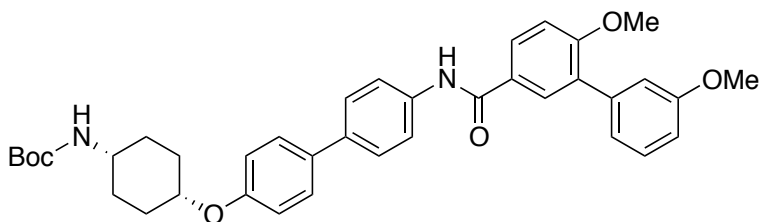
tert-Butyl ((1*r*,4*r*)-4-((4'-(3',6-dimethoxy-[1,1'-biphenyl]-3-ylcarboxamido)-[1,1'-biphenyl]-4-yl)oxy)cyclohexyl)carbamate (**5.72a**).

Compound **5.72a** was obtained following the procedure for the synthesis of **5.1** as a white amorphous solid (35%): ^1H NMR (500 MHz, Chloroform-*d*) δ 8.01 (s, 1H), 7.97 (dt, $J = 8.5, 2.4$ Hz, 1H), 7.89 – 7.83 (m, 1H), 7.58 (dd, $J = 8.7, 1.8$ Hz, 2H), 7.49 – 7.41 (m, 3H), 7.39 (d, $J = 8.9$ Hz, 1H), 7.32 (t, $J = 7.7$ Hz, 1H), 7.22 (dd, $J = 8.6, 1.8$ Hz, 1H), 7.10 (t, $J = 1.4$ Hz, 1H), 6.97 (s, 1H), 6.95 (d, $J = 8.9$ Hz, 1H), 6.88 (dd, $J = 8.4, 2.3$ Hz, 1H), 6.78 (d, $J = 8.4$ Hz, 1H), 4.60 – 4.55 (m, 1H), 4.32 (dt, $J = 9.5, 5.4$ Hz, 1H), 3.85 (s, 3H), 3.82 (s, 3H), 2.89 (dd, $J = 9.7, 3.3$ Hz, 1H), 2.16 – 2.09 (m, 2H), 2.04 – 1.97 (m, 2H), 1.78 – 1.69 (m, 4H), 1.47 (s, 9H). ^{13}C NMR (126 MHz, DMSO) δ 164.72, 158.99, 158.74, 138.88, 138.19, 138.17, 129.90, 129.25, 129.12, 127.39, 127.33, 126.16, 125.93, 121.80, 120.72, 116.11, 115.71, 115.22, 112.59, 111.43, 55.89, 55.13, 48.77, 30.37, 29.53. HRMS (ESI+), m/z $[\text{M}+\text{H}^+]$ calculated for $\text{C}_{38}\text{H}_{42}\text{N}_2\text{O}_6$ 623.3054; found 623.3067.



N-(4'-(((1*r*,4*r*)-4-Aminocyclohexyl)oxy)-[1,1'-biphenyl]-4-yl)-3',6-dimethoxy-[1,1'-biphenyl]-3-carboxamide (**5.19a**).

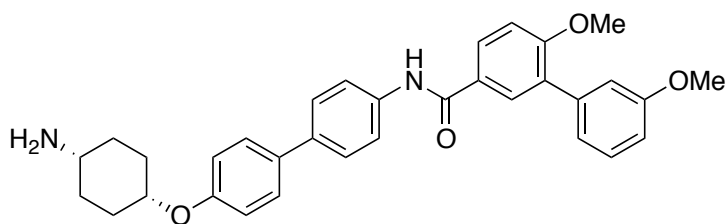
Compound **5.19a** was obtained following the procedure for the synthesis of **5.4a** as a white amorphous solid (70%): ^1H NMR (500 MHz, DMSO- d_6) δ 10.25 (s, 1H), 8.04 (dt, $J = 8.7, 2.2$ Hz, 1H), 8.01 – 7.98 (m, 1H), 7.86 (dd, $J = 9.0, 2.1$ Hz, 2H), 7.63 – 7.54 (m, 3H), 7.49 (d, $J = 8.6$ Hz, 1H), 7.37 (t, $J = 7.9$ Hz, 1H), 7.26 (dd, $J = 8.9, 1.5$ Hz, 1H), 7.14 (t, $J = 1.2$ Hz, 1H), 7.12 (s, 1H), 7.01 (d, $J = 8.7$ Hz, 1H), 6.95 (dd, $J = 8.2, 2.6$ Hz, 1H), 6.85 (d, $J = 8.6$ Hz, 1H), 4.30 (dt, $J = 9.7, 5.2$ Hz, 1H), 3.86 (s, 3H), 3.80 (s, 3H), 2.87 (dd, $J = 9.5, 3.7$ Hz, 1H), 2.13 – 2.06 (m, 1H), 2.06 – 1.99 (m, 1H), 1.93 (dd, $J = 9.5, 4.6$ Hz, 1H), 1.60 – 1.27 (m, 4H). ^{13}C NMR (126 MHz, DMSO) δ 164.72, 158.99, 158.74, 138.88, 138.19, 138.17, 129.90, 129.25, 129.12, 127.39, 127.33, 126.16, 125.93, 121.80, 120.72, 116.11, 115.71, 115.22, 112.59, 111.43, 55.89, 55.13, 48.77, 30.37, 29.53. HRMS (ESI+), m/z $[\text{M}+\text{Na}^+]$ calculated for $\text{C}_{33}\text{H}_{34}\text{N}_2\text{O}_4\text{Na}$ 545.2416; found 545.2399.



tert-Butyl ((1s,4s)-4-((4'-(3',6-dimethoxy-[1,1'-biphenyl]-3-yl)carboxamido)-[1,1'-biphenyl]-4-yl)oxy)cyclohexyl)carbamate (5.72b**).**

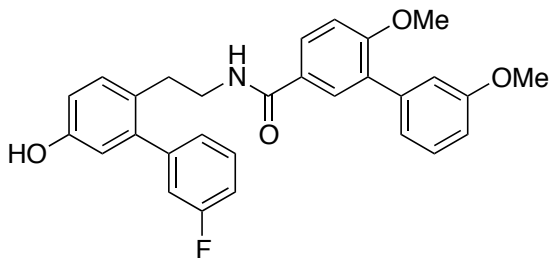
Compound **5.72b** was obtained following the procedure for the synthesis of **5.1** as a white amorphous solid (35%): ^1H NMR (500 MHz, Chloroform- d) δ 7.92 (dd, $J = 8.6, 2.4$ Hz, 1H), 7.89 (s, 1H), 7.83 (d, $J = 2.4$ Hz, 1H), 7.69 (d, $J = 8.6$ Hz, 2H), 7.54 (d, $J = 8.6$ Hz, 2H), 7.52 – 7.49 (m, 2H), 7.36 (t, $J = 7.9$ Hz, 1H), 7.12 (dt, $J = 7.6, 1.2$ Hz, 1H), 7.09 (dd, $J = 2.6, 1.6$ Hz, 1H), 7.05 (d, $J = 8.6$ Hz, 1H), 6.95 (d, $J = 8.8$ Hz, 1H), 6.92 (ddd, $J = 8.3, 2.6, 0.9$ Hz, 1H), 4.58 – 4.53 (m, 1H), 4.49 (dt, $J = 4.7, 2.3$ Hz, 1H), 3.88 (s, 3H), 3.85 (s, 3H), 3.57 (s, 1H), 2.06 – 1.98

(m, 2H), 1.81 – 1.73 (m, 2H), 1.71 – 1.58 (m, 4H), 1.45 (s, 9H). ¹³C NMR (126 MHz, CDCl₃) δ 165.49, 159.70, 157.18, 155.62, 139.20, 137.22, 133.46, 131.06, 129.93, 129.55, 128.79, 128.28, 127.56, 122.36, 120.83, 116.66, 115.68, 113.34, 111.43, 71.52, 56.24, 55.72, 53.22, 48.64, 28.83, 28.19. HRMS (ESI+), m/z [M+H⁺] calculated for C₃₈H₄₂N₂O₆ 623.3054; found 623.3027.



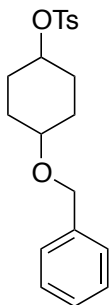
***N*-(4'-(((1*s*,4*s*)-4-Aminocyclohexyl)oxy)-[1,1'-biphenyl]-4-yl)-3',6-dimethoxy-[1,1'-biphenyl]-3-carboxamide (**5.19b**).**

Compound **5.19b** was obtained following the procedure for the synthesis of **5.4a** as a white amorphous solid (70%): ¹H NMR (500 MHz, DMSO-*d*₆) δ 10.24 (s, 1H), 8.03 (dd, *J* = 8.6, 2.4 Hz, 1H), 7.98 (d, *J* = 2.4 Hz, 1H), 7.86 – 7.83 (m, 2H), 7.62 – 7.57 (m, 4H), 7.36 (t, *J* = 7.9 Hz, 1H), 7.25 (d, *J* = 8.8 Hz, 1H), 7.12 (dt, *J* = 7.6, 1.2 Hz, 1H), 7.10 (dd, *J* = 2.6, 1.5 Hz, 1H), 7.04 – 7.01 (m, 2H), 6.95 (ddd, *J* = 8.3, 2.6, 1.0 Hz, 1H), 4.62 (dd, *J* = 4.3, 2.3 Hz, 1H), 3.86 (s, 3H), 3.80 (s, 3H), 3.10 (td, *J* = 8.9, 8.2, 4.0 Hz, 1H), 2.01 – 1.93 (m, 2H), 1.79 – 1.59 (m, 6H). ¹³C NMR (126 MHz, DMSO) δ 164.43, 158.68, 158.44, 155.92, 138.56, 137.91, 134.51, 132.02, 129.58, 128.95, 127.16, 126.62, 125.88, 121.49, 120.42, 116.18, 114.90, 112.30, 111.15, 69.50, 55.60, 54.83, 47.98, 26.70, 24.84. HRMS (ESI+), m/z [M+H⁺] calculated for C₃₃H₃₄N₂O₄ 523.2597; found 523.2600.



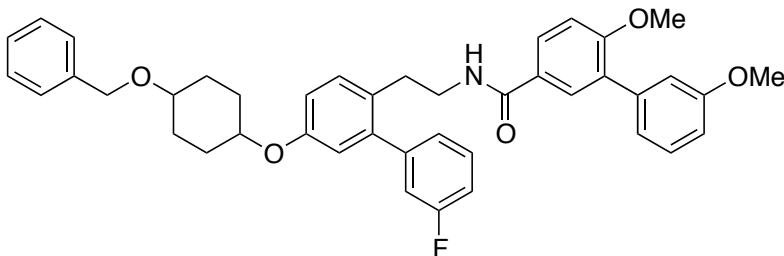
***N*-(2-(3'-Fluoro-5-hydroxy-[1,1'-biphenyl]-2-yl)ethyl)-3',6-dimethoxy-[1,1'-biphenyl]-3-carboxamide (5.80).**

Compound **5.80** was synthesized following the procedure reported in Chapter 3.



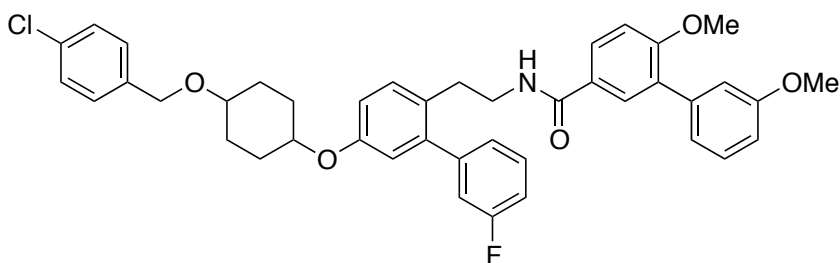
4-(Benzyloxy)cyclohexyl 4-methylbenzenesulfonate (5.84a).

Compound **5.84a** and related derivatives (**5.84a-d**) were synthesized following the procedure reported in Chapter 2.



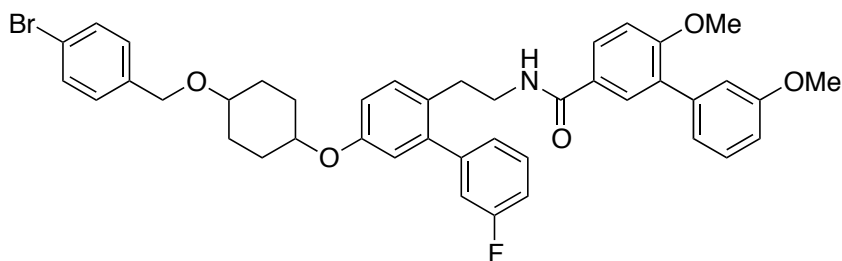
***N*-(2-(5-((4-(Benzyloxy)cyclohexyl)oxy)-3'-fluoro-[1,1'-biphenyl]-2-yl)ethyl)-3',6-dimethoxy-[1,1'-biphenyl]-3-carboxamide (5.20).**

Potassium carbonate (30 mg, 0.19 mmol) was added to a solution of **5.80** (45 mg, 0.16 mmol) in anhydrous DMF (1 mL) and stirred at rt for 30 min, before 4-(benzyloxy)cyclohexyl 4-methylbenzenesulfonate (75 mg, 0.19 mmol) and TBAI (7 mg, 0.016 mmol) were added. The solution was heated to 90 °C for 16h. Distilled water (3x 5 mL) was added to the mixture and the organic layer extracted with EtOAc. After removal of the solvent on a rotorevaporator, the crude mixture was purified by column chromatography (SiO₂, 1:10, MeOH: DCM) to give **5.20** as a white solid in 75% yield: ¹H NMR (500 MHz, Chloroform-d) δ 7.68 (dt, *J* = 8.6, 2.4 Hz, 1H), 7.57 (dd, *J* = 3.6, 2.4 Hz, 1H), 7.38 – 7.19 (m, 12H), 7.09 – 6.95 (m, 5H), 6.89 (dddd, *J* = 11.3, 8.5, 4.7, 2.0 Hz, 2H), 6.75 (dd, *J* = 8.6, 2.7 Hz, 1H), 5.90 (dt, *J* = 6.0, 2.7 Hz, 1H), 4.55 (s, 2H), 4.35 (dt, *J* = 6.6, 3.4 Hz, 1H), 4.29 (dt, *J* = 8.4, 4.2 Hz, 1H), 3.84 (d, *J* = 4.2 Hz, 6H), 3.53 – 3.42 (m, 3H), 2.84 (t, *J* = 7.1 Hz, 2H), 2.13 – 1.96 (m, 2H), 1.94 – 1.86 (m, 1H), 1.74 – 1.66 (m, 2H), 1.62 – 1.48 (m, 6H). ¹³C NMR (126 MHz, CDCl₃) δ 167.16, 163.87, 161.90, 159.66, 159.29, 156.51, 156.33, 139.35, 131.37, 130.75, 129.76, 129.46, 128.74, 128.36, 127.86, 127.79, 125.27, 122.35, 117.97, 116.45, 115.65, 115.64, 113.25, 111.17, 70.55, 70.13, 41.34, 34.71, 32.34, 30.35, 27.74, 23.11, 21.27, 14.54. HRMS (ESI+), *m/z* [M+H⁺] calculated for C₄₂H₄₃FNO₅ 660.3125; found 660.3128.



***N*-(2-(5-((4-(4-Chlorobenzyl)oxy)cyclohexyl)oxy)-3'-fluoro-[1,1'-biphenyl]-2-yl)ethyl)-3',6-dimethoxy-[1,1'-biphenyl]-3-carboxamide (**5.21**).**

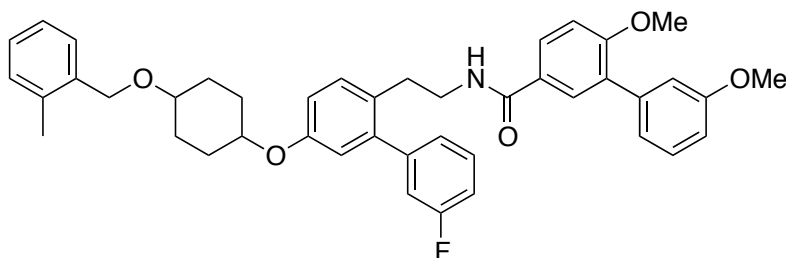
Compound **5.21** was obtained following the procedure for the synthesis of **5.20** as a white amorphous solid (70%): ^1H NMR (500 MHz, Chloroform- d) δ 7.68 (dd, $J = 8.6, 2.4$ Hz, 1H), 7.52 (d, $J = 2.4$ Hz, 1H), 7.48 – 7.43 (m, 3H), 7.37 – 7.31 (m, 1H), 7.30 – 7.27 (m, 1H), 7.22 (dd, $J = 8.9, 8.1$ Hz, 3H), 7.17 (d, $J = 8.3$ Hz, 1H), 7.10 – 7.07 (m, 1H), 7.02 (ddt, $J = 4.2, 2.5, 1.3$ Hz, 2H), 6.96 (d, $J = 8.5$ Hz, 2H), 6.91 (ddd, $J = 8.3, 2.6, 1.0$ Hz, 1H), 6.82 (dd, $J = 8.3, 2.7$ Hz, 1H), 6.71 (d, $J = 2.7$ Hz, 1H), 5.94 (t, $J = 5.8$ Hz, 1H), 4.47 (d, $J = 7.9$ Hz, 3H), 3.85 (d, $J = 3.4$ Hz, 6H), 3.78 – 3.65 (m, 2H), 3.50 – 3.40 (m, 3H), 2.83 (t, $J = 7.1$ Hz, 2H), 2.06 – 2.01 (m, 1H), 2.01 – 1.95 (m, 1H), 1.93 – 1.83 (m, 2H), 1.76 – 1.65 (m, 6H), 1.63 – 1.51 (m, 2H). ^{13}C NMR (126 MHz, CDCl_3) δ 167.19, 163.58, 159.32, 159.11, 154.70, 142.23, 139.05, 138.23, 131.58, 131.54, 131.26, 130.41, 129.94, 129.42, 129.24, 129.17, 129.08, 128.27, 127.76, 126.79, 124.94, 122.24, 121.27, 117.27, 116.27, 116.10, 115.58, 115.35, 114.29, 114.12, 112.82, 111.00, 69.56, 69.06, 41.05, 32.72, 31.98, 30.61, 29.39, 27.62. HRMS (ESI+), m/z $[\text{M}+\text{H}^+]$ calculated for $\text{C}_{42}\text{H}_{43}\text{ClFNO}_5$ 694.2736; found 694.2756.



***N*-(2-(5-((4-((4-Bromobenzyl)oxy)cyclohexyl)oxy)-3'-fluoro-[1,1'-biphenyl]-2-yl)ethyl)-3',6-dimethoxy-[1,1'-biphenyl]-3-carboxamide (5.22).**

Compound **5.22** was obtained following the procedure for the synthesis of **5.20** as a white amorphous solid (70%): ^1H NMR (500 MHz, Chloroform- d) δ 7.68 (dt, $J = 8.6, 2.2$ Hz, 1H), 7.57 (t, $J = 2.7$ Hz, 1H), 7.36 – 7.22 (m, 8H), 7.08 – 6.94 (m, 7H), 6.90 (dddd, $J = 9.2, 8.3, 2.5,$

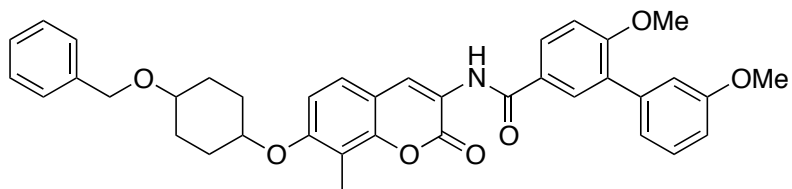
1.4 Hz, 2H), 6.75 (dd, $J = 8.3, 2.7$ Hz, 1H), 5.95 – 5.88 (m, 1H), 4.51 (s, 2H), 4.35 (dt, $J = 6.6, 3.4$ Hz, 1H), 4.31 – 4.24 (m, 1H), 3.84 (d, $J = 4.3$ Hz, 6H), 3.54 – 3.42 (m, 3H), 2.84 (t, $J = 7.1$ Hz, 2H), 2.15 – 1.95 (m, 3H), 1.93 – 1.83 (m, 1H), 1.75 – 1.65 (m, 2H), 1.63 – 1.49 (m, 2H). ^{13}C NMR (126 MHz, CDCl_3) δ 166.93, 161.64, 159.39, 159.03, 156.02, 142.19, 139.09, 137.66, 131.11, 130.49, 129.96, 129.49, 129.20, 128.88, 128.12, 126.98, 125.02, 122.09, 117.71, 116.18, 115.78, 115.39, 114.31, 112.98, 110.91, 69.54, 69.13, 41.10, 32.08, 30.09, 29.85, 28.45, 27.59, 27.45. HRMS (ESI+), m/z $[\text{M}+\text{H}^+]$ calculated for $\text{C}_{42}\text{H}_{43}\text{BrFNO}_5$ 738.2256; found 738.2245.



***N*-(2-(3'-Fluoro-5-((4-((2-methylbenzyl)oxy)cyclohexyl)oxy)-[1,1'-biphenyl]-2-yl)ethyl)-3',6-dimethoxy-[1,1'-biphenyl]-3-carboxamide (5.23).**

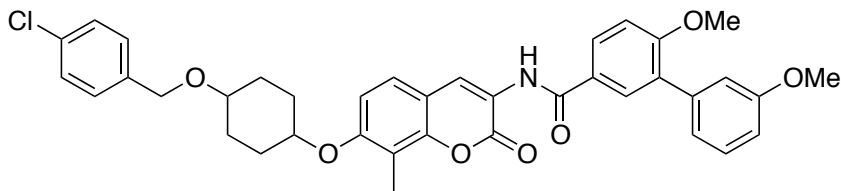
Compound **5.23** was obtained following the procedure for the synthesis of **5.20** as a white amorphous solid (70%): ^1H NMR (500 MHz, Chloroform- d) δ 7.68 (dt, $J = 8.6, 2.7$ Hz, 1H), 7.58 (t, $J = 2.6$ Hz, 1H), 7.39 – 7.29 (m, 2H), 7.24 (dd, $J = 8.5, 2.4$ Hz, 1H), 7.21 – 7.15 (m, 2H), 7.09 – 7.03 (m, 3H), 7.03 – 6.99 (m, 1H), 6.97 (d, $J = 8.7$ Hz, 1H), 6.89 (dddd, $J = 8.5, 7.8, 3.9, 2.3$ Hz, 2H), 6.76 (dd, $J = 6.6, 2.7$ Hz, 1H), 5.94 – 5.90 (m, 1H), 4.53 (s, 2H), 4.35 (dt, $J = 6.5, 3.3$ Hz, 1H), 4.29 (ddd, $J = 8.6, 4.8, 3.3$ Hz, 1H), 3.88 – 3.81 (m, 6H), 3.56 – 3.41 (m, 3H), 2.85 (t, $J = 7.1$ Hz, 2H), 2.34 (d, $J = 1.8$ Hz, 3H), 2.16 – 1.98 (m, 2H), 1.94 – 1.88 (m, 1H), 1.70 (tdd, $J = 12.9, 6.6, 3.5$ Hz, 2H), 1.62 – 1.50 (m, 3H). ^{13}C NMR (126 MHz, CDCl_3) δ 167.16, 163.85, 161.89, 159.64, 159.28, 156.50, 156.32, 142.42, 139.34, 137.16, 136.88, 131.35, 130.74, 130.60,

130.54, 130.20, 129.76, 129.45, 128.76, 128.73, 128.48, 128.36, 128.09, 127.99, 127.25, 126.22, 126.19, 125.26, 122.34, 117.98, 116.61, 116.44, 116.05, 115.63, 114.54, 114.38, 113.23, 111.16, 69.16, 68.77, 41.34, 32.33, 30.35, 30.10, 27.77, 19.27, 19.24. HRMS (ESI+), m/z $[M+H^+]$ calculated for $C_{43}H_{44}FNO_5$ 673.3205; found 673.3217.



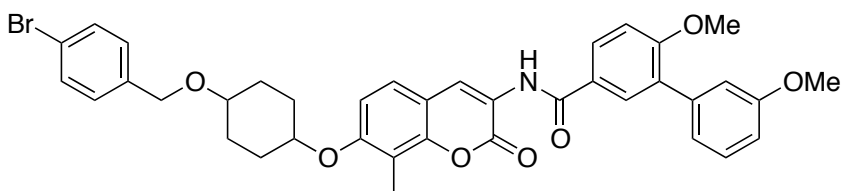
***N*-(7-((4-(Benzyloxy)cyclohexyl)oxy)-8-methyl-2-oxo-2*H*-chromen-3-yl)-3',6-dimethoxy-[1,1'-biphenyl]-3-carboxamide (5.24).**

Compound **5.24** was obtained following the procedure for the synthesis of **5.20** as a white amorphous solid (70%): 1H NMR (500 MHz, Chloroform- d) δ 8.80 (s, 1H), 8.70 (s, 1H), 7.95 – 7.87 (m, 2H), 7.39 – 7.31 (m, 7H), 7.13 (ddd, $J = 7.6, 1.6, 1.0$ Hz, 1H), 7.11 – 7.04 (m, 2H), 6.93 (ddd, $J = 8.3, 2.6, 1.0$ Hz, 1H), 6.89 (d, $J = 8.7$ Hz, 1H), 4.57 (s, 2H), 4.45 (dt, $J = 7.6, 4.0$ Hz, 1H), 3.90 (s, 3H), 3.86 (s, 3H), 3.57 (dt, $J = 7.8, 4.0$ Hz, 1H), 2.32 (s, 3H), 2.17 – 2.11 (m, 2H), 2.10 – 2.03 (m, 2H), 1.70 – 1.59 (m, 3H). ^{13}C NMR (126 MHz, $CDCl_3$) δ 165.64, 159.87, 159.73, 159.45, 157.45, 149.57, 139.01, 138.74, 131.13, 130.08, 129.32, 128.54, 128.30, 127.62, 126.25, 125.69, 124.60, 122.14, 121.63, 115.35, 113.29, 111.12, 110.75, 75.18, 74.98, 70.31, 56.03, 55.47, 28.03, 8.46. HRMS (ESI+), m/z $[M+H^+]$ calculated for $C_{38}H_{38}NO_7$ 620.2648; found 620.2637.



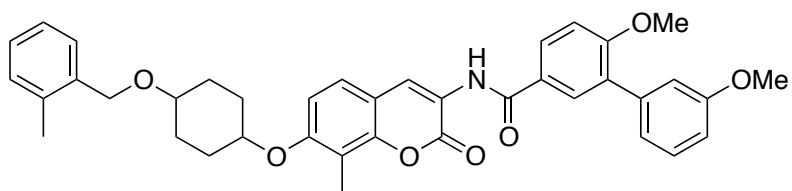
***N*-(7-((4-((4-Chlorobenzyl)oxy)cyclohexyl)oxy)-8-methyl-2-oxo-2*H*-chromen-3-yl)-3',6-dimethoxy-[1,1'-biphenyl]-3-carboxamide (5.25).**

Compound **5.25** was obtained following the procedure for the synthesis of **5.20** as a white amorphous solid (70%): ^1H NMR (500 MHz, Chloroform- d) δ 8.80 (s, 1H), 8.70 (s, 1H), 7.97 – 7.85 (m, 2H), 7.52 – 7.44 (m, 2H), 7.42 – 7.30 (m, 2H), 7.24 (d, J = 8.3 Hz, 2H), 7.14 – 7.12 (m, 1H), 7.09 (dd, J = 2.6, 1.6 Hz, 1H), 7.07 (d, J = 8.6 Hz, 1H), 6.96 (d, J = 0.7 Hz, 1H), 6.93 (ddd, J = 8.3, 2.6, 1.0 Hz, 1H), 6.89 (d, J = 8.7 Hz, 1H), 4.51 (s, 2H), 4.49 – 4.43 (m, 2H), 3.90 (s, 3H), 3.86 (s, 3H), 3.55 (dt, J = 7.8, 4.3 Hz, 1H), 2.32 (s, 3H), 2.17 – 2.10 (m, 2H), 2.09 – 2.00 (m, 3H), 1.72 – 1.59 (m, 3H). ^{13}C NMR (126 MHz, CDCl_3) δ 165.65, 159.88, 159.72, 159.45, 157.40, 149.57, 138.74, 138.06, 131.63, 131.14, 130.08, 129.32, 129.23, 128.98, 128.30, 126.24, 125.70, 124.59, 122.14, 121.44, 115.35, 113.29, 111.12, 110.73, 75.18, 75.04, 69.59, 34.46, 32.08, 30.10, 29.85, 27.93, 22.85, 21.01, 14.29, 8.46. HRMS (ESI+), m/z $[\text{M}+\text{H}^+]$ calculated for $\text{C}_{38}\text{H}_{37}\text{ClNO}_7$ 654.2259; found 654.2249.



***N*-(7-((4-((4-Bromobenzyl)oxy)cyclohexyl)oxy)-8-methyl-2-oxo-2*H*-chromen-3-yl)-3',6-dimethoxy-[1,1'-biphenyl]-3-carboxamide (5.26).**

Compound **5.26** was obtained following the procedure for the synthesis of **5.20** as a white amorphous solid (70%): ^1H NMR (500 MHz, Chloroform- d) δ 8.80 (s, 1H), 8.70 (s, 1H), 7.97 – 7.83 (m, 2H), 7.41 – 7.22 (m, 12H), 7.19 – 7.03 (m, 4H), 6.97 – 6.83 (m, 2H), 4.52 (s, 2H), 4.45 (dt, $J = 7.7, 4.0$ Hz, 1H), 3.90 (s, 3H), 3.86 (s, 3H), 3.55 (dt, $J = 7.8, 4.2$ Hz, 1H), 2.32 (s, 3H), 2.17 – 2.09 (m, 2H), 2.09 – 2.00 (m, 2H), 1.72 – 1.58 (m, 2H). ^{13}C NMR (126 MHz, CDCl_3) δ 165.89, 161.07, 160.13, 159.96, 159.70, 157.65, 149.82, 138.99, 137.78, 133.58, 131.39, 130.33, 129.57, 129.20, 129.15, 128.93, 128.55, 126.49, 125.95, 124.83, 122.40, 121.90, 115.61, 113.63, 113.54, 111.37, 110.98, 75.42, 75.30, 69.82, 30.35, 30.11, 28.22, 8.71. HRMS (ESI+), m/z $[\text{M}+\text{H}^+]$ calculated for $\text{C}_{38}\text{H}_{37}\text{BrNO}_7$ 698.1753; found 698.1758.



3',6-Dimethoxy-*N*-(8-methyl-7-((4-((2-methylbenzyl)oxy)cyclohexyl)oxy)chromen-3-yl)-[1,1'-biphenyl]-3-carboxamide (5.27).

Compound **5.27** was obtained following the procedure for the synthesis of **5.20** as a white amorphous solid (70%): ^1H NMR (500 MHz, Chloroform- d) δ 8.80 (s, 1H), 8.70 (s, 1H), 7.96 – 7.85 (m, 2H), 7.39 – 7.35 (m, 2H), 7.32 (d, $J = 8.6$ Hz, 1H), 7.22 – 7.15 (m, 4H), 7.13 (dt, $J = 7.6, 1.2$ Hz, 1H), 7.09 (dd, $J = 2.6, 1.5$ Hz, 1H), 7.07 (d, $J = 8.6$ Hz, 1H), 6.96 – 6.95 (m, 1H), 6.93 (ddd, $J = 8.3, 2.6, 0.9$ Hz, 1H), 6.88 (d, $J = 8.7$ Hz, 1H), 4.55 (s, 2H), 4.53 – 4.48 (m, 2H), 3.90 (s, 3H), 3.86 (s, 3H), 3.56 – 3.48 (m, 1H), 2.35 (d, $J = 5.5$ Hz, 6H), 2.11 – 2.00 (m, 2H), 1.95 – 1.87 (m, 2H), 1.8 ^{13}C NMR (126 MHz, CDCl_3) δ 165.90, 161.11, 160.12, 159.97, 159.70, 157.51, 149.87, 139.00, 137.03, 131.39, 130.62, 130.35, 129.57, 128.83, 128.53, 128.10, 128.05,

126.51, 126.22, 125.86, 124.84, 122.40, 121.86, 115.60, 113.55, 111.36, 110.77, 75.23, 73.80, 68.87, 34.71, 32.33, 30.35, 30.11, 28.15, 27.80, 23.10, 21.26, 19.28, 14.54, 8.77. HRMS (ESI+), m/z [M+H⁺] calculated for C₃₉H₄₀NO₇ 634.2805; found 634.2827.

References

1. Karagoz, G. E.; Rudiger, S. G. D., Hsp90 interaction with clients. *Trends in Biochemical Sciences* **2015**, *40* (2), 117-25.
2. Verma, S.; Goyal, S.; Jamal, S.; Singh, A.; Grover, A., Hsp90: Friends, clients and natural foes. *Biochimie* **2016**, *127*, 227-40.
3. Isaacs, J.; Whitesell, L., Hsp90 in Cancer: Beyond the Usual Suspects. *Advances in Cancer Research* **2016**, *129*.
4. Pratt, W. B.; Gestwicki, J. E.; Osawa, Y.; Lieberman, A. P., Targeting Hsp90/Hsp70-based protein quality control for treatment of adult onset neurodegenerative diseases. *Annual Review Pharmacology Toxicology* **2015**, *55*, 353-71.
5. Morimoto, R. I., Cells in Stress: Transcriptional Activation of Heat Shock Genes. *Science* **1993**, *259* (5100), 1409-1410.
6. Frydman, J.; Nimmegern, E.; Ohtsuka, K.; Hartl, F. U., Folding of nascent polypeptide chains in a high molecular mass assembly with molecular chaperones. *Nature* **1994**, *370*, 111-117.
7. Hanahan, D.; Weinberg, R. A., The Hallmarks of Cancer. *Cell* **2000**, *100*, 57-70.
8. Hanahan, D.; Weinberg, R. A., Hallmarks of cancer: the next generation. *Cell* **2011**, *144* (5), 646-74.

9. Miyata, Y.; Nakamoto, H.; Neckers, L., The Therapeutic Target Hsp90 and Cancer Hallmarks. *Current Pharmaceutical Design* **2013**, *19* (3), 347-365.
10. Trepel, J.; Mollapour, M.; Giaccone, G.; Neckers, L., Targeting the Dynamic HSP90 Complex in Cancer. *Nature Reviews Cancer* **2010**, *10* (8), 537-549.
11. Kamal, A.; Thao, L.; Sensintaffar, J.; Zhang, L.; Boehm, M. F.; Fritz, L. C.; Burrows, F. J., A high-affinity conformation of Hsp90 confers tumour selectivity on Hsp90 inhibitors. *Letters to Nature* **2003**, *425*, 407-410.
12. Neckers, L.; Workman, P., Hsp90 Molecular Chaperone Inhibitors: Are We There Yet? *Clinical Cancer Research : an official journal of the American Association for Cancer Research* **2012**, *18* (1), 64-76.
13. Whitesell, L.; Santagata, S.; Lin, N. U., Inhibiting HSP90 to Treat Cancer: A Strategy in Evolution. *Current Molecular Medicine* **2012**, *12* (9), 1108-1124.
14. Muth, A.; Crowley, V.; Khandelwal, A.; Mishra, S.; Zhao, J.; Hall, J.; Blagg, B. S., Development of radamide analogs as Grp94 inhibitors. *Bioorganic & Medicinal Chemistry* **2014**, *22* (15), 4083-98.
15. Peterson, L. B.; Eskew, J. D.; Vielhauer, G. A.; Blagg, B. S. J., The hERG Channel is Dependent Upon the Hsp90alpha Isoform for Maturation and Trafficking. *Molecular Pharmaceutics* **2012**, *9* (6), 1841-6.
16. Marcu, M. G.; Chadli, A.; Bouhouche, I.; Catelli, M.; Neckers, L. M., The Heat Shock Protein 90 Antagonist Novobiocin Interacts with a Previously Unrecognized ATP-binding Domain in the Carboxyl Terminus of the Chaperone. *The Journal of Biological Chemistry* **2000**, *275* (47), 37181-6.

17. Marcu, M. G.; Schulte, T. W.; Neckers, L., Novobiocin and Related Coumarins and Depletion of Heat Shock Protein 90-Dependent Signaling Proteins. *Journal of the National Cancer Institute* **2000**, *92* (3), 242-248.
18. Ansar, S.; Burlison, J. A.; Hadden, M. K.; Yu, X. M.; Desino, K. E.; Bean, J.; Neckers, L.; Audus, K. L.; Michaelis, M. L.; Blagg, B. S. J., A non-toxic Hsp90 inhibitor protects neurons from Abeta-induced toxicity. *Bioorganic & Medicinal Chemistry Letters* **2007**, *17* (7), 1984-90.
19. Yu, X. M.; Shen, G.; Neckers, L.; Blake, H.; Holzbeierlein, J.; Cronk, B.; Blagg, B. S. J., Hsp90 Inhibitors Identified From a Library of Novobiocin Analogues. *Journal of the American Chemical Society* **2005**, *127*, 12778-12779.
20. Kusuma, B. R.; Zhang, L.; Sundstrom, T.; Peterson, L. B.; Dobrowsky, R. T.; Blagg, B. S. J., Synthesis and evaluation of novologues as C-terminal Hsp90 inhibitors with cytoprotective activity against sensory neuron glucotoxicity. *Journal of Medicinal Chemistry* **2012**, *55* (12), 5797-812.
21. Yu, X. M.; Shen, G.; Blagg, B. S. J., Synthesis of (-)-Noviose from 2,3-O-Isopropylidene-D-erythronolactol. *Journal of Organic Chemistry* **2004**, *69*, 7375-7378.
22. Anyika, M.; McMullen, M.; Forsberg, L. K.; Dobrowsky, R. T.; Blagg, B. S. J., Development of Noviomimetics as C-Terminal Hsp90 Inhibitors. *ACS Medicinal Chemistry Letters* **2016**, *7* (1), 67-71.
23. Donnelly, A. C.; Mays, J. R.; Burlinson, J. A.; Nelson, J. T.; Vielhauer, G.; Holzbeierlein, J.; Blagg, B. S. J., The Design, Synthesis and Evaluation of Coumarin Ring Derivatives of the Novobiocin Scaffold that Exhibit Antiproliferative Activity. *Journal of Organic Chemistry* **2008**, *73*, 8901-8920.

24. Donnelly, A. C.; Zhao, H.; Kusuma, B. R.; Blagg, B. S. J., Cytotoxic Sugar Analogues of an Optimized Novobiocin Scaffold. *Medicinal Chemistry Communication* **2010**, *1* (2), 165-170.
25. Zhao, H.; Kusuma, B. R.; Blagg, B. S. J., Synthesis and Evaluation of Noviose Replacements on Novobiocin that Manifest Anti-proliferative Activity. *ACS Medicinal Chemistry Letters* **2010**, *1* (7), 311-315.
26. Zhao, H.; Blagg, B. S. J., Novobiocin Analogues with Second-Generation Noviose Surrogates. *Bioorganic & Medicinal Chemistry Letters* **2013**, *23* (2), 552-7.
27. Ghosh, S.; Shinogle, H. E.; Garg, G.; Vielhauer, G. A.; Holzbeierlein, J. M.; Dobrowsky, R. T.; Blagg, B. S., Hsp90 C-terminal inhibitors exhibit antimigratory activity by disrupting the Hsp90alpha/Aha1 complex in PC3-MM2 cells. *ACS Chemical Biology* **2015**, *10* (2), 577-90.
28. Mishra, S. J.; Ghosh, S.; Stothert, A. R.; Dickey, C. A.; Blagg, B. S., Transformation of the Non-Selective Aminocyclohexanol-Based Hsp90 Inhibitor into a Grp94-Selective Scaffold. *ACS Chemical Biology* **2017**, *12* (1), 244-253.
29. Li, W.; Sahu, D.; Tsen, F., Secreted Heat Shock Protein-90 (Hsp90) in Wound Healing and Cancer. *Biochimica et Biophysica Acta (BBA) - Molecular Cell Research* **2012**, *1823* (3), 730-741.
30. Zhao, H.; Moroni, E.; Colombo, G.; Blagg, B. S. J., Identification of a New Scaffold for Hsp90 C-Terminal Inhibition. *ACS Medicinal Chemistry Letters* **2014**, *5* (1), 84-88.
31. Blagg, B., S.J., Dobrowsky, Rick, T., Anyika, Mercy, Biphenyl Amides With Modified Ether Groups as Hsp90 Inhibitors and Hsp70. CA2952029 A1, **2015**.